

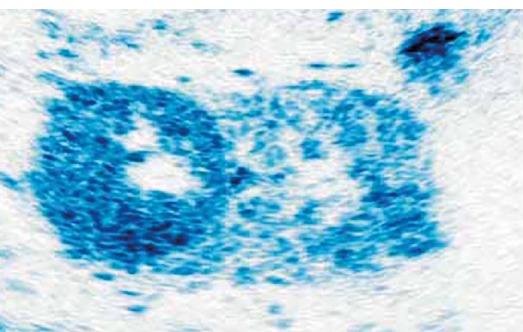
DGfN

MITTEILUNGEN

DER DEUTSCHEN GESELLSCHAFT FÜR NEPHROLOGIE

SUPPLEMENT 01/2022

Erscheinungsort: Berlin



ABSTRACTS

der 14. Jahrestagung der Deutschen Gesellschaft für Nephrologie
„Kongress für Nephrologie“ 2022
6. bis 9. Oktober 2022 in Berlin

INHALTSVERZEICHNIS

FREIE VORTRÄGE 5

FV01	5
FV02	5
FV03	6
FV04	7
FV05	7
FV06	8
FV07	9
FV08	10
FV09	10
FV10	11
FV11	12
FV12	13
FV13	13
FV14	15
FV15	16
FV16	16
FV17	17
FV18	18
FV19	20
FV20	21
FV21	22
FV22	23
FV23	23
FV24	24
FV25	25
FV26	27
FV27	29
FV28	30
FV29	31
FV30	31
FV31	32
FV32	33
FV33	33
FV34	34
FV35	35
FV36	36
FV37	36
FV38	37
FV39	38

POSTER 40

Akutes Nierenversagen	40
Diabetes	46
Chronisches Nierenversagen 1	52
Chronisches Nierenversagen 2	59
Chronisches Nierenversagen 3	68
Case Reports	80
COVID-19 1	90
COVID-19 2	97
Dialyse/Apherese 1	106
Dialyse/Apherese 2	114
Nierenphysiologie	124
Hypertensiologie	134
Digitale Nephrologie	142
Experimentelle Nephrologie 1	146
Experimentelle Nephrologie 2	154
Experimentelle Nephrologie 3	161
Experimentelle Nephrologie 4	170
Experimentelle Nephrologie 5	178
Experimentelle Nephrologie 6	186
Experimentelle Nephrologie 7	193
Glomerulonephritis und immunologische Krankheiten (klinisch)	202
Pädiatrische Nephrologie	213
Transplantation 1	215
Transplantation 2	225

AUTORENVERZEICHNIS 234

IMPRESSUM 247

FREIE VORTRÄGE

Chronic Kidney Disease I

FV01

Veränderungen des Volumenstatus mit Beginn einer Therapie mit SGLT2-Inhibitoren bei chronischer Nierenerkrankung

A. Schork; M.-L. Eberbach; D. J. Heister; B. N. Bohnert; N. Heyne; F. Artunc
Sektion Nieren- und Hochdruckkrankheiten, Universitätsklinikum, Medizinische Klinik IV, Eberhard Karls Universität Tübingen, Tübingen

Hintergrund: Überwässerung bei chronischer Nierenerkrankung (CKD) ist mit Proteinurie und Progression der CKD assoziiert. SGLT2-Inhibitoren können die Progression der CKD verlangsamen, ihr Effekt auf die Überwässerung bei CKD ist hingegen nicht bekannt.

Methode: In dieser longitudinalen Observationsstudie wurde der Volumenstatus mittels Bioimpedanzspektroskopie (BCM, Fresenius) bei n = 36 Patienten mit CKD (Genese hypertensiv/diabetisch n = 10, IgAN n = 13, andere n = 13; Alter Median 55 (IQR 38–68) Jahre; eGFR 46 ml/min/1,73 m² (33–64); Albuminurie 1851 mg/g Krea (467–3904)) bei Neubeginn eines SGLT2-Inhibitors (n = 31 Dapagliflozin 1 × 10 mg, n = 4 Dapagliflozin 1 × 5 mg, n = 1 Empagliflozin 2 × 10 mg) und nach 1 Woche, 1 Monat, 3 Monaten und 6 Monaten gemessen (bisher verfügbares Follow Up (FU): n = 33 Tag 6 (4–12), n = 30 Tag 35 (30–42), n = 25 Tag 98 (89–105), n = 18 Tag 187 (175–194)).

Ergebnisse: Die Glukosurie unter Einnahme eines SGLT2-Inhibitors stieg auf 0,55 (0,29–0,98) g/dl bzw. 10,3 (7,3–17,8) g/g Krea. Albuminurie bzw. eGFR nahmen nach 6 Monaten um 910 (101–1225) mg/g

Krea (Wilcoxon p = 0,0079) bzw. 5 (2–10) ml/min/1,73 m² (Wilcoxon p = 0,0031) ab. Gewicht bzw. BMI betrugen zu Beginn 79,6 (70,3–94,4) kg bzw. 26,3 (23,8–33,8) kg/m² und nahmen nach 6 Monaten tendenziell aber nicht signifikant ab. Die Überwässerung (Overhydration, OH) in der Kohorte zu Beginn lag bei +0,42 (–0,14 – +1,38) L/1,73 m² und nahm bereits am ersten bzw. zweiten FU (Tag 6 bzw. 35) um 0,4 (–0,2–0,9) L bzw. 0,5 (0,02–0,9) L ab (Wilcoxon p = 0,011 bzw. p = 0,002) und blieb im weiteren Verlauf stabil (Friedmann Test p = 0,010; Abnahme OH nach 6 Monaten gegenüber Beginn 0,6 (0,1–1,8) L, Wilcoxon p = 0,006). Die Abnahme der OH war umso größer, je höher der Ausgangswert der OH (Lineare Regr. p = 0,001). Das Extrazellulärwasser (ECW) nahm ebenfalls bereits beim ersten FU um 0,5 (–0,3–0,9) L/1,73 m² ab (p = 0,032) und blieb dann stabil. **Zusammenfassung:** Unter SGLT2-Inhibitoren kommt es bei CKD zu einer Reduktion einer (latent) Überwässerung. Dies stellt einen potentiellen Mechanismus der Nephroprotektion von SGLT2-Inhibitoren dar.

Mortalität an der Dialyse

FV02

Mortalitätsprädiktion mittels retinaler Gefäßanalyse im Langzeitverlauf bei Hämodialysepatienten

R. Günthner; L. Streese¹; S. Angermann; G. Lorenz; M. C. Braunisch; J. Matschkal; R. I. Hausinger; D. Stadler; B. Haller; K. Kotliar²; U. Heemann; H. Hanssen³; C. Schmaderer
II. Medizinische Klinik, Nephrologie, Klinikum rechts der Isar, Technische

Universität München, München;

¹ Departement für Sport, Bewegung und Gesundheit, Universität Basel, Basel/CH; ² Fachbereich 9 – Medizintechnik und Technomathematik, Fachhochschule Aachen, Jülich; ³ Bereich Sport- und Bewegungsmedizin, Department Sport, Bewegung und Gesundheit, Universität Basel, Basel/CH

Hintergrund: Retinale Gefäßdurchmesser dienen seit längerem als valide Biomarker für die Mortalitätsprädiktion in großen Populationsstudien. Eine Beeinträchtigung der mikrovaskulären Funktion retinaler Gefäße wurde bei Hämodialysepatienten bereits als Mortalitätsprädiktor im kurzfristigen Verlauf beschrieben. Wir untersuchten nun die Bedeutung der retinalen Gefäßanalyse für die Mortalitätsprädiktion von Hämodialysepatienten im Langzeitverlauf. **Methode:** Mit Hilfe der statischen retinalen Gefäßanalyse werden arterielläre und venuläre Durchmesser bestimmt. Bei der dynamischen Gefäßanalyse wird die Retina mit Flickerlicht stimuliert und die (physiologische) Dilatationsreaktion der Arteriolen (aMax) und Venolen (vMax) quantifiziert.

Ergebnisse: 275 Patienten (statische Analyse) bzw. 214 Patienten (dynamische Analyse) wurden für einen medianen Zeitraum von 73 Monaten beobachtet. Es starben 41 % (113/275) bzw. 36 % (76/214) der Patienten. Hinsichtlich der Flickerlicht-induzierten Dilatation ergab aMax im Median 1,6 [0,3–3,3]% und vMax 3,2 [2,0–5,1]%. Nach Einteilung der Patienten in Tertile entsprechend ihrer Gefäßreaktion hatten die Patienten im unteren vMax-Tertil ein deutlich verschlechtertes

5-Jahresüberleben, verglichen mit den Patienten im höchsten vMax-Terzil (50,6 % vs. 82,1 %). Dieser Unterschied war vor allem auf die erhöhte Inzidenz von Infektions-assoziierten Todesfällen im Terzil der Patienten mit niedrigem vMax zurückzuführen (21,7 % vs. 4,0 %). Die univariate Hazard ratio pro Standardabweichung von vMax betrug für die Gesamtmortalität 0,69 [0,54; 0,88] und war für die Infektions-assoziierte Mortalität sogar noch ausgeprägter (HR 0,53 [0,33; 0,83]). Nach multivariater Adjustierung zeigte sich weiterhin ein statistisch signifikanter Einfluss von vMax auf die Gesamtmortalität (HR 0,73 [0,54; 0,98]). Die statische Messung der Gefäßdurchmesser zeigte keine signifikante Assoziation mit der Mortalität.

Zusammenfassung: Durch die Ergebnisse der Langzeitbeobachtung konnte die Bedeutung der dynamischen retinalen Gefäßanalyse für die Mortalitätsprädiktion von Hämodialysepatienten gefestigt werden. Interessanterweise scheint dies hauptsächlich für die Infektions-assoziierte Mortalität eine Rolle zu spielen. Eine Untersuchung der statischen Gefäßdurchmesser zeigte hingegen keine Bedeutung für die Mortalitätsprädiktion.

Abstoßungstherapie

FV03

Molecular and cellular mechanisms of Lipocalin-2 mediated renoprotection in kidney transplantation

A. M. Pfeifferkorn¹; L. Zhao¹; M. Xu¹; A. Kusch²; R. Fritsche³; C. Erdogan¹; H. G. Schwelberger⁴; J. Pratschke; A. Patzak¹; F. Aigner⁵; I. M. Sauer; M. I. Ashraf

Experimentelle Chirurgie, Campus Virchow-Klinikum, Charité – Universitätsmedizin Berlin, Berlin; ¹ Institut für Translational Physiologie, Campus Charité Mitte, Charité – Universitätsmedizin Berlin, Berlin; ² Medizinische Klinik mit Schwerpunkt Internistische Intensivmedizin und Nephrologie, Campus Virchow-Klinikum, Charité – Universitätsmedizin Berlin, Berlin; ³ Metabolomics Platform, Berlin Institute of Health, Charité – Universitätsmedizin Berlin, Berlin; ⁴ Department of Visceral, Transplantation and Thoracic Surgery, Medical University of Innsbruck, Austria, Innsbruck/A; ⁵ Abteilung für Chirurgie, Barmherzige Brüder Krankenhaus Graz, Graz/A

Objective: While Lipocalin-2 (Lcn2) is an early marker of acute kidney injury, delayed graft function and acute rejection, our previous studies have delineated a renoprotective effect of recombinant Lcn2:Siderophore:Fe (rLcn2) in a mouse kidney transplantation (KTx) model. In this study, we primarily focus on the molecular and cellular processes triggering these effects, which have not yet been fully investigated to date.

Method: Kidneys were transplanted from Balb/c to C57Bl/6 mice (\pm rLcn2, 250 mg/kg) with subsequent phenotyping of adaptive and innate immune cells, isolated from graft, spleen, lymph nodes and blood by flow cytometry at post-operative day 3 and 7. Following syngeneic mouse KTx (cold ischemia time (CIT): 5.5 h, reperfusion (R): 24 h \pm rLcn2, 250 mg/kg) and culturing of isolated murine primary proximal tubular epithelial cells subjected to hypoxia/reoxygenation (H: 24 h/R:

0.5 h, 6 h, 12 h, 24 h \pm rLcn2, 1 μ g/ml) *in vitro*, intrarenal stress, inflammation and survival pathways were comprehensively scrutinized by multiplex signaling analysis. To determine the effect of rLcn2 on the physiology of renal microvessels, dilatation function of BAY 58-2667 (soluble guanylyl cyclase activator) on angiotensin II (Ang II)-precontracted murine afferent arterioles (AA) were examined following H/R (H:30min/R:10min) and syngeneic KTx (CIT: 5.5 h, R: 20 h) \pm rLcn2, apo-rLcn2 and deferoxamine (DFO).

Results: Although immune cell phenotyping revealed no extensive immunosuppressive or regulatory effect of rLcn2, administration of rLcn2 mitigated intragraft accumulation of total and particularly of activated (NKG2D+) CD8+ T cells, while the degranulation capacity and frequency of interferon γ (IFN γ)⁺ and perforin⁺ CD8+ T cells significantly subsided. Contradictory, rLcn2 treatment elicited no clear effect on stress, inflammation and survival signaling in murine kidney epithelia after H/R and KTx. Apart from this, rLcn2 not only circumvented H/R-induced loss in dilatation of isolated renal AA but also substantially improved cold ischemia-impaired vasodilatation. Moreover, while Fe free apo-rLcn2 could not ameliorate loss of vasodilatation, DFO reversed the protective effect of rLcn2, validating the iron-dependent effect.

Conclusion: rLcn2 protects mouse renal allografts from CD8+T cell mediated alloimmune response and attenuates ischemia reperfusion injury-induced loss in dilatation of renal AA both *in vitro* (H/R) and *in vivo* (KTx).

From bench to bedside – ANCA-assoziierte Vaskulitis

FV04

Urinary CD4+ T cell quantification identifies ANCA patients at risk for subsequent renal flares: Results of the prospective, multicenter Pre-Flared study

L. Prskalo; C. Skopnik¹;
J. Sonnemann²; N. Görlich²;
L. Wagner; E. Grothgar²; J. Klocke¹;
D. Metzke¹; U. Schneider²; A. Salama³;
M. Bieringer⁴; A. Schreiber; P. Enghard
Medizinische Klinik mit Schwerpunkt Nephrologie und Internistische Intensivmedizin, Campus Charité Mitte, Charité – Universitätsmedizin Berlin, Berlin; ¹Medizinische Klinik mit Schwerpunkt Nephrologie und Internistische Intensivmedizin, Campus Virchow-Klinikum, Charité – Universitätsmedizin Berlin, Berlin; ²Medizinische Klinik mit Schwerpunkt Rheumatologie und Klinische Immunologie, Campus Charité Mitte, Charité – Universitätsmedizin Berlin, Berlin; ³Department of Renal Medicine, Royal Free Hospital, University College London, London/UK; ⁴Klinik und Poliklinik für Kardiologie und Nephrologie, HELIOS Klinikum Berlin-Buch, Berlin

Objective: Patients with ANCA-associated vasculitis (AAV) are at risk for recurrent renal flares. Presently, there are no reliable biomarkers for flare prediction. Urinary CD4+ T cells have previously been reported to distinguish active renal involvement in AAV from AAV in stable remission, but it is currently unknown if they may predict future flares in quiescent disease.

Method: We prospectively collected urine samples from 112 AAV patients in remission (BVAS = 0) at three AAV clinics in two

hospitals (NCT04428398). 10 patients met the exclusion criteria; 102 patient samples were analyzed. Renal flares were defined as an increase in BVAS > 0 and at least one element of the renal BVAS or alternatively as new initiation of induction treatment. Using flow cytometry, urinary CD4+ and CD8+ T cell subsets were quantified. The primary end point was the prediction of renal relapse after six months using the initial CD4+ count.

Results: Of the 102 analyzed patients 10 developed a renal flare, 2 developed a non-renal flare and 90 remained in stable remission. The number of urinary CD4+ T cells predicted renal flares with an Receiver-Operator Characteristic (ROC) area under the curve (AUC) of 0.88. Urinary CD4+ T cells outperformed traditional biomarkers such as ANCA titers, hematuria, and proteinuria in renal flare prediction. Applying a cut-off of 490 CD4+ T cells per 100 ml urine yielded a sensitivity of 60 % and specificity of 97.8 % in identifying patients with future renal flares. A combination of urinary CD4+ T cells (> 50/100 ml) and PR3 ANCA levels (> 40IU/ml) increased the predictive value to the sensitivity of 100 % and specificity of 92 %. Furthermore, in the complete patient cohort (n = 102), the number of urinary CD4+ T cells correlated with loss of GFR (p < 0.01) and increase in proteinuria (p < 0.05) in the subsequent 6 months.

Conclusion: Urinary CD4+ T cell numbers identify AAV patients at risk for renal flares. Combining urinary CD4+ T cell numbers with ANCA levels may further improve flare prediction.

Covid bei Nierenerkrankten

FV05

Neutralization of the SARS-CoV-2 delta and omicron variants in previous non-responder kidney transplant recipients after short-term withdrawal of mycophenolic acid

L. Benning; C. Morath; T. Kühn¹;
M. Schaier; A. Blank²; P. Schnitzler³;
M. Zeier; R. Bartenschlager³;
T. H. Tran⁴; C. Speer
Medizinische Klinik I, Sektion Nephrologie, Medizinische Fakultät, Ruprecht-Karls-Universität Heidelberg, Heidelberg; ¹Nierenzentrum, Medizinische Fakultät, Ruprecht-Karls-Universität Heidelberg, Heidelberg; ²Klinische Pharmakologie und Pharmakoepidemiologie, Innere Medizin VI, Ruprecht-Karls-Universität Heidelberg, Heidelberg; ³Molekulare Virologie, Zentrum für Infektologie, Ruprecht-Karls-Universität Heidelberg, Heidelberg; ⁴Transplantationsimmunologie, Medizinische Fakultät, Ruprecht-Karls-Universität Heidelberg, Heidelberg

Objective: Seroconversion rates after COVID-19 vaccination are significantly lower in kidney transplant recipients (KTR) compared to healthy cohorts. Adaptive immunization strategies are urgently needed to ultimately protect these patients from COVID-19. In this single-center trial we aimed to determine whether short-term withdrawal of mycophenolic acid (MPA) increases immunogenicity of SARS-CoV-2 mRNA vaccination in KTR.

Method: 76 KTR with no seroresponse after at least three COVID-19 vaccinations were enrolled to receive an additional 100 µg mRNA-1273 vaccination. In 43 patients with stable graft function and a maintenance

immunosuppressive therapy consisting of a calcineurin inhibitor, MPA, and corticosteroids, MPA was withdrawn 5–7 days prior to vaccination and remained paused for 4 additional weeks after vaccination. Results were compared to 25 participants with continued maintenance therapy including MPA. SARS-CoV-2-specific antibodies were determined four weeks after vaccination. Neutralization of the delta and omicron variants was determined using a live-virus assay. In patients with MPA withdrawal, donor-specific anti-HLA antibodies (DSA) and donor-derived cell-free DNA (dd-cfDNA) were monitored before withdrawal and at follow-up.

Results: After vaccination, 24/69 (35 %) KTR showed anti-spike S1 IgG antibodies above the predefined cut-off, excluding 7 breakthrough infections that occurred during follow-up. Seroconversion rates and SARS-CoV-2

specific antibodies were significantly higher in patients in whom MPA was withdrawn prior to vaccination compared to those who remained on maintenance immunosuppression including MPA ($P = 0.006$, Figure 1A). Neutralization of the omicron variant was significantly impaired compared to neutralization of the delta variant ($P < 0.001$, Figure 1B). Higher anti-S1 IgG antibody levels were associated with better neutralization of the B.1.617.2 (delta) and B.1.1.529 (omicron) variants (Figure 1C). In patients with MPA withdrawal, graft function and dd-cfDNA remained stable. No acute rejection episodes occurred during short-term follow-up. However, resurgence of prior DSA was detected in 7 patients.

Conclusion: Our data show a significant improvement in humoral immune response after an additional vaccine dose in previous

non-responder KTR with at least three vaccine doses. The effect was most pronounced in KTR where MPA was withdrawn temporarily upon vaccination. Thus, MPA withdrawal seems reasonable to enhance seroconversion rates. For safety reasons, this may be applied in patients without current or previous DSA.

FV06

Kein Anhalt für persistierende Nierenerkrankung nach milder SARS-CoV-2 Infektion in der Hamburg City Health Study COVID Kohorte

C. Schmidt-Lauber; S. Hänzelmann; D. Fliser¹; A. Alabdo; M. T. Lindenmeyer; T. Renné²; E. L. Petersen³; T. Zeller⁴; F. Hausmann⁵; S. Blankenberg⁴; R. Twerenbold⁴; T. B. Huber
Nephrologie/Rheumatologie und Endokrinologie/Diabetologie, III. Medizinische Klinik,

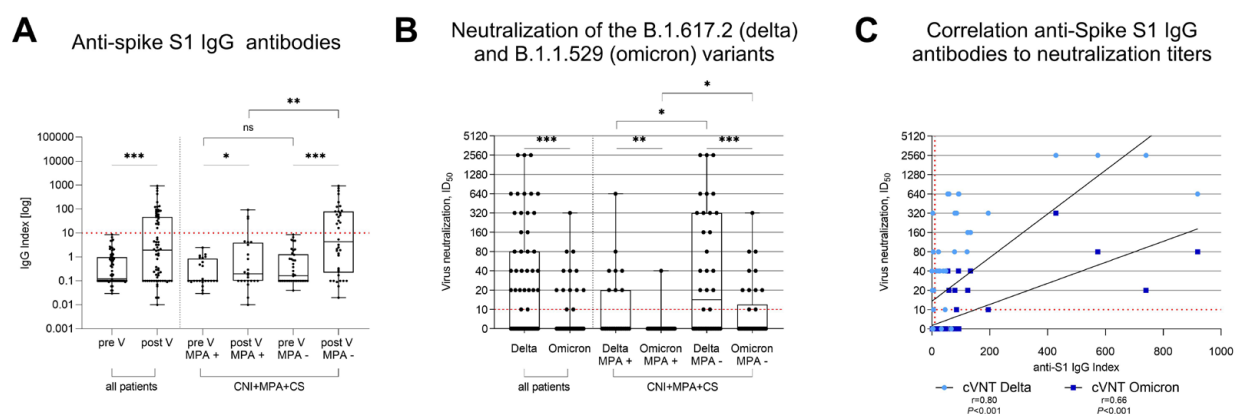


Figure 1: SARS-CoV-2 specific antibodies in 69 previous non-responder kidney transplant recipients after an additional mRNA-1273 vaccine dose (A) Anti-Spike S1 IgG antibodies in 69 KTR before and after vaccination, stratified for short-term withdrawal of MPA (B) Neutralization of the SARS-CoV-2 B.1.617.2 (delta) and the B.1.1.529 (omicron) variants by antibodies in sera of 69 KTR, stratified for short-term withdrawal of MPA (C) Correlation analysis of anti-S1 IgG results to cross-neutralization titers of the B.1.617.2 (delta) and the B.1.1.529 (omicron) variants CNI, calcineurin inhibitor; CS, corticosteroids; cVNT, conventional virus neutralization test; KTR, kidney transplant recipients; ID₅₀, inhibitory dilution 50; MFI, mean fluorescence intensity; MPA, mycophenolic acid; V, vaccination; r, Spearman's rho; *** $P < 0.001$; ** $P < 0.01$; * $P < 0.05$

Universitätsklinikum Hamburg-Eppendorf, Hamburg; ¹Nieren- und Hochdruckkrankheiten, Klinik für Innere Medizin IV, Universität des Saarlandes, Homburg/Saar; ²Institut für Klinische Chemie und Laboratoriumsmedizin, Universitätsklinikum Hamburg-Eppendorf, Hamburg; ³Epidemiologisches Studienzentrum, Universitätsklinikum Hamburg-Eppendorf, Hamburg; ⁴Klinik und Poliklinik für Kardiologie, Universitäres Herz- und Gefäßzentrum Hamburg, Universitätsklinikum Hamburg-Eppendorf, Hamburg; ⁵Institut für Medizinische Systembiologie, Universitätsklinikum Hamburg-Eppendorf, Hamburg

Hintergrund: Diverse Symptome und Organpathologien wurden nach einer Coronavirus Erkrankung 2019 (COVID-19) beschrieben, wobei renale Langzeitfolgen weitestgehend unbekannt sind. Diese Studie untersucht die renalen Folgen nach milder bis moderater COVID-19.

Methode: Diese Querschnittsstudie analysiert Patient:innen nach nicht-schwerer COVID-19 sowie gematchte Kontrollen ohne vorherige COVID-19. Die Rekrutierung erfolgte über die bevölkerungsbasierte Hamburg City Health Study (HCHS) sowie das dazugehörige COVID-Programm. Die HCHS ist eine prospektive populationsbasierte Kohortenstudie an zufällig ausgewählten Einwohner:innen der Stadt Hamburg. Während der COVID-19-Pandemie lud die Studie auch Individuen nach COVID-19 über Zeitungsankündigungen und ein offizielles COVID-19-Testzentrum ein. Die PCR-bestätigten Infektionen mussten mindestens 4 Monate vor Studieneinschluss aufgetreten sein. Alle Patient:innen waren zwischen 45 und 74 Jahre alt. Das Matching erfolgte nach Alter,

Geschlecht und Bildung. Als Hauptergebnisse wurden die nach Kreatinin und Cystatin C errechnete glomeruläre Filtrationsleistung (eGFR), Albuminurie, Dickkopf-3, Hämaturie und Leukozyturie festgelegt.

Ergebnisse: Die Post-COVID-Kohorte bestand aus 443, die non-COVID-Kohorte aus 1328 Personen. Die meisten Patient:innen hatten eine milde COVID-19, nur 31 Individuen wurden im Krankenhaus und niemand auf einer Intensivstation behandelt. Im Median lag die Infektion 9 Monate zurück. Das Risiko für eine chronische Nierenerkrankung (CNE), definiert als eine eGFR < 60 ml/min/1,73 m², (OR 0,9, adjustierter P Wert = 1,000) oder eine stark erhöhte Albuminurie (OR 0,73, adj. P = 0,630) war in der post-COVID-Kohorte nicht höher als in der non-COVID-Kohorte. Dies galt auch für frühe CNE-Stadien. Die mittlere eGFR war jedoch in der post-COVID-Kohorte leicht niedriger, selbst nach Adjustierung auf bekannte CNE-Risikofaktoren (beta -1,96, adj. P = 0,018). Wir fanden keine erhöhte Rate an Hämaturie, Leukozyturie oder Proteinurie in der post-COVID-Kohorte, was auf keine anhaltende systematische Nierenbeteiligung hindeutet. Dickkopf3 war bei post-COVID-Patienten sogar tendenziell niedriger, was darauf hinweist, dass in dieser Kohorte kein Risiko für eine anhaltende Abnahme der eGFR besteht (beta -72,66, adj. P = 0,072).

Zusammenfassung: Während es nach milder und moderater COVID-19 zu einem subklinischen Abfall der eGFR kommt, fanden wir keine Hinweise auf eine relevante Nierenerkrankung oder eine anhaltende Nierenbeteiligung nach nicht-schwerer COVID-19.

Ernährung

FV07

Microbial metabolites induce pro-inflammatory mechanisms in children with CKD

J. B. Holle; H. Bartolomaeus¹; U. Löber¹; F. Behrens²; T. U. P. Bartolomaeus¹; V. McParland¹; A. Thürmer³; J. Kirwan¹; N. Wilck¹; D. Müller
Klinik für Pädiatrie mit Schwerpunkt Nephrologie, Campus Virchow-Klinikum, Charité – Universitätsmedizin Berlin, Berlin; ¹ECRC-Kooperation von MDC und Charité, Experimental and Clinical Research Center, Berlin; ²Institut für Physiologie, Campus Charité Mitte, Charité – Universitätsmedizin Berlin, Berlin; ³Robert Koch Institute, Berlin

Objective: Controlling chronic inflammatory processes as a major risk factor for cardiovascular disease is of outstanding importance in chronic kidney disease (CKD) to reduce the rate of CKD-associated morbidity. The underlying mechanisms are incompletely understood, but may be linked to gut dysbiosis. We aim to describe the microbiota-immune interaction in a cohort of pediatric CKD, thus independent of confounding comorbidities frequently seen in adult patients.

Method: We analyzed the fecal microbiome, plasma metabolites and peripheral immune phenotypes in 48 children (normal kidney function, CKD stage G3–G4, G5 treated by hemodialysis (HD) or kidney transplantation) with a mean age of 10.6 ± 3.8 years.

Results: Serum TNF-α and sCD14 were stage-dependently elevated, indicating inflammation, gut barrier dysfunction and endotoxemia. We observed compositional and functional alterations of the

microbiome, including a diminished production of short-chain fatty acids. Plasma metabolite analysis revealed a stage-dependent increase of tryptophan metabolites of bacterial origin. Serum from HD patients activated the aryl hydrocarbon receptor and stimulated TNF- α production in monocytes, corresponding to a pro-inflammatory shift from classical to non-classical and intermediate monocytes. Moreover, unsupervised analysis of T cells revealed a loss of mucosa-associated invariant T (MAIT) cells and regulatory T cell subtypes in HD patients.

Conclusion: Gut barrier dysfunction and microbial metabolite imbalance mediate the pro-inflammatory immune phenotype, thereby driving the susceptibility to cardiovascular disease. The fact that these dysbiosis-driven immunological changes are already detectable in children with CKD, in whom comorbidities usually found in adults are absent, highlights the importance and the specificity of CKD-related microbiota-immune interaction for chronic inflammation. Based on this knowledge, the development of personalized dietary interventions and microbiota-targeted therapies represent a promising area of research to improve the prognosis of young and old CKD patients.

Digitale Pathologie

FV08

Hochdimensionale Bildgebung von neonatalen und adulten Nieren durch vereinfachten Gewebe-Clearing Ansatz

M. Preussner; J. Einloft; A. Hofmeister; S. Bedenbender; K. Roth¹; I. Grgic
Klinik für Innere Medizin, Nephrologie und Internistische Intensivmedizin,

Standort Marburg, Universitätsklinikum Gießen und Marburg GmbH, Marburg;
¹ Zelluläre Bildgebung, Zentrum für Tumor- und Immunbiologie, Philipps-Universität Marburg, Marburg

Hintergrund: Vorgänge der Glomerulogenese gelten als komplex. Insbesondere die zeitlich-räumliche Koordination während der Ausbildung der glomerulären Architektur ist noch unzureichend verstanden. Klassische histopathologische Methoden und Mikroskopiertechniken erlauben meist nur limitierte Darstellungs- und Rekonstruktionsmöglichkeiten von Prozessen in der reifenden Niere, die im Grunde nur in einem dreidimensionalen Kontext adäquat nachvollzogen werden können.

Methode: Um das schrittweise Konstituieren und Ausformen von podozytären Vorläuferzellen und gereiften Podozyten bei der Glomerulogenese longitudinal studieren zu können, verwendeten wir Nieren von transgenen Podo^{TRAP} Mäusen unterschiedlichen Alters in Kombination mit einem modifizierten Ethyl-Cinnamate (ECi)-basierten Clearing Ansatz, Immunostaining und 3D-Mikroskopie.

Ergebnisse: Die Wahl dieses Verfahrens sollte eine optische Transparenz im Nierengewebe herstellen und es so einer hochauflösenden 3D-Visualisierung zugänglich machen. Es gelang eine hochdimensionale Rekonstruktion und Quantifizierung der unterschiedlichen glomerulären Entwicklungsstadien (Nierenbläschen, S-Phase, Kapillarschlinge, maturierter Glomerulus) in transparenten Nieren von P0 bis P7 sowie adulten Podo^{TRAP} Mäusen. Die Kombination von ECi und anschließender

2-Photonen-Mikroskopie erzielte eine signifikant höhere Visualisierungstiefe gegenüber nicht-geklärten Nieren (~1500µm versus ~150µm). GFP-L10a⁺ Podozyten in ECi-behandelten Podo^{TRAP} Nieren konnten aufgrund ihrer robusten zellulären Epifluoreszenz prompt identifiziert werden, wobei die Signalintensität mit fortschreitender Reifung interessanterweise zunahm. Es gelang eine präzise und umfassende Quantifizierung der glomerulären Volumenzunahme während ihres Reifungsprozesses. Extraglomeruläre GFP-L10a⁺ mesenchymale Zellen zeichneten sich im Vergleich zu Podozyten durch eine deutlich schwächere eGFP-L10a Expression aus.

Zusammenfassung: Der kombinierte Ansatz aus ECi-Clearing und hochdimensionaler Mikroskopie in Podo^{TRAP} Nieren eignet sich für eine hochauflösende und umfängliche 3D-Bildgebung einschließlich Morphometrie von Glomeruli und Podozyten in kompletten neonatalen Mausnieren. Der Ansatz könnte u. a. für holistische histopathologische Analysen in verschiedenen glomerulären Krankheitsmodellen einschließlich der FSGS genutzt werden.

Glomeruläre Erkrankungen

FV09

Podocyte expression of the human PLA2R1 causes immune-mediated membranous nephropathy in mice

N. M. Tomas; S. Dehde¹; C. Meyer-Schwesinger²; I. Hermans-Borgmeyer; L. Seifert; J. Maybaum; R. Lucas; S. Köllner; M. Huang; O. Kretz; T. B. Huber; G. Zahner
Nephrologie/Rheumatologie und Endokrinologie/Diabetologie,

III. Medizinische Klinik, Universitätsklinikum Hamburg-Eppendorf, Hamburg; ¹ Heinrich-Pette-Institut für Experimentelle Virologie und Immunologie, Universitätsklinikum Hamburg-Eppendorf, Hamburg; ² Institut für Zelluläre und Integrative Physiologie, Universitätsklinikum Hamburg-Eppendorf, Hamburg

Objective: Antibody-mediated autoimmune pathologies like membranous nephropathy (MN) are difficult to model, particularly in the absence of target antigen expression in typical model organisms such as mice and rats – as it is the case for PLA2R1, the major autoantigen in this disease.

Method: We generated a mouse line expressing the full-length human PLA2R1 specifically in podocytes (hPLA2R1-positive mice). Mice were characterized during the first weeks of life using urinary albumin measurements, serum analyses, light microscopic and immunofluorescence microscopy as well as electron microscopy. The mouse line was also crossed to *Rag2*^{-/-} mice, which lack mature B and T lymphocytes.

Results: Human PLA2R1-positive mice were healthy after birth. Beginning from the age of three weeks, however, mice developed a nephrotic syndrome with progressive albuminuria and hyperlipidemia. This was preceded by the development of anti-PLA2R1 autoantibodies, which targeted the PLA2R1 extracellular domains that are also recognized by patient autoantibodies. After disease onset, histological analyses in hPLA2R1-positive mice revealed the typical morphological signs of MN with granular glomerular deposition of murine IgG in immunofluorescence and subepithelial

electron-dense deposits in electron microscopy. Importantly, hPLA2R1-positive *Rag2*^{-/-} mice did neither develop anti-PLA2R1 autoantibodies nor proteinuria.

Conclusion: Our work demonstrates that podocyte expression of human PLA2R1 in mice can induce membranous nephropathy with an underlying autoimmune pathogenesis.

Telemedizin und Social Media

FV10

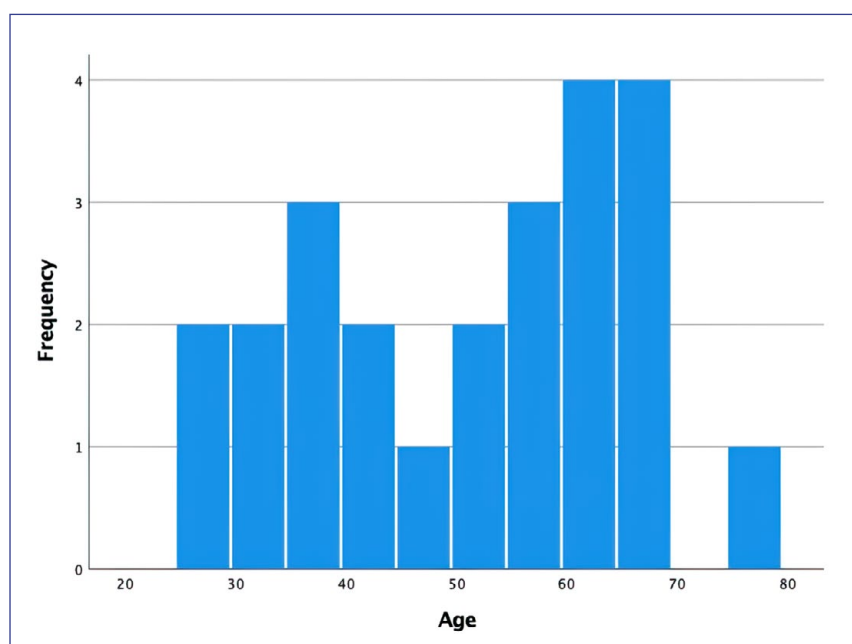
App-basierte Dokumentation und Unterstützung eines deutschen Heimdialyseprogramms – Eine Pilotstudie

S. Schricker; M. Schanz; T. Oberacker¹; M. Kimmel²; M. D. Alscher; M. Ketteler
Abteilung für Allgemeine Innere Medizin und Nephrologie, Robert-Bosch-Krankenhaus, Stuttgart; ¹Dr. Margarete Fischer-Bosch-Institut für Klinische

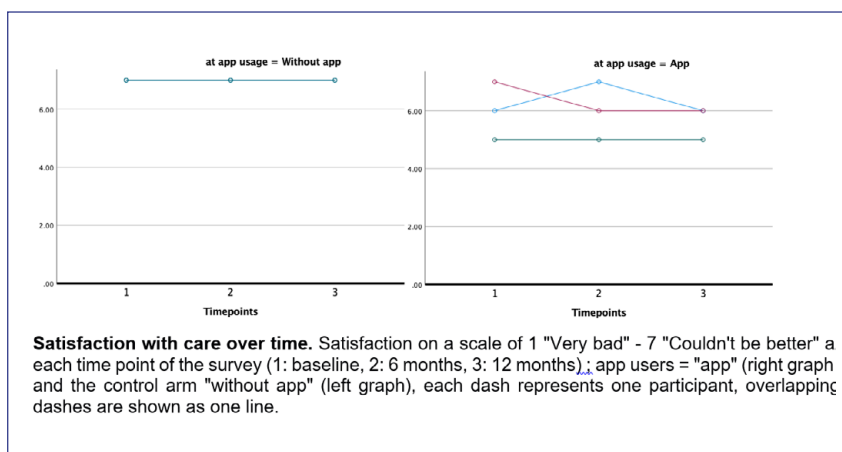
Pharmakologie, Robert-Bosch-Krankenhaus, Stuttgart; ² Klinik für Nieren-, Hochdruck- und Autoimmunerkrankungen, Zentrum für Innere Medizin, Alb Fils Kliniken – Klinik am Eichert, Göppingen

Hintergrund: Studien, die die Integration von Telemedizin in die Heimdialyseversorgung untersuchen, sind rar. Diese multizentrische, deutschlandweite prospektive Pilotstudie untersuchte die Auswirkungen und Akzeptanz einer App als Versorgungskonzept im Vergleich zu konventionell versorgten Patienten.

Methode: Zum Einsatz kam die „DiaApp“, ein tabletbasiertes Dokumentations- und Kommunikationssystem, das von der PHV entwickelt wurde. Die App wurde zwischen 2018 und 2019 von 25 Patienten in vier Dialysepraxen genutzt. Die Teilnehmer



FV10: Abb. 1



FV10: Abb. 2

konnten frei zwischen der App-Nutzung (App) und der bisherigen papierbasierten Dokumentation (Kontrolle) wählen. Prospektiv wurde Daten zur Demografie, unerwünschten Ereignissen sowie Fragebögen zur Lebensqualität (KDQL v1.3), Technikaffinität (TA-EG), Zufriedenheit mit der App (UTAUT) und Selbstvertrauen im Umgang mit chronischer Krankheit (SES6G) erhoben. Darüber hinaus wurden 5 qualitative Interviews über 90 min durchgeführt.

Ergebnisse: Von den 25 Teilnehmern nutzten 13 die App (52%). Die App-Nutzer waren tendenziell jünger, eher männlich (60%) und an der Peritonealdialyse ($n = 15$, 60%). Das mittlere Alter und der Dialyse-Jahrgang der App-Nutzer und der Kontrollen lagen bei 51 (38–60; 0) vs. 59 (37–64; 1) Jahren bzw. 51,5 (34–68; 3) vs. 38 (28–66; 5) Monaten. Die mittlere Nachbeobachtungszeit betrug 6,5 Monate und 12 Monate. App-Benutzer zeigten einen Trend (n.s.) zur größerem Selbstvertrauen im Umgang mit ihrer chronischen Krankheit (SES6G

Score App: 7,33, IQR: 6–8,83; Kontrollen: 7,17, IQR 6–7,83) und höhere Technikaffinität (in allen vier TA-EG Dimensionen). Insgesamt war das Bildungsniveau der Teilnehmer und die Behandlungszufriedenheit hoch. In den qualitativen Interviews gaben alle befragten App-Nutzer an, dass sie regelmäßig digitale Angebote in allen Lebensbereichen nutzen. Die App wurde insgesamt als nützlich empfunden. Den Patienten missfiel die Notwendigkeit eines speziellen Geräts. Informationen über die Krankheit suchten sie eher außerhalb der App, z.B. im Internet.

Zusammenfassung: In dieser Studie fanden wir keine signifikanten Unterschiede zwischen App-Nutzern und Kontrollen. Es traten keine unerwünschten Ereignisse auf. Vorteile flexibler digital gestützter Heimdialyseverfahren werden geschätzt. Gleichzeitig unterliegen Gesundheitsapps großen Erwartungen. Dies stellt die oft kostspielige Entwicklung solcher Anwendungen durch nicht-kommerzielle Anbieter und eine begrenzte Anzahl von Zielgruppen vor enorme Herausforderungen.

From bench to bedside – Glomerulosclerosis

FV11

Pathogenic role of cytotoxic CD8+ T cells in glomerulonephritis

A. Mueller; K. Neumann; G. Tiegs
Institut für Experimentelle Immunologie und Hepatologie, III. Medizinische Klinik, Universitätsklinikum Hamburg-Eppendorf, Hamburg

Objective: Glomerulonephritis (GN) is characterized by an immune-mediated inflammation of the glomeruli, leading to kidney damage and deterioration in renal function. Correlations between infiltrating CD8⁺ T cells and disease severity have already been described. There is increasing evidence for the pathogenic role of cytotoxic CD8⁺ T cells (CTL) in autoimmune diseases. However, their function in immune-mediated GN is less clear.

Method: Phenotypic characterization of renal CD8⁺ T-cell subsets in ANCA-GN patients was done by CITE-seq and scRNA-seq analyses. Nephrotoxic nephritis (NTN), as a model of murine crescentic GN, was induced in wild-type, *Cd8a*^{-/-}, and *Gzmb*^{-/-} mice, which were analyzed 8 days after NTN induction. The crescent formation, proteinuria, and IgG levels were determined to assess disease severity. Phenotype analysis of murine CD8⁺ T cells was done by flow cytometry. The expression of cleaved caspase-3 was analyzed in renal tissues from nephritic mice and ANCA-GN patients.

Results: We identified three distinct renal CD8⁺ T-cell subsets in ANCA-GN patients: effector CD8⁺ T cells (T_{eff}), memory CD8⁺ T cells (T_m) and tissue-resident memory CD8⁺ T cells (T_{rm}). CD8⁺ T_{eff}

were characterized by strong expression of granzyme B (GzmB), while CD8⁺ T_m predominantly expressed GzmK. We further determined low expression of granzymes by CD8⁺ T_m. In NTN, CTLs infiltrated the kidney. This was accompanied by increased GzmB-induced cleavage of caspase-3 in renal tissue, to induce apoptosis. Lack of CD8⁺ T cells in *Cd8a*^{-/-} mice ameliorated disease severity of NTN and reduced cleavage of caspase-3. The same findings were observed in *GzmB*^{-/-} mice.

Conclusion: We prove a pathogenic function of CTLs and the cytotoxic molecule GzmB in GN. Thus, mediators of cytotoxicity might be potential novel therapeutic targets in immune-mediated GN.

Lupus Nephritis

FV12

Macrophage subpopulations in the progression of HUS and lupus nephritis in pediatric patients

M. Sandersfeld; C. Daniel; M. Büttner-Herold; K. Amann; K. Benz¹

Institut für Nephropathologie, Universitätsklinikum, Friedrich-Alexander-Universität Erlangen-Nürnberg, Erlangen; ¹ Stabsstelle Transplantationen, Universitätsklinikum, Ärztliche Direktion, Friedrich-Alexander-Universität Erlangen-Nürnberg, Erlangen

Objective: Impaired renal function can be caused by various pathological processes. An important role in mediating renal injury is played by macrophages, which can possess either a pro-inflammatory (M1-like) or a more anti-inflammatory (M2-like) macrophage subtype. In this study, we aim to characterize the renal macrophage

subpopulations of pediatric patients with hemolytic uremic syndrome (HUS) and lupus nephritis (LN) and investigate whether they correlate with renal injury.

Method: Renal biopsies from 22 LN and 11 HUS pediatric patients collected at Erlangen University Hospital from 2000 to 2020 were included in this study. A group of pediatric kidney donors (n = 6) served as healthy controls. Immunofluorescence multi staining was used to mark iNOS+ M1-like, CD206+ M2a-like, CD163+M2c-like and CD68 as pan macrophage marker. Using semiquantitative scoring, glomerulosclerosis was analyzed in periodic acid Schiff stained sections followed by correlation with macrophage subpopulations.

Results: The M1-like macrophage phenotype could not exactly be detected since iNOS+ cells were missing in all kidney biopsies. Instead, CD68+ cells that were negative for CD163 and C206 were determined to be the M1-like subpopulation. The total number of CD68+ renal macrophages was significantly increased in patients with HUS compared to the control group and LN. M1-like CD68+CD163- macrophages were significantly increased 7.5-fold in HUS compared to the control group and 4.2-fold in LN. Even though the M2c-like CD68+CD163+ macrophage subpopulation dominated numerically, only a significant difference was observed between the control and HUS groups. The ratio of CD68+CD163-/CD68+CD163+ was also significantly higher in the HUS biopsies than in the controls, indicating an increased proportion of M1-like macrophages in HUS kidneys. Interestingly, M2a-like CD68+CD206+

macrophages were also significantly increased in HUS compared to control and LN, whereas CD68+CD206- numbers were comparable. In the LN kidney biopsies, the number of macrophages was higher on average than in the control group, but failed to reach the significance level. Furthermore, CD68+CD163- macrophages correlated significantly with kidney function and renal injury as assessed by serum creatinine (r = 0.769) and glomerulosclerosis (r = 0.550).

Conclusion: The correlation of M1-like macrophages with renal damage suggests a significant role of these cells in the pathogenesis of kidney disease and this cell type was particularly significantly increased in paediatric cases of HUS compared to controls and LN.

Clinical Science – Chronic Kidney Disease I

FV13

CKD im Alter – Daten zu Prävalenz und Verlauf über 8 Jahre in der Berliner Initiative Studie

T. Bothe; E. Schäffner; N. Mielke; A. Schneider; M. Barghout; M. van der Giet¹; M. K. Kuhlmann²; N. Ebert
Institut für Public Health, Charité – Universitätsmedizin Berlin, Berlin; ¹ Medizinische Klinik IV, Klinik für Nephrologie, Campus Benjamin Franklin, Charité – Universitätsmedizin Berlin, Berlin; ² Nephrologie, Klinik für Innere Medizin, Vivantes Klinikum im Friedrichshain, Berlin

Hintergrund: Es liegen wenige Ergebnisse zu Verläufen der geschätzten glomerulären Filtrationsrate (eGFR) in älteren Patient*innen vor. Die Beschreibung von eGFR Verläufen bei älteren Patient*innen

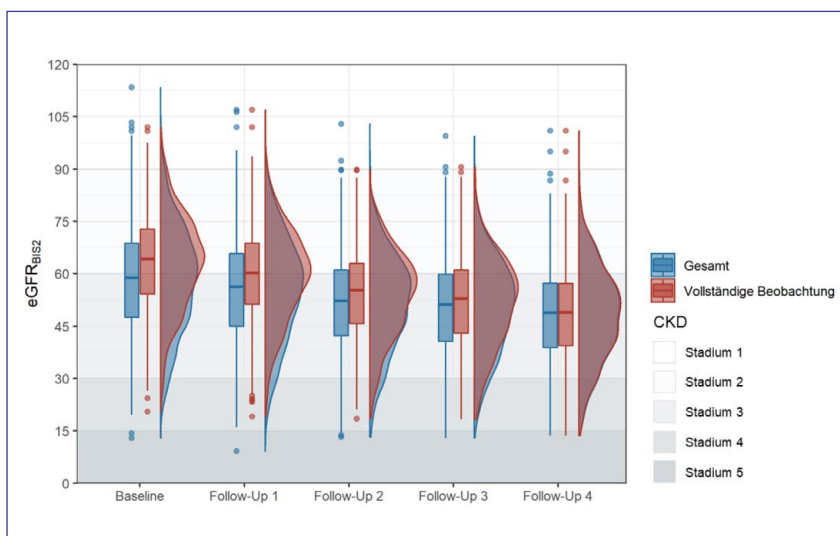
Tabelle 1: Soziodemographische Variablen und Prävalenz von CKD für beide Studienpopulationen.

Population	Variable	Baseline	Follow-Up 1	Follow-Up 2	Follow-Up 3	Follow-Up 4
Gesamt	N ¹	2.068	1.670	1.396	1.130	870
	Alter, MW (SD)	80,4 (6,7)	81,8 (6,4)	83,1 (6,1)	84,3 (5,6)	85,6 (5,3)
	Frauen, N (%)	1.088 (52,6)	889 (53,2)	754 (54,0)	618 (54,7)	487 (56,0)
	Verstorben ^{2,3} , N (%)	127 (6,1)	143 (8,6)	152 (10,9)	119 (10,5)	103 (11,8)
	eGFR _{BIS2} , MW (SD)	58,1 (15,2)	55,5 (15,0)	51,4 (13,6)	50,2 (13,5)	48,3 (13,3)
	eGFR _{EKFC} , MW (SD)	60,4 (15,9)	58,5 (16,2)	57,5 (16,0)	55,6 (15,8)	54,2 (15,9)
	CKD Stadien ⁴ , N (%)					
	Stadium 1	33 (1,6)	12 (0,7)	2 (0,1)	2 (0,2)	2 (0,2)
	Stadium 2	938 (45,4)	647 (38,7)	390 (27,9)	277 (24,5)	160 (18,4)
	Stadium 3	1.020 (49,3)	924 (55,3)	906 (64,9)	766 (67,8)	630 (72,4)
Vollständige Beobachtung ²	N	820	820	820	820	820
	Alter, MW (SD)	77,4 (5,3)	79,5 (5,2)	81,5 (5,3)	83,5 (5,3)	85,6 (5,3)
	Frauen, N (%)	450 (54,9)	450 (54,9)	450 (54,9)	450 (54,9)	450 (54,9)
	eGFR _{BIS2} , MW (SD)	63,3 (13,5)	59,7 (13,2)	54,3 (12,4)	51,9 (12,9)	48,4 (13,1)
	eGFR _{EKFC} , MW (SD)	65,4 (13,7)	62,4 (14,2)	60,3 (14,6)	57,2 (15,2)	54,3 (15,8)
	CKD Stadien ⁴ , N (%)					
	Stadium 1	19 (2,3)	7 (0,9)	0 (0,0)	1 (0,1)	2 (0,2)
	Stadium 2	487 (59,4)	409 (49,9)	282 (34,4)	231 (28,2)	146 (17,8)
	Stadium 3	304 (37,1)	393 (47,9)	509 (62,1)	547 (66,7)	602 (73,4)
	Stadium 4	10 (1,2)	11 (1,3)	29 (3,5)	41 (5,0)	69 (8,4)
	Stadium 5	0 (0,0)	0 (0,0)	0 (0,0)	0 (0,0)	1 (0,1)

¹ N bezieht sich auf die Personen mit validen eGFR-Messungen zu der jeweiligen Studienvisite. Aufgrund fehlender Laborwerte ausgeschlossen waren: N = 1, 29, 44, 36 und 74 (Baseline – Follow-Up 4). ² *Vollständige Beobachtung* bezieht sich auf Personen, die an jeder Studienvisite teilgenommen und valide eGFR Messungen zu jeder Visite haben.

³ Verstorben^{2,3} wurde berechnet als die Anzahl an Personen, die innerhalb von 2 Jahren nach ihrem jeweiligen Visitendatum verstorben sind. ⁴ CKD Stadien wurden berechnet mittels der eGFR_{BIS2}. *Abkürzungen:* MW: Mittelwert; SD: Standardabweichung.

FV13: Tab. 1



FV13: Abb. 1

Boxplots and flache Violinplots der eGFR_{visz} Verteilungen und CKD Stadien für beide Gruppen.

ist wichtig für ein besseres Verständnis der chronischen Nierenerkrankung (CKD) im hohen Alter. **Methode:** Die Berliner Initiative Studie (BIS), ist eine Alterskohorte mit N = 2.069 Teilnehmer*innen ≥ 70 Jahre. Nach einer Baseline-Visite (2010–2011) erfolgten im 2-Jahresabstand vier Follow-Up-Visiten. Über den Studienzeitraum von acht Jahren wurden die eGFR und CKD Stadien gemäß der KDIGO Leitlinien mittels der Kreatinin und Cystatin C-basierten BIS2-Formel (eGFR_{BIS2}) bestimmt. Zusätzlich wurde die Kreatinin-basierte EKFC Formel genutzt (eGFR_{EKFC}). In einer Sub-Analyse wurden alle Personen mit kompletter Beobachtung

eingeschlossen (nicht verstorben, bei jeder Visite mit validen eGFR-Messungen anwesend).

Ergebnisse: Das mittlere Alter zu Baseline lag bei 80,4 Jahren und 52,6 % waren Frauen. Die Prävalenz war am höchsten für CKD Stadien 2 (45,4 %) und 3 (49,3 %). Innerhalb von acht Jahren sank die Prävalenz von Stadium 1 und 2, wohingegen die von Stadium 3 und 4 konstant auf 72,4 bzw. 8,9 % anstieg. Die mittlere eGFR_{BIS2} sank über acht Jahre kontinuierlich von 58,1 auf 48,3 ml/min/1,73 m² ab. Mit der eGFR_{EKFC} ergab sich ein geringeres Absinken (60,4 auf 54,2 ml/min/1,73 m²). Die Subgruppe mit vollständiger Beobachtung (mittleres Alter: 77,4 Jahre) zeigte ähnliche Trends, jedoch mit einer initial höheren mittleren eGFR_{BIS2} (63,3 vs. 58,1 ml/min/1,73 m²) und einem stärkeren Absinken nach acht Jahren (63,3 auf 48,4 ml/min/1,73 m²).

Zusammenfassung: Über einen Zeitraum von acht Jahren sank die mittlere eGFR_{BIS2} der BIS-Studienteilnehmer*innen um 9,8 ml/min/1,73 m². Dies resultierte in einem kontinuierlichen Anstieg der Prävalenz von CKD Stadium 3 und 4 um 23,1 bzw. 5,3 %. Beim Berichten der CKD-Prävalenz für ältere Personen sollte deutlich sein, dass diese eng mit dem mittleren Alter der Studienbevölkerung zusammenhängt.

Apherese & Plasmapherese

FV14

Sicherheit therapeutischer Apherese im Kindes- und Jugendalter

J. Thumfart; A. Schaaf; C. Dorn¹; C. P. Schmitt²; S. Loos³;

N. Kanzelmeyer⁴; L. Pape⁵; D. Müller; L. T. Weber¹; C. Taylan¹

Klinik für Pädiatrie mit Schwerpunkt Nephrologie, Campus Virchow-Klinikum, Charité – Universitätsmedizin Berlin, Berlin; ¹Klinik und Poliklinik für Kinder- und Jugendmedizin, Universitätsklinikum, Universität zu Köln, Köln; ²Pädiatrische Nephrologie, Zentrum für Kinder- und Jugendmedizin, Ruprecht-Karls-Universität Heidelberg, Heidelberg; ³Pädiatrische Nephrologie, Klinik für Kinder- und Jugendmedizin, Universitätsklinikum Hamburg-Eppendorf, Hamburg; ⁴Abteilung II, Zentrum Kinderheilkunde und Jugendmedizin, Medizinische Hochschule Hannover, Hannover; ⁵Klinik für Pädiatrische Nephrologie, Universitätsklinikum Essen, Universität Duisburg-Essen, Essen

Hintergrund: Die therapeutische Apherese (TA) basiert auf den Prinzipien entweder gelöste pathogene Substanzen (z. B. Antikörper) aus dem Blutplasma zu entfernen, oder Plasmafaktoren zu ersetzen. Es erweitert die therapeutischen Möglichkeiten für eine Vielzahl von Krankheiten. Während es bereits umfangreiche Daten zur Sicherheit und Verträglichkeit bei Erwachsenen gibt, basieren die Daten in der Pädiatrie auf kleineren Beobachtungsstudien oder Fallberichten. Ziel dieser Analyse war es, spezifische Komplikationen der TA-Modalitäten – Plasmaaustausch (PE) und Immunadsorption (IA) – bei Kindern und Jugendlichen zu analysieren.

Methode: 298 Kinder und Jugendliche, die von 2008 bis 2018 in fünf kindernephrologischen Zentren mit TA behandelt wurden, wurden retrospektiv

analysiert. Insgesamt wurden 4.004 Behandlungen (2.287 PE und 1.717 IA) ausgewertet.

Ergebnisse: Indikationen für TA waren vor allem nephrologische und neurologische Erkrankungen. Die drei Hauptindikationen waren die Antikörper-vermittelte Transplantatabstoßung (13,4 %), das hämolytisch-urämische Syndrom, hauptsächlich mit neurologischer Beteiligung (12,8 %), und die AB0-inkompatible Transplantation (11,7 %). Komplikationen entwickelten sich in 440 der 4004 Sitzungen (11 %), von denen ein Drittel unspezifisch war (Übelkeit, Kopfschmerzen). IA wurde besser vertragen als PE. Komplikationen wurden in 9,5 % (n = 163) der IA gegenüber 12,1 % (277) der PE-Sitzungen (p < 0,001) berichtet. Bei der Betrachtung verschiedener Arten von Komplikationen traten in PE-Sitzungen signifikant mehr unspezifische/nicht-allergische Ereignisse (p = 0,02) und allergische Reaktionen auf (p < 0,001). Mehr Komplikationen traten bei PE bei Verwendung von Frischplasma (16,2 %; n = 145) im Vergleich zu Humanalbumin (14,5 %; n = 115) auf (p < 0,001). In der multivariaten Analyse war neben PE als Modalität ein höheres Patientenalter (> 14 Jahre) mit einer erhöhten Komplikationsrate assoziiert.

Zusammenfassung: In der bislang größten untersuchten pädiatrischen Kohorte konnte gezeigt werden, dass TA im Kindes- und Jugendalter ein sicheres Behandlungsverfahren ist. Die IA zeigte eine signifikant niedrigere Komplikationsrate als PE. Daher sollte IA vorzugsweise eingesetzt werden, wenn die Pathomechanismen der Grunderkrankung keine PE erfordern.

Genbasierte Therapien und neue Therapieansätze für rare diseases

FV15

Lifetime risk of autosomal recessive kidney diseases calculated from genetic databases

M. C. Braunisch; M. Menke¹; C. Großwinkelmann¹; K. M. Riedhammer; J. Comic¹; R. Günthner; L. Renders; C. Schmaderer; U. Heemann; M. Wagner¹; J. Höfele¹
 II. Medizinische Klinik, Nephrologie, Klinikum rechts der Isar, Technische Universität München, München;
¹Institut für Humangenetik, Klinikum rechts der Isar, Technische Universität München, München

Objective: Hereditary kidney diseases are a heterogeneous group of rare diseases. Age of onset primarily ranges between early childhood and adolescence. However, there are also adult-onset hereditary kidney diseases. Their marked clinical and genetic heterogeneity as well as referral and ascertainment biases render phenotype-based prevalence estimations difficult. Here we provide the calculated lifetime risk of autosomal recessive kidney diseases.

Method: Overall, 149 genes associated with autosomal recessive kidney diseases were included. Using the publicly available databases ClinVar, HGMD, and LOVD, disease-causing variants rated as (likely) pathogenic were collected and reevaluated according to the guidelines of the American College of Medical Genetics (ACMG) with current amendments by the Association for Clinical Genomic Science (ACGS) 2020. The minor allele frequency of identified variants was then collected in the Genome Aggregation Database (gnomAD)

and in our in-house exome database to estimate the lifetime risk.

Results: Overall, 9,541 variants were investigated in 149 analyzed genes. After reclassification according to ACMG 3,287 variants were excluded, leaving 6,254 disease-causing variants in the final dataset. The combined estimated lifetime risk of 149 investigated autosomal recessive kidney disease genes was 7.41 (4.48–12.53)/100,000 as calculated based on the in-house database, 12.15 (8.71–17.11)/100,000 in the European gnomAD dataset, and 8.67 (6.87–11.02)/100,000 in the global gnomAD dataset. The disorders with the highest lifetime risk (> 1 per 100,000) were those caused by variants in the genes *SLC12A3*, *BCS1L*, *PKHD1*, and *ALMS1* associated with Gitelman syndrome, renal tubular acidosis, autosomal recessive polycystic kidney disease, and nephronophthisis, respectively.

Conclusion: We provide a population-genetic estimation for the lifetime risk of autosomal recessive kidney diseases in different populations. Our findings suggest a substantial cumulative prevalence of autosomal recessive kidney diseases. The data will be essential for the identification of possible underestimated prevalences and therefore for resource allocation in therapy development and bio-medical research.

Chronic Kidney Disease II

FV16

Validierung der neuen „race free“ CKD-EPI Schätzformel in Personen im Alter von 70+

N. Ebert; H. Pottel¹; M. van der Giet²; M. K. Kuhlmann³; P. Delanaye⁴; E. Schäffner

Institut für Public Health, Charité – Universitätsmedizin Berlin, Berlin;

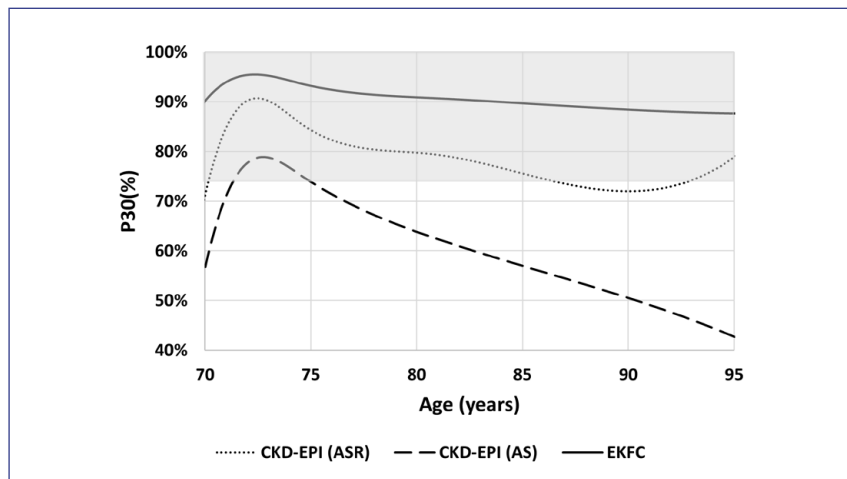
¹Public Health and Primary Care, University Leuven, Kortrijk/BE;

²Medizinische Klinik IV, Klinik für Nephrologie, Campus Benjamin Franklin, Charité – Universitätsmedizin Berlin, Berlin; ³Nephrologie, Klinik für Innere Medizin, Vivantes Klinikum im Friedrichshain, Berlin; ⁴Department of Dialysis, Université de Liège, Liège/BE

Hintergrund: Die häufig verwendete Kreatinin-basierte CKD-EPI (ASR)-Formel wurde jüngst überarbeitet (ASR: Alter, Geschlecht und „Race“), da sie in der Kritik stand, dass die integrierte „race“-Variable zur Ungleichbehandlung von schwarzen Patienten führe. Stattdessen wird nun von der National Kidney Foundation die neue „race free“ CKD-EPI (AS)-Formel in den USA empfohlen. Hierbei ist unklar, ob dies für alte Patienten sinnvoll ist. Die aktuelle Studie vergleicht die Schätzgenauigkeit der neuen CKD-EPI (AS)-Formel mit der CKD-EPI (ASR)-Formel und der in Europa neu entwickelten European Kidney Function Consortium (EKFC)-Formel. **Methode:** Daten von 570 Studienteilnehmern der „Berliner Initiative Studie“ (BIS), einer Bevölkerungs-basierten Kohorte, wurden analysiert. Als Referenzmethode wurde die gemessene GFR (mGFR) durch die invasive Iohexol-Plasmaclearance bestimmt. Sowohl die systematische Abweichung (Bias, geschätzte GFR (eGFR) minus mGFR) als auch die Präzision (Interquartilsabstand, IQR) und die Akkuratheit (P30, definiert als Prozentsatz der eGFR-Werte innerhalb von $\pm 30\%$ mGFR) wurden berechnet. Die CKD-EPI (ASR), CKD-EPI (AS)

All n = 570	Bias (95%CI)	IQR [Pct25; Pct75]	P30 (%)
CKD-EPI (ASR)	8.40 [7.0; 9.0]	12.8 [1.7; 14.4]	81.4 [78.2; 84.6]
CKD-EPI (AS)	13.0 [12.1; 14.0]	13.8 [6.0; 19.8]	66.5 [62.6; 70.4]
EKFC	1.6 [0.7; 2.7]	11.3 [-4.0; 7.3]	91.9 [89.7; 94.2]
age < 80y n = 362			
CKD-EPI (ASR)	8.5 [6.7; 9.8]	13.9 [1.2; 15.0]	84.0 [80.2; 87.8]
CKD-EPI (AS)	13.0 [11.6; 14.5]	14.6 [5.7; 20.3]	71.5 [66.9; 76.2]
EKFC	1.3 [0.6; 2.8]	11.9 [-4.1; 7.8]	93.1 [90.5; 95.7]
Age ≥ 80y n = 208			
CKD-EPI (ASR)	8.3 [6.7; 9.1]	11.9 [1.8; 13.6]	76.9 [71.1; 82.7]
CKD-EPI (AS)	13.1 [11.4; 14.2]	12.4 [6.5; 18.9]	57.7 [50.9; 64.5]
EKFC	2.0 [-0.3; 3.4]	10.4 [-4.0; 6.4]	89.9 [85.8; 94.0]
mGFR < 60 n = 273			
CKD-EPI (ASR)	8.8 [7.0; 10.0]	13.6 [1.7; 15.3]	67.8 [62.2; 73.3]
CKD-EPI (AS)	12.9 [11.5; 14.4]	14.7 [5.5; 20.2]	52.4 [46.4; 58.3]
EKFC	3.7 [2.7; 5.1]	11.5 [-2.3; 9.2]	85.0 [80.7; 89.2]
mGFR ≥ 60 n = 297			
CKD-EPI (ASR)	7.6 [6.3; 9.1]	12.6 [1.3; 13.9]	93.9 [91.2; 96.7]
CKD-EPI (AS)	13.1 [11.6; 14.5]	12.4 [6.7; 19.1]	79.5 [74.8; 84.1]
EKFC	-0.5 [-1.4; 0.8]	11.9 [-6.0; 5.8]	98.3 [96.8; 99.8]

FV16: Tab. 1



FV16: Abb. 1

P30 (%) nach Alter für CKD-EPI (ASR), CKD-EPI (AS) und EKFC. Grauschattierte Fläche: P30-Wert über 75 %.

und EKFC Formeln wurden anhand der mGFR extern validiert. **Ergebnisse:** Mittleres Alter der Studienprobanden war 78,5 Jahre, 57 % waren Männer, und die mittlere mGFR war 60,3 ml/min/1.73 m². Der mittlere Bias war am höchsten für die neue

CKD-EPI (AS)-Formel mit 13,0 im Vergleich zu 8,4 und 1,6 ml/min/1.73 m² für CKD-EPI (ASR) und EKFC-Formel (Tab. 1). Der P30-Wert war für die CKD-EPI (AS)- mit 67 % deutlich niedriger verglichen mit der CKD-EPI (ASR, 81 %)- und der

EKFC-Formel (92 %) (Abb. 1). Bei Hochaltrigen (≥ 80 Jahre) und Personen mit eingeschränkter Nierenfunktion (mGFR < 60) schnitt die neue CKD-EPI (AS)-Formel mit einem P30-Wert von 58 % bzw. 52 % noch schlechter ab. **Zusammenfassung:** Für die USA wird zur Diagnose der CKD die neue „race-free“ CKD-EPI (AS)-Formel empfohlen. Die aktuellen Studienergebnisse zeigen, dass es durch die Neueinführung der CKD-EPI (AS) sowohl zu einer erheblichen systematischen Überschätzung als auch einer deutlich schlechteren Vorhersage der geschätzten GFR bei älteren Patienten kommt. Bei Patienten mit GFR < 60 ml/min weist sie sogar noch einen deutlich schlechteren P30-Wert von nur 52 % auf. Für ältere Patienten besteht dadurch die Gefahr der Medikamentenüberdosierung und verspäteten CKD-Diagnosestellung.

FV17

TULP3 as a novel gene for progressive kidney, liver and heart degeneration in adult patients

C. Bergmann; E. Ott¹; D. Epting¹; E. Olinger²; J. Devane¹; E. Decker; A. Friedrich; N. Bachmann; G. Renschler³; T. Eisenberger; M. Börries⁴; P. Metzger⁴; A. Yilmaz⁵; I. Grünwald⁶; M. Konrad⁷; J. König⁷; B. Schlevogt⁸

Medizinische Genetik Mainz, Limbach Genetics GmbH, Mainz; ¹ Medizinische Klinik IV/ Abteilung Nephrologie, Universitätsklinikum, Albert-Ludwigs-Universität Freiburg, Freiburg; ² Faculty of Medical Sciences, Translational and Clinical Research Institute, Newcastle University, Newcastle/UK; ³ Institut für Biologie, Albert-Ludwigs-Universität, Freiburg; ⁴ Institut für Molekulare Medizin und Zellforschung,

Universitätsklinikum, Albert-Ludwigs-Universität Freiburg, Freiburg;

⁵Abteilung Kardiologie, Universitätsklinikum, Albert-Ludwigs-Universität Freiburg, Münster; ⁶Institut für Pathologie, Universitätsklinikum, Albert-Ludwigs-Universität Freiburg, Münster; ⁷Abteilung für pädiatrische Nephrologie, Universitäts-Kinderklinik, Westfälische Wilhelms Universität Münster, Münster; ⁸Abteilung Gastroenterologie, Universitätsklinikum, Albert-Ludwigs-Universität Freiburg, Freiburg

Objective: Organ fibrosis is a shared endpoint of many common human diseases, yet the underlying mechanisms are not well understood. Several pathways governed by the primary cilium, a sensory antenna present on most vertebrate cells, have been linked with the development of fibrosis. Diseases linked to the dysfunction of cilia usually start early in life and represent a considerable disease burden in paediatric patients.

Method: We performed massively parallel sequencing, clinical, imaging and centrally reviewed histopathological analysis involving eight unrelated families. Mechanistic studies were conducted using patient liver, heart and kidney biopsies, a vertebrate model and patient-derived cell systems.

Results: We detected biallelic deleterious variants in TULP3, a critical adapter protein for ciliary trafficking, in a total of 15 patients. Affected individuals presented with progressive degenerative disease manifestations in different organs including fibrocystic kidney disease, liver fibrosis and hypertrophic cardiomyopathy. Liver biopsies revealed a distinct fibrotic pattern not in line with ductal plate

malformation usually seen in paediatric ciliopathies and myocardial fibrosis followed an atypical pattern reminiscent of systemic disease with cardiac involvement. We recapitulated the human phenotype in zebrafish as a vertebrate model and confirmed disruption of critical ciliary cargo composition in several patient-derived primary cells. In addition, we validated a novel interaction between TULP3 and the nuclear deacetylase SIRT1, with roles in DNA damage repair and fibrosis. Increased levels of DNA damage were also seen in patient cells. Patient-cell based transcriptomic studies highlighted the upregulation of profibrotic pathways with gene clusters for hypertrophic cardiomyopathy, WNT and TGF beta signalling.

Conclusion: These findings identify a novel monogenic cause for progressive degenerative disease of major organs in which patients benefit from early detection and improved clinical management. Elucidation of mechanisms crucial for well-balancing DNA-damage repair and tissue maintenance will help guiding novel therapeutic avenues for this and similar genetic and non-genomic diseases.

Clinical Science – Chronic Kidney Disease II

FV18

Albuminurie im Alter – Daten zu Prävalenz und Verlauf über 8 Jahre in der Berliner Initiative Studie

T. Bothe; E. Schäffner; N. Mielke; A. Schneider; M. Barghouth; M. van der Giet¹; M. K. Kuhlmann²; N. Ebert
Institut für Public Health, Charité – Universitätsmedizin Berlin, Berlin;
¹Medizinische Klinik IV, Klinik für

Nephrologie, Campus Benjamin Franklin, Charité – Universitätsmedizin Berlin, Berlin; ²Nephrologie, Klinik für Innere Medizin, Vivantes Klinikum im Friedrichshain, Berlin

Hintergrund: Erkenntnisse zum Verlauf der Albumin-Kreatinin-Ratio (ACR) in älteren Personen sind rar. Diese zu beschreiben, ist wichtig, um die Relevanz von Albuminurie im hohen Alter besser zu verstehen.

Methode: Die Berliner Initiative Studie (BIS), ist eine Kohorte mit N = 2.069 Personen im Alter von 70+ Jahre. Die Baseline-Visite erfolgten in 2010 und 2011 mit vier Folgevisiten alle 2 Jahre. Das Vorliegen von Albuminurie (keine Albuminurie: ACR < 30 mg/g; Mikroalbuminurie: ACR 30–299 mg/g; Makroalbuminurie: ACR ≥ 300 mg/g) wurde zu allen Messzeitpunkte ermittelt. In einer Sub-Analyse wurden alle Personen mit kompletter Beobachtung eingeschlossen (nicht verstorben, bei jeder Visite mit validen ACR-Messungen anwesend).

Ergebnisse: Das mittlere Alter zu Baseline war 80,4 Jahren und 52,6 % waren Frauen. Die mediane ACR stieg von 10,7 zu Baseline auf 13,3 mg/g nach acht Jahren an, wobei die Prävalenz von Mikro- bzw. Makroalbuminurie nahezu stabil verblieb (21,6–25,3 % bzw. 3,3–4,1 %). Bei Personen mit kompletter Beobachtung stieg die mediane ACR von 7,3 auf 13,2 mg/g an, wobei die Prävalenzen von Mikro- bzw. Makroalbuminurie von 14,9 auf 25,6 % bzw. von 1,7 auf 3,3 % nach acht Jahren zunahm.

Zusammenfassung: Die Ergebnisse zeigen, dass die ACR und Prävalenzen von Mikroalbuminurie

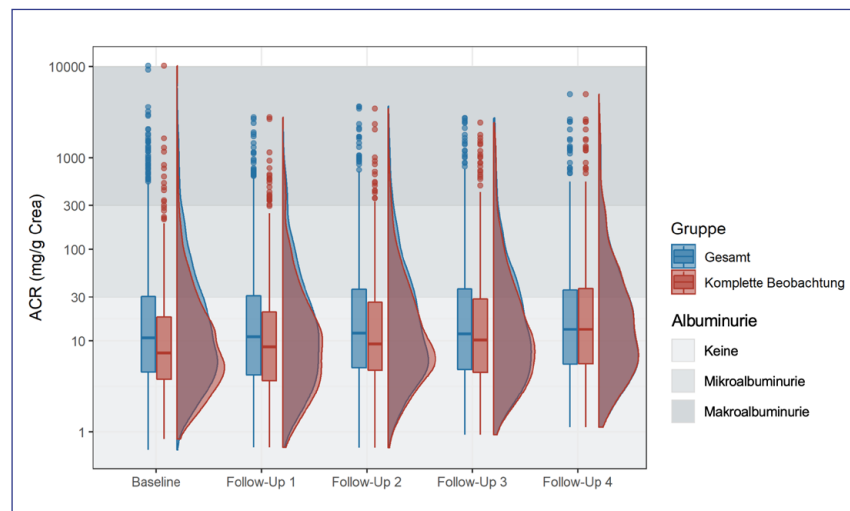
Tabelle 1: Soziodemographische Variablen und Prävalenz von Albuminurie für beide Studienpopulationen.

Population	Variable	Baseline	Follow-Up 1	Follow-Up 2	Follow-Up 3	Follow-Up 4
Gesamt	N ¹	2.055	1.667	1.411	1.086	845
	Alter, MW (SD)	80,4 (6,7)	81,8 (6,4)	83,0 (6,0)	84,2 (5,5)	85,6 (5,2)
	Frauen, N (%)	1.081 (52,6)	889 (53,3)	762 (54,0)	590 (54,3)	470 (55,6)
	Verstorben ^{2,3} , N (%)	125 (6,1)	143 (8,6)	146 (10,3)	107 (9,9)	94 (11,1)
	ACR, Median (q25; q75)	10,7 (4,5; 30,6)	11,0 (4,2; 31,1)	12,0 (5,0; 36,5)	11,8 (4,8; 36,9)	13,3 (5,4; 35,9)
	Urinstix _{valide} ⁴ , N (%) von N ¹	1.794 (87,3)	1.662 (99,7)	1.405 (99,6)	1.084 (99,8)	845 (100,0)
	-	1.510 (84,2)	1.184 (71,2)	1.119 (79,6)	841 (77,6)	669 (79,2)
	+	232 (12,9)	414 (24,9)	236 (16,8)	216 (19,9)	143 (16,9)
	++	44 (2,5)	44 (2,6)	36 (2,6)	21 (1,9)	21 (2,5)
	+++	8 (0,4)	20 (1,2)	14 (1,0)	6 (0,6)	12 (1,4)
	Albuminurie, N (%)					
	Keine (ACR < 30)	1.523 (74,1)	1.239 (74,3)	998 (70,7)	779 (71,7)	599 (70,9)
	Mikro (ACR 30-299)	458 (22,3)	360 (21,6)	357 (25,3)	264 (24,3)	218 (25,8)
	Makro (ACR ≥ 300)	74 (3,6)	68 (4,1)	56 (4,0)	43 (4,0)	28 (3,3)
Komplette Beobachtung ²	N	784	784	784	784	784
	Alter, MW (SD)	77,3 (5,2)	79,4 (5,2)	81,4 (5,2)	83,4 (5,2)	85,5 (5,2)
	Frauen, N (%)	422 (53,8)	422 (53,8)	422 (53,8)	422 (53,8)	422 (53,8)
	ACR, Median (q25; q75)	7,3 (3,7; 18,1)	8,6 (3,6; 20,6)	9,2 (4,7; 26,1)	10,1 (4,4; 28,3)	13,2 (5,5; 37,0)
	Urinstix _{valide} ⁴ , N (%)	654 (83,4)	782 (99,7)	781 (99,6)	782 (99,7)	784 (100,0)
	-	576 (88,1)	587 (75,1)	647 (82,8)	613 (78,4)	620 (79,1)
	+	70 (10,7)	178 (22,8)	113 (14,5)	155 (19,8)	133 (17,0)
	++	7 (1,1)	11 (1,4)	18 (2,3)	10 (1,3)	20 (2,6)
	+++	1 (0,2)	6 (0,8)	3 (0,4)	4 (0,5)	11 (1,4)
	Albuminurie, N (%)					
	Keine (ACR < 30)	654 (83,4)	644 (82,1)	606 (77,3)	599 (76,4)	557 (71,0)
	Mikro (ACR 30-299)	117 (14,9)	118 (15,1)	159 (20,3)	158 (20,2)	201 (25,6)
	Makro (ACR ≥ 300)	13 (1,7)	22 (2,8)	19 (2,4)	27 (3,4)	26 (3,3)

¹ N bezieht sich auf die Personen mit validen ACR-Messungen zu der jeweiligen Studienvisite. Aufgrund fehlender Laborwerte ausgeschlossen waren: N = 14, 32, 29, 80 und 99 (Baseline – Follow-Up 4). ² Vollständige Beobachtung bezieht sich auf Personen, die an jeder Studienvisite teilgenommen und valide ACR Messungen zu jeder Visite haben.

³ Verstorben^{2,3} wurde berechnet als die Anzahl an Personen, die innerhalb von 2 Jahren nach ihrem jeweiligen Visitedatum verstorben sind. ⁴ Urinstix_{valide} bezieht sich auf die Anzahl von Personen mit validen Urinstix-Messungen. Abkürzungen: MW: Mittelwert; SD: Standardabweichung; q25: 25. Perzentil; q75: 75. Perzentil.

FV18: Tab. 1



FV18: Abb. 1

über einen Beobachtungszeitraum von acht Jahren intra-individuell lediglich leicht um ca. 6 mg/g ansteigen. Die Messung der ACR unterliegt einer relativ hohen Varianz, so dass der Wert nur als Richtgröße angesehen werden sollte. Die Prävalenzen von Mikro- und Makroalbuminurie blieben bei ca. 25 % bzw. 4 % über den Beobachtungszeitraum nahezu stabil. Die Ergebnisse von Personen mit kompletter Beobachtung zeigten einen nahezu gleichen Trend.

FV19

Carotid Intima-Media-Thickness and atherosclerotic plaques are associated with renal function decline. A 14-year longitudinal population-based study

M. Goepfert; T. Ittermann¹; M. Dörr²; N. Friedrich³; H. Völzke⁴; T. Dabers⁵; S. B. Felix⁶; U. Schminke⁷; S. Stracke⁵; S. Freiin von Rheinbaben⁵

Abteilung für Nephrologie, Hochdruckkrankheiten und Dialyse, Klinik und Poliklinik für Innere Medizin A, Universität Greifswald, Greifswald; ¹ Study of Health in Pomerania – Klinisch-epidemiologische Forschung (SHIP-KEF), Institut für Community Medicine, Ernst-Moritz-Arndt-Universität Greifswald, Greifswald; ² Kardiologie, Angiologie, Intensivmedizin, Klinik und Poliklinik für Innere Medizin B, Universitätsmedizin Greifswald, Greifswald; ³ Institut für Klinische Chemie und Laboratoriumsmedizin, Greifswald, Greifswald; ⁴ Institut für Epidemiologie und

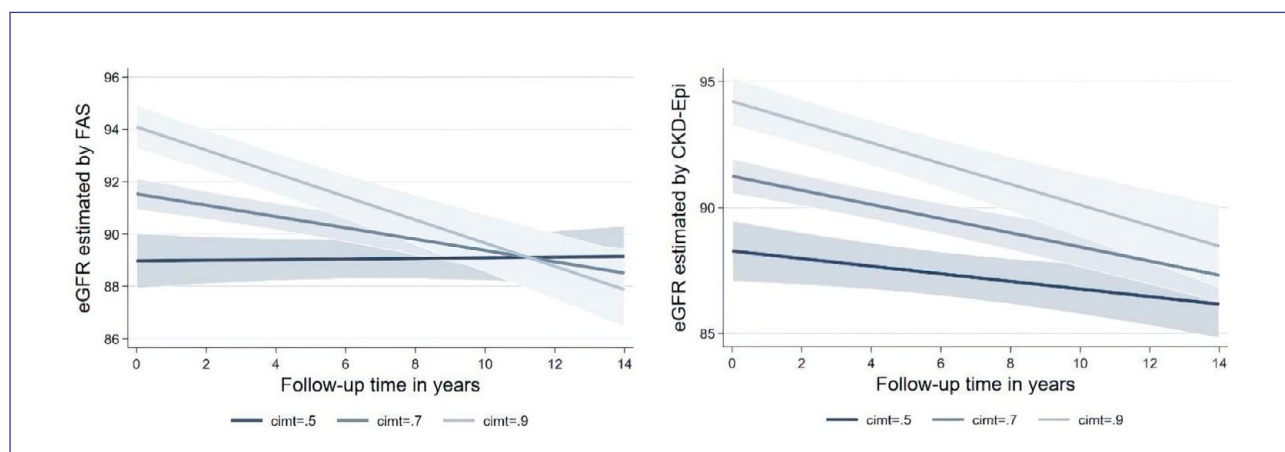
Sozialmedizin, Universitätsklinik Greifswald, Greifswald; ⁵ Abteilung für Nephrologie und Hypertensiologie, Klinik und Poliklinik für Innere Medizin A, Universitätsmedizin Greifswald, Greifswald; ⁶ Klinik und Poliklinik für Innere Medizin B, Universitätsklinikum, Ernst-Moritz-Arndt-Universität Greifswald, Greifswald; ⁷ Klinik und Poliklinik für Neurologie, Universität Greifswald, Greifswald

Objective: Atherosclerosis leads to numerous macroangiopathic complications such as coronary heart disease, stroke and renal artery stenosis. The underlying mechanisms are often similar to those causing chronic kidney disease e.g., hypertension or diabetes mellitus. In a longitudinal study we investigated if carotid Intima-Media-Thickness (cIMT) and carotid plaques as indicators for atherosclerosis are associated with renal function decline. We used two distinct

equations to calculate the estimated glomerular filtration rate (eGFR) in order to explore their suitability in the context of the study.

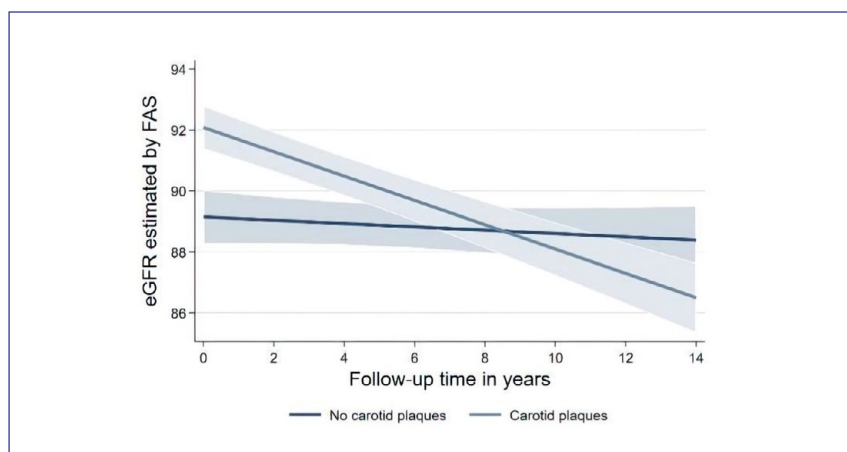
Method: In a population-based study, 2904 subjects with no predominant medical condition were observed over a follow-up of 14 years. Chronic kidney disease (CKD) is defined as eGFR < 60 ml/min/1.73 m² and albuminuria as urinary albumin-creatinine-ratio (ACR) > 30 mg/g, eGFR was calculated by full age spectrum (FAS) equation and Chronic Kidney Disease Epidemiology Collaboration (CKD-EPI) equation. The cIMT as well as carotid plaques were measured by standardized B-mode-ultrasound protocol. Mixed models were used to associate carotid parameters with change in renal function longitudinally.

Results: The age range was 20–79 years with a median of 54 years at baseline. In the longitudinal



FV19: Abb. 1

Association between eGFR values (ml/min/1.73 m²) calculated by FAS and CKD-EPI equation during the 14-year-Follow-up and three different cIMT values (0.5 mm, 0.7 mm, 0.9 mm) using mixed model (n = 2740). cIMT = carotid intima media thickness, eGFR = estimated glomerular filtration rate (ml/min/1.73m²), CKD-EPI equation = Chronic Kidney Disease Epidemiology Collaboration equation, FAS equation = full age spectrum equation. Values are adjusted for age, sex, waist circumference, education, type 2 diabetes mellitus, hypertension, triglyceride/HDL-cholesterol ratio, lipid-lowering drug intake, uric acid. Grey regions indicate the 95 %-confidence interval



FV19: Abb. 2

Association between eGFR values (ml/min/1.73 m²) calculated by FAS equation during the 14-year-Follow-up and the presence of carotid plaques using mixed model (n = 2740). eGFR = estimated glomerular filtration rate (ml/min/1.73m²), FAS equation = full age spectrum equation. Values are adjusted as previously described. Grey regions indicate the 95 %-confidence interval.

analyses subjects with a high cIMT showed a greater decrease in eGFR during the follow-up period than subjects with low cIMT (FAS-eGFR: $p < 0.001$, CKD-EPI-eGFR: $p = 0.006$). This effect was more evident for the FAS than for CKD-EPI equation. In subjects with at least one plaque, the decrease in eGFR calculated via FAS was significantly greater than in subjects without plaques ($p < 0.001$), but not significant for the eGFR calculated by the CKD-EPI equation. Additionally, plaque occurrence was associated with an increased risk of developing a CKD (CKD-EPI-eGFR: $p = 0.001$; FAS-eGFR: $p = 0.003$) as well as albuminuria. No such association was observed for the cIMT.

Conclusion: Atherosclerotic parameters, as defined by cIMT and carotid plaques, are associated with renal function decline in a population-based sample and should be considered as combined values in potential screenings. The FAS equation, in addition to the well-known CKD-EPI equation, represents a significant and appropriate formula for the analysed age group and should be incorporated into future studies.

Basic Science – Function

FV20

High throughput investigation of the metabolic flux of intact cortical kidney tubules

J. Jägers; N. Himmerkus¹; M. Chrysopoilou; F. Demir; A. Billing; N. Bogh; C. Westergaard Rasmussen; C. Lautsen; M. Bleich¹; M. Rinschen²
 Institut for Biomedicine, Aarhus University, Aarhus/DK; ¹Physiologisches Institut, Christian-Albrechts-Universität Kiel, Kiel; ²Nephrologie/Rheumatologie und Endokrinologie/Diabetologie, III. Medizinische Klinik, Universitätsklinikum Hamburg-Eppendorf, Hamburg

Objective: The proximal tubule epithelial cells, has to generate high amounts of ATP to reabsorb substances from urine, to retain essential metabolites. In case of kidney injury, the cells experience a metabolic shift. Current assays depend on cell culture and are limited to differentiate between aerobic and anaerobic metabolism. These assays cannot quantify the proximal tubules' capacity to reabsorb essential substances, excrete toxins or

metabolize different substrates in oxygen-independent pathways. To overcome these limitations, we measure the degree of metabolization of substrates directly in structurally intact cortical kidney tubules (KTCs).

Method: We generated a time-resolved, large-scale experimental setup to quantify the metabolic flux. We incubate isolated, intact, and vital KTCs with isotopic labelled substrates. Subsequently, we extracted isotopic labelled metabolites, that were generated by the KTCs during incubation, and analyzed them with UHPLC/QQQ-based mass spectroscopy-technology. This setup enables the identification and quantification of changes in the KTCs' capacity to metabolize different substrates and was applied to porcine and murine models of kidney injury and nephrotoxicity in a time course of 30 seconds up to 120 minutes.

Results: We could identify nephron segment-specific uptake and metabolization of glucose in six different micro dissected nephron segments. We observed pyruvate derived gluconeogenesis in micro dissected proximal straight tubules under treatment with ouabain and

oxidative stress. Additionally, we observed the concentration-dependent effect of arginine and lysine on uptake and metabolism of the respective other amino acid in a heterogeneous KTC suspension. We also proved the KTC suspension to allow for the analysis of carbohydrate metabolism during pharmacological SGLT2 inhibition of the glucose uptake and the gluconeogenic capacity of the KTCs. Furthermore, we tested whether calcineurin inhibitors show a toxic effect on gluconeogenic capacity of the KTCs, which may pave the way to toxicological evaluation of further substances. Finally, we transferred the setup to a clinically relevant model of porcine ischemia reperfusion injury and were able to observe the loss of gluconeogenesis and concomitant gain of glycolysis during the transition of acute kidney injury towards chronic kidney disease. **Conclusion:** We established a high-throughput analysis method for different metabolic activities and their comparison of intact nephron compartments applicable on different kidney disease

model. We could detect changes in the central carbon metabolism as well as determine uptake kinetics of carbohydrates and amino acids.

From bench to bedside – Acute kidney injury

FV21

suPAR inflames kidneys with T cells and aggravates septic acute kidney injury

C. Nußbag; C. Wei¹; E. Hahm¹; S. Hayek²; J. Li¹; F. Kälble; C. Speer; J. Eugen-Olsen³; E. Krautkrämer; M. Zeier; C. Morath; T. Brenner⁴; J. Reiser¹

Medizinische Klinik I, Sektion Nephrologie, Medizinische Fakultät, Ruprecht-Karls-Universität Heidelberg, Heidelberg; ¹Nephrology, Department of Internal Medicine, Rush University Medical Center, Chicago/USA;

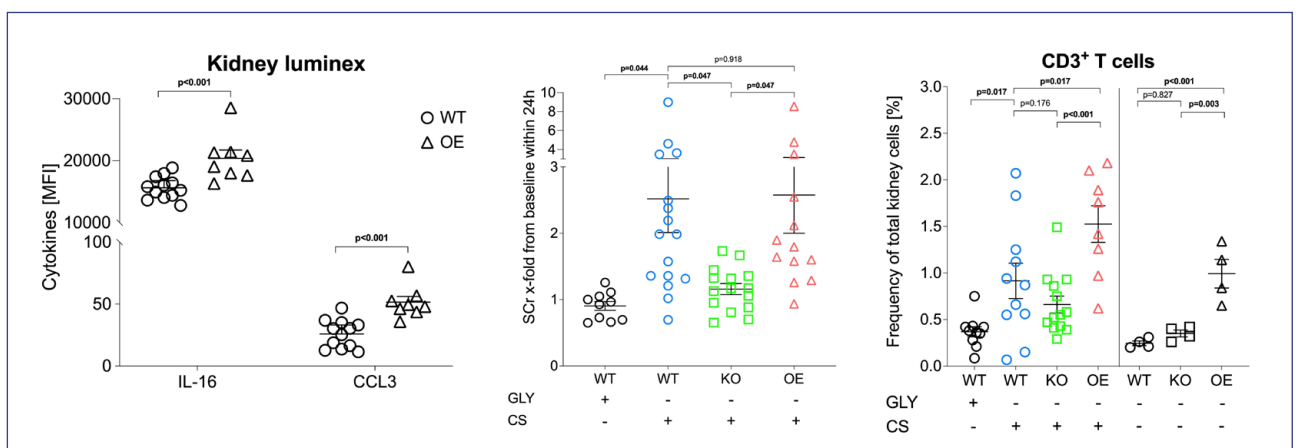
²Cardiovascular Disease, Internal Medicine, University of Michigan, Ann Arbor/USA; ³Department of Clinical Research, Copenhagen University Hospital Hvidovre, Hvidovre/DK;

⁴Klinik für Anästhesiologie und Intensivmedizin, Universitätsklinikum Essen, Essen

Objective: The soluble urokinase plasminogen activator receptor (suPAR) is an immune-derived glycoprotein implicated in the pathogenesis of acute kidney injury (AKI). Sepsis is a strong inducer of plasma suPAR levels and a known contributor to the development of AKI. We hypothesized that suPAR is involved in the pathophysiology of sepsis-related AKI.

Method: We used a polymicrobial model of sepsis (cecal slurry [CS] vs. glycerol [GLY]) in wild-type (WT), uPAR knock-out (KO, suPAR deficient), and transgenic suPAR-overexpressing (OE) mice. We compared measures of kidney function, tissue damage, and tissue inflammation in septic and untreated mice. Kidney tissue inflammation was quantified by kidney flow cytometry, immunohistostaining, and kidney luminex assay.

Results: Compared to WT, kidneys from untreated OE mice expressed high levels of interleukin-16 (IL-16) and C-C motif chemokine ligand 3 (CCL3); both involved in cell-mediated kidney injury and



FV21: Abb. 1

potent chemo-attractants for T and NK cells. Consistent with this expression pattern, we found significantly increased numbers of kidney T and NK cells in untreated OE mice, equaling numbers observed in septic WT mice. Further, high plasma suPAR aggravated sepsis-induced ultrastructural kidney damage, cellular apoptosis and kidney function impairment after 24 h of sepsis. In contrast, KO mice showed a strong protective effect against AKI. Kaplan-Meier analysis revealed a survival benefit of KO over OE mice (87 % vs. 50 %, $p=0.033$). The composition of kidney immune cells in sepsis was strongly influenced by varying suPAR plasma levels. Especially, numbers of kidney T cells were strongly linked to the extent of systemic suPAR elevation and kidney function impairment, with significant higher numbers in septic OE mice compared to septic WT and KO mice.

Conclusion: suPAR inflames the kidney with T cells potentially via local upregulation of IL-16 and CCL3. "SuPAR inflamed" kidneys react with increased kidney injury in sepsis which can potentially be improved by deleting suPAR. These findings hold great potential for new therapeutic strategies.

FV22

Urinary single-cell sequencing captures intrarenal injury and repair processes in human acute kidney injury

J. Klocke; S.J. Kim¹; C. Skopnik; C. Hinze²; A. Boltengagen¹; D. Metzke; E. Grothgar³; L. Prskalo³; L. Wagner³; P. Freund; N. Görlich⁴; F.D.R. Münch; K.M. Schmidt-Ott⁵; M.-F. Mashreghi⁶; C. Kocks¹; K.-U. Eckardt³; N. Rajewsky¹; P. Enghard³

Medizinische Klinik mit Schwerpunkt Nephrologie und Internistische Intensivmedizin, Campus Virchow-Klinikum, Charité – Universitätsmedizin Berlin, Berlin; ¹*Berlin Institute for Medical Systems Biology, Max-Delbrück-Center für Molekulare Medizin, Berlin;* ²*Medizinische Klinik mit Schwerpunkt Nephrologie und Internistische Intensivmedizin, Campus Benjamin Franklin, Charité – Universitätsmedizin Berlin, Berlin;* ³*Medizinische Klinik mit Schwerpunkt Nephrologie und Internistische Intensivmedizin, Campus Charité Mitte, Charité – Universitätsmedizin Berlin, Berlin;* ⁴*Medizinische Klinik mit Schwerpunkt Rheumatologie und Klinische Immunologie, Campus Charité Mitte, Charité – Universitätsmedizin Berlin, Berlin;* ⁵*Klinik für Nieren- und Hochdruckerkrankungen, Zentrum für Innere Medizin, Medizinische Hochschule Hannover, Hannover;* ⁶*Deutsches Rheuma-Forschungszentrum, Berlin*

Objective: Acute kidney injury (AKI) is a major health issue, the outcome of which depends primarily on damage and reparative processes of tubular epithelial cells (TEC). Mechanisms underlying AKI remain incompletely understood, specific therapies are lacking and monitoring the course of AKI in clinical routine is confined to measuring urine output and plasma levels of filtration markers.

Method: Here we demonstrate feasibility and potential of a novel approach to assess the cellular and molecular dynamics of AKI by establishing a robust urine-to-single cell RNA sequencing (scRNA-seq) pipeline for excreted kidney cells via flow cytometry sorting. We analyzed 42,608 single cell

transcriptomes of 40 urine samples from 32 AKI patients and compared our data with reference material from human AKI post-mortem biopsies and published mouse data.

Results: We demonstrate that urine-excreted TEC are mostly derived from distal nephron segments and are more abundant in patients with severe kidney injury. Their transcriptomes mirror intrarenal pathology and reflect distinct injury and repair processes, including oxidative stress, inflammation, and tissue rearrangement. We also describe a potentially AKI-specific abundant urinary excretion of adaptive progenitor-like cells.

Conclusion: In conclusion, single cell transcriptomics of kidney cells excreted in urine provides non-invasive, unprecedented insight into cellular processes underlying AKI, thereby opening novel opportunities for target identification, AKI sub-categorization and monitoring of natural disease course and interventions.

Dialyse

FV23

Der Einfluss von Surveillance und intensivierten Präventionsmaßnahmen in der ambulanten Dialyse auf Hämodialyse assoziierte Infektionen: Eine multizentrische randomisierte kontrollierte Interventionsstudie im stepped wedge Design

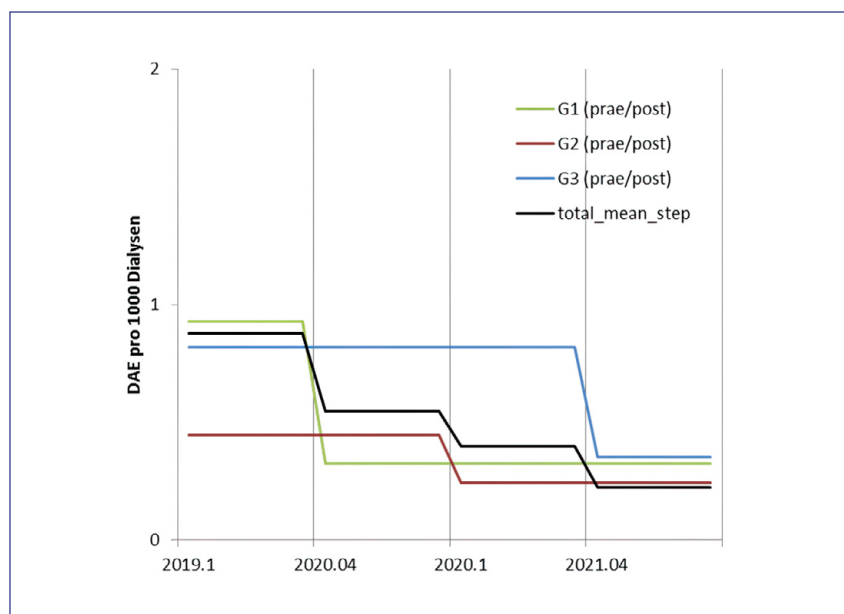
T. Kramer; B. Weikert; F. Schwab; J. Clausmeyer; C. Graf-Allgeier¹; P. Gastmeier; C. Geffers
Institut für Hygiene und Umweltmedizin, Campus Benjamin Franklin, Charité – Universitätsmedizin Berlin, Berlin; ¹Hygiene und Arbeitsschutz, PHV, Bad Homburg

Hintergrund: Es existieren nur wenige Daten zur epidemiologie Dialyse assoziierten Infektionen und effektiven Präventionsstrategien. Ziel dieser Studie ist es die Machbarkeit eines Surveillancesystems für die Erfassung von Infektionen in ambulanten Dialysezentren zu eruieren und den Effekt einer multimodalen Interventions Strategie auf die Infektionen zu untersuchen.

Methode: In 43 ambulanten Dialysezentren wurde zwischen September 2019 und Oktober 2021 eine prospektive Surveillance dialyse assoziierter Infektionen durchgeführt. Direkte Beobachtung der Händehygiene Compliance erfolgte halbjährlich durch externe Fachkräfte.

In der Interventionsphase erhielten die Zentren eine eingehende Schulung, Schulungs- und Erringermaterial. Leitungen erhielten in Onlinetreffen Rückmeldung zu den gemessenen Infektions- und Compliance raten. Diese wurde darauf hin im Zentrum besprochen, Ursachen analysiert, Ziele festgelegt und Maßnahmen abgeleitet.

Ergebnisse: Insgesamt wurden 12.519 Patient:innen mit 4.278.648 hämodialyse Behandlungen in diese Studie eingeschlossen. Insgesamt wurden 706 Dialyse assoziierte Infektionen während des Studienzeitraums dokumentiert. Die ZVK assoziierten Infektionsraten reduzierten sich von 2,39 Infektionen/1000 Dialysen (95 % CI 2,15–2,64) auf 0,99 Infektionen/1000 Dialysen (95 % CI 0,84–1,15). Die Graft assoziierten Infektionsraten reduzierten sich von 0,58 Infektionen/1000 Dialysen (95 % CI 0,38–0,84) auf 0,27 Infektionen/1000 Dialysen (95 % CI 0,15–0,45). Bei Shunt assoziierten Infektionen reduzierten sich



FV23: Abb. 1

die Infektionsraten von 0,19 Infektionen/1000 Dialysen (95 % CI 0,15–0,23) auf 0,07 Infektionen/1000 Dialysen (95 % CI 0,05–0,1). Die Compliance der Händedesinfektion steigerte sich im Median von 58,2 % (95 % CI 57,0–59,0) auf 64,6 % (95 % CI 63,4–65,5).

Zusammenfassung: Das Surveillancesystem zur Erfassung von Dialyse assoziierten Infektionen und die direkte Beobachtung der Händehygiene Compliance konnten erfolgreich in den ambulanten Zentren implementiert werden. Die Multimodale Interventionsstrategie führte zur effektiven Reduzierung von Dialyse assoziierten Infektionen.

Xenotransplantation und Organoide

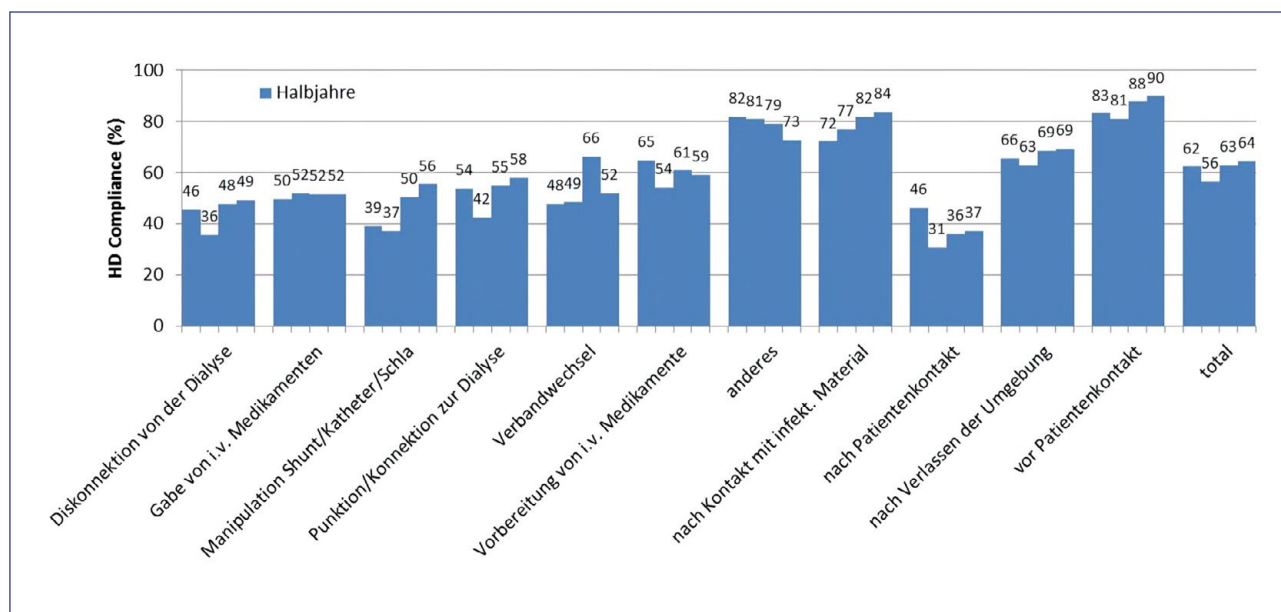
FV24

Spatial expression of kidney-specific genes in human iPSC-derived renal organoids

J. Dilz; I. Auge; S. Reuter¹; R. Mrowka

Experimentelle Nephrologie, Klinik für Innere Medizin III, Friedrich-Schiller-Universität Jena, Jena; ¹ThIMEDOP – Thüringer Innovationszentrum für Medizintechnik-Lösungen, Friedrich-Schiller-Universität Jena, Jena

Objective: Kidney organoids derived from human induced pluripotent stem cells (hiPSCs) allow studying of complex 3D interactions of cells in a tissue complex and provide attractive ex vivo platforms for disease modeling and organogenesis. During embryogenesis, not only temporal cues but also spatial signals from neighboring cells are crucial for determining tissue development. We aimed at investigating the spatial expression of kidney-specific genes in hiPSC-derived renal organoids using RNA-fluorescence in situ hybridization. In previous qPCR analysis, we showed enhanced gene expression for the podocyte marker genes NPHS1 and



FV23: Abb. 2

NPHS2 as well as for SLC12A1, marking the thick ascending limb of the loop of Henle (LOH), rendering these genes promising targets for further investigation.

Method: Renal organoids were generated from hiPSCs in suspension culture. Three different batches of 14-day-old organoids were analyzed. Following standard histological procedures, organoids were embedded in paraffin and sectioned. RNA-fluorescence in situ hybridization was executed according to the RNAscope Multiplex protocol. Samples were mounted and imaged with confocal laser scanning microscopy.

Results: Renal tubular structures, represented by circularly arranged nuclei with a lumen in the center, were clearly visible throughout the specimen. A focus-like distribution of hybridization signals for NPHS1, NPHS2, and SLC12A1 was co-localized in circular structures clearly distinct from renal tubules. Fluorescence signals for SLC12A1 could

also be detected adjacent to the foci. In detail imaging, strong partially co-localized nuclear hybridization signals for both NPHS1 and SLC12A1 could be detected along with fine dot-like and evenly distributed signals for NPHS2.

Conclusion: The co-expression of NPHS1 and NPHS2 in the foci suggests the presence of podocyte-like cells in putative glomerular structures in the organoids. Because renal organoids are most similar to fetal kidneys in the first trimester, the co-expression of SLC12A1, marking the LOH in mature kidneys, and podocyte marker genes may indicate an early developmental state. SLC12A1 expression near glomerular structures suggests the development of macula densa cells in the LOH. We were able to demonstrate the distinct expression of kidney-specific genes using RNA-fluorescence in situ hybridization, implying the development of glomerular structures in

renal organoids. This could pose to be a powerful method to determine the maturation stage of renal organoids and aid in the translation of experimental findings onto human nephrogenesis.

From bench to bedside – IgA Nephritis

FV25

Efficacy and safety of iptacopan in IgA nephropathy: Results of a randomized double-blind placebo-controlled Phase 2 study at 6 months

A. Schreiber¹; J. Barratt¹; B. Rovin²; H. Zhang³; N. Kashihara⁴; B. Maes⁵; D. V. Rizk⁶; H. N. Trimarchi⁷; B. Sprangers⁸; M. Meier⁹; D. Kollins⁹; W. Wang¹⁰; A. Magirr⁹; V. Perkovic¹¹
Medizinische Klinik mit Schwerpunkt Nephrologie und Internistische Intensivmedizin, Campus Charité Mitte, Charité – Universitätsmedizin Berlin, Berlin; ¹ Department of Respiratory Sciences, University of

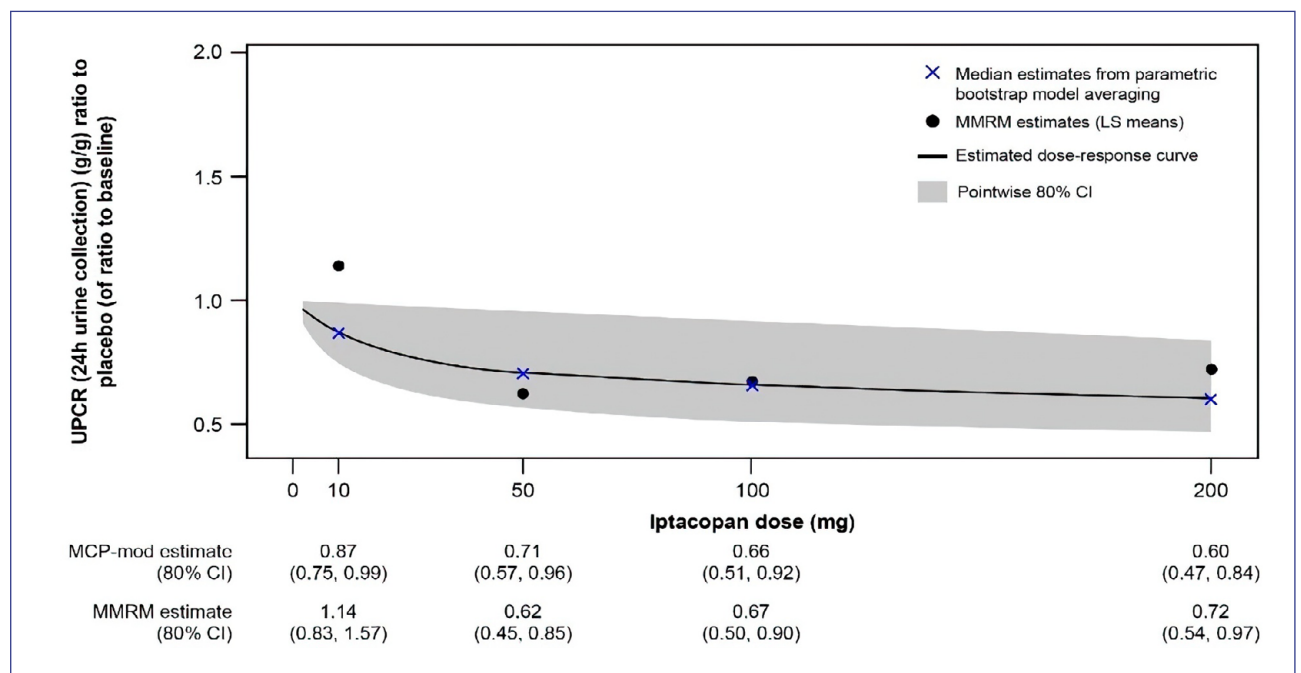
Leicester, Leicester/UK; ² Division of Nephrology, Wexner Medical Center, The Ohio State University, Columbus/USA; ³ Renal Division, Institute of Nephrology, Peking University, Beijing/CN; ⁴ Department of Nephrology and Hypertension, Kawasaki Medical School, Kurashiki Okayama/J; ⁵ AZ Delta, Department of Nephrology, Roeselare/BE; ⁶ Division of Nephrology, Department of Medicine, University of Alabama at Birmingham, Birmingham/USA; ⁷ Nephrology Service and Kidney Transplantation Unit, Hospital Británico de Buenos Aires, Buenos Aires/RA; ⁸ Department of Microbiology, Immunology and Transplantation, Rega Institute for Medical Research, University Hospitals Leuven, KU Leuven, Leuven/BE; ⁹ Novartis Pharma AG, Basel/CH; ¹⁰ Novartis Pharmaceuticals Corporation, East Hanover/USA; ¹¹ University of New South Wales, Sydney/AUS

Objective: No approved targeted therapies currently exist for IgA nephropathy (IgAN). Targeting the alternative complement pathway (AP) is a therapeutic strategy given its role in the pathogenesis of IgAN. Iptacopan (LNP023) is a first-in-class, oral, potent and highly selective inhibitor of factor B of AP.

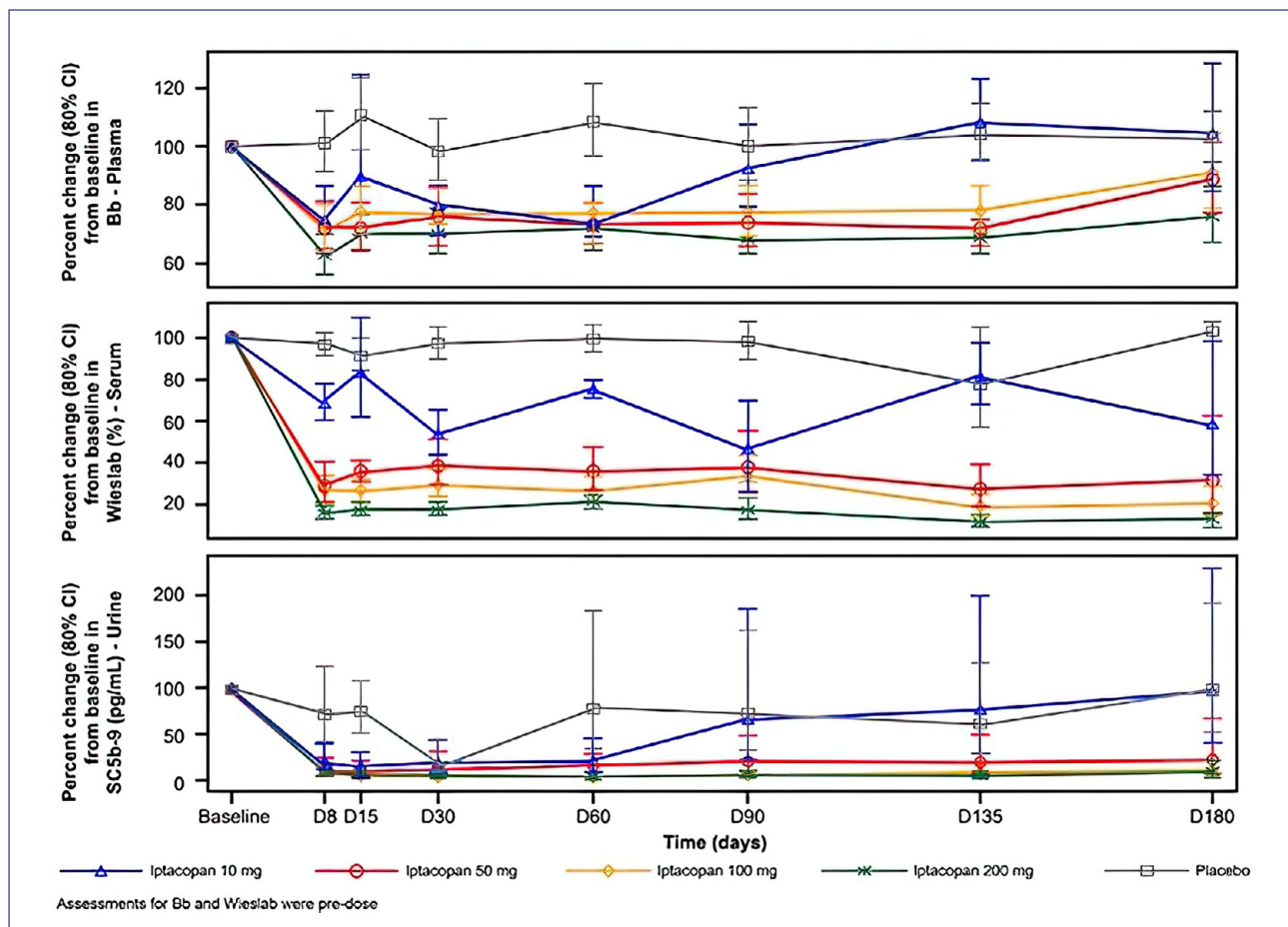
Method: This randomized, double-blind, dose-ranging, parallel-group adaptive design Phase 2 study (NCT03373461) enrolled patients with biopsy-confirmed IgAN, urine protein-to-creatinine ratio (UPCR) ≥ 0.8 g/g or urine protein ≥ 0.75 g/24 h, and estimated glomerular filtration rate (eGFR) ≥ 30 mL/min/1.73 m². Part 1 of the study enrolled patients for a 3-month and Part 2 enrolled patients for a 6-month treatment period; both Parts comprised a 3-month treatment-free follow-up.

Patients were randomized to one of the four iptacopan arms (10, 50, 100 [in Part 2 only], and 200 mg bid) or placebo. In this analysis, we report efficacy, safety and biomarker data assessed at 6 months.

Results: 46 and 66 patients were randomized in Parts 1 and 2, respectively. In Part 2, 58 patients completed 6 months of treatment. Demographic and baseline characteristics were generally well-balanced across all arms. The primary analysis yielded a statistically significant dose-response effect (1-sided $p = 0.038$) of iptacopan versus placebo at 3 months, with maximal reduction in UPCR achieved with iptacopan 200 mg bid (23 %; 80 % CI: 8–34 % using MCP-mod). UPCR continued to decrease between 3 and 6 months in the higher dosed iptacopan arms in Part 2, albeit with a wider 80 %



FV25: Abb. 1



FV25: Abb. 2

CI reflecting the smaller sample size. A *Post hoc* analysis of pooled data from Parts 1 and 2 was performed indicating UPCR reduction from baseline up to 6 months in iptacopan 200 mg bid arm by up to 40 % (80 % CI: 16–53 % using MCP-mod model) and at least 28 % (80 % CI: 3–46 % using MMRM model) versus placebo (Figure 1). Sustained inhibition of AP biomarkers including plasma Bb, serum Wieslab, and urinary C5b-9 through 6 months was also observed with all doses of iptacopan above 10 mg bid (Figure 2). Iptacopan had a well-tolerated safety profile.

Conclusion: Iptacopan was well tolerated and led to continuous reduction in proteinuria and strong inhibition of AP activity through 6 months in patients with IgAN. These data are consistent with previous findings from the interim analysis and support further evaluation of iptacopan in the ongoing Phase 3 APPLAUSE-IgAN trial (NCT04578834).

Clinical Science – Pädiatrische Nephrologie

FV26

The genetic landscape and clinical spectrum in a cohort of 601 nephronophthisis patients.

F. Petzold; M. Zaidan¹; K. Billot²; X. Chen²; V. Morinière³; P. Krug²; C. C. Jeanpierre²; K. Tory⁴; O. Boyer⁵; A. Burgun⁶; A. Servais⁷; A. Benmerah²; L. Heidet⁵; N. Garcelon⁸; C. Antignac²; S. Saunier²

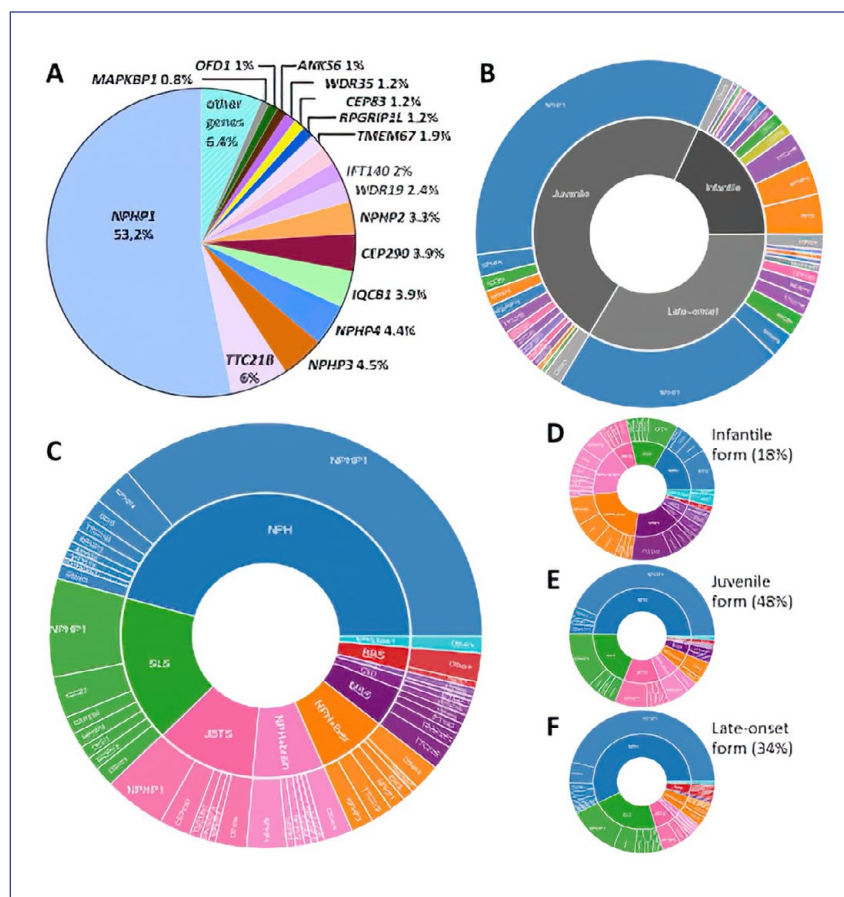
Sektion Nephrologie, Klinik für Endokrinologie und Nephrologie, Universitätsklinikum Leipzig, Leipzig; ¹ Department of Nephrology, Dialysis, Transplantation,

Bicêtre University Hospital, Paris-Saclay University, Le Kremlin-Bicêtre/F; ² Laboratory of Inherited Kidney Diseases, Imagine Institute, Université de Paris, Paris/F; ³ Department of Genetics, Necker Hospital, Université de Paris, Paris/F; ⁴ MTA-SE Lendület Nephrogenetic Laboratory, 1st Department of Pediatrics, Semmelweis University, Budapest/H; ⁵ Department of Pediatric Nephrology, Necker Hospital, Université de Paris, Paris/F; ⁶ Department of Medical Informatics, Necker Hospital, Université de Paris, Paris/F; ⁷ Nephrology and Transplantation Department, Necker Hospital, Université de Paris, Paris/F; ⁸ Imagine Institute, Université de Paris, Paris/F

Objective: Ciliopathies comprise severe disorders that affect several organs including kidneys, eyes, CNS, liver, bone and heart. Renal involvement is one of the most common, and results in CKD due to nephronophthisis (NPH), an autosomal recessive form of chronic tubulointerstitial nephritis. In this study, we report one of the worldwide biggest cohorts of NPH patients captured over the last three decades.

Method: Inclusion criteria were i) a clinical diagnosis of NPH and ii) an identified genetic variant in known ciliopathy-associated genes. Genetic analyses included conventional PCR, NGS gene panel, and WES.

Results: 1167 NPH patients underwent genetic analysis, which identified 788 causal variants (138 novel) in 38 ciliopathy genes in 601 individuals. The majority of patients (53 %) bore pathogenic variants in *NPHP1*. Each remaining gene represented less than 6 % of cases. Beyond that, we related the clinical spectrum of other ciliopathy genes (*OFD1*, *SCLT1*, *WDR35*,

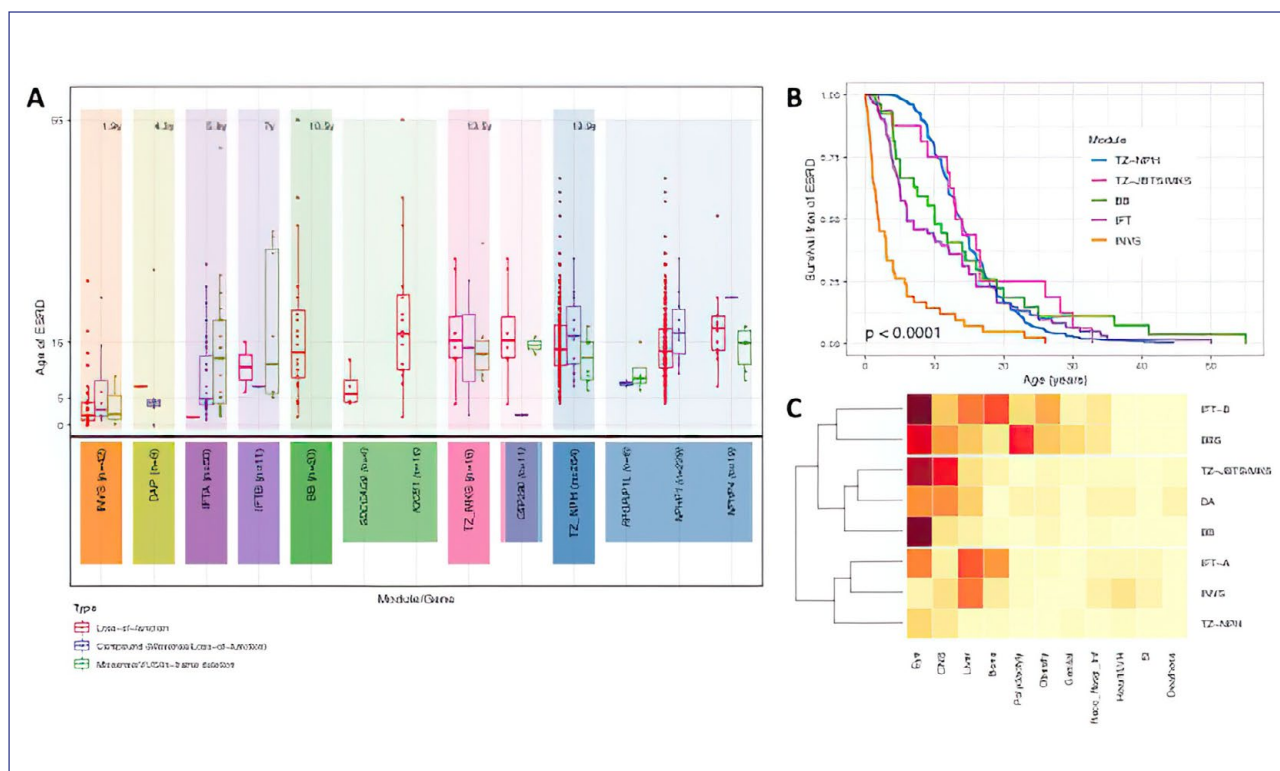


FV26: Abb. 1

Relative frequencies of disease causing genes in the cohort. B Distribution of causative genes related to the age of ESKD, where the causative genes of the infantile form (< 5 years) vary widely from the juvenile (5–15 years) and late-onset form (> 15 years). C Relative fractions of NPH an *saue* mutations in the overall cohort, and related to the group of patients with infantile (D), juvenile (E) and late-onset form (F). NPH isolated nephronophthisis, SS Senior-Løken syndrome, JBTS Joubert syndrome, MSS Saldino-Mainzer syndrome, CED cranioectodermal dysplasia, JATD Asphyxiating thoracic dystrophy, BBS Bardet-Biedl syndrome.

IFT43, *CPLANE1*) to NPH (Fig. 1A). **NPH-related CKD profile and ESKD progression risk.** At mean 13 years, 76 % of the patients had progressed to ESKD, of which 18 % had an infantile form, and nearly half (48 %) exhibited juvenile NPH, while the remaining 34 % exhibited a late-onset disease (Fig. 1B). Kidney ultrasound findings revealed

hyperechogenicity, cysts, small size and corticomedullary dedifferentiation in 56 %, 43 %, 32 % and 26 % of cases, respectively. **Ciliopathies-related extrarenal features and syndromic forms.** Extrarenal manifestations were observed in 54 % of patients. Eye involvement represented the predominant feature (37 %), either isolated as Senior-Løken



FV25: Abb. 2

A Age of ESKD dependent on the affected gene/compartment and the type of mutation (Loss-of-function (nonsense, frameshift, splice) vs. compound (LoF and missense/VUS/in-frame deletion) vs. missense/VUS/In-frame deletion). B The Kidney survival by ciliary modules. C Correlation between the different ciliary modules and main organ involvement revealed three groups of main phenotypes.

syndrome (MIM #266900) (17%), or with other extrarenal disorders. The second major extrarenal symptom was cerebellar hypoplasia (11%), and correspond to Joubert syndrome (MIM #609583). Skeletal malformations as common features of ciliopathies (13%) were mainly related to hands and feet. Liver abnormalities, heart involvement, and finally *situs inversus* were more rarely observed (8%, 4%, and 3%) (Fig. 1C, D, E, F). Hereby, we emerged significant genotype-phenotype correlations between both, the CKD profile and the extrarenal organ involvement, relating to the mutation type, the affected gene, and moreover the belonging ciliary module (Fig. 2).

Conclusion: In our cohort of 601 NPH patients, which is characterized by a great genetic and clinical heterogeneity, we extended the number of disease-causing variants and genes and delineated genotype-phenotype correlations giving implications in diagnose NPH patients including late NPH in adult patients.

Basic Science – Inflammation

FV27

Immune checkpoint molecule BTLA attenuates inflammation and glomerular damage in experimental glomerulonephritis

P. Diefenhardt; M. Braumann; T. Schömig; B. Trinsch; C. Sierra-Gonzalez; B. Schermer; C. Kurts¹; P. T. Brinkkötter; T. Benzinger; S. Brähler
Nephrologie, Rheumatologie, Diabetologie und Allgemeine Innere Medizin, Klinik II für Innere Medizin, Universitätsklinikum Köln, Köln;
¹ Institut für Experimentelle Immunologie, Medizinische Fakultät, Rheinische Friedrich-Wilhelms-Universität Bonn, Bonn

Objective: Overshooting immune responses mediated by T-cells in the kidney may lead to acute, crescentic Glomerulonephritis (GN). For successful T-cell activation, different signals need to play in concert. Accordingly, interference with these pathways might represent a viable treatment option for GN. One of these signal molecules, B and T Lymphocyte Attenuator (BTLA), was shown to mediate anti-inflammatory effects in other T-cell mediated disease models. Its role during glomerular inflammation, however, remains unclear. Here we aimed to elucidate the function of BTLA signaling in the kidney using a mouse model of acute GN and evaluated BTLA as a therapeutic target.

Method: Nephrotoxic nephritis (NTN) was induced in wild type (wt) and BTLA knock out (BTLA-KO) mice. In addition, an agonistic anti-BTLA antibody was administered i.v. into wt mice after NTN induction to evaluate its therapeutic potential. Functional readouts included albuminuria and BUN concentration. Histological damage was assessed 10 days after NTN induction in all groups using PAS stained tissue slides. Flow cytometry was performed to analyse renal and systemic immunity and IHC was used to visualize and quantify renal T-cell infiltration. Additional *in vitro* assays revealed the impact of BTLA deficiency on the function of T-cell subsets.

Results: Knockout of BTLA resulted in aggravation of NTN. Quantification and characterization of renal immune cells revealed an increase in pro-inflammatory Tbet⁺ Th1 cells. Systemically, nephritic BTLA-KO mice showed a significant reduction of Foxp3⁺ T

regulatory cells. Activation of BTLA through administration of an agonistic anti-BTLA-antibody attenuated NTN by reducing the frequencies of Th1 and Th17 cells in the nephritic kidney and increasing systemic Treg frequencies. *In vitro* Treg suppression assays revealed an evasion of Treg mediated suppression by BTLA deficient T effector cells.

Conclusion: BTLA signaling attenuates inflammation in experimental GN directly through suppression of pro-inflammatory T effector cells in the kidney as well as indirectly through induction of differentiation and/or proliferation of anti-inflammatory T regulatory cells. Activation of BTLA signaling by agonistic antibodies represents an effective treatment strategy in NTN.

Nephrogenetik

FV28

Circadian clock genes compensate *nphp* mutations in zebrafish

N. Kayser; F. Zaiser; A. C. Veenstra; H. Wang; B. Göcmen; P. Eckert; A. Köttgen¹; G. Walz; T. A. Yakulov
Medizinische Klinik IV/ Abteilung Nephrologie, Universitätsklinikum, Albert-Ludwigs-Universität Freiburg, Freiburg; ¹Institut für Genetische Epidemiologie, Universitätsklinikum, Albert-Ludwigs-Universität Freiburg, Freiburg

Nephronophthisis (NPH) is the most common hereditary condition leading to end-stage renal disease in childhood. Over 25 NPH-related genes have been identified that predominantly localize to primary cilia. Therefore, NPH is considered a ciliopathy. The zebrafish pronephros model, using morpholino oligonucleotides (MO) to deplete target genes, has been extensively used to

characterize human ciliopathy phenotypes. However, discrepancies between MO and genetically defined mutant zebrafish lines have questioned this approach. Here, we analyzed zebrafish with mutations in the *nphp1-4-8* module, and compared the mutation-associated ciliopathy manifestations with the results observed after MO-based depletion of *nphp1*, *nphp4*, and *nphp8*. All zebrafish lines with defined *nphp1*, *nphp4*, or *nphp8* mutations were viable. MO-mediated depletion resulted in glomerular cyst and cloaca malformation; these ciliopathy-typical manifestations were observed at a much lower frequency in zebrafish embryos with defined *nphp* mutations, and decreased from the first (F1) to the second maternal zygotic (F2) generation, despite lacking maternal RNA contribution. While zebrafish embryos with mutations in one *nphp* gene became more sensitive to MO-based depletion of additional *nphp* genes, successive genetic compensation from the F1 to the F2 generation was supported by the observation that *nphp4*-deficient mutants became partially refractory to MO-based *nphp4* depletion. To address the underlying compensatory mechanisms, the transcriptome of *nphp8* mutant zebrafish embryos was compared to wildtype siblings. This approach revealed a striking upregulation of circadian clock genes in *nphp8* mutant zebrafish embryos. MO-mediated depletion of the clock genes *cry1a* and *cry5* caused ciliopathy phenotypes in wildtype embryos, and increased the frequency of glomerular cysts in maternal zygotic *nphp8* mutant embryos. Importantly, co-injection of *cry1a* and *cry5* mRNA rescued the ciliopathy-related phenotypes in *nphp1*, *nphp4* or *nphp8*-depleted

zebrafish embryos. Our findings indicate that upregulation of circadian clock genes ameliorates the loss of *nphp* genes. Identifying genetic networks that compensate ciliopathy-associated defects in zebrafish may provide a new conceptual approach to combat these rare but serious human hereditary diseases.

Machine learning

FV29

Oxford Classification by machine learning

N. Altini; C. Delprete; F. Berloco; B. Prencipe; A. Brunetti; C. Mohan¹; S. Rizvi²; P. A. Cicalese²; H. V. Nguyen²; P. Pontrelli³; F. Pesce³; M. Rossini³; L. Gesualdo⁴; V. Bevilacqua; J. U. Becker⁵

Department of Electrical and Information Engineering, Polytechnic University of Bari, Bari/I; ¹ Biomedical Engineering & Medicine, University of Houston, Houston/USA; ² Department of Electrical & Computer Engineering, University of Houston, Houston/USA; ³ Department of Emergency and Organ Transplantation, Nephrology, Dialysis and Transplantation Unit, University of Bari "Aldo Moro", Bari/I; ⁴ Division of Nephrology, Department of Emergency and Organ Transplantation, University clinic of Bari, "Aldo Moro" Medicine School Bari, Bari/I; ⁵ Institut für Pathologie, Universität zu Köln, Köln

Objective: The Oxford Classification for IgA glomerulonephritis (IgA-GN) is the most successful example of an evidence-based nephropathology classification system. With a machine learning approach we aim to develop a model for the automatic analysis of large biopsy cohorts with perfect reproducibility and minimal human effort.

Method: We used a set of 4703 glomerular image crops from PAS sections of biopsies with IgA-GN. All crops were labelled by an expert nephropathologist for the M score as "indeterminate", "yes"/"no", the E scores as "yes"/"no", the S score as "global glomerulosclerosis"/"segmental glomerulosclerosis"/"no glomerulosclerosis", the C score as "yes"/"no". We trained several neural network architectures for the M, E, S, C classifiers and compared the performance with standard metrics. The dataset was split into 80%/20%/20% for training, testing and validation. Dataset dysbalance was addressed with ADASYN. We trained for 500 epochs.

Results: The frequency of expert labels regarding M were 42%/30%/28% for "yes"/"no"/"indeterminate", regarding E was 2%/98% for "yes"/"no", regarding S was 23%/13%/64% for "global glomerulosclerosis"/"segmental glomerulosclerosis"/"no glomerulosclerosis", regarding C was 6%/95% for "yes"/"no".

Overall best-performing network architectures were two iterations of ResNet. Accuracy, Precision, Sensitivity, F1 Score and AUC for M reached .729, .686-.872, .493-.952, .574-.859, for E reached .866, .162, .552, .879, .250, .807, for S reached .838, .475-.948, .200-.958, .669-.985, .282-.910, .805-.986, for C reached .806, .230, .760, .809, .354, .864.

Conclusion: Modern network architectures, pretrained on ImageNet, deliver promising results for the replication of expert labels for the glomerular components of the Oxford Classification. However, larger training sets are needed to overcome the dysbalance of rare lesions like E and C in randomly generated datasets.

Together with our automatic segmentation models, we will generate larger datasets from more institutions and will employ them in an end-to-end protocol, rendering M, E, S, C outputs for the input of unsegmented whole slide images.

From bench to bedside – Complement und Niere

FV30

Intrarenal synthesis of complement C3 localized to distinct vascular compartments in ANCA-associated renal vasculitis

S. Hakroush; B. Tampe¹
Institut für Pathologie, Universitätsmedizin Göttingen, Georg-August-Universität, Göttingen; ¹ Klinik für Nephrologie und Rheumatologie, Universitätsmedizin Göttingen, Georg-August-Universität, Göttingen

Objective: Anti-neutrophil cytoplasmic antibody (ANCA)-associated vasculitis (AAV) is a small vessel vasculitis affecting multiple organ systems, including the kidney. The activation of the complement system contributes essentially to its pathogenesis by autoantibody-antigen recognition directed against host cells in ANCA-associated renal vasculitis. The measurement of serum complement C3 with immunoassays is routinely used in clinical practice to determine and monitor complement activation. Importantly, C3 hypocomplementemia is only present in a minor subset of ANCA-associated renal vasculitis. These observations suggest that intrarenal synthesis of distinct complement components might contribute to kidney injury in renal vasculitis.

Method: A total number of 43 kidney biopsies with ANCA-associated

renal vasculitis were retrospectively included between 2015 till 2020. Intrarenal complement C3c localized to distinct vascular compartments (including small-sized arteries, capillaries, and venules) was evaluated. Publicly available transcriptome array datasets for C3 expression (encoded by C3) from Nephroseq (www.nephroseq.org, May 2022, University of Michigan, Ann Arbor, MI).

Results: Immunostaining confirmed presence of C3c deposits localized to either the glomerular tuft, interlobular arteries, peritubular capillaries, or venules in ANCA-associated renal vasculitis. Glomerular C3c deposits correlated positively with serum levels of complement C3c ($p = 0.011$), indicating that intrarenal complement deposition occurs independent of systemic activation of the complement system and further supporting intrarenal synthesis of complement C3. To confirm transcriptional induction of intrarenal C3, we next extracted transcriptome datasets for C3 mRNA expression specifically from microdissected tubulointerstitial and glomerular compartments. As compared to healthy controls, we observed a significant induction of C3 mRNA transcripts in the tubulointerstitial ($p < 0.0001$) and glomerular compartments of renal vasculitis ($p < 0.0001$). Intrarenal C3 mRNA expression correlated with impaired kidney function in the tubulointerstitial and glomerular compartments of renal vasculitis. Gene set enrichment analysis in the whole dataset linking intrarenal C3 synthesis to potential signaling pathways differing between tubulointerstitial and glomerular C3 synthesis.

Conclusion: In summary, intrarenal synthesis of complement C3 is present in distinct vascular compartments of ANCA-associated renal vasculitis. This is especially relevant because clinical trials currently investigate inhibition of the complement system in ANCA-associated renal vasculitis.

Was wir über seltene Erkrankungen wissen sollten

FV31

Genetic variants in ARHGEF6 cause congenital anomalies of the kidneys and urinary tract in humans, mice, and frogs

V. Klämbt¹; F. Buerger¹; C. Wang¹; T. Naert²; A.-C. Weiss³; E. Lai¹; S. Shril¹; S. Schneider¹; L. Schierbaum¹; M. R. Bekheirnia⁴; M. Joosten⁵; A. Vivante⁶; E. Banne⁷; S. Mane⁸; R. Lifton⁸; A. Kispert³; K.-D. Fischer⁹; S. Lienkamp²; M. Zegers¹⁰; F. Hildebrandt¹

Klinik für Pädiatrie mit Schwerpunkt Nephrologie, Campus Virchow-Klinikum, Charité – Universitätsmedizin Berlin, Berlin; ¹ Division of Nephrology, Boston Children's Hospital, Harvard Medical School, Boston/USA; ² Anatomisches Institut, Medizinische Fakultät, Universität Zürich, Zürich/CH; ³ Institut für Molekularbiologie, Medizinische Hochschule Hannover, Hannover; ⁴ Molecular and Human Genetics, Baylor College of Medicine, Houston/USA; ⁵ University Medical Center Rotterdam, Rotterdam/NL; ⁶ Division of Nephrology, Sheba Medical Center, Sackler Faculty of Medicine, Tel-Hashomer/IL; ⁷ Hebrew University and Hadassah Medical School, Jerusalem/IL; ⁸ Yale University School of Medicine, New Haven/USA; ⁹ Institut für Biochemie und Zellbiologie,

Otto-von-Guericke-Universität Magdeburg, Magdeburg; ¹⁰ Radboud University Medical Center, Nijmegen/NL

Objective: Congenital anomalies of the kidney and urinary tract (CAKUT) are the most common cause of end-stage renal disease during childhood. More than 40 disease genes for monogenic, isolated CAKUT have been described; however, pathogenic variants in these genes only explain 20 % of cases. Thus, broader genetic heterogeneity is evident.

Method: Here, we performed exome sequencing (ES) in a cohort of 1265 families with CAKUT to further characterize the genetic etiology of this disease.

Results: We detected six hemizygous variants in the gene *ARHGEF6* in six unrelated families with CAKUT. Overexpression of *ARHGEF6* wild type but not proband-derived mutant proteins increased CDC42/RAC1 activity, induced lamellipodia formation and stimulated PARVA-dependent cell spreading. Furthermore, *ARHGEF6* mutant proteins displayed loss-of-interaction with the PARVA, a described murine CAKUT protein, in co-immunoprecipitation assays. 3D cell culture of MDCK cells revealed a reduced lumen formation when expressing *ARHGEF6* mutant proteins. Finally, *in vivo* *Arhgef6* knockout models in *Xenopus* and mouse replicated the proband's disease by exerting different features of CAKUT.

Conclusion: We conclude that deleterious variants in *ARHGEF6* may cause dysregulation of integrin-parvin-RAC1/CDC42 signaling, thereby leading to CAKUT.

Basic Science – Tubulus und Interstitium

FV32

Regulatorische DNA-Elemente aus primären tubulären Zellen überlappen mit GWAS-Daten zur Nierenfunktion

R. Krüger; K.J. Stanzick¹; V. Lauer; S. Naas; K. Stark¹; M. Gorski¹; M. Schiffer; I. Heid¹; J. Schödel
Medizinische Klinik 4, Nephrologie und Hypertensiologie, Universitätsklinikum, Friedrich-Alexander-Universität Erlangen-Nürnberg, Erlangen; ¹Institut für Epidemiologie und Präventivmedizin, Universitätsklinikum, Universität Regensburg, Regensburg

Hintergrund: Durch genomweite Assoziationsstudien (GWAS) konnten Tausende von genetischen Varianten identifiziert werden, die mit einer verminderten Nierenfunktion und chronischen Nierenerkrankungen (*Chronic kidney disease*, CKD) in Verbindung stehen. Die meisten der identifizierten genetischen Varianten befinden sich in intronischen oder nicht kodierenden Regionen des menschlichen Genoms. Die Kartierung dieser Varianten und die Charakterisierung ihrer möglichen Funktion stellt eine wichtige Hürde zum besseren Verständnis der genetischen Prädisposition für eine reduzierte Nierenfunktion dar.

Methode: Wir verwendeten den genomweiten *Assay for Transposase-Accessible Chromatin using sequencing* (ATAC-seq) in primären Tubuluszellen zur Identifizierung von regulatorischen DNA-Elementen. Hierfür wurden primäre Tubuluszellen (PTC) verwendet, die aus gesunden Anteilen von vier Tumornephrektomien isoliert wurden. Für eine weitere

Filterung wurden zusätzlich öffentliche ATAC-seq Daten aus der gesamten Niere (n = 15) und aus Einzelzellkernen aus dem Nierenkortex (n = 5) eingesetzt (Accelerating Medicines Partnership in Common Metabolic Diseases (AMP-CMD), 2022; Muto et al., 2021). Die so erhaltenen Daten wurden mit 38,306 publizierten Varianten verglichen, die in einer GWAS meta-analysis zur eGFR mit mehr als 1 Mio. Individuen priorisiert worden waren (Stanzick et al., 2021).

Ergebnisse: Aus den ATAC-seq-Daten aus PTC erstellten wir eine genomweite Landschaft der Chromatinzugänglichkeit, die ca. 110,000 Konsensregionen umfasst. Die zelluläre Identität wurde validiert, indem man diese Stellen mit öffentlich zugänglichen epigenetischen Datensätzen aus ENCODE verglich. Die Überlappung der GWAS Varianten mit dem offenen Chromatin der PTC ergab eine Reduktion der Varianten auf 1402. Eine weitere Filterung mit veröffentlichten ATAC-seq Daten für die gesamte Niere und snATAC-seq Daten ergab letztendlich ein Set von 150 priorisierten SNPs.

Zusammenfassung: Unser genomweiter Atlas der Chromatinzugänglichkeit und -aktivität in PTC bietet einen wertvollen Referenzdatensatz für die Untersuchung des Einflusses genetischer Variation auf die Genexpression im Tubulussystem. Wir haben dadurch mehrere SNP-assoziierte regulatorische Elemente identifiziert, die dem beobachteten Effekt auf die eGFR funktionell zugrunde liegen könnten. Aktuell evaluieren wir diese mögliche Beziehung zwischen genetischer Variation und Genexpression im Tubulussystem experimentell.

Transplantation

FV33

Five-year follow-up of a phase I trial of donor-derived modified immune cell infusion in kidney transplantation

M. Schaier; C. Morath; L. Wang¹; C. Kleist²; G. Opelz²; T.H. Tran²; S. Scherer²; C. Süsal³; E. Ibrahim³; M. Aly; C. Alvarez²; F. Kälble; C. Speer; L. Benning; C. Nußhag¹; L. Pego da Silva; C. Sommerer; A. Hückelhoven-Krauss¹; D. Czock⁴; A. Mehrabi⁵; C. Schwab⁶; R. Waldherr⁶; P. Schnitzler⁷; U. Merle¹; G.A. Böhmig⁸; C. Müller-Tidow¹; J. Reiser⁹; M. Zeier; M. Schmitt¹; P. Terness³; A. Schmitt¹; V. Daniel³
Medizinische Klinik I, Sektion Nephrologie, Medizinische Fakultät, Ruprecht-Karls-Universität Heidelberg, Heidelberg; ¹Gastroenterologie, Infektionskrankheiten, Vergiftungen, Klinik für Innere Medizin IV, Universitätsklinikum Heidelberg, Heidelberg; ²Transplantationsimmunologie, Medizinische Fakultät, Ruprecht-Karls-Universität Heidelberg, Heidelberg; ³Abteilung Transplantationsimmunologie, Institut für Immunologie und Serologie, Ruprecht-Karls-Universität Heidelberg, Heidelberg; ⁴Klinische Pharmakologie und Pharmakoepidemiologie, Medizinische Klinik, Universitätsklinikum Heidelberg, Heidelberg; ⁵Klinik für Allgemein-, Viszeral- und Transplantationschirurgie, Medizinische Fakultät, Ruprecht-Karls-Universität Heidelberg, Heidelberg; ⁶Pathologisches Institut, Klinikum der Universität Heidelberg, Heidelberg; ⁷Molekulare Virologie, Zentrum für Infektologie, Ruprecht-Karls-Universität Heidelberg, Heidelberg; ⁸Klinische Abteilung für Nephrologie und Dialyse, Universitätsklinik für Innere Medizin III, Medizinische Universität Wien,

Wien/A; ⁹ Nephrology, Departement of Internal Medicine, Rush University Medical Center, Chicago/USA

Objective: The administration of modified immune cells (MIC) prior to kidney transplantation led to specific immunosuppression against the allogeneic donor and a significant increase in regulatory B lymphocytes (Breg). We now wanted to investigate how this approach affects the clinical course of treated patients.

Method: Ten patients from a phase I clinical trial who had received MIC infusions before kidney transplantation were compared to 15 matched standard-risk recipients. Follow-up was until year five after surgery.

Results: The 10 MIC patients had an excellent clinical course with stable kidney graft function and showed no donor-specific human leukocyte antigen antibodies (DSA) or acute rejections during follow-up. In contrast, 1 of 15 controls died (A) and 5 of 15 controls developed DSA (log rank $P = 0.046$) (B). While the number of patients with a non-opportunistic infection did not differ significantly between groups ($P = 0.36$), opportunistic

infections were reported more frequently in controls (log rank $P = 0.033$) (C). Compared to controls, MIC patients were found to have a trend towards a higher COVID-19 anti-S1 IgG index after vaccination with a median of 53 vs. 2 ($P = 0.16$). Importantly, the four MIC patients who had received the highest MIC cell dose 7 days before surgery and were on low immunosuppression during follow-up, continued to show absent anti-donor T lymphocyte reactivity in vitro and high CD19⁺CD24^{hi}CD38^{hi} transitional Breg as well as CD19⁺CD24^{hi}CD27⁺ memory Breg.

Conclusion: MIC infusions together with reduced conventional immunosuppression were associated with lower de novo DSA development and lower rates of opportunistic infections. In the future, MIC infusions could contribute to graft protection while reducing the side effects of immunosuppressive therapy.

FV34

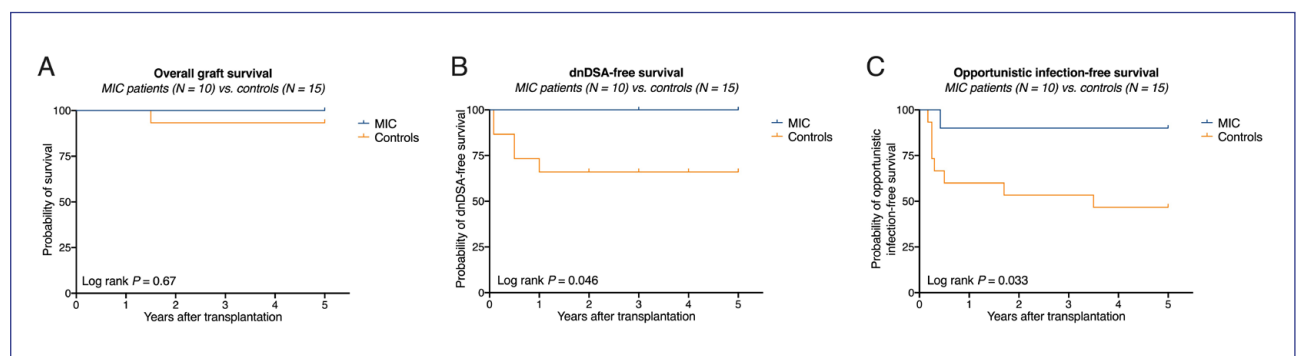
Regional differences in waiting time prior to kidney transplantation in Germany

D. Zecher; J. Wadewitz¹; F. Zeman²; A. Rahmel¹; I. Tieken³; B. Banas

Abteilung für Nephrologie, Universitätsklinikum, Universität Regensburg, Regensburg; ¹ Deutsche Stiftung Organtransplantation, Frankfurt a. M.; ² Zentrum für Klinische Studien, Universitätsklinikum, Universität Regensburg, Regensburg; ³ Eurotransplant Foundation, Leiden/NL

Objective: Organ allocation algorithms promote regional allocation to keep ischemia times short. Whereas in the common Eurotransplant (ET) kidney allocation scheme (ETKAS), a regional bonus is integrated into a complex algorithm, the ET senior program (ESP) is primarily based on regional allocation. Little is known, however, how these algorithms influence regional waiting times prior to kidney transplantation (KTX) in Germany.

Method: We performed a retrospective cohort study including all patients that received a kidney-only graft under standard circumstances during 24 months in Germany ($n = 2053$). We used simple and multiple linear regression to study regional differences in waiting time prior to KTX between the seven organ procurement regions in ETKAS and the



FV33: Abb. 1

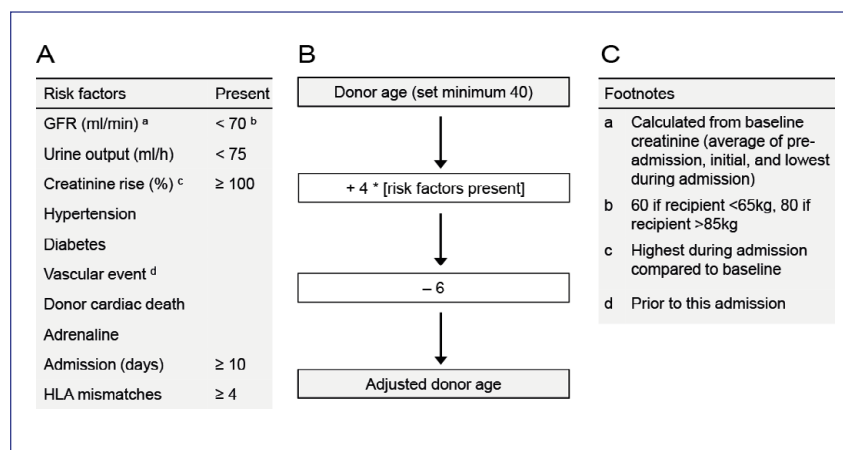
15 ESP subregions established by the *Deutsche Stiftung Organtransplantation* (DSO). The impact of the number of regionally procured kidneys on waiting time was also investigated. **Results:** In both exploratory analyses and multiple linear regression models, we found significant regional differences in median waiting time of up to 1.7 years in ETKAS and 4.4 years in the ESP. The ratio of the number of patients waitlisted in a certain region to the number of kidneys procured in that region correlated with waiting time in ETKAS (R^2 0.70). In the ESP, the ratio of the number of patients listed in a subregion to the number of subregionally procured and transplanted kidneys also correlated with waiting time, albeit to a lower degree (R^2 0.62). **Conclusion:** In Germany, waiting time is profoundly influenced by where a patient is listed for KTX. These results question the equity of the current allocation algorithms.

FV35

Adjusted Donor Age Score als Tool zur Charakterisierung von Verstorbenspendernieren: Validierung für das Heidelberger Eurotransplant Kollektiv

C. F. Mahler¹; F. Friedl¹; D. Ashby¹; C. Nußbag²; C. Speer¹; L. Benning¹; D. Göth¹; M. Schaier¹; M. Mieth³; A. Mehrabi³; M. Zeier¹; C. Morath¹; F. Kälble

Medizinische Klinik I, Sektion Nephrologie, Medizinische Fakultät, Ruprecht-Karls-Universität Heidelberg, Heidelberg; ¹ Hammersmith Hospital, Imperial College London, London/UK; ² Gastroenterologie, Infektionskrankheiten, Vergiftungen, Klinik für Innere Medizin



FV35: Abb. 1

IV, Universitätsklinikum Heidelberg, Heidelberg; ³ Klinik für Allgemein-, Viszeral- und Transplantationschirurgie, Medizinische Fakultät, Ruprecht-Karls-Universität Heidelberg, Heidelberg

Hintergrund: Bestehende Scores zur Charakterisierung von Spendernieren wie KDRI oder KDPI (Kidney Donor Risk Index/Kidney Donor Profile Index) sind für die multimorbide Spenderpopulation von eingeschränkter Aussagekraft und für Patienten schwer verständlich. Um diese Probleme zu adressieren, wurde in Großbritannien der Adjusted Donor Age (ADA)-Score entwickelt. Dieser moduliert das Spenderalter anhand von Risikofaktoren und teilt das Spenderrisiko in Quintilen ein (A-C günstig, D moderat, E ungünstig). Ziel der vorliegenden Studie ist es, den ADA-Score erstmals an einem deutschen Eurotransplant Zentrum zu validieren und unserer Organannahme-Strategie gegenüberzustellen.

Methode: Es erfolgte die retrospektive Erfassung aller Nierentransplantationen nach Verstorbenspende an unserem Zentrum zwischen 2019 und 2021. Die

Spender-assoziierten Risikofaktoren wurden anhand der Eurotransplantdaten erhoben und darauf basierend der ADA berechnet. Die Prognosegüte wurde anhand der Transplantatfunktion nach drei Monaten analysiert.

Ergebnisse: Von 463 Organangeboten von 409 Spendern im Alter von 14–94 Jahren wurden 173 akzeptiert und transplantiert. Nach drei Monaten lag die eGFR bei 84 % der Empfänger über 30 ml/min/1,75 m². In 8 % der Fälle kam es zu einem Transplantatversagen. Eine höhere ADA-Quintile war mit einem schlechteren Transplantationsergebnis verbunden (Drei-Monats-eGFR < 30 ml/min bei 0, 3, 13, 21 und 46 % der Patienten, $p < 0.003$, chi-square test). Für Patienten mit guter Transplantatfunktion war die Drei-Monats-eGFR deutlich mit dem *adjusted donor age* assoziiert ($R = 0,56$, $p < 0.001$) und nahm mit höherer ADA-Quintile ab (64, 60, 49, 37 und 28 ml/min respektive)

Zusammenfassung: ADA ist ein geeigneter Score zur Charakterisierung von Verstorbenspendernieren vor Transplantation. In unserem Spenderkollektiv zeigte sich eine

gute Prognosegüte für die Transplantatfunktion nach drei Monaten. Obwohl Organe mit ADA > 80 Jahren ein erhöhtes Risiko für Transplantatversagen aufweisen, weisen > 50 % der Patienten in dieser Gruppe eine exzellente Transplantatfunktion auf. Ziel weiterer Untersuchungen wird sein, diese Gruppe besser zu differenzieren und so den ADA-Score an die spezifischen Eigenschaften des Eurotransplant-Spenderpools anzupassen.

Basic Science – Hypertonie

FV36

High potassium intake aggravates cardiovascular damage accompanied by premature senescence in hypertensive apolipoproteinE-KO mice under high salt diet

D. Arifaj; A. Lang¹; M. Yakoub; M. Rahman; L. Hering; S. Temme; L. C. Rump; N. Gerdes¹; J. Stegbauer
Klinik für Nephrologie, Universitätsklinikum, Heinrich-Heine-Universität Düsseldorf, Düsseldorf; ¹Institut für Molekulare Kardiologie, Universitätsklinikum Düsseldorf, Heinrich-Heine-Universität Düsseldorf, Düsseldorf

Objective: Increased sodium intake aggravates cardiovascular diseases. Salt substitute containing potassium chloride improves cardiovascular outcome in hypertensive patients with high cardiovascular risk. Until now, it is not known whether the positive outcome can be accredited to potassium (K⁺) supplementation or sodium reduction. Here, we investigate the role of high K⁺ intake on the development of hypertensive cardiac damage in the presence or absence of high salt diet.

Method: 8–10 weeks old apolipoproteinE-deficient mice (apoE-KO) were fed a normal K⁺ (0,55 %) or high K⁺ (5 %) diet throughout the whole experimental period. Two weeks after diet start, apoE-KO mice were infused with angiotensin (Ang)II (500ng/kg/min) for 28 days. Hypertensive cardiac damage was assessed by MRI, immunohistochemistry, FACS analysis and quantitative PCR.

Results: High K⁺ diet increased serum K⁺ levels significantly compared to apoE-KO fed a normal K⁺ diet (5.3 ± 1.2 vs. 3.9 ± 0.4 mmol/L, $p < 0.05$). Interestingly, high K⁺ diet did not affect blood pressure or cardiac function in apoE-KO mice chronically infused with AngII. As expected, aldosterone excretion was increased in AngII infused apoE-KO mice fed a high K⁺ diet compared to a normal K⁺ diet (132 ± 20 vs 8 ± 18 ng/24 h, $p < 0.01$). To evaluate the consequence of K⁺ mediated aldosterone secretion for hypertensive cardiovascular damage, we additionally treated our high K⁺ group with high salt diet (1 % NaCl) in the drinking water throughout the experiment. High K⁺ induced aldosterone production in the presence of high NaCl intake aggravated hypertensive cardiac damage characterized by significantly higher left ventricular mass, more cardiac fibrosis and inflammation as well as lower ejection fraction compared to mice fed a high K⁺ or a high NaCl diet solely. Furthermore, the simultaneous intake of high K⁺/NaCl diet, induced higher mitochondrial ROS production in cardiac endothelial cells compared to high K⁺ or

high NaCl diet alone. As a consequence, cellular senescence markers such as p16 and p21 were significantly higher in apoE-KO mice fed a high K⁺/NaCl diet. Of note, co-treatment with spironolactone (50 mg/kg/day), significantly attenuated cardiovascular damage and cellular senescence in mice fed a high K⁺/NaCl diet.

Conclusion: High K⁺ diet compared to normal K⁺ diet does not have a beneficial effect on hypertensive cardiac damage in apoE-KO mice. Moreover, the present study indicates that potassium-induced aldosterone production aggravates the detrimental effect of high salt intake on cardiac health in hypertension by influencing cardiac senescence.

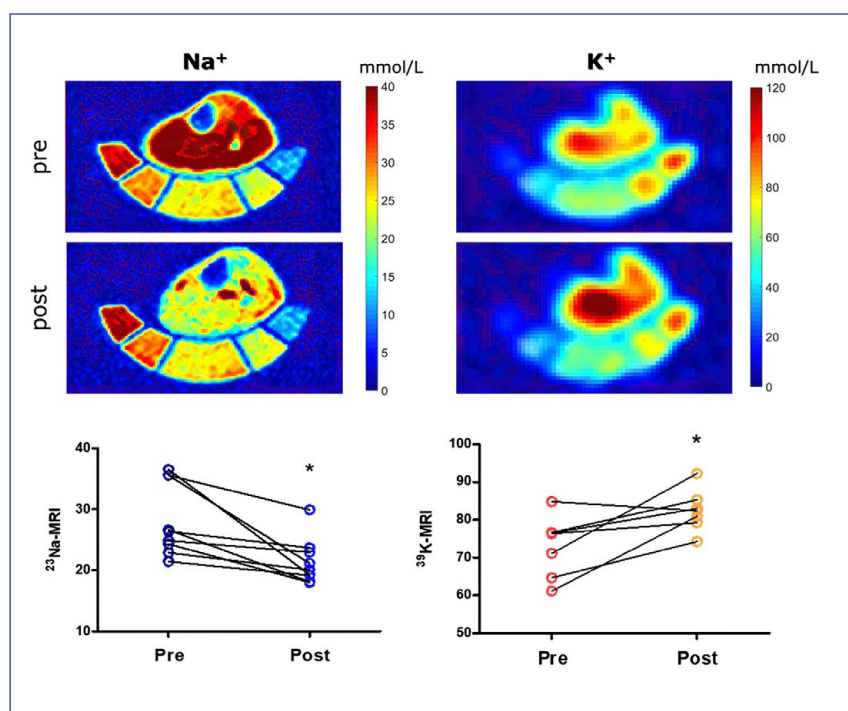
FV37

Tissue Potassium Depletion in Patients with Primary Hyperaldosteronism detected by 39K-Magnetic Resonance Imaging

C. Kopp; A. Dahlmann; P. Linz¹; L. Gast¹; M. Uder¹; M. Schiffer; A. Nagel¹

Medizinische Klinik 4, Nephrologie und Hypertensiologie, Universitätsklinikum, Friedrich-Alexander-Universität Erlangen-Nürnberg, Erlangen; ¹Institut für Radiologie, Universitätsklinikum, Friedrich-Alexander-Universität Erlangen-Nürnberg, Erlangen

Objective: Although 98 % percent of K⁺ is located intracellularly, current clinical diagnostics solely rely on assessment of extracellular K⁺ concentration. Recently, technical advances in magnetic resonance imaging (MRI) enabled non-invasive analysis of tissue K⁺ homeostasis in vivo. In animal models of mineralocorticoid



FV37: Abb. 1

excess, intracellular Na⁺/K⁺-exchange could be identified in skeletal muscle by invasive methods such as chemical analysis. We hypothesized that primary hyperaldosteronism results in K⁺ depletion of skeletal muscle in humans and can be visualized by ³⁹K MRI.

Method: We conducted a prospective, observational study in 9 patients with the confirmed diagnosis of primary hyperaldosteronism. Muscle K⁺ and Na⁺ were directly assessed by a 7 Tesla magnetic resonance imaging system and a ³⁹K/²³Na volume coil before treatment (either removal of an adrenal adenoma or administration of a mineralocorticoid-antagonist) and three months after initiation of treatment. Additionally, blood pressure, bioimpedance measurements and blood as well as urine samples were obtained.

Results: In patients with primary hyperaldosteronism a high muscle Na⁺ concentration could be detected (28.2 ± 6.0 mmol/l, n = 9), which decreased to 21.6 ± 3.7 mmol/l ($p < 0.05$) after successful treatment, consistent with former ²³Na MRI investigations in these patients. In contrast, muscle K⁺ was found to be reduced to a concentration of 73.1 ± 8.1 mmol/l (n = 7) and increased upon treatment to 82.5 ± 5.5 mmol/l, $p < 0.05$. These tissue electrolyte shifts could not be explained by changes in serum electrolyte concentration (Na⁺ 142 ± 3 vs. 140 ± 2 mmol/l; K⁺ 3.2 ± 0.4 vs. 4.1 ± 0.5 mmol/l).

Conclusion: In our work, we detected K⁺ depletion in hyperaldosteronism for the first time in humans, which could be reversed upon successful treatment. Thus,

skeletal muscle seems to represent a variable intracellular K⁺ reservoir. ³⁹K MRI might evolve as a novel tool to assess previously unrecognized tissue K⁺ alterations in various electrolyte disorders.

PD/Heimdialyse

FV38

Matched-Control Study on off-label DOAC therapy and other anti-thrombotic therapies for atrial fibrillation in HD-patients based on DN-Network data

K. A. Brensing; H. Omran¹; H. Reichel²; F.-P. Tillmann³; J. Duttlinger³

Dialyse-Abteilung, Nierenzentrum Bonn-Bad Godesberg, Bonn; ¹ Medizinische Klinik, Kardiologie, St. Marienhospital, Bonn; ² Nephrologisches Zentrum Villingen-Schwenningen, Villingen-Schwenningen; ³ WiNe Wissenschaftliches Institut für Nephrologie, Verband Deutsche Nierenzentren e. V., Düsseldorf

Objective: Hemodialysis patients (HD-pts) with atrial fibrillation (AF) are at high risk for cardiovascular events, major bleeds and rapid vascular/valvular calcification. Benefit of vitamin-K based oral anticoagulation (VK-OAC) or direct-acting OAC drugs (DOACs) is debated for missing prospective trials and off-label of DOACs in HD-pts. We studied DOACs and other anti-thrombotic therapies in a larger HD-cohort.

Method: We analyzed pseudonymized benchmark data of the dialysis center network (Verband Deutsche Nierenzentren, DN). Diagnoses were coded by "International Classification of Diseases (ICD)" and "Anatomical Therapeutic Chemical (ATC)" drug code. De-novo events were analysed (2019-2021).

Results: In 2019, 2477 (19 %) of 12903 HD-pts had coded AF. Baseline CHA2DS2-VASc (4,2/1,5 Mean/SD) and HAS-BLED (3.4/0.9) risk-scores indicated high risk for adverse events. Charlson Comorbidity Index (= CCI) was high (8,7/2.8) and median observation time was 2.2 yrs (Range: 0.1–3 yrs.). Beside HD-related heparin five main approaches were applied: No active therapy, VK-OAC, DOAC, heparin-based therapy (Heparin) or 1–2 anti-thrombocyte drugs (Aspirin/Clopidogrel = Asp/Clop). 632 pts (25 %) changed therapy, but 1845 pts (75 %) had unchanged therapy and were used for outcome analysis. Risk-scores overestimated de-novo events: Total 3-yr events were rare (4.7 %) and similar for all therapies, especially for cerebral ischemic events (2.1 %, range 1.5–2.4; NS). Pts on any anti-thrombotic therapy had similar overall events as without active therapy (2.2 vs. 3.2 %) including cerebral adverse events (ischemic: 1.9 vs. 1.3 %; bleeds: 0.3 vs. 0.3 %; NS). Kaplan-Meier survival was analyzed by matched controls (adjusted risk-factors: age/HR 1.05, female/HR 0.78, CCI/HR 1.07, albumin/HR 0.93). Total 3-yr mortality was high (46 %). Median survival on heparin-therapy (1.8 yrs) was significantly lower than on Asp/Clop (2.5 yrs; $p < 0.05$) or VK-OAC (2.5 yrs; $p < 0.001$) but similar to no active therapy (2.0 yrs). DOAC pts ($n = 66$; 4 % of cohort) had highest 3-yr survival rate (55 %), but matched data showed no survival benefit to other (active/no active) therapies (NS).

Conclusion: Our large study showed that CHA2DS2-VASc and HAS-BLED scores were not predictive in HD-pts with AF. Cerebral

ischemic events were rare (0.6 %/yr) and similar for all therapies suggesting benefit of regular HD heparin-supply. Asp/Clop results in same survival as VK-OAC but with less bleeding and same cerebral events, thus HD-pts with AF can be treated safely with Asp/Clop and avoid VK-OAC. Current DOAC data revealed no safety concern and no benefit regarding events and survival.

FV39

Uremia modulates endothelial expression of vasculoprotective Krüppel-like factor 2 (KLF2) through an activator protein 1 (AP1) dependent transcriptional mechanism

H. Zhao; D. Wu; K. Budde¹; J. Witowski²; D. Zickler; R. A. Catar
Medizinische Klinik mit Schwerpunkt Internistische Intensivmedizin und Nephrologie, Campus Virchow-Klinikum, Charité – Universitätsmedizin Berlin, Berlin; ¹ Medizinische Klinik mit Schwerpunkt Nephrologie und Internistische Intensivmedizin, Campus Charité Mitte, Charité – Universitätsmedizin Berlin, Berlin; ² Department of Pathophysiology, Poznan University of Medical Sciences, Poznan/PL

Objective: Endothelial dysfunction is a major complication in uremic patients undergoing hemodialysis (HD). Krüppel-like factor 2 (KLF2) is crucially involved in the maintenance of vascular homeostasis and protection against atherosclerosis. Here, we assessed the detrimental effect of uremia on KLF2 expression and its transcriptional regulation by vascular endothelial cells (ECs).

Method: 40 patients were enrolled in a randomized controlled clinical

trial. To test for relevant inflammation markers PCR array was used. Cytokines release was determined by ELISA. ERK and AKT pathways were measured by western blot. ERK-AP-1 mediating KLF2 regulation was measured by promoter assay and EMSA. Inhibitory studies with AP1 and ERK blockers were used as final prove.

Results: Uremic serum (US) was collected from 14 patients treated with HD and respective healthy serum (HS) was obtained from 14 matched healthy control individuals. The addition of US but not HS to ECs in our *in vitro* model resulted in a time- and dose-dependent decrease in KLF2 mRNA expression (64 ± 6 % reduction after 24-h exposure to 5 % US), which was associated with a concomitant reduced activity of the KLF2 gene promoter region. Progressive promoter 5'-deletions and electro-mobility-shift-assays revealed that the inhibitory effect of US was mediated by the transcription factor AP-1/c-FOS and identified the promoter region responsible for its binding. Accordingly, the pharmacological blockade of AP-1 abolished the inhibitory effect of US on KLF2 promoter activity and KLF2 mRNA expression. To see if these changes had functional significance, IL-8 mRNA expression in ECs was assessed. Compared to ECs treated with HS, cells exposed to US expressed 3 ± 0.21 -fold more IL-8 mRNA. This increase could be reduced either by treating cells with an AP-1 inhibitor or by overexpressing KLF2 with an appropriate plasmid. Finally, ECs were exposed pairwise to sera obtained from 40 clinical study patients

undergoing HD, which used alternately standard high-flux (HF) dialyzers and novel medium cut-off (MCO) membranes (PERCI-I and PERC-I clinical.trials.gov registered studies). ECs treated with MCO sera expressed significantly more KLF2 mRNA compared to when exposed to HF sera ($p < 0.05$). Further, *in vivo* validation studies in patient derived tissue biopsies are currently ongoing.

Conclusion: Uremia decreases the expression of KLF2 in ECs through a mechanism that involves transcription factor AP-1 and contributes to increased IL-8 expression by ECs. Reduction in endothelial KLF2 expression is less pronounced during HD with MCO dialyzers.

POSTER

Akutes Nierenversagen

P001

Combined single nuclei RNA and ATAC-sequencing reveal long-term effects of adaptive and maladaptive repair after acute kidney injury

L. Gerhardt; K. Koppitch; S. Cho;
A. McMahon

Department of Stem Cell Biology and
Regenerative Medicine, University of
Southern California, Los Angeles/USA

Objective: Acute kidney injury (AKI) triggers a proliferative response as part of the intrinsic repair program that can result in adaptive or maladaptive repair of proximal tubule cells (PTCs). Maladaptive PTCs contribute to disease progression from AKI to chronic kidney disease (CKD), but the cellular and molecular understanding underlying the adaptive and maladaptive repair trajectories is limited.

Method: We used genetic fate-mapping to label and trace proliferating (*Ki67*⁺) cells after ischemia-reperfusion injury. Combined snRNA- and ATAC-seq of lineage-traced cells isolated by FACS at 4 weeks and 6 months after AKI and controls was performed to generate a final dataset of 83,315 high-quality nuclei (after quality control and doublet removal). Published snRNA-seq data was used to assess transcriptomic changes early after AKI.

Results: Labeling *Ki67*⁺ cells early after AKI revealed a broad proliferative response in kidney epithelial and non-epithelial cells, which was preceded by cell type-specific and global gene expression changes, such as downregulation of genes involved in transmembrane transport processes and

upregulation of immediate early response genes. A heterogeneous population of maladaptive PTCs derived from all proximal tubule segments persisted until 6 months after AKI, although decreasing in abundance in time post AKI. Combined profiling of gene expression and chromatin accessibility in the same cell showed a specific activation of the transcription factors Rbpj, Klf6, Runx1 and Creb5 as well as of members of the NF- κ B and the AP-1 family in maladaptive PTCs, accompanied by corresponding changes in target gene expression. Regulatory factors of adaptively repaired PTCs, such as Maf and Hnf4a, were downregulated in maladaptive PTCs. Comparison of adaptively repaired PTCs with control PTCs suggested long-term effects of AKI on the transcriptional state of PTCs, including reduced expression of genes encoding critical transmembrane transport proteins.

Conclusion: This study provides the first combined snRNA- and snATAC-seq atlas of healthy and injured kidney tissue, defines the regulatory landscape of PTCs after adaptive and maladaptive repair and reveals long-term effects of AKI on PTCs even following adaptive repair.

P002

GSDMD is required for control of necroptotic cell death in AKI

A. Brucker; W. Tonnus; K. Flade;
J. U. Becker¹; F. Shao²; C. Hugo;
A. Linkermann

Medizinische Klinik III, Nephrologie,
Universitätsklinikum Carl Gustav
Carus, Technische Universität Dresden,
Dresden; ¹ Institut für Pathologie,
Universität zu Köln, Köln; ² National
Institute of Biological Sciences (NIBS),
Beijing/CN

Objective: Within the last decade, it has been established that necrotic rather than apoptotic cell death critically mediates acute tubular necrosis in AKI. While the involvement of necroptosis and ferroptosis has been established, the role of pyroptosis, the third major form of necrosis, remains unclear in AKI. This form of regulated necrosis requires proteolytic activation of members of the gasdermin family and is considered highly immunogenic. Thus, we aimed to investigate the role of pyroptosis and its mechanism of action in AKI.

Method: Immunohistochemistry (IHC) was utilized to detect gasdermin D (GSDMD) in kidney samples of mice after ischemia/reperfusion injury (IRI). Furthermore, gasdermin-deficient mice were investigated in IRI and cisplatin-induced AKI and cisplatin-induced AKI. Mechanistic approaches involved the isolation of renal tubules for studies on cell death propagation and standard biochemistry to detect protein expression kinetics. Finally, MLKL/GSDMD^{dko} mice were generated to investigate the interplay of these caspase-dependent forms of regulated necrosis in AKI.

Results: In GSDMD-IHC of kidney samples after IRI, we detected as specific signal surrounding necrotic tubules. No such signal was detectable within the tubular compartment at any time. Unexpectedly, GSDMD^{dko} mice exhibited higher levels of serum creatinine and serum urea as well as more severe tubular damage compared to wild type controls. Unlike whole kidney lysates, freshly isolated renal tubules do not express the GSDMD protein. In isolated

renal tubules, no changes in kinetics of cell death propagation were detectable upon genetic GSDMD deficiency. In addition, we generated combined necroptosis/pyroptosis-deficient MLKL/GSDMD^{dko} mice. Here, we demonstrate that co-deletion of MLKL rescued the sensitization of GSDMD^{dko} mice. Comparable effects were seen in cisplatin-induced AKI.

Conclusion: Our study reveals an unexpected protective role of GSDMD in AKI. Our mechanistic studies indicate the effect of GSDMD to function outside the tubular compartment, specifically surrounding areas of tubular necrosis. This infiltrate appears to limit tubular necroptosis in a non-cell autonomous manner. Alongside with these mechanistic insights, our data urge caution when inhibition of pyroptosis is therapeutically considered.

P003

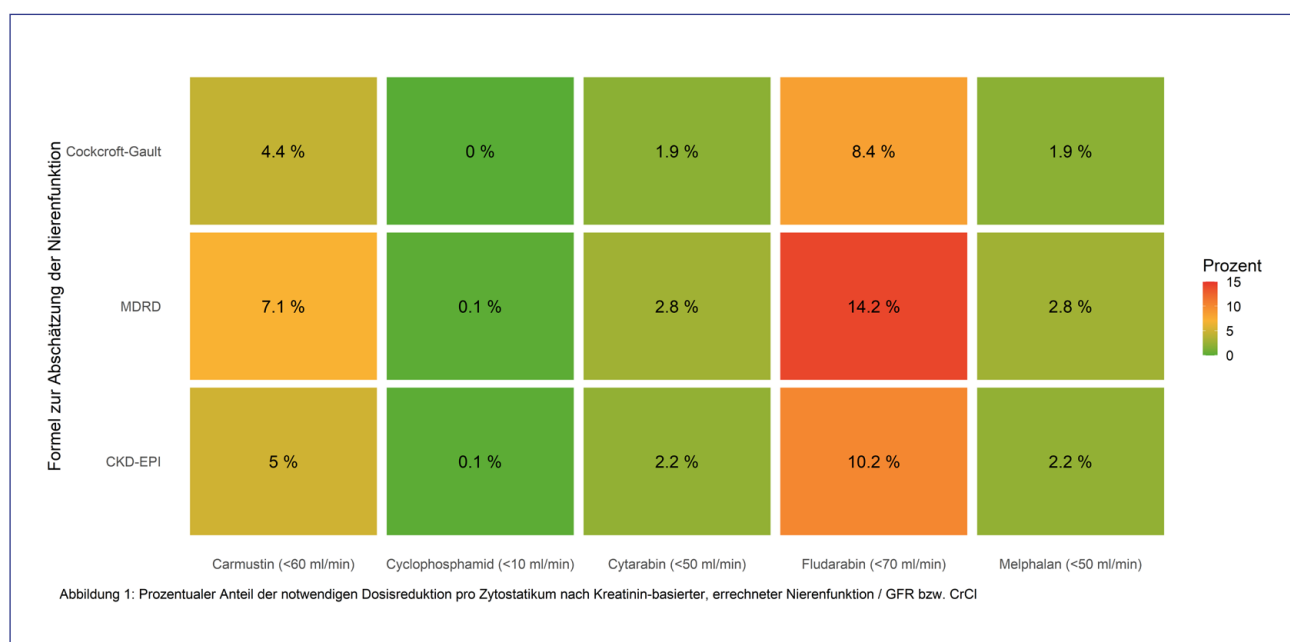
Ein Serumkreatinin – verschiedene Chemotherapeutika-Dosierungen: Formeln zur Abschätzung der Nierenfunktion haben Einfluss auf die Intensität der Konditionierung (N = 959)

L.-M. Heinze; N. Brüder; S. R. Talbot¹; E. Dammann; S. Köhler²; A. Ganser; M. Eder; M. Heuser; J. T. Kielstein³; G. Beutel

Abteilung für Hämatologie, Hämostaseologie, Onkologie und Stammzelltransplantation, Zentrum für Innere Medizin, Medizinische Hochschule Hannover, Hannover; ¹Institut für Versuchstierkunde und Zentrales Tierlaboratorium, Medizinische Hochschule Hannover, Hannover; ²Enterprise Clinical Research Data Warehouse, Medizinische Hochschule Hannover, Hannover; ³Nephrologie | Rheumatologie | Blutreinigungsverfahren, Medizinische Klinik V, Städtisches Klinikum Braunschweig, Braunschweig

Hintergrund: Die allogene Stammzelltransplantation (SZT) ist für Hochrisiko-Patient:innen mit hämatologischen Erkrankungen häufig die einzig kurative Therapie. Die Konditionierungstherapie der SZT basiert überwiegend auf dem Einsatz klassischer Zytostatika. Bei eingeschränkter Nierenfunktion ist in Abhängigkeit der verwendeten Zytostatika eine Dosisreduktion notwendig. Ziel unserer Untersuchung ist es, verschiedene Formeln zur Abschätzung der Nierenfunktion – Kreatininclearance (CrCl) und geschätzte glomeruläre Filtrationsrate (eGFR) – und die resultierende Dosisreduktion der Chemotherapeutika zu vergleichen.

Methode: Zwischen dem 01.01.2003 und dem 31.12.2020 wurden an unserem Zentrum 1.394 allogene SZT durchgeführt. Bei 959 Patienten konnten die klinischen Daten mit



P003: Abb. 1

Serum-Kreatininwerten (N = 92.229) aus dem Data Warehouse angereichert werden. Auf Basis der i) Cockcroft-Gault-ii) MDRD- und iii) CKD-EPI-Formel erfolgte vor Beginn der Konditionierungstherapie die Bestimmung der CrCl bzw. eGFR. Für einen Vergleich wurde jeweils die CrCl/eGFR aus den zur Baseline vorliegenden Kreatininwerten ermittelt und gemäß KDIGO Stadium G1 bis G5 klassifiziert. Anhand aktueller Dosierungsempfehlungen wurde basierend auf den verschiedenen Methoden zur Abschätzung der CrCl/eGFR die erforderliche Dosisreduktion für jedes Zytostatikum berechnet.

Ergebnisse: CrCl/eGFR zeigen je nach verwendeter Formel unterschiedliche Ergebnisse. Der Anteil an Patienten mit reduzierter GFR < 60 ml/min lag vor Beginn der Konditionierungstherapie mit Cockcroft-Gault bei 4,4 %, mit MDRD bei 7,1 % und mit CKD-EPI bei 5,0 %. Die Notwendigkeit zur Dosisreduktion der Zytostatika variierte zwischen 0,1 % für Cyclophosphamid und 5,8 % für Fludarabin. Beispielhaft beruht die Dosierungsempfehlung von Fludarabin laut Fachinformation auf der Bestimmung der CrCl und würde in 8,4 % der Fälle dosisreduziert werden müssen. Nach MDRD läge der Prozentsatz bei 14,2 % und somit um 5,8 % höher. Generell zeigt sich, dass die nach Cockcroft-Gault berechnete CrCl in nur wenigen Fällen zu einer Dosisreduktion der Zytostatika führt, die MDRD-Formel hingegen den höchsten Prozentsatz einer Dosisreduktion erforderlich macht (Abb. 1).

Zusammenfassung: Die Dosierung vieler Zytostatika erfolgt nach Cockcroft-Gault. Diese sonst nicht mehr in der Klinik verwendete Formel

schätzt die Nierenfunktion deutlich besser als die CKD-EPI- und die MDRD-Formel. Für die Optimierung von Therapieerfolg und Toxizität ist eine korrekte und schnelle Bestimmung der Nierenfunktion erforderlich, welche durch die aktuell verwendeten Formeln erschwert wird.

P004

Preoperative Fasting Time as a Risk Factor for Development of Acute Kidney Injury after Elective Cardiac Surgery – a Pilot Study

M. Schanz; N. Schmid¹; T. Oberacker²; N. Göbel³; U. Franke³; M. D. Alscher; S. Schricker; M. Ketteler
Abteilung für Allgemeine Innere Medizin und Nephrologie, Robert-Bosch-Krankenhaus, Stuttgart; ¹Medizinische Informatik/Biostatistik, Robert-Bosch-Krankenhaus, Stuttgart; ²Dr. Margarete Fischer-Bosch-Institut für Klinische Pharmakologie, Robert-Bosch-Krankenhaus, Stuttgart; ³Abteilung für Herz- und Gefäßchirurgie, Robert-Bosch-Krankenhaus, Stuttgart

Objective: Acute kidney injury (AKI) is associated with high morbidity and mortality, therefore prevention is important. The aim of this study was to systematically assess AKI incidence after elective cardiac surgery depending on the preoperative fasting time.

Method: This retrospective single-center study included n = 89 patients who underwent elective cardiac surgery with cardiopulmonary bypass. All patients scheduled for surgery the next day stop eating and drinking at midnight, irrespective the time of surgery. Patients who underwent surgery in the 2nd half of the day were assigned to the late group, cutoff time 11 a. m. (n = 45). AKI was classified

according to the full definition of Kidney Disease: Improving Global Outcomes (KDIGO), including urinary output, and recorded within 72 hours after cardiac surgery.

Results: In our cohort overall AKI incidence was 50.5 % (45/89) within 72 hours. Relevant baseline parameters were similar between early and late group (Table 1). Interestingly, total AKI and stage 1 AKI incidence was significant (p = 0.03) higher in the late group (62.2 %) compared to the early group (38.6 %). Logistic regression analysis confirmed significant impact (p = 0.02) of preoperative fasting time on AKI incidence. No evidence of relevant confounding factors was detected (Table 2). The significant influence of body mass index on AKI incidence (p = 0.009) is expected, since obesity is a known risk factor.

Conclusion: For the first time, this pilot study provides evidence that preoperative fasting time may be a potential risk factor for the development of AKI after elective cardiac surgery. In clinical routine, this could highlight the relevance of preoperative measures to prevent postoperative AKI.

P005

Dexamethason senkt die Ferroptose-Schwelle durch Glukokortikoidrezeptor abhängige Dipeptidase-1 Expression und Glutathion Depletion

W. Tonnus; A. von Mäßenhausen; N. Zamora Gonzalez; F. Maremonti; A. Belavgeni; C. Meyer; K. Beer; P. Hoppenz; C. Hugo; A. Linkermann
Medizinische Klinik III, Nephrologie, Universitätsklinikum Carl Gustav Carus, Technische Universität Dresden, Dresden

Hintergrund: Dexamethason ist ein synthetisches Glukokortikoid, welches für viele Indikationen eingesetzt wird, der Einsatz ist jedoch durch zahlreiche dosisabhängige Nebenwirkungen limitiert. Ferroptose ist eine eisenkatalysierte Form der regulierten Nekrose, die u. a. im akuten Nierenversagen eine wichtige Rolle spielt. Bei der Ferroptose kommt es zur vermehrte Oxidation von membranären Phospholipiden was letztendlich zu einem Einreißen der Zellmembran führt. In dieser Arbeit sollte untersucht werden, auf welche Weise dexamethason die Ferroptose reguliert.

Methode: In Zellkultur wurde der Einfluss der Vorbehandlung unterschiedlicher Steroidhormone auf regulierten Zelltod wurde via FACS untersucht. Standardmethoden der Biochemie wurden für die mechanistische Aufarbeitung verwendet, der Glutathiongehalt der Zellen wurde via Massenspektrometrie untersucht. Weiterhin wurden murine Nierentubuli aufgereinigt und die Kinetik von Zelltod nach Behandlung mit Dexamethason untersucht.

Ergebnisse: Die Vorbehandlung mit Dexamethason *in vitro* führte zu einer erhöhten Sensitivität für Ferroptose unter Depletion von GSH; dieser Effekt war nicht nach Vorbehandlung mit dem Mineralokortikoid Aldosteron oder Dehydroepiandrosteron nachweisbar. Mechanistisch zeigte sich, dass die Sensitivierung für Ferroptose mit Steroidrezeptor-abhängigen Depletierung von GSH einherging. Während Dexamethason keinen Einfluss auf die Expression Ferroptose-regulieren der Proteine hatte, konnten wir mit Hilfe von mRNA-Sequenzierung eine erhöhte Expression des Glutathion-metabolisierenden Proteins

Dipeptidase-1 (DPEP1) nach Dexamethason-behandlung identifizieren. Dies konnten wir auf Proteinebene bestätigen. In Übereinstimmung mit diesen Daten revertierte der Knockdown von DPEP1 die erhöhte Ferroptosesensitivität nach Dexamethasonbehandlung. Auch in frisch isolierten murinen Nierentubuli führte die Behandlung mit Dexamethason zur vermehrten Tubulusnekrose, die durch Ferroptoseinhibition, den DPEP1-Inhibitor Cilastatin oder den Knockout von DPEP1 revertiert werden konnte.

Zusammenfassung: Zusammenfassend wurde gezeigt, dass Dexamethason gegenüber Ferroptose sensitiviert und dies durch eine Glukokortikoidrezeptor-abhängige erhöhte Expression von DPEP1 und Glutathion-Depletion zustande kommt. Dieser neue Mechanismus hat sowohl klinische als auch therapeutische Implikationen. Er könnte von Dexamethason hervorgerufenen Nebenwirkungen erklären und identifiziert DPEP1 als therapeutische Zielstruktur.

P006

How does acute kidney injury affect metabolic compensation of respiratory acidosis in patients with acute exacerbation of COPD in the intensive care unit. A retrospective study.

K. Göttfried; F. Marcy; T. Schröder; P. Enghard¹

Medizinische Klinik mit Schwerpunkt Internistische Intensivmedizin und Nephrologie, Campus Virchow-Klinikum, Charité – Universitätsmedizin Berlin, Berlin; ¹ Medizinische Klinik mit Schwerpunkt Nephrologie und Internistische Intensivmedizin, Campus Charité Mitte, Charité – Universitätsmedizin Berlin, Berlin

Objective: Chronic Obstructive Pulmonary Disease (COPD) is the third leading cause of death worldwide. Acute exacerbation (AECOPD) can lead to severe respiratory acidosis which is associated with poor outcome and often requires treatment in an intensive care unit (ICU). Renal retention of bicarbonate is one of the main mechanisms compensating acidosis. Acute kidney injury (AKI) is a common complication in ICU-patients and can affect the metabolic compensation mechanisms of acid-base-disorders. The aim of this analysis was to objectify the influence of AKI on metabolic compensation of respiratory acidosis in AECOPD and to look for predictors of poor outcome.

Method: The clinical data of 498 patients who were admitted with AECOPD to medical intensive care unit from 2009 to 2021 was retrospectively analysed. Considering KDIGO criteria the study population was divided into a group presenting an AKI (AKI) and a group with stable kidney function (NOAKI). Cox regression model was used to inspect survival adjusting for sex, age, time on ventilator and the SOFA score. Daily measurements of pH, arterial carbon dioxide partial pressure ($p_a\text{CO}_2$) and concentration of bicarbonate (HCO_3^-) were analysed within a correlation analysis with respect to the degree of kidney injury.

Results: 278 patients (55,8 %) suffered from an AKI. From those patients 139 (50 %) presented an AKI stage 3. Patients with AKI had a higher initial SOFA score (6 vs. 3), were intubated more often (53,6 vs. 13,6 %) and ventilated longer (92 vs. 14 h). They were also treated longer in the ICU (8 vs. 3 days). The

ICU mortality in the group with AKI was higher (16,2 vs. 4,5 %). The concentration of HCO_3^- (25,8 vs. 27,5 mmol/l on day 1) in relation to the p_aCO_2 (68,5 vs. 61,8 mmHg on day 1) was significantly lower in the AKI-group during their whole stay in the ICU ($\text{HCO}_3^-/\text{p}_a\text{CO}_2$ 0,38 vs. 0,45 on day 1; $p = 0,001$). The pH in this group was also lower during their whole ICU treatment (7,23 vs. 7,28 on day 1; $p = 0,001$). The concentrations of HCO_3^- in relation to the p_aCO_2 of patients with AKI stage 3 were lower than those of patients with AKI stages 1 and 2. The values of patients with AKI stages 1 and 2 were nearly similar to patients without AKI. The lowest HCO_3^- and pH and highest p_aCO_2 were found in the patients in need of acute dialysis.

Conclusion: Acute kidney injury affects metabolic compensation of respiratory acidosis in patients with acute exacerbation of COPD in ICU.

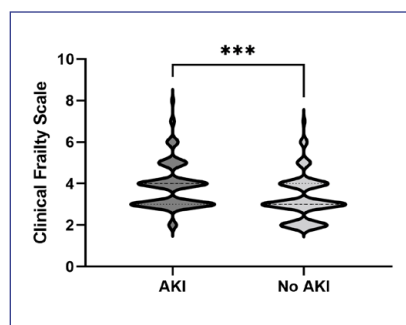
P007

Frailty as tested by the Clinical Frailty Scale is a risk factor for hepatorenal syndrome in patients with liver cirrhosis

E. M. Schleicher; W. M. Kremer; V. Kalampoka; S. J. Gairing; L. Kaps; J. M. Schattenberg; P. R. Galle; M.-A. Wörns¹; M. Nagel¹; J. Weinmann-Menke; C. Labenz

Medizinische Klinik und Poliklinik I, Universitätsklinikum, Johannes-Gutenberg-Universität Mainz, Mainz; ¹Klinik für Gastroenterologie, Hämatologie und internistische Onkologie, Endokrinologie, Klinikum Dortmund, Dortmund

Objective: Hepatorenal syndrome (HRS-AKI) is a frequent complication in patients with liver cirrhosis and is associated with a

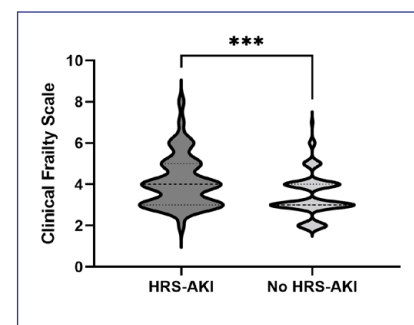


P007: Abb. 1

poor prognosis. Identifying prognostic factors regarding the development of HRS-AKI is of pivotal importance to identify patients in need of preventive measures. Frailty is common in patients with liver cirrhosis and increases the vulnerability to internal and external stressors. The aim of this study was to investigate the impact of frailty, as defined by the validated Clinical Frailty Scale (CFS), on the risk of acute kidney injury (AKI) and HRS-AKI in hospitalized patients with liver cirrhosis.

Method: We retrospectively analyzed data of 201 non-elective hospitalized patients with liver cirrhosis without higher degrees of chronic kidney disease. Data were captured within the first 24 hours of hospital admission, and frailty was assessed using the CFS. Patients were followed for the development of AKI and HRS-AKI during the hospital stay.

Results: Median CFS was 3 (IQR 3; 4) and 34 (16.9 %) patients were frail (CFS > 4); median MELD 17 (IQR 12; 24). During the hospital stay, 110 (54.7 %) and 49 (24.3 %) patients developed AKI or HRS-AKI, respectively. Patients suffering from AKI or HRS-AKI had a significantly higher CFS than patients without AKI ($p < 0.001$ each).



P007: Abb. 2

In multivariable analyses, a higher CFS was independently associated with the development of AKI (OR 1.467, 95 % CI 1.065–2.021) in the total cohort and HRS-AKI (OR 1.809, 95 % CI 1.263–2.591) in the subcohort of patients with a history of ascites. Additionally, there was a strong association between frailty and HRS-AKI (OR 3.717, 95 % CI 1.456–9.491).

Conclusion: Frailty in patients with liver cirrhosis is associated with AKI and HRS-AKI. In this context, the CFS seems to be a reliable tool to identify high-risk patients at hospital admission in whom preventive measures should be initiated.

P008

Urinary biomarkers to predict acute kidney damage and mortality in COVID-19

D. Racovitan; M. Hogeweg; A. Doevelaar; M. Seidel; B. Rohn; S. Bettag; S. Rieckmann; N. Babel; F. S. Seibert; T. H. Westhoff
Centrum für Translationale Medizin, Medizinische Klinik I, Marien Hospital Herne, Ruhr-Universität Bochum, Herne

Objective: Acute kidney injury (AKI) is a frequent condition in patients hospitalized for COVID-19. There are only few reports on the use of urinary biomarkers in

COVID-19 and no data comparing the prognostic use of individual biomarkers in the prediction of adverse outcome so far.

Method: We performed a prospective monocentric study on the value of urinary biomarkers to predict the composite endpoint of a transfer to the intensive care unit (ICU), the need for renal replacement therapy (RRT), mechanical ventilation, and in-hospital mortality. 41 patients hospitalized for COVID-19 were enrolled in this study. Urine samples were obtained shortly after admission in order to assess neutrophil gelatinase-associated lipocalin (NGAL), kidney injury molecule-1 (KIM-1), calprotectin, and vanin-1.

Results: We identified calprotectin as a predictor of a severe course of the disease, requiring intensive care treatment (AUC 0.728, $p = 0.016$). Positive and negative predictive values were 78.6 % and 76.9 %, respectively), using a cut-off concentration of 127.8 ng/ml. NGAL tended to predict COVID-19 associated AKI without reaching statistical significance (AUC 0.669, $p = 0.053$). The best parameter in the prediction of in-hospital mortality was NGAL as well (AUC 0.674, $p = 0.077$). KIM-1 and vanin-1 did not reach significance for any of the investigated endpoints.

Conclusion: While KIM-1 and vanin-1 did not provide prognostic clinical information in the context of COVID-19, the present study shows that urinary calprotectin and NGAL concentrations are independent predictors of an adverse course of the disease. Calprotectin and NGAL may thereby constitute helpful adjuncts in the identification of patients at increased

risk, who may benefit from upcoming antiviral agents to SARS-CoV-2.

P009

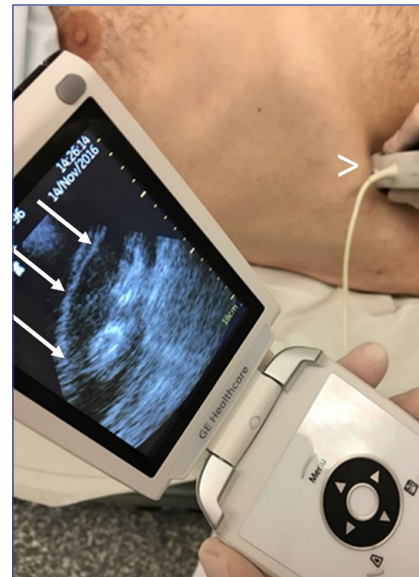
Bettseitiger Taschenultraschall in der Nephrologie

K. Hollerieth; M.-T. Vo-Cong; S. Preuß; S. Kemmner; K. Stock
II. Medizinische Klinik, Nephrologie, Klinikum rechts der Isar, Technische Universität München, München

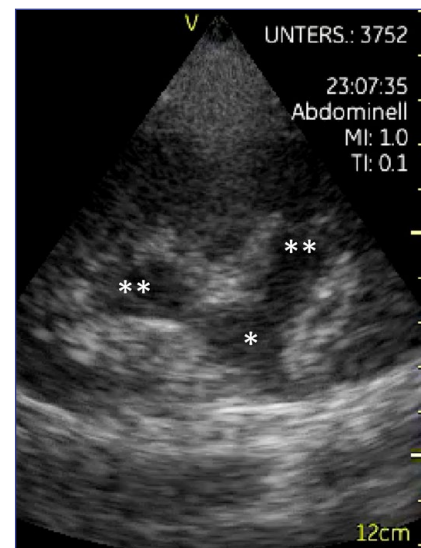
Hintergrund: Der Einsatz von Taschenultraschallgeräten in der medizinischen Diagnostik hält mehr und mehr Einzug in den klinischen Alltag. Obwohl die EF-SUMB (European Federation of Societies for Ultrasound in Medicine and Biology) ein Positionspapier über deren Nutzung veröffentlicht hat¹, lag der wissenschaftliche Fokus bisher nicht auf deren Anwendung in der nephrologischen Routine. Das Ziel unserer Arbeit war die Evaluation der bettseitigen Anwendung von Taschenultraschallgeräten im Rahmen von nephrologischen Fragestellungen.

Methode: Insgesamt 27 Untersucher (alle Ärzte mit mindestens 6 Monaten Ultraschall Erfahrung) führten 280 bettseitige Untersuchungen mittels Taschenultraschallgerät im Rahmen der klinischen Routine durch.

Ergebnisse: Die häufigsten Indikationen waren die Abklärung einer möglichen Hydronephrose (147), die sonographische Evaluation des Volumenmanagements inkl. Erfassung der Weite und Atemvariabilität der Vena cava inferior (196), der Detektion von Pleura- bzw. Perikardergüssen und Aszites (113) sowie die Beurteilung der Restharnbildung (52). In 90 % konnten spezifische klinische Fragestellungen allein



P009: Abb. 1



P009: Abb. 2

durch die Anwendung des Taschenultraschallgeräts geklärt werden.

Zusammenfassung: Taschenultraschall kann im nephrologischen Bereich für gezielte Fragestellungen oder für bettseitige Verlaufsuntersuchungen nach vorheriger Diagnose mittels High-end-Ultraschall eingesetzt werden, sowohl im stationären

als auch im ambulanten Bereich. Unter Berücksichtigung der technischen Limitationen kann die Sonographie mittels Taschenultraschallgerät in den Händen eines erfahrenen Untersuchers somit ein Zeit- und Kosten-effizientes Tool sein.²

¹ DOI: 10.1055/a-0783-2303

² DOI: 10.1007/s00345-022-04018-y

P010

Diskrepantes Verhalten zwischen der errechneten und der gemessenen glomerulären Filtrationsrate nach herzchirurgischen Eingriffen

W. Ribitsch; F. Wagner¹; A. Meinitzer²; L. Pflanzl-Knizacek¹; M. Hafner¹; S. Hatzl³; P. Eller⁴; I. Mursic⁵; W. Toller⁶; M. Schörghuber⁶; L. Queisser³; S. Zitta; G. Schilcher³
Klinische Abteilung für Nephrologie und Hämodialyse, Universitätsklinik für Innere Medizin, Medizinische Universität Graz, Graz/A; ¹ CBmed – Center for Biomarker Research in Medicine, Graz/A; ² Klinisches Institut für Medizinische und Chemische Labor Diagnostik, Medizinische Universität Graz, Graz/A; ³ Allgemeine Intensivstation, Universitätsklinik für Innere Medizin, Medizinische Universität Graz, Graz/A; ⁴ Internistische Intensivmedizin, Universitätsklinik für Innere Medizin, Medizinische Universität Graz, Graz/A; ⁵ Klinische Abteilung für Endokrinologie, Universitätsklinik für Innere Medizin, Medizinische Universität Graz, Graz/A; ⁶ Universitätsklinik für Anästhesiologie und Intensivmedizin, Medizinische Universität Graz, Graz/A

Hintergrund: Nach herzchirurgischen Eingriffen sind sowohl ein Kreatininanstieg als auch ein Kreatininabfall mit einer erhöhten Mortalität assoziiert. Das Serumkreatinin und die daraus errechnete eGFR

unterliegen jedoch zahlreichen bekannten Limitationen, die eine postoperative Einschätzung der tatsächlichen Nierenfunktion erschweren. Ziel der vorliegenden Studie war daher bei Patienten mit herzchirurgischen Eingriffen eine perioperative Evaluierung der Nierenfunktion mittels herkömmlicher Messmethoden durchzuführen und diese mit dem Goldstandard zu vergleichen.

Methode: In dieser prospektiven Observationsstudie wurden bei Patienten mit herzchirurgischen Eingriffen an der Herz-Lungen-Maschine vor, unmittelbar nach sowie 24 h nach OP die eGFR nach CKD-EPI (eGFR) bestimmt und eine Volumenadjustierung mittels Korrekturfaktor nach Morand und Myers (eGFRcorr) durchgeführt. Zu denselben Messpunkten wurden zudem eine Iohexol-Clearance (mGFR) nach der Bolusmethode (Accupaque 300mgJ/ml GE Healthcare® auf einem Hochdruckflüssigkeitschromatographen B. S. N. s. r.l®, Castelleone CR, Italien) sowie eine 6 h Kreatinin-Clearance (CrCl) bestimmt.

Ergebnisse: Es wurden 25 Patienten (5 Frauen, Alter 66 ± 10 Jahre, aortocoronarer Bypass $n = 5$, Klappenersatz $n = 20$) eingeschlossen. Die mGFR fiel von präoperativ 84 ± 17 ml/min auf 72 ± 22 ml/min ab ($p = 0,01$) und stieg 24 h nach OP wieder auf 78 ± 22 ml/min (n.s.) an. Die CrCl fiel ebenso von 84 ± 33 ml/min auf 58 ± 23 ml/min postoperativ ab ($p = 0,004$) und stieg 24 h post OP wieder auf 78 ± 43 ml/min (n.s.) an. Die eGFR stieg von 73 ± 13 ml/min postoperativ auf 88 ± 12 ml/min an ($p < 0,001$) und fiel 24 h post OP wieder auf 82 ± 18 ml (n.s.) ab. Ebenso stieg die volumenadjustierte eGFRcorr

von 73 ± 13 ml/min auf 91 ± 15 ml/min ($p = 0,01$) und fiel 24 h post OP wieder auf 76 ± 19 ml/min (n.s.) ab.

Zusammenfassung: Nach herzchirurgischen Eingriffen mit Herz-Lungen-Maschine kam es nur zu einem Abfall der gemessenen glomerulären Filtrationsrate, während sowohl die eGFR nach CKD-EPI als auch die volumenadjustierte eGFR einen Anstieg zeigten. Ein Verdünnungseffekt durch perioperative Volumengabe lag somit nicht vor. Die Daten unterstreichen die Unzuverlässigkeit der Kreatinin-basierten eGFR-Bestimmung im postoperativen Setting und haben Implikationen für die Diagnostik des postoperativen akuten Nierenversagens. Der in der Literatur beschriebene negative Effekt eines postoperativen Kreatininabfalls auf die Prognose von Patienten ist ebenso zu hinterfragen.

Diabetes

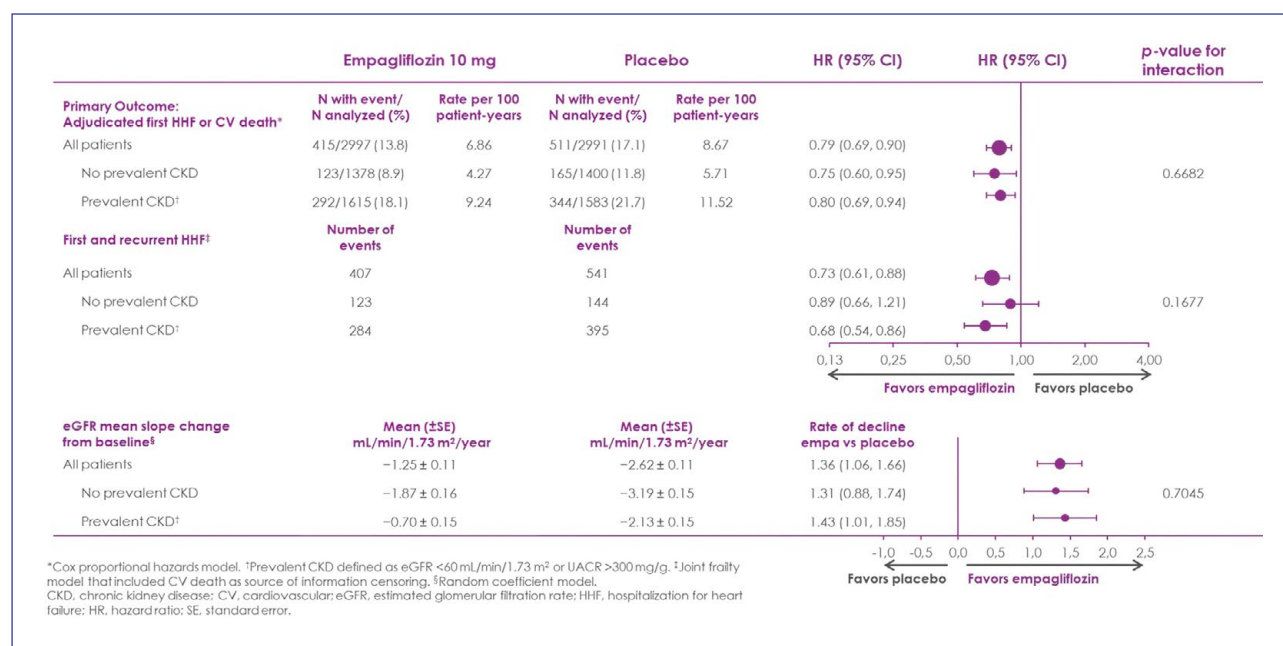
P011

EMPEROR-Preserved: Empagliflozin and Outcomes in Heart Failure with a preserved ejection fraction and Chronic Kidney Disease

C. Wanner on behalf of the EMPEROR Study Group

Medizinische Klinik und Poliklinik I, Abteilung für Nephrologie, Universitätsklinikum, Julius-Maximilians-Universität Würzburg, Würzburg

Objective: In EMPEROR-Preserved, empagliflozin reduced cardiovascular death and heart failure hospitalizations and slowed the progressive decline in glomerular function in heart failure and a preserved ejection fraction (HFpEF), with or without diabetes. We explored the effect of empagliflozin on cardiovascular



P011: Abb. 1

and kidney endpoints, across the spectrum of kidney function.

Method: 5988 patients were randomized, of whom 3198 (53 %) had prevalent chronic kidney disease (CKD) (eGFR < 60 ml/min/1.73 m² or an

UACR > 300 mg/g). The key outcomes were (1) a composite of cardiovascular death or hospitalization for heart failure; (2) total hospitalizations for heart failure, and (3) eGFR slope. The median follow-up was 26 months.

Results: Patients with prevalent CKD had a higher rate of CV and kidney events. Overall, empagliflozin reduced the risk of cardiovascular death and hospitalization for heart failure by 21 % ($p < 0.001$), reduced total hospitalizations for heart failure by 27 % ($p < 0.001$) and significantly slowed the yearly decline in eGFR (Difference: 1.36 mL/min/1.73 m² per year, $p < 0.001$). In this present CKD subgroup analysis,

all three benefits were seen consistently in patients with and without CKD (figure) and were apparent even in patients with severe impairment (eGFR from 20 to 30 ml/min/1.73 m²). Empagliflozin was well tolerated regardless of the level of baseline kidney function.

Conclusion: In patients with HFpEF, empagliflozin reduced serious heart failure events and slowed the decline in glomerular function, regardless of the presence or absence of CKD and across a broad spectrum of baseline kidney function.

P012

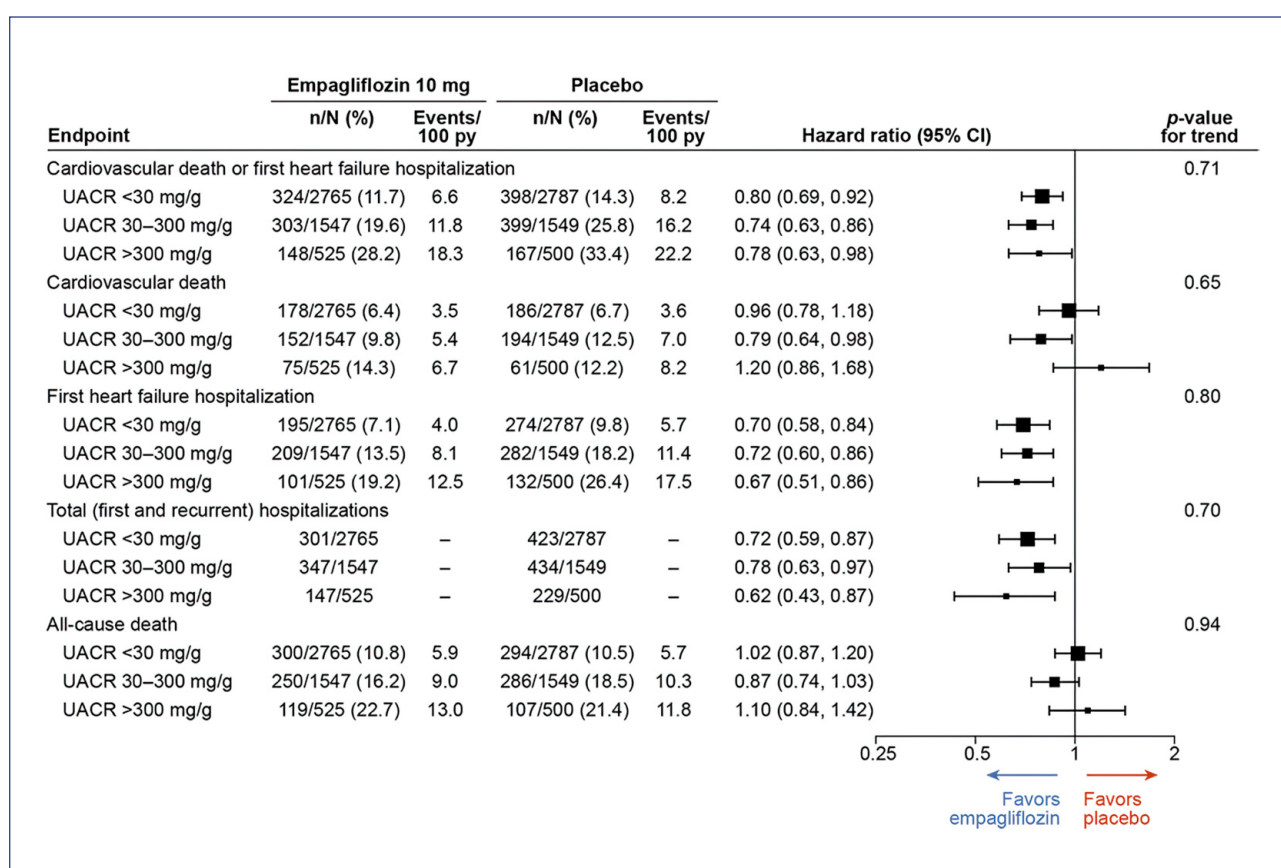
Albuminuria in Heart Failure and the Effect of Empagliflozin: an analysis from EMPEROR-Pooled

C. Wanner on behalf of the EMPEROR Study Group

Medizinische Klinik und Poliklinik I, Abteilung für Nephrologie, Universitätsklinikum, Julius-Maximilians-Universität Würzburg, Würzburg

Objective: Albuminuria, routinely assessed as spot urine albumin-to-creatinine ratio (UACR), indicates structural damage of the glomerular filtration barrier and is associated with worse renal and cardiovascular outcomes. SGLT2 inhibitors reduce UACR in patients with type 2 diabetes (T2D), but the effect in patients with heart failure (HF) is less well studied. To analyze the effect of empagliflozin on the study outcomes across the baseline levels of albuminuria and study the effect of empagliflozin on albuminuria in patients with HF across a wide range of ejection fractions.

Method: EMPEROR-Pooled combined individual patient data from EMPEROR-Reduced and EMPEROR-Preserved. Patients were randomized to either empagliflozin or placebo. Cox models were used to study the effect of empagliflozin on macroalbuminuria and on the study outcomes across albuminuria levels.



P012: Abb. 1

Results: A total of 9673 patients were included. Compared to patients with UACR < 30 mg/g (normoalbuminuria, n = 5552), those with UACR > 300 mg/g (macroalbuminuria, n = 1025) were younger, more frequently non-White, obese, men, with T2D and had higher levels of NT-proBNP, lower eGFR and less frequent use of ACEi/ARBs and MRAs. An increase in events was observed with higher UACR levels. The effect of empagliflozin was consistent across UACR categories (interaction > 0.05 for all studied outcomes, Figure 1). Among the 8648 patients without macroalbuminuria (UACR ≤ 300 mg/g) at baseline, treatment

with empagliflozin reduced the incidence of new macroalbuminuria: 5.7 vs. 7.1 events per 100 person-years, HR 0.81, 95 %CI 0.70–0.94, P = 0.005. Among the 1025 patients with macroalbuminuria at baseline, treatment with empagliflozin increased the rate of remission to sustained normo- or microalbuminuria: HR 1.31, 95 %CI 1.07–1.59, P = 0.009.

Conclusion: Empagliflozin reduced HF hospitalizations or cardiovascular death irrespective of albuminuria levels at baseline, reduced the progression to macroalbuminuria and reverted macroalbuminuria more frequently than placebo.

P013

Annexin A2 contributes to kidney injury by activating the NF-kappa B signaling pathway in diabetic nephropathy

L. Chen; S. Xie; W. Zou

Department of nephropathy, Sun Yat-sen University, Zhuhai/CN

Objective: Diabetic nephropathy (DN), has become the leading course of end-stage kidney disease across the world. Excessive inflammation in the tubular compartment leads to tubular injury and kidney function decline. Annexin A2 (ANXA2), an endogenous pro-inflammatory molecule, has been shown to be involved in

the development of atherosclerosis, another diabetic complication. But its relation to kidney inflammation in DN remains unknown. In this work, we explored the potential role of Annexin A2 (ANXA2) in kidney inflammation in DN.

Method: Gene expression data from GSE30122 and GSE47185, two diabetic nephropathy-related datasets, were downloaded from the GEO database and analyzed using the GEO2R online tool. The association of tubular ANXA2 expression levels with GFR of the DN cohort in the NEPTUNE data set was analyzed. GSEA analysis in DN samples with higher ANXA2 expression versus lower ANXA2 expression based on the GSE30122 dataset was performed. An STZ-induced type I diabetes mellitus mouse model was established. Human kidney tubular epithelial cells (HK2) were stimulated with low or high glucose in vitro. qPCR and Western blot were performed to measure the expression levels of ANXA2 and inflammatory-related molecules. Dual-luciferase activity experiment was used to detect NF- κ B transcription activity.

Results: Bioinformatic analysis showed that the mRNA level of ANXA2 was significantly elevated in the tubulointerstitial compartment of DN patients compared to healthy individuals (3.6 folds in the GSE30122 dataset, and 1.9 folds in the GSE47185 dataset, respectively). ANXA2 expression levels negatively correlated with GFR, implicating a deleterious effect of tubular ANXA2. ANXA2 expression was positively correlated with KEGG CYTOKINE_CYTOKINE_RECEPTOR_INTERACTION and CHEMOKINE_SIGNALING_PATHWAY, suggesting a role of ANXA2 in kidney

inflammation. Anxa2 and multiple inflammatory factors were up-regulated in the kidneys of STZ-induced diabetic mice. High glucose treatment dramatically upregulated the expression levels of ANXA2 and multiple inflammatory factors and increased the NF- κ B transcription activity in HK2 cells. Silencing ANXA2 via siRNA significantly blunted these increases.

Conclusion: In the present study, we provide evidence that ANXA2 may contribute to kidney inflammation by activating the NF- κ B pathway. Further experiments should be performed to investigate how high glucose increases ANXA2 levels and whether blocking ANXA2 via shRNA could reduce kidney inflammation and improve kidney function in mouse models of diabetic nephropathy.

P014

Renal proteasomal activity is impaired in a type-2 diabetes mouse model

L. Heintz; M. Wang; S. Liu¹; J. Brand; S. Zielinski; T.B. Huber¹; T. Wiech²; D. Loreth; W. Sachs; C. Meyer-Schwesinger
Institut für Zelluläre und Integrative Physiologie, Zentrum für Experimentelle Medizin, Universitätsklinikum Hamburg-Eppendorf, Hamburg;
¹*Nephrologie/Rheumatologie und Endokrinologie/Diabetologie, III. Medizinische Klinik, Universitätsklinikum Hamburg-Eppendorf, Hamburg;*
²*Institut für Pathologie, Sektion Nephropathologie, Zentrum für Diagnostik, Universitätsklinikum Hamburg-Eppendorf, Hamburg*

Objective: In contrast to the significance of the autophagosomal-lysosomal pathway (ALP) in diabetic

nephropathy (DN), little is known about the involvement of the ubiquitin-proteasome system (UPS). Therefore, this study aimed at characterising important players of this degradative system in both glomeruli and total kidney tissue in a DN type 2 model (BTBR ob/ob mice) at an early (8 weeks) and a late stage (ca. 20 weeks) of disease. We focused on the assessment of proteasomal subtype composition, the actual proteolytic activity and how these relate to cell-type specific mRNA and protein levels of the corresponding proteasomal subunits.

Method: Proteasome subtype composition and activity was quantified via in-gel activity assays and activity-based probes targeting the proteolytic subunits. Transcript and protein levels of important UPS and ALP players were assessed via RNAseq (both bulk and single cell) and Western blot analysis. The protein abundance of proteasomal proteins was correlated with the resulting catalytic activities. Immunohistochemical analyses in mice and patient biopsies with diabetic nephropathy were used to identify the renal cell-types which exhibited changes in proteasome abundance.

Results: Using activity-based probes and in-gel activity assays, a decrease in proteasomal catalytic activity was observed in diabetic glomerular and kidney tissue, both for different proteasome subtypes and catalytic subunits, partly due to a down-regulation of proteasomal components on the protein level. These effects were exacerbated with disease progression as the impairment was stronger at 20 than at 8 weeks. Interestingly, most proteasomal subunits were not regulated on the mRNA level. K48-ubiquitin, which

commonly targets substrates for proteasomal degradation, showed a mild accumulation in glomeruli at 8 weeks, and a decrease in kidney at 8 and 20 weeks, especially in male mice. Immunohistochemical staining of proteasomal proteolytic subunits revealed an accumulation and aggregation in glomerular endothelial cells and podocytes, but not in mesangial cells in BTBR ob/ob mice and patient biopsies.

Conclusion: In the BTBR ob/ob mouse model of diabetic type-2 nephropathy, renal proteasomal activity is already reduced at 8 weeks, especially in non-glomerular cells. Similarly altered glomerular cell-type expression patterns between ob/ob and patient biopsies indicate a common pathophysiological proteasomal disturbance in diabetic nephropathy.

P015

Influence of Carnosine and Carnosinase-1 on diabetes-induced afferent arteriole vasodilation: implications for glomerular hemodynamics

M. A. Rodriguez-Niño; D. O. Pastene Maldonado; S. Hettler; B. K. Krämer; B. A. Yard; J. van den Born¹
Nephrologie, Endokrinologie, Rheumatologie, V. Medizinische Klinik, Universitätsmedizin Mannheim, Mannheim; ¹ Nephrology, Univ Med Center Groningen, State University Groningen, Groningen/NL

Objective: Dysregulation in glomerular hemodynamics favors hyperfiltration in diabetic kidney disease (DKD). Although carnosine supplementation ameliorates features of DKD, its effect on glomerular vasoregulation is not known. We assessed the influence of carnosine

and carnosinase-1 (CN1) on afferent glomerular arteriole vasodilation and its association with glomerular size, hypertrophy and nephrin expression in diabetic BTBR^{ob/ob} mice.

Method: Two cohorts of mice including appropriate controls were studied i.e., diabetic mice receiving oral carnosine supplementation (cohort 1) and human CN1 (hCN1) transgenic (TG) diabetic mice (cohort 2). Lumen area ratio (LAR) of the afferent arterioles and glomerular parameters were measured by conventional histology. Three-dimensional analysis using a tissue clearing strategy was also employed.

Results: In both cohorts, LAR was significantly larger in diabetic BTBR^{ob/ob} vs non-diabetic BTBR^{wt/ob} mice (0.41 ± 0.05 vs 0.26 ± 0.07 ; $p < 0.0001$) and (0.42 ± 0.06 vs 0.29 ± 0.04 ; $p < 0.0001$), and associated with glomerular size (cohort 1: $r = 0.55$, $p = 0.001$; cohort 2: $r = 0.89$, $p < 0.0001$). LAR was partially normalized by oral carnosine supplementation (0.34 ± 0.05 vs 0.41 ± 0.05 ; $p = 0.004$), but did not differ between hCN1 TG and wild type (WT) BTBR^{ob/ob} mice. In hCN1 TG mice, serum CN1 concentrations correlated with LAR ($r = 0.90$; $p = 0.006$). Diabetic mice displayed decreased nephrin expression and increased glomerular hypertrophy. This was not significantly different in hCN1 TG BTBR^{ob/ob} mice ($p = 0.06$ and $p = 0.08$, respectively).

Conclusion: Carnosine and CN1 may affect intra-glomerular pressure in an opposing manner through regulation of afferent arteriolar tone. This study corroborates previous findings on the role of carnosine in the progression of DKD.

P016

Identification of mitochondrial dysfunction-related hub genes in diabetic kidney disease

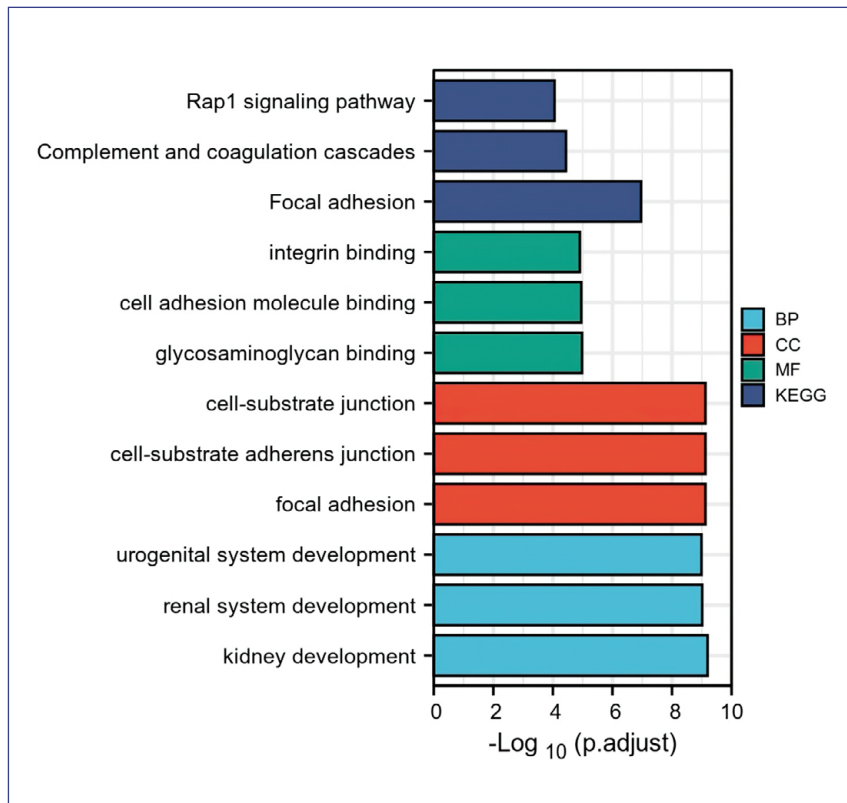
S. Wu

The Fifth Affiliated Hospital of Sun Yat-sen University, Zhuhai/CN

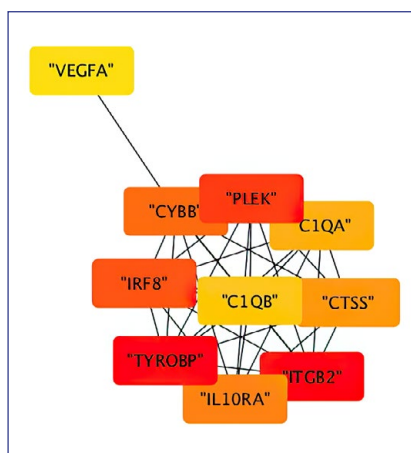
Objective: Diabetic kidney disease is the most important complication of diabetes and is becoming the most important cause of new-onset chronic renal failure. Mitochondrial dysfunction in podocytes is a typical feature of kidney injury but precedes the clinical manifestations of DKD. This study was designed to explore the potential role of mitochondrial dysfunction-related genes associated with DKD.

Method: GSE30528 from the Gene Expression Omnibus (GEO) database was downloaded, after which the differentially expressed genes (DEGs) were identified between DKD and healthy samples. The list of mitochondrial dysfunction-related genes (MDRGs) was downloaded and sorted out from the Genecards database. Then the list was intersected with the DEGs of GSE30528. The overlapping genes were defined as MDRDEGs and were further arranged into Gene Ontology (GO) terms and Kyoto Encyclopedia of Genes and Genomes (KEGG) pathway enrichment analyses to explore their functional roles. Finally, a protein-protein interaction (PPI) network was constructed to identify the hub genes.

Results: 429 differentially expressed mRNAs, including 143 up-regulated and 286 down-regulated mRNAs, were obtained in GSE30528. 8334 MDRGs were obtained from the Genecards database and were



P016: Abb. 1



P016: Abb. 2

intersected with the DEGs in GSE30528. 221 MDRDEGs were obtained. These genes were mainly enriched in kidney development, renal system development, urogenital

system development, and other biological processes (BPs). In addition, MDRDEGs were also involved in the Rap1 signaling pathway, Complement and coagulation cascades, and Focal adhesion pathway in diabetic complications. Top 10 genes, TYROBP, ITGB2, PLEK, IRF8, CYBB, IL10RA, CTSS, C1QA, C1QB, and VEGFA were identified as hub genes associated with DKD.

Conclusion: TYROBP, ITGB2, PLEK, IRF8, CYBB, IL10RA, CTSS, C1QA, C1QB, and VEGFA are involved in the process of DKD, which can be used as molecular targets for the intervention of DKD. Independent studies are warranted to validate the identified genes and further translate them into clinical utility.

P017

Empagliflozin and the risk of nephrolithiasis

P. Balasubramanian; C. Wanner¹;
J. O. P. Ferreira²; A. P. Ofstad³;
A. Elsaesser⁴; B. Zinman⁵;
S. E. Inzucchi⁶

Section of Endocrinology and Metabolism, Yale School of Medicine, New Haven/USA; ¹ Medizinische Klinik und Poliklinik I, Abteilung für Nephrologie, Universitätsklinikum, Julius-Maximilians-Universität Würzburg, Würzburg; ² Centre d'Investigation Clinique-Plurithématique Inserm CIC-P 1433, CHRU Nancy Brabois, Université de Lorraine, Nancy/F; ³ Boehringer Ingelheim Norway KS, Asker/N; ⁴ Boehringer Ingelheim Pharma GmbH & Co. KG, Ingelheim am Rhein; ⁵ The Lunenfeld-Tanenbaum Research Institute, Division of Endocrinology, Mount Sinai Hospital, University of Toronto, Toronto/CDN; ⁶ Section of Endocrinology, School of Medicine, Yale University, New Haven/USA

Objective: Nephrolithiasis is a common disease. In addition to pain, often severe, it can lead to urinary tract infections and acute kidney injury. Type 2 diabetes (T2D) is a well-known risk factor for nephrolithiasis. Recently in an observational study of patients with T2D, use of sodium-glucose transport-protein 2 (SGLT2) inhibitors as glucose lowering agents was associated with a 49 % lower risk of nephrolithiasis when compared with use of glucagon-like peptide 1 (GLP-1) receptor agonists. We examined, prospectively, the association between renal stone disease and the use of the SGLT2 inhibitor empagliflozin, using existing data from randomized clinical trials.

Method: Pooled data from 15,081 patients with T2D treated with empagliflozin (10,177) or placebo (4,904) from 20 phase I-IV randomized, placebo-controlled trials including the large cardiovascular outcome trial, EMPA-REG OUTCOME, were included in this analysis. Incident urinary tract stone events were captured using a pre-defined collection of MedDRA terms: nephrolithiasis, renal colic, ureterolithiasis, calculus bladder, calculus urinary, calculus urethral, and nephrocalcinosis. A sensitivity analysis used a narrower definition by excluding the terms renal colic and nephrocalcinosis. Incidence rate ratios (IRR) and 95 % confidence intervals (CI) were calculated using the relative risk estimate stratified by study.

Results: The median exposure to study drug was 543 (placebo) and 549 (empagliflozin 10 or 25 mg) days. We found that a total of 183 patients experienced an incident urolithiasis during follow-up (79 in placebo, 104 in pooled empagliflozin) yielding annual incidence rates of 1.01 versus 0.63 events per 100 patient years in placebo and empagliflozin, respectively. All but one event occurred in patients with no prior history of urinary tract stones. The IRR was 0.64 (95 % CI 0.48, 0.86), in favor of empagliflozin. In the sensitivity analysis, now restricted to nephrolithiasis, ureterolithiasis, calculus bladder, calculus urinary, and calculus urethral, the results were similar (IRR, empagliflozin vs. placebo, 0.62 [95 % CI 0.45, 0.85]).

Conclusion: As compared to placebo, use of empagliflozin was associated with an approximate 40 % reduction in the risk of urolithiasis in

patients with T2D. Based on these initial observations, mechanistic studies to elucidate the mediator(s) of this seemingly protective effect and dedicated randomized prospective clinical trials appear warranted in patients with renal stone disease.

P018

Hämodynamische Modulation der glomerulären Filtration durch kombinierte SGLT2 und ACE Hemmung in STZ-diabetischen Mäusen

*H. Kröger; F. Kessel; J. Sradnick; V. T. Todorov; F. Gemhardt; C. Hugo
Medizinische Klinik III, Nephrologie,
Universitätsklinikum Carl Gustav
Carus, Technische Universität Dresden,
Dresden*

Hintergrund: Eine der häufigsten Ursachen für chronische Nierenerkrankungen im Endstadium ist die diabetische Nephropathie. Gängige Behandlungsstrategien mit SGLT2 Inhibitoren oder ACE-Hemmern zeigen renoprotektive Effekte. Der zugrundeliegende renoprotektive Mechanismus der kombinierten Therapie von SGLT2 Inhibition und ACE-Hemmern ist nicht vollständig verstanden. Daher haben wir die hämodynamischen Veränderungen in einzelnen Glomeruli als Antwort auf SGLT2 und/oder ACE Inhibition in diabetischen Mäusen untersucht.

Methode: Männlichen C57BL/6-Mäusen wurde Streptozotocin (STZ) injiziert, um Diabetes mellitus Typ 1 hervorzurufen. Nach fünf Wochen Diabetes wurden die Mäuse drei Tage lang mit Enalapril, Empagliflozin oder Enalapril/Empagliflozin behandelt. Mittels longitudinaler Intravitalmikroskopie wurde die *single nephron GFR* (snGFR) und die Veränderungen des afferenten und efferenten

Arterioldurchmessers während ACE und/oder SGLT2 Inhibition von einzelnen Glomeruli gemessen.

Ergebnisse: Die STZ-diabetischen Mäuse zeigten eine signifikante Hyperfiltration (Kontrolle $1003.0 \pm 190.5 \mu\text{l/min/100 g b.w}$ vs. diabetisch $1329.4 \pm 309.6 \mu\text{l/min/100 g b.w}$, $p < 0.05$). Die Enalapril Behandlung reduzierte die snGFR und führte zur einer signifikanten Dilation der efferenten Arteriole ($12.55 \pm 1.46 \mu\text{m}$ vs. Kontrolle $11.92 \pm 1.04 \mu\text{m}$, $p < 0.05$). Die snGFR wurde durch die Empagliflozin Behandlung reduziert. Gleichzeitig führte die Empagliflozin Behandlung zu einer Vasokonstriktion der afferenten Arteriole ($11.19 \pm 2.55 \mu\text{m}$ vs. Kontrolle $12.35 \pm 1.32 \mu\text{m}$, $p < 0.05$). Die kombinierte Behandlung mit Enalapril und Empagliflozin führte zur Reduktion der snGFR jedoch ohne jegliche Veränderung im Durchmesser der afferenten oder efferenten Arteriole.

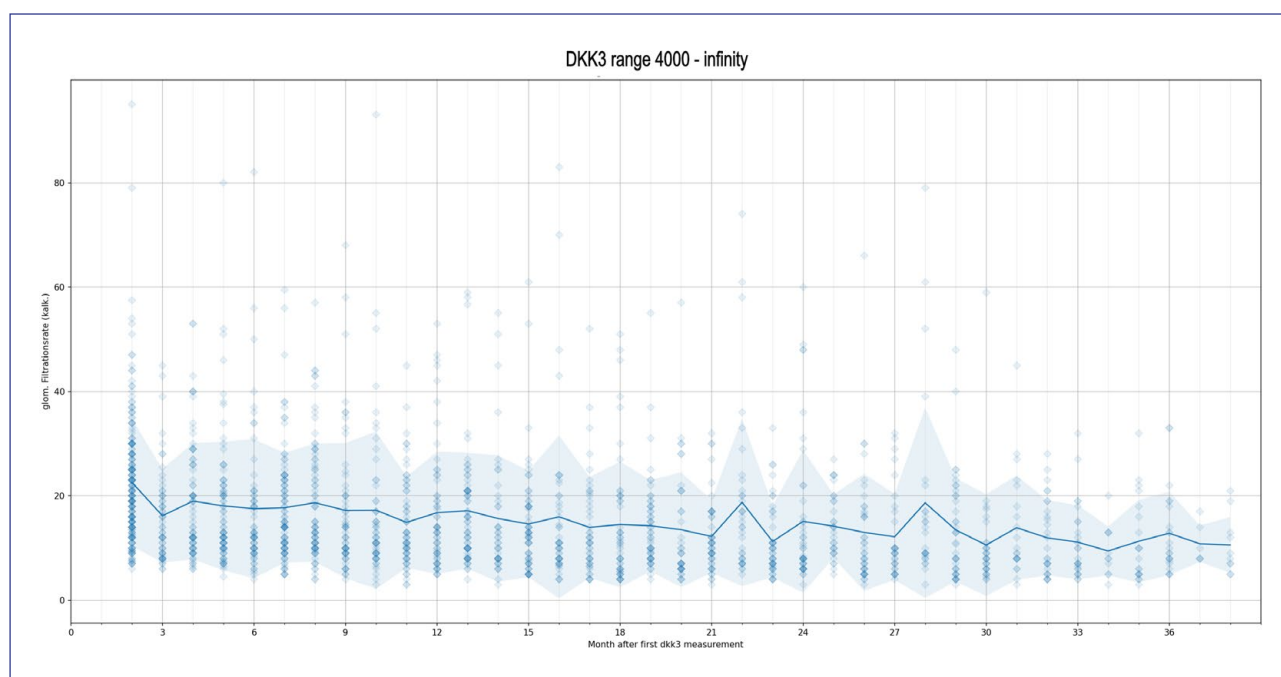
Zusammenfassung: SGLT2 Inhibitoren und ACE-Hemmer regulieren die Kontraktilität der afferenten und efferenten Arteriole und haben dabei einen positiven Einfluss auf die glomeruläre Filtration in frühen Stadien des Diabetes mellitus. Der genaue Mechanismus der Kombinationstherapie gilt es dabei noch weiter zu untersuchen.

Chronisches Nierenversagen 1

P019

Evaluation of the biomarker Dickkopf 3 in more than 1100 CKD patients of a German single center cohort using algorithm-based data analysis

*T. Weinreich; E. Seibert;
E. Brohammer¹; M. Rüb¹; F. Geblen;
A. Sikora¹; B. Hohenstein*



P019: Abb. 1

Nephrologisches Zentrum Villingen-Schwenningen, Villingen-Schwenningen;
¹ Künstliche Intelligenz – Software Solutions, Hahn-Schickard-Gesellschaft für angewandte Forschung e. V., Villingen-Schwenningen

Objective: Dickkopf 3 (DKK3) has been identified as a urinary biomarker. Values above 4000 pg/mg creatinine (Cr) were linked with a higher risk of short-term decline of kidney function (J Am Soc Nephrol 29: 2722–2733). However, as of today, there is little experience with DKK3 as a risk marker in everyday clinical practice. We used algorithm-based data analysis to evaluate the potential dependence of DKK3 in a cohort from a large single center in Germany.
Method: DKK3 was measured in all CKD patients in our center October 1st 2018 till Dec. 31 2019, together with calculated GFR (eGFR)

and urinary albumin/creatinine ratio (UACR). Kidney transplant patients were excluded. Until the end of follow-up Dec 31st 2021, repeated measurements were performed for all parameters. Data analysis was performed using MD-Explorer (Bio-ArtProducts, Rostock, Germany) and Python with multiple libraries. Linear regression models were applied in patients for DKK3, eGFR and UACR. Comparison of the models was performed with a two-sided Kolmogorov-Smirnov test.

Results: 1206 DKK3 measurements were performed in 1103 patients (621 male, age 70yrs, eGFR 29,41 ml/min/1.73qm, UACR 800 mg/g). 134 patients died during follow-up. DKK3 mean was 2905 pg/mg Cr (max. 20000, 75 % percentile 3800). 121 pts had DKK3 > 4000. At the end of follow-up 7 % of patients with DKK3 < 4000 (initial

eGFR 17.6) versus 39.6 % of patients with DKK3 > 4000 (initial eGFR 15.7) underwent dialysis. Compared to eGFR and UACR at baseline, DKK3 > 4000 performed best to predict eGFR loss over the next 12 months.

Conclusion: In this cohort of CKD patients, DKK3 > 4000 at baseline predicted the eGFR slope better than eGFR or UACR at baseline. DKK3 > 4000 reflected a higher risk of progression towards ESRD in patients with similar baseline eGFR levels.

P020

Einfluss verschiedener Serumkreatinin-Bestimmungsmethoden auf die Graduierung der chronischen Nierenkrankheit (CKD)

K. Boss; S. Stolpe¹; A. Müller²; L. Volbracht²; A. Stang³; B. Kowall¹; A. Kribben

Klinik für Nephrologie, Universitätsklinikum, Universität Duisburg-Essen, Essen; ¹ Institut für Medizinische Informatik, Biometrie und Epidemiologie (IMIBE), Universitätsklinikum Essen, Universität Duisburg-Essen, Essen; ² Zentrallabor, Universitätsklinikum Essen, Universität Duisburg-Essen, Essen; ³ Zentrum für Klinische Epidemiologie, Institut für Medizinische Informatik, Biometrie und Epidemiologie, Universitätsklinikum Essen, Essen

Hintergrund: Serumkreatinin ist der wichtigste Parameter zur Abschätzung der glomerulären Filtrationsrate (eGFR), anhand derer eine CKD graduiert wird. Dabei wird Serumkreatinin überwiegend entweder mittels Jaffe- oder enzymatischer Methode bestimmt. Abweichungen zwischen den Messergebnissen beider Methoden können sich auf die eGFR auswirken. Eine potenzielle Differenz der eGFR ist dabei von klinischer Bedeutung.

Methode: Alle Bestimmungen des Serumkreatinins mittels Jaffe- und enzymatischer Methode in derselben Serumprobe von Erwachsenen bei Erstvorstellung, die zwischen 2008–2020 in ambulanter oder stationärer Behandlung der Universitätsklinik waren, wurden ausgewertet. Zur Bestimmung der Differenz zwischen den Messmethoden wurde ein Bland-Altman-Plot, zur Bestimmung der eGFR die CKD-EPI Formel für Serumkreatinin (2009) verwendet. Das CKD-Stadium wurde nur anhand der eGFR als Marker für die Nierenfunktion festgelegt, ohne Berücksichtigung von Markern für einen Nierenschaden.

Ergebnisse: Bei 53.916 Patienten wurden Serumkreatinin-Doppelbestimmungen durchgeführt und ausgewertet, davon 51,6 % aus

ambulant, 41,1 % aus stationären und 7,3 % aus intensivmedizinischen Aufenthalten. Der Anteil der Frauen lag bei 47,9 %, der Altersdurchschnitt bei 64,2 Jahren, der Median bei 70 Jahren. Das mit der Jaffe-Methode bestimmte Serumkreatinin war durchschnittlich 0,13 mg/dl höher (Upper Limit 0,74, Lower Limit -0,48 mg/dl), als das mit der enzymatischen Methode bestimmte Serumkreatinin, wodurch die eGFR mittels Jaffe-Serumkreatinin 3,5 ml/min/1,73 m² niedriger war (Lower Limit -17,42, Upper Limit -10,43 ml/min/1,73 m²). Dies ergab in 37 % aller Fälle ein unterschiedliches CKD-Stadium, wobei der Anteil der unterschiedlichen Klassifizierungen in den Stadien G1/G2 (50,4 %), G2/G3a (35,9 %) und G3a/G3b (46,9 %) am größten war (G3b/G4 18,3 %, G4/G5 5,4 %, G5/G4 2,8 %).

Zusammenfassung: Der Unterschied der Serumkreatininmessung mittels Jaffe- oder enzymatischer Methode hat bei mehr als einem Drittel der Fälle einen relevanten Einfluss auf die Zuordnung in ein CKD-Stadium.

P021

Genauere Einordnung von Biopsiebefunden bei Patienten mit fokalsegmentaler Glomerulosklerose und Glomerulopathien mittels molekulargenetischer Untersuchung

A. Zellner; K. M. Riedhammer¹; C. Schaaf¹; M. Büttner-Herold²; P.-H. Kuhn³; M. C. Braunisch¹; J. Comic; L. Renders¹; C. Schmaderer¹; U. Heemann¹; J. Höfele

Institut für Humangenetik, Klinikum rechts der Isar, Technische Universität München, München; ¹ II. Medizinische Klinik, Nephrologie, Klinikum rechts der Isar, Technische Universität München,

München; ² Institut für Nephropathologie, Universitätsklinikum, Friedrich-Alexander-Universität Erlangen-Nürnberg, Erlangen; ³ Institut für Allgemeine Pathologie und Pathologische Anatomie, Technische Universität München, München

Hintergrund: Bei Erwachsenen mit chronischer Niereninsuffizienz liegt in ca. 10 % der Fälle eine erbliche Ursache zugrunde. Wichtige Vertreter erblicher Nierenkrankheiten sind das Alport-Syndrom und erbliche Podozytopathien, welche häufig das histologische Bild einer fokalsegmentalen Glomerulosklerose (FSGS) zeigen. Die FSGS ist ein histologischer Befund verschiedener Ätiologien (primär, erblich/genetisch, sekundär). Gerade bei vermuteter glomerulärer Erkrankung ist die Nierenbiopsie diagnostischer Goldstandard. Ziel dieser Studie war es, die morphologischen Veränderungen von Nierenbiopsien bei Patienten mit genetisch gesicherten erblichen Nierenkrankheiten zu evaluieren.

Methode: Retrospektive Studie mit einer Kohorte von 18 Patienten mit genetisch gesicherter erblicher Nierenkrankheit und vorausgegangener Nierenbiopsie. Systematische Zweitbefundung der Biopsien durch eine Nephropathologin (genetische Diagnose bei Zweitbefundung unbekannt). Vergleich der biopsischen Ergebnisse mit den Ergebnissen der molekulargenetischen Analyse.

Ergebnisse: Genetisch waren in der Kohorte krankheitsverursachende Varianten in folgenden Genen repräsentiert: COL4A3, COL4A5, WT1, DAAM2, INF2, UMOD, MUC1, ADCK4, NPHP4, TRIM8, CD2AP, NPHS2. Die Biopsien zeigten vorwiegend glomeruläre Vernarbungen

und ein unspezifisches Schädigungsmuster. Ein Patient mit der histologischen Diagnose eines Alport-Syndroms konnte genetisch als X-chromosomales Alport-Syndrom bestätigt werden (Korrelation Histologie und Genetik).

Zusammenfassung: In dieser Studie bei Patienten mit erblichen Nierenkrankheiten, bei denen eine Nierenbiopsie erfolgt ist, ermöglichte die molekulargenetische Diagnostik eine präzisere Krankheitszuordnung und damit Informationen zur Prognose/Rekurrenz im Transplantat/möglichen extrarenalen Phänotypen/Vererbung. Pathologische Befunde können Hinweise auf eine erbliche Krankheit geben und helfen, gezielt genetische Untersuchungen zu veranlassen (z. B. beim Alport-Syndrom). Durch eine genetische Diagnostik kann man jedoch auch Fälle einordnen, für die bisher keine typischen morphologischen Kriterien beschrieben sind. Es müssten zahlreiche Fälle der jeweiligen Krankheit analysiert werden, um gemeinsame histopathologische Kriterien zu etablieren, was aufgrund der rasch fortschreitenden Entdeckung von neuen krankheitsassoziierten Genen und der Seltenheit der jeweiligen Krankheit eine Herausforderung darstellt. Alternativ könnten in Zukunft molekulare Methoden wie MALDI-Imaging diese Veränderungen visualisieren.

P022

Prävalenz von Perikardergüssen bei autosomal-dominanter polyzystischer Nierenerkrankung

J. S. Jost; T. F. Kaireit¹; B. Auber²; H. Haller; K. M. Schmidt-Ott; V. C. Wulfmeyer; R. Schmitt
Klinik für Nieren- und Hochdruck-
erkrankungen, Zentrum für Innere

Medizin, Medizinische Hochschule Hannover, Hannover; ¹ Institut für Diagnostische und interventionelle Radiologie, Medizinische Hochschule Hannover, Hannover; ² Institut für Humangenetik, Medizinische Hochschule Hannover, Hannover

Hintergrund: Die autosomal dominante polyzystische Nierenerkrankung (ADPKD) geht mit zahlreichen extrarenalen Manifestationen einher, zu denen unter anderem auch Perikardergüsse (PE) zählen. Die Ätiologie für das vermehrte Auftreten von PE bei ADPKD ist noch ungeklärt. Ein Polycystin 1-assoziiierter Bindegewebsdefekt mit einer resultierenden erhöhten Gewebedurchlässigkeit wird als ursächlich vermutet. Bisherige Studien fanden in dieser Patientengruppe eine Prävalenz von bis zu 35 %. Ziel der aktuellen Untersuchung ist die Erhebung der Häufigkeit von PE bei ADPKD sowie möglicherweise einflussnehmender Kofaktoren.

Methode: Retrospektiv wurden interne und externe Schnittbilduntersuchungen (CT, MRT) der hiesigen Studienambulanz hinsichtlich des Vorliegens eines Perikardergusses untersucht. Perikardiale Flüssigkeitsansammlungen mit einer Saumbreite ≥ 4 mm gemessen in coronaler oder transversaler Schichtführung wurde als PE gewertet. Weitere erhobene Parameter: Alter, Geschlecht, Body-Mass-Index, Nierenretentionsparameter, Proteinurie, Mayo-Klasse, arterieller Hypertonus, Vorliegen einer antihypertensiven Therapie, eingeteilt nach Wirkstoffklassen, (Empfehlung zur) Tolvaptantherapie und Autoimmunerkrankungen.

Ergebnisse: In der Kohorte der 208 Patienten (39,7 % Männern und

60,3 % Frauen) lag bei 17 (8,2 %) Personen ein PE vor. Dabei ist eine deutliche Überrepräsentation des weiblichen Geschlechts von 82,3 % in der Gruppe mit PE zu beobachten, die nicht alleine auf die ungleiche Geschlechterverteilung zurückzuführen ist. Hinsichtlich der Nierenretentionsparameter waren beide Gruppen vergleichbar (eGFR $63,51 \pm 1,95$ ml/min/1,73 m² ohne PE vs. $64,29 \pm 7,64$ ml/min/1,73 m² bei PE; $p=0,91$). Anhand der Mayo Klassifikation ergab sich kein Hinweis auf eine raschere Progredienz der ADPKD in einer der Gruppen. Vor allem bei ausgedehnteren Ergüssen ≥ 8 mm ließen sich in fast allen Fällen Komorbiditäten nachweisen, die auf andere Ätiologien des PE rückschließen lassen.

Zusammenfassung: Im Vergleich zu bisherigen Publikationen liegt die Prävalenz für Perikardergüsse bei ADPKD in unserer Population mit 8,2 %, bis zu 4-fach niedriger. Frauen scheinen überproportional betroffen zu sein (Prävalenz PE bei Frauen 10,1 % vs. Männer 3,8 %). Im Management der ADPKD sollte auch ein neu aufgetretener, nicht akut behandlungsbedürftiger PE bei ADPKD einer weiteren Abklärung zugeführt werden, bevor die ADPKD als ursächlich angenommen werden kann.

P023

Kardioresnale Protektion mit Empagliflozin bei Patienten mit chronischer Niereninsuffizienz – Baselinecharakteristika der klinischen randomisierten EMPA-KIDNEY Studie

V. Cejka; S. Brenner; S. Ghavampour; C. Wanner für die deutsche EMPA-KIDNEY Studiengruppe¹

Deutsches Zentrum für Herzinsuffizienz, Universitätsklinikum Würzburg, Würzburg; ¹ Medizinische Klinik und Poliklinik I, Abteilung für Nephrologie, Universitätsklinikum, Julius-Maximilians-Universität Würzburg, Würzburg

Hintergrund: Der Benefit einer SGLT2-Inhibitorentherapie bei Patienten mit chronischer Niereninsuffizienz (CKD) konnte in mehreren klinischen Studien nachgewiesen werden. Dennoch besteht weiterhin eine unzureichende Evidenzlage für Patienten ohne Diabetes mellitus (DM), mit fortgeschrittener Einschränkung der Nierenfunktion und geringgradiger Albuminurie.

Methode: EMPA-KIDNEY ist eine internationale multizentrische klinische randomisierte Placebo-kontrollierte Studie, die den Effekt von Empagliflozin 10 mg/d untersucht. Der primäre kombinierte Endpunkt ist kardiovaskulärer Tod oder Progression der Niereninsuffizienz. Eingeschlossen wurden erwachsene Patienten mit CKD, mit und ohne DM, mit geschätzter glomerulärer Filtrationsrate (eGFR) ≥ 20 und < 45 ml/min/1,73 m², oder ≥ 45 und < 90 ml/min/1,73 m² mit Albuminurie (uACR) ≥ 200 mg/g Kreatinin oder Proteinurie ≥ 300 mg/g Kreatinin.

Ergebnisse: Es konnten 6609 Teilnehmer in 8 Ländern weltweit randomisiert werden, 1269 (18 %) davon in 34 deutschen Studienzentren. Mithilfe des Mainfranken-Netzwerks niedergelassener Nephrologen konnte das Zentrum Würzburg mit 173 Randomisierungen einen substantiellen Beitrag dazu leisten. Charakteristika der gesamten Studienpopulation bei Baseline waren: Alter $63,8 \pm 13,9$ (Mittelwert,

SD) Jahre, 2192 (33 %) Frauen, eGFR $37,5 \pm 14,8$ (Mittelwert, SD) ml/min/1,73 m², uACR 412 [94–1190] (Median, IQR) mg/g Kreatinin. Insgesamt hatten 3570 (54 %) keinen DM, bei 2280 (34 %) war die eGFR < 30 ml/min/1,73 m², bei 3194 (48 %) war uACR < 300 mg/g Kreatinin. Als primäre Nierenerkrankung hatten 2057 (31 %) eine diabetische Nephropathie, 1669 (25 %) hatten eine Glomerulopathie (einschl. 12 % mit IgA-Nephropathie) und 1445 (22 %) hatten eine hypertensive/renovaskuläre Nephropathie.

Zusammenfassung: EMPA-KIDNEY ist bislang die größte klinische Studie, die den Effekt des SGLT-2 Inhibitors Empagliflozin bei Patienten mit CKD untersucht. Die Studienpopulation ist repräsentativ für ein breites Spektrum der Niereninsuffizienz und beinhaltet bislang untererforschte Patientengruppen, z. B. nicht-Diabetiker ohne Albuminurie oder Patienten mit primärer Glomerulopathie. Die Ergebnisse der Studie werden diese Lücke mit der benötigten randomisierten Evidenz beleuchten. Eine neue Technik der zentralen Patientenrekrutierung aus einem Netzwerk wird dargestellt und kann als Beispiel für Studien mit seltenen Erkrankungen dienen.

P024

Entwicklung von Qualitätsindikatoren für die ambulante Versorgung von Patienten mit chronischer Nierenkrankheit

S. Kiel; L. Dröge; E. Sierocinski; S. Stracke; E. Schäffner¹; N. Ebert¹; N. Mielke¹; T. Bothe¹; J.-F. O. Chenot
Abteilung für Nephrologie und Hypertensiologie, Klinik und Poliklinik für Innere Medizin A, Universitätsmedizin Greifswald, Greifswald;

¹ Institut für Public Health, Charité – Universitätsmedizin Berlin, Berlin

Hintergrund: Für die Beurteilung der Qualität der Versorgung von Patient*innen mit nicht dialysepflichtiger chronischer Nierenkrankheit (CKD) sind Qualitätsindikatoren (QI) essentiell. Ziel war es, zwei Qualitätsindikatoren-Sets basierend auf Abrechnungsdaten, z. B. von Krankenkassen, und auf Datenerhebung in Praxen (Chart Review) zu entwickeln. Der Fokus lag dabei auf Patient*innen ≥ 70 Jahre.

Methode: In einem ersten Schritt wurden QIs basierend auf den Empfehlungen der nationalen S3-Leitlinie CKD und aus einem Review von bereits existierenden internationalen Qualitätsindikatoren vorgeschlagen. Diese wurden in einem interdisziplinären mehrstufigen Delphi-Verfahren mit zweistufiger Onlinebefragung und abschließender Konsensuskonferenz mit N = 6 Expert*innen der Allgemeinmedizin, Nephrologie, Geriatrie und Patient*innenvertretung in Bezug auf Relevanz, Wissenschaftlichkeit und Praktikabilität gewertet und in eine Rangordnung gebracht.

Ergebnisse: Es wurde ein Inzidenzindikator als Bezugsgröße für die Versorgung von Patient*innen mit neu diagnostizierter CKD und ein Prävalenzindikator für die Versorgung bereits vorhandener CKD konsentiert. Insgesamt wurden 21 Prozessindikatoren mit dem Fokus Screening, Diagnose, Monitoring und Therapie ausgewählt. Bei der Auswahl spielten Annahmen über die derzeitige Versorgungsqualität eine Rolle. Für die Routinedatenindikatoren wurden die QIs Vermeidung der Verordnung von NSAR, die Bestimmung der Albumin-Kreatinin-Ratio

bei Erstdiagnose, Überweisung in die Nephrologie bei eGFR < 30 ml/min und Urinstreifentest auf Hämaturie bei Erstdiagnose als hochrangig eingestuft. Beim Chartreview wurde die Blutdruckkontrolle, die mit Abrechnungsdaten nicht abgebildet werden kann, als höchstrangig eingestuft.

Zusammenfassung: Die konsentierten Indikatoren-Sets sollen ein Monitoring der ambulanten Versorgungsqualität von Patient*innen mit CKD erlauben. Der Anteil der CKD-Patient*innen, die empfohlene (unerwünschte) medizinische Maßnahmen erhalten, soll im Rahmen des Innovationsfonds-Projektes GUIDAGE-CKD evaluiert und anhand umfangreicher Daten von Krankenkassen evaluiert werden.

P025

Effect of severe lipid metabolism disorder on renal function – a prospective cross-sectional study

N. Lewandowski; R. M. Spitthöver; A. L. Kahl¹; N. Mülling; A. Kribben; W. Reinhardt

Klinik für Nephrologie, Universitätsklinikum, Universität Duisburg-Essen, Essen; ¹ Institut für Med. Psychologie, Universitätsklinik, Universität Duisburg-Essen, Essen

Objective: Renal dysfunction causes dyslipidemia in the course of its progression with consecutive lipid metabolism disorder requiring therapy. However only a few other studies have described that the severity of dyslipidemia and the various regimen may also influence renal function.

Method: In a prospective unicentric cross-sectional study a total of n = 214 prevalent patients (105 women, 109 men, 18–86 years) were investigated and divided into four

groups based on the severity and the therapeutic regimen of an existing lipid metabolism disorder: a lipid apheresis-treated group (LA n = 72), a drug-treated group (MG n = 54), a diabetes group (DG n = 45) and a control group (KG n = 43). These groups were studied for the prevalence of renal impairment. In particular, age, sex, BMI, blood pressure, abdominal circumference, fat metabolism parameters (Lp(a), HDL-C, LDL-C), renal parameters (serum creatinine (s-crea), GFR, urea), as well as urinary protein excretion (total urinary protein (tp)) and urinary albumin (alb) were examined and compared with each other for a precise analysis.

Results: Lipid apheresis therapy leads to an effective lowering of LDL-C, as well as to a reduction in the presumably protective HDL-C. S-crea is significantly higher in the LA, MG and DG, compared to the KG ($p = .002$), the GFR is correspondingly lower ($p = .014$), whereby the significantly lower age of the KG ($p < .001$) (13–15 yrs.) must be considered. On the other hand proteinuria was not elevated in the LA- and the MG-group, compared to KG. Here, a better blood pressure setting of the LA also seems to have a protective influence on the renal function ($p = .002$). The Lp(a), which could not be lowered to the norm under apheresis, showed a negative influence on kidney function with positive correlation to s-crea ($p = .002$) and urinary tp ($p = .017$), as well as a negative correlation to GFR ($p = .028$). HDL-C correlated negatively with BMI ($p > .001$) and s-crea ($p < .001$). Additionally, significantly higher HDL-C levels were seen in female patients across all groups ($p < .001$).

LDL-C had no significant effect on kidney parameters. In addition to Lp(a) and HDL-C, age, blood pressure, BMI and abdominal circumference were expected to have the strongest influence on GFR.

Conclusion: Thus, Lp(a) and HDL-C seem to have the greatest impact on renal function, whereas the influence of LDL-C can be neglected. Also, lipid apheresis is not associated with higher proteinuria.

P026

Expression of Interferon regulatory factor 8 (IRF8) and its association with infections in patients with end-stage renal disease

J. Friebus-Kardash; F. Kuang¹; T. Peitz; U. Eisenberger; A. Kribben; K. S. Lang¹; M. Jahn

Klinik für Nephrologie, Universitätsklinikum, Universität Duisburg-Essen, Essen; ¹ Institut für Immunologie, Universitätsklinikum, Universität Duisburg-Essen, Essen

Objective: Patients having end-stage renal disease (ESRD) have dysfunction of innate and adaptive immune system responses accounting for susceptibility to infections. The transcriptional factor IRF8 (interferon regulatory factor 8) which is mainly expressed on differentiated plasmacytoid dendritic cells (pDCs) and conventional dendritic cells is essential for maturation of dendritic cells, monocytes and macrophages and contributes to protection from bacterial infections. The current study was designed to analyze the expression pattern of IRF8 in patients on dialysis and to assess IRF8 as a risk factor for infections in this patient population.

Method: The study comprised 92 patients who were treated with

dialysis therapy and 44 healthy controls. Dialysis patients were free of clinical and laboratory signs of infection at the time of analysis. Different population of leukocytes and intracellular expression of IRF8 were measured using flow cytometry.

Results: The number of pDCs was significantly reduced in dialysis patients compared with control group. Indeed natural killer cells, classical and intermediate monocytes and macrophages were significantly higher in dialysis patients than in controls. Dialysis patients exhibited a significantly decreased number of IRF8 positive pDCs and myeloid DCs (mDCs) ($p = 0.0003$, $p = 0.0001$) and increased number of IRF8 positive classical, intermediate and nonclassical monocytes ($p = 0.0001$, $p = 0.0001$, $p = 0.0001$). The IRF8 expression on pDCs, mDCs and classical monocytes was significantly lower in dialysis patients than controls.

A significant decline in the number of IRF8 positive pDCs and classical monocytes ($p = 0.009$, $p = 0.05$) as well as a significantly reduced IRF8 expression on pDCs, mDCs and classical monocytes ($p = 0.003$, $p = 0.05$, $p = 0.04$) were observed in the group of dialysis patients who experienced severe infections including sepsis, pneumonia and pyelonephritis within the first year after analysis compared to ESRD patients without infection. Additionally, we detected an association of the number IRF8 expressing mDCs, classical and intermediate monocytes with serum concentration of protein in the group of dialysis patients. The time on dialysis therapy correlated with the number of IRF8 positive pDCs and mDCs.

Conclusion: We identified a decrease of IRF8 expression on dendritic cells and a rise of IRF8 expression on monocytes in dialysis patients with ESRD compared to healthy controls. Our results suggest reduced IRF8 expression on dendritic cells and monocytes as a potential risk factor predisposing dialysis patients for severe infections.

P027

Pre-existing anti-drug antibodies in Fabry disease show a reduced cross-reactivity against pegunigalsidase-alfa

M. Lenders; S. Pollmann; M. Terlinden; E. Brand

Allg. Innere Medizin sowie Nieren- und Hochdruckkrankheiten und Rheumatologie, Medizinische Klinik D, Westfälische Wilhelms-Universität Münster, Münster

Objective: Anti-drug antibodies (ADAs) against approved recombinant α -galactosidase A (AGAL) significantly limit therapeutic benefits of enzyme replacement therapy in Fabry disease. Here, we analyzed the cross-reactivity of pre-existing ADAs against agalsidase-alfa and agalsidase-beta from 49 patients with Fabry disease (FD) against the novel PEGylated enzyme pegunigalsidase-alfa (PRX-102).

Method: We used enzyme inhibition assays and classical ELISAs to determine affinities (dissociation constant [K_d]) and cross-reactions of ADAs against three recombinant AGALs. Furthermore, we used cell culture experiments to analyze the impact of ADAs on enzyme uptake in endothelial AGAL-deficient cells.

Results: The affinity of purified anti-AGAL antibodies from pooled patient sera was significantly lower for PRX-102 compared

to agalsidase-alfa and agalsidase-beta (both $p < 0.05$). Pull-down experiments revealed the presence of masked epitopes on PRX-102, possibly due to PEGylation. ADA titers in sera ($\mu\text{g/ml}$) and corresponding inhibitory capacities against agalsidase-alfa and agalsidase-beta were measured in male FD patients, showing strong correlations ($r^2 = 0.9978$ and $r^2 = 0.4930$, both $p < 0.001$). Affinity of ADAs of individual patients against PRX-102 (K_d : $3.55 \pm 2.72 \mu\text{Mol}$) were significantly lower compared to agalsidase-alfa (K_d : $1.99 \pm 1.26 \mu\text{Mol}$) and agalsidase-beta (K_d : $2.18 \pm 1.51 \mu\text{Mol}$) (both $p < 0.0001$). Cross-ELISAs confirmed the presence of potentially masked epitopes on PRX-102. Importantly, inhibition measurements also revealed a 30 % reduction in inhibitory capacity of pre-existing ADAs towards PRX-102. Enzyme uptake experiments in AGAL-deficient EA.hy926 cells demonstrated less inhibitory effect of ADAs on cellular PRX-102 uptake.

Conclusion: We conclude that due to the reduced affinity of pre-existing ADAs, ADA-affected patients might benefit from a therapy switch to PRX-102.

P028

Characteristics and Outcomes of Chronic Kidney Disease patients stratified for prevalent Heart Failure: Results from the German Cohort of a Multinational Retrospective Observational Study

J. Leiner; V. Pellisier; S. König; C. Schanner; P. Schmitz; J. Bodegard¹; D. Anderson²; R. Kühlen³; G. Hindricks; A. Bollmann
Abteilung für Rhythmologie, Universität Leipzig, Herzzentrum Leipzig, Leipzig

Heart Institute GmbH, Leipzig; ¹ Astra Zeneca GmbH, Oslo/N; ² Astra Zeneca GmbH, Wedel; ³ Klinik für Intensivmedizin, HELIOS Klinikum Berlin-Buch, Berlin

Objective: Heart Failure (HF) represents one of the most common comorbidities in patients with chronic kidney disease (CKD) and has significant impact on patients' outcomes. The multinational CaReMe study (observational study to highlight the epidemiology and healthcare burden of Cardiovascular-REnal-METabolic diseases) with the here presented German sub-study assesses inpatient characteristics, comorbidities, and burden of care in CKD patients stratified for prevalent HF.

Method: This study utilized administrative data of inpatient cases from 89 Helios hospitals from 01/01/2016 to 02/28/2022 by extracting ICD-10- and OPS-encoded discharge diagnoses and procedures. Cases that fulfilled a prespecified CKD definition (main discharge diagnosis CKD or comparable combination of ICD-10- and OPS-codes) were further analyzed including a description of patient characteristics and event rates during hospital readmissions within the observational period. Endpoints were stratified for prevalent HF at index case.

Results: The CKD patient cohort included in the presented analysis comprised 48,034 CKD patients (mean age 73.8 ± 13.1 , 44 % female) and HF was present in 42.9 %. HF patients were older (76.5 ± 10.8 vs. 71.5 ± 14.3 years, $p < 0.001$), less likely to be female and were characterized by higher prevalence of distinct comorbidities such as hypertension (77.3 % vs. 67.1 %, $p < 0.001$),

atrial fibrillation/flutter (46.3 % vs. 20.5 %, $p < 0.001$), ischemic heart disease (16.4 % vs. 6.0 %, $p < 0.001$) and diabetes mellitus type 2 (54.1 % vs. 42.6 %, $p < 0.001$). HF patients more frequently required dialysis during index hospitalization (44.3 % vs. 38.9 %, $p < 0.001$). In-hospital mortality among index cases (16.6 % vs. 6.8 %, $p < 0.001$) as well as during follow-up (8.7 % vs. 5.8 %, $p < 0.001$) was substantially increased in HF patients. Time-to-event analyses showed a significantly lower mean duration until first re-hospitalization (175.9 ± 266 vs. 212.7 ± 308.9 days, $p < 0.001$) in HF patients. Re-admission numbers in HF patients were mostly driven by hospitalizations due to end stage renal disease, cardiorenal disease and HF. Event numbers for end stage renal disease or dialysis were higher in non-HF patients (36.1 % vs. 30.1 %, $p < 0.001$).

Conclusion: In this nationwide German inpatient cohort, 43 % of CKD patients have diagnosed HF that decisively worsens the patient's prognosis. However, also non-HF patients are at high risk for developing end stage renal disease. Interdisciplinary strategies to improve quality of care for patients with cardiorenal disease are desirable.

Chronisches Nierenversagen 2

P029

Sekundärprophylaxe nach kardioembolischem Apoplex in Abhängigkeit der CKD; eine Querschnittsanalyse aus der Nephro-, Neuro- und Kardiokohorte der GANI_MED-Studie

M. Scheuch; S. Freiin von Rheinbaben; R. Hoffmann; N. Endlich¹; K. Endlich¹; U. Lendeckel²; R. Rettig³; T. Petsch; T. Dabers; S. Stracke

Abteilung für Nephrologie und Hypertensiologie, Klinik und Poliklinik für Innere Medizin A, Universitätsmedizin Greifswald, Greifswald;

¹ Institut für Anatomie und Zellbiologie, Universitätsmedizin Greifswald, Greifswald; ² Institut für Medizinische Biochemie und Molekularbiologie, Universitätsklinikum, Universitätsmedizin Greifswald, Greifswald; ³ Institut für Physiologie, Universitätsmedizin Greifswald, Greifswald

Hintergrund: Die Prävalenz von Vorhofflimmern (VHF) liegt mit zirka 20 % bei Patient*innen mit chronischer Nierenerkrankung (CKD) 2–3 mal höher als in der Normalbevölkerung. Die Verwendung von Antikoagulanzen bei CKD wird kontrovers diskutiert, da diese in höheren CKD Stadien nicht zugelassen sind oder unerwünschte Ereignisse wie Blutungsneigung eintreten können. Wir analysierten daher in einer Querschnittsstudie CKD Patient*innen auf eine Anamnese für VHF bzw. Apoplex und die entsprechende medikamentöse Sekundärprophylaxe.

Methode: Wir betrachteten insgesamt 1.322 Patient*innen der GANI_MED-Studie (Greifswald Approach to Individualized Medicine). Für die Auswertung wurden ein standardisierter Fragebogen mit Anamnese sowie Untersuchungen des Klinikaufenthaltes mit den entsprechenden Laborparameter herangezogen.

Ergebnisse: Insgesamt wiesen 314/1.322 (23,8 %) Patient*innen VHF auf, insgesamt 370 (28,0 %) Patient*innen erlitten einen Apoplex, entweder kardioembolisch oder arteriosklerotisch bedingt. Bei insgesamt 156 Personen war VHF an der Genese des Apoplex beteiligt.

Verglichen mit Patient*innen ohne VHF zeigten Patient*innen mit VHF eine um 8 ml/min niedrigere GFR (\bar{O} 53 \pm 28 vs. 62 \pm 32 ml/min; $p < 0.001$). Insbesondere im Stadium G4 wiesen 38,1 % (ein Plus von 14,3 %) aller Patient*innen ein VHF auf. Anders als bei VHF konnten keine Zusammenhänge zwischen einer Änderung der Nierenfunktion und der Prävalenz von Apoplex beobachtet werden. Bei den 156 Personen mit der Beteiligung von VHF an der Genese von Apoplex, erhielten 51 Patient*innen (32,7 %) nur ASS oder ADP-Rezeptor-Antagonisten (ARA). Von 77 Personen mit gemischt arteriosklerotisch-kardioembolischem Apoplex wurden nur 14 mit ASS/ARA und Vollantikoagulation behandelt (18,2 %). Insgesamt erhielten nur 64,8 % eine leitliniengerechte Sekundärprophylaxe entsprechend der Ursache des Schlaganfalls. **Zusammenfassung:** Mit zunehmendem Alter steigt das Risiko für CKD-Patient*innen zusätzlich an VHF zu erkranken. Im Fall eines Schlaganfalls wird ungeachtet der Ursache in ca. 23 % der Fälle nicht leitliniengerecht therapiert. Insbesondere bei multiplen Schlaganfällen mit unterschiedlichen Ursachen wird häufig nur eine der Ursachen medikamentös behandelt.

P030

COL4A5 Gly624Asp is the predominant variant in patients with Alport spectrum in a bicentric cohort in Eastern Germany

B. M. Krüger; A. Jens¹; R. Schönauer¹; J. de Fallois; J. Halbritter¹; M. Schüller¹
Sektion Nephrologie, Klinik für Endokrinologie und Nephrologie, Universitätsklinikum Leipzig, Leipzig; ¹ Medizinische Klinik mit Schwerpunkt Nephrologie

und Internistische Intensivmedizin, Campus Charité Mitte, Charité – Universitätsmedizin Berlin, Berlin

Objective: Pathogenic variants in genes encoding for the glomerular basement membrane (GBM), namely variants affecting COL4A3-5, are the second most common cause of inherited chronic kidney disease (Groopman et al, NEJM, 2019). The spectrum of kidney diseases associated with COL4A3-5 has extended from classic Alport syndrome (AS) to FSGS without extrarenal manifestation, leading to the terminology Alport spectrum. Yet, there is insufficient knowledge concerning correlations between specific pathogenic variants in COL4A3-5 and different clinical phenotypes. Therefore, we aimed to assess genotype-phenotype correlations in a bicentric cohort of patients with the clinical and/or genetic diagnosis of AS.

Method: Recruited patients with AS/TBMN/FSGS and/or a diagnostic variant in one of the COL4A3-5 genes were characterized using electronic medical records, patient questionnaires and telephone interviews. Statistical analysis is done by GraphPad Prism and SPSS.

Results: Preliminary analysis includes 148 individuals with the clinical and/or genetic diagnosis of AS. Of these, 96 % had a diagnostic variant in one of the COL4A3-5 genes. In 64.9 %, we detected variants in COL4A5 gene (X-linked), while 31.1 % of the cases harbored variants in either COL4A4 or COL4A3 (autosomal). Furthermore, in the remaining 4 %, digenicity was observed. Overall, biallelic or hemizygous variant carriers reached end-stage kidney failure (ESKF) earlier

than monoallelic variant carriers. The mean age at onset of ESKF was 32.4 years (SD 12,2) in men and 43.3 years (SD 15.9) in women. While hypacusis was present in almost 44 %, pathologies of the eyes in less than one quarter of the cohort. The most commonly found variant accounting for about 15 % of the total cohort was COL4A5 Gly624Asp.

Conclusion: Preliminary analyses of our bicentric cohort illustrate the clinical and genetic spectrum of COL4A3-5 alteration. Specific genotype-phenotype correlations are yet to be evaluated. However, predominance of the Central and Eastern European COL4A5 founder mutation Gly624Asp (Zurowska et al, *Kidney Int*, 2021) was confirmed, known to be associated with milder course of disease.

P031

Incidence of hospitalisation with community-acquired infections in the German Chronic Kidney Disease study

F. K. Kotsis; H. Bächle; A. Esser; I. Steinbrenner; P. Sekula¹; H. Meiselbach²; H. Stockmann³; H. U. Zacharias⁴; C. Sommerer⁵; M. Busch⁶; H. Weissensteiner⁷; S. Schönherr⁷; L. Forer⁷; F. Kronenberg⁷; A. Köttgen; K.-U. Eckardt³; U. T. Schultheiß; all GCKD Investigators

Medizin IV, Nephrologie und Institut für genetische Epidemiologie, Universitätsklinikum, Albert-Ludwigs-Universität Freiburg, Freiburg; ¹ Department für Medizinische Biometrie und

Medizinische Informatik, Albert-Ludwigs-Universität Freiburg, Freiburg; ² Medizinische Klinik 4, Nephrologie und Hypertensiologie, Universitätsklinikum, Friedrich-Alexander-Universität Erlangen-Nürnberg, Erlangen;

³ Medizinische Klinik mit Schwerpunkt

Nephrologie und Internistische Intensivmedizin, Campus Charité Mitte, Charité – Universitätsmedizin Berlin, Berlin; ⁴*Institut für Klinische Molekularbiologie (IKMB), Christian-Albrechts-Universität Kiel, Kiel;* ⁵*Medizinische Klinik I, Sektion Nephrologie, Medizinische Fakultät, Ruprecht-Karls-Universität Heidelberg, Heidelberg;* ⁶*Abteilung für Nephrologie, Klinik für Innere Medizin III, Friedrich-Schiller-Universität Jena, Jena;* ⁷*Department für Medizinische Genetik, Molekulare und Klinische Pharmakologie, Medizinische Universität Innsbruck, Innsbruck/A*

Objective: Chronic Kidney Disease (CKD) is a global health problem with a high prevalence and is associated with a markedly increased risk for cardiovascular- and non-cardiovascular complications. Several studies in patients with advanced CKD requiring dialysis identified infections as the most common non-cardiovascular comorbidity and second leading cause of death in this population. Patients with mild to moderate CKD without kidney replacement therapy seem to be at higher risk for infections compared to patients without CKD; however, data are limited.

Method: We evaluated 5217 German Chronic Kidney Disease (GCKD) study participants during a follow-up period of 6.5 years. Based on a standardized event catalogue, incident hospitalization due to community-acquired infection events were adjudicated by trained physicians. Infections were assigned to 10 categories: respiratory, genitourinary, skin and musculoskeletal system, gastrointestinal, endocarditis, implant or catheter associated, nervous system, others, infection with unclear focus, or due

to COVID-19. Furthermore, hospital discharge letters and death certificates were screened in more detail for available data on pathogen spectrum, antibiotic agents, previous immunosuppressive treatment and indications of a septic course.

Results: During the observation period of 6.5 years, 2006 infection events (including recurrent events) were in 1208 participants observed. Overall of 680 patients had died and the second leading cause of death was infection (n = 146). Majority of the infections were respiratory and genitourinary infections. Prevalent diseases such as diabetes (51.3 % vs. 28.6 %) or cardiovascular disease (42.6 % vs. 25.1 %) were more common baseline characteristics in participants with infection compared to without it. About one-fourth of the infections occurred under immunosuppressive treatment.

Conclusion: Community-acquired infections are a major, but under-recognized complication in patients with moderate CKD contributing to adverse outcomes. This study of participants with CKD not requiring dialysis provides data on: (i) infection rates, (ii) organ specificity, (iii) pathogen spectrum and treatment. This data will serve as a basis for future studies that may determine specific diagnostic, preventive, and therapeutic interventions in this vulnerable patient population.

P032

Cyclosporine-A mediated anemia and capillary rarefaction is ameliorated by Phd-inhibitor daprodustat.

R. Labes; L. Brinkmann; V. A. Kulow¹; K. Rögner; S. Mathia; B. Balcersek;

*P. B. Persson; C. Rosenberger¹; M. Fäßling
Institut für Translational Physiologie, Campus Charité Mitte, Charité – Universitätsmedizin Berlin, Berlin;
¹ Medizinische Klinik mit Schwerpunkt Nephrologie, Campus Charité Mitte, Charité – Universitätsmedizin Berlin, Berlin*

Objective: Treatment with the immunosuppressive calcineurine inhibitor Cyclosporine-A (CsA) is associated with nephrotoxicity and anemia. In organ transplantation and various autoimmune diseases, CsA is used for its immunosuppressive effects. CsA alters protein phosphorylation by inhibition of the phosphatase calcineurin. The pathophysiology of CsA induced kidney damage and anemia remains unclear. Daprodustat represents an activator of the hypoxia inducible factor and is designed for the treatment of renal anemia. In this study, we investigated the effect of daprodustat on CsA induced kidney injury and anemia, having a special focus on the phospho-proteome.

Method: Mice were treated daily with CsA (80 mg/kg BW) and/or daprodustat (10 mg/kg BW) by oral gavage for up to 8 weeks. Blood samples were taken to evaluate kidney function and anemia. Kidney injury markers were assessed by qPCR and immunofluorescence. Kidney homogenates were used for large scale phospho-proteomic analysis including gene set enrichment analysis. To examine capillary density kidney slices were stained for the endothelial marker CD31 by immunofluorescence.

Results: After 8 weeks of daily CsA treatment, mice showed anemia and elevated kidney injury markers

Kim-1, Ng2, Dkk3 as well as vimentin. While anemia could be ameliorated by daprodustat, renal injury markers remained unaffected. Nevertheless, phospho-proteomic analysis revealed 79 proteins changed at expression and 86 proteins at phosphorylation level by CsA. When combined with daprodustat, the expression of 95 proteins were altered but only 6 at the phosphorylation level. Daprodustat alone showed only marginal effects on its own. Under CsA and daprodustat/CsA treatment, angiogenesis-related pathways were among the top enriched candidates as shown by gene set enrichment analyses. Immunofluorescence staining for CD31 revealed capillary rarefaction by CsA which could be prevented by daprodustat.

Conclusion: This study provides a detailed renal phospho-proteomic map under CsA, daprodustat or daprodustat/CsA treatment. We demonstrate that chronic CsA treatment induces capillary rarefaction and anemia. Daprodustat on top of CsA prevents CsA induced effects on microcirculation and Hb. Data suggest that the protective action of daprodustat involves changes in the renal phosphorylation response to CsA.

P033

Characteristics and Outcomes of Chronic Kidney Disease patients stratified for prevalent Diabetes Mellitus: Results from the German Cohort of a Multinational Retrospective Observational Study

J. Leiner; V. Pellissier; S. König; C. Schanner; P. Schmitz; J. Bodegard¹; D. Anderson²; R. Kühlen³; G. Hindricks; A. Bollmann
Abteilung für Rhythmologie, Universität Leipzig, Herzzentrum Leipzig, Leipzig

Heart Institute GmbH, Leipzig; ¹ Astra Zeneca GmbH, Oslo/N; ² Astra Zeneca GmbH, Wedel; ³ Klinik für Intensivmedizin, HELIOS Klinikum Berlin-Buch, Berlin

Objective: Diabetes mellitus type 2 (T2DM) is the leading cause of chronic kidney disease (CKD) worldwide. Both conditions substantially worsen patients' prognosis. The ongoing multinational CaReMe study (observational study to highlight the epidemiology and healthcare burden of Cardiovascular-REnal-METabolic diseases) with the here presented German sub-study assesses inpatient characteristics, comorbidities, and burden of care in CKD patients stratified for prevalent T2 DM.

Method: This study utilized administrative data of inpatient cases from 89 Helios hospitals from 01/01/2016 to 02/28/2022 by extracting ICD-10-encoded discharge diagnoses and OPS-encoded procedures. Cases that fulfilled a previously developed CKD definition (main discharge diagnosis CKD or comparable combination of ICD-10- and OPS-codes) were further analyzed including a description of patient characteristics and pre-defined event rates during hospital readmissions within the observational period. Endpoints were stratified for prevalent T2 DM at index case.

Results: In total, 48,034 CKD patients were included in the presented analysis (mean age 73.8 ± 13.1 , 44 % female) and 47.9 % had an encoded T2 DM diagnosis. T2 DM patients were older (75 ± 10.6 vs. 72.7 ± 14.9 years, $p < 0.001$) but gender distribution was similar. Comorbidities such as hypertension (74.6 % vs. 69.2 %, $p < 0.001$), heart failure (51.9 % vs. 40.5 %, $p < 0.001$), atrial fibrillation/flutter (35.5 % vs. 29.5 %, $p < 0.001$), and ischemic heart disease (12.8 % vs. 8.8 %, $p < 0.001$) were more common in T2 DM patients. Non-T2 DM patients showed more advanced CKD at index case as indicated by the proportion of end stage renal disease (52.7 % vs. 47.5 %, $p < 0.001$) and need for dialysis (43.1 % vs. 39.5 %, $p < 0.001$). Index in-hospital mortality was significantly higher in T2 DM patients (11.8 % vs. 10.8 %, $p < 0.001$), driven mostly by cardiovascular deaths. During follow-up, in-hospital mortality in T2 DM patients was higher (7.6 % vs. 6.6 %, $p < 0.001$) as were event numbers for cardiorenal disease, myocardial infarction and heart failure. Non-T2 DM patients were more frequently re-hospitalized due to end stage renal disease or dialysis (36.8 % vs. 29.7 %, $p < 0.001$).

Conclusion: T2 DM is common among CKD patients. In this nationwide German patient cohort, CKD-T2 DM patients are characterized by a higher prevalence of cardiovascular diseases that appear to be the major determinants of adverse outcomes. Interestingly, CKD was more advanced in non-T2 DM patients possibly suggesting closer and more regular follow-up care in the outpatient sector due to concomitant T2 DM.

Conclusion: T2 DM is common among CKD patients. In this nationwide German patient cohort, CKD-T2 DM patients are characterized by a higher prevalence of cardiovascular diseases that appear to be the major determinants of adverse outcomes. Interestingly, CKD was more advanced in non-T2 DM patients possibly suggesting closer and more regular follow-up care in the outpatient sector due to concomitant T2 DM.

P034

REVEAL-CKD: Die Prävalenz nicht diagnostizierter chronischer Niereninsuffizienz im Frühstadium in Deutschland

M. P. Schneider; E. Peach¹; S. Barone²; S. Kumar³; N. Tangri⁴
Medizinische Klinik 4, Nephrologie und Hypertensiologie,

Universitätsklinikum, Friedrich-Alexander-Universität Erlangen-Nürnberg, Erlangen;
¹BioPharmaceuticals Business Unit, Global Medical Affairs, AstraZeneca, Cambridge/UK; ²Global Medical Affairs, AstraZeneca, Gaithersburg/USA; ³Real World Data Science, Global Medical Affairs, AstraZeneca, Gaithersburg/USA; ⁴Section of Nephrology, Max Rady College of Medicine, University of Manitoba, Winnipeg/CDN

Hintergrund: Chronische Niereninsuffizienz (CKD) betrifft ca. 10 % der Weltbevölkerung. Die frühzeitige Erkennung ist wesentlich, um den Krankheitsverlauf zu verlangsamen und das Patienten-Outcome zu verbessern. Die REVEAL-CKD-Studie untersuchte die Prävalenz nicht diagnostizierter,

früher CKD (Stadium 3) und die damit verbundenen Faktoren.

Methode: REVEAL-CKD ist eine multinationale Beobachtungsstudie, die Sekundärdaten aus elektronischen Gesundheits- und Versicherungsdatenbanken verwendet. In Deutschland wurden die Datenbank "Disease Analyzer" (IQVIA, Frankfurt) verwendet, die aus elektronischen Krankenakten, anonymisierten Longitudinaldaten zu Arzneimittelverordnungen, Diagnosen und medizinischen Daten einer repräsentativen Stichprobe von > 1.200 deutschlandweiten Allgemeinmedizin- und Lungenfacharztpraxen besteht. Die Studienkohorte umfasste Patienten im Alter von ≥ 18 Jahren von 2015–2021 mit zwei aufeinanderfolgenden Messungen der geschätzten glomerulären Filtrationsrate (eGFR)

≥ 30 und < 60 ml/min/1,73 m², erfasst zwischen > 90 und ≤ 730 Tagen. Der Tag der zweiten qualifizierenden eGFR war das Indexdatum. Eine nicht diagnostizierte CKD war als das Fehlen eines CKD-Diagnoseschlüssels vor der ersten, und bis zu sechs Monate nach der zweiten eGFR definiert. Die Prävalenz wurde als das Verhältnis nicht diagnostizierter Patienten zu allen Personen berechnet, die die Studieneinschlusskriterien erfüllen.

Ergebnisse: Die deutsche Studienkohorte umfasste 26.767 Patienten, die die eGFR-Kriterien für CKD im Stadium 3 erfüllten. Das mediane Alter zum Indexdatum war 79 Jahre (IQR: 72; 84) und 58 % waren Frauen. Der Gesamtanteil an Patienten mit nicht diagnostizierter CKD im Stadium 3 lag bei 84,3 % (95 %-KI: 83,8; 84,7) und war bei Männern, Personen < 45 Jahre und Patienten mit Komorbiditäten zu Studienbeginn niedriger (Tabelle 1). Bei 5 % (N = 1.157) der zum Indexdatum nicht diagnostizierten Patienten (N = 23.302) wurde während des Follow-Ups eine CKD im Stadium 3 diagnostiziert, mit einer medianen Zeit bis zur Diagnose von 109 Tagen (IQR: 22; 238).

Zusammenfassung: In Deutschland lag in einer großen Datenbank ambulanter Patienten, die die eGFR-Kriterien erfüllten, eine hohe Prävalenz nicht diagnostizierter, früher CKD vor. Diese Ergebnisse verdeutlichen, dass die Früherkennung der CKD verbessert werden muss, um den Einsatz gezielter, evidenzbasierter Therapien zu gewährleisten, die das Risiko für eine Krankheitsprogression verringern und das Patienten-Outcome verbessern.

Variable	Gesamt, n	Nicht diagnostizierte CKD, n	Anteil nicht diagnostizierter CKD, % (95 %-KI)
GESAMT	26.767	22.557	84,27% (83,84%; 84,71%)
ALTER BEI INDEXDATUM (JAHRE)			
<45	66	46	69,70% (58,61%; 80,78%)
45–64	2.431	1.957	80,50% (78,93%; 82,08%)
65–74	6.032	5.088	84,35% (83,43%; 85,27%)
≥ 75	18.238	15.466	84,80% (84,28%; 85,32%)
GESCHLECHT			
FRAUEN	15.551	13.384	86,07% (85,52%; 86,61%)
MÄNNER	11.216	9.173	81,78% (81,07%; 82,50%)
TYP-2-DIABETES			
NEIN	20.697	18.097	87,44% (86,99%; 87,89%)
JA	6.070	4.460	73,48% (72,37%; 74,59%)
HERZINSUFFIZIENZ			
NEIN	22.403	19.239	85,88% (85,42%; 86,33%)
JA	4.364	3.318	76,03% (74,76%; 77,30%)
HYPERTONIE			
NEIN	25.264	21.612	85,54% (85,11%; 85,98%)
JA	1.503	945	62,87% (60,43%; 65,32%)

P034: Tab. 1

P035**Safety of Roxadustat Versus Erythropoiesis-Stimulating Agents for Treatment of Anemia in Patients With Chronic Kidney Disease Incident to or Not Receiving Dialysis: Pooled Analysis of Four Phase 3 Studies**

F. Dellanna; J. Barratt¹; J. Portoles²; G. Choukroun³; L. De Nicola⁴; M. Reusch⁵; J. Young⁶; N. Dimkovic⁷
 MVZ DaVita Rhein-Ruhr GmbH, Düsseldorf; ¹ Department of Respiratory Sciences, University of Leicester, Leicester/UK; ² Hospital Universitario Puerta de Hierro, Madrid/E; ³ CHU Amiens Picardie and Jules Verne University, Amiens/F; ⁴ University of Campania, Naples/I; ⁵ Guard Therapeutics International AB, Stockholm/S; ⁶ Astellas Pharma, Inc, Northbrook/USA; ⁷ University of Belgrade, Belgrad/SRB

Objective: Patients with late-stage chronic kidney disease (CKD) who are non-dialysis-dependent (NDD) or incident to dialysis (ID) (eg, initiated dialysis within the last 4 months) or dialysis-dependent (DD) represent a vulnerable population at increased risk for morbidity and mortality despite significant clinical advancements in recent years. How may the safety of roxadustat in patients with NDD or ID-DD CKD be further elucidated?

Method: In this post hoc exploratory analysis, safety results from eligible patients with anemia of CKD enrolled in four phase 3, randomized, open-label studies [NDD (DOLOMITES) or ID-DD (SIERRAS, HIMALAYAS, ROCKIES)] were pooled and compared roxadustat to an erythropoiesis-stimulating agent (ESA). Endpoints were time to major adverse cardiovascular

event (MACE; myocardial infarction, stroke, and all-cause mortality [ACM]) and MACE+ (MACE plus congestive heart failure or unstable angina requiring hospitalization), ACM, and treatment-emergent adverse events (TEAEs).

MACE and MACE+ were evaluated for non-inferiority using hazard ratios (HRs) at 1.8- and 1.3-upper margins, respectively, and 95 % confidence intervals (CIs). TEAEs were descriptively summarized.

Results: In total, 2142 patients were evaluated (1083 roxadustat; 1059 ESA; 616 NDD; 1526 ID-DD). Roxadustat was non-inferior to ESA for risk of MACE (HR 0.79, 95 % CI 0.61–1.02) and MACE+ (HR 0.78, 95 % CI 0.62–0.98) with a consistent finding for ACM (HR 0.78, 95 % CI 0.57–1.05). TEAEs were generally comparable between roxadustat and ESA groups, including any TEAE (incidence rate per 100 patient-exposure years [IR/100 PEY] 56.1 vs 53.5), TEAEs leading to discontinuation of study drug (IR/100 PEY 6.7 vs 5.1), and TEAEs leading to death (IR/100 PEY 6.9 vs 7.4). The most frequent (IR/100 PEY) TEAEs were hypertension (roxadustat 12.8, ESA 12.3), end-stage kidney disease (roxadustat 6.6, ESA 6.1), diarrhea (roxadustat 7.1, ESA 4.8), and hyperkalemia (roxadustat 4.3, ESA 4.8).

Conclusion: There was no evidence of an increased risk of cardiovascular events or mortality with roxadustat compared with ESA in patients with anemia who have NDD or ID-DD CKD. Although TEAE development occurred commonly in both the roxadustat and ESA groups, patients infrequently discontinued a study drug because of an adverse event.

P036**Cardiovascular Safety of Roxadustat Versus Erythropoiesis-Stimulating Agents for Treatment of Anemia in Patients With Chronic Kidney Disease Incident to or Not Receiving Dialysis: Pooled Subgroup Analysis of Four Phase 3 Studies**

F. Dellanna; J. Barratt¹; J. Portoles²; G. Choukroun³; L. De Nicola⁴; M. Reusch⁵; J. Young⁶; A. Jiletcovici⁷; N. Dimkovic⁸
 MVZ DaVita Rhein-Ruhr GmbH, Düsseldorf; ¹ Department of Respiratory Sciences, University of Leicester, Leicester/UK; ² Hospital Universitario Puerta de Hierro, Madrid/E; ³ CHU Amiens Picardie and Jules Verne University, Amiens/F; ⁴ PO S. M. d. P. Incurabili, Second University of Naples, Naples/I; ⁵ Guard Therapeutics International AB, Stockholm/S; ⁶ Astellas Pharma, Inc, Chicago/USA; ⁷ Astellas Pharma, Inc., Chicago/USA; ⁸ University of Belgrade, Belgrad/SRB

Objective: How do baseline characteristics affect cardiovascular safety in patients with anemia of chronic kidney disease (CKD) who are non-dialysis-dependent (NDD) or incident to dialysis (ID-DD) receiving roxadustat or an erythropoiesis-stimulating agent (ESA)?

Method: In this post hoc exploratory analysis, cardiovascular safety results from eligible patients with anemia of CKD enrolled in four phase 3 studies (NDD [DOLOMITES] or ID-DD [SIERRAS, HIMALAYAS, ROCKIES]) were pooled and compared between roxadustat and ESA. Time to major adverse cardiovascular event (MACE), MACE+, and all-cause mortality (ACM) were evaluated in baseline

Endpoint/Parameter	Non-Dialysis-Dependent/Incident to Dialysis (NDD/ID-DD)	
	Roxadustat (n=1078)	ESA (n=1051)
CFB in hemoglobin (g/dL) to Weeks 28-52, regardless of rescue therapy		
Baseline, mean (SD)	9.04 (1.15)	9.05 (1.12)
CFB, mean (SD)	2.06 (1.36)	1.90 (1.31)
LS mean (95% CI)	1.85 (1.734, 1.966)	1.65 (1.534, 1.765)
LSMD (95% CI)	0.20 (0.038, 0.362)	
P-value	0.0153	
CFB in serum iron (µg/dL) to Week 20		
Baseline, mean (SD)	65.39 (26.56)	64.21 (26.76)
CFB, mean (SD)	5.04 (32.93)	-0.37 (32.76)
LS mean (95% CI)	6.93 (4.122, 9.735)	-0.29 (-3.065, 2.486)
LSMD (95% CI)	7.22 (3.337, 11.099)	
P-value	0.0003	
CFB in ferritin (µg/L) to Week 20		
Baseline, mean (SD)	384.75 (352.97)	373.63 (312.13)
CFB, mean (SD)	-139.92 (244.26)	-107.57 (230.93)
LS mean (95% CI)	-118.57 (-138.008, -99.140)	-108.50 (-127.885, -89.114)
LSMD (95% CI)	-10.07 (-37.031, 16.881)	
P-value	0.4637	
CFB in TIBC to Week 20		
Baseline, mean (SD)	44.82 (8.97)	44.57 (8.61)
CFB, mean (SD)	7.55 (8.03)	0.56 (6.05)
LS mean (95% CI)	6.77 (5.894, 7.651)	0.49 (-0.370, 1.358)
LSMD (95% CI)	6.28 (5.074, 7.484)	
P-value	<0.0001	
CFB in TSAT (%) to Week 20		
Baseline, mean (SD)	27.35 (10.81)	27.17 (10.40)
CFB, mean (SD)	-1.44 (12.17)	-0.66 (10.95)
LS mean (95% CI)	-0.17 (-1.176, -0.828)	-0.37 (-1.364, 0.617)
LSMD (95% CI)	0.20 (-1.184, 1.583)	
P-value	0.7774	
Proportion of patients using IV iron as rescue therapy up to Week 52		
IV iron, n (%)	36.5%	49.1%
95% CI	0.34, 0.39	0.46, 0.52
Odds ratio (95% CI)	0.52 (0.42, 0.63)	
P-value	<0.0001	

CFB, change from baseline; ESA, erythropoiesis-stimulating agent; IV, intravenous; LS, least squares; LSMD, least squares mean difference; TIBC, total iron-binding capacity; TSAT, transferrin saturation.

characteristics subgroups. End-points were evaluated descriptively for consistency with prior reported main cardiovascular safety analyses in this population. Hazard ratios (HRs) and 95 % confidence intervals (CIs) were compared between roxadustat and ESA. The analysis period was the “on-treatment plus 7 days” time frame.

Results: In total, 2142 patients were evaluated (1083 roxadustat, 1059 ESA; 616 NDD, 1526 ID-DD). Roxadustat was comparable to ESA for risk of MACE and MACE+ with a consistent finding for ACM in most subgroups, which was consistent with main cardiovascular safety analyses outcomes, including male sex (MACE: HR 0.66, 95 % CI 0.47–0.92; MACE+: HR 0.65, 95 % CI 0.48–0.87; ACM: HR 0.64, 95 % CI 0.43–0.95), United States region (MACE+: HR 0.60, 95 % CI 0.36–0.99), prior smoker (MACE: HR 0.36, 95 % CI 0.19–0.68; MACE+: HR 0.48, 95 % CI 0.27–0.85; ACM: HR 0.28, 95 % CI 0.12–0.64), baseline hemoglobin ≥ 8 g/dL (MACE: HR 0.74, 95 % CI 0.55–0.99; MACE+: HR 0.75, 95 % CI 0.58–0.97; ACM: HR 0.68, 95 % CI 0.48–0.97), prior statin use (MACE+: HR 0.58, 95 % CI 0.34–1.00), peritoneal dialysis (MACE+: HR 0.26, 95 % CI 0.08–0.87), no history of diabetes mellitus (MACE+: HR 0.62, 95 % CI 0.42–0.90), no history of coronary artery disease (MACE: HR 0.70, 95 % CI 0.52–0.95; MACE+: HR 0.71, 95 % CI 0.54–0.93; ACM: HR 0.65, 95 % CI 0.45–0.92), no history of congestive heart failure (MACE: HR 0.65, 95 % CI 0.43–0.97; MACE+: HR 0.60, 95 % CI 0.41–0.87; ACM: HR 0.57, 95 % CI 0.35–0.93), transferrin saturation ≥ 20 % (MACE+: HR 0.71, 95 % CI 0.53–0.93), and

ferritin ≥ 100 mcg/L (MACE+: HR 0.77, 95 % CI 0.60–0.99) (Figure).

Conclusion: The risks of MACE, MACE+, and ACM between roxadustat and ESA were consistent with the main cardiovascular safety analyses in the pooled NDD or ID-DD CKD population across most baseline characteristic subgroups with no evidence of increased cardiovascular risk compared with ESA.

P037

Iron Parameters in Patients Treated With Roxadustat for Anemia Associated With Chronic Kidney Disease: Post Hoc Analysis of the Non-Dialysis-Dependent or Incident Dialysis Population From Four Phase 3 Studies

F. Dellanna¹; J. Barratt¹; J. Portoles²; G. Choukroun³; L. De Nicola⁴; M. Reusch⁵; J. Young⁶; A. Jiletcovici⁶
MVZ DaVita Rhein-Ruhr GmbH, Düsseldorf; ¹ Department of Respiratory Sciences, University of Leicester, Leicester/UK; ² Hospital Universitario Puerta de Hierro, Madrid/E; ³ CHU Amiens Picardie and Jules Verne University, Amiens/F; ⁴ University of Campania, Naples/I; ⁵ Guard Therapeutics International AB, Stockholm/S; ⁶ Astellas Pharma, Inc, Northbrook/USA

Objective: Anemia is a common complication in patients with chronic kidney disease (CKD) who are non-dialysis-dependent (NDD) or incident dialysis-dependent (ID-DD) (ie, initiated dialysis within the last 4 months). Does treatment with roxadustat improve iron metabolism parameters in patients with anemia of CKD who were NDD/ID-DD compared to an erythropoiesis-stimulating agent (ESA)?

Method: The results of four phase 3, randomized, open-label

studies (NDD [DOLOMITES]; ID-DD [HIMALAYAS, SIERRAS, ROCKIES]) comparing oral roxadustat to an ESA (darbepoetin alfa or epoetin alfa) for patients with anemia of CKD were pooled in this post hoc exploratory analysis. Iron metabolism parameters (serum iron, ferritin, total iron-binding capacity [TIBC], transferrin saturation [TSAT]), hemoglobin, and proportion of patients using intravenous (IV) iron supplementation were measured at various intervals within the 52-week efficacy evaluation period in patients with NDD or ID-DD CKD. The Figure displays change from baseline (CFB), least squares mean difference (LSMD), 95 % confidence interval (95 % CI), and *P* value for each iron metabolism parameter.

Results: In total, 2129 patients were evaluated (1078 roxadustat, 1051 ESA). Hemoglobin levels increased from baseline to Weeks 28–52 for patients receiving roxadustat with NDD/ID-DD CKD compared to ESA active controls (*P* = 0.0153). Treatment with roxadustat was associated with increased serum iron (*P* = 0.0003) and TIBC (*P* < 0.0001) from baseline to Week 20 compared to treatment with ESA. Ferritin and TSAT did not significantly change from baseline to Week 20 in patients with NDD/ID-DD CKD receiving roxadustat. Fewer patients receiving roxadustat received IV iron supplementation at Week 52 (*P* < 0.0001).

Conclusion: Compared with ESA, roxadustat treatment was associated with improvement in iron metabolism while achieving a statistically significant increase in hemoglobin levels in patients with anemia of NDD or ID-DD CKD.

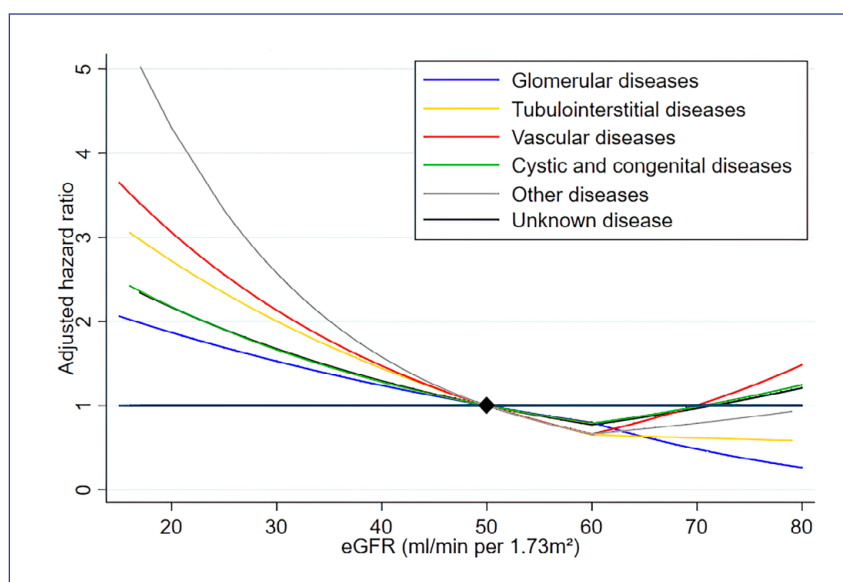
P038

Consistency of the Association between Measures of Chronic Kidney Disease and Mortality in the GCKD Cohort, Stratified by Cause of Kidney Disease

J. Scheppach; A. H. Arsiwala¹;
M. P. Schneider²; M. Grams³; J. Coresh³;
K.-U. Eckardt

Medizinische Klinik mit Schwerpunkt Nephrologie und Internistische Intensivmedizin, Campus Charité Mitte, Charité – Universitätsmedizin Berlin, Berlin; ¹Dr. Vasantrao Pawar Medical College, Hospital and Research Centre, Nashik/IND; ²Medizinische Klinik 4, Nephrologie und Hypertensiologie, Universitätsklinikum, Friedrich-Alexander-Universität Erlangen-Nürnberg, Erlangen; ³Bloomberg School of Public Health, Johns Hopkins University, Baltimore/USA

Objective: Chronic kidney disease is a considerable global public health burden affecting more than 10 % of the world's population and leading to increased morbidity and mortality. It is classified based on cause of kidney disease, estimated glomerular filtration rate (eGFR) and albuminuria, but risk prediction is mainly based on eGFR and albuminuria. To better understand the impact of cause of kidney disease on mortality risk, we evaluated its impact on the association between kidney disease measures and all-cause mortality. **Method:** We studied 5,214 adult patients with mild to moderate chronic kidney disease in the German Chronic Kidney Disease (GCKD) study, where the treating nephrologists assessed the leading cause of kidney disease. We grouped causes according to the kidney disease: Improving Global



P038: Abb. 1

Adjusted HR of the interaction between cause of kidney disease and the association of eGFR and mortality, reference at 50 ml/min per 1.73 m², spline at 60 ml/min per 1.73 m².

Adjusted for age, sex, systolic blood pressure, smoking, diabetes, body mass index, history of cardiovascular and log-UACR.

Outcomes (KDIGO) guideline into the categories of glomerular diseases, tubulointerstitial diseases, vascular diseases, cystic and congenital diseases, other diseases and unknown disease. The independent and joint association of eGFR and urinary albumin-creatinine-ratio (UACR) with all-cause mortality was assessed using Cox proportional hazards models, using age, sex, systolic blood pressure, smoking, diabetes, body mass index and history of cardiovascular disease as covariates. We tested for interaction between eGFR and UACR with cause of kidney disease in a Cox proportional hazards model. **Results:** We observed 707 deaths over 6.5 years of follow-up. Risk of mortality increased with lower eGFR and higher UACR in each of the causes of kidney disease. Compared to the reference category

of eGFR ≥ 60 ml/min per 1.73 m² and UACR < 30 mg/g, the risk of death during 6.5 years of follow-up in the category with eGFR < 30 ml/min and UACR > 300 mg/g was increased threefold (HR: 3.02, 95 % CI: 1.57–5.80, $p = 0.001$). Interaction terms between eGFR and cause of kidney disease as well as between albuminuria and cause of kidney disease did not show evidence of interaction.

Conclusion: Both lower eGFR and higher albuminuria were independent risk factors for all-cause mortality in patients with chronic kidney disease. There was no interaction between the cause of kidney disease and kidney disease measures in the prediction of death from all causes. KDIGO staging of mortality risk by eGFR and albuminuria is valid across different causes of kidney disease.

P039

Vitamin D Status and Its Association with Parathyroid Hormone in 23,134 Outpatients

X. Chen; C. Chu; C. Doebis¹; Y. Xiong²; Y. Cao; B. K. Krämer³; V. von Baehr¹; B. Hoher³

Medizinische Klinik mit Schwerpunkt Nephrologie, Campus Charité Mitte, Charité – Universitätsmedizin Berlin, Berlin; ¹IMD Institut für Medizinische Diagnostik Berlin-Potsdam GbR, Berlin; ²Physiologie und Pathophysiologie der Ernährung, Institut für Ernährungswissenschaft, Universität Potsdam, Potsdam; ³Nephrologie, Endokrinologie, Rheumatologie, V. Medizinische Klinik, Universitätsmedizin Mannheim, Mannheim

Objective: In vitro studies indicate that 25-hydroxyvitamin D3 (25(OH)D3) and 1,25-dihydroxyvitamin D3 (1,25(OH)2D3) inhibits the synthesis of parathyroid hormone (PTH). The degree of PTH inhibition in humans by circulating 25(OH)D and 1,25(OH)2D may be different. Moreover, age and sex as well as confounding factors like calcium and phosphate may likewise affect the relationship between

vitamin D and PTH in humans. However, this was not done so far in adequately powered studies.

Method: We investigated the relationship between 25(OH)D as well as 1,25(OH)2D and intact parathyroid hormone (iPTH) in 23,134 outpatients (age mean: 59.81 years) from the Berlin-Brandenburg area of Germany with normal serum creatinine considering confounding factors like age, sex, calcium and phosphate.

Results: 25(OH)D and iPTH were inversely correlated ($r = -0.17$, $p < 0.0001$). The inverse linear correlation was observed over the entire spectrum of 25(OH)D concentrations – from low 25(OH)D concentrations to very high 25(OH)D concentrations. Multiple linear regression analysis revealed that this correlation was independent of age, sex, creatinine, calcium and phosphate (unstandardized coefficients B: -0.16 , $p < 0.0001$). However, 1,25(OH)2D was only positively associated with iPTH in women ($r = 0.05$, $p = 0.033$) and in the subgroup of patients with lower 25(OH)D (25(OH)D < 40 ng/ml) ($r = 0.09$, $p < 0.0001$), which was also presented in multiple linear

regression analysis (unstandardized coefficients B: 0.20 , $p = 0.001$).

Conclusion: Circulating 1,25(OH)2D does not contribute substantially to the regulation of PTH in middle aged and vitamin D sufficient outpatients from the Berlin-Brandenburg area of Germany with normal kidney function. Presumably, serum 25(OH)D that is converted to 1,25(OH)2D after uptake in the parathyroid chief cells plays the critical role.

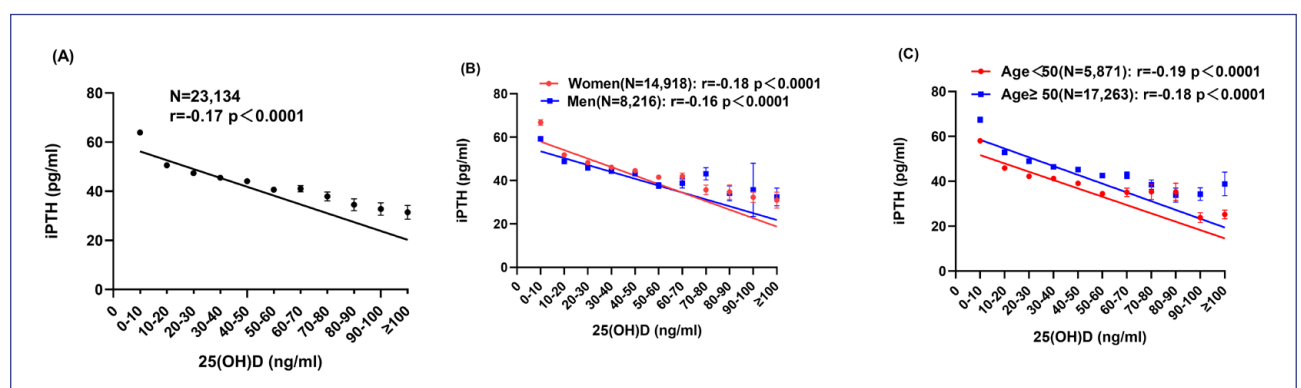
Chronisches Nierenversagen 3

P040

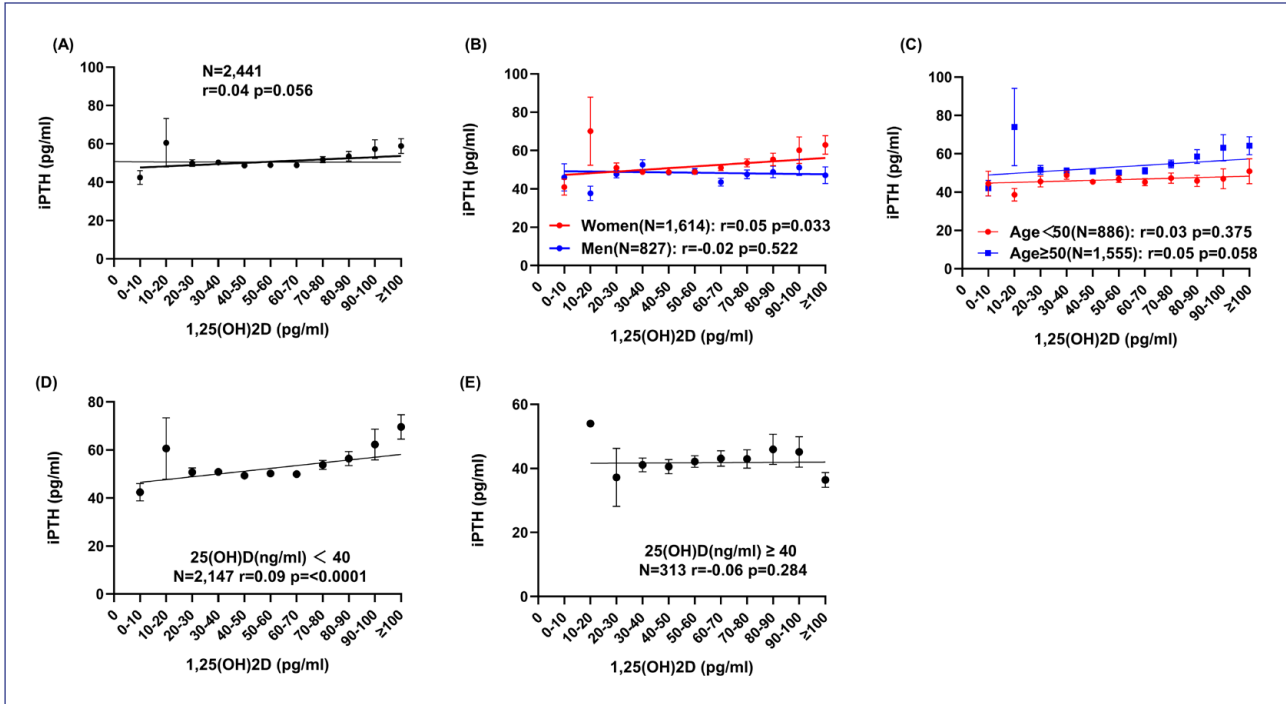
GUIDAGE-CKD – Leitlinien-gerechte Versorgung alter Patient*innen mit chronischer Nierenerkrankung

T. Bothe; E. Schäffner; N. Mielke; A. Schneider; M. Barghouth; D. Huscher¹; J.-F. O. Chenot²; C. Heintze³; N. Ebert

Institut für Public Health, Charité – Universitätsmedizin Berlin, Berlin; ¹Institut für Biometrie und Klinische Epidemiologie, Charité – Universitätsmedizin Berlin, Berlin; ²Abteilung für Nephrologie und Hypertensiologie, Klinik und Poliklinik für Innere Medizin A, Universitätsmedizin



P039: Abb. 1



P039: Abb. 2

Tabelle 1: Soziodemographische Variablen und Prävalenz von CKD für beide Studienpopulationen.

Population	Variable	Baseline	Follow-Up 1	Follow-Up 2	Follow-Up 3	Follow-Up 4
Gesamt	N ¹	2.068	1.670	1.396	1.130	870
	Alter, MW (SD)	80,4 (6,7)	81,8 (6,4)	83,1 (6,1)	84,3 (5,6)	85,6 (5,3)
	Frauen, N (%)	1.088 (52,6)	889 (53,2)	754 (54,0)	618 (54,7)	487 (56,0)
	Verstorben ³ , N (%)	127 (6,1)	143 (8,6)	152 (10,9)	119 (10,5)	103 (11,8)
	eGFR _{BISZ} , MW (SD)	58,1 (15,2)	55,5 (15,0)	51,4 (13,6)	50,2 (13,5)	48,3 (13,3)
	eGFR _{CKD} , MW (SD)	60,4 (15,9)	58,5 (16,2)	57,5 (16,0)	55,6 (15,8)	54,2 (15,9)
	CKD Stadien ⁴ , N (%)					
	Stadium 1	33 (1,6)	12 (0,7)	2 (0,1)	2 (0,2)	2 (0,2)
	Stadium 2	938 (45,4)	647 (38,7)	390 (27,9)	277 (24,5)	160 (18,4)
	Stadium 3	1.020 (49,3)	924 (55,3)	906 (64,9)	766 (67,8)	630 (72,4)
	Stadium 4	75 (3,6)	86 (5,1)	95 (6,8)	83 (7,3)	77 (8,9)
	Stadium 5	2 (0,1)	1 (0,1)	3 (0,2)	2 (0,2)	1 (0,1)
Vollständige Beobachtung ²	N	820	820	820	820	820
	Alter, MW (SD)	77,4 (5,3)	79,5 (5,2)	81,5 (5,3)	83,5 (5,3)	85,6 (5,3)
	Frauen, N (%)	450 (54,9)	450 (54,9)	450 (54,9)	450 (54,9)	450 (54,9)
	eGFR _{BISZ} , MW (SD)	63,3 (13,5)	59,7 (13,2)	54,3 (12,4)	51,9 (12,9)	48,4 (13,1)
	eGFR _{CKD} , MW (SD)	65,4 (13,7)	62,4 (14,2)	60,3 (14,6)	57,2 (15,2)	54,3 (15,8)
	CKD Stadien ⁴ , N (%)					
	Stadium 1	19 (2,3)	7 (0,9)	0 (0,0)	1 (0,1)	2 (0,2)
	Stadium 2	487 (59,4)	409 (49,9)	282 (34,4)	231 (28,2)	146 (17,8)
	Stadium 3	304 (37,1)	393 (47,9)	509 (62,1)	547 (66,7)	602 (73,4)
	Stadium 4	10 (1,2)	11 (1,3)	29 (3,5)	41 (5,0)	69 (8,4)
	Stadium 5	0 (0,0)	0 (0,0)	0 (0,0)	0 (0,0)	1 (0,1)

¹ N bezieht sich auf die Personen mit validen eGFR-Messungen zu der jeweiligen Studienvsiste. Aufgrund fehlender Laborwerte ausgeschlossen waren: N = 1, 29, 44, 36 und 74 (Baseline – Follow-Up 4). ² Vollständige Beobachtung bezieht sich auf Personen, die an jeder Studienvsiste teilgenommen und valide eGFR Messungen zu jeder Vsiste haben.

³ Verstorben₂ wurde berechnet als die Anzahl an Personen, die innerhalb von 2 Jahren nach ihrem jeweiligen Visitedatum verstorben sind. ⁴ CKD Stadien wurden berechnet mittels der eGFR_{BISZ}. Abkürzungen: MW: Mittelwert; SD: Standardabweichung.

P040: Tab. 1

Greifswald, Greifswald; ³ Institut für Allgemeinmedizin, Charité – Universitätsmedizin Berlin, Berlin

Hintergrund: Aufgrund des demographischen Wandels steigt die Bedeutsamkeit von chronischen Erkrankungen, auch von chronischer Nierenerkrankung (CKD). Über die ambulante hausärztliche leitliniengerechte Versorgungssituation von älteren Patient*innen mit CKD bestehen derzeit wenige Kenntnisse.

Methode: In 4 konsekutiven Modulen sollen im Rahmen des Innovationsfonds-Projektes GUIDAGE-CKD Qualitätsindikatoren (QI) der ambulanten hausärztlichen Versorgung für ältere Patient*innen mit CKD entwickelt und validiert werden. Dafür werden QIs anhand von Leitlinien entwickelt und durch Expert*innen konsentiert (Modul 1). Im Anschluss werden Operationalisierungen der QIs in GKV-Routinedaten der AOK Nordost durch Abgleiche mit Primärdaten selbiger Studienteilnehmer*innen (alle AOK-versichert) anhand der Berliner Initiative Studie (BIS) validiert (Modul 2). Diese sollen genutzt werden, um die Versorgungssituation anhand umfangreicher Routinedaten von N = 250.000 Versicherten zu untersuchen (Modul 3). Anschließend sollen Hindernisse und Lösungsansätze für die Leitlinienimplementierung durch Interviews mit Hausarzt*innen identifiziert werden (Modul 4). **Ergebnisse:** Die Entwicklung der QIs aus Modul 1 ist abgeschlossen. Ein konsentiertes finalisiertes Set von 8 QIs befindet sich derzeit in der Vorbereitung zur Veröffentlichung. **Zusammenfassung:** GUIDAGE-CKD bietet die Möglichkeit, unter Einbeziehung verschiedener

Perspektiven (Nephrologie, Allgemeinmedizin, Geriatrie, Patient*innenvertretung) eine umfassende Beschreibung der hausärztlichen Versorgungssituation von älteren Patient*innen mit CKD zu ermöglichen und Unter- bzw. Überversorgung aufzudecken. Dies kann potentiell zu einer Verbesserung der Versorgungssituation für ältere CKD-Patient*innen und Behandelnde beitragen.

P041

Modeling disease progression by age-adjusted liver volumes and genetic determination in polycystic liver disorders

D. Sierks; R. Schönauer¹; A. Friedrich²; E. Hantmann¹; N. Linder³; J. Fischer⁴; A. Herber⁴; C. Bergmann²; T. Berg⁴; J. Halbritter¹

Sektion Nephrologie, Klinik für Endokrinologie und Nephrologie, Universitätsklinikum Leipzig, Leipzig; ¹ Medizinische Klinik mit Schwerpunkt Nephrologie und Internistische Intensivmedizin, Campus Charité Mitte, Charité – Universitätsmedizin Berlin, Berlin; ² Medizinische Genetik Mainz, Limbach Genetics GmbH, Mainz; ³ Radiologie, Universitätsklinikum, Leipzig; ⁴ Fachbereich Gastroenterologie/Hepatologie, Medizinische Klinik und Poliklinik II, Universitätsklinikum Leipzig A. ö. R., Leipzig

Objective: Polycystic liver disease (PLD) manifests with numerous fluid-filled cysts scattered throughout the liver parenchyma. PLD most commonly develops in females, either as extra-renal manifestation of autosomal-dominant polycystic kidney disease (ADPKD) or as isolated polycystic liver disease (ADPLD). Despite known genetic causes, clinical variability challenges patient

counselling and timely risk prediction is hampered by a lack of genotype-phenotype correlations and prognostic imaging classifications.

Method: We analyzed a cohort of 80 deeply-characterized PLD patients for the underlying genetic defect. Identified genotypes were correlated with total liver and kidney volume (TLV/TKV), organ function, co-morbidities, and clinical endpoints.

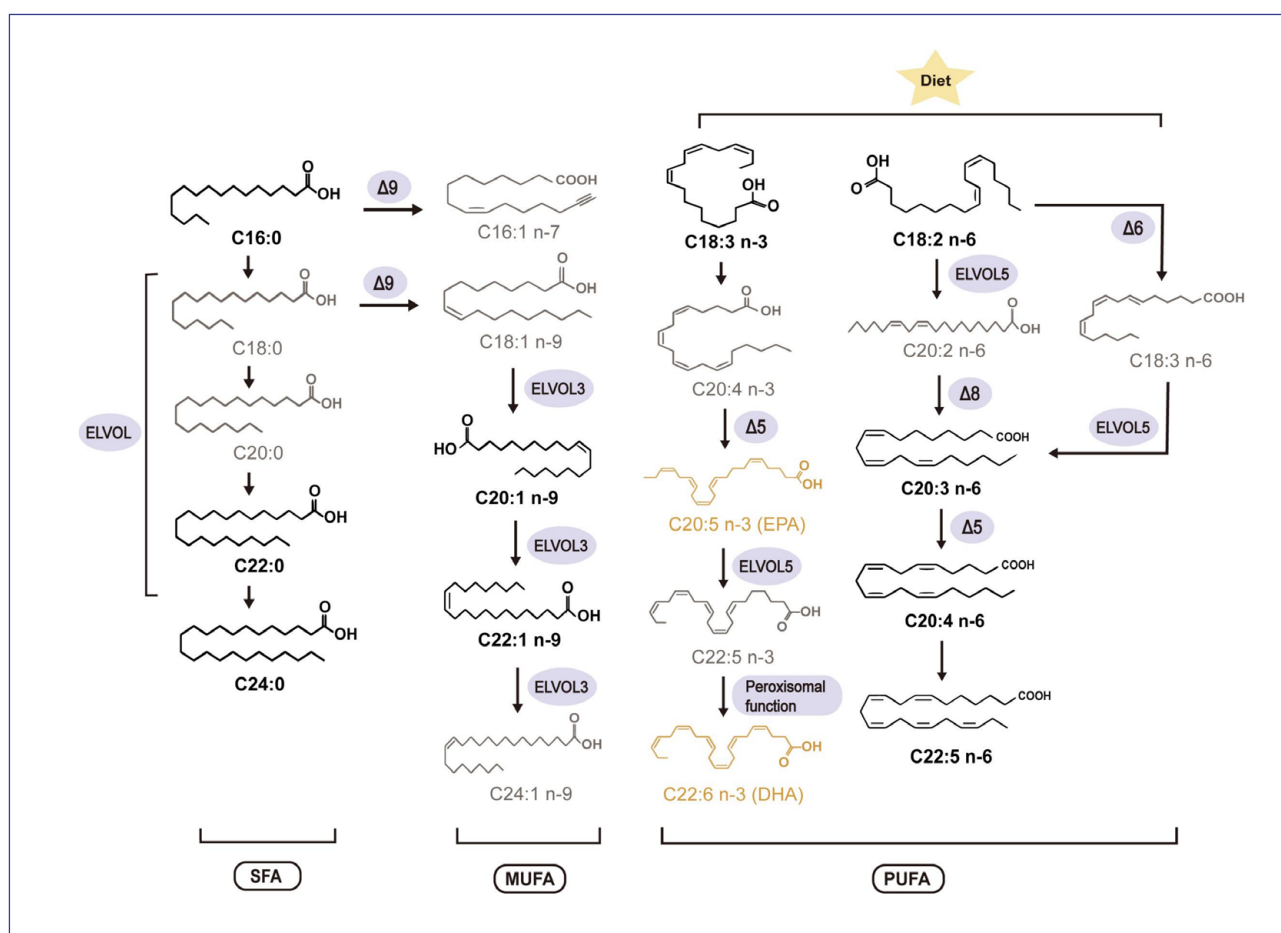
Results: Monoallelic diagnostic variants were identified in 60 (75 %) patients, 38 (48 %) of which pertained to ADPKD-gene variants (*PKD1*, *PKD2*, *GANAB*) and 22 (27 %) to ADPLD-gene variants (*PRKCSH*, *SEC63*). Disease severity defined by age at waitlisting for liver transplantation and first liver complication was significantly more pronounced in mutation carriers as compared to patients without genetic diagnoses. While current imaging classifications proved unable to differentiate between severe and moderate courses, grouping by estimated age-adjusted TLV progression yielded significant risk discrimination.

Conclusion: This study underlines the predictive value of providing a molecular diagnosis for patients with PLD. By defining groups of age- and height-adjusted TLV, we propose a novel imaging-based risk-classification in order to improve individual prognostication and personalized clinical management.

P042

Bioakkumulation von langkettigen Fettsäuren im Blut während der Hämodialyse

T. Liu; I. Dogan; M. Rothe¹; J. Reichardt²; F. Knauf³; M. Gollasch; F. C. Luft; B. Gollasch⁴ ECRC-Kooperation von MDC und Charité,



P042: Abb. 1

Experimental and Clinical Research Center, Berlin; ¹ Lipidomix GmbH, Berlin; ² Medizinische Klinik mit Schwerpunkt Internistische Intensivmedizin und Nephrologie, Campus Virchow-Klinikum, Charité – Universitätsmedizin Berlin, Berlin; ³ Medizinische Klinik mit Schwerpunkt Nephrologie und Internistische Intensivmedizin, Campus Charité Mitte, Charité – Universitätsmedizin Berlin, Berlin; ⁴ Klinik und Poliklinik für Kardiologie und Nephrologie, HELIOS Klinikum Berlin-Buch, Berlin

Objective: Long-chain fatty acids (LCFAs) serve as energy sources, components of cell

membranes, and precursors for signaling molecules. Uremia alters LCFA metabolism so that the risk of cardiovascular events in chronic kidney disease (CKD) is increased. End-stage renal disease (ESRD) patients undergoing dialysis are particularly affected and their hemodialysis (HD) treatment could influence blood LCFA bioaccumulation and transformation. Our previous studies have shown that a single HD session increased some fatty acids in the arteries. This study is the first to use the arteriovenous (AV) differences of LCFAs to respond to their biotransformation,

either by release, storage, or consumption in vivo. The aim is to further understand the specific effects of HD on LCFAs.

Method: We selected 12 participants to collect arterial blood from arteriovenous fistulas and peripheral venous blood from the ipsilateral upper extremity before and after hemodialysis and measured LCFAs in erythrocytes and plasma by high performance liquid chromatography-mass spectrometry.

Results: We observed that differences in arterial and venous LCFAs contents within erythrocytes (AV differences) were affected

Table 1. Effects of hemodialysis on individual fatty acids in RBC in the CKD patients before (Pre-HD) and at cessation (Post-HD) of hemodialysis

Fatty Acids	Chain	Pre-HD Median (IQR)				Post-HD Median (IQR)			
		pre-HD Arterial	pre-HD Venous	p value, t test	pre-HD A-V difference	post-HD Arterial	post-HD Venous	p value, t test	post-HD A-V difference
				(# paired Wilcoxon test)				(# paired Wilcoxon test)	
Total-RBC (µg/g)									
Myristic Acid	C14:0	22.83 (17.21–26.87)	26.27(19.64–29.9)	0.084	-2.47 (-6.70–0.20)	26.09(19.78–31.59)	22.34(20.05–36.54)	0.465	0.29 (-4.18–2.78)
Myristolein acid	C14:1 n-5	0.12 (0–0.31)	0.04 (0–0.26)	0.889#	0 (-0.14–0.06)	0.30 (0–0.53)	0.13 (0.05–0.60)	0.182#	-0.06 (-0.19–0.00)
Palmitic acid	C16:0	338.15 (267.59–458.51)	400.18 (294.72–538.39)	0.032	-40.61 (-152.84–0.79)	367.43 (304.75–437.36)	343.50 (293.53–500.62)	0.308#	-5.55 (-78.39–30.19)
Palmitoleic acid	C16:1 n-7	16.34 (12.68–20.67)	20.82(14.82–21.7)	0.091	-2.96 (-6.93–0.11)	17.38(14.05–21.25)	17.99 (13.76–28.05)	0.083	-0.95 (-8.51–0.51)
Stearic acid	C18:0	244.11 (212.57–299.70)	236.32 (227.66–389.72)	0.05#	-30.10 (-88.64–0.08)	229.34 (219.53–263.88)	233.45 (212.47–281.02)	0.583#	-2.16 (-12.04–7.65)
Oleic acid	C18:1 n-9	281.48 (269.48–321.05)	340.48 (276.50–421.20)	0.06#	-31.17 (-53.72–1.62)	318.61 (299.01–371.41)	348.14 (292.85–372.47)	0.269	0.69 (-52.06–9.26)
Linoleic acid	C18:2 n-6	224.08 (210.52–245.12)	283.47 (208.23–314.04)	0.041#	-27.40 (-62.49–1.26)	233.85 (224.40–307.23)	261.82(220.05–285.12)	0.48#	-3.81 (-58.30–14.18)
α-Linoleic acid	C18:3 n-3 alpha	4.47 (2.93–5.83)	4.80(3.55–9.54)	0.034#	-1.13 (-1.73–0.27)	4.79 (3.94–8.60)	5.39 (4.01–8.29)	0.53#	-0.20 (-0.85–0.54)
Eicosenoic acid	C20:1 n-9	5.77 (4.36–7.05)	6.74 (5.83–7.28)	0.031	-0.39 (-2.04–0.09)	5.78 (4.81–6.50)	6.06 (4.89–6.91)	0.084#	-0.55 (-0.90–0.08)
Eicosa-dienoic acid	C20:2 n-6	4.07 (3.37–4.71)	4.52 (4.20–5.11)	0.18	-0.19 (-0.89–0.05)	4.07 (3.70–4.42)	4.08 (3.97–4.39)	0.239#	-0.05 (-0.26–0.03)
Dihomo-γ-Linoleic acid	C20:3 n-6	32.67 (25.93–36.58)	39.14(34.52–41.1)	0.013	-4.21 (-7.15–0.53)	33.33(29.99–37.48)	33.25 (27.50–38.73)	0.741	0.18 (-4.75–2.72)
Arachidonic acid	C20:4 n-6	269.51 (261.38–284.76)	280.99 (265.66–368.67)	0.015#	-16.98 (-64.07–7.21)	298.17 (278.64–311.91)	292.51 (279.77–297.85)	0.281	15.27 (-13.87–23.51)
Eicosapenta-enoic acid	C20:5 n-3	12.14 (8.77–15.25)	13.31(8.18–15.87)	0.738	-1.15 (-3.98–0.325)	13.53 (9.58–15.27)	12.40 (9.47–14.47)	0.465	-0.08 (-1.21–1.70)
Docosanoate	C22:0	2.67 (2.25–4.06)	3.14 (2.48–6.08)	0.019#	-0.60 (-2.53–0.07)	2.84 (2.55–4.02)	3.06 (2.44–3.64)	0.638#	0.04 (-0.30–0.45)
Erucic acid	C22:1 n-9	6.34 (6.01–7.58)	7.86 (7.41–10.78)	0.019#	-1.25 (-4.76–0.81)	6.28 (5.79–6.63)	6.75 (6.03–7.20)	0.308#	-0.47 (-1.13–0.28)
Docosa-pentaenoic acid ω-3	C22:5 n-3	36.45(34.87–39.67)	40.71 (37.68–51.77)	0.084#	-2.10 (-7.69–1.23)	39.81 (37.32–43.06)	38.28 (37.40–41.89)	0.399	1.19 (-1.34–2.49)
Docosapentaenoic acid ω-6	C22:5 n-6	4.76 (3.29–5.37)	5.63 (4.83–6.07)	0.012	-0.80 (-1.36–0.42)	4.88 (3.96–5.81)	5.26 (4.57–5.58)	0.574	-0.08 (-0.33–0.28)
Docosahexa-enoic acid	C22:6 n-3	197.74 (167.70–213.22)	200.35 (173.02–240.19)	0.088	-26.82 (-42.02–2.05)	192.05 (166.18–226.80)	190.91 (169.06–223.00)	0.59	2.53 (-10.01–9.29)
Lignoceric acid	C24:0	5.30 (4.36–7.14)	6.62 (5.32–11.02)	0.032	-1.44 (-3.46–0.20)	5.39 (4.74–6.76)	5.56 (4.53–7.14)	0.239#	0.62 (-0.42–1.05)
Nervonic acid	C24:1 n-9	10.63 (8.84–12.71)	12.09 (11.19–13.12)	0.112	-0.14 (-3.93–0.27)	11.45 (9.68–13.23)	10.57 (9.73–13.22)	0.921	0.24 (-0.72–0.85)

Notes: A, arterial blood; V, venous blood. Median (IQR). A-V difference; arteriovenous difference.

Table 2. Effects of hemodialysis on total fatty acids in RBC in the CKD patients before (Pre-HD) and at cessation (Post-HD) of hemodialysis.

Fatty Acids	Pre-HD Median (IQR)				Post-HD Median (IQR)			
	pre-HD	pre-HD	p value, t test	pre-HD A-V	post-HD	post-HD	p value, t test	post-HD A-V
	Arterial	Venous	(# paired Wilcoxon test)	difference	Arterial	Venous	(# paired Wilcoxon test)	difference
Total-RBC (µg/g)								
Total SFA	595.703	670.018		-56.325	624.941	591.402		-28.462
	(513.040	(553.384	0.027	(-277.577	(551.351	(534.765	0.182#	(-94.268 –
	-757.739)	-972.688)		-2.217)	-746.70)	-831.952)		36.130)
Total MUFA	322.825	387.006		-46.965	376.076	394.564		-5.169
	(305.306	(329.542	0.034#	(-63.638 –9.095)	(332.646	(330.508	0.188	(-62.982 –
	-380.602)	-476.590)			-409.804)	-432.247)		7.602)
PUFA n-3	257.166	261.911		-37.862	246.884	246.460		4.399
	(218.402	(235.961	0.078	(-48.270 –4.691)	(223.435	(218.649	0.579	(-11.394 –
	-273.419)	-312.850)			-303.050)	-284.657)		14.169)
PUFA n-6	538.579	625.916		-46.288	588.363	605.591		15.263
	(527.422	(544.230	0.008#	(-97.802	(554.219	(539.772	0.814#	(-80.730 –
	-560.087)	-707.882)		-19.074)	-649.017)	-637.355)		38.335)
Total-PUFA	784.818	905.273		-78.630	876.443	843.795		33.365
	(758.405	(795.178	0.023#	(-162.449	(778.130	(801.30	0.937#	(-92.123 –
	-818.550)	-1041.732)		-37.522)	-892.759)	-888.677)		67.535)

Notes: A, arterial blood; V, venous blood. Median (IQR). A-V difference; arterio-venous difference.

P042: Tab. 2

Table 3. Effect of hemodialysis on polyunsaturated fatty acid ratios in RBC in the CKD patients before (Pre-HD) and at cessation (Post-HD) of hemodialysis.

Ratio	Pre-HD Median (IQR)			Post-HD Median (IQR)		
	pre-HD Arterial	pre-HD Venous	p value, t test	post-HD Arterial	post-HD Venous	p value, t test
			(# paired Wilcoxon test)			(# paired Wilcoxon test)
Total-RBC						
Omega-3 quotient	11.07 (9.63–13.06)	11.37 (7.71 –12.17)	0.776	11.37 (9.73 –12.38)	11.37 (8.30 –12.54)	0.217
DHA+EPA/AA	0.75 (0.59 –0.82)	0.65 (0.52 –0.90)	0.835	0.73 (0.56 –0.80)	0.70 (0.61 –0.81)	0.851
EPA/AA	0.04 (0.03 –0.05)	0.03 (0.03 –0.05)	0.445	0.04 (0.03 –0.05)	0.04 (0.03 –0.05)	0.575
DHA/AA	0.71 (0.57 –0.76)	0.62 (0.50 –0.84)	0.908	0.69 (0.52 –0.73)	0.66 (0.58 –0.74)	0.759
DHA/EPA	16.1(12.81 –18.59)	15.26 (14.59 –21.71)	0.814#	16.42 (12.26 –18.76)	17.38 (13.46 –20.36)	0.929
n-3/n-6	0.44 (0.44 –0.49)	0.41 (0.35 –0.50)	0.822	0.44 (0.36 –0.48)	0.41 (0.38 –0.46)	0.356

Notes: A, arterial blood; V, venous blood. Median (IQR).

P042: Tab. 3

by HD treatment. Numerous saturated fatty acids (SFA), monounsaturated fatty acids (MUFA), and polyunsaturated fatty acids (PUFA) n-6 showed negative AV differences, accumulated during peripheral tissue perfusion of the upper limbs, in erythrocytes before HD (Table 1–2). HD reduced these differences. The omega-3 quotient {[Eicosapentaenoic acid (EPA) + docosahexaenoic acid (DHA)]/total FAs} in the erythrocyte membranes was not affected by HD in either arterial or venous blood (Table 3). However, LCFAs in plasma did not show any differences (Results not presented). To see whether desaturase activities were affected by single HD treatment, we calculated the following ratios: C18:3 n-6/C18:2 n-6 ratio, representing $\Delta 6D$, C20:4 n-6/C20:3 n-6 ratio, representing $\Delta 5D$, C16:1 n-7/C16:0 and C18:1 n-9/C18:0 ratios, representing $\Delta 9D$ and DHA/DPA peroxisome functions, respectively (Figure 1). The results show that pre-HD or post-HD values were not statistically significant in either plasma or erythrocytes.

Conclusion: Our data demonstrate that AV differences in fatty acids status of LCFAs are present and active in mature erythrocytes and their bioaccumulation is sensitive to single HD treatment.

P043

Assoziationen der Schilddrüsenfunktion mit einer erniedrigten geschätzten glomerulären Filtrationsrate und Albuminurie – Ergebnisse einer populations-basierten Studie

T. Ittermann¹; S. Frein von Rheinbaben¹; M. Markus²; M. Dörr²; A. Steveling³; M. Nauck⁴; H. Völzke⁵; S. Stracke¹

Study of Health in Pomerania – Klinisch-epidemiologische Forschung (SHIP-KEF), Institut für Community Medicine, Ernst-Moritz-Arndt-Universität Greifswald, Greifswald; ¹ Abteilung für Nephrologie und Hypertensiologie, Klinik und Poliklinik für Innere Medizin A, Universitätsmedizin Greifswald, Greifswald; ² Kardiologie, Angiologie, Intensivmedizin, Klinik und Poliklinik für Innere Medizin B, Universitätsmedizin Greifswald, Greifswald; ³ Endokrinologie, Klinik und Poliklinik für Innere Medizin A, Ernst-Moritz-Arndt-Universität Greifswald, Greifswald; ⁴ Institut für Klinische Chemie und Laboratoriumsmedizin, Universitätsmedizin Greifswald, Greifswald; ⁵ Institut für Epidemiologie und Sozialmedizin, Universitätsklinik Greifswald, Greifswald

Objective: The severity of chronic kidney disease can be estimated by the “Kidney Disease Improving Global Outcomes” (KDIGO) definition, which uses measurements of glomerular filtration rate (GFR) and albuminuria. Low GFR and albuminuria are both risk factors for cardiovascular events and mortality. Hypothyroidism may be associated

with a low glomerular filtration rate (GFR) via a reduced renal blood flow. Likewise, hypothyroidism may lead to an increased risk for albuminuria due to its effect on the cardiovascular system. The aim of our study was to investigate associations of thyroid hormone levels with estimated GFR (eGFR) and albuminuria in a population-based setting.

Method: We analysed cross-sectional data from 6,136 individuals of a population-based study without self-reported kidney disease. eGFR was defined creatinine-based according to the FAS formula.

Low eGFR was defined as an eGFR < 60 mL/min. Albuminuria was defined as an albumin-creatinine-ratio ≥ 30 mg/g. Serum levels of thyroid-stimulating hormone (TSH), free triiodothyronine (fT3), and free thyroxine (fT4) were measured. Associations of thyroid hormone levels with eGFR and albuminuria were analysed by logistic regression models adjusted for confounding.

Results: High TSH, low fT3, and high fT4 were associated with a low eGFR. Serum levels of TSH and fT4 were positively associated

	Low eGFR	Albuminuria
	Odds ratio (95% confidence interval)	Odds ratio (95% confidence interval)
TSH; mIU/L	1.14 (1.07; 1.21)*	1.06 (1.02; 1.11)*
fT3; pmol/L	0.58 (0.49; 0.69)*	0.89 (0.78; 1.02)
fT4; pmol/L	1.05 (1.01; 1.10)*	1.05 (1.01; 1.08)*

Logistic regression models adjusted for age, sex, and smoking.
*p<0.05

P043: Abb. 1

with albuminuria, while the inverse association between serum fT3 levels and albuminuria missed statistical significance.

Conclusion: The observed associations of high TSH and low fT3 with a low eGFR argue for an association of hypothyroidism with a lower renal function. Associations of thyroid hormone levels with albuminuria showed a less clear picture. The observation that both TSH and fT4 were positively associated with a low eGFR and albuminuria needs further investigation.

P044

Nephrogenetische Fälle aus der humangenetischen Praxis – eine retrospektive Studie

U. T. Schultheiß¹; T. Hermle¹; N. Meier²; A. Köttgen; J. Kohlbase²

Medizin IV, Nephrologie und Institut für genetische Epidemiologie, Universitätsklinikum, Albert-Ludwigs-Universität Freiburg, Freiburg; ¹ Medizinische Klinik IV/ Abteilung Nephrologie, Universitätsklinikum, Albert-Ludwigs-Universität Freiburg, Freiburg; ² Synlab MVZ Humangenetik Freiburg, Freiburg

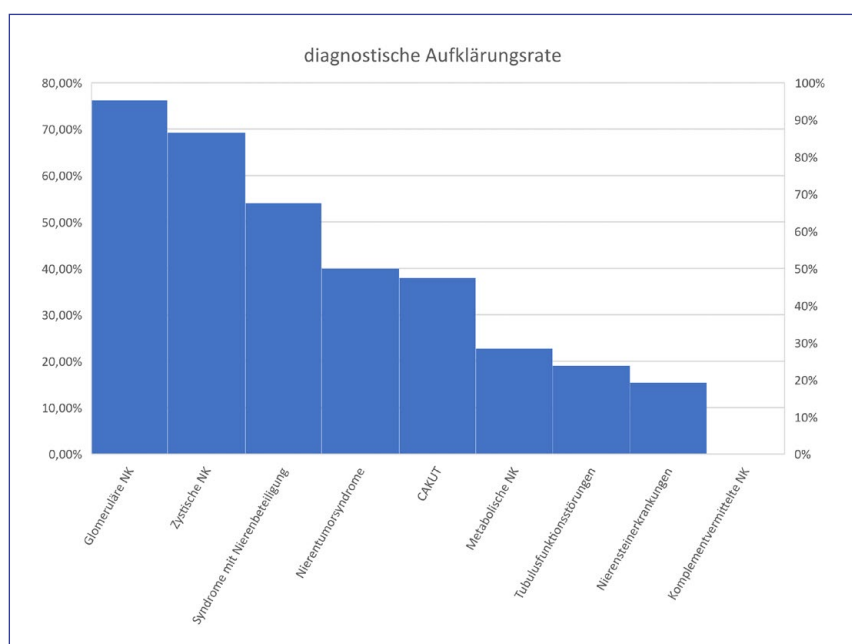
Hintergrund: Chronische Nierenerkrankung (CKD) kann genetisch bedingt sein. Es gibt > 600 Gene, die mit einer Nieren/Urogenitalerkrankung assoziiert sind. Bei positiver Familienanamnese für terminale Niereninsuffizienz (KF) haben Familienmitglieder ein 7-fach erhöhtes Risiko, auch eine KF zu entwickeln. Bei Patienten mit monogener Ursache der Nierenerkrankung (NK) in großen CKD/KRT-Patienten-Kohorten lagen in 63 % aller Fälle Mutationen in sechs bekannten Genen vor (*PKD1*, *PKD2*, *COL4A5*, *COL4A3*, *COL4A4*, *UMOD*). Wir führten eine retrospektive Auswertung

nephrogenetischer Fälle in einer allgemein-humangenetischen Praxis.

Methode: Über einen data mining Ansatz im Praxisinformationssystem wurden über 3 Jahre (2018–2022) Anfragen aus dem nephrogenetischen Spektrum extrahiert. Erkrankungen wurden in nephrogenetische Kategorien unterteilt: metabolische NK, zystische NK, kongenitale Anomalien der Niere und des Urogenitaltrakts (CAKUT), Nierensteinerkrankungen, Tubulusfunktionsstörungen, glomeruläre NK, Nierentumorsyndrome, komplementvermittelte NK, und sonstige syndromale Phänotypen mit Nierenbeteiligung. **Ergebnisse:** In drei Jahren wurden 353 nephrogenetische Anfragen inklusive 225 Betroffener mit einem nephrogenetischen Phänotyp und Überträger-Status-Anfragen untersucht. Innerhalb des nephrogenetischen Spektrums kamen die meisten Anfragen zu metabolischen

NK (21 %; inkl. Morbus Fabry, Cystinose, familiäres Mittelmeerfieber), 20 % zu Tubulusfunktionsstörungen (keine Anfrage zu *UMOD*), 14 % zu CAKUT, 12 % zu zystischen NK (> 69 % *PKD*-Gene), 10 % zu glomerulären NK (> 95 % Alport-Syndrom), 6 % zu Nierensteinerkrankungen, 5 % zu Nierentumorsyndrom und 1 % zu komplementvermittelten NK. Die diagnostische Aufklärungsrate bewegte sich zwischen 76 % für glomeruläre NK und 0 % für komplementvermittelte NK. Abbildung 1 gibt einen Überblick über die diagnostische Aufklärungsrate.

Zusammenfassung: Genetische Diagnostik wird aufgrund bedeutender Implikationen für Diagnosestellung, Behandlung, Patientenmanagement und Familienplanung bei CKD Patienten immer wichtiger. Obwohl bekannt ist, dass die meisten CKD Patienten



P044: Abb. 1

mit genetischen NK aus dem Bereich der zystischen/glomerulären NK stammen, scheinen diese Patienten nicht am häufigsten zur Abklärung überwiesen zu werden. Es ist wichtig, dass Nephrolog*innen bei diesen Kategorien an die Abklärung einer genetischen Ursache denken.

P045

Protein carbamylation is associated with increased mortality in patients with CKD: results from the EQUAL study

T. Foltmann¹; A. Haug; N. Chesnaye¹; G. Porto²; M. P. Szymczak³; M. Evans⁴; F. Caskey⁵; A. H. Berg⁶; C. Drechsler; C. Wanner

Medizinische Klinik und Poliklinik I, Abteilung für Nephrologie, Universitätsklinikum, Julius-Maximilians-Universität Würzburg, Würzburg;

¹ Department of Medical Informatics, ERA Registry, University of Amsterdam, Amsterdam/NL; ² Istituto di Fisiologia Clinica CNR, Pisa/I; ³ Department of Nephrology and Transplantation Medicine, Wrocław Medical University, Wrocław/PL; ⁴ Department of Clinical Science, Intervention and Technology, Karolinska Institute, Stockholm/S; ⁵ Population Health Sciences, University of Bristol, Bristol/UK; ⁶ Department of Pathology and Laboratory Medicine, Cedars-Sinai Medical Center, Los Angeles/USA

Objective: Urea that accumulates in CKD patients' blood sometimes spontaneously decomposes to reactive isocyanate which can irreversibly bind to lysine side chains of serum proteins in a reaction called carbamylation and can change proteins' function. Recent studies suggest a direct link between protein carbamylation and the pathogenesis of cardiovascular events and

all-cause mortality in dialysis patients. It is unclear whether protein carbamylation also plays a significant role in CKD patients not requiring dialysis. We investigated the hypothesis that carbamylation of albumin (C-Alb) is already present in patients with advanced CKD and is associated with increased mortality. We used a large patient population of the international EQUAL study.

Method: The European Quality Study on treatment in advanced chronic kidney disease (EQUAL) is a multicentre prospective cohort study of the ERA. CKD patients ≥ 65 years old from six countries (NL, DE, UK, IT, PL, SE) were recruited and followed up for four years. The study participants were non-dialysis patients with advanced stage of kidney disease at inclusion ($\text{eGFR} \leq 20 \text{ ml/min/1.73 m}^2$) and before starting dialysis therapy or transplantation. In a subgroup of 1114 patients, the C-Alb concentration was measured at the baseline visit using combined liquid chromatography and mass spectrometry.

Results: C-Alb correlated significantly with age, creatinine, urea, and negatively with eGFR; but not with total albumin. The mean C-Alb value was $13.47 \pm 6.54 \text{ mmol/mol}$. Men had higher C-Alb values than women (13.91 vs. 12.69 mmol/mol , $p = 0.003$), as did patients with chronic heart failure compared to patients without heart failure (15.35 vs. 13.10 mmol/mol , $p = < 0.001$). Patients in the highest C-Alb quartile had twice the mortality compared with patients from the lowest C-Alb quartile (HR 2.01, CI 95 % 1.53–2.64, $p = < 0.001$). Analyses were adjusted for potential confounders including age, sex, GFR, urea, albumin, Hb, K, PO_4 , EPO

medication and pre-existing conditions (diabetes, CVD, PVD, CHF, cerebrovascular disease, systolic BP, BMI). The adjusted risk of mortality was still significantly increased by 60 % for patients in the fourth quartile compared with patients in the first quartile (HR 1.59, CI95 % 1.06–2.39, $p = 0.025$).

Conclusion: In conclusion, we show that in non-dialysis patients, increased levels of protein carbamylation are associated with higher mortality. C-Alb may be of potential use as a risk marker in patients with CKD not yet on dialysis.

P046

Ernährungsgewohnheiten von Dialysepatienten im Vergleich zu ihrer Körperzusammensetzung

M. Zeiler; D. Stadler; C. Schmaderer II. Medizinische Klinik, Nephrologie, Klinikum rechts der Isar, Technische Universität München, München

Hintergrund: Im Spektrum der Komorbiditäten und Risikofaktoren von HD-Patienten rückt die Mangelernährung immer mehr in den wissenschaftlichen Fokus. Die zugrundeliegenden pathologischen Vorgänge (Protein-Energy-Wasting, Mikroinflammation) wurden in früheren Studien bereits untersucht. Ziel dieser Studie ist nun die Untersuchung eines möglichen Einflusses der Nährstoffaufnahme und Ernährungsgewohnheiten auf biochemische Surrogat-Marker sowie die Körperzusammensetzung.

Methode: Für die Diagnostik einer Mangelernährung wurden biochemische Surrogat-Parameter (Albumin, Transferrin) und die Körperzusammensetzung mittels bioelektrischer Impedanzanalyse (BIA) (Magermasse (LTM),

Körperfettmasse (ATM), aktive Zellmasse (BCM)) gemessen. Zur Erfassung der täglichen Nährstoffaufnahme und des subjektiven Essverhaltens unter Dialysetherapie wurde ein retrospektiver Fragebogen basierend auf dem Survey of Lifestyle, Attitudes and Nutrition (SLAN)-Fragebogen erstellt. Die Ergebnisse wurden mit einer in Alter und Geschlecht gematchten Kontrolle verglichen.

Ergebnisse: Zwischen den Vergleichsgruppen konnte ein signifikanter Unterschied in den laborchemischen Surrogat-Parametern der HD-Patienten ($n = 35$) festgestellt werden (Albumin: $3,98 \text{ g/dl} \pm 0,36$ vs. $4,72 \text{ g/dl} \pm 0,26$, $p < 0,001$; Transferrin: 178 mg/dl [$165,0\text{--}201,3$] vs. 269 mg/dl [$231,5\text{--}289,0$], $p < 0,001$). Bezüglich der Körperzusammensetzung konnte eine signifikant erhöhte ATM festgestellt werden, LTM und BCM waren an der unteren Signifikanzgrenze erniedrigt (ATM: $40,1 \text{ kg}$ [$31,6\text{--}60,2$] vs. $33,3 \text{ kg}$ [$26,2\text{--}43,6$], $p < 0,042$; LTM: $46,56 \%$ [$32,5\text{--}57,6$] vs. $51,3 \%$ [$43,2\text{--}57,5$], $p = 0,052$; BCM: $17,7 \text{ kg}$ [$12,0\text{--}49,7$] vs. $20,9 \text{ kg}$ [$15,5\text{--}24,3$], $p = 0,068$). Es bestand kein signifikanter Unterschied in der täglichen Nährstoffaufnahme. Im Vergleich zu den Ernährungsempfehlungen (KDIGO) zeigten sich signifikante Abweichungen für die Fett-, Ballaststoff-, Natrium-, Kalium- und Phosphatzufuhr. Es konnten keine signifikanten Korrelationen zwischen der täglichen Ernährung und der Körperzusammensetzung sowie zwischen Ernährung und biochemischen Markern festgestellt werden.

Zusammenfassung: Die Ergebnisse stimmen mit früheren Studien überein. Die geringen Korrelationen zwischen der Ernährung und

den biochemischen Markern bzw. der BIA ist durch diverse Einflussgrößen wie Inflammation, Überwässerung, Komorbiditäten und der Grunderkrankung sowie der Kohortengröße erklärbar. Daher sollte dies in einer größeren Stichprobe weiter untersucht und bestätigt werden.

P047

Validierung und Vergleich einer neuen Methode für eine schnelle und einfache Quantifizierung von Iohexol im Rahmen der Nierenfunktionsmessung

M. Babic; C. Goblisch¹; M. Tölle¹; M. Schuchardt¹; M. van der Giet¹; A.-M. Schulz¹

Medizinische Klinik für Nephrologie – Hochschulambulanz, Campus Benjamin Franklin, Charité – Universitätsmedizin Berlin, Berlin; ¹ Medizinische Klinik IV, Klinik für Nephrologie, Campus Benjamin Franklin, Charité – Universitätsmedizin Berlin, Berlin

Hintergrund: Die exakte Bestimmung einer Nierenfunktion (mGFR) im Alltag ist in der Regel sehr zeitaufwendig, in der Routine nur schwierig durchzuführen und kaum verfügbar. Die genutzten Abschätzungsformeln (eGFR) haben eine Variabilität von 20 %. Für eine präzise Bestimmung eignet sich die Methode nicht. Eine Nierenfunktionsmessung kann präzise mittels exogener Marker, wie dem Iohexol, durchführen. Die derzeitigen verwandten Iohexol-Methoden sind aber in der Präanalytik und Analytik aufwendig, sodass diese sich bisher nicht in der Routine durchsetzen können. Hier haben wir eine neue Iohexol-Bestimmungsmethode getestet, die seit dem Mai 2022 als zugelassenes Kit für die einfache und schnelle Nierenfunktionsmessung

zur Verfügung steht (Nephrolytix, Berlin)

Methode: Die Methode kombiniert eine Ein-Schritt Probenvorbereitung mittels Filter und einer chromatographischen schnellen Separation über ein UHPLC-DAD-System (Hitachi). Die Methode wurde auf den Quantifizierungsbereich überprüft, ebenso Präzision, Variabilität und Genauigkeit. Es wurde bei 40 Patienten die Nierenfunktion bestimmt und mit herkömmlicher Nierenfunktionsmessung (Fällung-HPLC-UV).

Ergebnisse: Die Methode wurde validiert mit einem linearen Bereich von $8,6\text{--}500 \text{ mg/ml}$ Iohexol in humanem Serum. Die Ungenauigkeit innerhalb eines Tages bzw. zwischen verschiedenen Tagen lag bei $\leq 0,8 \%$ and $\leq 1,84 \%$. Die Genauigkeiten innerhalb eines Tages und auch zwischen verschiedenen Tagen lag bei $-1,12 \%$ bis $1,04 \%$ bzw. zwischen $1,24 \%$ bis $0,1 \%$. Die Probenvorbereitungszeit liegt nach Probeneingang bei 20 min und die Messzeit der Probe bei 90 sek. Von der Blutprobe bis zum Messwert vergehen in der Regel 45–60 min. Beim Vergleich von 120 Blutproben von 40 Patienten zeigt sich in der Nierenfunktionsbestimmung eine Abweichung von $1,2 \%$, d. h. $46,2 \text{ ml/min}$ (HPLC) vs. $46,8 \text{ ml/min}$ (UPLC).

Zusammenfassung: Die neue vereinfachte Methode für die Iohexolmethode konnte erfolgreich validiert werden und zeigt eine exzellente Präzision und Genauigkeit. Die Methode basiert auf einer einfachen Probenvorbereitung im 96-Well-Format, wodurch Robustheit, eine hoher Probendurchsatz und eine Automatisierung sich erreichen lässt. Die neue Methode konnte erfolgreich

die Iohexol-Konzentration im humanen Serum bestimmen, um somit auch die Nierenfunktion zu bestimmen. Die Einfachheit der Methode bietet die Möglichkeit, diese auch in der klinischen Routine einfach einzusetzen.

P048

In vivo inhibition of TRPC6 by SH045 attenuates renal fibrosis in the New Zealand obese (NZO) mouse model of metabolic syndrome

Y. Xu; Z. Zheng¹; U. Krügel²; M. Schaefer²; T. Grune³; B. Nürnberg⁴; M.-B. Köhler¹; M. Gollasch; D. Tsvetkov; L. Marko¹

Klinik und Poliklinik für Innere Medizin D – Geriatrie, Universitätsmedizin Greifswald, Greifswald; ¹ECRC-Kooperation von MDC und Charité, Experimental and Clinical Research Center, Berlin; ²Rudolf-Boehm-Institut für Pharmakologie und Toxikologie, Universität Leipzig, Leipzig; ³Wissenschaftlicher Direktor, Deutsches Institut für Ernährungsforschung, Nuthetal; ⁴Institut für Experimentelle und Klinische Pharmakologie und Toxikologie, Universitätsklinikum, Eberhard Karls Universität, Tübingen

Objective: Metabolic syndrome is a significant public health challenge worldwide and associated with adverse renal and cardiovascular outcomes. Mice lacking the transient receptor potential cation channel subfamily C member 6 (TRPC6) have ameliorated renal outcome in the accelerated renal fibrosis model, unilateral ureteral obstruction (UUO). Therefore, pharmacological inhibition of TRPC6 could be a promising therapeutic intervention in progressive tubulo-interstitial fibrosis in hypertension and metabolic

syndrome. In the present study, we hypothesized that the novel selective TRPC6 inhibitor SH045 (larixyl N-methylcarbamate) may ameliorate UUO-accelerated renal fibrosis in New Zealand obese (NZO) mouse model, which is a polygenic model of metabolic syndrome.

Method: We used SH045, the pharmacological inhibitor of TRPC6, to treat NZO mice. We evaluated renal outcomes 7 days after UUO. SH045 (20 mg/kg) was applied daily by intraperitoneal injection. Renal inflammation and tubulointerstitial fibrosis were determined by quantitative real-time (qRT)-PCR and histological analysis.

Results: *In vivo* inhibition of TRPC6 by SH045 markedly decreased mRNA expression of pro-fibrotic markers (*Col1a1*, *Col3a1*, *Col4a1*, *Acta2*, *Ccn2*, *Fn1*) and chemokines (*Cxcl1*, *Ccl5*, *Ccr2*) in UUO kidneys of NZO mice compared to kidneys of vehicle-treated animals. Furthermore, renal inflammatory cell infiltration (F4/80+ and CD4+) and tubulointerstitial fibrosis (Sirius red, fibronectin, and α -SMA staining) were ameliorated in SH045 treated NZO mice.

Conclusion: We conclude that pharmacological inhibition of TRPC6 might be a promising antifibrotic therapeutic agent to treat progressive tubulo-interstitial fibrosis in hypertension and metabolic syndrome.

P049

Progression der chronischen Niereninsuffizienz ist mit zunehmender Eryptose und Anämie assoziiert

L. Schaefer; R. Bissinger; F. Artunc
Sektion Nieren- und Hochdruckkrankheiten, Universitätsklinikum,

Medizinische Klinik IV, Eberhard Karls Universität Tübingen, Tübingen

Hintergrund: Die chronische Niereninsuffizienz (CKD) ist häufig mit einer renalen Anämie vergesellschaftet, welche die Leistungsfähigkeit und Lebensqualität der Patienten erheblich einschränkt. Bei Häm- und Peritonealdialysepatienten konnte gezeigt werden, dass die Erythrozyten prozentual vermehrt von einem vorzeitigen Zelltod (Eryptose) betroffen sind. Es gab vereinzelt Hinweise darauf, dass die Eryptose auch bei nicht-dialysepflichtigen Patienten zur Anämie beiträgt, allerdings fehlen hierzu Querschnittstudien.

Methode: In die Querschnittstudie wurden n = 122 Patienten aller CKD-Stadien einbezogen (G1: n = 8, G2: n = 12; G3a: n = 16, G3b: n = 34; G4: n = 39; G5: n = 13) und mit Blutproben einer gesunden Kontrollgruppe verglichen (Blutspender, n = 133). Aus Blut- und Urinproben aller Teilnehmer wurden die relevanten Nierenfunktions- und Anämieparameter bestimmt. Unmittelbar nach der Blutentnahme wurde die Eryptoserate entsprechend des Anteils der Erythrozyten mit Phosphatidylserin-Exposition über Bindung von Annexin V durchflusszytometrisch bestimmt. Die Quantifizierung der Retikulozyten erfolgte ebenfalls per Durchflusszytometrie.

Ergebnisse: Die untersuchte Patientenkohorte wies im Vergleich zur Kontrollgruppe signifikant niedrigere Hämoglobin (Hb)-Werte auf ($12,4 \pm 2,6$ g/dl (Median \pm Interquartilsabstand) in der CKD- vs. $13,8 \pm 1,8$ g/dl in der Kontrollgruppe, $p < 0,001$). Dabei war der Hb-Wert stadienabhängig vermindert ($12,9 \pm 2,6$ g/dl in Stadium G1 und $9,4 \pm 1,6$ g/dl in Stadium G5)

und korrelierte univariat signifikant positiv mit der geschätzten glomerulären Filtrationsrate (eGFR) der Patienten ($r = 0,51$, $p < 0,001$). Die Eryptoserate war bei den Patienten signifikant höher als bei den Kontrollpersonen ($1,05 \pm 0,47\%$ vs. $0,76 \pm 0,39\%$) und nahm mit zunehmendem CKD-Stadium zu ($0,82 \pm 0,38\%$ in Stadium G1 und $1,34 \pm 0,41\%$ in Stadium G5). Sie korrelierte univariat signifikant negativ mit der eGFR ($r = -0,27$, $p = 0,002$) und dem Hb-Wert ($r = -0,31$, $p < 0,001$) der Patienten. Die Anämie bestand trotz gesteigerter Retikulozytenzahlen ($1,22 \pm 0,71\%$ vs. $0,85 \pm 0,53\%$, $p < 0,001$) und nicht-signifikant erhöhter Erythropoetinspiegel im Plasma ($9,9 \pm 8\%$ vs. $9,5 \pm 5,3\%$; $p > 0,05$).

Zusammenfassung: Eine gesteigerte Eryptose tritt bereits bei nicht-dialysepflichtiger chronischer Niereninsuffizienz auf und nimmt mit zunehmendem CKD-Stadium zu. Die erhöhte Eryptose könnte zur renalen Anämie beitragen.

P050

Das Urämietoxin Indoxylsulfat ist ein Induktor der Caspase-4, nicht jedoch der Caspase-1-Aktivierung in monozytären THP-1 Zellen

C. Ulrich; S. Markau; M. Girndt
SP Nephrologie, Rheumatologie und Endokrinologie, Universitätsklinik und Poliklinik für Innere Medizin II, Martin-Luther-Universität Halle-Wittenberg, Halle (Saale)

Hintergrund: Eine Vielzahl von Urämietoxinen trägt zur entzündlichen Konstellation in Hämodialysepatienten bei. Das Protein-gebunden Urämietoxin Indoxylsulfat (IS) nimmt dabei eine besonders

prominente Rolle ein. Es scheint über seine inflammatorische Wirkung die Progression von renalen und kardiovaskulären Erkrankungen zu befördern. Entzündung wird durch unterschiedliche Mechanismen getriggert. Eine Variante, die bei chronisch Nierenkranken ausgeprägt zu sein scheint, stellt der inflammatorische Zelltod (Pyroptose) dar, bei dem, durch Caspase-1 und/oder Caspase-4 getriggert, inflammatorische Mediatoren (u. a. IL-1 β) nach Zellerstörung freigesetzt werden. Es stellt sich die Frage, inwieweit dieses Urämietoxin zur monozytären Caspase-1 und/oder Caspase-4-Aktivierung beiträgt?

Methode: IS induzierte Effekte wurden in der monozytären Zelllinie THP-1 untersucht. Hierzu wurden die pyroptotischen Analysen in undifferenzierten Zellen, die potentielle Freisetzung von IL-1 β in differenzierten THP-1 Zellen (100 nM Phorbol-Myristat-Acetat) analysiert. Physiologische wie supra-physiologische IS Konzentrationen wurden eingesetzt (1–4 mM). Die Caspase-1 und Caspase-4 Aktivierung wurde in durchflusszytometrischen und luminometrischen Assay mithilfe Caspase-spezifischer Substrate wie -Inhibitoren durchgeführt. Die IL-1 β Aktivität wurde mittels ELISA-Technik bzw. mittels der IL-1 β Indikatorzelllinie HEK-Blue™ IL-1 β ermittelt.

Ergebnisse: Durchflusszytometrische Analysen zeigen, dass die Pyroptose-rate (7-AAD + Caspase+) bereits bei Zugabe von 1 mM IS, einer IS-Menge, die in Hämodialysepatienten nachgewiesen worden ist, signifikant erhöht war. Diese Daten konnten in einem luminometrischen Assay, der im Gegensatz zu dem durchflusszytometrischen

Assay mit einem anderen Caspase-1-spezifischen Substrat arbeitet (Ac-WEHD-aminoluciferin vs. FAM-YVAD-FMK), bestätigt werden. Darüber hinaus konnte eine IS-induzierte (2 mM) Caspaseaktivität durch Zugabe des NLRP3 Inflammasome-spezifischen Induktors Nigericin (21 μ M) signifikant gesteigert werden. Da insbesondere das Caspase-Substrat Ac-WEHD eine breitere Spezifität aufzuweisen scheint – es erkennt sowohl Caspase-1, als auch Caspase 4 – wurden spezifische Caspase-Inhibitoren getestet. Unter Einsatz des Caspase-1-spezifischen Inhibitors Ac-YVAD-CHO (2 μ M) konnten lediglich die Nigericin-, nicht jedoch die IS-vermittelten Effekte inhibiert werden. Zusatz des Caspase-4-spezifischen Inhibitors Ac-LEVD-CHO (2 μ M) führte zu einer kompletten Inhibition der durch IS induzierten Caspase (Kontrolle: 100 %, IS: $128 \pm 12\%$, IS + Ac-LEVD: $81 \pm 22\%$, IS + AC-YVAD: $107 \pm 15\%$; IS vs. IS + Ac-LEVD, $p < 0,001$). mRNA-Analysen ergaben, dass IS sowohl die Expression der Caspase-1, der Caspase-4 als auch der pro-IL1 β mRNA erhöht. Protein-Analysen zeigen sowohl im ELISA als auch bei Analyse der IL-1 β Indikatorzelllinie HEK-Blue™, dass IS nicht zur Freisetzung des inflammatorischen Zytokins IL-1 β beiträgt.

Zusammenfassung: Die Analyse Indoxylsulfat-vermittelter Effekt im monozytären THP-1 Zellmodell zeigt, dass dieses Urämietoxin die Caspase-4, nicht jedoch die Caspase-1 aktiviert. Somit scheint IS den Zelltod in THP-1 Zellen zu induzieren, ohne den für die Caspase-1 typische IL-1 β Freisetzung-Pathway (NLRP3 Inflammasom) zu tangieren.

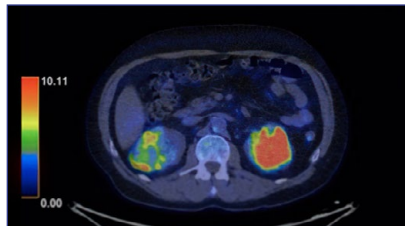
Case Reports

P051

Der Nutzen von PET-CT und immunmodulatorischer Therapie bei steroidrefraktärer IgG4-assoziiierter Nephritis und retroperitonealer Fibrose

M. Babic; M. Tölle¹; M. Schuchardt¹; K.-U. Eckardt²; M. van der Giet¹
Medizinische Klinik für Nephrologie – Hochschulambulanz, Campus Benjamin Franklin, Charité – Universitätsmedizin Berlin, Berlin; ¹Medizinische Klinik IV, Klinik für Nephrologie, Campus Benjamin Franklin, Charité – Universitätsmedizin Berlin, Berlin; ²Medizinische Klinik mit Schwerpunkt Nephrologie und Internistische Intensivmedizin, Campus Charité Mitte, Charité – Universitätsmedizin Berlin, Berlin

Hintergrund: IgG4-assoziierte Erkrankungen sind eine heterogene Gruppe fibroinflammatorischer Prozesse mit unklarer Ätiologie, deren Diagnostik und Therapie im klinischen Alltag herausfordernd ist. Klinische Empfehlungen beruhen weit überwiegend auf retrospektiven Daten und die Definition dieser Krankheitsentität ist noch Forschungsgegenstand. PET-CT Untersuchungen zur Bestimmung der Krankheitsaktivität und die medikamentöse B-Zell-Depletion stellen hierbei wertvolle Werkzeuge dar, wie der folgende Fall aufzeigt. **Methode:** Wir berichten von einem 64-jährigen Patienten mit langem Krankheitsverlauf von Schwäche, Gewichtsverlust, Sicca-Symptomatik und chronischer Niereninsuffizienz. Die Zuweisung erfolgte nach komplexer Immuntherapie mit Prednisolon, Hydroxychloroquin und Methotrexat mit dem

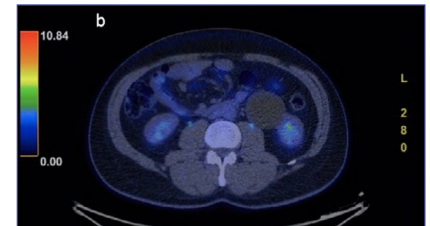


P051: Abb. 1

Hohe entzündliche Aktivität der Grunderkrankung in beiden Nieren

Verdacht eines Sjögren-Syndroms. Bei serologischem Nachweis eines Komplementverbrauchs und Hypergammaglobulinämie führten wir eine Nierenbiopsie durch, welche eine tubulointerstitielle Nephritis mit zahlreichen IgG4 positiven Plasmazellen ergab. Zur Evaluation der Krankheitsaktivität führten wir eine PET-CT durch, in welcher eine hochfluoride retroperitoneale Fibrose, Periaortitis, tubulointerstitielle Nephritis, Sialadenitis und Pankreatitis zur Darstellung kam. Aufgrund dieser Befunde diagnostizierten wir eine IgG4-assoziierte Erkrankung mit hoher Aktivität und leiteten eine Steroidinduktionstherapie sowie immunmodulatorische Therapie mit vier Zyklen Rituximab ein. Die Krankheitsaktivität und der Therapieerfolg wurden durch regelmäßige PET-CT-Untersuchungen überwacht.

Ergebnisse: Die immunmodulatorische Therapie mit Rituximab führte zu einem Ansprechen mit sinkender systemischer Inflammation. Durch die Verlaufskontrollen mittels PET-CT in 6-monatigem Abstand konnte ein klinisch apparentes Rezidiv mithilfe einer frühzeitigen wiederholten immunmodulatorischen Therapie verhindert werden. Nach vier Zyklen Rituximab konnte keine entzündliche Aktivität mehr in einem



P051: Abb. 2

Kein Nachweis einer entzündlichen Aktivität nach vier Zyklen immunmodulatorischer Therapie mit Rituximab

der vormals beteiligten Organe mittels PET-CT nachgewiesen werden.

Zusammenfassung: Dieser Fall demonstriert den diagnostischen Wert von PET-CT-Untersuchungen zur Verlaufskontrolle und die Effektivität von Rituximab bei steroidrefraktärer IgG4-assoziiierter retroperitonealer Fibrose und interstitieller Nephritis.

P052

Extensive ¹⁷⁷Lu-PSMA radio-ligand therapy can lead to radiation nephropathy with renal thrombotic microangiopathy-like picture

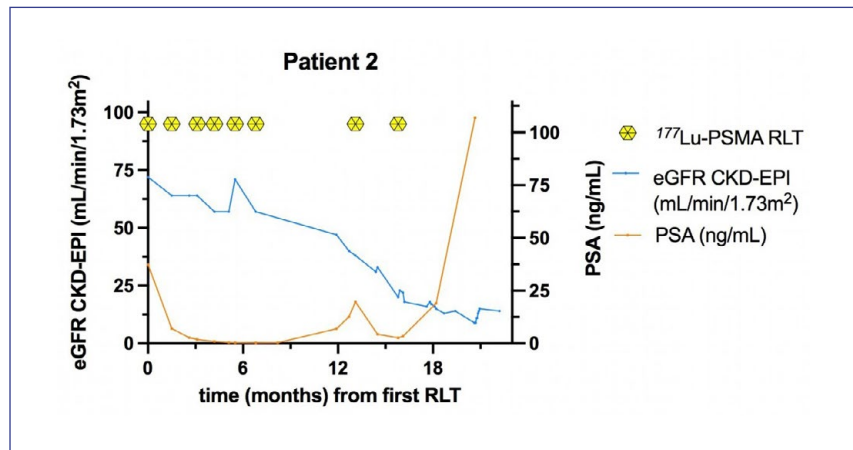
H. Schäfer; S. Mayr¹; M. Büttner-Herold²; C. A. Böger³; U. Heemann; M. Eiber⁴; R. Tauber⁵; C. Schmaderer
II. Medizinische Klinik, Nephrologie, Klinikum rechts der Isar, Technische Universität München, München; ¹Abteilung für Nephrologie, Klinikum rechts der Isar, Technische Universität München, München; ²Institut für Nephropathologie, Universitätsklinikum, Friedrich-Alexander-Universität Erlangen-Nürnberg, Erlangen; ³Medizinischen Abteilung – Nephrologie, Klinikum Traunstein, Kliniken Südostbayern, Traunstein; ⁴Abteilung für Nuklearmedizin, Klinikum rechts der Isar, Technische Universität München, München; ⁵Abteilung für Urologie, Klinikum

rechts der Isar, Technische Universität München, München

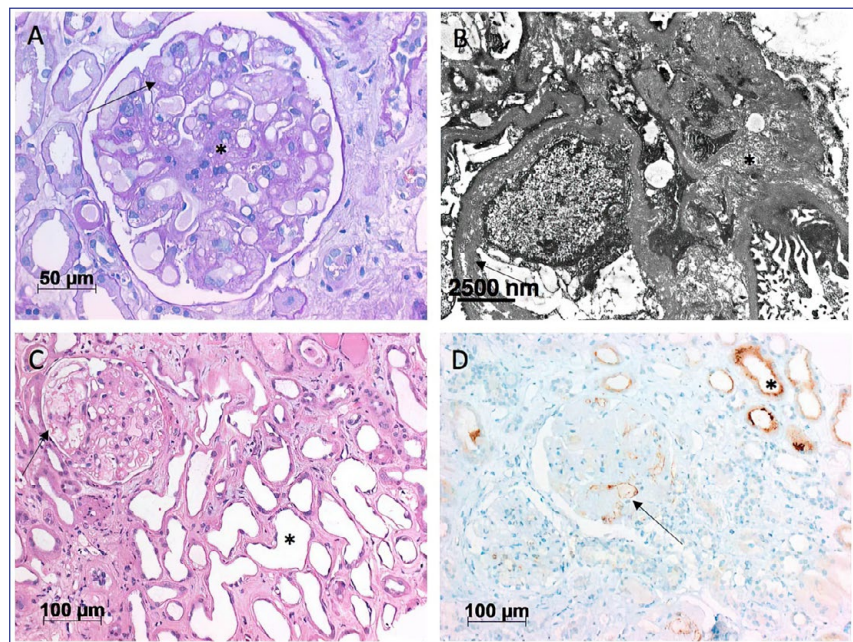
Objective: Lutetium-177 prostate-specific membrane antigen radioligand therapy (^{177}Lu -PSMA RLT) is an increasingly used therapy for metastatic, castration-resistant prostate cancer (mCRPC). It delivers β -radiation to cells expressing PSMA and high accumulation of the radiopharmaceutical in the kidneys has been shown. Recently, ^{177}Lu -PSMA RLT was approved by the FDA due to prolonged, progression-free survival. Here, we report three cases of radiation nephropathy with severe chronic kidney disease (CKD) with biopsy-proven renal thrombotic microangiopathy (TMA) following extensive treatment with ^{177}Lu -PSMA RLT.

Method: A total number of 301 patients were treated with ^{177}Lu -PSMA RLT at our center with 31 of them receiving more than six cycles. Three patients developed a substantial decrease in estimated glomerular filtration rate (eGFR) and underwent kidney biopsy. In addition to routine pathological work-up, kidney biopsies were stained using a monoclonal antibody against PSMA.

Results: We report three cases of mCRPC receiving high activities of ^{177}Lu -PSMA RLT (8–10 cycles, cumulative activity 54.8–69.5 GBq). High absorbed renal doses lead to Common Terminology Criteria for Adverse Events (CTCAE) grade 3–4 CKD seen in 10 % (3/31) of patients receiving more than six RLT cycles. The onset of CKD was 12 to 17 months after the first RLT cycle and progressed after RLT cessation. In all three patients, kidney biopsy revealed TMA and severe ATI. No



P052: Abb. 1



P052: Abb. 2

systemic signs of TMA were present. A timeline and kidney biopsies are shown in Figure 1 and 2. **Conclusion:** ^{177}Lu -PSMA accumulates in and is excreted by the kidneys potentially causing radiation-induced nephrotoxicity. So far only mild toxicities have been reported. We report three cases with severe CKD. Kidney biopsy

results are reminiscent of TMA with TMA being known as the histologic correlate of radiation nephropathy. Radiation nephropathy is a late-onset renal dysfunction exerting dose-dependent toxicity. It remains unclear as to whether patients receiving standard RLT are also at risk of developing radiation nephropathy.

P053**CAKUT is variably associated with a PHIP-related syndrome of obesity and neurodevelopmental delay**

J. de Fallois; T. Wagner¹; E. Decker¹; C. Bergmann¹; K. Platzer²; W.K. Chung³; J. Halbritter⁴
 Sektion Nephrologie, Klinik für Endokrinologie und Nephrologie, Universitätsklinikum Leipzig, Leipzig; ¹Medizinische Genetik Mainz, Limbach Genetics GmbH, Mainz; ²Institut für Human-genetik, Leipzig, Leipzig; ³Department of Medicine, Medical Center, Columbia University, New York/USA; ⁴Medizinische Klinik mit Schwerpunkt Nephrologie und Internistische Intensivmedizin, Campus Charité Mitte, Charité – Universitätsmedizin Berlin, Berlin

Objective: Monoallelic pathogenic variants in *PHIP* (*Pleckstrin homology domain-interacting protein*) lead to Chung-Jansen syndrome (CJS OMIM_# 617991), characterized by developmental delay, intellectual disability, obesity, and dysmorphic features. Prompted by a patient with CJS and congenital anomalies of the kidney and urinary tract (CAKUT), we sought to systematically review available cohorts and published cases regarding the frequency of CAKUT in patients with *PHIP* haploinsufficiency.

Method: Exome sequencing (ES), multiplex ligation-dependent probe amplification (MLPA), familial segregation analysis, and reverse phenotyping. Critical review of existing CJS cohorts and cases (n = 83) for the presence of kidney or urogenital anomalies.

Results: The index patient presented with end-stage kidney failure at the age of 40 years. As medical

history, she revealed congenital bilateral hydronephrosis due to ureterovesical junction obstruction. The family further reported developmental delay since infancy resulting in adult intellectual disability. At clinical examination, the patient showed obesity (BMI 35.6) and dysmorphic facial features. ES identified a heterozygous truncating variant in *PHIP* (NM_017934.7: c.241C > T p.(Arg81*) affecting the eight β -propeller-forming WD40 repeat domain. Furthermore, no additional genetic variants in known or candidate CAKUT-genes were found by ES and MLPA. Parental segregation analysis demonstrated the *de novo* status of the *PHIP* variant, thereby confirming the genetic diagnosis of CJS with CAKUT in the proband. Clinical review of additional patients with CJS (Columbia-cohort, Leipzig database, and published cases; n = 83) revealed four additional patients with a CAKUT phenotype: i) vesicoureteral reflux, ii) hypo-dysplastic kidneys, iii) horseshoe kidney, and iv) ureterocele with recurrent urinary tract infections. Furthermore, five patients displayed genital abnormalities (micro- or cryptorchidism). Single cell transcriptomic databases support the role of *PHIP* during human nephrogenesis with high expression in nephron progenitor and tubular precursor cells at 17 weeks of gestation.

Conclusion: Among genetically unresolved patients with a syndromic CAKUT phenotype of neurodevelopmental delay and obesity, sequence aberrations in *PHIP* should be considered. Conversely, patients with diagnosed CJS should be monitored for kidney and urogenital anomalies as

part of the phenotypic spectrum (at least 10 % in our review).

P054**MPGN und ein großes Fragezeichen**

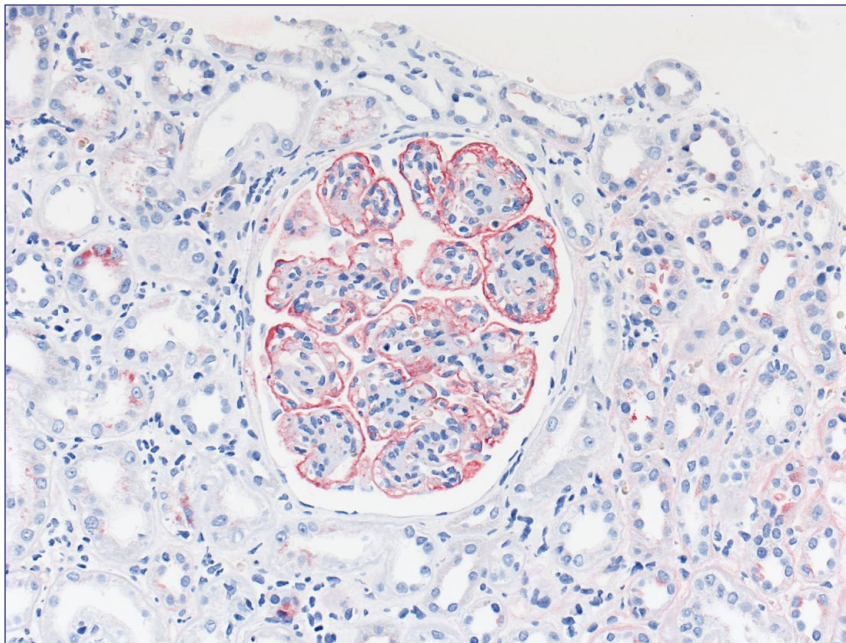
M. Løyen; T. Wiech¹; M. Gohl²; W. Clasen

Klinik für Innere Medizin und Nephrologie/Dialyse, Herz-Jesu-Krankenhaus Hilstrup GmbH, Münster; ¹Institut für Pathologie, Sektion Nephropathologie, Zentrum für Diagnostik, Universitätsklinikum Hamburg-Eppendorf, Hamburg; ²Labor Enders, Stuttgart

Hintergrund: Die differentialdiagnostische Abklärung einer membranoproliferativen Glomerulonephritis erfordert zunächst die Abgrenzung einer C3-Glomerulopathie von einer Immunkomplexnephritis. Ursachen der immunkomplexvermittelten MPGN sind häufig infektiöse Erkrankungen. Wir berichten über eine seltenere Endokarditisform, deren Erkennung wesentliche therapeutische Konsequenzen für die renale Prognose hat.

Methode: Der 62jährige Patient wurde im September 2021 wegen einer ausgeprägten Anämie (Hb 6,4 g/dl) stationär internistisch sowie ambulant hämato-onkologisch untersucht. Eine Ursache für die Anämie konnte nicht ermittelt werden. Ein halbes Jahr später wurde ein schweres nephrotisches Syndrom diagnostiziert und in unserer Klinik eine Nierenbiopsie durchgeführt. In seiner Freizeit unternahm der 62jährige Patient ausgedehnte Fahrradtouren im Münsterland. In diesem Gebiet wird eine intensive Schafzucht betrieben.

Ergebnisse: Die nephropathologische Analyse des Nierenbiopsats wies morphologisch eine eindeutige



P054: Abb. 1

MPGN vom Immunkomplex-Typ mit Aktivierung des klassischen Komplementweges nach. Bei der differentialdiagnostischen Abklärung der MPGN konnte eine (postendokarditisch) destruierte bikuspidale angelegte Aortenklappe ohne frische Vegetationen dargestellt werden. Serologisch wurde anhand anti-Phase I-Antikörpern die typische Konstellation einer chronischen *Coxiella burnetii*-Infektion (Q-Fieber, von engl. "Query": Fragezeichen) nachgewiesen. Die Anamnese mit Kontakt zu Schafen war typisch. Die Genese der immunkomplexvermittelten MPGN war damit geklärt. Die Behandlung der chronischen Q-Fieber-Infektion erfolgt mit einer Kombinationstherapie mit Hydroxychloroquin (3×200 mg/d) und Doxycyclin (2×100 mg/d) über mindestens 18–24 Monate. Die Nierenfunktion hat sich jetzt 2 Monate nach Therapiebeginn deutlich verbessert, das nephrotische

Syndrom ist regredient. Ein Herzklappenersatz ist im Verlauf geplant.

Zusammenfassung: Die differentialdiagnostische Abklärung von immunkomplexvermittelten MPGN erfordert eine enge interdisziplinäre Zusammenarbeit. Das Erkennen einer Q-Fieber-Endokarditis als infektiöse Ursache der Immunkomplexbildung hat für die Therapie und Prognose der MPGN weitreichende Konsequenzen.

P055

Acute interstitial nephritis after vaccination with BNT162b2

S. Rieckmann; F. S. Seibert; M. Hogeweg; S. Bertram; A. Doevelaar; K. Amann¹; N. Babel; T. H. Westhoff
Centrum für Translationale Medizin, Medizinische Klinik I, Marien Hospital Herne, Ruhr-Universität Bochum, Herne; ¹ Institut für Nephropathologie, Universitätsklinikum, Friedrich-Alexander-Universität Erlangen-Nürnberg, Erlangen

Objective: mRNA based vaccination strategies to SARS-CoV-2 have shown high efficacy and a very low incidence of serious side effects. Inflammatory side effects have predominantly been described for the heart in terms of myocarditis. The present reports show that the vaccine can induce interstitial inflammation in the kidney as well. We present three cases of biopsy proven acute interstitial nephritis after BNT162b2 vaccination, one of them requiring temporary dialysis. Physicians should be aware of this complication since it is highly responsive to steroids.

Results: A 63-year-old male, an 18-year-old male and a 25-year-old female without any medical history were admitted to hospital for acute kidney injury three to six weeks after vaccination. Kidney biopsies disclosed very similar histological findings with interstitial edema, lymphoplasmacellular infiltration with eosinophil granulocytes, and acute tubular necrosis consistent with acute interstitial nephritis (AIN). History and laboratory findings did not reveal any alternative etiologic factors. There were neither typical causes of AIN like drugs or infections, nor a systemic entity like IgG4 disease or sarcoidosis. All nasopharyngeal swabs for SARS-CoV-2 RT-PCR remained negative, as well as supplemental analysis of SARS-CoV-2 nucleocapsid antibodies, so that we concluded that BNT162b2 vaccination was the only apparent trigger for AIN. Whereas acute kidney injury was rather mild in the young male patient (maximum serum creatinine concentration 1.7 mg/dl), it was severe in the young female (initial serum creatinine concentration 11.7 mg/dl) and even required

immediate hemodialysis in the 63-year-old patient (initial serum creatinine concentration 19 mg/dl). All cases were rapidly responsive to steroid treatment and recovered after approximately two weeks.

Conclusion: The present case reports describe AIN as a rare, but potentially serious side effect of mRNA vaccination to SARS-CoV-2. Thus, vaccine-related inflammatory side effects may also occur in the kidney. Physicians should be aware of this rare, but potentially serious complication and its excellent responsiveness to steroid treatment.

P056

A case of Herpes simplex esophagitis presenting 25 years after kidney transplantation

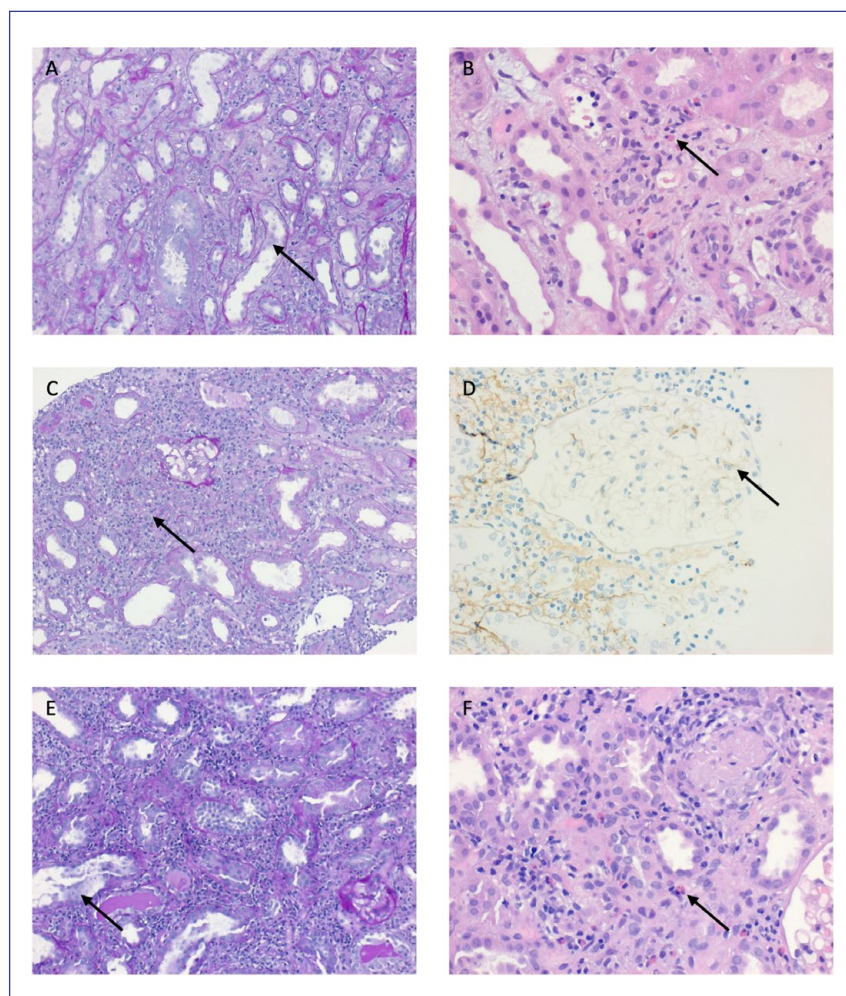
R. Wolf; A. Samadova; T. Kuschnerer; V. Paul; T. Dabers; S. Freim von Rheinbaben; S. Stracke
Abteilung für Nephrologie und Hypertensiologie, Klinik und Poliklinik für Innere Medizin A, Universitätsmedizin Greifswald, Greifswald

Objective: Herpes simplex virus (HSV) infection of the esophagus, an uncommon condition in immunocompetent hosts, can be seen in transplant patients, either as reactivation of viral persistence or as primary infection. Common symptoms reported by patients are dysphagia and odynophagia, with epigastric pain or hiccups.

Results: We report the case of a 66-year-old male patient, presenting with dysphagia und odynophagia, occurring after solid as well as liquid meals, accompanied by postprandial coughing and an unintentional weight loss of 15 kg in a timespan of one year. In 1995, the patient had received a renal transplant, due to

ANCA-associated Vasculitis (AAV), leading to end-stage renal disease in 1994. Immunosuppressive regime comprised cyclosporine (CsA), MMF and prednisolone. In 2014, he was diagnosed with retroperitoneal marginal zone lymphoma which was cured by 40 Gy radiation therapy. In 3/2022, he presented with deteriorating transplant function (creatinine 365 µmol/l, eGFR 15 ml/min, BUN 37 mmol/l). Esophago-gastroduodenoscopy (EGD) showed extensively inflamed tissue in the lower part of the esophagus with

a subsequent narrowing of the lumen. Biopsies confirmed acute ulcerative esophagitis, most likely due to acidic reflux. High-dose therapy with proton-pump inhibitors yielded only slight improvement. Repeat biopsies showed the presence of HSV. Therapy with aciclovir was initiated and MMF reduced, leading to a significant improvement in symptoms but worsened kidney function and caused neurotoxicity. We discontinued aciclovir and CsA. After viral resistance testing, famciclovir was given for



P055: Abb. 1

1 month and an EGD 4 months after first presentation, no residual lesions in the esophagus were seen. Immunosuppression was continued with MMF 1.5 g/d and prednisolone 5 mg/d only. Renal function improved (creatinine 218 µmol/l, eGFR 26 ml/min, BUN 17 mmol/l).

Conclusion: Most cases of HSV esophagitis occur under intensified immunosuppression. Antiviral treatment should be initiated immediately after diagnosis, because of possible fatal complications, like bleeding and even perforation. Our case is remarkable because we saw HSV esophagitis 25 years after kidney transplantation and during perceived maintenance immunosuppression. For our patient, CsA levels of 90–100 ng/ml, 1.5 g MMF and 5 mg prednisolone/d were too much. Research is needed on individualizing long term immunosuppression in older patients.

P057

Thrombotische Mikroangiopathie (TMA) mit akuter Nierenschädigung – seltene Verlaufsform bei idiopathic Multicentric Castleman Disease (iMCD)

F. Bamukhaiar; T. M. Meyer; A. Ahmed¹; A. Dellmann²; J. H. Bräsen³; K. Rifai⁴; J. T. Kielstein
Nephrologie | Rheumatologie | Blutreinigungsverfahren, Medizinische Klinik V, Städtisches Klinikum Braunschweig, Braunschweig; ¹ Praxis für Hämatologie und Onkologie (MVZ), Städtisches Klinikum Braunschweig, Braunschweig; ² Institut für Pathologie, Städtisches Klinikum Braunschweig, Braunschweig; ³ Nephropathologie, Institut für Pathologie, Medizinische Hochschule Hannover, Hannover; ⁴ Klinik für Innere Medizin – Gastroenterologie, Städtisches Klinikum Wolfenbüttel, Wolfenbüttel

Hintergrund: Die thrombotische Mikroangiopathie (TMA) ist eine seltene, aber potentiell lebensbedrohliche Erkrankung, die bei Auftreten häufig mit der Trias hämolytische Anämie, Thrombozytopenie und schweren Endorganschäden einhergeht und dann in vielen Fällen dem HUS, der TTP oder dem aHUS zugeordnet werden kann. Aber auch andere Erkrankungen (autoimmunologisch, lymphoproliferativ, maligne art. Hypertonie, Infektionen, Medikamente) können sekundär eine TMA auslösen.

Methode: Ein 30-jähriger, bislang gesunder Patient wurde uns mit einer akuten Nierenschädigung (AKIN 3) zugewiesen. Bei massiver hydropischer Dekompensation war vor Durchführung der Nierenbiopsie eine akute Dialyseanleitung zum Flüssigkeitsentzug über einen zentral-venösen Katheter notwendig. Die im Verlauf durchgeführte Nierenbiopsie zeigte histologisch überraschend das morphologische Bild einer TMA ohne Zeichen einer Glomerulonephritis oder interstitiellen Nephritis. Angesichts der biopsisch gesicherten TMA starteten wir mit Plasmapherese einschl. hochdosierten Glukokortikoiden. Laborchemisch konnten wir ein HUS und eine TTP sowie andere typische sekundäre TMA-Auslöser ausschließen. Die Laborparameter zeigten eine Coombs-positive hämolytische Anämie (Hb 6,2 g/dl) mit Thrombozytopenie (98.000/ul) und eine polyklonale Hypergammaglobulinämie (16 g/l) mit Hypalbuminämie (22 g/l). Die sich anschließende Umfelddiagnostik einschl. der Suche nach einem Infektfokus bot unauffälligen Befunde. In der Vordiagnostik fielen bildgebend neben einer multifokalen LK-Vergrößerung eine

Splenomegalie auf. Die Punktion eines Leisten-LK erbrachte histologisch ein plasmazellreiches Infiltrat (LANA-1 negativ) ohne Hinweis auf eine Tbc, was uns auf die Verdachtsdiagnose eines Morbus Castleman lenkte (HIV-, HHV-8-PCR negativ). Entsprechend der Consensus-Konferenz "idiopathic multicentric Castleman disease" (iMCD) konnten wir die Diagnose eines iMCD sichern und begannen mit einer IL-6 Blockade (Siltuximab).

Ergebnisse: Bereits unter Glukokortikoiden konnte ein erfolgreicher Dialyseauslass erfolgen. Die Gabe von Siltuximab wurde in 3 Wochen-Abständen fortgesetzt, so dass im Verlauf die Kortikosteroide getapert wurden. Nach der 3. Siltuximab-Gabe zeigte sich eine vollständige Erholung der Nierenfunktion.

Zusammenfassung: Dieser klinische Fall einer TMA mit renaler Beteiligung zeigt die Notwendigkeit einer engen interdisziplinären Zusammenarbeit im Sinne einer Hämato-Onko-Nephrologie und (Nephro-)Pathologie, um potentiell lebensbedrohliche Erkrankungen rasch diagnostizieren und therapieren zu können.

P058

Detection of perfusion defects by multiparametric fMRI in a kidney allograft recipient with acute kidney injury and inconsistent conventional diagnostic procedures.

D. J. Heister; C. Zhang¹; P. Martirosian¹; F. Seith¹; A. L. Birkenfeld; N. Heyne; M. Guthoff
Sektion Nieren- und Hochdruckkrankheiten, Universitätsklinikum, Medizinische Klinik IV, Eberhard Karls Universität Tübingen, Tübingen; ¹ Diagnostische und Interventionelle

*Radiologie, Eberhard Karls Universität
Tübingen, Tübingen*

Objective: Decline in renal allograft function can be caused by a variety of factors. Laboratory tests and imaging techniques such as (duplex-) ultrasound help to delineate the underlying cause, in many cases however, allograft biopsy is the only diagnostic procedure to clarify the reason for the impaired allograft function. Yet, even with this invasive method, a definite diagnosis cannot always be made. Therefore, additional diagnostic tools are needed, with multiparametric functional magnetic resonance imaging (fMRI), combining oxygenation (blood oxygen-dependant MRI [BOLD, T2* mapping]), diffusion (diffusion weighted imaging [DWI]) and perfusion (arterial spin labelling [ASL]), being an option.

Method: A 36-year-old female kidney transplant recipient presented with progressive decline in allograft function. Clinical examination did not reveal any cause for graft dysfunction. Laboratory tests showed progressive renal functional impairment with an increase in plasma creatinine to a maximum of 5.9 mg/dl and an eGFR of 8,1 ml/min/1,73 m² (MDRD). Ultrasound demonstrated normal perfusion with resistance indices (RI) of 0,6–0,7. Repeat kidney biopsy were performed, which showed acute tubular epithelial damage with less than 5 % tubular atrophy and interstitial fibrosis. In both histological examinations there was no evidence of acute cellular or humoral rejection or polyomavirus infection. In addition, computer tomography angiography (CT-A) and MRI of the transplanted kidney were performed.

Results: The CT-A was indicative of a kink in the renal artery with otherwise inconspicuous vascular imaging. In contrast, multiparametric fMRI showed a clearly reduced global perfusion of the transplant kidney. Based on the findings, an angiography of the transplant kidney was performed including embolization of an arterio-venous malformation and stent angioplasty of the renal artery. In follow-up, renal function improved to a plasma creatinine of 2.2 mg/dl and an eGFR of 25,1 ml/min/1,73 m² (MDRD).

Conclusion: Multiparametric fMRI examination may present a valuable additional tool to delineate underlying causes of a decline in renal allograft function. Prospective studies are warranted and currently in preparation.

P059

Total plasma exchange and high cut-off hemodialysis are able to remove significant amounts of vitamin D metabolites in vitamin-D induced hypercalcemic crisis

D.J. Heister; B.N. Bohnert; N. Heyne; F. Artunc

Sektion Nieren- und Hochdruckkrankheiten, Universitätsklinikum, Medizinische Klinik IV, Eberhard Karls Universität Tübingen, Tübingen

Objective: We report on a 33-year-old male patient with life-threatening hypercalcemic crisis caused by self-induced vitamin-D intoxication, after taking cumulatively around 7,000,000–10,000,000 I.U. of vitamin D₃ within approximately one year. Given the binding of vitamin D metabolites to the vitamin D binding protein (59 kDa), we have found in a previous pilot case that extracorporeal treatments

such as total plasma exchange with replacement by human albumin (TPE-HA) and high cut-off hemodialysis (HCO-HD) are able to reduce vitamin D metabolites from the plasma. However, the exact amount removed remains unknown.

Method: We performed extracorporeal treatments using sustained low efficient dialysis (SLED, one session) and intermittent hemodialysis (iHD, three sessions) to correct hypercalcemia. To remove vitamin D metabolites, we performed four sessions of TPE-HA with an exchange volume of 2.5–3.5 L corresponding to 0.61–0.85 of the plasma volume and three 6 h sessions of HCO-HD using the Theralite dialyzer. We compared their efficacy to remove vitamin D metabolites from the spent plasma and dialysate.

Results: On admission, total and ionized plasma calcium concentration was 4.0 mmol/L and 2.19 mmol/L, respectively. Plasma 25-OH-vitamin D₃ was elevated to 1280 nmol/L. In addition to forced diuresis and one-time administration of zoledronic acid, we performed a total of eleven extracorporeal treatments, starting on the admission day. We were able to achieve a rapid and lasting reduction in plasma calcium concentrations (from 4.0 mmol/L to 2.2 mmol/L). In addition, we were able to reduce plasma 25-OH-vitamin D₃ concentration by 70 % (from 1280 nmol/L to 383 nmol/L) and 1,25-OH-vitamin D₃ concentrations by 66 % (from 178 nmol/L to 61 nmol/L) at the time of hospital discharge. The reduction rate for 25-OH-vitamin D₃ seemed to be higher after TPE-HA (42–60 %) compared to HCO-HD (33–47 %). In contrast, the 1,25-OH-vitamin D₃

reduction rate was not different between the two methods (14–29 % for TPE-HA vs. 15–29 % for HCO-HD). TPE-HA tended to remove quantitatively more 25-OH-vitamin D₃ (1045 nmol to 2557 nmol vs. 660 nmol) and 1,25-OH-vitamin D₃ (161 pmol to 450 pmol vs. 134 pmol) than HCO-HD.

Conclusion: Extracorporeal treatments such as TPE-HA and HCO-HD are able to remove significant amounts of vitamin D metabolites from the body. Compared to HCO-HD, a single session of TPE-HD tended to remove more vitamin D metabolites.

P060

Von COVID-19 zum Goodpasture-Syndrom – eine Fallvorstellung

L. Greipel; M. Gutting; N. Kanzelmeyer
Klinik für pädiatrische Nieren-, Leber- und Stoffwechselerkrankungen, Zentrum Kinderheilkunde und Jugendmedizin, Medizinische Hochschule Hannover, Hannover

Hintergrund: Wie wichtig ist eine frühe Diagnosestellung, welche Therapie hilft?

Methode: Es wird der Fall einer 16-jährigen Patientin mit einem langwierigen und ungewöhnlichen Verlauf eines Goodpasture-Syndroms vorgestellt.

Ergebnisse: Die vorher gesunde Patientin erkrankte im Januar 2021 an COVID-19 mit mildem Verlauf. Sechs Monate später traten Belastungsdyspnoe und hohes Fieber auf. CT Thorax und Lungenfunktionsuntersuchungen bei persistierender respiratorischer Symptomatik im Juli und September 2021 zeigten eine obstruktive Ventilationsstörung. Zwischenzeitlich erhielt die Patientin Prednisolon

intravenös, Azithromycin oral, Salbutamol und Fluticason/Salmeterol inhalativ. Nach insgesamt drei Krankenhausaufenthalten traten im Oktober 2021 hohes Fieber, Erbrechen, starke Belastungsdyspnoe, Makrohämaturie sowie Sauerstoffbedarf und blutiges Bronchialsekret auf. Das Kreatinin stieg bis auf 726 µmol/L (09/2021: 54 µmol/L). Eine Nierenbiopsie zeigte eine hochgradige extrakapilläre proliferative und nekrotisierende Glomerulonephritis sowie ausgedehnte Halbmondformationen. Die Lungenbiopsie ergab Zeichen einer alveolären Hämorrhagie. Korrelierend hierzu waren die anti-Glomeruläre Basalmembran (GBM) Titer nicht messbar hoch, sodass die Diagnose Goodpasture-Syndrom gestellt wurde. Initial erfolgten drei Methylprednisolon-Pulse je 1 g mit anschließend Prednisolon oral (2 mg/kg/Tag) und zusätzlich einer Immunsuppression mit Mycophenolatmofetil (MMF) 2 g/Tag. Insgesamt erhielt die Patientin 21 Plasmapheresen, 21 Immunadsorptionen und sechs Rituximab-Gaben sowie einmalig Immunglobuline bis Februar 2022. Zweimalig waren die anti-GBM Titer unter der Therapie auf 65 U/mL und 10 U/mL angestiegen. Bei trotz niedriger anti-GBM Titer persistierender Diarrhoe und Abgeschlagenheit wurde von Cellcept (MMF) auf Myfortic (Mycophenolat) umgestellt. Aktuell ist die Patientin unter Myfortic (720 mg/Tag) und Prednisolon (0,5 mg/kg/Tag) mit anti-GBM Titern unter 7 U/mL seit Mitte Februar 2022 stabil. Es besteht intermittierender nächtlicher Sauerstoffbedarf. Seit Ende Oktober 2021 ist die Patientin hämodialysepflichtig.

Zusammenfassung: Bei einer protrahierten respiratorischen Symptomatik wurde die Diagnosestellung durch die initiale COVID-19-Infektion verzögert. Die aggressive Therapie mit Plasmapheresen, Cortison und einer Immunsuppression mit Rituximab und MMF konnte die anti-GBM Titer dauerhaft senken. Einerseits wird die Dringlichkeit der frühzeitigen Diagnosestellung und des zügigen Therapiebeginns verdeutlicht und andererseits gezeigt, dass eine aggressive Therapie zur Senkung der anti-GBM Titer nötig ist.

P061

Transarterielle Chemoembolisation zur Therapie einer schweren therapie-refraktären Hyperkalzämie

B. Gießmann; C. Jackisch; N. Riling¹; K. de Groot

Medizinische Klinik III, Sana Klinikum Offenbach GmbH, Offenbach; ¹ Radiologie und Nuklearmedizin, Sana Klinikum Offenbach GmbH, Offenbach

Hintergrund: Wir berichten über eine 73 Jahre alte Patientin mit ausgeprägter, oligosymptomatischer Hyperkalzämie bis 3,99 mmol/l, welche als Zufallsbefund in einer hausärztlichen Laborkontrolle aufgefallen war. Elf Jahre zuvor war ein bifokales Mammakarzinom rechts diagnostiziert worden, welches brusterhaltend in kurativer Intention operiert wurde. Es schloss sich eine adjuvante antihormonelle Therapie mit einem Aromatasehemmer (Letrozol) und eine sekundäre Axilladissektion an. CT-morphologisch zeigte sich eine solitäre 11 × 10 × 10 cm messende, hypervaskularisierte, solide fokale Leberläsion im rechten Leberlappen

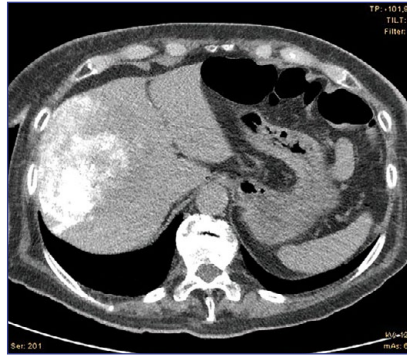


P061: Abb. 1

die sich bioptisch als metastatische Absiedelung eines klinisch vorbekannten Mammakarzinoms herausstellte. Ursache der schweren Hyperkalzämie war eine paraneoplastischen Sekretion von Parathormon-related Peptide (PTHrP) durch eine solitäre, hormonaktive Lebermetastase eines Mammakarzinomrezidivs.

Methode: Es erfolgte zunächst eine konservative Kalziumsenkung mit intravenöser Volumen- und Bisphosphonatgabe sowie die Einleitung einer Therapie mit Aromatasehemmer (Exemestan) und CDK4/6-Inhibitor (Palbociclib). Bei anhaltender Hyperkalzämie erfolgte dann die Einleitung einer intermittierenden Hämodialyse unter der sich die Hyperkalzämie als therapierefraktär erwies. Zur Reduktion der hormonaktiven Tumormasse erfolgte eine transarterielle Chemoembolisation (TACE) mit einer Kombination aus Mitomycin, Epirubicin, Lipiodol und Polyvinyl-Alkohol. Durch die TACE konnte hier etwa 50–60 % der großen solitären Lebermetastase destruiert werden, erkennbar an der Anreicherung des Embolisats in der Metastase im postinterventionell erfolgten CT.

Ergebnisse: Postinterventionell zeigte die Patientin auch in Dialyseauslass ein in den Normbereich



P061: Abb. 2

abfallendes Serumkalzium. PTHrP war zuletzt nicht in erhöhter Konzentration messbar. Die Patientin wurde in gutem Allgemeinzustand und beschwerdefrei wieder in die ambulante Nachsorge entlassen, in der sich die Metastase als größenregredient erwies.

Zusammenfassung: PTHrP wird von vielen Tumorentitäten gebildet und ist ein wichtiger Parameter bei Patienten mit Hyperkalzämie und supprimiertem Parathormon. Bei solitären, hormonaktiven Lebertumoren stellt eine transarterielle Chemoembolisation (TACE) eine Option zur raschen Tumordestruktion und anhaltenden Kalziumsenkung dar.

P062

The management of haemodialysis catheter associated right atrial thrombus – a case report

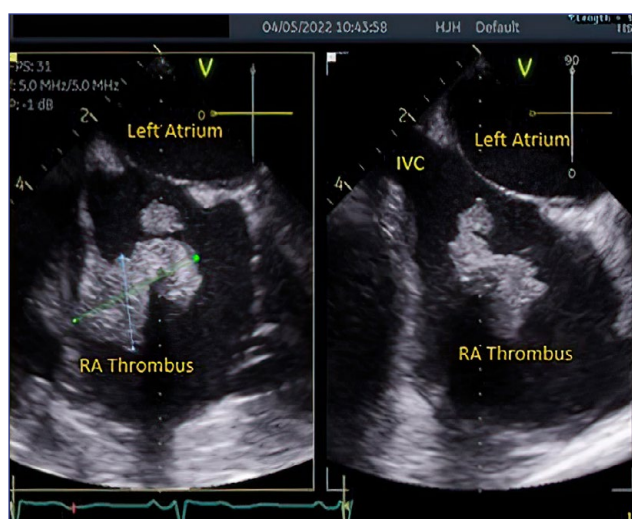
Z. M. Tun; L. Moore; S. Hussain;
R. Brown; M. Schulz
Nephrology, Royal Liverpool University
Hospital, Liverpool/UK

Introduction: A tunnelled line is a form of dialysis access that is commonly used for haemodialysis patients. The incidence of catheter related atrial thrombus (CRAT) is relatively common but exact incidence

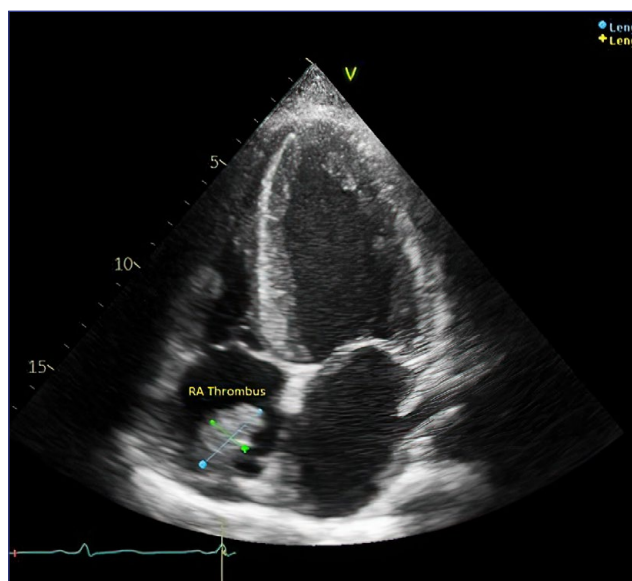
is unknown (2–29 %)¹ as most cases are asymptomatic. Potential complications include pulmonary embolism, systemic embolism and haemodynamic instability. Management of CRAT is variable. We report a case of CRAT and its successful management by thrombolysis via the tunnelled line.

Patient Description: A 29 year old male with chronic kidney disease stage 5 secondary to diabetic nephropathy was commenced on haemodialysis via right internal jugular tunnelled line. Chest x-ray confirmed the tip of the catheter was in the right atrium. Citralock 46.7 % was used in both catheter lumens post dialysis. He was not on antiplatelet or anticoagulation medications. A transthoracic echocardiogram (TTE) before line insertion showed severe left ventricular systolic impairment. A repeat TTE five months later, and two months after tunnelled line insertion, showed a large 3.1×2.4 cm right atrial mass. Therapeutic low molecular weight heparin was commenced. Transoesophageal echocardiogram confirmed thrombus adherent to the catheter tip and atrial wall. The nephrology radiology MDT opted for thrombolysis therapy via tunnelled line (IV alteplase 10 mg bolus over 2 minutes then IV alteplase 85 mg infusion over 2 hours (total 1.5 mg/kg)). Repeat TTE showed a reduction in thrombus size to 2.9×1.6 cm. The tunnelled line was removed without embolic complications and intravenous heparin continued whilst loading on warfarin.

Discussion: Since the catheter is pro-thrombogenic², catheter removal is recommended due to the risks of complications



P062: Abb. 1
Transoesophageal echocardiogram (04/05/2022), bi-plane image, X-plane (Left) showing 4 chamber view focused on right atrium showing thrombus (3.1 cm x 2.4 cm) attached to the right atrial wall. (Right) Perpendicular plane



P062: Abb. 2
Transthoracic echocardiogram (05/05/2022), Apical 4 chamber view, 1 day post intracardiac thrombolysis and commencement of intravenous unfractionated heparin showing relative reduction of clot size (2.9 cm x 1.6 cm) in the right atrium.

and recurrence. There are multiple CRAT management strategies including removal of the catheter alone, systemic anticoagulation, surgical thrombectomy and catheter directed thrombolysis^{3,4}. As there are no recognised guidelines, treatment is based on clinical judgement, experience and available resources. A similar study managed large CRAT with thrombolysis via the tunnelled line leading to

a 96% reduction in thrombus volume⁵. There are a limited number of reported cases of thrombolysis via tunnelled line for CRAT, which is a suitable management option in selected cases. Further studies need to assess thrombolysis via tunnelled line for CRAT including timing and dose administration, with consideration given to routine screening for CRAT due to its asymptomatic nature and significant risks.

P063

The use of prolonged-release tacrolimus twice a day (BID) might be beneficial for selected kidney transplant recipients

L. Füesl; L. Kreuzer; K. Nierychlewski¹; B. Meiser; M. Schwarz¹; M. Fischeder; S. Kemmner²

Medizinische Klinik und Poliklinik IV – Nephrologisches Zentrum, Klinikum Großhadern, Ludwig-Maximilians-Universität München, München; ¹ Institut für Labormedizin, Ludwig-Maximilians-Universität München, München; ² II. Medizinische Klinik, Nephrologie, Klinikum rechts der Isar, Technische Universität München, München

Objective: Tacrolimus either as prolonged- or immediate-release is part of the standard immunosuppressive therapy in kidney transplant recipients. It is known to have a highly variable metabolism rate and a narrow therapeutic window that requires close drug monitoring and individual dosing. Thereby fast tacrolimus metabolism is associated with reduced kidney transplant survival.

Method: We describe a case of a 47 y old female transplant recipient, who presented with declining kidney transplant function over time. The patient had a high immunological risk constellation, and the tacrolimus trough levels were in the lower target range despite high doses administered. The graft biopsy revealed typical signs of calcineurin inhibitor toxicity in the absence of acute or chronic rejection, and especially without any evidence of transplant glomerulopathy. Exceedingly high serum levels of immediate-release tacrolimus were confirmed in the area under the concentration

time curve (AUC). Switching to a belatacept- or mTOR inhibitor-based regimen was not possible in this special case. Therefore, prolonged-release tacrolimus twice daily in adjusted dosage was administered in order to reduce progress of CNI toxicity as well as to secure an optimal therapeutic drug level.

Results: After the change in medication, the AUC for oral tacrolimus as well as the transplant function improved despite higher tacrolimus trough levels and a lower total dose administered.

Conclusion: The administration of prolonged-release tacrolimus twice-daily might be beneficial for selected patients, and especially for patients with fast tacrolimus metabolism. However, this use is off-label and should be critically discussed by the transplant community. The performance of the AUC for oral tacrolimus is necessary to identify high serum levels that are known to cause renal toxicity. The AUC should be further done to ensure optimal adjustment of the medication dosage, especially in the use of prolonged-release tacrolimus twice daily.

COVID-19 1

P064

Molnupiravir (Lagevrio®) als Monotherapie bei SARS-CoV2-infizierten Patienten nach Nierentransplantation

K. Boss; M. J. Konik¹; H. Rohn¹; M. Lindemann²; A. Kribben; O. Witzke¹; A. Gäckler
Klinik für Nephrologie, Universitätsklinikum, Universität Duisburg-Essen, Essen; ¹ Klinik für Infektiologie, Universitätsklinikum, Universität Duisburg-Essen, Essen; ² Institut für Transfusionsmedizin,

Universitätsklinikum Essen, Universität Duisburg-Essen, Essen

Hintergrund: Seit Ende Dezember 2021 ist das oral anwendbare antivirale Medikament Molnupiravir in Deutschland zur Behandlung nicht hospitalisierter Patienten mit SARS-CoV2-Infektion ohne Sauerstoffbedarf, aber mit erhöhtem Risiko für einen schweren Krankheitsverlauf, verfügbar. Daten zur Wirksamkeit und Sicherheit von Molnupiravir als Monotherapie bei Patienten nach Nierentransplantation wurden bislang nicht publiziert.

Methode: In einer retrospektiven Beobachtungsstudie wurden Daten von 13 nierentransplantierten Patienten mit immunsuppressiver Triple-Therapie und < 5 Tage bestehender, PCR-gesicherter, mild symptomatischer SARS-CoV2-Infektion, ausgewertet, die bei fehlender Verfügbarkeit eines wirksamen Antikörpers im Zeitraum 01-02/2022 mit Molnupiravir als Monotherapie behandelt wurden. Alle Patienten hatten eine eGFR > 30 ml/min/1,73 m² bei Therapiebeginn.

Ergebnisse: 9/13 Patienten waren männlich (Alter 33–65, Median 46 Jahre). Zwischen Transplantation und SARS-CoV2-Infektion lagen 96–2288 Tage. Der SARS-CoV2-Antikörpertiter war bei 3 Patienten prä-Infektion nicht bekannt, bei 6 Patienten negativ und bei 4 Patienten positiv (range 43–1370 BAU/ml). Kein Patient berichtete von Medikamenten-assoziierten Nebenwirkungen. Es traten keine Thrombozytopenie oder Leberwerterhöhung auf. 9/13 Patienten zeigten einen unkomplizierten Krankheitsverlauf. Die Patientin mit dem kürzesten Abstand zur Transplantation musste im Verlauf bei

respiratorischer Insuffizienz intensivmedizinisch behandelt werden. Zwei Patienten erhielten 18 bzw. 22 Tage nach Symptombeginn bei persistierendem Antigenbefund mit Temperaturerhöhungen und Allgemeinsymptomatik das zwischenzeitlich verfügbare Sotrovimab. Hiervon war ein Patient erst 6 Monate transplantiert, der andere hatte eine Abstoßungstherapie im Vorjahr erhalten und hatte einen negativen Antikörpertiter. Ein ungeimpfter Patient nach AB0-inkompatibler Lebendnierenspende vor < 6 Monaten entwickelte ein akutes Transplantatversagen mit SARS-CoV2-Infiltration der Niere. 2/4 Patienten mit komplikativem Verlauf entwickelten im Rahmen der Infektion weder eine B- noch eine T-Zell-Antwort.

Zusammenfassung: Eine Monotherapie mit Molnupiravir kann auch bei Nierentransplantierten eingesetzt werden, erscheint jedoch insbesondere bei hoher Immunsuppression unzureichend.

P065

COVID-19-assoziiertes akutes Nierentransplantatversagen nach AB0-inkompatibler Lebendspende

K. Boss; M. J. Konik¹; J. H. Bräsen²; J. Schmitz²; C. Jürgens; A. Kribben; O. Witzke¹; S. Dölff¹; A. Gäckler
Klinik für Nephrologie, Universitätsklinikum, Universität Duisburg-Essen, Essen; ¹ Klinik für Infektiologie, Universitätsklinikum, Universität Duisburg-Essen, Essen; ² Nephropathologie, Institut für Pathologie, Medizinische Hochschule Hannover, Hannover

Hintergrund: Immunsuppressive Therapie geht mit einem erhöhten Risiko für schwere Verläufe einer SARS-CoV2-Infektion einher,

mit häufig verzögerter Virus-Clearance. Wir berichten über ein akutes Nierentransplantatversagen bei persistierender SARS-CoV-2-Infektion bei einem Patienten mit absoluter B-Zell-Depletion nach Gabe von Rituximab bei erfolgter AB0-inkompatibler Nierenlebenspende.

Ergebnisse: Bei einem 34-jährigen, ungeimpften Patienten wird vier Monate nach Transplantation eine SARS-CoV2-Infektion mittels PCR diagnostiziert. Es bestand eine Tripple-Immunsuppression mit Tacrolimus, MMF und Prednison. Bei einer eGFR von 44 ml/min/1,73 m² und zu diesem Zeitpunkt nicht verfügbarer Antikörperprophylaxe erfolgte bei dem nur minimal symptomatischen Patienten und Ablehnung einer stationären Aufnahme zur Remdesivirgabe zunächst eine Therapie mit Molnupiravir. Im Verlauf trat ein akutes Nierentransplantatversagen auf. Bei biopischem Nachweis einer akuten T-Zell-rejektion mit schwerem akuten Tubulusepithelschaden mit nur geringer interstitieller Fibrose und Tubulusatrophie (BANFF Kat. 4 IB) sowie einer Borderline-Abstoßung (BANFF Kat. 3) im Rahmen einer zweiten Biopsie erfolgte jeweils ein Steroidstoß, sowie im Rahmen der zweiten Biopsie die Gabe intravenöser Immunglobuline (iViG). Bindende HLA-IgG-Antikörper lagen nicht vor. Etwa 8 Wochen nach erstmaligem Nachweis einer SARS-CoV-2-Infektion entwickelte der Patient eine COVID-19 Pneumonie mit bakterieller Superinfektion, welche antiinfektiv mit Tazobactam/Piperacillin und Clarithromycin sowie immunmodulatorisch mit Dexamethason und erneuten iViG behandelt wurde. Bei unverändert eingeschränkter Transplantatfunktion

erfolgte eine erneute Biopsie, formal mit Nachweis einer akuten T-Zellrejektion. Mittels Fluoreszenz-in-situ-Hybridisierung konnten jedoch in großen Teilen der Tubuli SARS-CoV-2-Viren nachgewiesen werden. Nach 9 Wochen andauern der SARS-CoV2-Infektion mit einem Cycle Threshold zwischen 22–28 konnten beim Patienten weder Anti-SARS-CoV2-IgG noch eine SARS-CoV2-spezifische zelluläre Immunantwort nachgewiesen werden, sodass die Gabe von Remdesivir und des zwischenzeitlich verfügbaren Sotrovimab erfolgten. Darunter konnten eine SARS-CoV-2-Clearance, der Nachweis von Anti-SARS-CoV2-IgG und eine Besserung der Transplantatfunktion erzielt werden.

Zusammenfassung: Die fehlende Virus-Clearance kann bei Immunsupprimierten auch spät zu Komplikationen einer SARS-CoV2-Infektion führen. Zudem sind atypische Manifestationen wie Infiltration eines Nierentransplantats mit einer Abstoßung vortäuschenden Entzündung möglich.

P066

Generation of potentially inhibitory Autoantibodies to ADAMTS13 in Coronavirus Disease 2019

A. Doevelaar; M. Bachmann¹; B. Hölzer; F. S. Seibert; B. Rohn; P. Zgoura; O. Witzke²; U. Dittmer³; T. Brenner⁴; K. Paniskaki; S. Yilmaz¹; R. Dittmer⁵; S. Schneppenheim⁵; J. Wilhelm⁶; N. Babel; U. Budde⁵; T. H. Westhoff
Centrum für Translationale Medizin, Medizinische Klinik I, Marien Hospital Herne, Ruhr-Universität Bochum, Herne; ¹ Bereich Intensivmedizin und Beatmungsmedizin, Lungen- und Thoraxklinik Hamburg, Asklepios Klinik Harburg, Hamburg; ² Klinik

für Infektiologie, Universitätsklinikum, Universität Duisburg-Essen, Essen;

³ Institut für Virologie, Universitätsklinikum, Universität Duisburg-Essen, Essen; ⁴ Klinik für Anästhesiologie und Intensivmedizin, Universitätsklinikum Essen, Essen; ⁵ Abteilung für Hämostaseologie, MEDILYS Labor-gesellschaft mbH, Hamburg; ⁶ Institut für Pathologie, Universitätsklinikum Gießen und Marburg GmbH, Gießen

Objective: It has recently been shown that von Willebrand factor (vWf) multimers contribute to immunothrombosis in Coronavirus disease 2019 (COVID-19). Since COVID-19 is associated with an increased risk of autoreactivity, the present study investigates, whether the generation of autoantibodies to ADAMTS13 contributes to this finding.

Method: In this observational prospective controlled multicenter study blood samples and clinical data of patients hospitalized for COVID-19 were collected from April to November 2020.

Results: The study included 156 individuals with 90 patients having confirmed COVID-19 of moderate to critical severity. 30 healthy individuals and 36 critically ill ICU patients without COVID-19 served as controls. ADAMTS13 antibodies occurred in 31 (34.4%) COVID-19 patients. Antibodies occurred more often in critically ill COVID-19 patients (55.9%) than non-COVID-19 ICU patients and healthy controls (5.6% and 6.7%; $p < 0.001$), respectively. Generation of ADAMTS13 antibodies in COVID-19 was associated with lower ADAMTS13 activity (56.5%, interquartile range (IQR) 21.25 vs. 71.5%, IQR 24.25, $p = 0.0041$), increased disease severity (severe or

critical in 90 % vs. 62.3 %, $p = 0.019$), and a trend to higher mortality (35.5 % vs. 18.6 %, $p = 0.077$). Median time to antibody development was 11 days after first positive SARS-CoV-2-PCR specimen. Gel analysis of vWf multimers resembled the constellation in patients with TTP. **Conclusion:** The present study demonstrates for the first time, that generation of ADAMTS13 antibodies is frequent in COVID-19, associated with lower ADAMTS13 activity and increased risk of an adverse disease

course. These findings provide a rationale to include ADAMTS13 antibodies in the diagnostic workup of SARS-CoV-2 infections.

P067
Renal injury and inflammatory response in new onset IgA Nephropathy after infection with SARS-Cov-2 or Covid-19 vaccination.

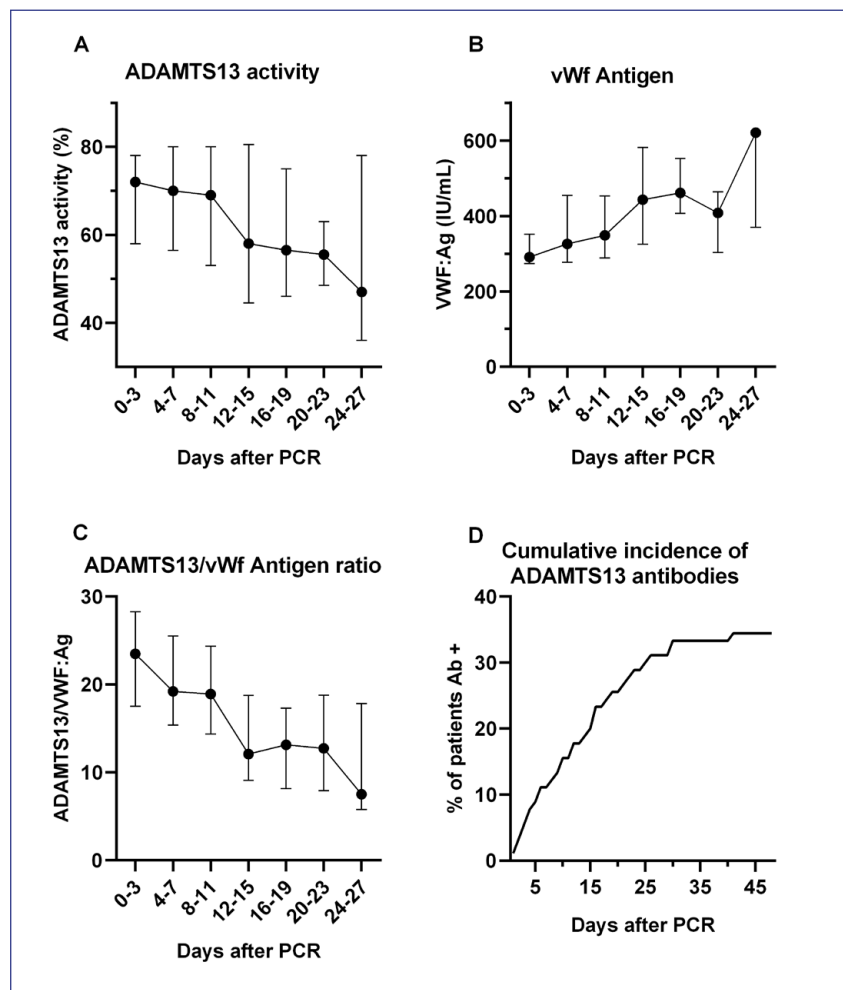
N. Hussein; E. Vonbrunn; C. Eck; M. Büttner-Herold; K. Amann; C. Daniel

Institut für Nephropathologie, Universitätsklinikum, Friedrich-Alexander-Universität Erlangen-Nürnberg, Erlangen

Objective: After infection with SARS-Cov-2 or vaccination against COVID-19, some patients develop kidney diseases, including minimal change nephrotic syndrome and IgA Nephropathy (IgAN). Here we characterized renal injury and inflammatory response in biopsies from patients with new onset IgAN diagnosed promptly after COVID-19 disease or vaccination.

Method: Eleven kidney biopsies from patients who developed IgAN after SARS-Cov-2 infection and 6 from patients with new onset IgAN after vaccination against COVID-19 were diagnosed at Department of Nephropathology, FAU Erlangen-Nuremberg. Biopsies from patients with IgAN who had no prior COVID-19 disease ($n = 10$) and zero-time biopsies from transplants (ZB; $n = 6$) served as controls. Kidney function was assessed by measurement of serum creatinine and kidney injury by analysis of nephrin-positive podocyte loss, detection of Pax-8 positive parietal epithelial cells on the glomerular tuft and IF/TA. Macrophages and granulocytes were detected by triple staining of CD68, CD163 and myeloperoxidase.

Results: Significant podocyte loss, as assessed by nephrin staining, was observed in all three IgAN groups compared to ZB, as well as Pax8-positive parietal epithelial cells on glomerular tuft. The serum creatinine, as a marker of kidney function, was on average 1.8–3.5-fold higher in the IgAN groups compared to ZB, but did not reach



P066: Abb. 1

significance level due to small sample numbers. IF/TA was below 20 % in most investigated biopsies. No significant differences in renal function or injury were observed between different IgAN groups. While CD68 + CD163 + MPO+, CD68 + CD163-MPO+ and CD68 + CD163 + MPO- (M2c-like macrophages) inflammatory cells were significantly increased in both COVID-19 IgAN groups, significant increase of CD68-CD163 + MPO-cells compared to ZB control was restricted to IgAN w/o COVID-19 group (11.7 ± 8.1 vs 0.8 ± 0.9 cells/mm²). CD68 + CD163-MPO- M1-like macrophages and CD68-CD163-MPO+ neutrophils tended to be higher in all IgAN groups but failed to reach the level of significance.

Conclusion: Changes in kidney function and renal damage was comparable in all three investigated IgAN groups independent on experience of COVID-19 or vaccination. Renal macrophage and neutrophil invasion tended to be higher in COVID-19 IgAN groups. However, no significant differences in inflammation were observed in direct comparisons of IgAN groups.

P068

Cellular immune response to SARS-CoV-2 vaccination among kidney transplant patients with and without COVID-19 infection

S. Landmann; M. Kantauskaitė; J. Lamberti; I. Tometten; L. Müller¹; J. Hillebrandt; M. Kittel; T. Kolb; K. Ivens; E. Königshausen; L. C. Rump; J. Timm¹; J. Stegbauer
Klinik für Nephrologie, Universitätsklinikum, Heinrich-Heine-Universität Düsseldorf, Düsseldorf;
¹ Virologie, Universitätsklinikum,

Heinrich-Heine-Universität Düsseldorf, Düsseldorf

Objective: Kidney transplant recipients (KTRs) demonstrate low humoral response following SARS-CoV-2 vaccination and remain susceptible to the infection. Various booster vaccination schemes were developed to overcome this obstacle, however proved to succeed only in certain cases. It is believed, however, that KTRs develop cellular immune response which plays an important additional role in protection against severe infection. Therefore, we ought to measure immune cell response among KTRs who were vaccinated at least 3 times and compare it KTRs after vaccination and COVID-19 infection.

Method: SARS-CoV-2-specific T cells and antibodies were quantified approximately four months (median 16, IQR 15–18 weeks) after the third or fourth SARS-CoV-2 vaccination among 103 KTRs after vaccination, 15 KTRs after vaccination and COVID-19 infection and 21 healthy controls. T cell response were quantified by a commercially available standardized Interferon gamma (IFN γ) release assay (T.SPOT COVID Test) and antibody levels against SARS-CoV-2 spike protein were measured using the SARS-CoV 2-QuantVac ELISA (Euroimmun). For the T-cell response > 7 IFN γ spots (= spot forming units, SFU)/2.5 \times 10⁵ PBMCs were considered positive whereas seroconversion was defined by antibody levels above 35.2 BAU/ml. Clinical and demographic data were retrieved from patients records.

Results: In line with the impaired humoral immune response, the spike-specific T cell response was

also significantly lower among KTRs in comparison to healthy controls. In addition to that, KTRs after vaccination had median values of 5 (1–9) SFU/2.5 \times 10⁵ PBMCs which was significantly lower to the ones observed among KTRs after vaccination and COVID-19 infection (18 (9–30) SFU/2.5 \times 10⁵ PBMCs, $p < 0.05$). In only vaccinated KTRs a positive correlation (R 0.39, $p < 0.05$) between antibody level and cellular response was observed. Vaccinated and recovered from infection KTRs did not demonstrate such a correlation. Factors associated with positive cellular immune response after the vaccination were antibody level above 35,2 BAU/ml (OR 5.85, 95 CI% 1.88–18.21), time after the transplantation (OR 1.00, 95 CI% 0.99–1.01) and the use of vector vaccine (OR 3.76, 95 CI% 1.09–12.89). Indeed, 24 % KTRs vaccinated with vector vaccine developed cellular immunity. Although KTRs vaccinated with mRNA vaccines showed similar antibody levels, positive T-cell response was observed in only 10 % KTRs

Conclusion: Humoral immune response correlates well with cellular immune response and is more potent after COVID-19 infection.

P069

SARS-CoV-2 associated infections and mortality in dialysis patients in central Germany – a multicenter prospective trial

S. Kamalanabhaiah; C. Ostermaier; L. Dahmen; I. Lettermann-Nass¹; K. Volland¹; R. Gefßner²; J. Hoyer; C. Keller¹; C. S. Haas
Klinik für Innere Medizin, Nephrologie und Internistische Intensivmedizin, Standort Marburg, Universitätsklinikum Gießen und Marburg GmbH,

Marburg; ¹Institut für Virologie, Philipps Universität, Marburg; ²Institut für Laboratoriumsmedizin und Pathobiochemie, Philipps Universität, Marburg

Objective: Dialysis patients are at great risk for contracting COVID-19 during the pandemic as they have limited options to self-isolate. In fact, they have to appear at their dialysis centers on a regular basis to receive their life-saving treatment. In this course, they are forced to be in close contact with ambulance or taxi drivers, co-patients and health care workers, setting them at risk of contracting COVID-19. It has been postulated that dialysis patients might be more affected than the general population concerning disease severity and mortality. The objective of this study is to assess incidence of SARS-CoV-2 infection as well as clinical course of COVID-19 and its mortality.

Method: We conducted a prospective, multicenter study in chronic hemodialysis patients in 12 dialysis centers in central Germany, starting April 2020. PCR testing and antibody blood sampling was performed at the start as well after 9 and 12 months. Basic data was assessed, means of transportation and kind of residence were evaluated specifically with regard of risk for infection. At any time point, COVID-19 associated symptoms were logged, and fatalities were counted during the ongoing pandemic with its particular waves of virus variants. Data was compared to the local general population.

Results: 874 of 1004 screened patients participated in the study. Medium age was 69.8 ± 14.2 years with 62.1 % males. Taxi or ambulance were the means of transportation

in 86.5 %, 7.6 % lived in a nursing home. A total of 77 patients (8.8 %) acquired COVID-19. Demographic data did not differ between diseased and healthy patients except for residency (22.1 % vs. 6.1 % in nursing homes, $p < 0.001$): the odds ratio to get COVID-19 was significantly higher in dialysis patients living in nursing homes compared to those in home care (OR 3.76, 95 % CI 2.05–6.87). Like in the general population, the highest infection rate was observed with the alpha variant, whereas the delta variant did not affect the dialysis centers. Omicron on the other hand was highly present. Mortality was highest during the alpha variant wave (29.1 %), but was lower in delta (14.2 %) and lowest in omicron infections (0.3 %). Overall infections and mortality in dialysis patients decreased with immunization status, either through prior infection or vaccination in nursing homes. Of note, cumulative 2-years mortality in this cohort (37.3 %) was barely impacted by COVID-19 associated death.

Conclusion: COVID-19 immunization in hemodialysis patients highly effective preventing spreading the virus from nursing homes to dialysis centers. General morbidity status in dialysis patients seems to be more relevant to outcome than intercurrent infections with COVID-19.

P070

Kidney infiltrating SARS-CoV-2 T cells

U. Stervbo; J. Kurek; M. Anft; T. Roch; T.H. Westhoff; N. Babel
Centrum für Translationale Medizin, Medizinische Klinik I, Marien Hospital Herne, Ruhr-Universität Bochum, Herne

Objective: Kidney transplantation is associated with an increased risk of severe COVID-19 disease. The viral entry receptor ACE-2 is also found on cells of the kidney, making these a possible target during an infection, which could have detrimental effect on the kidney function. This effect could be caused by an uncontrolled viral replication or through cellular immunity towards the infected cells, leading to tissue destruction. Here we present two cases of kidney transplant patients, who suffered impaired kidney function during and acute SARS-CoV-2 infection.

Method: The possible role of cellular immunity towards SARS-CoV-2 infected kidney cells was assessed through AIRR-seq by NGS of the T cell receptor (TCR) of whole biopsies and SARS-CoV-2 specific T cells of the peripheral blood. SARS-CoV-2 specific T cells were isolated from peripheral blood by overnight stimulation with an overlapping peptide pool of SARS-CoV-2 S-protein (Wuhan variant) and subsequent isolation by MACS using antibodies and beads against CD154 and CD137. By comparing the TCRs of these two samples, we can assess the specificity of the kidney infiltrating T cells. One kidney transplant donor was a living relative which enabled us to setup a mixed lymphocyte reaction to further evaluate acute rejection, as a cause of decreased kidney function.

Results: From patient 1 we obtained 1.7×10^7 reads from the S-protein specific T-cells, and 2.5×10^6 reads from the biopsy. Of these, we identified 127,310 distinct clonotypes in the peripheral blood, but 0 in the kidney biopsy. This lack of T cell infiltration was confirmed by

conventional histology, and exclude a T cell driven etiology. From patient 2 we obtained 9.8×10^6 reads from the kidney biopsy, 9.5×10^6 reads from the S-protein specific T-cells, and 5.7×10^6 reads from the mixed lymphocyte reaction. This translated into 104,760, 24,743, and 5,312 distinct clonotypes, respectively. Here, 11.1 % of the repertoire of the kidney infiltrating T cells were identical to S-protein specific T-cells in the periphery, and only 3.12 % of the repertoire was identical to donor reactive TCRs.

Conclusion: AIRR-Seq of whole biopsies is a method to evaluate T cell infiltration and the specificity of these infiltrating T cells. We find, that one patient had no T cell associated complications, while another patient had an infiltration of predominantly SARS-CoV-2 specific T cells, indicating SARS-CoV-2a leading cause of the kidney function deterioration.

P071

A vector-based vaccine dose after three doses of mRNA-based COVID-19 vaccination does not substantially improve humoral SARS-CoV-2 immunity in renal transplant recipient

B. Rohn; A. Blázquez-Navarro¹; T. L. Meister²; E. Vidal Blanco³; K. Paniskaki⁴; M. Anft; J. Wellenkötter⁵; T. Giglio⁵; S. Pfaender²; U. Stervbo; O. Cinkilic¹; T. H. Westhoff; N. Babel
Centrum für Translationale Medizin, Medizinische Klinik I, Marien Hospital Herne, Ruhr-Universität Bochum, Herne; ¹ Berlin-Brandenburg Center für Regenerative Therapien, Charité – Universitätsmedizin Berlin, Berlin; ² Department of Molecular and Medical Virology, Marien Hospital Herne, University

Hospital of the Ruhr-University Bochum, Herne; ³ Department of Molecular and Medical Virology, Ruhr-University Bochum, Bochum; ⁴ Klinik für Infektiologie, Universitätsklinikum, Universität Duisburg-Essen, Essen; ⁵ Dialysezentrum Schwerte, Schwerte

Objective: Kidney transplant recipients (KTX) are at high risk for a severe Coronavirus disease 2019 (COVID-19) manifestation. Vaccination against the severe acute respiratory syndrome coronavirus 2 (SARS-CoV-2) is the most efficient measure to protect this vulnerable population. However, even after the application of three doses of an mRNA-based vaccine, about 25 % of kidney transplant recipients remain seronegative. Due to the proven superiority of heterologous mRNA and vector-based COVID-19 vaccine regimens, we hypothesized that a fourth booster vaccination with the vector-based Ad26.COV2.S vaccine can induced immunity in hitherto seronegative KTX.

Method: A cohort of 20 KTX vaccinated three times with an mRNA-based vaccine but showing low or no SARS-CoV-2 reactive IgG was vaccinated with the vector-based vaccine Ad26.COV2.S. SARS-CoV-2 S-protein-specific antibodies were determined by ELISA and S-protein-reactive T cells were quantified by flow cytometry.

Results: The vaccination induced seroconversion in only two out of 13 seronegative KTX. In 6 out of 7 KTX with low level of SARS-CoV-2 specific antibodies, a slight increase of the titers could be observed. In KTX with increasing antibody titers, the median titer developed from 3.7 [0.6–35.9] to 50.0 [11.3–342.9]. The functional

SARS-CoV-2-reactive CD4 and CD8T-cell response could be enhanced in approximately 30 % to 60 % of the KTX. The CD4 T-cell response did correlate neither with the antibody titers nor with the neutralization capacity.

Conclusion: Boosting with the vector-based vaccine Ad26.COV2.S did only moderately enhance the humoral immunity in previous low-responders and most KTX non-responders remained seronegative. However, the SARS-CoV-2 reactive T cell response, which may protect against severe disease manifestation, could be enhanced in the majority of the KTX.

P072

Improvement of HBV seroconversion rate following COVID-19 boost in hemodialysis patients with initial lack of HBV vaccination response

M. Anft; K. Paniskaki; T. Giglio¹; J. Wellenkötter¹; A. Blázquez-Navarro²; T. L. Meister³; U. Stervbo; S. Pfaender³; T. H. Westhoff; O. Cinkilic¹; N. Babel
Centrum für Translationale Medizin, Medizinische Klinik I, Marien Hospital Herne, Ruhr-Universität Bochum, Herne; ¹ Dialysezentrum Schwerte, Schwerte; ² Berlin-Brandenburg Center für Regenerative Therapien, Charité – Universitätsmedizin Berlin, Berlin; ³ Department of Molecular and Medical Virology, Marien Hospital Herne, University Hospital of the Ruhr-University Bochum, Herne

Objective: Epidemiological studies in humans and experimental animal data have clearly demonstrated that exposure or infection with one pathogen can induce and/or modify the immune response against another unrelated pathogen.

The mechanism of this phenomenon, known as heterologous immunity, has not been elucidated in humans in details. Hemodialysis patients (HD) are known to be immunocompromised and a high degree of vaccination non-responders is observed in this population. The aim of this study was to assess the effect of heterologous immunity in context of HBV and COVID-19 vaccination in HD.

Method: We analyzed the adaptive immunity against SARS-CoV-2 and HBsAg in 16 hemodialysis patients (HD) following consecutive HBV and COVID-19 vaccination boosts applied three weeks apart each other. All patients were HBV vaccination non-responders (following 4 doses of Engerix), and no- or low-responder following prime-boost vaccination with Comirnaty. Titers of binding antibodies as well as neutralizing antibodies against HBV, SARS-CoV-2 WT, delta and omicron were estimated in follow up by ELISA and SARS-CoV-2 spike-protein (S-protein) pseudovirus assays, respectively. T cell immunity reactive against SARS-CoV-2 and HBV was analyzed by multiparameter flow cytometry. T cell receptor (TCR) repertoires of HBsAg- and S-protein-reactive T cells were analyzed by NGS.

Results: Three weeks after the third SARS-CoV-2 vaccination, all 16 HD were able to develop a protective humoral immunity against SARS-CoV-2 wild-type, delta VOC and omicron VOC. Interestingly, while no HBsAg seroconversion could be observed 4 weeks following an HBV vaccination boost, 6 out of 16 initial HBV vaccination non-responders demonstrated seroconversion with median Ab

titers of 123.5 IU/mL [53.5–129]. Three weeks after the SARS-CoV-2 boost, HBsAg- T cells were detectable in all vaccinated patients without differences between humoral responders and non-responders. Additionally, we found no overlapping TCR repertoire in HBsAg- and S-protein-reactive T cells.

Conclusion: 6 out of 16 HBV vaccination non-responders on HD therapy were able to generate antibodies against HBV after COVID-19 vaccination. Since no TCR overlap could be detected between S-protein- and HBsAg-reactive T cells, unspecific activation following COVID-19 immunization rather than cross-reactivity appears to contribute to the development heterologous HBV immunity. Our data might have important implication for the vaccination regime for immunocompromised patients such as hemodialysis and transplant patients. However, further analyses are required to validate our observations.

P073

Inferior humoral and sustained cellular immunity against SARS-CoV-2 wild type and omicron VOC in hemodialysis patients immunized with three SARS-CoV-2 vaccine doses compared to four doses

M. Anft; O. Cinkilic¹; A. Blázquez-Navarro²; T. L. Meister³; U. Stervbo; S. Pfaender³; T. H. Westhoff; N. Babel
Centrum für Translationale Medizin, Medizinische Klinik I, Marien Hospital Herne, Ruhr-Universität Bochum, Herne; ¹ Dialysezentrum Schwerte, Schwerte; ² Berlin-Brandenburger Center für Regenerative Therapien, Charité – Universitätsmedizin Berlin, Berlin; ³ Department of Molecular and Medical Virology, Marien Hospital

Herne, University Hospital of the Ruhr-University Bochum, Herne

Objective: For immunocompromised patients including renal transplant and hemodialysis patients, the fourth vaccination is of special relevance. The aim of the present study was to evaluate the immunogenicity of a fourth mRNA-based vaccination (BNT162b2) in comparison to three vaccination doses in hemodialysis patients.

Method: We analyzed the adaptive immunity against SARS-CoV-2 wild type and omicron VOCs in a cohort of hemodialysis patients (n = 40) following third vaccination dose compared to fourth dose. Titers of binding antibodies as well as neutralizing antibodies against WT and omicron were estimated by ELISA and SARS-CoV-2 spike-protein (S-protein) pseudovirus assays, respectively. T cell immunity reactive against WT- and omicron-derived S-protein was analyzed by multiparameter flow cytometry.

Results: All patients demonstrated seroconversion with significantly higher titers of binding and omicron-specific neutralizing antibodies after four compared to three vaccine doses. As expected, fourth vaccination led to a significant increase in titers of omicron-specific neutralizing antibodies, whereas a significant decline in neutralizing antibody titers was observed between 6 and 12 weeks following third vaccination if the fourth dose was not applied. Of interest, we demonstrated a significant correlation between titers of binding and omicron-specific neutralizing antibodies with ROC demonstrating a higher AUC for wild type as compared to omicron. Notably,

we did not detect significant differences in humoral or cellular immunity in patients, which received COVID-19 vector vaccine from Johnson&Johnson or mRNA vaccine BNT162b2 as a third vaccine doses as it was previously reported.

Conclusion: In line with the improved seroconversion rate in transplant patients, our data demonstrate an improved omicron-specific humoral immunity following fourth mRNA vaccination dose as compared to three-dose vaccination regimen in hemodialysis patients. In contrast to the humoral immunity, the cellular immunity remained stable in follow up, without magnitude increase of wild type or omicron S-protein specific T cells in patients, which received four vaccine doses. Even though adequate neutralization titers have been observed following third dose, the significant titer decline observed in follow up justifies the fourth dose in this vulnerable population subgroup.

P074

Inferior cellular and humoral immunity against Omicron and Delta VOC compared to SARS-CoV-2 wild-type in hemodialysis patients immunized with four SARS-CoV-2 vaccine doses

M. Anft; A. Blázquez-Navarro¹; M. Fröhnert²; L. Fricke²; T. L. Meister³; U. Stervbo; S. Pfaender³; T. H. Westhoff; N. Babel

Centrum für Translationale Medizin, Medizinische Klinik I, Marien Hospital Herne, Ruhr-Universität Bochum, Herne; ¹Berlin-Brandenburger Center für Regenerative Therapien, Charité – Universitätsmedizin Berlin, Berlin; ²Dialyse Bochum, Bochum; ³Department of Molecular and Medical Virology, Marien

Hospital Herne, University Hospital of the Ruhr-University Bochum, Herne

Objective: With the domination of the less lethal but highly infectious SARS-CoV-2 variant of concern (VOC) Omicron (B.1.1.529), many countries have moved to dismantle or completely end protective measures in order to initiate the endemization of SARS-CoV-2. This makes it even more important to protect high risk groups with effective vaccination procedures. The objective of this study was to investigate how protective the immune response of hemodialysis patients, immunized with four doses of SARS-CoV-2 vaccine, is against Omicron VOC compared with wild-type or Delta VOC.

Method: We analyzed the cellular and humoral immunity in a cohort of hemodialysis patients (N = 42). Titers of neutralizing antibodies against wild-type, Delta and Omicron were estimated by SARS-CoV-2 spike-protein (S-protein) pseudovirus assays. T cell immunity reactive against wild-type, Delta- and Omicron-derived S-protein were analyzed by multiparameter flow cytometry. The analyses were performed 8–9 weeks following the fourth doses.

Results: The hemodialysis patients had a clear seroconversion after four doses of SARS-CoV-2 vaccination with a significantly higher titer of neutralizing antibodies against wild-type compared to Delta or Omicron S-Protein (Median [IQR]_{ND50} = 2117 [663–2560]; 759 [276–2560]; 439 [160–1180] respectively) and in addition significantly more neutralizing antibodies against Delta compared to Omicron. Although the number of patients

with a detectable CD4 T cell immune response was nearly identical (40–41 of 42 patients), the magnitude of the response was significantly lower against overlapping peptide pools (OPPs) of Omicron and Delta VOC compared to wild-type. In contrast, significant fewer patients showed a detectable CD8 T cell response against Omicron but not Delta compared to wild-type although the magnitude was not different after ex-vivo stimulation with peptides from the three SARS-CoV-2 variants. In addition, SARS-CoV-2 specific CD4⁺ T cells showed significantly lower production of Th1 cytokines IFN γ and TNF after ex vivo stimulation with Omicron and Delta compared with wild-type OPPs.

Conclusion: In line with the results from the general populations, hemodialysis patients show a clearly decreased humoral and cellular immune response against Omicron but also Delta VOC compared with SARS-CoV-2 wild-type after four doses of vaccination.

COVID-19 2

P075

Longitudinal immune responses after a third BNT162b and mixed fourth mRNA-1273 COVID-19 vaccination in patients on hemodialysis

K. Lürken
Gemeinschaftspraxis für Nieren- und Hochdruckkrankheiten, Eickenhof Dialyse, Langenhagen

Objective: Hemodialysis patients respond poorly to vaccination and are at risk for severe COVID-19. Therefore, dialysis patients were among the first for

which a fourth COVID-19 vaccination was recommended. We aimed to assess the impact of the vaccination schedule on response rates.

Method: We analyzed immunity against the receptor-binding domain (RBD) and ACE-binding inhibition of variants of concern including Omicron using multiplex-based IgG measurements and performed IFN γ release assay (IGRA) to measure SARS-CoV-2 specific T cell responses. We studied healthy controls (n = 33) and dialysis patients (n = 52) after triple BNT162b2 (Biontech) vaccination and the latter after a subsequent fourth dose of 100 μ g mRNA-1273 (Moderna).

Results: After the third BNT162b2 vaccination, anti-RBD IgG and ACE2 binding inhibition of the Wuhan type (WT) were significantly lower in dialysis patients when compared to controls. Both groups gained significantly higher titers compared to after the second vaccination, with 85 % of dialysis patients having significant ACE2 WT binding inhibition above a 20 % threshold. Three months later, anti-RBD IgG and ACE2 binding inhibition had declined significantly in dialysis patients. Whilst 60 % maintained ACE2 WT binding inhibition, only 10 % revealed efficient ACE2 binding inhibition towards Omicron. Importantly, the fourth vaccination with mRNA-1273 strongly augmented humoral immunity against both Spike and RBD WT. Similarly, the fourth vaccination increased the rate of dialysis patients with significant ACE2 binding inhibition towards Omicron RBD from 10 % to 83 %. Modest declines in SARS-CoV-2 S1-specific T cell responses in dialysis patients and controls after the second vaccination were restored by the

third BNT162b2 vaccination and moderately increased by the fourth vaccination with mRNA-1273.

Conclusion: A fourth mRNA-1273 standard dose after triple BNT162b2 vaccination in hemodialysis patients lead to efficient humoral responses against Omicron. Our data confirm current STIKO recommendation and suggest that other immune-impaired individuals may benefit from this mixed mRNA vaccination regimen.

P076

Increasing but insufficient neutralizing activity against Omicron-BA.1 after a second booster dose of mRNA-1273 vaccine in chronic hemodialysis patients

E. Ovcary; S. Patyna¹; N. Kohmer²; E. Heckel-Kratz³; S. Ciesek²; H. Rabenau²; I. A. Hauser¹; K. de Groot⁴

*KfH Nierenzentrum, Offenbach;
¹ Medizinische Klinik III, Nephrologie, Universitätsklinikum, Johann Wolfgang Goethe-Universität, Frankfurt a. M.;
² Institut für Virologie, Universitätsklinikum, Johann Wolfgang Goethe-Universität, Frankfurt a. M.;
³ KfH Nierenzentrum Groß-Gerau, Groß-Gerau;
⁴ Medizinische Klinik III, Sana Klinikum Offenbach, Offenbach*

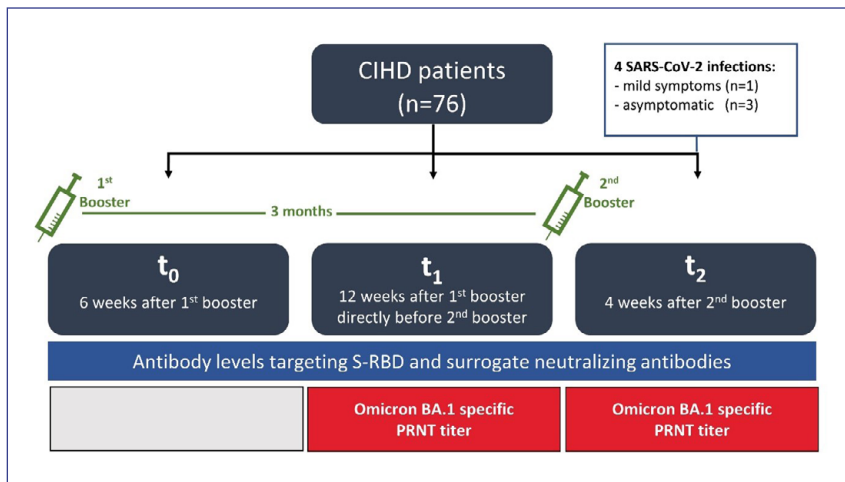
Objective: Untersuchung der humoralen Impfantwort chronischer Dialysepatient*innen vor und nach der vierten Impfung mit einem mRNA-Impfstoff. Vergleich der Neutralisation des Wildtyp-Virus gegenüber der Variante Omikron B.1.1.529/BA.1.

Method: We prospectively investigated 76 hemodialysis patients and measured neutralizing AB titer specific for BA.1 with a plaque reduction neutralization test (PRNT)

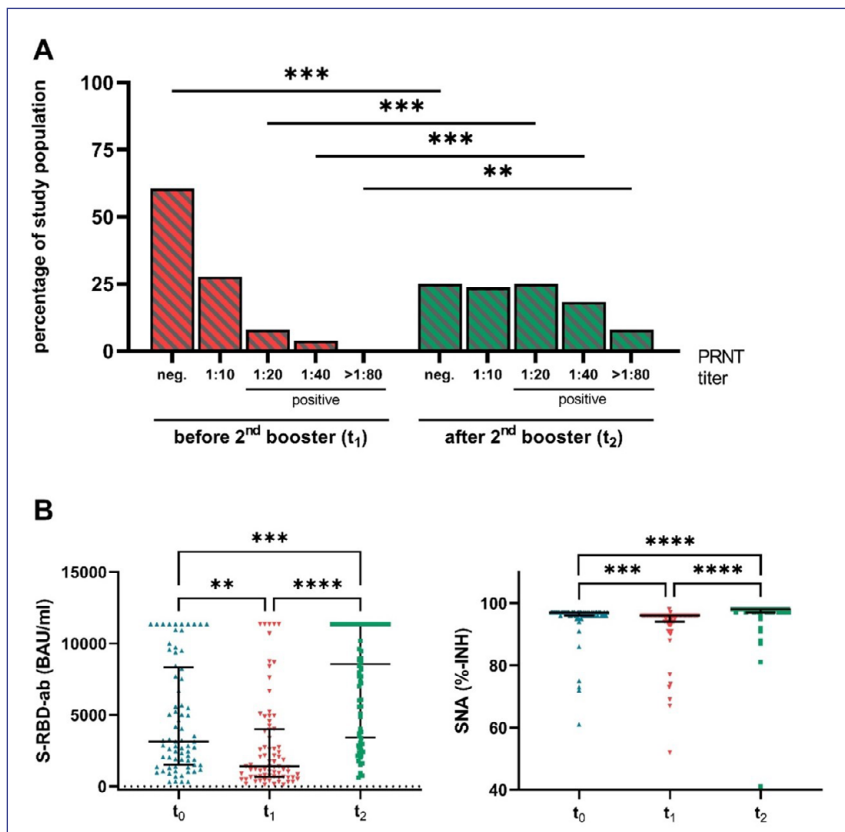
before and four weeks after second booster vaccine (mRNA-1273, Moderna). We assessed AB levels targeting SARS-CoV-2 spike receptor binding domain (S-RBD, Abbott GmbH, Wiesbaden, Germany) and surrogate neutralizing antibodies (SNA, GenScript Biotech, Piscataway Township, NJ, USA) against wild-type. P.S. Es wurden insgesamt 116 Patient*innen rekrutiert. Die Ergebnisse weiterer 40 Pat. befinden sich in der Auswertung.

Results: The BA.1 specific PRNT revealed, that only 11.8 % (9/76) of our patients were positive (titer \geq 1:20) before the second booster, without titers above 1:80 dilution. Four weeks after the second booster, 51.3 % (39/76) showed positive results in BA.1 specific PRNT, which is a 4.3-fold increase compared to positivity rate before the second booster ($p < 0.001$). We observed a 6-fold increase in S-RBD-AB levels ($p < 0.0001$) after the second booster and a response rate for SNA of 98.7 % (75/76). Four patients were infected by SARS-CoV-2 after the second booster. One had mild symptoms, three were asymptomatic, detected by PCR or positive nucleocapsid antibodies test.

Conclusion: Our findings reveal a high response rate for SNA against wild-type after the second booster, whereas the BA.1 specific neutralizing AB response rate achieved only 51.3 %. This limited neutralizing potency against BA.1 refers to an immune evasion of AB-mediated neutralization. Further studies have to elucidate whether Omicron-matched vaccines can enhance the neutralizing activity against Omicron variants to sufficiently protect this highly vulnerable population.



P076: Abb. 1



P076: Abb. 2

P077

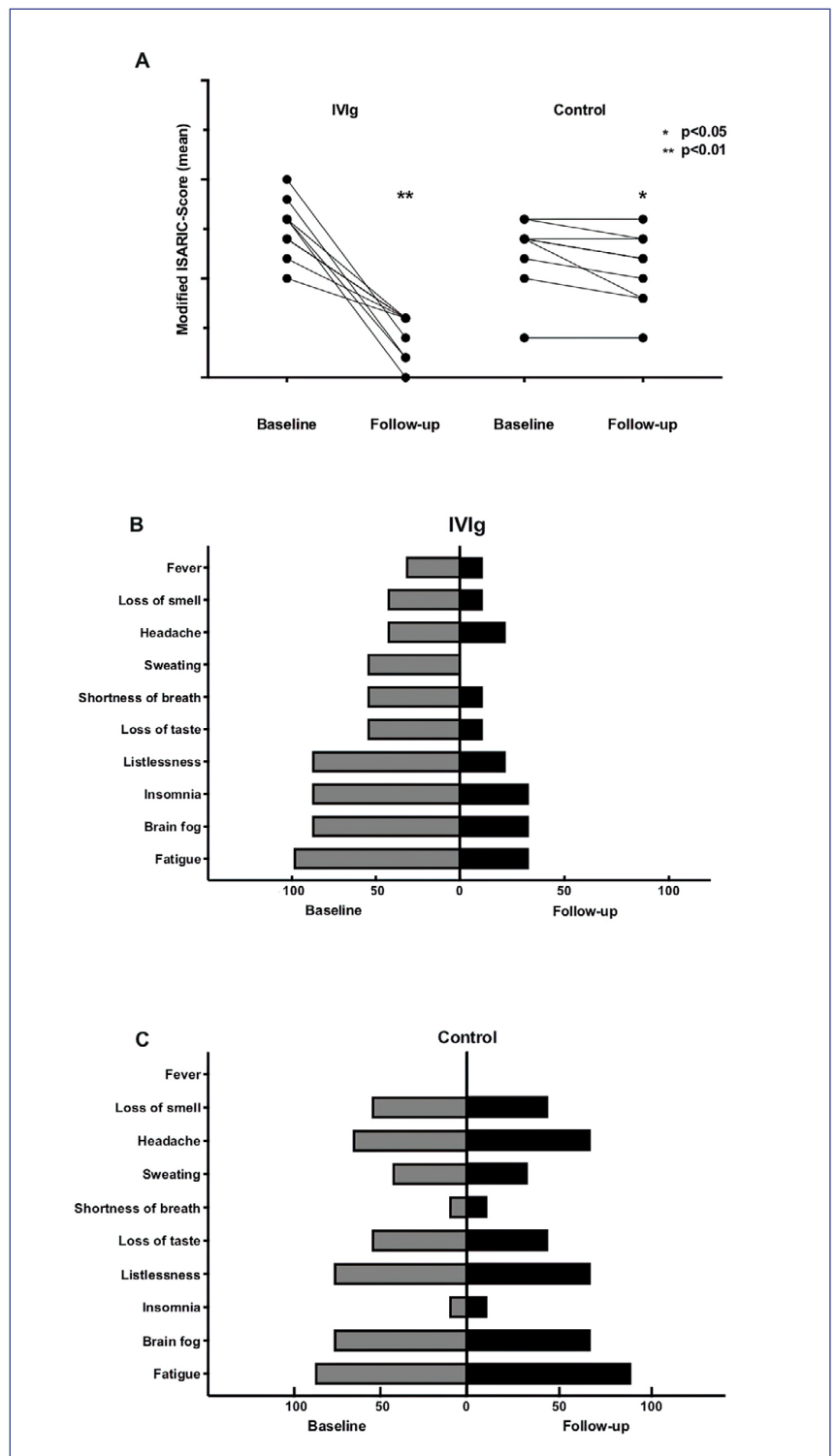
Immunglobuline in der Therapie von Post-COVID: Eine Fall-Kontroll-Studie

M. Hogeweg; A. Doevelaar;
S. Rieckmann; F. S. Seibert;
D. Scholten¹; M. Segelmacher¹;
N. Babel; T. H. Westhoff
Centrum für Translationale Medizin,
Medizinische Klinik I, Marien Hospital
Herne, Ruhr-Universität Bochum,
Herne; ¹ Medizinische Klinik, Marien-
hospital Witten, Ruhr-Universität
Bochum, Witten

Methode: In der vorliegenden retrospektiven Fall-Kontroll-Studie wurden 10 Patienten, welche neben supportiver Maßnahmen (Sport/ Gesprächstherapie/ Atemübungen) über 3–4 Monate hinweg Immunglobuline erhielten (Gruppe 1), mit 10 Patienten verglichen, die lediglich oben genannte supportive Maßnahmen in einer spezialisierten Post-COVID-Ambulanz erhielten (Gruppe 2). Die zum Vergleich dienenden Symptome der Patienten wurden sowohl zum Zeitpunkt der Erstdiagnose als auch beim Follow-Up mittels eines 19 Punkte umfassenden Fragebogen, basierend auf dem ISARIC COVID-19 follow-up study protocol, quantifiziert.

Ergebnisse: Die Studienpopulation war homogen in Bezug auf Alter, Komorbiditäten und Zeit seit der SARS-CoV-2-Infektion. Der mittlere Ausgangswert des modifizierten ISARIC-Scores betrug 8 in Gruppe 1 und 7 in Gruppe 2. Beim Follow-Up sank der Score signifikant auf 3 in Gruppe 1 und 6 in Gruppe 2. Alle Patienten aus Gruppe 1 berichteten über eine Symptomlinderung, während dies nur bei 6 (60 %) der Patienten in Gruppe 2 der Fall war.

Zusammenfassung: Die vorliegende Studie zeigt, dass IVIg eine vielversprechende Säule in der Behandlung des schweren Post-COVID-Syndroms sein könnte. So berichteten die Patienten unter IVIg-Therapie von einer wesentlich stärkeren Linderung der Symptomatik als die Patienten, welche nur eine supportive Therapie erhielten. Interessanterweise sprachen vor allem die für den Alltag einschränkendsten Symptome Müdigkeit, Antriebslosigkeit sowie Brainfog auf den Therapieansatz an. In Anbetracht der hohen physischen und psychischen Belastung, der daraus resultierenden Beeinträchtigung der täglichen Funktionsfähigkeit und des bisherigen Fehlens einer spezifischen Behandlung sind diese Ergebnisse vielversprechend. Zu den wahrscheinlichsten pathophysiologischen Mechanismen von Post-COVID gehören neben virusspezifischen pathophysiologischen Veränderungen auch immunologische Aberrationen als Reaktion auf die akute Infektion, die zu autoimmunvermittelten Schäden führen. IVIg enthalten ein breites Spektrum an anti-idiotypischen Antikörpern, die die schädlichen Autoimmunantikörper neutralisieren. Dieser Mechanismus ist auch bei Post-COVID wahrscheinlich, da er die AK-vermittelte Autoimmunität ohne die Nebenwirkungen einer systemischen Immunsuppression behebt. Während dies der erste Bericht über den Einsatz von IVIg bei Post-COVID ist, hat sich die Verabreichung von IVIg bei schweren Verläufen von COVID-19 bereits als hilfreich erwiesen.



P077: Abb. 1

P078

COVID-19: Impfbereitschaft und Informationsbedürfnisse medizinischer Fachkräfte Kommunizieren wir richtig?

C. Holzmänn-Littig; C. Schaaf; U. Heemann; L. Renders; T. Assali¹; M. Popp²; F. Fichtner³; P. Kranke²; M. C. Braunisch; J. Lühnen⁴; A. Steckelberg⁴; J. J. Meerpohl⁵; C. Schmaderer; C. Seeber³

II. Medizinische Klinik, Nephrologie, Klinikum rechts der Isar, Technische Universität München, München;

¹Abteilung für Nephrologie, Klinikum rechts der Isar, Technische Universität München, München; ²Institut für Allgemeinmedizin, Universitätsklinikum Würzburg, Würzburg; ³Klinik und Poliklinik für Anästhesiologie und Intensivtherapie, Universitätsklinikum Leipzig, Universität Leipzig, Leipzig;

⁴Institut für Gesundheits- und Pflegewissenschaft, Medizinische Fakultät, Martin-Luther-Universität Halle-Wittenberg, Halle (Saale); ⁵Institut für Evidenz in der Medizin, Universitätsklinikum Freiburg, Universität Freiburg, Freiburg

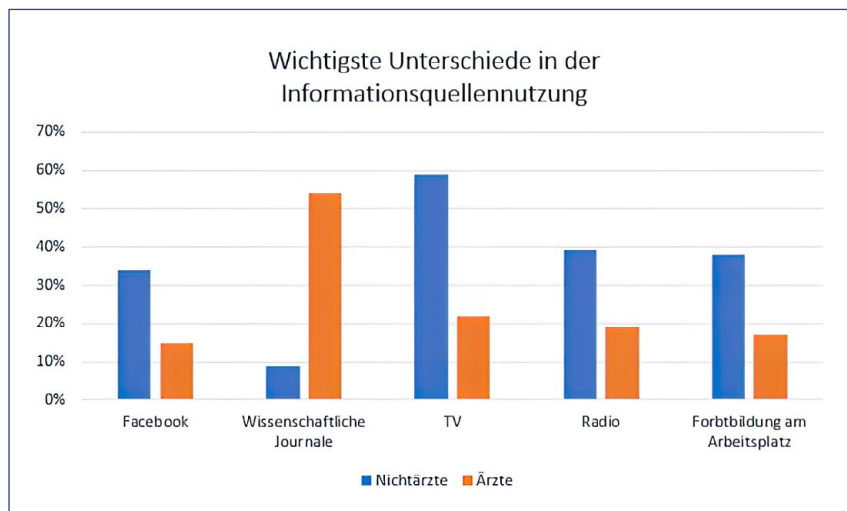
Hintergrund: Die COVID-19-Pandemie stellt in der Dialyse, Transplantationsmedizin und stationären Versorgung eine immense Belastung dar. Wenngleich die Impf-raten medizinischen Fachpersonals in Deutschland hoch sind, gibt es weiter Impflücken, teils unzureichende Beachtung von Hygienemaßnahmen und lokale Ausbruchsgeschehen. Neben niedrigem Alter und ambulanter Tätigkeit sind mangelndes institutionelles Vertrauen, Angst vor Nebenwirkungen sowie eine Impfabablehnung im persönlichen Umfeld Risikofaktoren für eine Impfabablehnung. (Holzmänn-Littig et al., 2021) Es bestehen Hinweise auf Clusterbildungen. (Holzmänn-Littig et al. 2022) Somit stellt sich die Frage nach der optimalen Kommunikation mit Mitarbeitenden des Gesundheitswesens, um optimal auf die nächsten Wellen vorbereitet zu sein.

Methode: Im CEOsyst-Projekt wurden die bevorzugten Informationskanäle einzelner Berufsgruppen mit 309 Teilnehmenden im

Dezember 2020 mittels offener Online-Surveys untersucht. Die Ergebnisse wurden deskriptiv ausgewertet. Freitextantworten wurden induktiv kategorisiert und anschließend deskriptiv ausgewertet.

Ergebnisse: Die insgesamt am meisten geforderten Informationskanäle zu COVID-19-Themen waren Newsletter (57 %), institutionelle Websites (56 %) sowie wissenschaftliche Journale (48 %). Bei Nichtärzten war Facebook ($p = 0.002$) signifikant häufiger genutzt als bei Ärzten. Wissenschaftliche Journale wurden signifikant häufiger von Ärzten ($p < 0.001$) genutzt, TV ($p < 0.001$) und Radio signifikant häufiger von Nichtärzten ($p < 0.001$). Fortbildungsveranstaltungen am Arbeitsplatz wurden signifikant häufiger von Nichtärzten gefordert ($p < 0.001$).

Zusammenfassung: Die Pandemie wird wahrscheinlich auch in den nächsten Jahren eine große Bürde in der Nephrologie darstellen. Zur Konsolidierung des Erreichten ist optimale Kommunikation mit allen medizinischen Fachkräften erforderlich. Nichtärzte verwenden seltener wissenschaftliche Quellen, auch, da ihnen wissenschaftliche Journale kaum zur Verfügung stehen. Gezielte Informationen über das aktuelle Infektionsgeschehen, Infektionsmechanismen, Risiken und Vorteile der Impfung sowie Hygienemaßnahmen sollten direkt per Newsletter, aber auch in regelmäßigen Fortbildungsveranstaltungen kommuniziert werden, um eine gezielte Information aller Berufsgruppen zu gewährleisten, mögliche Cluster direkt anzusprechen und so eine optimale Vorbereitung für die nächsten Wellen zu gewährleisten.



P078: Abb. 1

P079**Management und Verlauf der SARS-Cov-2 Pandemie in einem deutschen Dialyse-Netzwerk**

T. Krüger; M. Milster¹; W. Kleophas
DaVita Clinical Research Deutschland
GmbH, Düsseldorf; ¹ DaVita Deutschland
AG, Hamburg

Hintergrund: Die globale Covid-19 Pandemie ist für Dialysepatienten ein besonderes Risiko, die Covid-assoziierte Mortalität der Dialysepatienten ist im Vergleich zur Bevölkerung erhöht. Aus dem DaVita Netzwerk präsentieren wir den Verlauf der SARS-CoV-2-Infektionen aus 65 deutschen Zentren mit rund 3.300 aktiven Dialysepatienten sowie gut 1.500 Angestellten.

Methode: Zur Reduktion des Infektionsrisikos wurde ein Triage-System eingeführt, welches den Umgang mit Dialysepatienten regelt. Die Triage richtet sich nach klinischen Symptomen, Abstrichresultat sowie Kontakt zu bestätigten positiven Patienten und bestimmt eine mögliche Dialyse in Isolation. Kurz nach Verfügbarkeit von Antigen-Schnelltests wurde der routinemäßige Einsatz sowohl bei Dialysepatienten als auch beim medizinischen Personal als Screening eingeführt. Zudem wurden neben generellen Hygienemaßnahmen ein Ampel-System implementiert, welches je nach lokaler Inzidenz weitere Maßnahmen wie Besuchsverbot, Kohortenisolation, Bereichspflege und Einzelfahrten vorsah. Im Verlauf der Pandemie wurde in diesem System zusätzlich die Impfsituation erfasst.

Ergebnisse: Der Inzidenzverlauf reflektiert den der Gesamtbevölkerung. Das Maximum der Inzidenz verzeichneten wir Ende 2021. Aktuell beträgt die kumulative

Gesamtzahl positiv getesteter Patienten 1545 Fälle, was einer Rate von etwa 48 % der Patienten entspricht (deutschlandweit offiziell Stand April 2022 rund 30,4 %). In Bezug auf die Infektionsrate je Zentrum liegen innerhalb des Netzwerks deutliche Unterschiede vor, welche von 1 % bis 65 % reicht. Die Mortalitätsrate von SARS-CoV-2 unter den positiv getesteten Dialysepatienten lag Stand April 2022 kumulativ bei 10,2 % (158/1545; aktuell deutschlandweit rund 0,5 %). Im Verlauf von 2021 zeigt sich ab Ende 2021 eine deutlich reduzierte Covid-assoziierte Mortalität. Diese ging von rund 23 % bis August 2021 auf 1,5 % im April 2022 zurück. Aktuell sind rund 84,9 % der Patienten mindestens 3fach geimpft.

Zusammenfassung: Das Infektionsgeschehen konnte innerhalb der Standorte effektiv kontrolliert werden. Durch Routinetestungen mag eine höhere Covid-Inzidenz erfasst worden sein als in der Bevölkerung. Die deutlich regrediente infektassoziierte Mortalität ist möglicherweise auf Impfungen und die mildere Omikron Variante zurückzuführenden.

P080**The impact of chronic heart failure in patients with chronic kidney disease suffering from COVID-19: data from the Lean European Open Survey on SARS-CoV-2 infected patients (LEOSS)**

F. S. Seibert; N. Timmesfeld¹;
J. Lanznaster²; C. E. M. Jakobs³;
P. Zgoura; M. M. Rüttrich⁴;
A. Doevelaar; A. Hemmersbach¹;
C. Spinner⁵; S. Bertram; M. Stecher³;
M. Vehreschild⁶; K. Wille⁷; N. Babel;
B.-E. O. Jensen⁸; T. H. Westhoff

Centrum für Translationale Medizin,
Medizinische Klinik I, Marien Hospital
Herne, Ruhr-Universität Bochum,
Herne; ¹ Biometry & Epidemiology,
Department of Medical Informatics,
Ruhr-Universität Bochum, Bochum;
² Department of Internal Medicine,
University of Passau, Passau;
³ Medizinische Klinik I, Universitäts-
klinikum Köln, Köln; ⁴ Abteilung
Hämatologie / Internistische Onko-
logie, Klinik für Innere Medizin II,
Universitätsklinikum Jena, Jena;
⁵ II. Medizinische Klinik und Poliklinik,
Klinikum rechts der Isar, Technische
Universität München, München;
⁶ Medizinische Klinik II, Infektiologie,
Universitätsklinikum, Johann Wolfgang
Goethe-Universität, Frankfurt a. M.;
⁷ Klinik für Hämatologie, Onkologie,
Hämostaseologie und Palliativmedizin,
Johannes Wesling Klinikum Minden,
Minden; ⁸ Klinik für Gastroenterologie,
Hepatology, Infektiologie, Universitäts-
klinikum, Heinrich-Heine-Universität
Düsseldorf, Düsseldorf

Objective: A rapid understanding of pathomechanisms of COVID-19 and the identification of patients at risk, remains crucial in this pandemic. Hence, patients with chronic kidney disease (CKD) are prone to face a severe course of the disease. Amongst these, dialysis patients with cardio-renal syndrome as the underlying aetiology, show the highest mortality. We investigated the impact of chronic heart failure (CHF) in patients with CKD in the Lean European Open Survey on SARS-CoV-2-Infected Patients (LEOSS). **Method:** Data from the LEOSS registry documented from March 2020 until October 2021 were evaluated. LEOSS is an international non-interventional multi-center cohort study established in March 2020 in

order to address the lack of information on the epidemiology and the clinical course of COVID-19. Only patients with CKD and in-hospital stay were included in the analysis. Patients with liver cirrhosis and age younger than 18 years were excluded. Primary endpoint was all-cause mortality, secondary endpoints consisted of acute on chronic kidney injury, the need for intensive care, renal replacement therapy, and invasive ventilation.

Results: 721 patients were diagnosed with CKD, from which 243 patients suffered from additional CHF. Patients with CKD plus CHF were older ($p < 0.001$) and were more likely to have COPD ($p = 0.015$). An overall of 177 (24.5 %) patients in the CKD group without CHF died from all causes, compared to 93 (38.3 %) patients in the group with simultaneous CKD and CHF ($p < 0.001$). After an adjustment for age, body mass index, presence of COPD or hypertension as comorbidities, this difference remained significant ($OR = 1.65$, 95 %-CI [1.18–2.30], $p = 0.003$ from logistic regression model).

Conclusion: CKD and CHF are risk factors for a severe the course of a SARS-CoV-2 infection and its complications. Patients with a coincidence of CKD and CHF are an extremely vulnerable population, who may thereby benefit from an early treatment with antiviral agents.

P081

Impact of Moderna mRNA-1273 Booster Vaccine on Fully Vaccinated High-Risk Chronic Dialysis Patients after Loss of Humoral Response

S. Patyna; T. S. Eckes¹; L. Weiß; B. F. Koch; S. Sudowe²; A. Oftring¹;

N. Kohmer³; H. Rabenau³; S. Ciesek³; D. Avaniadi; R. Steiner; I. A. Hauser; J. M. Pfeilschifter¹; C. Betz

Medizinische Klinik III, Nephrologie, Universitätsklinikum, Johann Wolfgang Goethe-Universität, Frankfurt a. M.;

¹Institut für Allgemeine Pharmakologie und Toxikologie, Universitätsklinikum, Johann Wolfgang Goethe-Universität, Frankfurt a. M.; ²GANZIMMUN Diagnostics AG, Mainz; ³Institut für Virologie, Universitätsklinikum, Johann Wolfgang Goethe-Universität, Frankfurt a. M.

Objective: The current coronavirus disease 2019 (COVID-19) pandemic confronts our society with a global threat that particularly concerns patients with compromised immune systems, either due to immunosuppressive therapy or diseases associated with impaired immune response. Patients with end-stage renal disease (ESRD) undergoing chronic intermittent hemodialysis (CIHD) are affected by lower humoral and cellular immunity. For this reason, severe acute respiratory syndrome coronavirus-2 (SARS-CoV-2) infection and chronic dialysis patients make a particular dangerous relationship.

Method: We investigated the humoral and cellular immune response of 42 CIHD patients who had received two doses of SARS-CoV-2 vaccine, and again after a booster vaccine with mRNA-1273 six months later. We measured antibody levels and SARS-CoV-2-specific surrogate neutralizing antibodies (SNA). Functional T cell immune response to vaccination was assessed by quantifying interferon- γ (IFN- γ) and IL-2 secreting T cells specific for SARS-CoV-2 using an ELISpot assay.

Results: Our data reveal a moderate immune response after the second dose of vaccination, with significantly decreasing SARS-CoV-2-specific antibody levels and less than half of the study group showed neutralizing antibodies six months afterwards. Booster vaccines increased the humoral response dramatically and led to a response rate of 89.2 % for antibody levels and a response rate of 94.6 % for SNA. Measurement in a no response/low response (NR/LR) subgroup of our cohort, which differed from the whole group in age and rate of immunosuppressive drugs, indicated failure of a corresponding T cell response after the booster vaccine.

Conclusion: A third dose of SARS-CoV-2 mRNA-1273 vaccine in high-risk CIHD patients increased the magnitude and the neutralizing capacity of SARS-CoV-2-specific antibodies, even in the NR/LR subgroup. The relevance of a repeated booster vaccination after a certain period to enhance immunity against SARS-CoV-2 provides an incentive for the next inoculation campaign for these immunocompromised CIHD patients.

P082

Impact of Hypertension on long-term Humoral and Cellular Response to SARS-CoV-2 Infection

C. Chu; A. Schönbrunn¹; K. Klemm²; V. von Baehr¹; B. K. Krämer³; S. Elitok²; B. Hoher³

Medizinische Klinik mit Schwerpunkt Nephrologie, Campus Charité Mitte, Charité – Universitätsmedizin Berlin, Berlin; ¹IMD Institut für Medizinische Diagnostik Berlin-Potsdam GbR, Berlin;

²Klinik für Nephrologie und Endokrinologie/Diabetologie, Zentrum für Innere Medizin II, Klinikum Ernst von

Bergmann gGmbH, Potsdam; ³ Nephrologie, Endokrinologie, Rheumatologie, V. Medizinische Klinik, Universitätsmedizin Mannheim, Mannheim

Objective: It was shown that hypertension delays SARS CoV-2 viral clearance and exacerbates airway hyper-inflammation in the respiratory tract. However, it is unknown whether hypertension determines the long-term cellular and humoral response to SARS CoV-2.

Method: Health care workers (HCWs) after an outbreak of SARS CoV-2 infections were recruited. Two groups were analyzed, infected and fully vaccinated HCWs. Clinical data were recorded. Blood was drawn and the humoral and cellular immune responses were examined.

Results: 5–14 months (median 7 months) after detection of SARS CoV-2 infection, blood was taken to analyze humoral response (S1 IgG and SARS CoV-2 neutralizing antibodies) and cellular (T cell responses to SARS-CoV-2 with Lymphocyte Transformation Test). Infected hypertensive HCWs more often developed anosmia, and myalgia and needed to be hospitalized as compared to non-hypertensive HCWs. The long-term humoral and cellular immune response was significantly strengthened in hypertensive versus normotensive infected HCWs. Multivariate regression analysis revealed that only hypertension but not age, BMI, sex, diabetes, smoking, COPD, asthma, and time between PCR positivity and blood taking was independently associated with the humoral and cellular response to SARS CoV-2 infection.

Conclusion: In conclusion, SARS CoV-2 infection strengthened

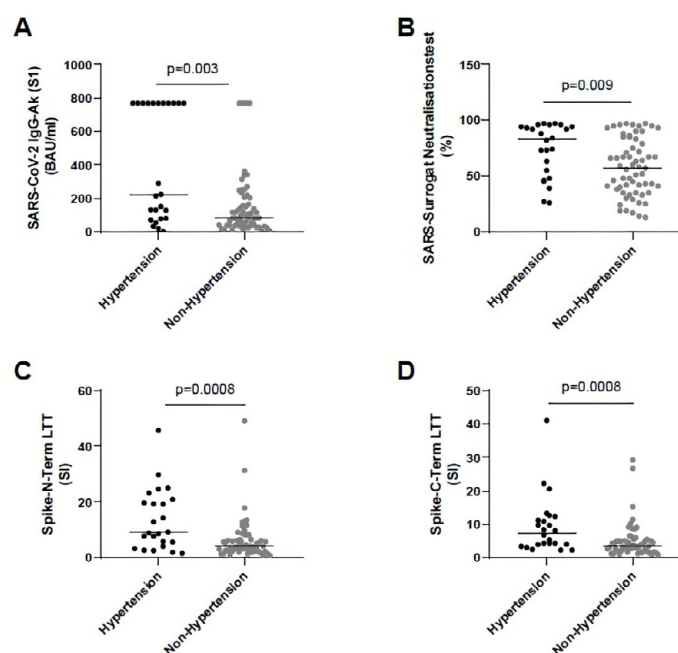


Figure 1. (A) SARS-CoV-2 IgG-Ak (S1) (BAU/ml) in SARS-CoV-2 infected health care workers (HCWs) with and without hypertension. (B) SARS surrogate neutralization test (%) in SARS-CoV-2 infected HCWs with and without hypertension. (C) Spike-N-Term LTT (SI) in SARS-CoV-2 infected HCWs with and without hypertension. (D) Spike-C-Term LTT (SI) in SARS-CoV-2 infected HCWs with and without hypertension. Lines show median. Comparison was made by Mann-Whitney U test.

P082: Abb. 1

humoral and cellular immune response to SARS CoV-2 infection in hypertensive HCWs independent of other risk factors and also severity of symptoms.

P083 Immunogenicity, efficacy and harms of additional SARS-CoV-2 booster vaccination for kidney transplant recipients: a systematic review

R. I. Hausinger; Q. Bachmann; N. Kreuzberger¹; N. Hannane; T. Crone-Raue; I. Monsefi¹; U. Heemann; N. Skoetz¹; C. Schmaderer
II. Medizinische Klinik, Nephrologie, Klinikum rechts der Isar, Technische

Universität München, München;
¹ Abteilung für evidenzbasierte Onkologie – Innere Medizin I, Uniklinik Köln, Universität Köln, Köln

Objective: COVID-19 is a pandemic respiratory disease caused by severe acute respiratory syndrome coronavirus 2 (SARS-CoV-2). By today, it has led to over 6 million deaths worldwide. Mutations of the virus are emerging rapidly and enhance its ability of immune-evasion, thereby not only altering transmissibility and disease severity, but also permitting it to escape established disease control measures such as vaccines and virus-directed

therapies. Even though reduced vaccine efficacy has been shown against variants of concern like the recently evolved omicron strain, vaccination against SARS-CoV-2 is still substantial in preventing hospitalization and death and thus ending the pandemic. Whilst low fatality rates have been reported for the general population, a high mortality has been documented for kidney transplant recipients (KTRs), who have the highest risk for non-response to seroconversion among the immunocompromised and development of severe disease. In this systematic review, we give an overview of the existing evidence of benefits and harms of additional SARS-CoV-2 vaccine doses in KTRs.

Method: We searched the following databases and registries: Cochrane COVID-19 Study register, the Web of Science Citation Index and Emerging Sources Citation Index and the WHO COVID-19 Global literature on coronavirus. Then, we synthesized evidence from all existing prospective studies on the benefits and harms of additional booster doses of SARS-CoV-2-vaccines for KTRs. We considered studies investigating the effects of at least 3 doses of all of the SARS-CoV-2 vaccines granted Emergency Use listing by the WHO.

Results: We report evidence from single-arm studies and from studies comparing different vaccines. Our main outcomes of interest were: breakthrough infections, humoral and cellular immune response. We also report on important graft-related adverse events such as De-novo formation of donor specific antibodies or acute graft rejection. Subgroup analysis was done for age, different immunosuppressive

regimens, transplant vintage, diabetes and living vs. cadaveric graft recipients to identify patients at high risk for failure of seroresponse.

Conclusion: Due to the overwhelming pace of the pandemic, well-conducted randomized controlled studies are rare. The heterogeneity in the measurement of humoral and cellular immunity due to different assays complicates the task to summarize these studies. Nonetheless, to our knowledge this is the first systematic review to achieve an analysis of the existing literature on KTRs with more than 2 COVID-19 vaccine doses.

P084

Der Verlauf von COVID-19 Infektionen mit der Omikron-Variante ist auch bei geimpften chronischen Dialysepatienten mit einer dramatischen Reduktion der Sterblichkeit verbunden

T. Weinreich; D. Lojko; F. Gehlen; D. Draganova; E. Seibert; O. Hergesell; B. Hohenstein

Nephrologisches Zentrum Villingen-Schwenningen, Villingen-Schwenningen

Hintergrund: Die COVID-19 Pandemie läuft seit März 2020 und hat weltweit dramatische Konsequenzen für alle Menschen. Bereits früh wurde gezeigt, dass Patienten mit chronischer Nierenerkrankung und Dialysepflichtigkeit ein deutlich erhöhtes Risiko haben an den Folgen dieser Erkrankung zu versterben. Wir charakterisierten unsere Kohorte von Dialysepatienten und berichteten (Dialyse aktuell 2021; 25(05/06): 214–219), dass die Sterblichkeit während der ersten beiden Wellen im Kollektiv unserer Dialysepatienten bei rund 17 % lag. Die Einführung

der Schutzimpfungen, Verbreitung der Omikron-Variante und ein verbessertes klinisches Management sowie die Verfügbarkeit von Antikörpertherapien haben die Sterblichkeit in der Allgemeinbevölkerung deutlich reduziert.

Methode: In der vorliegenden Analyse wurde nochmals der Verlauf der Infektionen bei Dialysepatienten unseres Zentrum im Abgleich zu den Daten aus 2020/2021 betrachtet. Um trotz im Verlauf fehlender genetischer Routinetestung überwiegend Fälle mit der Omikron-Variante zu selektionieren wurde gezielt der Zeitraum ab Januar 2022 herangezogen, da sich seither Omikron als klar dominant durchgesetzt hatte. Alle Fälle einer erkannten COVID-19 Infektion zwischen Januar und April 2022 wurden betrachtet und hinsichtlich Hospitalisierung und Mortalität nachbetrachtet.

Ergebnisse: In unserem Zentrum kam es in diesem Zeitraum zu 145 mittels PCR bestätigten COVID-19 Infektionen. Die Therapie der Patienten erfolgte nach aktuellen Leitlinien. Patienten mit zusätzlicher Immunsuppression, ohne Impfschutz oder mit fehlendem Nachweis von SARS-CoV-2 IgG Antikörpern erhielten eine Einmaldosis Sotrovimab. 17 Patienten (11,7 %) mussten im Rahmen der Infektion hospitalisiert werden. Vier Patienten verstarben an und mit der Infektion (2,1 %). Die 3 verstorbenen Patienten waren alle männlich: 90J, ungeimpft; 81J, 4x geimpft unter Rituximab; 72J, 4x geimpft mit hepatorenalem Syndrom und reduziertem Allgemeinzustand. Der Versorgungsaufwand war im Vergleich zu unserem vorausgehenden

Bericht mit bis zu 20 isolierten und kohortierten COVID-19 Patienten weiterhin extrem hoch.

Zusammenfassung: Schutzimpfungen und bessere Therapieoptionen haben unter der Omikronvariante zu einem dramatischen Rückgang der Hospitalisierung und vor allem tödlicher Verläufe bei chronischen Dialysepatienten (2 % vs. 17 %) geführt. COVID-19 stellt auch mit besseren Therapieoptionen weiterhin eine extreme, personal- und kostenintensive Herausforderung für die Versorgung chronischer Dialysepatienten dar.

P085

Antibody response to COVID-19 vaccination in dialysis patients – a prospective multicenter analysis over 18 months

C. Ostermaier; S. Kamalanabhaiah; I. Lettermann-Nass¹; K. Volland¹; C. Keller¹; J. Hoyer; C. S. Haas
Klinik für Innere Medizin, Nephrologie und Internistische Intensivmedizin, Standort Marburg, Universitätsklinikum Gießen und Marburg GmbH, Marburg; ¹ Institut für Virologie, Philipps Universität, Marburg

Objective: Dialysis patients are considered to be at increased risk for SARS-CoV-2 infection. People with chronic underlying diseases are prone to higher morbidity and mortality when infected. Thus, dialysis patients were prioritized for early COVID-19 vaccination. However, early data suggested that seroconversion rates are relatively low in this population, consistent with the reduced response rate following vaccination against hepatitis B, pneumococcus or influenza. The objective of this study is to evaluate the effectiveness of COVID-19 vaccines in this

special cohort with respect to seroconversion and to identify potential risk factors for non-responding.

Method: We conducted a prospective, multicenter study in 4 dialysis facilities in central Germany, starting in April 2021. Patients in a chronic hemodialysis program were included after informed consent was obtained. Blood samples were taken prior to first vaccination, before second vaccination, 7–14 days after second vaccination, as well as 60 and 120 days after full vaccination for long-term follow-up. At any study time point, results of COVID-19 antigen tests as well as clinical symptoms were assessed. Furthermore, similarly data was obtained for first or second booster vaccination. Blood samples for antibody titers were drawn – if applicable – at day 30, 90, 150 and 210 following booster vaccination. Basic data including underlying condition, comorbidities, lab results, seroresponse to hepatitis B vaccination, immunosuppression and other medication was assessed to identify potential risk factors. Antibody response was defined above a value of 7.1 BAU per liter.

Results: A total of 320 patients participated in the study. After 2 vaccinations, 288 individuals remained for evaluation; of these, 270 (= 93 %) developed an adequate antibody response. Although the majority of patients had received an mRNA vaccine, there was no significant difference in the overall response rates compared to vector based vaccines. Age and immunosuppressive medication were found to be significant risk factors for non-responsiveness to COVID-19 vaccination ($p < 0.05$). Infections clearly dropped following immunization. Of note, 6 months

after full vaccination, antibody titers significantly declined. Both, first and second booster doses resulted in a notable increase of antibody titers: during the omicron wave, no COVID-19 associated hospital admissions were observed.

Conclusion: COVID-19 vaccination is highly effective in hemodialysis patients. Like in the general population, only age and immunosuppression are notable risk factors for not responding to vaccination, thereby having a potential impact on outcome, especially for the wave to come.

Dialyse/Apherese 1

P086

Caplacizumab for Acquired Thrombotic Thrombocytopenic Purpura (aTTP): Long-term Safety and Efficacy in the Post-HERCULES Study

M. Scully; J. de la Rubia¹; K. Pavenski²; A. Metjian³; P. Knöbl⁴; F. Peyvandi⁵; S. Cataland⁶; P. Coppo⁷; J. Kremer Hovinga⁸; J. Minkue Mi Edou⁹; R. de Passos Sousa¹⁰; F. Callewaert¹¹; S. Gunawardena¹²; J. Lin¹²
Department of Hematology, University College London Hospitals NHS Trust, London/UK; ¹ Department of Hematology, Hospital Universitario Dr. Peset, Valencia/E; ² Departments of Medicine and Laboratory Medicine, St. Michael's Hospital, University of Toronto, Toronto/CDN; ³ Anschutz Medical Center, University of Colorado, Aurora/USA; ⁴ Klinische Abteilung für Hämatologie und Hämostaseologie, Universitätsklinik für Innere Medizin I, Medizinische Universität Wien, Wien/A; ⁵ Angelo Bianchi Bonomi Hemophilia and Thrombosis Center, Fondazione IRCCS Ca'Granda Ospedale Maggiore Policlinico, University of Milan,

Milan/I; ⁶ Division of Hematology, Department of Internal Medicine, Ohio State University, Columbus/USA; ⁷ Department of Hematology, Saint-Antoine University Hospital, Paris/F; ⁸ Department of Hematology and Central Hematology Laboratory, Inselspital, Bern University Hospital, University of Bern, Bern/CH; ⁹ Medical Affairs, Sanofi Aventis, Ghent/BE; ¹⁰ Medical Affairs, Sanofi Aventis, Porto Salvo/P; ¹¹ formerly Sanofi, Diegem/BE; ¹² Sanofi, Cambridge/USA

Objective: The post-HERCULES trial (NCT02878603) investigated long-term safety and efficacy of caplacizumab, and repeat use, in patients with acquired thrombotic thrombocytopenic purpura (aTTP). **Method:** For 3 years after completing the HERCULES trial, patients could participate in post-HERCULES and attend twice-yearly visits. Patients could receive open-label (OL) caplacizumab with plasma exchange (PEX) and immunosuppression (IS) upon aTTP recurrence. Safety, TTP-related events (recurrence, mortality, or major thromboembolic events), and pharmacodynamics/immunogenicity were analyzed in defined patient populations:

- ITO [intention-to-observe] (n = 104): all enrolled patients, grouped according to caplacizumab treatment during HERCULES (randomized or switched to OL after exacerbation).
- Efficacy ITO (n = 78): patients without aTTP recurrence during HERCULES or prior to post-HERCULES
- Recurrence (n = 19): patients with ≥ 1 recurrence during post-HERCULES

- Repeat-use (n = 9): patient subset treated \geq twice with caplacizumab.

Results: Of 104 patients enrolled in post-HERCULES, 75 received caplacizumab with PEX + IS during HERCULES (caplacizumab group) and 29 PEX + IS only (placebo group). Incidence of adverse events (AEs) and serious AEs was similar in both groups. In the ITO population, 11/75 (15 %) caplacizumab treated patients and 8/29 (28 %) placebo patients had a recurrence. In the efficacy ITO population, TTP-related events occurred in 8 % (4/49) versus 38 % (11/29) of patients randomized to caplacizumab and placebo, respectively. Of 19 patients with ≥ 1 recurrence, 13 received caplacizumab. Recurrences were resolved (12/13) or resolving (1/13) for all patients treated with caplacizumab, including 9 patients with repeat caplacizumab use. One patient who did not receive caplacizumab at any time died due to TTP recurrence. Safety profile of caplacizumab for treatment of recurrence was consistent with that in HERCULES with headache and constipation (n = 3 each) being the most common treatment-emergent AEs during the first recurrence (n = 13). In the repeat-use population (n = 9), bleeding events were reported in 5/9 patients (56 %) for the first recurrence; 2 patients had a serious treatment-related bleeding event; anti-drug antibodies were found in 2 patients. **Conclusion:** The long-term safety profile of caplacizumab with PEX + IS was similar to that of PEX + IS alone. Repeat caplacizumab use was efficacious and no new safety signals occurred.

P087

Inzidenz der Dialysebehandlung von Patienten mit terminaler Niereninsuffizienz, sowie Mortalität und relevante Endpunkte für die Lebensqualität nach Dialysebeginn in Deutschland

B. Kolbrink; K. Schüssel¹; F. A. von Samson-Himmelstjerna; G. Esser; U. Kunzendorf; K. Schulte
Klinik für Nieren- und Hochdruckkrankheiten, Campus Kiel, Universitätsklinikum Schleswig-Holstein, Kiel;
¹ Wissenschaftliches Institut der Allgemeinen Ortskrankenkassen, Berlin

Hintergrund: Deutschland ist eine Ausnahme unter den Industriestaaten, da es kein umfassendes Dialyseregister führt. Es ist unbekannt, wie viele Menschen in Deutschland eine chronische Dialysebehandlung beginnen und wie die Prognose dieser Patienten ist. Das Ziel dieser Studie war die Beschreibung der Inzidenz der chronischen Dialysebehandlung sowie patientenrelevanter Endpunkte zur Mortalität, Hospitalisation und Verschlechterung des Pflegegrads nach Dialysebeginn.

Methode: Datengrundlage für diese retrospektive Beobachtungsstudie waren anonymisierte Krankenkassenroutinedaten von AOK-versicherten Personen aus den Jahren 2016 bis 2020. Hieraus identifizierten wir alle im Jahr 2017 inzidenten chronischen Dialysepatienten anhand der Kombination der Diagnose „terminale Niereninsuffizienz“ (ICD N18.5) und der Abrechnung von Dialysebehandlungen (OPS 8-854.2 bis 8-854.5, 8-855, 8-857, GONr. 13610 oder 13611). Betrachtet wurden hierbei ambulante und stationäre Behandlungsdaten. Nach Dialysebeginn wurde ein Zeitraum von bis

zu 4 Jahren (bis Ende 2020) beobachtet. Als Endpunkte wurden Todesfälle, Krankenhausaufnahmen sowie eine Verschlechterung des Pflegegrads ausgewertet. **Ergebnisse:** Der Datensatz umfasste 2017 mit knapp 23 Millionen durchgängig AOK-versicherten Personen ca. ein Drittel aller gesetzlich Krankenversicherten in Deutschland. Von diesen begannen 10.328 eine chronische Dialysebehandlung (Inzidenzrate 454 je 1 Million Personenjahre). Der Anteil der Patienten mit Peritonealdialyse betrug 4,2 %. Eine AV-Fistel bereits vor Beginn der Dialyse hatten 21,1 % der Dialysepatienten. Die erste Dialysebehandlung wurde bei dem Großteil der Patienten (7.324 Patienten entsprechend 70,9 %) im Krankenhaus durchgeführt, und 865 (11,8 %) dieser Patienten verstarben im selben Krankenhausaufenthalt. Die 1-Jahres-Mortalität der inzidenten chronischen Dialysepatienten betrug 33,8 %. Eine Verschlechterung des Pflegegrads trat bei 27,1 % der Patienten im ersten Jahr nach Dialysebeginn auf. Zudem mussten innerhalb eines Jahres 82,8 % aller inzidenten chronischen Dialysepatienten erneut stationär in Krankenhäusern behandelt werden.

Zusammenfassung: In der untersuchten Kohorte zeigte sich im internationalen Vergleich eine hohe Inzidenz chronischer Dialysebehandlungen, doch die Patienten scheinen unzureichend auf den Beginn der Dialyse vorbereitet zu sein. Die Mortalität der Dialysepatienten ist sehr hoch, ebenso wie das Risiko von Hospitalisationen sowie eine Verschlechterung des Pflegegrads als Ausdruck der verschlechterten Alltagsfunktionalität.

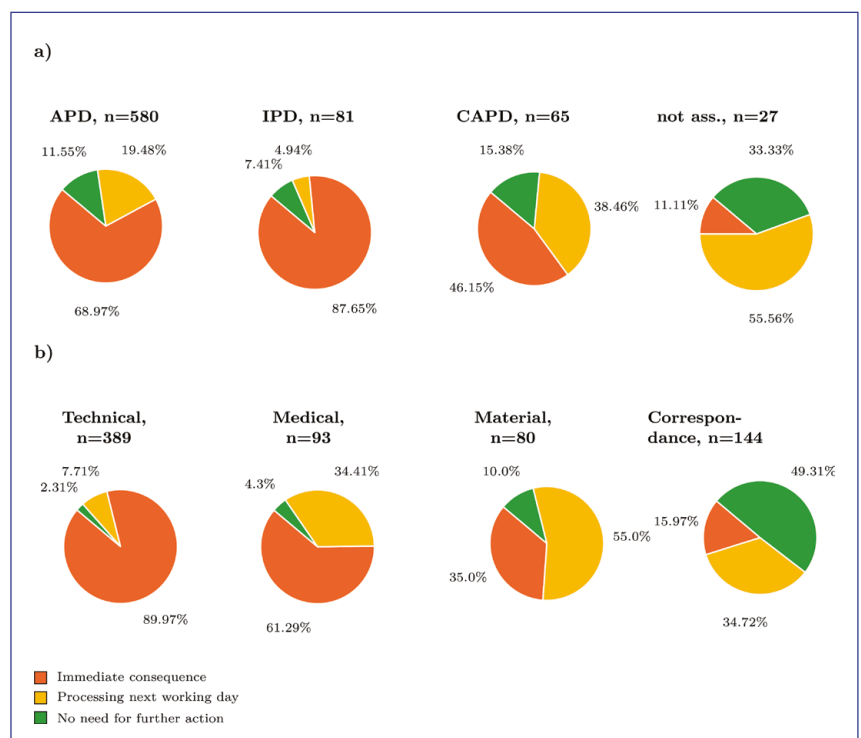
P088 Kategorisierung und Analyse von Notfällen in der telefonischen Rufbereitschaft für Peritonealdialysepatienten. Erfahrungen eines Referenzzentrums.

C. Albert; S. Richter; P. Kalk;
R. P. Woitas; A. Albert
Diaverum MVZ Am Neuen Garten,
Potsdam

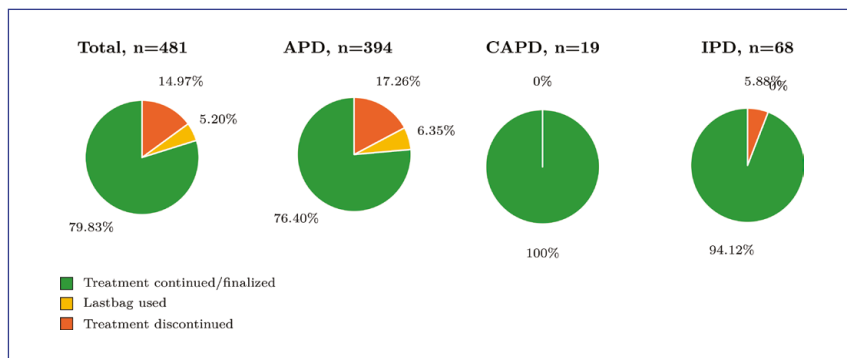
Hintergrund: Kategorisierung und Analyse medizinischer oder technischer Notfälle von Patienten mit ambulanter Peritonealdialyse (PD), die einen telefonischen PD-Bereitschaftsdienst eines Referenzzentrums außerhalb der regulären Sprechzeiten anrufen.

Methode: Wir analysierten retrospektiv die Probleme der Patienten, die an den PD-Bereitschaftsdienst

adressiert wurden. Anrufe im Beobachtungszeitraum (2015–2021) wurden systematisch nach technisch/prozeduralen, medizinischen, Material-bezogenen oder sonstiger Korrespondenz kategorisiert und auf Notwendigkeit und Dringlichkeit analysiert. Die Hauptbeschwerden, Lösungsansatz und die Assoziation der Patienten mit der aktuellen PD-Behandlung und -Modalität wurden in kurzen Protokollen von der diensthabenden PD-Pflegekraft dokumentiert. Die Ergebnisse wurden danach klassifiziert, ob die Patienten ihre Behandlungen erfolgreich beginnen, fortsetzen oder beenden konnten oder ob zusätzliche Interventionen erforderlich waren. **Ergebnisse:** Insgesamt wurden 753 Anrufe kategorisiert und ausgewertet. Anrufe wurden



P088: Abb. 1



P088: Abb. 2

hauptsächlich gegen 6:49 und 18:28 Uhr getätigt. (je \pm 2:36 h). 504 Anrufe (66,9 % aller Anrufe) hatten eine „unmittelbare Konsequenz“. Bei 69,4 % (N = 350) dieser Anrufe handelte es sich um technische/prozedurale, bei 11,3 % (N = 57) um medizinische, bei 5,6 % (N = 28) um Material-bezogene Probleme und bei 4,6 % (N = 23) um sonstige Korrespondenz. Als dringlich wurden auch Anrufe gewertet, welche auf (I) PD bezogen waren, die in einem akademischen Lehrkrankenhaus als Konsilleistung durchgeführt wurden (Abb. 1b + N = 47). Probleme, die den Verlauf der PD-Behandlung unterbrechen, wurden in 481 Fällen identifiziert. In 79,83 % (N = 384) dieser Anrufe war es den Patienten nach telefonischer Rücksprache möglich, ihre Behandlung zu beginnen, fortzusetzen oder final abzuschließen. In 5,2 % der Fälle erfolgte ein Last-Bag-Wechsel, was kumulativ in 85,03 % eine Fortsetzung der Therapie ermöglichte. In 35 Fällen wurde geraten, zu Untersuchung oder Therapieanpassung die Praxis zum frühestmöglichen Zeitpunkt aufzusuchen; in acht Fällen war eine akute Hospitalisierung erforderlich (4,65 % bzw. 1,06 % aller Anrufe).

Zusammenfassung: Der PD-Bereitschaftsdienst bietet Patienten Unterstützung bei akuten und möglicherweise drohenden Komplikationen, bzw. unterstützt und berät im Vorgehen, um die verschriebene Behandlung erfolgreich fortsetzen, wieder aufnehmen oder abschließen zu können. Medizinische Unterstützung kann das Risiko von unerwünschten Ereignissen vermindern und im eingetretenen Fall eine rasche Diagnostik und Therapie vermitteln.

P089

Durchführbarkeit und Funktionalität einer Sonographie-gesteuerten Anlage von Vorhofkathetern zur Hämodialyse und Positionierung im Vergleich zur Durchleuchtungs-gestützten Anlage

M. Kächele; L. Bettac; H. Herrmann; A. Brandt; U. Ludwig; B. Schröppel; L. S. Schulte-Kemna

Innere Medizin I, Sektion Nephrologie, Zentrum für Innere Medizin, Universitätsklinikum Ulm, Ulm

Hintergrund: Die für die Anlage von permanenten Vorhofkathetern zur Hämodialyse notwendige radiologische Durchleuchtung (RAD) erfordert eine entsprechende strukturelle und personelle Infrastruktur

und exponiert den Patienten ionisierender Strahlung. Es wurde unlängst über die Durchführbarkeit der Sonographie-gestützte Positionierung von Vorhofkathetern berichtet. Dieses Vorgehen sollte an einem größeren Kollektiv erneut analysiert werden und die Position der Katheter im rechten Vorhof mit der bei einer Durchleuchtungs-gestützten Anlage verglichen werden.

Methode: Wir werteten prospektiv erfasste Untersuchungsdaten von 134 Patienten, die eine doppelumige Vorhofkatheteranlage in unserer Klinik zwischen Januar 2020 und Dezember 2021 erhielten, hinsichtlich Durchführbarkeit, Sicherheit und Katheterfunktion aus. Insgesamt konnten 1844 Kathetertage beurteilt werden. Wir verglichen darüber hinaus die Position der Katheter in der Röntgenübersichtsaufnahme im retrospektiven Vergleich mit 50 Vorhofkathetern, die mittels RAD angelegt wurden. Dabei unterschieden wir folgende Positionen: Vena cava superior (VCS), cavo-atrialer Übergang (CAJ), rechter Vorhof (RA). **Ergebnisse:** Das Durchschnittsalter betrug 65 Jahre (58 % männlich). Der Vorhofkatheter wurde in 117 (87 %) Fällen in die rechte Jugularvene angelegt. Die primäre Erfolgsrate für Funktion und Position betrug 98,5 % (n = 132). Die Anlage und Positionierung war in 130 Fällen (97 %) mit alleiniger sonographischer Lagekontrolle möglich, bei 4 Patienten mit Hilfe einer zusätzlichen intrakardialen EKG Ableitung oder agitierter Kochsalzlösung, wovon 1 Katheter aufgrund des abschließenden Röntgenbildes revidiert wurde. Eine weitere Revision erfolgte wegen Knickbildung am jugulären

Umschlagspunkt. 2 (1,5 %) Patienten verstarben < 48 h nach dem Eingriff. Katheter-bedingte Infektionen traten im Nachbeobachtungszeitraum nicht auf. Der effektive Blutfluss betrug im Mittel 292 ± 39 ml/min. Nur 1 Katheter wurde > 4 Tage nach Andialyse mit einem effektiven Blutfluss < 250 ml/min befahren. Unter den sonographisch platzierten Kathetern lagen 6 % in der VCS (RAD 24 %), 70 % im CAJ (RAD 60 %) und 24 % im RA (RAD 16 %) und waren damit signifikant unterschiedlich ($p = 0,002$), mit einem höheren Anteil an Kathetern im Zielbereich (CAJ, RA) mittels sonographischer Technik.

Zusammenfassung: Die Anlage von Vorhofkathetern mittels Sonographie stellt eine zuverlässig durchführbare und hinsichtlich Funktionalität und Positionierung gute Alternative zur Durchleuchtungs-gestützten Anlage dar.

P090

IL-17 primes human peritoneal mesothelial cells for VEGF production through IL-6 trans-signaling

R. A. Catar; E. Kawka¹; H. Zhao; D. Wu; J. Witowski¹
Medizinische Klinik mit Schwerpunkt Internistische Intensivmedizin und Nephrologie, Campus Virchow-Klinikum, Charité – Universitätsmedizin Berlin, Berlin; ¹ Department of Pathophysiology, Poznan University of Medical Sciences, Poznan/PL

Objective: IL-17 is believed to contribute significantly to peritoneal homeostasis during peritoneal dialysis (PD), while vascular endothelial growth factor (VEGF) is thought to be a driver of adverse angiogenesis and peritoneal

membrane remodeling in PD. The effect of IL-17 on VEGF synthesis by human peritoneal mesothelial cells (HPMCs) has long been postulated but not fully characterized. Here, we examined the mechanisms by which IL-17 can modulate VEGF production by HPMCs. **Method:** HPMCs were isolated from normal omentum. VEGF mRNA and protein levels were measured by RT-qPCR and ELISA, respectively. The involvement of transcriptional factors was assessed by transient transfections with VEGF promoter constructs, EMSA, ChIP, and siRNA silencing. **Results:** IL-17 alone had little effect on VEGF mRNA expression and VEGF release by HPMCs. However, VEGF production could be greatly increased when IL-17 was applied together with soluble IL-6 receptor (sIL-6R). This effect was associated with VEGF promoter activation through a region containing the binding site for transcription factor AP-1. Inhibition of AP-1 abolished the stimulating effect of IL-17+sIL-6R on VEGF expression. Also, neutralization of IL-6 with either anti-IL-6 antibodies or IL-6-targeting siRNA eliminated the effect of IL-17+sIL-6R, suggesting that IL-6 acts as an intermediate. Accordingly, silencing STAT3, a key mediator of IL-6 signaling, abolished the effect of IL-17+sIL-6R on AP-1 induction and VEGF production. **Conclusion:** IL-17 contributes to VEGF production in HPMCs by inducing IL-6, which, by acting together with sIL-6R in a trans-signaling mechanism, stimulates AP-1-controlled VEGF synthesis. This complex mechanism suggests that IL-17 may impact on

peritoneal vascularity, although it does not itself have a major direct effect on VEGF production.

P091

A prospective cross over study on the effects of medium cut-off membranes on T cellular and serologic immune phenotypes in hemodialysis.

G. Lorenz; Y. Bonnie Shen; C. Scheid; M. Eckermann; S. Hornung; J. Cardoso; M. Lech¹; A. Ribeiro¹; B. Haller; R. I. Hausinger; C. Holzmann-Littig; D. Steubl; M. C. Braunisch; R. Günthner; A. Poschenrieder; U. Heemann; C. Schmaderer
II. Medizinische Klinik, Nephrologie, Klinikum rechts der Isar, Technische Universität München, München; ¹ Nephrologisches Zentrum, Medizinische Poliklinik Innenstadt, Ludwig-Maximilians-Universität München, München

Objective: Extended cut off filtration by medium cut off membranes (MCO) has been shown to be safe in maintenance hemodialysis (HD). The notion of using them for the control of chronic low-grade inflammation and positively influencing cellular immune aberrations seems tempting.

Method: We conducted an open label, multicenter, randomized, 90day 2-phase cross over clinical trial (MCO- versus high flux-HD). 46 patients underwent randomization of which 34 completed the study. Dialysate- or pre- and post-dialysis serum inflammatory mediators were assayed for each study visit. Ex vivo T cell activation was assessed from cryopreserved leucocytes by flow cytometry. Linear mixed models were used to compare treatment modalities,

with serum MCP-1 levels as the predefined primary endpoint.

Results: Filtration/dialysate concentrations of most mediators, including MCP-1 (mean \pm SD: 10.5 ± 5.9 vs. 5.1 ± 3.8 pg/ml, $p < 0.001$) were significantly increased during MCO- versus high flux-HD. However, except for the largest mediator studied, i.e., YKL-40, this did not confer any advantages for single session elimination kinetics (post-HD mean \pm SD: 360 ± 334 vs. 564 ± 422 pg/ml, $p < 0.001$). No sustained reduction of any of the studied mediators was found. Still, the long-term reduction of CD69+ ($p = 0.01$) and PD1+ ($p = 0.02$) activated CD4+ T cells was striking

Conclusion: In contrast to other uremic middle molecules, increased filtration during MCO-HD is compensated for by compartment redistribution or increased production during dialysis in the case of most inflammatory mediators. Long-term reduction over a 3-month period was not possible. Nevertheless, lasting effects on the T-cell phenotype were seen.

P092

Extracorporeal light chain elimination with medium cut off (MCO) membrane hemodialysis is as effective as high cut off (HCO) membrane hemodialysis and less lavish – a preliminary study

C. Schaaf; M. C. Braunisch;
C. Holzmann-Littig; F. Pfister¹;
L. Hannemann; R. I. Hausinger;
C. Schmaderer; L. Renders;
U. Heemann; C. Küchle

II. Medizinische Klinik, Nephrologie,
Klinikum rechts der Isar, Technische
Universität München, München;

¹Institut für Nephropathologie,

Universitätsklinikum, Friedrich-Alexander-Universität Erlangen-Nürnberg, Erlangen

Objective: To determine the efficacy of free light chain (FLC) removal by regular dialysis equipment (high-flux filtration) with medium cut off (MCO) membrane hemodialysis (HD) as an adjuvant treatment to standard chemotherapy for patients with acute kidney failure complicating multiple myeloma (MM).

Method: 55 patients with dialysis-dependent renal failure secondary to MM were treated with MCO-HD (50 patients) and HCO-HD (5 patients) as an internal control, each with four hours duration. Measurement of FLC serum concentration as well as kidney function, total protein and immunoglobulins was performed before and after hemodialysis single or multiple sessions.

Results: The population average age was 68 years, mainly male (23 female, 32 male patients). Over the whole dialysis treatment period with MCO-HD, FLC kappa was reduced significantly by 57 % ($p < 0.05$) and FLC lambda by 46 % ($p < 0.05$). Renal function improved significantly and continuously from starting creatinine 5.7 mg/dl before dialysis to 1.9 mg/dl ($p < 0.05$) after one year. Single dialysis data showed a reduction of 56 % in kappa and 37 % in lambda serum FLC concentration, independent of the MM subtype ($p < 0.05$). In the analyzed subgroups of MM (only kappa, only lambda, all kappa, all lambda type MM) reduction of FLC kappa was significantly higher compared to FLC lambda in all subgroups, as expected by the different sizes of the light chains. No significant alteration of

total protein and immunoglobulins by MCO-HD could be found.

Conclusion: MCO filter-based dialysis is comparably effective, technically easier and less cost-intensive as HCO dialysis in terms of FLC elimination. Kidney function recovery in MM patients is achievable.

P093

Schwere und langanhaltende Veränderung des Albumin-Redox-Zustands durch Plasmapherese

K. Boss; M. Stettner¹; F. Szezanowski¹;
A. K. Mausberg¹; M. Paar²; R. Pul¹;
C. Kleinschnitz¹; K. Öttl²; A. Kribben
Klinik für Nephrologie, Universitätsklinikum, Universität Duisburg-Essen, Essen; ¹Klinik für Neurologie, Universitätsklinikum, Universität Duisburg-Essen, Essen; ²Institut für Physiologische Chemie, Zentrum für Physiologische Medizin, Medizinische Universität Graz, Graz/A

Hintergrund: Plasmapherese (PS) ist eine etablierte Form der therapeutischen Apherese zur Behandlung einer Vielzahl nephrologischer und neurologischer Erkrankungen. Hier wurde untersucht, ob das zugeführte kommerzielle Albumin die Albuminmenge und den Albumin-Redox-Status von Patienten verändert, was sich auf die funktionellen Eigenschaften des Albumins und das Niveau des oxidativen Stresses auswirken kann.

Methode: 20 Patienten ohne Leber- oder Nierenfunktionseinschränkung erhielten fünf PS-Behandlungen. Albuminmenge und Albumin-Redox-Status wurden vor und nach den fünf PS-Behandlungen, 12 Tage nach der letzten PS-Behandlung, sowie in der infundierten Albuminlösung bestimmt. Die Kontrollgruppe bestand aus 13

mit Immunadsorption behandelten Patienten, bei denen kein Albumin hinzugefügt wurde. Der Albumin-Redox-Status wurde durch Fraktionierung in reduziertes humanes Mercaptalbumin (HMA), reversibel oxidiertes humanes Non-Mercaptalbumin 1 (HNA-1) und irreversibel oxidiertes humanes Non-Mercaptalbumin 2 (HNA-2) mittels Hochleistungsflüssigkeitschromatographie (HPLC) bestimmt.

Ergebnisse: Die Albuminmenge blieb im Verlauf der fünf PS-Behandlungen konstant ($4,1 \pm 0,6$ mg/dl vs. $4,3 \pm 0,4$ mg/dl). Irreversibel oxidiertes HNA-2 stieg im Verlauf von fünf PS-Behandlungen von $2,5 \pm 1,4$ % auf $13,4 \pm 4,2$ % ($P < 0,01$) und blieb auch 12 Tage nach der letzten PS-Behandlung deutlich erhöht ($8,6 \pm 2,1$ %, $P < 0,05$). Der HNA-2-Anteil in der Infusionslösung betrug 18,8 %. In der Kontrollgruppe stieg HNA-2 im Verlauf der 5 Behandlungen mäßig an, blieb aber unter 5 %, was einem Anteil wie bei Gesunden entspricht. Die Albuminmenge sank um 15 % ($P < 0,01$).
Zusammenfassung: Plasmapherese führt zu einer schwerwiegenden und langanhaltenden Veränderung des Albumin-Redox-Status, was eine neue potenzielle Nebenwirkung darstellt, die das Niveau des oxidativen Stresses beeinflussen könnte.

P094

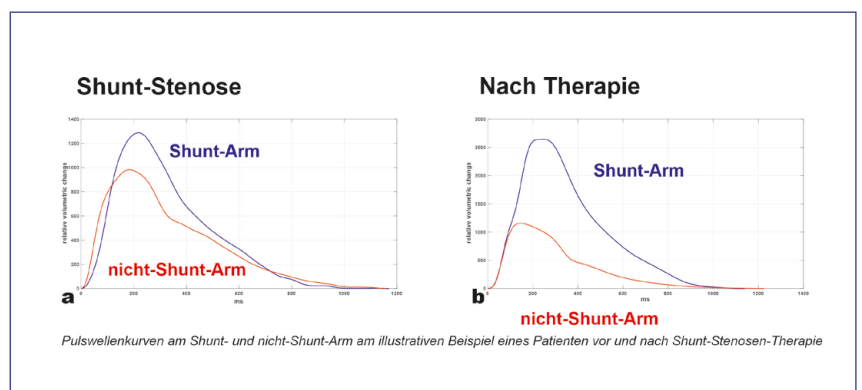
Ateriovenöse-Oszillometrie zur Shuntfunktionsdiagnostik

V. Busch¹; J. Streis¹; N. Mueller²; S. Müller³; F. S. Seibert⁴; T. Felderhoff⁵; T. H. Westhoff⁴

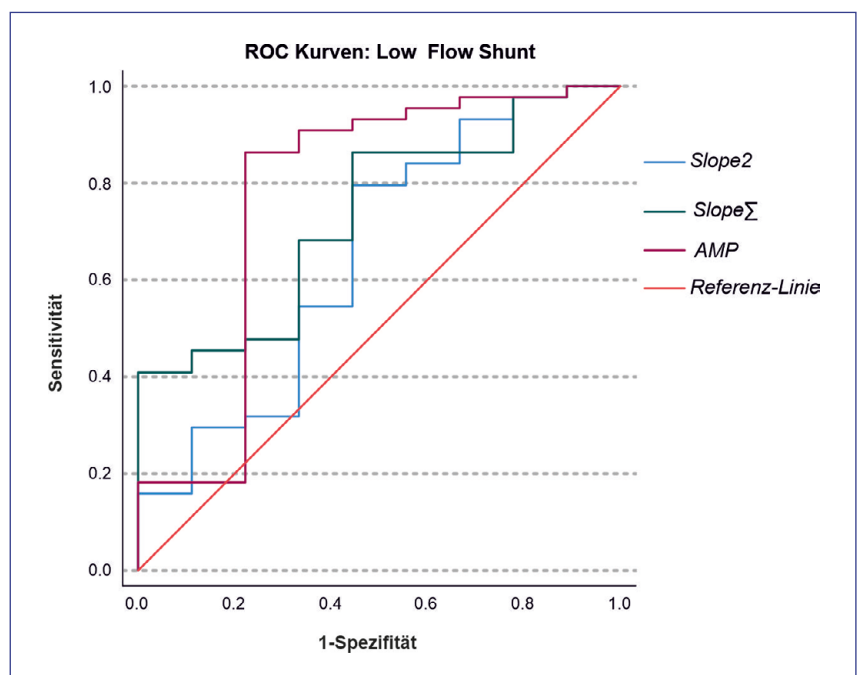
Nephrologie/Dialyse/Lipidapherese, Diavital Dialysezentrum Kamen, Kamen; ¹ Pleiger Maschinenbau GmbH & Co. KG, Witten; ² Onkologie, Medizinische Klinik III,

Ludwig-Maximilian Universität, München; ³ Institut für Diskrete Mathematik und Geometrie, Technische Universität Wien, Wien/A; ⁴ Centrum für Translationale Medizin, Medizinische Klinik I, Marien Hospital Herne, Ruhr-Universität Bochum, Herne; ⁵ Fachbereich Informationstechnik, Bereich: Medizinische Informationstechnik, Fachhochschule Dortmund, Dortmund

Hintergrund: In einer früheren Studie wurde gezeigt, dass die Pulswellenanalyse mittels Tonometrie zur Shuntfunktionsdiagnostik geeignet sein kann. Die hier vorgelegte Studie untersucht, ob die benutzerfreundlichere oszillometrische Pulswellenanalyse ebenfalls zur Shuntdiagnostik geeignet ist und in der Lage ist, einen



P094: Abb. 1



P094: Abb. 2

N	Alter	BMI	Geschlecht	Unter/Oberarm-Fistel	Diabetes	Permanentes VHF	KHK	HF/EF
53 (100 %)	66 ± 2.2 [Jahre]	25.6 ± 0.6 [kg/m ²]	2.53 [m/w]	2.31	30 (56.6 %)	17 (32.1 %)	18 (34 %)	5 (9.4 %)

P094: Tab. 1

Shunt-Fluss unter 500 ml/min („low flow Shunt“) zu detektieren.

Methode: Bei 53 Patienten mit nativer Fistel wurden Pulswellen beidseitig mit dem Vicorder®-Gerät an der A. brachialis gemessen. Nachfolgend analysierten wir die normalisierten digitalisierten Kurven in einer spezifisch programmierten Matlab®-Umgebung. Entsprechend früheren Ergebnissen stand die durchschnittliche Steigung in den vier Abschnitten der Pulsweite zwischen dem Fusspunkt, dem systolischen Maximum (T1), dem ersten diastolischen Extrempunkt und dem Ende der Pulsweite im Fokus. Primär wurden die Steigung im zweiten Abschnitt (slope2) und die Summe aller vier Abschnitte (slopeΣ) analysiert. Darüber hinaus wurde die Amplitude der Änderung des nicht-kalibrierten relativen Füllvolumens der Messmanschette des Vicorder®-Gerät innerhalb eines Herzzyklus (AMP) betrachtet (eindrückliche Effekte in ersten Messungen). Das Shunt-Minutenvolumen wurde duplexsonographisch gemessen.

Ergebnisse: Es fanden sich signifikante Unterschiede in den Pulswellenkonturen am Shunt- und nicht-Shunt-Arm. Die Mediane am Shunt-Arm/nicht-Shunt-Arm von slope2, slopeΣ und AMP betrugen -0.00150/-0.00322 [relative Amplitude/ms, $p < 0.001$], 0.01094/0.01187 [relative Amplitude/ms, $p = 0.006$] und 1850/725 [relative Volumenänderung, $p < 0.001$] (Wilcoxon Test). T1 stellte sich am Shunt-Arm

verzögert dar (204 ± 3.4 ms versus 162 ± 5.3 ms Shunt/nicht-Shunt-Arm, $p < 0.001$). In der ROC-Analyse der Messwerte am Shunt-Arm zur Detektion eines Shunt-Flusses < 500 ml/min zeigten sich AUC's (mit CI) von 0.652 (0.437–0.866, $p = 0.167$) für slope 2, 0.732 (0.566–0.899, $p = 0.006$) für slopeΣ und 0.775 (0.56–0.991, $p = 0.012$) für AMP.

Zusammenfassung: Eine Shunt-funktionsdiagnostik mittels Pulswellen-Oszillometrie stellt eine einfach handhabbare und vielversprechende Anwendung zur Detektion einer Low-Flow Fistel dar.

P095

Vorhofkatheter in der Dialyse – zu Unrecht verdammt?

A. Buckenmayer; B. Möller; C. Ostermaier; J. Hoyer; C. S. Haas
Klinik für Innere Medizin, Nephrologie und Internistische Intensivmedizin, Standort Marburg, Universitätsklinikum Gießen und Marburg GmbH, Marburg

Hintergrund: AV-Shunts gelten bisher als Goldstandard beim Zugang für Dialysepatienten, Vorhofkatheter (VHK) sind eine mögliche Alternative. Bei älteren und multimorbiden Patienten werden VHKs oft als permanenter Zugang genutzt, aufgrund ihres Risikos für Komplikationen sind sie aber nicht unumstritten. Unklar ist, inwiefern VHK-Komplikationen das klinische Outcome mitbeeinflussen. Ziel dieser Studie war die quantitative und qualitative Analyse von

VHK-assoziierten Komplikationen in einem universitären Setting.

Methode: Retrospektiv wurden alle Patienten, die von JAN 2015–JUN 2021 über einen VHK dialysierten, erfasst. Untersucht wurden Tragedauer, Gründe von Im- und Explantation, sowie Komplikationen der VHKs in Abhängigkeit von Komorbiditäten (Diabetes, Hypertonus, Herzinsuffizienz, pAVK, Demenz), Alter und prognostizierter sowie tatsächlicher 6-Monats-Mortalität (Cohen Modell).

Ergebnisse: Insgesamt wurden 478 VHKs bei 351 Patienten analysiert. Mit 66,5 Jahren war das mittlere Alter dieser Kohorte vergleichbar mit dem aller Dialysepatienten in Deutschland. Häufigster Grund für die Anlage eines VHK war die Einleitung der Dialysetherapie, die durchschnittliche Nutzungsdauer lag bei 309 Tagen. Bei 31,1 % war das Versterben der Patienten Grund für Beendigung der VHK-Nutzung, bei 26,9 % erfolgte ein Verfahrenswechsel (Dialyse via Shunt, Umstellung auf Peritonealdialyse, Nierentransplantation) oder die Beendigung der Dialysetherapie. Häufigkeit und Art von Komplikationen (Dysfunktion, Thrombusbildung, Infektion, Tod) waren altersunabhängig. VHK-Infektionen waren mit 0,6/1.000 Kathetertagen ein eher seltenes Ereignis. pAVK, Herzinsuffizienz und Demenz zeigten eine signifikante Assoziation mit erhöhtem Risiko für eine Komplikation ($p < 0,05$). Interessanterweise lag die tatsächliche 6-Monats-Mortalität mit 14,3 %

deutlich unter dem prognostizierten Wert (19,6 %, $p < 0,05$).

Zusammenfassung: Wir konnten zeigen, dass: (1) VHK am häufigsten zur Dialyseeinleitung implantiert und mit durchschnittlich 10 Monaten relativ lange genutzt werden; (2) schwere Komplikationen selten auftreten; (3) VHK-assoziierte Komplikationen altersunabhängig, aber mit bestimmten Komorbiditäten assoziiert sind; und (4) Dialysepatienten mit VHK länger als prognostiziert leben. Die Daten suggerieren, dass VHKs per se nicht unbedingt einen inferioren Zugangsweg darstellen, und dass das bisherige Dogma „fistula first, catheter last“ möglicherweise zugunsten einer differenzierten Wahl verlassen werden sollte.

P096

An den Kohlendioxidpartialdruck ($p\text{CO}_2$) adaptierte Bicarbonat-Zielwerte bei kontinuierlicher Nierenersatztherapie (CKRT) – Zwischenergebnisse der prospektiv randomisierten BigBIC Studie

J. V. Kunz; H. Stockmann¹; M. Fähndrich; M. Pigorsch²; N. Bethke¹; H. Peters¹; A. Krüger¹; K.-U. Eckardt¹; D. Khadzhynov¹; P. Enghard¹
Medizinische Klinik mit Schwerpunkt Nephrologie und Internistische Intensivmedizin, Campus Virchow-Klinikum, Charité – Universitätsmedizin Berlin, Berlin; ¹ Medizinische Klinik mit Schwerpunkt Nephrologie und Internistische Intensivmedizin, Campus Charité Mitte, Charité – Universitätsmedizin Berlin, Berlin; ² Institut für Biometrie und klinische Epidemiologie, Charité – Universitätsmedizin Berlin, Berlin

Hintergrund: Bei lungenprotektiv beatmeten ARDS-Patient:innen ist die CO_2 Retention ein häufiges

Problem. Physiologisch wird bei intakter Nierenfunktion unter CO_2 Retention mehr Bicarbonat (HCO_3^-) rückresorbiert. Eine solche Kompensation ist bei CKRT mit Citratantikoagulation (Citrat-CKRT) zwar möglich, aktuell aber nicht als Therapiestandard vorgesehen.

Methode: Lungenprotektiv beatmete ARDS-Patient:innen mit CO_2 Retention (arterieller $p\text{CO}_2 > 55$ mmHg) und Indikation zur CKRT wurden in eine prospektive Feasibility-Pilotstudie eingeschlossen und 1:1 randomisiert. In der Interventionsgruppe wird durch Anpassung des Blut-zu-Dialysatverhältnisses ein an den $p\text{CO}_2$ adaptiertes HCO_3^- angestrebt, das entsprechend der physiologischen renalen Kompensation berechnet wird: Ziel $\text{HCO}_3^- = ((p\text{CO}_2 - 45 \text{ mmHg}) / 10 \text{ mmHg}) * 4 \text{ mmol/l} + 24 \text{ mmol/l}$. In der Kontrollgruppe beträgt das Ziel HCO_3^- 24 mmol/l. Primärer Endpunkt ist das HCO_3^- nach 72 h. In diese Pilotstudie sollen 40 Patient:innen eingeschlossen werden. Die Studie wurde von der zuständigen Ethikkommission genehmigt und im Deutschen Register für klinische Studien registriert (DRKS00026177). **Ergebnisse:** Aktuell wurden 20 Patient:innen randomisiert. Nach Ausschluss von zwei Patient:innen (1x Rückzugs der Einwilligung, 1x Protokollverletzung) wurden 10 Patient:innen in der Interventionsgruppe und 8 in der Kontrollgruppe ausgewertet. Bei Studieneinschluss unterschied sich das HCO_3^- in beiden Gruppen nicht (Interventionsgruppe 26,1 mmol/l ($\pm 2,3$); Kontrollgruppe 25,8 mmol/l ($\pm 2,4$)). Bereits innerhalb der ersten 24 Stunden zeigten sich in der Interventionsgruppe steigende

HCO_3^- Werte (29,1 mmol/l ($\pm 1,5$)) im Vergleich zur Kontrollgruppe (25,5 mmol/l ($\pm 2,2$)). Nach 72 h sahen wir in der Interventionsgruppe weiterhin relevant höhere HCO_3^- Spiegel (29,1 mmol/l ($\pm 2,3$) vs. 25,3 mmol/l ($\pm 1,9$)). Unter Anhebung der HCO_3^- Konzentration konnte in der Interventionsgruppe bei etwa gleichbleibendem Atemminutenvolumen keine zusätzliche CO_2 Retention beobachtet werden. In der Interventionsgruppe trat am sechsten Studientag bei zwei Patient:innen eine Citratakkumulation auf, verglichen mit keinem Ereignis in der Kontrollgruppe. In beiden Gruppen verstarben jeweils zwei Patient:innen im Interventionszeitraum.

Zusammenfassung: Die systemische HCO_3^- Konzentration lässt sich unter Citrat-CKRT schnell und sicher anheben. Die $p\text{CO}_2$ adaptierte CKRT könnte dazu beitragen, eine lungenprotektive Beatmung trotz Hyperkapnie beizubehalten.

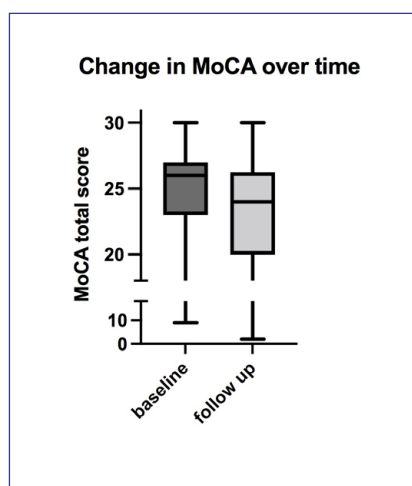
Dialyse/Apherese 2

P097

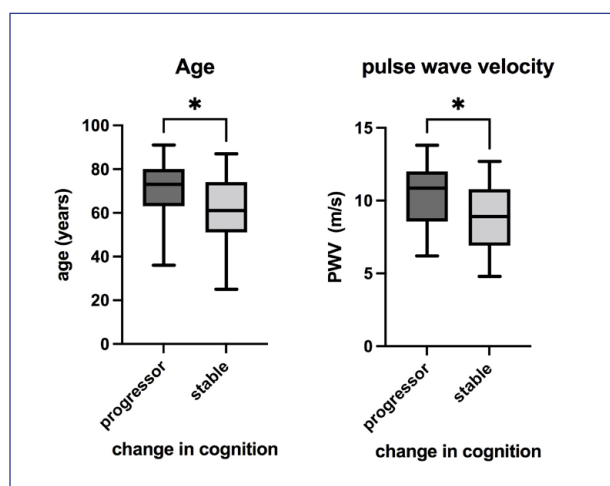
Risk factors associated with a decline in cognitive function in hemodialysis patients

H. Schäfer; S. Angermann; U. Heemann; C. Schmaderer
II. Medizinische Klinik, Nephrologie, Klinikum rechts der Isar, Technische Universität München, München

Objective: Cognitive impairment is common in dialysis patients and associated with adverse health outcomes. The pathogenesis is unclear, but cerebrovascular disease is likely to be the leading cause. Different risk factors for cognitive decline have been described so far



P097: Abb. 1



P097: Abb. 2

with age and lower diastolic blood pressure being the most prominent. We examined the potential relationship between declining cognitive function and different categories of risk factors focusing on pulse wave velocity (PWV) as a marker of arterial stiffness.

Method: 150 hemodialysis patients underwent cognitive testing using Montreal Cognitive Assessment (MoCA). 90 patients had a follow-up MoCA approximately 2 years later. Demographic data including socioeconomic and cardiovascular risk factors, dialysis-associated risk factors and risk factors for vascular calcification and hemodynamics including PWV were analyzed. PWV was measured noninvasively as a continuous measurement over 24 hours and calculations of PWV were derived from an oscillometric pulse contour analysis. To evaluate risk factors associated with cognitive decline patients were split into two groups according to their initial and follow-up MoCA results. Those who had a normal (≥ 24 points) MoCA at baseline and progressed to a MoCA within

pathological range (< 24 points) were summarized as progressors, all other patients were summarized as non-progressors.

Results: Follow-up MoCA results were significantly lower compared to baseline (Figure 1). 25 of the 90 patients (28 %) had a MoCA score within the pathological range (< 24 points) at baseline. 19 of the 90 patients (21 %) had a MoCA score at baseline within the normal range (≥ 24 points) and progressed to a pathological MoCA score at follow up. Higher Age was independently associated with a decline in cognitive function. A significant between groups difference was seen for PWV with higher values being associated with a declining cognitive function, however, after adjustment for confounders this tendency lost statistical significance (Figure 2). There were no further significant differences between the two groups regarding socioeconomic and cardiovascular risk factors, dialysis-associated risk factors and risk factors for vascular calcification and hemodynamics. Figure 1 and 2.

Conclusion: Decline of cognitive function in patients on hemodialysis is a common observation. Risk factors for declining cognition are age and potentially arterial stiffness measured by PWV. More patients are needed to evaluate a potential role of arterial stiffness assessment as a screening tool in hemodialysis patients.

P098

Ergebnisse des medizinischen Qualitätsmanagements und Ereignismanagements im KfH

K. Jüttner; K. Göbel; J. Messer; M. Masannek¹; D. Bach¹; J. Beige²
Medizin, Kuratorium für Dialyse und Nierentransplantation e. V., Neu-Isenburg; ¹ KfH-Hauptverwaltung, KfH Kuratorium für Dialyse und Nierentransplantation e. V., Neu-Isenburg; ² Nephrologie und KfH Nierenzentrum, Klinikum St. Georg, Leipzig

Hintergrund: Qualitätsmanagement (QM) generell und in der Medizin im Besonderen ist idealerweise ein bidirektionaler Prozess. Im Bereich Medizin des Kuratorium für Dialyse und

Nierentransplantation e. V. (KfH) werden dazu Qualitätsrichtlinien erarbeitet und kommuniziert und andererseits ein aktives zentrales Ereignis- und Maßnahmenmanagement (ZEMM) praktiziert, welches perspektivisch Rückwirkungen auf die Erstellung von Richtlinien und Empfehlungen haben wird.

Methode: Basiert auf § 4, Abs. 2 QM-Richtlinie G-BA und einer KfH Gesamtbetriebsvereinbarung, Darstellung der zentralen Befunde aus ZEMM vom 1.8.2020 (Initiierung) – 30.4.2022 Verwendung einer IT-Plattform (Intrafox) mit folgenden Meldungskategorien: Medizinische Ereignisse mit Patientenschaden, Arzneimitteln und/oder Medizinprodukten (Pflichtmeldungen), Patientenbeschwerden, Qualitätsbeanstandungen

Ergebnisse: Bei ca. 3,5 Mio durchgeführten KfH-Zentrumsdialysebehandlungen im Erfassungszeitraum wurden von 158 Zentren (68 Zentren keine Meldung) insgesamt 1200 Ereignisse gemeldet, davon im vollständig erfassten Jahr 2021 600, die detailliert dargestellt werden können: 503 medizinische Ereignisse (davon 58 mit Patientenschaden), 73 Medizinprodukte-Ereignisse, 24 Arzneimittelereignisse. Unter den med. Ereignissen führen Blutverluste (141, davon 11 kritische aber non-fatale Dislokationen) und Stürze (73). 109 mal waren stationäre Behandlungen nötig, es kam zu drei bekannten Todesfällen in sekundärem Zusammenhang zu Ereignissen.

Zusammenfassung: Die im KfH gewählte Plattform und Erhebungsmethodik erbringt umfangreiche QM-Erkenntnisse durch Ereignisdaten, die vergleichbar sind mit Literaturdaten, z. B. im Bereich der

kritischen Dislokationen. Somit ergibt sich ein sinnvoller Ansatz zur gezielten Beeinflussung (Zurückdrängung) solcher Ereignisse z. B. durch Richtlinien- und Empfehlungsdisein und Qualitätskonferenzen. Ein ganzheitliches, durch ZEMM rück-gekoppeltes QM ist ein Mehrwert zentraler Dialyseprovider.

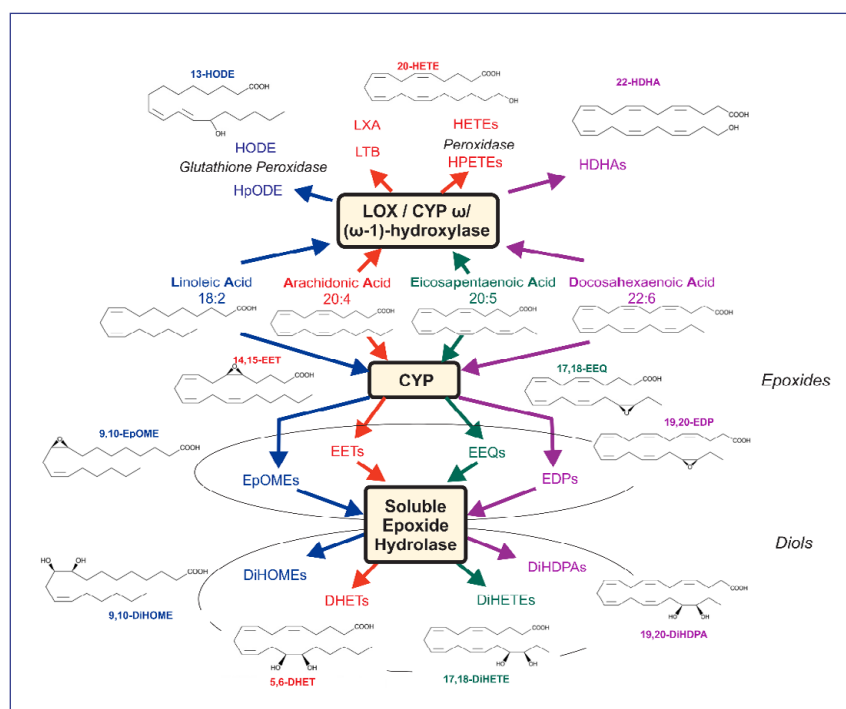
P099 Hemodialysis and Plasma Oxylipin Biotransformation in Peripheral Tissue

T. Liu; I. Dogan; M. Rothe¹; J. V. Kunz²; F. Knauf³; M. Gollasch; F. C. Luft; B. Gollasch⁴

ECRC-Kooperation von MDC und Charité, Experimental and Clinical Research Center, Berlin; ¹ Lipidomix GmbH, Berlin; ² Medizinische Klinik mit Schwerpunkt Nephrologie und Internistische Intensivmedizin,

Campus Virchow-Klinikum, Charité – Universitätsmedizin Berlin, Berlin; ³ Medizinische Klinik mit Schwerpunkt Nephrologie und Internistische Intensivmedizin, Campus Charité Mitte, Charité – Universitätsmedizin Berlin, Berlin; ⁴ Klinik und Poliklinik für Kardiologie und Nephrologie, HELIOS Klinikum Berlin-Buch, Berlin

Objective: The role of polyunsaturated fatty acids (PUFA) and their oxidative metabolites on the development and progression of cardiovascular disease have been extensively studied. However, it is unclear whether abnormal biometabolism of these oxylipins occurs in the context of end-stage renal disease patients undergoing hemodialysis (HD). Our previous studies have shown that a single HD session increased some



P099: Abb. 1

Table 1. Effects of hemodialysis on oxylipins in the CKD patients before (Pre-HD) and at cessation (Post-HD) of hemodialysis.

Amount ng/ml	pre-HD Arterial	pre-HD Venous	p value, t test (# paired Wilcoxon test)	pre-HD A-V difference	post-HD Arterial	post-HD Venous	p value, t test (# paired Wilcoxon test)	post-HD A-V difference
CYP epoxy-metabolites								
5,6-EET	25.24 ±22.80	16.80 ±15.37	0.325	8.156 ±22.08	37.07 ±16.68	61.84 ±21.09	0.003 #	-24.77 ±17.42
8,9-EET	10.52 ±10.90	7.27 ±6.68	0.806	3.13 ±11.45	13.31 ±5.65	22.40 ±7.86	0.002 #	-9.09 ±6.79
11,12-EET	9.95 ±10.08	7.04 ±6.84	0.806	2.70 ±10.22	14.23 ±6.68	25.69 ±9.18	0.002 #	-11.46 ±7.50
14,15-EET	12.56 ±12.54	9.67 ±9.49	0.538	2.63 ±12.46	19.09 ±9.30	35.69 ±13.58	0.002 #	-16.60 ±10.90
5,6-DHET	1.15±0.55	1.07 ±0.59	0.389	0.12 ±0.18	1.37 ±0.59	1.28 ±0.62	0.177 #	0.09 ±0.22
8,9-DHET	1.74 ±1.58	1.61 ±1.36	0.806	0.16 ±0.43	1.61 ±1.12	1.25 ±0.98	0.004 #	0.36 ±0.40
11,12-DHET	0.44 ±0.22	0.42 ±0.20	0.902	0.03 ±0.09	0.52 ±0.20	0.47 ±0.19	0.005	0.05 ±0.05
14,15-DHET	0.42 ±0.10	0.37 ±0.08	0.252	0.05 ±0.09	0.49 ±0.13	0.42 ±0.10	0.132	0.07 ±0.15
7,8-EDP	4.52 ±4.37	3.29 ±3.18	0.951	1.19 ±4.79	6.01 ±2.69	10.44 ±3.56	0.002 #	-4.43 ±2.24
10,11-EDP	4.48 ±4.40	3.34 ±3.09	0.806	1.05 ±4.56	6.64 ±3.08	11.93 ±3.93	<0,001	-5.30 ±2.52
13,14-EDP	3.39 ±3.50	2.66 ±2.82	0.806	0.65 ±3.68	4.82 ±2.21	7.82 ±2.62	<0,001	-3.00 ±1.94
16,17-EDP	2.97 ±2.88	2.19 ±2.04	0.806	0.75 ±2.85	3.83 ±1.69	5.54 ±2.02	0.008	-1.70 ±1.84
19,20-EDP	5.56 ±5.39	3.97 ±3.15	1	1.47 ±5.61	8.68 ±3.86	16.31 ±6.27	0.002 #	-7.64 ±3.78
7,8-DiHDPA	0.45 ±0.25	0.41 ±0.23	0.498	0.04 ±0.04	0.49 ±0.23	0.45 ±0.22	0.021	0.04 ±0.06
10,11-DiHDPA	0.13 ±0.04	0.12 ±0.03	0.664	0.01 ±0.02	0.14 ±0.05	0.13 ±0.05	0.031	0.01 ±0.02
13,14-DiHDPA	0.09 ±0.03	0.08 ±0.02	0.65	0.01 ±0.01	0.10 ±0.04	0.10 ±0.04	0.55	-0.01 ±0.03
16,17-DiHDPA	0.09 ±0.04	0.09 ±0.03	0.886	0.00 ±0.01	0.12 ±0.05	0.10 ±0.05	0.168	0.01 ±0.03
19,20-DiHDPA	0.84 ±0.41	0.83 ±0.37	0.943	0.04 ±0.07	0.95 ±0.41	0.91 ±0.43	0.393	0.04 ±0.16
5,6-EEQ	0.01 ± 0	0	0.23	-0.01 ± 0.00	0.01± 0.01	0.01 ± 0.01	0.004 #	0
8,9-EEQ	1.45 ±1.23	1.00 ±0.70	0.498	0.43 ±1.38	2.61 ±1.77	4.39 ±1.58	0.008 #	-1.78 ±1.65
11,12-EEQ	0.95 ±0.83	0.72 ±0.48	0.806	0.23±0.93	1.81 ±1.23	3.50 ±1.37	0.003 #	-1.69 ±1.18
14,15-EEQ	0.94 ±0.71	0.70 ±0.45	0.343 #	0.22 ±0.82	1.75 ±1.22	3.27 ±1.32	0.004 #	-1.52 ±1.30
17,18-EEQ	1.68 ±1.39	1.39 ±0.85	0.543 #	0.26 ±1.49	2.96 ±2.10	6.26 ±2.28	0.002 #	-3.30 ±2.03
5,6-DiHETE	1.53 ±0.93	1.37 ±0.71	0.622 #	0.32 ±0.87	2.04 ±1.50	1.69 ±0.83	0.53 #	0.35 ±1.28
8,9-DiHETE	0.09 ±0.04	0.09 ±0.03	0.667 #	0.01 ±0.04	0.11 ±0.06	0.10 ±0.04	0.36	0.01 ±0.05
11,12-DiHETE	0.05 ±0.04	0.04 ±0.01	0.806	0.01 ±0.04	0.06 ±0.06	0.04 ±0.01	0.099 #	0.02 ±0.06
14,15-DiHETE	0.05 ±0.02	0.05 ±0.01	0.364 #	0.01 ±0.02	0.05±0.02	0.05 ±0.02	0.49	0.01 ±0.02
17,18-DiHETE	0.21 ±0.08	0.21 ±0.08	0.981 #	0.00 ±0.07	0.28 ±0.12	0.25 ±0.11	0.253	0.03 ±0.09
9,10-EpOME	33.02 ±31.08	22.60 ±12.96	0.806	9.97 ±32.03	51.72 ±18.84	93.59 ±36.50	0.002 #	-41.86 ±26.99
12,13-EpOME	30.98 ±26.77	20.70 ±11.08	0.46	9.79 ±27.74	46.91 ±15.04	79.72 ±23.68	<0,001	-32.81 ±15.40
9,10-DiHOME	4.15 ±1.79	3.30 ±1.71	0.085	0.75 ±0.99	5.60 ±2.79	5.65 ±2.47	0.954 #	-0.05 ±2.79
12,13-DiHOME	4.98 ±1.94	3.90 ±1.63	0.161 #	0.99 ±1.66	6.96 ±3.79	6.93 ±3.38	0.875 #	0.03 ±2.83

Notes: Mean±SD. A-V ; arteriovenous .

Table 2. Effects of hemodialysis on plasma oxylipins in the CKD patients before (Pre-HD) and at cessation (Post-HD) of hemodialysis

Amount ng/ml	pre-HD Arterial	post-HD Arterial	p-Value, t-Test (# Paired Wilcoxon Test)	pre-HD Venous	post-HD Venous	p-Value, t-Test (# Paired Wilcoxon Test)
CYP epoxy-metabolites						
5,6-EET	25.24 ±22.80	37.07 ±16.68	0.042 #	16.80 ±15.37	61.84 ±21.09	0.002 #
8,9-EET	10.52 ±10.90	13.31 ±5.65	0.042 #	7.27 ±6.68	22.40 ±7.86	0.002 #
11,12-EET	9.95 ±10.08	14.23 ±6.68	0.036 #	7.04 ±6.84	25.69 ±9.18	0.002 #
14,15-EET	12.56 ±12.54	19.09 ±9.30	0.031 #	9.67 ±9.49	35.69 ±13.58	0.002 #
5,6-DHET	1.15±0.55	1.37 ±0.59	0.176 #	1.07 ±0.59	1.28 ±0.62	0.012 #
8,9-DHET	1.74 ±1.58	1.61 ±1.12	0.902 #	1.61 ±1.36	1.25 ±0.98	0.012 #
11,12-DHET	0.44 ±0.22	0.52 ±0.20	0.176 #	0.42 ±0.20	0.47 ±0.19	0.056
14,15-DHET	0.42 ±0.10	0.49 ±0.13	0.124	0.37 ±0.08	0.42 ±0.10	0.07
7,8-EDP	4.52 ±4.37	6.01 ±2.69	0.097 #	3.29 ±3.18	10.44 ±3.56	0.002 #
10,11-EDP	4.48 ±4.40	6.64 ±3.08	0.056 #	3.34 ±3.09	11.93 ±3.93	0.002 #
13,14-EDP	3.39 ±3.50	4.82 ±2.21	0.097 #	2.66 ±2.82	7.82 ±2.62	0.002 #
16,17-EDP	2.97 ±2.88	3.83 ±1.69	0.085 #	2.19 ±2.04	5.54 ±2.02	0.002 #
19,20-EDP	5.56 ±5.39	8.68 ±3.86	0.056 #	3.97 ±3.15	16.31 ±6.27	0.002 #
7,8-DiHDPA	0.45 ±0.25	0.49 ±0.23	0.58 #	0.41 ±0.23	0.45 ±0.22	0.158 #
10,11-DiHDPA	0.13 ±0.04	0.14 ±0.05	0.371	0.12 ±0.03	0.13 ±0.05	0.475
13,14-DiHDPA	0.09 ±0.03	0.10 ±0.04	0.473	0.08 ±0.02	0.10 ±0.04	0.054
16,17-DiHDPA	0.09 ±0.04	0.12 ±0.05	0.195	0.09 ±0.03	0.10 ±0.05	0.313
19,20-DiHDPA	0.84 ±0.41	0.95 ±0.41	0.506	0.83 ±0.37	0.91 ±0.43	0.25
5,6-EEQ	0.01 ± 0	0.01± 0.01	0.069 #	0	0.01 ± 0.01	0.002 #
8,9-EEQ	1.45 ±1.23	2.61 ±1.77	0.036 #	1.00 ±0.70	4.39 ±1.58	<0,001
11,12-EEQ	0.95 ±0.83	1.81 ±1.23	0.042 #	0.72 ±0.48	3.50 ±1.37	0.002 #
14,15-EEQ	0.94 ±0.71	1.75 ±1.22	0.065 #	0.70 ±0.45	3.27 ±1.32	0.002 #
17,18-EEQ	1.68 ±1.39	2.96 ±2.10	0.085 #	1.39 ±0.85	6.26 ±2.28	0.002 #
5,6-DiHETE	1.53 ±0.93	2.04 ±1.50	0.356 #	1.37 ±0.71	1.69 ±0.83	<0,001
8,9-DiHETE	0.09 ±0.04	0.11 ±0.06	0.389 #	0.09 ±0.03	0.10 ±0.04	0.376
11,12-DiHETE	0.05 ±0.04	0.06 ±0.06	0.255 #	0.04 ±0.01	0.04 ±0.01	0.451
14,15-DiHETE	0.05 ±0.02	0.05±0.02	0.916	0.05 ±0.01	0.05 ±0.02	0.458
17,18-DiHETE	0.21 ±0.08	0.28 ±0.12	0.152	0.21 ±0.08	0.25 ±0.11	0.129
9,10-EpOME	33.02 ±31.08	51.72 ±18.84	0.023 #	22.60 ±12.96	93.59 ±36.50	0.002 #
12,13-EpOME	30.98 ±26.77	46.91 ±15.04	0.023 #	20.70 ±11.08	79.72 ±23.68	0.002 #
9,10-DiHOME	4.15 ±1.79	5.60 ±2.79	0.176 #	3.30 ±1.71	5.65 ±2.47	0.006 #
12,13-DiHOME	4.98 ±1.94	6.96 ±3.79	0.135	3.90 ±1.63	6.93 ±3.38	0.01 #

Notes: Mean±SD.

oxylipins in the arteries. This study was the first to use the arteriovenous (AV) differences of metabolites to respond to their biometabolic direction, either release, storage, or biotransformation in vivo. The aim was to further understand

the effects of HD on the metabolism of different oxylipins. **Method:** We collected arterial and peripheral venous blood from 12 hemodialysis patients and measured oxylipins catalyzed by cytochrome P450 (CYP 450)

and lipoxygenase (LOX)/CYP ω /(ω -1)-hydroxylase by high-performance liquid chromatography-mass spectrometry.

Results: Comparing the AV differences between CYP450, LOX, and LOX/CYP ω /(ω -1)-hydroxylase

Table 3. Effects of hemodialysis on plasma oxylipins and their ratios in the CKD patients before (Pre-HD) and at cessation (Post-HD) of hemodialysis

Amount ng/ml	pre-HD Arterial	pre-HD Venous	p value, t test (# paired Wilcoxon test)	post-HD Arterial	post-HD Venous	p value, t test (# paired Wilcoxon test)	pre-HD Venous	post-HD Venous	p value, t test (# paired Wilcoxon test)
5,6-DHET/5,6-EET	0.07 \pm 0.05	0.09 \pm 0.06	0.617	0.04 \pm 0.03	0.02 \pm 0.01	0.002 #	0.09 \pm 0.06	0.02 \pm 0.01	0.002 #
8,9-DHET/8,9-EET	0.27 \pm 0.26	0.29 \pm 0.25	0.854 #	0.13 \pm 0.06	0.06 \pm 0.05	0.002 #	0.29 \pm 0.25	0.06 \pm 0.05	0.002 #
11,12-DHET/11,12-EET	0.08 \pm 0.06	0.09 \pm 0.07	0.926 #	0.04 \pm 0.02	0.02 \pm 0.01	0.002 #	0.09 \pm 0.07	0.02 \pm 0.01	0.002 #
14,15-DHET/14,15-EET	0.07 \pm 0.04	0.06 \pm 0.03	0.485	0.03 \pm 0.02	0.01 \pm 0.00	0.002 #	0.06 \pm 0.03	0.01 \pm 0.00	0.002 #
7,8-DiHDP/7,8-EDP	0.17 \pm 0.14	0.57 \pm 1.47	0.622 #	0.09 \pm 0.04	0.05 \pm 0.03	0.002 #	0.57 \pm 1.47	0.05 \pm 0.03	0.002 #
10,11-DiHDP/10,11-EDP	0.05 \pm 0.04	0.05 \pm 0.03	0.859	0.03 \pm 0.01	0.01 \pm 0.00	0.002 #	0.05 \pm 0.03	0.01 \pm 0.00	0.002 #
13,14-DiHDP/13,14-EDP	0.05 \pm 0.03	0.05 \pm 0.03	0.855	0.02 \pm 0.01	0.01 \pm 0.00	0.01 #	0.05 \pm 0.03	0.01 \pm 0.00	0.002 #
16,17-DiHDP/16,17-EDP	0.06 \pm 0.04	0.06 \pm 0.03	0.755	0.03 \pm 0.01	0.02 \pm 0.01	0.008	0.06 \pm 0.03	0.02 \pm 0.01	0.003 #
19,20-DiHDP/19,20-EDP	0.27 \pm 0.22	0.29 \pm 0.19	0.806 #	0.12 \pm 0.05	0.06 \pm 0.03	0.002 #	0.29 \pm 0.20	0.06 \pm 0.03	0.002 #
5,6-DiHETE/5,6-EEQ	483.30 \pm 348.21	599.01 \pm 431.60	0.49	274.72 \pm 163.71	121.89 \pm 63.09	0.001	599.01 \pm 431.60	121.89 \pm 63.09	0.002 #
8,9-DiHETE/8,9-EEQ	0.10 \pm 0.07	0.13 \pm 0.09	0.372	0.05 \pm 0.03	0.02 \pm 0.01	0.002 #	0.13 \pm 0.09	0.02 \pm 0.01	0.002 #
11,12-DiHETE/11,12-EEQ	0.11 \pm 0.15	0.06 \pm 0.03	0.806 #	0.06 \pm 0.11	0.01 \pm 0.00	0.002 #	0.06 \pm 0.03	0.01 \pm 0.00	0.002 #
14,15-DiHETE/14,15-EEQ	0.10 \pm 0.09	0.08 \pm 0.03	0.854 #	0.04 \pm 0.05	0.02 \pm 0.00	0.003 #	0.08 \pm 0.03	0.02 \pm 0.00	0.002 #
17,18-DiHETE/17,18-EEQ	0.23 \pm 0.16	0.22 \pm 0.16	0.667 #	0.14 \pm 0.15	0.04 \pm 0.01	0.002 #	0.22 \pm 0.16	0.04 \pm 0.01	0.002 #
9,10-DiHOME/9,10-EpOME	0.18 \pm 0.09	0.17 \pm 0.11	0.58 #	0.13 \pm 0.09	0.06 \pm 0.02	0.01 #	0.17 \pm 0.11	0.06 \pm 0.02	0.003 #
12,13-DiHOME/12,13-EpOME	0.23 \pm 0.10	0.21 \pm 0.10	0.356 #	0.16 \pm 0.11	0.09 \pm 0.03	0.008 #	0.21 \pm 0.10	0.08 \pm 0.03	0.003 #
Ratio(5,6-DHET+8,9-DHET+11,12-DHET+14,15-DHET)/(5,6-EET+8,9-EET +11,12 EET +14,15-EET)	0.11 \pm 0.09	0.12 \pm 0.09	1 #	0.05 \pm 0.03	0.03 \pm 0.01	0.002 #	0.12 \pm 0.09	0.03 \pm 0.01	0.002 #
Ratio(7,8-DiHDP+10,11-DiHDP+13,14-DiHDP+16,17-DiHDP+19,20-DiHDP)/(7,8-EDP+10,11-EDP+13,14-EDP+16,17-EDP +19,20-EDP)	0.14 \pm 0.11	0.15 \pm 0.11	0.902 #	0.07 \pm 0.02	0.03 \pm 0.01	0.002 #	0.15 \pm 0.11	0.03 \pm 0.01	0.002 #
Ratio(5,6-DiHETE+8,9-DiHETE+11,12-DiHETE +14,15-DiHETE+17,18-DiHETE)/(5,6-EEQ+8,9-EEQ+11,12-EEQ+14,15-EEQ+17,18-EEQ)	0.65 \pm 0.44	0.63 \pm 0.41	0.909	0.34 \pm 0.20	0.13 \pm 0.07	0.002 #	0.63 \pm 0.41	0.13 \pm 0.07	0.002 #
Ratio (9,10-DiHOME+12,13-DiHOME)/(9,10-EpOME+12,13-EpOME)	0.20 \pm 0.08	0.19 \pm 0.10	0.58 #	0.14 \pm 0.10	0.07 \pm 0.03	0.008 #	0.19 \pm 0.10	0.07 \pm 0.03	0.003 #

Notes: Mean \pm SD.

metabolites, we discovered that linolenic acid (LA), arachidonic acid (AA), docosahexaenoic acid (DHA), and eicosapentaenoic acid (EPA)-derived CYP450 metabolites exhibited significant negative AV differences after HD relative to those before HD (Table-1), but not LOX/CYP $\omega/(\omega-1)$ -hydroxylase metabolites (Results were not presented). These differences were mainly accounted for by the pronounced elevation of CYP450 metabolites in peripheral veins after HD (Table-2). Considering that CYP450 metabolites are mainly hydrolyzed *in vivo* by soluble epoxide hydrolase (sEH) to diols with low bioactivity or harmful biological effects (Figure 1). We expressed the activity of sEH using the ratio of diol/epoxy metabolite. We observed a positive AV difference in all diols/epoxy metabolites ratio after HD, largely due to a considerable decrease in their ratio in veins after HD (Table-3). This would interpret the accumulation and release of individual CYP450 metabolites in peripheral tissues after HD as described above.

Conclusion: Our data demonstrate that most epoxide metabolites derived from PU-FAs accumulate in plasma after HD, probably due to stimulation by dialysis blood perfusion, which may have deleterious effects on the circulation.

P100

Hemodialysis and biotransformation of erythrocyte epoxy fatty acids in peripheral tissue

T. Liu

ECRC-Kooperation von MDC und Charité, Experimental and Clinical Research Center, Berlin

Objective: Cardiovascular disease is the leading cause of mortality in patients with renal failure. Red blood cells (RBCs) are potential reservoirs for epoxy fatty acids (oxylipins) that regulate cardiovascular function. Hemoglobin exhibits pseudo-lipoxygenase activity *in vitro*. We previously assessed the impact of single hemodialysis (HD) treatment on RBC epoxy fatty acids status in circulating arterial blood and found that eicosanoids in oxygenated RBCs could be particularly vulnerable in chronic kidney disease and hemodialysis. The purpose of the present study was to evaluate the differences of RBC epoxy fatty acids profiles in arterial and venous blood *in vivo* (AV differences) from patients treated by HD treatment.

Method: We collected arterial and venous blood samples in upper limbs from 12 end-stage renal disease (ESRD) patients (age 72 ± 12 years) before and after HD treatment. We measured oxylipins derived from cytochrome P450 (CYP) monooxygenase and lipoxygenase (LOX)/CYP $\omega/(\omega-1)$ -hydroxylase pathways in RBCs by LC-MS/MS tandem mass spectrometry.

Results: Our data demonstrate arteriovenous differences in LOX pathway metabolites in RBCs after dialysis, including numerous hydroxyeicosatetraenoic acids (HETEs), hydroxydocosahexaenoic acids (HDHAs) and hydroxyeicosapentaenoic acids (HEPEs). We detected more pronounced changes in free metabolites in RBCs after HD, as compared with the total RBC compartment. Hemodialysis treatment did not affect the majority of CYP and CYP $\omega/(\omega-1)$ -hydroxylase products in RBCs.

Conclusion: Our data indicate that erythro-metabolites of the LOX pathway are influenced by renal-replacement therapies, which could have deleterious effects in the circulation.

P101

Sicherheit und Leistung des Clearum™ High Flux Hämodialysator

T. Krüger; F. Dellanna; W. Kleophas; C. McClure¹; S. Manfredini²

MVZ DaVita Rhein-Ruhr GmbH, Düsseldorf; ¹ Minneapolis/USA;

² Medtronic Bellco S. r. l., Mirandola/I

Hintergrund: Clearum™ ist ein neuer dampfsterilisierter high flux Dialysator für die Behandlung von Patienten mit terminaler Niereninsuffizienz an Hämodialyse (HD) oder Hämodiafiltration (HDF) online. Diese klinische Studie untersucht die Sicherheit und Leistung des Clearum HS Hämodialysator auf die Elimination von kleinen wie mittelgroßen urämischen Toxinen.

Methode: Eine prospektive, interventionelle, nicht-randomisierte Studie mit zwanzig (20) Patienten an HD. Der Clearum HS Dialysator wurde mit Dialysatoren der Fresenius FX-Serie zu Beginn (baseline Kontrolle) verglichen. Die Dauer der Studie umfasste 2 Wochen mit FX Dialysatoren (Kontrolle), anschließend 6 Wochen mit dem Clearum HS Dialysator bei 3x wöchentlicher high flux Hämodialyse. Der primäre Endpunkt war die mittlere Harnstoffreduktion durch Dialyse; sekundäre Endpunkte waren berichtete Nebenwirkungen, dialysebedingte β -2-Mikroglobulin Reduktion und Albuminreduktion,

Veränderung von Interleukin-6 (IL-6) und C-reaktives Protein (CRP) sowie von Koagulationsparametern.

Ergebnisse: 19 der 20 Teilnehmer beendeten die Studie. Das primäre Ziel der mittleren Harnstoffreduktion von $> 65\%$ wurde erreicht. Es gab diesbezüglich keinen signifikanten Unterschied zwischen den Clearum HS und Fresenius FX-Dialysator Serien ($p = 0.97$). Die Zahl der berichteten Nebenwirkungen war in beiden Phasen gleich (Clearum: 20 Ereignisse, FX: 21 Ereignisse). Es wurden keine auf die Dialysatoren bezogene Nebenwirkungen berichtet. Die Reduktion von β -2-Mikroglobulin war mit dem Clearum HS Dialysator statistisch größer als mit der FX-Dialysator Serie (67.0% versus 54.1% ; $p < 0.0001$). Prädialytische IL-6 und CRP Konzentrationen, postdialytische Streifigkeit des Dialysators und Thrombin-anti-Thrombin Werte waren unter den Clearum HS und FX-Serien vergleichbar. Albumin Serumwerte blieben über den Verlauf der gesamten 6-wöchigen Studie mit dem Clearum HS Dialysator stabil ohne nennenswerte Unterschiede verglichen mit der Fresenius FX-Dialysator Serie. **Zusammenfassung:** Die Clearum HS Dialysatoren zeigten eine ausreichende Effizienz und Sicherheit ohne berichtete Dialysator-assoziierte Nebenwirkungen.

P102

The blood to extracellular volume relationship is stable and in the physiologic range in chronic haemodialysis patients

S. Kron; D. Schneditz¹; J. Kron²
Medizinische Klinik mit Schwerpunkt Nephrologie, Campus Charité Mitte, Charité – Universitätsmedizin

Berlin, Berlin; ¹Institut für Physiologie, Medizinische Universität Graz, Graz/A; ²KfH Nierenzentrum Berlin-Köpenick, Berlin

Objective: Blood volume (BV) is approximately one third of the extracellular volume (ECV) under physiologic conditions [Guyton]. In haemodialysis patients without renal function, extracellular volume is expanded because fluid is accumulated in the interdialytic period. This volume excess has to be removed during dialysis by ultrafiltration of blood. The question therefore arises, a) how is this volume excess distributed between intra- and extravascular compartments in dialysis patients, and b) how is this distribution affected by ultrafiltration?

Method: Blood and extracellular volumes were measured in 79 stable chronic haemodialysis patients with moderate volume overload (1.85 ± 1.22 L). Immediately before treatment, ECV and volume overload were evaluated by bioimpedance spectroscopy using the Body Composition Monitor (FMC). ECV at the end of treatment was calculated by subtracting the intra-dialytic weight loss from pre-dialysis ECV. The actual BV at the beginning of dialysis was determined by indicator dilution, using an online infusate bolus of 240 mL which was administered immediately after the beginning of the dialysis session and subsequent calculation using the data of the relative blood volume monitor integrated in the HDF machine 5008 (FMC). BV at the end of dialysis session was calculated from the measurement of BV at the beginning and the relative BV at the end of dialysis.

Results: The ratio of BV (5.76 ± 1.54 L) to ECV (17.91 ± 3.90 L) was 0.321 ± 0.039 at dialysis start, and 0.319 ± 0.040 at dialysis end (BV 5.20 ± 1.41 L, ECV 16.22 ± 3.57 L). The mean difference between pre- and post-dialysis was -0.002 ± 0.018 . There were strong correlations ($p < 0.001$) between BV and ECV both at the beginning ($r = 0.88$) and at the end ($r = 0.88$) of dialysis.

Conclusion: In stable haemodialysis patients with moderate volume overload, the ratio between blood volume and extracellular volume is a) close to $1/3$ assumed under physiologic conditions, and b) this ratio remains unchanged in spite of rapid volume removal by ultrafiltration. Despite the lack of kidney function, the mechanisms to adequately distribute volume excess between intra- and extravascular seem to be maintained. This is the first time that these relationships are reported in dialysis patients.

P103

Das „Trockengewicht“: The never ending story

J. Kron; T. Leimbach; K. Bielik; C. Engler; S. Kron¹
KfH Nierenzentrum Berlin-Köpenick, Berlin; ¹Medizinische Klinik mit Schwerpunkt Nephrologie, Campus Charité Mitte, Charité – Universitätsmedizin Berlin, Berlin

Hintergrund: Das optimale Dialyse-Endgewicht soll einerseits garantieren, dass es während der Dialyse zu keinen volumenbedingten Komplikationen kommt und andererseits am Ende der Dialyse keine volumenbedingte Belastung des kardio-vaskulären Systems besteht. Die Einschätzung

des „Trockengewichtes“ erfolgt in der Regel klinisch. In dieser Arbeit wurde untersucht, welchen Beitrag die Bioimpedanz-Analyse (BIA) bei der Festsetzung des Dialyse-Endgewichtes liefern kann.

Methode: Bei 79 Patienten wurde mittels BIA (Body Composition Monitor, FMC) der Volumenüberschuss (VO) vor der Dialyse bestimmt und mit dem Gewicht über dem Trockengewicht verglichen. Es wurde dabei das aktuelle Trockengewicht der klinischen Routine berücksichtigt. Am Beginn der Dialysebehandlung wurde das absolute Blutvolumen (BV) mittels Indikator-Dilution bestimmt. Nach Infusion eines Bolus von 240 ml Dialysat als Postdilution über die Notfalltaste des Gerätes 5008 (FMC) und dem nachfolgenden Anstieg des relativen Blutvolumens (RBV) wurde das absolute BV und das spezifische BV (ml/kg) berechnet.

Ergebnisse: Vor Dialyse wurde ein VO von $1,85 \pm 1,22$ L gemessen. Das Gewicht lag um $1,72 \pm 0,90$ kg über dem Trockengewicht. Median waren mit $1,7$ L bzw. kg beide Parameter sogar identisch. Der VO mittels BIA zeigt jedoch eine erheblich breitere Streuung als die klinische Einschätzung ($-0,7$ – $4,6$ L vs. $0,2$ – $3,8$ kg). Trotz der nur geringen Unterschiede bestand zwischen beiden Parametern nur eine schwache ($r = 0,258$), aber noch signifikante ($p = 0,022$) Korrelation. Zwischen dem VO und dem spezifischen BV bestand eine signifikante ($p < 0,0001$) Korrelation ($r = 0,440$), nicht jedoch zwischen dem Gewicht über dem klinisch eingeschätzten Trockengewicht und dem spezifischen BV ($r = 0,115$).

Zusammenfassung: Die BIA korreliert besser mit dem Blutvolumen

als das rein klinisch festgesetzte Trockengewicht. Sie sollte deshalb häufiger routinemäßig zur Anwendung gelangen. Die klinische Beurteilung des Volumenstatus erwies sich in dieser Untersuchung als unzureichend. Der permanenten Anpassung des Trockengewichtes wird in der klinischen Routine offensichtlich nicht immer die notwendige Beachtung geschenkt. Hier bedarf es dringender Verbesserungen. Es bleibt zu hoffen, dass die Ergebnisse nur rein zentrums-spezifisch sind und keine Verallgemeinerung zulassen.

P104

Kann aus den Bioimpedanzanalyse-Daten auf das Blutvolumen geschlossen werden?

S. Kron; D. Schneditz¹; T. Leimbach²; K. Biolik²; J. Kron²

Medizinische Klinik mit Schwerpunkt Nephrologie, Campus Charité Mitte, Charité – Universitätsmedizin Berlin, Berlin; ¹Institut für Physiologie, Medizinische Universität Graz, Graz/A; ²KfH Nierenzentrum Berlin-Köpenick, Berlin

Hintergrund: Das Verhältnis von Blutvolumen (BV) und Extrazellulärvolumen (EZV) ist unter physiologischen Bedingungen 1 zu 3 [Guyton] und wird in der Mikrozirkulation durch die Starling-Kräfte und die vaskuläre Compliance gesteuert. Da die Bioimpedanz-Analyse ein etabliertes Verfahren ist, das in vielen Dialyseeinrichtungen routinemäßig eingesetzt wird, die Blutvolumenmessung hingegen einen beträchtlichen Aufwand erfordert, sollte in einem Modell das BV aus dem EZV errechnet und mit den gemessenen Werten verglichen werden.

Methode: Bei 79 chronischen Hämodialysepatienten wurde

unmittelbar vor Dialyse das EZV mit der Bioimpedanz-Spektroskopie (Body Composition Monitor, FMC) gemessen. Das absolute Blutvolumen (BV) wurde mittels Indikator-Dilution bestimmt. Nach Infusion eines Bolus von 240 ml Dialysat als Postdilution über die Notfalltaste des Gerätes 5008 (FMC) und dem nachfolgenden Anstieg des relativen Blutvolumens (RBV) wurde das absolute BV und das spezifische BV (ml/kg) berechnet. Für das Modell wurde zunächst in einem ersten Schritt die Ratio aus tatsächlich gemessenem BV und EZV berechnet. Anschließend wurde der Mittelwert der Ratio ($0,32$) mit dem EZV multipliziert und somit ein fiktives BV berechnet. Dieses wurde mit dem tatsächlich gemessenem BV verglichen.

Ergebnisse: Das Verhältnis von gemessenem BV ($5,76 \pm 1,54$ L) zum EZV ($17,91 \pm 3,90$ L) betrug im Mittel $0,321 \pm 0,039$, median $0,317$ mit einer Range von $0,249$ bis $0,396$.

Aus der Multiplikation des EZV mit $0,32$ würde sich ein berechnetes BV von $5,73 \pm 1,25$ L ergeben. In der Gesamtbetrachtung sind die gemessenen und die kalkulierten Blutvolumina fast vollständig identisch (spezifisches BV gemessen $77,3 \pm 9,6$ ml/kg, berechnet $77,6 \pm 8,5$ ml/kg). Es bestand jedoch eine erhebliche Streuung. Die absolute Abweichung betrug median $5,4$ ml/kg schwankt jedoch zwischen $-31,2$ und $18,3$ ml/kg.

Zusammenfassung: Bei den meisten Patienten ist eine relativ gute Abschätzung des BV aus dem EZV möglich. Insofern hat die BIA einen hohen Stellenwert beim Volumenmanagement und sollte deshalb routinemäßige zur Anwendung kommen. Bei Patienten, bei denen die Ratio von BV zu EZV

stärker vom physiologischen Verhältnis abweicht (z. B. bei Herzinsuffizienz, Hypalbuminämie, Entzündung usw.), würde eine Orientierung an den BIA-Daten hingegen zu einer Fehleinschätzung für die zu planende Ultrafiltration führen. Diese Ergebnisse bestätigen die klinische Erfahrung.

P105

Das vaskuläre Refilling wird vom bestehenden Verhältnis von Blutvolumen zu Extrazellulärvolumen beeinflusst

J. Kron; D. Schmeditz¹; T. Leimbach; K. Biolik; S. Kron²
KfH Nierenzentrum Berlin-Köpenick, Berlin; ¹Institut für Physiologie, Medizinische Universität Graz, Graz/A; ²Medizinische Klinik mit Schwerpunkt Nephrologie, Campus Charité Mitte, Charité – Universitätsmedizin Berlin, Berlin

Hintergrund: Das Verhältnis von Blutvolumen (BV) und Extrazellulärvolumen (EZV) ist unter physiologischen Bedingungen 1 zu 3 [Guyton]. Dies scheint auch für stabile chronische Hämodialysepatienten zu gelten. Ziel der Arbeit war es zu untersuchen, wie sich Abweichungen vom physiologischen Verhältnis der BV-EZV-Ratio auf das vaskuläre Refilling auswirken.

Methode: Bei 79 chronischen Hämodialysepatienten wurde unmittelbar vor Dialyse das EZV mit der Bioimpedanz-Spektroskopie (Body Composition Monitor, FMC) gemessen. Das absolute BV wurde mittels Indikator-Dilution bestimmt. Nach Infusion eines Bolus von 240 ml Dialysat als Postdilution über die Notfalltaste des Gerätes 5008 (FMC) und dem nachfolgenden Anstieg des relativen Blutvolumens (RBV) wurde

das absolute BV berechnet. Das Refilling-Volumen wurde aus dem Ultrafiltrationsvolumen (UFV) und der Differenz des absoluten BV vor und nach der Dialyse berechnet: Refilling-Volumen = UFV – (absolutes BV_{Beginn} – absolutes BV_{Ende}). Die Refilling-Fraktion ist das Verhältnis von Refilling-Volumen zu UFV: Refilling-Fraktion = Refilling-Volumen/UFV

Ergebnisse: Das Verhältnis von BV (5,76 ± 1,54 L) zum EZV (17,91 ± 3,90 L) betrug vor Dialyse im Mittel 0,321 ± 0,039, median 0,317 mit einer Range von 0,249 bis 0,396. Die BV-EZV-Ratio blieb auch nach der Dialyse mit 0,319 ± 0,040 weitgehend konstant. Die intraindividuelle Differenz (vor-nach) war mit -0,002 ± 0,018 außerordentlich gering. Die Refilling-Fraktion betrug 0,749 ± 0,094, daher $\frac{3}{4}$ des UF-Volumens. Zwischen der BV-EZV-Ratio und der Refilling-Fraktion bestand eine signifikante negative Korrelation ($r = -0.412$; $p < 0.001$). Die Refilling-Fraktionen der Patienten mit einer BV-EZV-Ratio über und unter 0,32 unterschieden sich signifikant ($< 0,32$: 0,783 ± 0,100; $> 0,32$: 0,715 ± 0,077; jeweils $p < 0,01$). Die Höhe der Differenz der BV-EZV-Ratio vor und nach Dialyse korreliert sowohl mit dem Refilling-Volumen ($r = 0.617$) als auch der Refilling-Fraktion ($r = 0.592$; jeweils $p < 0.001$).

Zusammenfassung: Das Verhältnis von BV zu EZV bleibt während der Dialyse weitgehend konstant. Es ist somit ein wichtiger Einflussfaktor auf das vaskuläre Refilling: Je höher die Ratio, desto geringer das Refilling, und umgekehrt. Wenn auch die individuellen Differenzen der Ratio vor und nach Dialyse sehr gering sind, wird das

Verhältnis durch das Refilling tendenziell in Richtung des physiologischen Gleichgewichts reguliert.

P106

Safety and efficacy of the Genius dialysis system: A retrospective data analysis

T. Burkhardt; J. Grenz; D. Göth; F. Kälble; C. Speer; L. Benning; C. Sommerer; M. Zeier; C. Morath; C. Nussbag
Medizinische Klinik I, Sektion Nephrologie, Medizinische Fakultät, Ruprecht-Karls-Universität Heidelberg, Heidelberg

Objective: The incidence of acute kidney injury (AKI) is steadily rising and is associated with high morbidity and mortality. Cost-intensive continuous kidney replacement therapies (KRT) – based on the principle of hemo(dia)filtration – represent the predominant procedure on German intensive care units (ICU). Hybrid techniques such as the Genius system are intended to combine the benefits of classical hemodialysis and continuous KRT at lower costs. The system can be used as sustained low efficiency dialysis (SLED) or intermittent hemodialysis (IHD). However, to date, there are limited data on the safety and efficacy of Genius dialysis procedures in critically ill patients.

Method: A retrospective data analysis of all Genius dialysis treatments at a German University Hospital in 2009. A total of 2658 procedures in 434 critically ill patients were evaluated based on Genius treatment protocols, medical reports, and laboratory values.

Results: The primary causes for ICU admission were abdominal disorders, cardiovascular problems, sepsis and pulmonary complications

with 41.2 %, 31.6 %, 11.8 % and 5.5 %, respectively. Hepatorenal syndrome occurred in 9.2 % of all cases. The median age was 64.8 years and 34.3 % of patients (n = 149) were female. 365 patients (84.1 %) suffered from AKI and 69 patients (15.9 %) had preexisting, dialysis-dependent kidney failure. Approximately half of all patients (n = 224, 51.6 %) were mechanically ventilated and 68.2 % required vasopressors. Patients with AKI received on average nine treatments over 10.5 hours. The median number of KRT-free days at day 28 after initiation of KRT was 14 days. 317 treatments were performed as IHD and 2341 treatments as SLED. The mean net ultrafiltration was -1625 mL and the mean effective blood flow was 119 mL/min. Central venous catheters were the main modality of vascular access (94,8 %). Heparin was given continuously in 70.1 % and as a bolus in 13.5 % of treatments, 0,2 % received citrate and 11,8 % had no anticoagulation. The overall rate of reported complications related to the Genius dialysis system was 29.3 % - none of them considered as severe. Clotting occurred in 21.9 % (n = 581), catheter dysfunction in 9.2 % (n = 244) and technical defect in 0.2 % (n = 6) of all procedures. Hypothermia, hemolysis or air embolism were not observed.

Conclusion: The Genius dialysis system offers a safe and effective alternative for the treatment of critically ill patients with acute or chronic kidney failure.

P107

Low-density lipoprotein apheresis is associated with removal of SARS-CoV-2 antibodies

S. Bertram; T. Pfab¹; C. Albert¹; S. Schmidt²; J. Passfall³; M. Haesner³;

M. Seidel; B. Hölzer; F. S. Seibert; A. Doevelaar; B. Rohn; P. Zgoura; N. Babel; T. H. Westhoff
Centrum für Translationale Medizin, Medizinische Klinik I, Marien Hospital Herne, Ruhr-Universität Bochum, Herne; ¹ Diaverum MVZ Am Neuen Garten Potsdam, Potsdam; ² Dialyse Praxis Fürstenwalde und Königs Wusterhausen, Fürstenwalde; ³ Nierenzentrum Charlottenburg, Berlin

Objective: Low-density lipoprotein apheresis is not specific to lipoproteins but removes immunoglobulins as well. It remains elusive, whether protective SARS-CoV-2 antibodies after vaccination from COVID-19 are eliminated as well.

Method: A cross-sectional case-control study on 55 patients undergoing weekly lipoprotein apheresis and 21 patients with comparable comorbidities and epidemiology not undergoing apheresis. SARS-CoV-2 IgG was assessed in all patients prior to apheresis and in 38 patients both before and after apheresis.

Results: SARS-CoV-2 IgG concentrations before a session of lipoprotein apheresis were comparable to control patients not undergoing apheresis (1727 IU/mL, IQR 365-2500) vs. 1652 IU/mL, (IQR 408.8-2500), p = 0.78). SARS-CoV-2 IgG concentrations were reduced by lipoprotein apheresis from 1656 IU/mL (IQR 540.5-2500) prior to 1305 IU/mL (IQR 449-2500) afterwards (p < 0.0001).

Conclusion: Lipoprotein apheresis removes SARS-CoV-2 IgG. The average elimination rate was 21.2 %. In the present population of patients undergoing apheresis once weekly, however, the elimination did not lead to inferior concentrations

compared to patients not undergoing lipoprotein apheresis.

Nierenphysiologie

P108

Modulation of the NO-sGC-cGMP pathway for dilating descending vasa recta after hypoxia/re-oxygenation

M. Xu; F. B. Lichtenberger; C. Erdogan; P. B. Persson; A. Patzak; P. H. Khedkar
Institut für Translationale Physiologie, Campus Charité Mitte, Charité – Universitätsmedizin Berlin, Berlin

Objective: Impairment of renal medullary blood flow holds a key position in the development of acute kidney injury (AKI). Hypoxia is involved in the pathogenesis of renal damage and can influence the function of renal microvessels. Dilating these vessels improves renal medullary flow, and this may be renoprotective. Here, we characterize the NO-sGC-cGMP signaling pathway in descending vasa recta (DVR), and test potential vasodilators after hypoxia/re-oxygenation.

Method: Rat DVR were isolated and perfused under isobaric conditions. A hypoxia chamber was used to provide the hypoxia (0.1 % oxygen) environment.

Results: Sildenafil, a PDE5 inhibitor (10⁻⁶ mol/l), induced vasodilatation in angiotensin II (Ang II, 10⁻⁶ mol/l)-pre-constricted vessels. In L-NAME (10⁻⁴ mol/l) pre-treated and Ang II (10⁻⁶ mol/l) pre-constricted vessels, BAY 60-2770, an sGC activator (10⁻⁶ mol/l), dilated vessels NO-independently. The application of Ang II (10⁻¹² to 10⁻⁶ mol/l) showed a stronger constriction effect in vessels after hypoxia/re-oxygenation. Sildenafil failed to dilate the

vessels after hypoxia/re-oxygenation. SNP, an NO donor (10^{-3} mol/l), and BAY 60-2770 both induced dilatation in DVR, while BAY 60-2770 dilated DVR faster than SNP under these conditions.

Conclusion: The results emphasize the role of the NO-sGC-cGMP signaling pathway in regulating the tone of renal medullary micro-vessels. The sGC activator BAY 60-2770 seems to be the best choice to restore renal blood flow after hypoxia/re-oxygenation compared to SNP as well as sildenafil.

P109

Einfluss von Aldosteron auf die Entwicklung einer Diuretika-Resistenz bei Mäusen

D. Essigke; M. Z. Kalo; B. N. Bohnert; F. Artunc

Sektion Nieren- und Hochdruckkrankheiten, Universitätsklinikum, Medizinische Klinik IV, Eberhard Karls Universität Tübingen, Tübingen

Hintergrund: Diuretika sind Medikamente zur Korrektur einer renalen Wasser- und Natriumretention. Gegenregulatorisch kann jedoch eine Diuretika-Resistenz induziert werden, welche die diuretische Wirkung abschwächt. Über die Entstehung der Diuretika-Resistenz ist wenig bekannt. Diese Studie untersucht, ob Aldosteron eine Rolle bei der Entstehung der Diuretika-Resistenz spielt.

Methode: Die Fragestellung wurde an Aldosteron-Synthase defizienten (AS-ko n = 6-19) und Wildtyp-Mäusen (wt n = 6-13) untersucht, die mit den Diuretika Furosemid (Natrium-Kalium-2-Chlorid-Transporter (NKCC2)-Blockade), HCT (Natrium-Chlorid-Cotransporter (NCC)-Blockade)

und Triamteren (Blocker des epithelialen Natriumkanals (ENaC)) entweder mit einer einmaligen Dosis oder kontinuierlich über 4 Tage behandelt wurden.

Ergebnisse: Die akute Gabe aller Diuretika führte bei den Tieren unabhängig vom Genotyp zu einer signifikanten Gewichtsabnahme über 6 h. Alle Diuretika stimulierten bei beiden Genotypen die Natriurese, die höchsten Werte erreichte hierbei Furosemid. Während der U-Na+/K+-Quotient bei Furosemid und HCT um einen zwischen den Genotypen vergleichbaren Faktor anstieg (HCT wt $2,5 \pm 0,4$ vs AS-ko $2,4 \pm 0,2$; Furosemid wt $4,7 \pm 0,7$ vs. AS-ko $4,2 \pm 0,6$), war dieser nach der Triamteren für die wt-Mäuse höher als für die AS-ko Mäuse ($8,3 \pm 1,3$ vs $3,2 \pm 0,3$). Bei der Diuretika-Gabe über 4 Tage zeigten beide Gruppen unter HCT als Korrelat einer Diuretika-Resistenz ein konstantes Körpergewicht. Unter Furosemid zeigten AS-ko Mäuse einen signifikant größeren Gewichtsverlust an Tag 4 als die wt-Tiere (wt $-4,6 \pm 1$ % vs AS-ko -17 ± 2 %), Natriurese und Kaliurese waren vergleichbar. Unter Triamteren kam es bei beiden Genotypen zu einer Gewichtsabnahme (wt -15 ± 3 % AS-ko vs 20 ± 2 % an Tag 3), die Gabe musste bei allen AS-ko Mäusen an Tag 3 beendet werden, da die Versuchsabbruchkriterien (Gewichtsverlust > 20 %) erreicht wurden. Diese entwickelten eine metabolische Azidose (pH $6,9 \pm 0,03$, stdHCO₃ $6,8 \pm 1$ mmol/l) und Hyperkaliämie ($9,63 \pm 0,75$ mmol/l). Bei wt-Mäusen stieg das Plasma-Aldosteron unter Furosemid und HCT nur tendenziell an, Triamteren induzierte einen signifikanten Anstieg auf das 6-fache der Kontrollwerte.

Zusammenfassung: Aldosteron scheint für die Ausbildung einer Diuretika-Resistenz auf eine NCC-Blockade nicht essenziell zu sein. Hingegen ist es bei der Entwicklung einer Diuretika-Resistenz bei NKCC2-Blockade beteiligt und spielt unter ENaC-Blockade eine entscheidende Rolle.

P110

Furosemide rescues hypercalciuria in Familial Hypomagnesaemia with Hypercalciuria and Nephrocalcinosis model

N. Kriuchkova; T. Breiderhoff¹; D. Müller²; D. E. Yilmaz³; H. Demirci³; D. Günzel¹; N. Himmerkus⁴; M. Bleich⁴; P. B. Persson; K. Mutig
Institut für Translational Physiologie, Campus Charité Mitte, Charité – Universitätsmedizin Berlin, Berlin;

¹ Institut für Klinische Physiologie, Campus Benjamin Franklin, Charité – Universitätsmedizin Berlin, Berlin;

² Klinik für Pädiatrie mit Schwerpunkt Nephrologie, Campus Virchow-Klinikum, Charité – Universitätsmedizin Berlin, Berlin; ³ Institut für Vegetative Anatomie, Campus Charité Mitte, Charité – Universitätsmedizin Berlin, Berlin; ⁴ Physiologisches Institut, Christian-Albrechts-Universität Kiel, Kiel

Objective: Perturbed calcium homeostasis limits life expectancy of patients with Familial Hypomagnesaemia with Hypercalciuria and Nephrocalcinosis (FHHNC). This rare disease occurs by loss-of-function mutations in the CLDN16 gene, causing impaired paracellular reabsorption of divalent cations along the cortical thick ascending limb. Only partial compensation takes place in the distal convoluted tubule (DCT) and connecting tubule (CNT), where the

transient receptor potential channel V5 (TRPV5) mediates transcellular Ca^{2+} reabsorption.

Method: The loop diuretic furosemide induces compensatory activation of these segments. Thus we test, whether furosemide alleviates hypercalciuria in *Cldn16*-deficient mice (*Cldn16*^{-/-}).

Results: Compared to WT, *Cldn16*^{-/-} mice showed higher fractional Ca^{2+} excretion (FE Ca^{2+}) and compensatory stimulation of Ca^{2+} transport protein at baseline. Furosemide significantly reduced FE Ca^{2+} in *Cldn16*^{-/-} mice. Analysis of proximal and distal Ca^{2+} transport systems revealed increased TRPV5 expression and abundance in the late DCT, CNT, and in principal cells of cortical and outer medullary collecting ducts (CD), explaining the therapeutic effect of furosemide.

Conclusion: In conclusion, furosemide restored hypercalciuria to nearly normal values in this functional model for FHHNC, which may be explained by functional plasticity of the distal nephron and CD enabling increased transcellular Ca^{2+} transport via TRPV5.

P111

The transcriptional regulator AP-2 α maintains epithelial differentiation and tubular diameter of renal collecting ducts in adult mice

J. Leiz¹; S. Cao¹; F. Boivin; C. Hinze¹; K. M. Schmidt-Ott¹

Medizinische Klinik mit Schwerpunkt Nephrologie und Internistische Intensivmedizin, Campus Benjamin Franklin, Charité – Universitätsmedizin Berlin, Berlin; ¹ Klinik für Nieren- und Hochdruckerkrankungen, Zentrum für Innere Medizin, Medizinische Hochschule Hannover, Hannover

Objective: The transcriptional regulator AP-2 α (encoded by *Tfap2a*) is part of the AP-2 transcription factor family. Heterozygous mutations of *TFAP2A* in humans result in branchio-oculo-facial syndrome (BOFS), which is associated with renal anomalies in 35 % of patients. Recent studies have shown that mice with a collecting duct-specific knockout of AP-2 α display a progressive tubular dilation of medullary collecting ducts. Molecular mechanisms leading to these renal anomalies are still unknown.

Method: Mice carrying a collecting duct-specific knockout of AP-2 α (*Hoxb7:Tfap2a*^{fl/fl}) were generated. In addition, inner medullary collecting duct (IMCD3) cells were engineered to harbour a CRISPR/Cas9-induced knock out of AP-2 α . Deregulated genes were identified by bulk and single-nucleus mRNA-sequencing and validated by in situ hybridization.

Results: Histomorphological analyses of our mouse model confirmed a progressive tubular dilation of outer medullary collecting ducts in adult mice. Integrative analysis of single-nucleus and bulk RNA-sequencing for kidneys of 3-months-old *Hoxb7:Tfap2a*^{fl/fl} mice and littermate controls indicated deregulated expression of genes associated with cell adhesion and WNT signaling pathways. Identical pathways were deregulated in AP-2 α -deficient IMCD3 cells when compared to controls. Genes deregulated in *Tfap2a*-deficient collecting ducts included the tight junction component *Cldn8* and the Wnt signaling factor *Wnt9b*. Their decreased mRNA expression was confirmed by in-situ hybridization. Both genes have previously

been implicated in the development of congenital renal anomalies and defects in tubulogenesis.

Conclusion: Taken together our study indicates that *Tfap2a* is maintaining epithelial differentiation and tubular diameter in collecting ducts, providing insights into potential molecular mechanisms causing renal defects observed in BOFS.

P112

High-fat, sucrose and salt-rich diet during rat spermatogenesis lead to the development of chronic kidney disease in the female offspring of the F2 generation

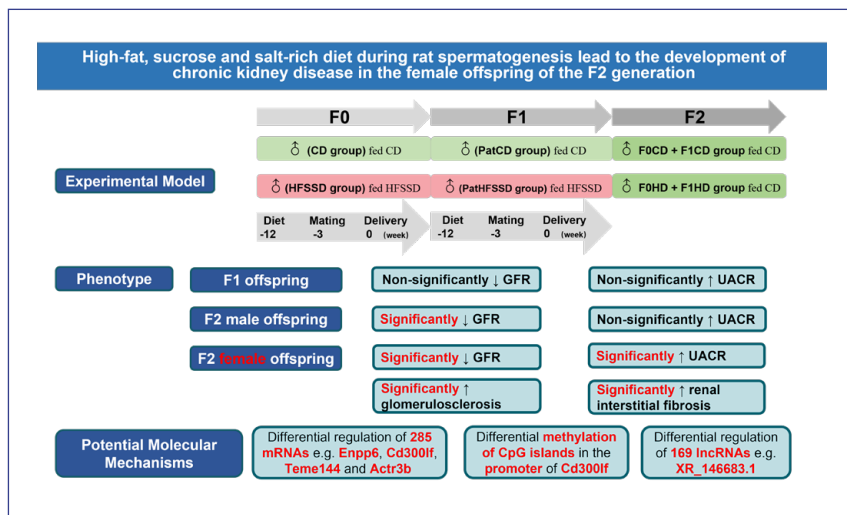
X. Zhang

Freie Universität Berlin, Berlin

Objective: Effects of feeding male rats during spermatogenesis a high-fat, high-sucrose and high-salt diet (HFSSD) over two generations (F0 and F1) on renal outcomes are unknown. In the current study, we analyzed the effect of feeding male rats a high-fat, high-sucrose and high-salt diet (HFSSD) over two generations (F0 and F1) on their offspring's (F2) kidney function.

Method: Male F0 and F1 rats were fed either control diet (F0CD + F1CD) or HFSSD (F0HD + F1HD). The outcomes were glomerular filtration rate and urinary albumin excretion in F1 and F2 offspring. If both outcomes were altered a morphological and molecular assessment was done.

Results: F2 offspring of both sexes had a decreased GFR. However, increased urinary albumin excretion was only observed in female F2 F0HD + F1HD offspring compared with controls. F0HD + F1HD female F2 offspring developed glomerulosclerosis (+31 %; $p < 0.01$)



P112: Abb. 1

and increased renal interstitial fibrosis (+52 %; $p < 0.05$). RNA sequencing followed by qRT-PCR validation showed that four genes (*Enpp6*, *Tmem144*, *Cd300lf*, and *Actr3b*) were differentially regulated in the kidneys of female F2 offspring. lncRNA XR-146683.1 expression decreased in female F0HD + F1HD F2 offspring and its expression was ($r = 0.44$, $p = 0.027$) correlated with the expression of *Tmem144*. Methylation of CpG islands in the promoter region of the *Cd300lf* gene was increased ($p = 0.001$) in female F2 F0HD + F1HD offspring compared to controls. Promoter CpG island methylation rate of *Cd300lf* was inversely correlated with *Cd300lf* mRNA expression in F2 female offspring ($r = -0.483$, $p = 0.012$). *Cd300lf* mRNA expression was inversely correlated with the urinary albumin-to-creatinine ratio in female F2 offspring ($r = -0.588$, $p = 0.005$).

Conclusion: Paternal pre-conceptional unhealthy diet given for two generations predispose female F2 offspring to chronic kidney

disease due to epigenetic alterations of renal gene expression. Particularly, *Cd300lf* gene promoter methylation was inversely associated with *Cd300lf* mRNA expression and *Cd300lf* mRNA expression itself was inversely associated with urinary albumin excretion in F2 female offspring whose fathers and grandfathers got a pre-conceptional unhealthy diet.

P113 Interaktion von Megalin und FcRn während der Endozytose

L. Klie; E. Dahlke; Y. Anan; F. Theilig
Forschung für Nieren- und Volumenregulation, Anatomisches Institut, Christian-Albrechts-Universität zu Kiel, Kiel

Hintergrund: Die Endozytose von gefilterten Proteinen ist eine der Hauptaufgaben des proximalen Tubulus in der Niere. Über den neonatalen Fc-Rezeptor (FcRn) ist bekannt, dass er Albumin transzytiert. Allerdings ist die Ligandenbindung von Albumin an FcRn abhängig von einem sauren pH (pH 6). Es

ist bisher unklar, in welchem Kompartiment der Zelle FcRn seine Liganden bindet. Megalin endozytiert zahlreiche Proteine, darunter Albumin, und ist daher möglicherweise eine Voraussetzung für die Transzytose von Albumin. Aktuell ist nicht bekannt, ob Megalin und FcRn interagieren, um einen korrekten Ablauf der Endozytose zu gewährleisten.

Methode: Wir haben die Interaktion von Megalin/FcRn mittels bimolekularer Fluoreszenz Komplektierung (BiFC) und Co-Immunpräzipitationen untersucht. Um die Dynamik der Interaktionen zu analysieren, haben wir Endozytose-Assays und hochauflösende Fluoreszenzmikroskopie (STED) verwendet. **Ergebnisse:** Unter Verwendung von BiFC- und Co-IP-Analysen, konnten wir eine Interaktion zwischen Megalin und FcRn beobachten. 8 h nach transients Transfektion interagierten beide Proteine bereits im Golgi, später zusätzlich in verschiedenen endosomalen Kompartimenten. Die Interaktion zwischen Megalin/FcRn war spezifisch, da keine Interaktion zwischen FcRn/Amnionless (der „Membrananker“ von Cubilin – ein anderer Albuminrezeptor) detektiert wurde. Unter Verwendung trunkierter Proteine identifizierten wir eine Bindung von FcRn an der extrazellulären Domäne von Megalin. Die Interaktion von Megalin/FcRn wurde durch die Inhibierung der Ligandenbindungsdomäne durch RAP oder durch Ansäuern des pHs (pH 5,5) nicht beeinflusst. Durch die Zugabe von Albumin (Ligand für Megalin und FcRn) oder Lactoglobulin (spezifisch für Megalin) wurde die Co-Lokalisation von Megalin/FcRn in Clathrin-Vesikeln und frühen Endosomen (letztes

nur für Albumin) gesteigert. Keine Veränderung der Interaktion wurde für Recycling-Endosomen und eine Reduktion in späten Endosomen/Lysosomen detektiert.

Zusammenfassung: Megalin und FcRn interagieren spezifisch miteinander und weisen möglicherweise die gleichen Sorting-Signale auf, da beide Proteine gemeinsam transportiert werden. Die Co-Lokalisation von Megalin/FcRn ist in frühen endosomalen Kompartimenten während der Endozytose erhöht, was eine funktionelle Ähnlichkeit impliziert.

P114

Knockout of renal BPGM provokes spontaneous kidney injury

V.A. Kulow; K. Rögner¹; R. Labes¹; P.B. Persson¹; C. Rosenberger; M. Fäßling¹

Medizinische Klinik mit Schwerpunkt Nephrologie, Campus Charité Mitte, Charité – Universitätsmedizin Berlin, Berlin; ¹Institut für Translational Physiologie, Campus Charité Mitte, Charité – Universitätsmedizin Berlin, Berlin

Objective: In erythrocytes, 2,3-bisphosphoglycerate mutase (BPGM) is crucial for the production of 2,3-bisphosphoglycerate (2,3-BPG) which reduce oxygen binding to hemoglobin and improves oxygen delivery to the tissue. We have recently shown that BPGM is expressed in mainly distal convoluted tubules (DCT) and connecting tubules (CNT) of the kidney under physiological conditions and is upregulated in rhabdomyolysis-induced acute kidney injury. While BPGM function is only described in erythrocytes, little is known about its function in other cells and

organs. We, thus, aim to rule out the renal BPGM function by using an inducible knockout model.

Method: We used a doxycycline-inducible tubular specific *Bpgm* knockout mouse-model (Pax8CreB-PGM^{fl/fl}). After 4 d of BPGM knockout, mice were sacrificed and organs were harvested. Quantitative PCR served to measure key factors of kidney injury. Paraffined kidneys served for PAS staining and for immunofluoreszenz (IF) studies against the kidney injury markers KIM-1 and NGAL, the proximal tubule marker Megalin, the proliferation marker Ki-67, Vimentin and the immune cell markers CD-3 (T-cells), Ly-6G (neutrophils) and F4/80 (macrophages).

Results: BPGM-KO mice showed increased levels of kidney injury markers NGAL and KIM-1 already 4 days after knockout induction. Immunofluorescence studies indicated that KIM-1 and NGAL were upregulated exclusively in the proximal part of the nephron. Notably, we have shown in previous studies that BPGM expression is limited to the distal part of the nephron, mainly distal convoluted tubules (DCT) and connecting tubules (CNT). Furthermore, KIM-1 positive proximal tubules showed indications for epithelial to mesenchymal transition (EMT) and are surrounded by F4/80 positive macrophages.

Conclusion: Here we show that BPGM is involved in maintaining the nephron well-being. A deficit in renal BPGM rapidly leads to kidney injury and the dedifferentiation of proximal tubules into mesenchymal cells through EMT. Our findings indicate a novel feedback mechanism in the signaling from distal

to proximal tubules with BPGM expressing cells as signal transmitter.

P115

Cellular Function of renal 2,3-Bisphosphoglycerate Mutase (BPGM)

K. Rögner; V.A. Kulow¹; R. Labes; N. Berndt²; P.B. Persson; C. Rosenberger¹; M. Fäßling

Institut für Translational Physiologie, Campus Charité Mitte, Charité – Universitätsmedizin Berlin, Berlin; ¹Medizinische Klinik mit Schwerpunkt Nephrologie, Campus Charité Mitte, Charité – Universitätsmedizin Berlin, Berlin; ²Institut für Kardiovaskuläre Computer-assistierte Medizin, Charité Universitätsmedizin Berlin, Berlin

Objective: In erythrocytes, 2,3-bisphosphoglycerate mutase (BPGM) promotes the conversion of 1,3-bisphosphoglycerate (1,3-BPG) to 2,3-bisphosphoglycerate (2,3-BPG) in a reaction known as the Rapoport-Luebering shunt in glycolysis. So far, the only acknowledged role of 2,3-BPG is to improve tissue oxygenation by favoring dissociation of oxygen from hemoglobin. However, little is known about the function of BPGM in other cells and organs. We have recently shown that BPGM is expressed in renal tubular cells and is upregulated in acute kidney injury (AKI). What is more, various stress stimuli *in vitro*, such as hypoxic and hyperosmotic stress, alter BPGM expression. Hence, we aim to seek for intracellular functions of renal BPGM and propose that BPGM has a renoprotective function.

Method: Experiments were performed in mouse embryonic fibroblast (MEF) cells that show robust BPGM expression. Cells were

subjected to hypertonic stress and compared to iso-osmolar controls. *Bpgm* knockdown was achieved using short interfering RNA. Samples were analyzed at proteomic and transcriptomic (Next Generation Sequencing: NGS) level. Cell culture supernatants were collected and glucose and lactate were measured using an ABL800 Flex PLUS Radiometer. Experimental approaches and computer modelling served for verification of the results from pathway enrichment analysis. Terminal deoxynucleotidyl transferase dUTP nick end labeling (TUNEL) assay and protein detection of active caspase 3 (CASP3) served for detection of apoptosis. Reactive oxygen species (ROS) were measured with 2',7'-dichlorofluorescein diacetate Assay. qPCR and Western Blotting served for detection of mRNA and protein levels, respectively.

Results: Knockdown of *Bpgm* *in vitro* led to significant changes in various cellular pathways, such as glucose metabolism, ROS and apoptosis. Lack of BPGM resulted in increase of anaerobic glycolysis. In addition, a kinetic model of renal glucose metabolism presenting the glycolytic, gluconeogenic, and polyol pathways verified these observations. Hypertonic stress caused increase of apoptosis and ROS levels, which was significantly more severe in cells with *Bpgm* knockdown.

Conclusion: Taken together, our data indicate that BPGM suppresses glycolysis, enhances antioxidant activity and protects renal cells against certain stress forms. Therefore, we propose that BPGM represents a protective factor promoting ROS resistance and cell survival.

P116 Different murine models of kidney injury exhibit a dysregulated polyamine system in favour of its catabolism

T. Sieckmann; N. Ögel; S. Kelterborn; F. Boivin¹; G. Schley²; M. Fäbbling; M. I. Ashraf³; M. Reichel⁴; E. Vigolo⁵; A. Hartner⁶; F. Knauf⁴; C. Rosenberger⁷; F. Aigner⁸; K. M. Schmidt-Ott⁹; H. Scholz; K. M. Kirschner
Institut für Translational Physiologie, Campus Charité Mitte, Charité – Universitätsmedizin Berlin, Berlin; ¹ Medizinische Klinik mit Schwerpunkt Nephrologie und Internistische Intensivmedizin, Campus Benjamin Franklin, Charité – Universitätsmedizin Berlin, Berlin; ² Medizinische Klinik 4, Nephrologie und Hypertensiologie, Universitätsklinikum, Friedrich-Alexander-Universität Erlangen-Nürnberg, Erlangen; ³ Chirurgischen Klinik, Experimentelle Chirurgie, Campus Virchow-Klinikum, Charité – Universitätsmedizin Berlin, Berlin; ⁴ Medizinische Klinik mit Schwerpunkt Nephrologie und Internistische Intensivmedizin, Campus Charité Mitte, Charité – Universitätsmedizin Berlin, Berlin; ⁵ ECRC-Kooperation von MDC und Charité, Experimental and Clinical Research Center, Berlin; ⁶ Kinder- und Jugendklinik, Pädiatrische Nephrologie, Universitätsklinikum, Friedrich-Alexander-Universität Erlangen-Nürnberg, Erlangen; ⁷ Medizinische Klinik mit Schwerpunkt Nephrologie, Campus Charité Mitte, Charité – Universitätsmedizin Berlin, Berlin; ⁸ Abteilung für Chirurgie, Barmherzige Brüder Krankenhaus Graz, Graz/A; ⁹ Klinik für Nieren- und Hochdruck-erkrankungen, Zentrum für Innere Medizin, Medizinische Hochschule Hannover, Hannover

Objective: The polyamines putrescine, spermidine and spermine are organic polycations that regulate fundamental cell functions including proliferation and differentiation. We hypothesise that different forms of acute and chronic kidney injury lead to similar changes in the expression patterns of the polyamine system.

Method: RT-qPCR and RNAScope were used to analyse expression of genes involved in polyamine homeostasis in different murine models of acute and chronic kidney injury. RNA sequencing data from the NCBI Gene Omnibus database were evaluated for changes the polyamine system in human kidney transplant recipients. We used mouse embryonic kidney explants to screen for stress stimuli regulating the expression changes observed in the in-vivo models. Using reporter assays, siRNA knockdown and RNA stability assays, we elucidated the molecular mechanisms behind the expression changes.

Results: Within all kidney injury models, the expression of catabolic enzymes (*Aoc1* and *Sat1*) was upregulated, and the anabolic enzymes (*Odc1*, *Sms*) were downregulated. Upregulation of the polyamine catabolizing enzyme *Aoc1* was the most striking change. Similar changes especially for *AOC1* were observed in RNA sequencing data sets of transplanted donor kidneys in humans. The increase of *Aoc1* after kidney injury by ischemia-reperfusion was located to injured but regenerating proximal tubules. Using reporter gene and RNA-stability assays, we showed that increased *Aoc1* expression is based on mRNA-stabilization and transcriptional activation via NFAT5. Notably, the *Aoc1*

splice variant, which shows the most prominent changes after kidney injury contains an additional set of 22 amino acids N-terminally. These amino acid sequence lead to an altered subcellular localization and increased secretion of AOC1. To elucidate the function of AOC1 in kidney injury we could show by overexpression that AOC1 elevates autophagy.

Conclusion: Different models of kidney injury exhibit a similar pattern of dysregulation of the polyamine system with the most striking change being the upregulation of *Aoc1* in damaged but regenerating proximal tubules. Using hyperosmolarity as a stimulus, we established a model to study polyamine function and provide first insights into the regulation of *Aoc1* under damaging conditions.

P117

Humane proximale Tubuluszellen exprimieren in vivo und in vitro das Chemokin CCL26, das chemotaktisch auf humane Monozyten wirkt

J. Schmitz; N. Brauns¹; A. M. Breloh¹; M. Flehsig¹; H. Haller¹; J. H. Bräsen; S. von Vietinghoff²

Nephropathologie, Institut für Pathologie, Medizinische Hochschule Hannover, Hannover; ¹ Klinik für Nieren- und Hochdruckerkrankungen, Zentrum für Innere Medizin, Medizinische Hochschule Hannover, Hannover; ² Sektion für Nephrologie, Medizinische Klinik und Poliklinik I, Universitätsmedizin Bonn, Bonn

Hintergrund: Die akute Infektabwehr in der Niere wird entscheidend durch die Zytokinproduktion residenter Nierenzellen mobilisiert. Wir haben kürzlich die Induktion des Chemokins CCL26

durch hyperosmolares NaCl wie es in der Nierenmedulla zu finden ist beschrieben. Hier untersuchen wir seine Expression und Regulation im humanen Nierengewebe.

Methode: CCL26 wurde per Immunhistochemie/-fluoreszenz und RNA-FISH in Nierenbiopsien von Patientenkohorten und im gesunden Gewebe nachgewiesen und mit Tubuluszell- und myeloiden Markern korreliert.

Ergebnisse: CCL26 wurde in der menschlichen Niere von proximalem Tubulusepithel exprimiert. Es war in der Medulla stärker als im Kortex nachzuweisen. CCL26 induzierte die Migration von Monozyten in vitro und verbesserte ihre bakterizide Wirkung. In der gesunden menschlichen Niere waren im Mark mehr Monozyten als im Kortex nachzuweisen. Die medulläre Monozytendichte korrelierte mit der tubulären CCL26 Expression. Um CCL26 exprimierende Tubuli fand sich eine deutliche Monozytenanreicherung.

Zusammenfassung: Unsere Daten zeigen, dass CCL26 vom proximalen Tubulusepithel in der humanen Niere exprimiert wird und mit dem Auftreten von CD14⁺ Monozyten korreliert. Seine Regulation durch NaCl könnte der differentiellen Expression in den renalen Kompartimenten zugrundeliegen.

P118

Cathepsin B activates ENaC channels

M. Westermann; M. Saudenova; G. Ohrenschall; M. Schewe¹; T. Baukrowitz¹; F. Theilig
Anatomisches Institut, Christian-Albrechts-Universität zu Kiel, Kiel;
¹ Physiologisches Institut, Christian-Albrechts-Universität zu Kiel, Kiel

Objective: Patients with nephrotic syndrome (NS) often present symptoms of volume retention, such as edema formation or hypertension. The primary dysregulation in sodium handling involves an inappropriate activation of the epithelial sodium channel (ENaC). Our previous studies showed that lysosomal protease cathepsin B (CatB) increases ENaC activity leading to hypertension early in nephrotic syndrome. The aim of this study is to investigate molecular mechanisms of how CatB regulates ENaC activity.

Method: *Xenopus laevis* oocytes and cathepsin B deficient (Ctsb^{-/-}) mouse collecting duct cells mpkCCDcl14 were used for western blot and immunohistochemistry analyses following exposure to purified CatB. Amiloride-sensitive Na⁺ currents were also assessed using patch clamp technique.

Results: Western blot analyzed on *Xenopus laevis* oocytes showed that treatment with CatB leads to higher ENaC stability as well as triggering α ENaC cleavage. In order to analyze CatB cleavage site, glycine at P3' in α ENaC was replaced for a larger amino acid (isoleucine) and suppressed CatB-induced ENaC currents were observed. Similarly, suppressive effect was observed after replacement of two N-glycosylated asparagines in the palm and knuckle domains of α ENaC, which are important for shear force sensing. Western blot analyzes on Ctsb^{-/-} mpkCCDcl14 cells revealed significantly increased expression of full length α ENaC subunit and cleaved α ENaC fragments after treatment with CatB. Moreover, Ctsb^{-/-} mpkCCDcl14 cells treated with CatB showed upregulation of ERK1/2 MAP kinase pathway.

Conclusion: Our data suggest that CatB could activate ENaC through increasing its stability as well as the cleavage of α ENaC. Our preliminary results imply that this ENaC activation could possibly rely on N-glycosylated asparagines in the palm and knuckle domains of α ENaC. In addition to that, we also found that ERK1/2 MAP kinase pathway might be involved in CatB-dependent regulation of ENaC.

P119

Short-term fasting elevates circulating fibroblast growth factor 23 (FGF23) through ketone body β -hydroxybutyrate

M. Feger; J. Alber; A. Grund¹;
M. Leifheit-Nestler¹; D. Haffner¹;
M. Föller

Institut für Physiologie, Universität Hohenheim, Stuttgart; ¹ Klinik für Pädiatrische Nieren-, Leber- und Stoffwechselerkrankungen, Zentrum für Kinder- und Jugendmedizin, Medizinische Hochschule Hannover, Hannover

Objective: Phosphate and vitamin D homeostasis are controlled by fibroblast growth factor 23 (FGF23) from bone. FGF23 suppresses renal sodium-dependent phosphate transporter NaPiIIa (Slc34a1) and enhances 24-hydroxylase (Cyp24a1), the key enzyme for inactivating $1,25(\text{OH})_2\text{D}_3$, active vitamin D. Hyperphosphatemia and further mechanisms result in early elevation of plasma FGF23 in patients with chronic kidney disease (CKD). Plasma FGF23 correlates with cardiovascular outcomes not only in kidney disease, but also in other acute and chronic disorders.

Fasting stimulates the production of ketone bodies like β -hydroxybutyrate. Given the relevance of FGF23 as a disease biomarker, we investigated whether short-term fasting (16 h) impacts on FGF23 production through ketogenesis. **Method:** Osteoblast-like UMR106 cells and isolated neonatal rat ventricular myocytes (NRVM) were treated with β -hydroxybutyrate. Wild type mice were fasted overnight or fed ad libitum, blood parameters were determined by enzyme-linked immunoassay (ELISA) or colorimetric methods, and gene expression by quantitative real-time polymerase chain reaction (qRT-PCR). **Results:** β -hydroxybutyrate stimulated FGF23 production in UMR106 cells in a nuclear factor kappa-light-chain enhancer of activated B-cells (NF κ B)-dependent manner, and in cardiomyocytes. Compared to fed animals, fasted mice exhibited higher β -hydroxybutyrate, C-terminal and intact FGF23 serum levels, cardiac Fgf23 and renal Cyp24a1 expression, and lower $1,25(\text{OH})_2\text{D}_3$ serum concentration as well as renal Slc34a1 and aKlotho (Kl) expression. In contrast, Fgf23 expression in bone and serum phosphate, calcium (Ca_{2+}) and parathyroid hormone (PTH) concentration were not significantly affected by fasting.

Conclusion: Short-term fasting increased FGF23 production at least in part through ketone body β -hydroxybutyrate, an effect of high clinical relevance in view of the increasing use of FGF23 as a surrogate parameter in clinical monitoring of diseases. The fasting state of patients is therefore likely to strongly affect plasma FGF23.

P120

Lactic acid induces fibroblast growth factor 23 (FGF23) production in UMR106 osteoblast-like cells

J. Alber; M. Föller

Institut für Physiologie, Universität Hohenheim, Stuttgart

Objective: Endocrine and paracrine fibroblast growth factor 23 (FGF23) is a protein predominantly produced by bone cells with strong impact on phosphate and vitamin D metabolism by targeting the kidney. Plasma FGF23 concentration early rises in kidney and cardiovascular diseases correlating with progression and outcome. Lactic acid is generated in anaerobic glycolysis. Lactic acidosis is the consequence of various physiological and pathological conditions and may be fatal. Since FGF23 production is stimulated by inflammation and lactic acid induces pro-inflammatory signaling, we investigated whether and how lactic acid influences FGF23.

Method: Experiments were performed in UMR106 osteoblast-like cells, Fgf23 mRNA levels estimated from quantitative real-time polymerase chain reaction, and FGF23 protein determined by enzyme-linked immunosorbent assay.

Results: Lactic acid dose-dependently induced Fgf23 gene expression and up-regulated FGF23 synthesis. Also, Na⁺-lactate as well as formic acid and acetic acid up-regulated Fgf23. The lactic acid effect was significantly attenuated by nuclear factor kappa-light-chain enhancer of activated B-cells (NF κ B) inhibitors wogonin and withaferin A.

Conclusion: Lactic acid induces FGF23 production, an effect at least

in part mediated by NF κ B. Lactic acidosis may, therefore, be paralleled by a surge in plasma FGF23.

P121

Unraveling Fundamental Mechanisms of Uromodulin Quality Control and Their Role in Uromodulin-associated Chronic Kidney Disease

S. Bazua-Valenti; M. Dvela-Levitt¹; K. Keller; S. Carr; N. Himmerkus²; M. Bleich²; K. Mutig³; S. Bachmann⁴; M. Kost-Alimova; A. Greka
Broad Institute, Cambridge/USA; ¹The Mina and Everard Goodman Faculty of Life Sciences, Bar-Ilan University, Ramat-Gan/IL; ²Physiologisches Institut, Christian-Albrechts-Universität Kiel, Kiel; ³Institut für Translatioinal Physiologie, Campus Charité Mitte, Charité – Universitätsmedizin Berlin, Berlin; ⁴Institut für Vegetative Anatomie, Campus Charité Mitte, Charité – Universitätsmedizin Berlin, Berlin

Objective: UMOD is an abundant glycosylphosphatidylinositol-anchored protein exclusively expressed in the Thick Ascending Limb of the Loop of Henle (TALH) and the early Distal Convoluted Tubule (DCT1). When properly folded, UMOD transits from the ER to the apical membrane via the Golgi apparatus, however, its specific trafficking partners and quality control mechanisms involved need more clarification. Mutations in UMOD cause UMOD-related autosomal-dominant tubulointerstitial kidney disease (ADTKD-UMOD), characterized by progressive Chronic Kidney Disease (CKD). Mutations disrupt protein folding and promote ER retention, triggering ER-stress pathways and apoptosis. It was recently demonstrated that another

mutant misfolded kidney protein, the Mucin family member MUC1, is trapped in TMED9 cargo receptor-containing vesicles and can be released by treatment with the compound BRD4780. We hypothesize that a similar pathogenic quality control mechanism may be active in ADTKD-UMOD.

Method: Localization and interactomes of UMOD was assessed in HEK-293 cells co-transfected with wild type (wt) or mutant (C126R) human UMOD by quantitative mass spectrometry-based affinity proteomics. We then tested the effect of BRD4780 on UMOD trafficking in isolated TALH from C57BL/6 mice. Finally, we conducted *in vivo* studies in heterozygous (UMOD⁺/C125R) mice (homologous to human C126R).

Results: Several interactors, including members of the TMED family, were enriched in mutant UMOD interactome. Protein complex immunoprecipitation (Co-IP) in lysates of HEK293 cells co-transfected with wt or mutant UMOD and interacting protein candidates confirmed these results. Interestingly, when TMEDs are overexpressed, the immature non-glycosylated form of UMOD is more abundant, suggesting that immature UMOD is entrapped in early secretory compartments. In isolated tubules, we found BRD4780 promotes UMOD trafficking to the apical membrane. *In vivo*, we found increased expression of members of the TMED family and treatment with BRD4780 triggered the release of trapped mutant UMOD, as assessed by Western Blot of kidney lysates and immunofluorescence microscopy of tissue from wt, UMOD⁺/C125R.

Conclusion: In summary, our results suggest that UMOD interacts with the TMED family, possibly mediating the pathogenic quality control mechanisms responsible for toxic ER-retention and accumulation. Shedding light on these new molecular mechanisms may unmask new therapeutic strategies for the treatment of ADTKD-UMOD and possibly other UMOD-related CKD pathologies.

P122

Tight junction component-encoding gene regulation in renal collecting duct principal cells

S. Cao; J. Leiz; C. Hinze; F. Boivin; K. M. Schmidt-Ott¹
Medizinische Klinik mit Schwerpunkt Nephrologie und Internistische Intensivmedizin, Campus Benjamin Franklin, Charité – Universitätsmedizin Berlin, Berlin; ¹Klinik für Nieren- und Hochdruckerkrankungen, Zentrum für Innere Medizin, Medizinische Hochschule Hannover, Hannover

Objective: To identify and characterize novel transcription factors that regulate tight junction biogenesis.

Method: We conducted bioinformatic predictions based on mouse and human single-nuclei sequencing data sets and performed *in situ* hybridization on mouse kidney sections and CRISPRi-based knock-down experiments in inner medullary collecting duct 3 (IMCD3) cells.

Results: Renal single-cell regulatory network prediction based on coregulation and motif enrichment identified a series of candidate collecting duct principal cell transcription factors predicted to be important for tight junction-encoding gene regulation, which included

the transcription factor Ets homologous factor (Ehf). In situ hybridization validated co-expression of Ehf and its predicted target claudin 8 (Cldn8) in mouse collecting ducts *in vivo*. *In vitro* CRISPRi-mediated knockdown of Ehf in IMCD3 cells was successfully achieved and its effects on tight junction component-encoding gene expression are currently being evaluated.

Conclusion: Preliminary data suggest that the transcription factor Ehf regulates tight junction component-encoding genes in renal collecting ducts.

P123

Unterschiedliche Löslichkeit mit Detergenzien von Claudin-10

L. Pinckert; C. Quintanova;
N. Himmerkus; M. Bleich
Physiologisches Institut, Christian-Albrechts-Universität Kiel, Kiel

Hintergrund: Claudin-10 ist ein Tight Junction (TJ)-Protein, das sowohl in der TJ (junctional) als auch ausserhalb, in der basolateralen Membran, vorliegen kann (extrajunctional). Im proximalen Tubulus (PT) kommt Claudin-10 (Splicevariante 10a) hauptsächlich junctional vor, im dicken aufsteigenden Ast der Henle-Schleife (TAL) als Splicevariante 10b auch extrajunctional. Luminale und basolaterale Membranen haben unterschiedliche Eigenschaften. Dies führte zu unserer Hypothese, dass junctionale und extrajunctionale Lokalisation von Claudin-10 mit unterschiedlicher Membranlipidverankerung assoziiert ist. Dazu untersuchten wir die Herauslösung von Claudin-10 und anderen, basolateralen Proteinen aus dem Membranlipidverbund mit den

Detergenzien Triton X-100 (neutral) und SDS (anionisch).

Methode: An frisch isolierten PT und TAL von C57 BL/6-Mäusen wurde die Lokalisation von Claudin-10, Na⁺/K⁺-ATPase (NKA) sowie der Cl-Kanal-Untereinheit Barttin mittels Immunfluoreszenz-Färbung (IF) untersucht. Für Western Blot-Analysen (WB) wurden PT und TAL zunächst segmentweise gesammelt, dann sequenziell in Triton X-100 (1 %) und SDS (1 %) gelöst und schliesslich zusammen mit dem verbliebenen Pellet untersucht.

Ergebnisse: In der TAL bestätigte die IF im Einzeltubulus die Lokalisation der untersuchten Proteine. Barttin und NKA waren ausschliesslich basolateral entlang der gesamten, stark eingefalteten Membran lokalisiert. Die Claudin-10-Färbung zeigte neben mäandrierenden linienförmigen TJ ebenfalls sehr ausgeprägte Präsenz in den basolateralen Einfaltungen. Der WB ergab für Barttin und NKA, dass bereits ca. 87–93 % des Proteins mit Triton in Lösung gebracht werden konnten und nach SDS-Extraktion (ca. 5–12 %) nur noch ein Bruchteil im Pellet ungelöst blieb (ca. 1–2 %). Claudin-10 war nur zu ca. 73 % mit Triton löslich, 23 % wurden noch mit SDS extrahiert und mit ca. 4 % blieb deutlich mehr ungelöst im Pellet. Auch im PT war NKA in der IF basolateral lokalisiert, Claudin-10 jedoch nur in TJ. Die Extraktion mit Triton war im Vergleich weniger effektiv und lag für NKA noch bei 54 % (25 % SDS-löslich, 21 % Pellet). Die Triton-Löslichkeit für Claudin-10 lag mit 40 % allerdings deutlich niedriger als die SDS-Extraktion (52 %), 8 % verblieben ungelöst im Pellet.

Zusammenfassung: Wir spekulieren, dass der niedrigere Anteil an Triton-Löslichkeit für Claudin-10 im PT auf die ausschliesslich junctionale Lokalisation von Claudin-10 zurückzuführen ist. Entsprechend zeigt sich in der TAL der hohe extrajunctionale Anteil von Claudin-10 in NKA- und Barttin-ähnlichen Löslichkeitseigenschaften.

P124

AMP-dependent kinase (AMPK) stimulates the expression of α Klotho

L. Wolf; M. Feger; M. Föller
Institut für Physiologie, Universität
Hohenheim, Stuttgart

Objective: α Klotho is expressed as a transmembrane protein in the kidney and regulates, together with fibroblast growth factor 23, an endocrine factor from bone, phosphate and vitamin D metabolism. Soluble Klotho originates from cleavage of its transmembrane form and regulates various intracellular processes. α Klotho deficiency results in rapid aging, and its overexpression expands life span. α Klotho has anti-inflammatory, antioxidant effects and is nephro- and cardioprotective. AMP-dependent kinase (AMPK) is ubiquitously expressed and contributes to restoring cellular energy stores in energy deficiency. Also, AMPK has nephro- and cardioprotective effects. Here, we studied whether AMPK regulates α Klotho gene expression.

Method: Experiments were performed in Madin-Darby canine kidney (MDCK) and normal rat kidney (NRK 52E) tubular cells. Using qRT-PCR, we measured α Klotho mRNA transcripts upon pharmacological

manipulation or siRNA-mediated knockdown of AMPK α .

Results: AMPK activator 5-aminoimidazole-4-carboxamide ribonucleotide (AICAR) significantly enhanced α Klotho gene expression, an effect significantly reduced in the presence of AMPK inhibitor compound C or siRNA specifically targeting AMPK subunits α 1 and α 2. Similarly, AMPK activators metformin and phenformin up-regulated α Klotho transcripts. **Conclusion:** AMPK is a powerful inducer of α Klotho. This effect is likely to contribute to the beneficial effects associated with AMPK activation with metformin or AICAR.

P125

Oncostatin M is a regulator of fibroblast growth factor 23 (FGF23) in UMR106 osteoblast-like cells

S. Münz, M. Föller

Institut für Physiologie, Universität Hohenheim, Stuttgart

Objective: Renal phosphate and vitamin D metabolism is under the control of fibroblast growth factor 23 (FGF23), an endocrine and paracrine factor produced in bone and other tissues. FGF23 formation is stimulated by 1,25(OH) $_2$ D $_3$, active vitamin D, or parathyroid hormone (PTH), which are further regulators of phosphate homeostasis. In renal, inflammatory, and further diseases, plasma FGF23 reflects disease stage and activity and correlates with outcomes. Cytokine oncostatin M is part of the IL-6 family and regulates remodeling and PTH effects in bone as well as cardiac FGF23 production in heart failure, effects mediated by glycoprotein

gp130. IL-6 is a strong stimulator of FGF23. Here, we studied whether oncostatin M is a regulator of FGF23 in bone cells.

Method: Experiments were performed in UMR106 osteoblast-like cells, Fgf23 mRNA was determined by qRT-PCR, FGF23 protein by ELISA, and oncostatin M receptor gene knock-out accomplished by RNAi.

Results: Oncostatin M dose-dependently up-regulated *Fgf23* gene expression and FGF23 protein synthesis. The oncostatin M effect on FGF23 was mediated by oncostatin M receptor and gp130.

Conclusion: Oncostatin M is a powerful regulator of FGF23 through oncostatin M receptor and gp130 in UMR106 osteoblasts.

Hypertensiologie

P126

An equivocal role of vitamin D3 and calcium supplementation on smooth muscle cell calcification

W. Pustlausk; T. Roch; P. Wehler; T. H. Westhoff¹; S. Geißler; N. Babel¹
Berlin-Brandenburger Center für Regenerative Therapien, Charité – Universitätsmedizin Berlin, Berlin;
¹ Centrum für Translationale Medizin, Medizinische Klinik I, Marien Hospital Herne, Ruhr-Universität Bochum, Herne

Objective: Increased life expectancy together with postmenopausal hormonal changes, obesity, lack of physical activity, and vitamin D3 (VitD) deficiency pose an increased risk for the development of osteoporosis. Patients suffering from osteoporosis, have an increased risk for falls and fragility fractures, causing loss of

independence and mobility, or even death. Supplementation with VitD alone or in combination with calcium (Ca) is a well established therapy to strengthen bone mineral density in osteoporotic patients. However, studies on secondary effects in the vascular system remain controversial. So far, no distinct beneficial effects of VitD supplementation on the cardiovascular system were described, while vascular calcification seems to be increased in animal models. Here we investigate potential effects of VitD and Ca on vascular calcification using an *in vitro* model for the osteogenic differentiation of human smooth muscle cells (SMC).

Method: Human SMC were induced to undergo osteogenic differentiation in the presence of increasing concentrations of VitD (Decostriol), Ca (calcium gluconate) or combinations thereof. Metabolic activity of the SMC, cell counts, and deposition of calcified matrix were assessed.

Results: Increasing concentrations of VitD decreased the metabolic activity of SMC compared to controls and showed detrimental effects on the cell count. On the contrary, supplementation with Ca slightly enhanced the metabolic activity of SMC, irrespective of the concentration used and did not affect the cell count. Addition of Ca to cultures partially reversed the VitD induced reduction of metabolic activity and cell numbers. Despite cytotoxic effects, increased VitD concentrations distinctly reduced SMC calcification, while Ca substantially increased deposition of calcified matrix, even without osteogenic stimulation of SMC. Interestingly, combined treatment with Ca and

VitD further enhanced deposition of calcified matrix compared to Ca or VitD supplementation alone.

Conclusion: Supplementation of osteoporotic patients with VitD might have inhibitory potential on SMC calcification but may exhibit cytotoxic effects. On the contrary, Ca alone or in combination with VitD increases SMC calcification. Our data highlight the need to carefully assess vascular calcification in patients receiving Ca- and VitD-based therapies.

P127

Novel therapeutic options in the cardiorenal syndrome: the AT2-agonist VIF improves recovery after myocardial infarction in mice

A. Baleanu-Curaj; K. Quach;

A. Kindelan Lohse; J. Jankowski

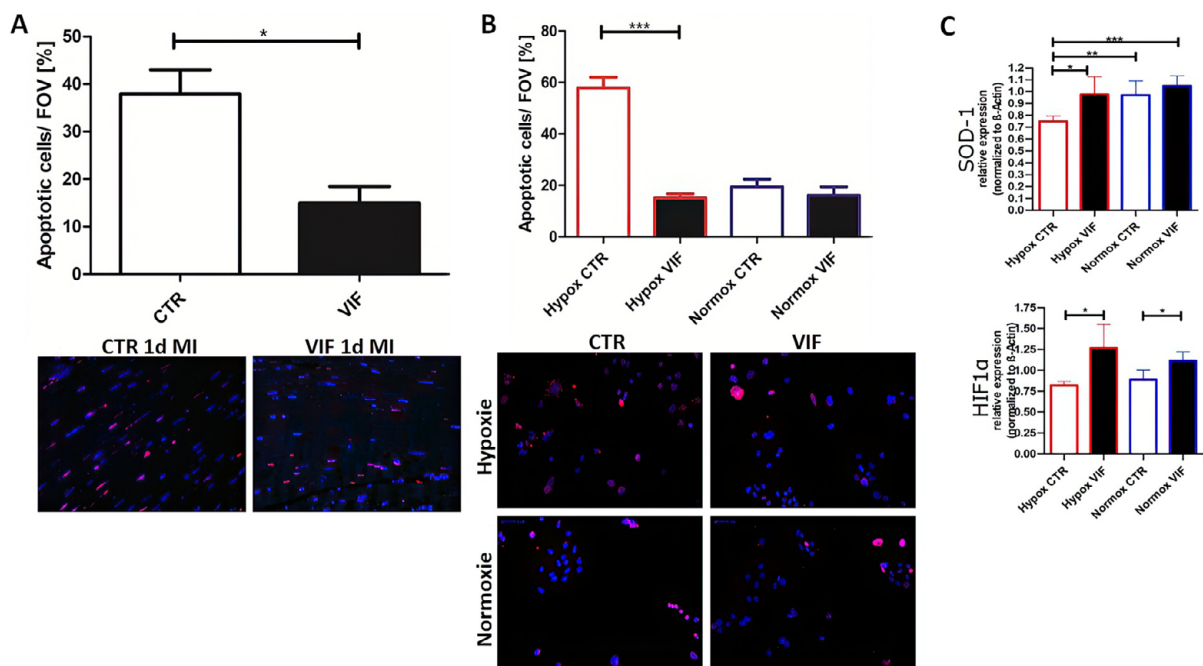
Institut für Molekulare Herz-Kreislaufforschung, Universitätsklinikum, Rheinisch-Westfälische Technische Hochschule Aachen, Aachen

Objective: Blood pressure (BP) regulation is essential in cardiorenal syndrome, and a main regulator of BP is the renin-angiotensin-aldosterone system, which makes it a key target in drug therapy following an acute myocardial infarction (MI). The 'vasoconstriction-inhibiting factor' (VIF) is a novel peptide targeting the AngII receptor 2. High plasma concentrations of VIF have been measured in both patients with chronic kidney disease (CKD) and heart failure (HF). In the current study, we hypothesized that increased plasma concentrations of VIF in patients suffering from CKD and

HF might have additional protective effects in the healing process of MI.

Method: Eight weeks old wild type mice subjected to MI were treated with VIF starting with day-1 post-MI for 2 weeks. BP and left ventricular (LV)-ejection fraction (EF) were measured at day-28 post-MI in VIF-treated and untreated groups, as well as in mice treated with β -blocker. Additionally, the recruitment of inflammatory cells in the infarcted area was assessed in paraffin sections. Moreover, VIF-induced cardiomyocyte protection against hypoxia injury was assessed both *in vivo* and as well *ex vivo* using HL-1 cells by performing immunofluorescence analysis and RT-PCR.

Results: VIF treatment preserved the BP (Figure 1A) and significantly improved the LV-EF ($p = 0,002$) in



P127: Abb. 1

VIF-treated mice (Figure 1B and C), in contrast with the VIF-untreated mice which developed significant-high BP and low LV-EF upon MI-induction ($p = 0.002$). Additionally, VIF treatment induced a significant decrease in the infarction size (Figure 1D) from 50.5 % of the LV volume in the untreated mice to 26.3 % in the VIF-treated mice ($p = 0.047$) by improving the cardiomyocyte's survival in the infarcted area ($p = 0.010$) as evaluated with TUNEL-analysis of day-1 post-MI histological heart tissue slides (Figure 2A). Moreover, VIF-induced cardiomyocyte protection against hypoxia damage was confirmed by a decrease in apoptotic HL-1 cells upon VIF-treatment under hypoxic conditions (Figure 2B). The protective effect of VIF was identified as well on the gene level by upregulation of HIF1 α and SOD1 when investigated with RT-PCR (Figure 2C). Furthermore, an increased level of reparatory monocyte recruitment at day-4 and day-7 post-MI was measured in VIF-treated mice in comparison with the untreated mice (Figure 1E).

Conclusion: VIF treatment preserved BP and the healing process after MI by protecting the cardiomyocytes against ischemia and sustaining the reparatory process resulting in a smaller scar size and a preserved LV-EF.

P128

Transient high salt intake aggravates immune cell-mediated vascular injury in angiotensin II infused apoE-KO mice

J. Stegbauer; M. Yakoub; C. Alter¹; P. Bouvain¹; D. Arifaj; L. Hering; M. Rahman; U. Flögel¹; L. C. Rump; S. Temme

Klinik für Nephrologie, Universitätsklinikum, Heinrich-Heine-Universität Düsseldorf, Düsseldorf; ¹ Institut für Molekulare Kardiologie, Universitätsklinikum Düsseldorf, Heinrich-Heine-Universität Düsseldorf, Düsseldorf

Objective: Chronic high salt intake is a major risk factor for cardiovascular diseases. Excessive chronic salt intake shapes immune differentiation, and thereby contributes to the pathogenesis of vascular injury. However, it remains unclear how salt intake primes immune responses and thereby aggravates vascular injury in response to a subsequent stimulus. Therefore, we investigate whether transient high salt diet prior to a second hit affects hypertensive vascular injury such as abdominal aortic aneurysm (AAA) and atherosclerosis by influencing the immune response.

Method: ApolipoproteinE (ApoE)-KO mice received either drinking water containing 1 % NaCl (transiently high salt intake) or normal tap water (controls) for 14 days followed by a 7 days washout period. After the washout period, apoE-KO mice were infused with angiotensin II (AngII) (1000ng/kg/min) for 10 days. The washout period was done to exclude direct effects of salt on the vasculature. AAA was assessed by magnetic resonance imaging (MRI). On day 10, mice were sacrificed, and atherosclerosis, inflammation as well as immune cell infiltration was assessed by FACS, rt-PCR and immunohistochemistry.

Results: After chronic AngII infusion, cumulative AAA incidence, as well as atherosclerosis were significantly higher and the survival rate significantly lower in apoE-KO mice transiently treated with high

salt compared to the control group. During AngII infusion, no differences were depicted in the blood pressure between the two groups. As a result of transient high salt intake, the frequency of infiltrated aortic T cells, neutrophils and monocytes was increased after Ang II infusion. Moreover, transient high salt intake promoted the differentiation of T-cells into Th1, Th17, effector memory CD4/CD8 T-cells, and CD69 pro-inflammatory phenotypes. Accelerated vascular inflammation and injury induced by transient high salt intake was accompanied by increased elastase expression levels as well as elastic fibre breakdowns suggesting an effect of salt on neutrophil function. Interestingly, high salt did not exert an effect on neutrophil migration in vitro. When co-culturing neutrophils with T cells polarized into effector T cells under high salt conditions, the neutrophil migration capacity was higher compared to co-cultures with T cells polarized into effector T cells under control conditions. These results suggest a relevant crosstalk between T cells and neutrophils.

Conclusion: Our data suggest that transient high salt intake aggravates vascular injury and inflammation during AngII infusion. This effect seems to be caused by a salt-induced shift in the immune cell response to a proinflammatory immune cell phenotype.

P129

Dickkopf-3 in patients with resistant hypertension

A.-K. Schäfer; D. Pieper; H. Dihazi; G. H. Dihazi; S. Lüders¹; M. J. Koziol; M. Wallbach
Abteilung Nephrologie und Rheumatologie, Universitätsmedizin Göttingen,

Göttingen; ¹ *Fachbereich II: Nephrologie, Innere Medizin, St. Josefs-Hospital Cloppenburg gGmbH, Cloppenburg*

Objective: Patients with resistant hypertension show increased risk of chronic kidney disease and progression to end-stage renal disease, however individual course is often not predictable. Assessing urinary Dickkopf-3 (uDKK3), a stress-induced, tubular epithelial-derived profibrotic glycoprotein, may provide insights about ongoing tubulointerstitial fibrosis and eGFR decline. However, data on uDKK3 levels in patients with resistant hypertension are limited so far.

Method: Patients with resistant hypertension were included in this analysis. Clinical and laboratory follow-up were up to 24 months. Spot urine collection, blood pressure measurements and assessment of renal function were performed within a prospective observational trial investigating baroreflex activation therapy. For this retrospective analysis, uDKK3 levels within the first 6 months of the study were determined in the collected urine spots using a commercial ELISA kit. eGFR slopes, measured by CKD EPI formula, were assessed up to 24 months post BAT implantation. Patients were divided into those with high and low eGFR loss (average ≥ 3.5 vs. < 3.5 ml/min/1.73 m²/year) and into those with high and low uDKK3 levels (≥ 400 vs. < 400 pg/mg creatinine), respectively. Correlation analysis of uDKK3 levels with changes of eGFR was performed.

Results: 31 patients were included in the study. Median uDKK3 level was 303 (IQR 715) pg/mg creatinine. At inclusion, patients were

58 \pm 13 years old, 13 (42 %) were women, mean BMI was 33 \pm 6 kg/m², 16 patients (52 %) had diabetes mellitus, 20 (65 %) had a history of smoking and on average they took 6.6 \pm 1.5 antihypertensive drugs. Mean office blood pressure was 171 \pm 23/90 \pm 19 mmHg. In patients with an average eGFR loss ≥ 3.5 ml/min/1.73 m²/year (n = 13), significantly higher uDKK3 levels were measured in the first 6 months (646 (IQR 2306) vs. 180 (IQR 242) pg/mg creatinine, p = 0.0412). The other way round, patients with uDKK3 levels ≥ 400 pg/mg creatinine (n = 11) showed a significant higher eGFR loss compared to patients with lower uDKK3 levels (n = 20, -6.4 \pm 4.7 vs. 0.0 \pm 7.6 ml/min/1.73 m²/year, p = 0.0172). Within the entire cohort, there was a significant correlation between the uDKK3 levels and changes of eGFR at the latest follow up (Spearman r = -0.3714, p = 0.0397).

Conclusion: In patients with resistant hypertension, high uDKK3 levels are associated with a higher loss of eGFR. Further studies are needed to confirm this results and to test whether blood pressure lowering therapies might influence uDKK3 levels according to their nephroprotective effects.

P130

Role of human T cells in hypertension and hypertensive organ damage

M. Rahman; L. Hering; M. Yakoub; D. Arifaj; M. Kantauskaitė; L. C. Rump; J. Stegbauer
Klinik für Nephrologie, Universitätsklinikum, Heinrich-Heine-Universität Düsseldorf, Düsseldorf

Objective: Inflammatory processes seem to influence the development of hypertension. Animal studies suggest that adaptive immunity, in particular T cells contribute to the development hypertension. However, due to the complex pathophysiological interactions in humans, the impact of human T cells in the development of hypertension and hypertensive organ damage is still unknown.

Method: To investigate the impact of human T cells in hypertension, we transferred T cells from treatment resistant hypertensive patients (TRH) and healthy controls into immunodeficient NOD.Cg-Prkdcscid H2-K1tm1Bpe H2-D1tm1Bpe Il2rgtm1Wjl/SzJ (NSG-(KbDb)null) mice to establish a humanized mouse model. Hypertension was induced by chronic angiotensin (Ang)II (500ng/kg/min) infusion for 14 days.

Results: PBMCs from RHT or healthy controls were transferred to NSG-(KbDb) null mice. After ensuring proper T cell engraftment, blood pressure was continuously measured by radiotelemetry. Systolic blood pressure did not differ at baseline between both groups (128 \pm 5 vs. 133 \pm 4 mmHg, n = 6). However, systolic blood pressure in response to AngII was increased in NSG-(KbDb) null mice receiving PBMCs from TRH compared to controls (week 1: 133 \pm 6 vs. 162 \pm 3 mmHg, n = 6, p < 0.01; week 2: 141 \pm 6 vs. 158 \pm 7 mmHg, n = 5-6, p < 0.05). Moreover, endothelial-dependent vasorelaxation was significantly impaired in isolated perfused kidneys of NSG-(KbDb) null mice receiving PBMCs from TRH compared to controls (n = 4-5). In addition, proportions of splenic and

renal effector memory CD4 and CD4 Th17 cells of NSG-(KbDb) null mice engrafted with PBMCs from TRH were significantly higher compared to controls. Furthermore, renal mRNA expression of TNF- α derived from human T-cells (1.5 ± 0.2 vs. 1.00 ± 0.1 , $p < 0.05$, $n = 5-6$) as well as renal perivascular T cell infiltration were significantly higher in NSG-(KbDb) null mice engrafted with PBMCs from TRH compared to controls. Overnight incubation of aortic rings with human TNF- α significantly impaired endothelial function compared to untreated aortic rings ($p < 0.01$, $n = 3-5$). Finally, NSG-(KbDb) null mice engrafted with PBMC from TRH were treated with the TNF- α inhibitor etanercept. TNF- α inhibition attenuated systolic blood pressure response to Ang II compared to untreated mice (132 ± 1 vs. 160 ± 2 mmHg, $p < 0.01$, $n = 6$).

Conclusion: The present results suggest that pro-inflammatory cytokines released by human T cells from patients with resistant hypertension seem to have a pathophysiological relevance in the genesis of human hypertension and hypertensive organ damage.

P131
Does Gender affect electrophysiological properties of neurons with axons from the kidney?

K. Rodionova; T. Ditting; J. Döllner; N. Cordasic; K. F. Hilgers; P. Linz¹; C. Ott; R. E. Schmieder; M. Schiffer; K. Amann²; R. Veelken
 Medizinische Klinik 4, Nephrologie und Hypertensiologie, Universitätsklinikum, Friedrich-Alexander-Universität Erlangen-Nürnberg, Erlangen; ¹ Radiologisches Institut, Universitätsklinikum,

Friedrich-Alexander-Universität Erlangen-Nürnberg, Erlangen; ² Institut für Nephropathologie, Universitätsklinikum, Friedrich-Alexander-Universität Erlangen-Nürnberg, Erlangen

Objective: Previously we reported on a complex composition of afferent nerves from the kidney comprising highly active tonic and less active phasic neurons. The portion of the latter is significantly increased in renal inflammation and hypertension likely impairing the sympathetic control by afferent renal nerves. Androgens were reported to act on sensitive afferent nerve structures. Hence we wanted to test the hypothesis that the function of neurons with renal afferents is subject to sexual dimorphism.

Method: Three groups of Sprague Dawley rats (male, female and ovariectomized female) were investigated. Renal neurons were retrogradely labeled with DiI. In culture, labeled dorsal root ganglion neurons (DRG Th11-L2) with renal afferents were investigated electrophysiologically using current clamp mode to assess action potential generation during current injection (neurons were characterized as tonic highly active (> 5 action potentials, AP) and phasic less active neurons (≤ 5 AP upon stimulation)). Rats were matched for body weight and age.

Results: In neurons from male and female rats, the relation of tonic highly active neurons to less active phasic neurons did not differ significantly (82 % tonic neurons in male vs. 79 % in female, z-test). No significant differences in the firing pattern of renal neurons were also observed in ovariectomized females

as compared to males and females that were not ovariectomized. Threshold of action potential generation and duration of action potentials did likewise not differ between the various groups investigated.

Conclusion: Although sexual dimorphism may occur in the nervous control of visceral organs like the kidney it proved to be not obvious with respect to the afferent innervation from the kidney. In how far afferent renal nerve fibers from male and females may have a different influence on central sympathetic outflow remains to be determined.

P132
Afferent Neurons of the Kidney with Impaired Firing Pattern in Inflammation – Role of Sodium and Potassium Currents

K. Rodionova; R. Veelken; K. F. Hilgers; P. Linz¹; C. Ott; R. E. Schmieder; M. Schiffer; K. Amann²; T. Ditting
 Medizinische Klinik 4, Nephrologie und Hypertensiologie, Universitätsklinikum, Friedrich-Alexander-Universität Erlangen-Nürnberg, Erlangen; ¹ Radiologisches Institut, Universitätsklinikum, Friedrich-Alexander-Universität Erlangen-Nürnberg, Erlangen; ² Institut für Nephropathologie, Universitätsklinikum, Friedrich-Alexander-Universität Erlangen-Nürnberg, Erlangen

Objective: Previously, we reported that peripheral neurons with renal afferents involved in sympathetic control exhibit a predominantly tonic firing pattern of higher frequency that is reduced to low frequencies (phasic firing pattern) in renal inflammation. Now, we wanted to test the hypothesis that the reduction in firing activity

during inflammation is due to special tonic neurons switching from higher to low frequencies.

Method: Renal subcapsular staining (DiI) for identification of neurons with renal projection (RANs). Cultivated neurons incubated with the chemokine CXCL1 (1,5 nmol/ml) for 12 hours prior to electrophysiology. Current clamp used to characterize neurons as “tonic”, i.e. sustained action potential (AP) firing or “phasic”, i.e. < 5 APs upon stimulation. Membrane currents investigated by increasing clamp voltage. Data analyzed: renal vs. non-renal and tonic vs. phasic neurons.

Results: Renal neurons exposed to CXCL1 showed a decrease of tonic firing pattern compared to controls (35,6 % vs. 57 %, $P < 0.05$). Phasic neurons exhibited higher Na^+ and K^+ currents than tonic neurons in controls resulting in shorter APs ($3.7 \pm 0,3$ vs. $6.1 \pm 0,6$ ms, $P < 0,01$). In neurons incubated with CXCL1, Na^+ and K^+ peak currents increased (Na^+ : -969 ± 47 vs. -758 ± 47 nA/pF, $P < 0.01$; K^+ : 707 ± 22 vs. 558 ± 31 nA/pF, $P < 0.01$) in phasic, but were unchanged in tonic neurons. Incubated phasic neurons showed a much broader range of Na^+ currents ($[-365 - -1429$ nA] vs. $[-412 - -4273$ nA]; $P < 0.05$); similar to tonic neurons.

Conclusion: The enlarged number of renal phasic neurons incubated with CXCL1 showed significantly increased membrane currents resembling the broad range of Na^+ currents seen in tonic neurons. These findings suggest that a subgroup of tonic neurons switched to a phasic response pattern in inflammation

while other mechanisms become less likely (e.g. recruitment of formerly silent phasic neurons).

P133

Synchronisierte 24-Stunden Blutdruckmessungen an beiden Armen zeigen klinisch relevante Unterschiede: Ein Weckruf für Diagnose und Behandlung der Hypertonie

*T.L. Bothe; A. Patzak; N. Pilz
Institut für Translational Physiologie, Campus Charité Mitte, Charité – Universitätsmedizin Berlin, Berlin*

Hintergrund: Manschettenbasierte 24-h Blutdruck (BD) -Messungen sind der Goldstandard für die Diagnose und das Therapiemonitoring der Hypertonie. Die klinische Bedeutung ambulanter BD-Messungen ist weithin etabliert. Unsere Studie möchte die Messunterschiede in parallellaufenden und synchronisierten Langzeit-BD-Messungen an beiden Armen quantifizieren. Das Verständnis der Ursachen von resultierenden Messunsicherheiten kann das zukünftige klinische Management verbessern und Vertrauen in alternative, manschettenfreie Systeme stärken.

Methode: Wir haben in 52 jungen Erwachsenen zeitgleich an beiden Armen Langzeit-BD-messungen durchgeführt. Zwei Manschettengeräte (BoSo TM-2430) wurden für den simultanen Messbeginn synchronisiert. Zusätzlich haben wir die Druckkurven der Manschetten und den hydrostatischen Druck zwischen den beiden Manschetten aufgezeichnet. Anschließend haben wir die Kurven auf Störungen untersucht und waren in der Lage, die hydrostatischen Unterschiede zwischen den Manschetten zu korrigieren. Dieses

Vorgehen erlaubte uns nicht nur das Ausmaß der Messunsicherheit zu quantifizieren, sondern auch Ursachen und Maßnahmen zu deren Eindämmung zu untersuchen.

Ergebnisse: Die gemessenen Blutdruckwerte der beiden Arme zeigten Limits of Agreement im Bland-Altman-Diagramm von > 33 mmHg für systolische und > 30 mmHg für diastolische Werte über 24-h. Die Abweichungen am Tag waren größer als in der Nacht (systolisch: > 35 mmHg vs. > 27 mmHg und diastolisch: > 32 mmHg vs. 24 mmHg). Die lineare Regression ergab $R^2 = 0.39$ ($p < 0.001$) für systolische und $R^2 = 0.20$ ($p < 0.001$) für diastolische Werte. Der Ausschluss fehlerhafter Messungen verbesserte die Limits of Agreement auf > 23 mmHg für systolische und > 19 mmHg für diastolische Werte. Folglich verbesserte sich die Korrelation auf $R^2 = 0.54$ ($p < 0.001$) und $R^2 = 0.35$ ($p < 0.001$). Die Korrektur der hydrostatischen Effekte hatte einen vernachlässigbaren Effekt.

Zusammenfassung: Der Vergleich zweier Langzeit-BD-Messungen an unterschiedlichen Armen zeigte große Messunterschiede mit möglichen Auswirkungen auf die klinische Bewertung einer Hypertonie. Der Ausschluss gestörter Pumpkurven, die nicht von der konventionellen Software erkannt wurden, verringerte die Unsicherheit, die allerdings weiterhin in bedenklich hohem Ausmaß bestand. Diese Ergebnisse sind ein Imperativ für weitere Untersuchungen zur klinischen Bedeutung der Messunsicherheit. Zudem implizieren sie die zuversichtliche Adaptation alternativer BD-Messmethoden, die ähnliche Messunsicherheiten zeigen können.

P134**Circulating monocytes from patients with primary aldosteronism display exhaustion upon LPS stimulation**

M. Kantauskaite; K. Bolten; M. Yakoub; F. Srugies; C. Schmidt; B. Duvnjak; T. Kolb; E. Königshausen; L. C. Rump; J. Stegbauer

Klinik für Nephrologie, Universitätsklinikum, Heinrich-Heine-Universität Düsseldorf, Düsseldorf

Objective: Aldosterone excess present in primary aldosteronism (PA) plays a critical role in the development of endothelial dysfunction, oxidative stress and chronic inflammation, which contributes to aggravated hypertensive organ damage. According to animal studies, aldosterone-induced immune cell activation directly contributes to the vascular injury. As the monocytes are the main immune cells interacting with vascular wall during the injury, we proposed that patients with PA would demonstrate activated monocytes which would be resolved by the treatment.

Method: Monocytes from patients (N=9) before and 3 months after the treatment (N=9) and healthy individuals (N=6) were seeded into 96-well plates at 200000 cell/well in RPMI 1640 Dutch-modified culture medium (PAN Biotech) supplemented with 10 µg/mL gentamicin, 10 mmol/L Glutamax, 10 mmol/L pyruvate, 10 mM HEPES and 10 % fetal bovine serum. After 4 hour rest time the cells were exposed to 10 ng/ml Lipopolysaccharides (LPS) O111:B4 from E.coli for 24 hours. After the incubation supernatants were collected for cytokine, chemokine

and growth factor measurements using Bio-Plex Pro Human Cytokine 17-plex Assay. Clinical and laboratory data were collected from patients records.

Results: Before the treatment patients with PA displayed significantly higher concentrations of following cytokines and growth factors than healthy controls: G-CSF, IFN-γ, TNF-α, IL-6, IL-10, IL-8, IL-17, MCP-1. Moreover, before the treatment Aldosterone-Renin-Quotient (ARQ) correlated positively with IL-6 (r 0.667, p = 0.05) and MCP-1 (r 0.883, p = 0.002). After the treatment was initiated, we have observed normalized blood pressure (median 139/85 mmHg vs 130/80 mmHg, p < 0.05) and significantly lower ARQ (83 (59–261) vs 13 (3.6–9.4), p < 0.05). In addition, cytokine levels in monocyte supernatants normalized and reach levels similar to healthy controls. Upon the stimulation with LPS patients with PA demonstrated a blunted immune response with lower cytokine concentrations whereas the treatment restored the cytokine response upon LPS stimulation. Moreover, lower IL-6 (r -0.766, p = 0.27), TNF-α (r -0.802, p = 0.017) and G-CSF (r -0.719, p = 0.045) concentration upon LPS stimulation was associated with higher diastolic blood pressure.

Conclusion: Patients with primary aldosteronism demonstrate higher cytokine levels at a steady state and a type of reversible endotoxin tolerance upon stimulation which might contribute to the increase in blood pressure.

P135**Metformin treatment decreases blood pressure but does not****ameliorate hypertensive cardio-renal damage in a double transgenic rat model**

H. Bartolomaeus; M. I. Wimmer; C.-Y. Chen; S. Kedziora; V. Vecera; O. Popatenko; T. U. P. Bartolomaeus; V. H. Jarquin-Diaz; U. Löber; N. Haase; S. Forslund; D. N. Müller; N. Wilck
ECRC-Kooperation von MDC und Charité, Experimental and Clinical Research Center, Berlin

Objective: Metformin (Met) is used as a first-line treatment in type II diabetes and is hence widely used among patients suffering from cardiovascular diseases (CVD). Met treatment is associated with decreased mortality from CVD. The mechanisms of action are broad and not sufficiently understood. In humans, Met treatment is associated with functional changes in the gut microbiome, leading to enhanced production of protective short-chain fatty acids (SCFA), but also potentially harmful lipopolysaccharides (LPS). Our study aims to examine the effects of Met in a rat model of RAAS-mediated hypertension with cardio-renal damage.

Method: Four-week-old double transgenic rats (dTGR, transgenic for human renin and angiotensinogen) were treated with oral Metformin (Met) or Vehicle (Veh) for 3 weeks. Untreated seven-week-old SD rats were included as healthy controls. Flow cytometry, echocardiography, radiotelemetric blood pressure measurements, clinical chemistry and gene expression analyses were employed to analyze the clinical and immune phenotype of the kidney and the heart. **Results:** Met treatment did not influence survival nor did it lead to lactate acidosis. Met-treated dTGR

had a significantly lower blood pressure than Veh-treated dTGR. Interestingly, the decreased blood pressure was accompanied by an increased cardiac hypertrophy. In line with a worsened cardiac damage, echocardiographic systolic and diastolic function was deteriorated. Matching, plasma BNP and cardiac beta-to-alpha MHC ratio were higher in Met-treated dTGR. Hypertensive kidney damage, as assessed by urinary albumin to creatinine ratio and plasma creatinine, was not affected by Met treatment. However, mRNA expression of kidney damage markers *Ngal* and *Kim1* were increased. The intestine, spleen, kidney and heart of dTGR showed a strong inflammatory phenotype with increases in both adaptive (e.g. T cells) and innate (e.g. macrophages) immune cell subsets in comparison to healthy SD rats, but virtually no differences could be observed between Met and Veh treated dTGR. Metagenomic shotgun sequencing of the fecal microbiota showed no large-scale taxonomic alterations between Veh and Met treated dTGR.

Conclusion: In our study, we observed a worsened phenotype of hypertensive rats treated with Met. To the best of our knowledge, previous studies found improved outcomes of Met treatment in hypertension models. Since the dTGR model is known for its strong phenotype, potential beneficial effects could have been outweighed by side effects like increased LPS production potential. Whether the aggravated phenotype is due to increased LPS translocation (leaky gut) is currently under investigation.

P136

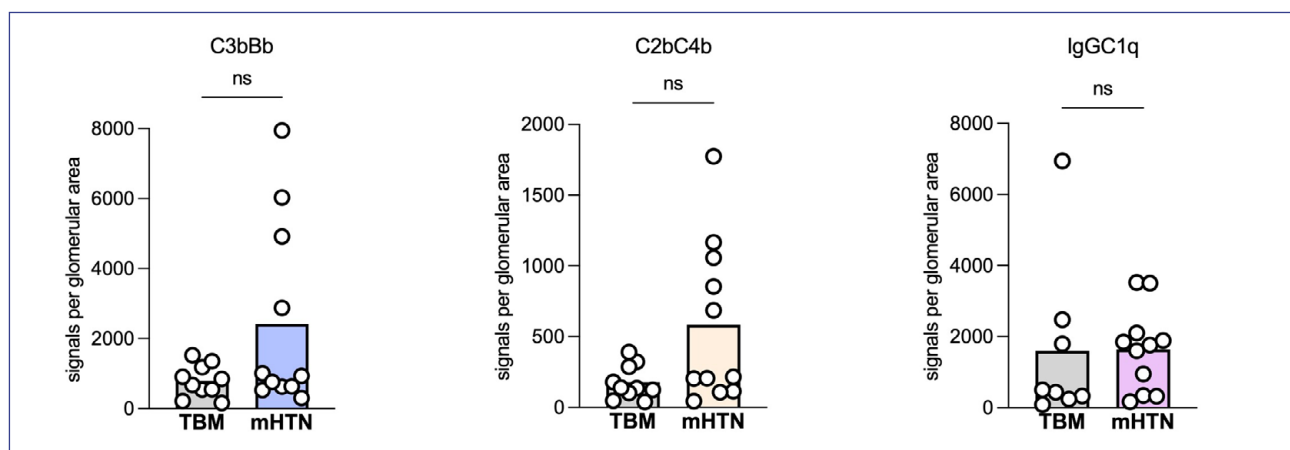
Die Rolle des Komplementsystems bei der Pathogenese der malignen Nephrosklerose

E. Alba-Schmidt; T. Schmidt¹; T.B. Huber; N.M. Tomas; T. Wiech²; U. Wenzel
Nephrologie/Rheumatologie und Endokrinologie/Diabetologie, III. Medizinische Klinik, Universitätsklinikum Hamburg-Eppendorf, Hamburg; ¹Abteilung für Nephrologie/Osteologie, III. Medizinische Klinik, Universitätsklinikum

Hamburg-Eppendorf, Hamburg;

²Institut für Pathologie, Sektion Nephropathologie, Zentrum für Diagnostik, Universitätsklinikum Hamburg-Eppendorf, Hamburg

Hintergrund: Das Komplementsystem ist ein Teil der angeborenen Immunität, das den Wirt vor einer feindlichen mikrobiellen Umgebung schützt und Gewebe- und Zellintegrität durch die Eliminierung veränderter Zellen aufrechterhält. Experimentelle Daten beweisen eine Rolle des Komplementsystems bei hypertensiven Endorganschäden. Die sogenannte maligne Nephrosklerose ist die schwerste Form der hypertensiven Endorganschädigung und kann zur terminalen Niereninsuffizienz führen. Es ist unklar, welche Mechanismen den Übergang von hypertensiver Nephropathie zur malignen Nephrosklerose bewirken. Daten aus dem „Limburg Renal Registry“ haben kürzlich suggeriert, dass Komplementaktivierung maligne Nephrosklerose verursacht (Kidney Int 91:1420, 2017). Die Autoren sehen die Komplementblockade damit



P136: Abb. 1

als therapeutische Option bei maligner Nephrosklerose. Immunhistochemisch findet sich in der Niere eine starke Komplementablagerung. Unklar ist aber, ob es sich dabei um Aktivität oder nur „Trapping“ der Komplementproteine handelt. Der Proximity Ligation Assay (in situ PLA) ist eine biochemische Methode zum histologischen Nachweis von Protein-Protein-Interaktionen. Sie erlaubt das Detektieren, die Lokalisierung und Quantifizierung der direkten Protein-Protein Interaktion der Komplementproteine (30–40 nm) und damit Aktivierung der Konvertasen im Gewebe.

Methode: Wir analysierten Nierenbiopsien von 11 Patienten mit maligner Nephrosklerose. Histologisch zeigten alle Fälle die klassischen „Onion Skin“ Gefäßveränderungen. Bei keinem Patienten gab es Anhalt für ein aHUS. Als Kontrollen dienten Patienten mit biopsisch gesicherter dünner Basalmembran (n = 10). Mit C4b/C2b wurden der klassische/Lektin, mit IgG/C1q der klassische und C3b/Bb der alternative Weg untersucht. Die Analyse der Glomeruli erfolgte automatisiert mittels einer von uns entwickelten deep learning software und die der Gefäße manuell.

Ergebnisse: Verglichen mit den Kontrollbiopsien zeigte sich keine signifikante Aktivierung (Signale/mm²) des klassischen (1639 ± 350 vs. 1604 ± 820, p = 0.49), des klassischen/Lektin (585 ± 171 vs. 177 ± 37, p = 0.49) oder des alternativen Wegs (2416 ± 805 vs. 797 ± 145, p = 0.28). Auch in den Gefäßen fand sich keine signifikante Aktivierung.

Zusammenfassung: Diese Daten beweisen, dass keine intrarenale

Aktivierung der drei Komplementwege bei Patienten mit maligner Nephrosklerose vorliegt. Im Gegensatz zu den Limburgdaten sehen wir damit aktuell keine Indikation für eine Komplementblockade bei maligner Nephrosklerose.

Digitale Nephrologie

P137

Improving the prediction of the renal function in kidney transplant patients

F. Westphal; U. Jehn; H. Pavenstädt; S. Reuter

Allg. Innere Medizin und Notaufnahme sowie Nieren- und Hochdruckkrankheiten und Rheumatologie, Medizinische Klinik D, Westfälische Wilhelms-Universität Münster, Münster

Objective: Maintaining the function of a renal transplant is a major challenge after a successful kidney transplantation. Currently, health professionals address this challenge by many follow-up appointments, including interviews, laboratory tests, and ultrasound examinations. Despite of these efforts, some patients lose kidney function rather quickly. Identifying patients at high risk of losing renal function could improve the follow-up strategy.

Method: Our single-centre study cohort consists of patients who received a kidney transplantation between 2007 and 2017 and were followed for five years. Exclusion of all patients with incomplete data entries resulted in 472 patients. Those were divided randomly into two groups (80 % training data and 20 % validation data). All patients were classified using the eGFR (CKD-EPI) five years after transplantation with a threshold

of 60 ml/min. Random Forest Classifiers were trained to predict the eGFR five years after transplantation using 5-fold cross-validation and optimisation by a grid search with multiple hyperparameters. The independent variables consisted of multiple donor and recipient properties. All calculations were performed using Python 3.

Results: Five years after transplantation, 311 of 472 patients had an eGFR below 60 ml/min. Including only the independent variables available at the time of kidney transplantation, the Random Forest Classifier models achieved prediction accuracies of up to 81 % for the training data and 71 % for the test data. Testing the best model with the validation data resulted in an accuracy of 73 %. Next, we trained a second set of Random Forest Classifier models. This time, we expanded the set of independent variables to include parameters of the renal function three months after transplantation. This improved the prediction accuracies to 88 % for the training data and 80 % for the test data. Testing our final model with the validation data confirmed these results by achieving a prediction accuracy of 82 %.

Conclusion: Random Forest Classifier models can be used to predict the kidney function five years after transplantation with satisfying accuracy. The accuracy of the models improves when they are trained with data obtained 3 months after transplantation. Therefore, such models can be used at different stages of the follow-up strategy to predict the renal function of patients, and can be used to initiate prevention strategies. It is expected that further models trained on larger cohorts will provide better predictions.

P138**Virtual reality-assisted CAPD / APD training in peritoneal dialysis: A pilot evaluation of trainer and patient perception**

P. Zgoura; A. Müller¹; B. Bader²; M. Baecker²; B. Kantzow³; M. Sayer⁴; O. Weckbach¹; B. Arntjen⁵; A. Kaczmarek⁵; N. Heyne⁴
 Centrum für Translationale Medizin, Medizinische Klinik I, Marien Hospital Herne, Ruhr-Universität Bochum, Herne; ¹Nierenzentrum Weinheim, Weinheim; ²MVZ DaVita Nierenzentrum Berlin-Britz, Berlin-Neukölln; MVZ DaVita Nierenzentrum Berlin-Britz, Berlin-Neukölln; ³Weltenmacher GmbH, Düsseldorf; ⁴Sektion Nieren- und Hochdruckkrankheiten, Universitätsklinikum, Medizinische Klinik IV, Eberhard Karls Universität Tübingen, Tübingen; Nierenzentrum Weinheim, Weinheim; Baxter Deutschland GmbH, Unterschleißheim; ⁵Baxter Deutschland GmbH, Unterschleißheim

Objective: Virtual reality (VR) is an evolving technology, increasingly used in different medical settings such as training of medical professionals in endoscopic or surgical procedures. In this context, immersive VR simulation has been shown to improve training efficacy and outcome. Less data is available on the use in patient education and training or delivery of medical intervention. To address this topic, a pilot evaluation is conducted to assess feasibility and usability of VR-assisted training for continuous ambulatory- (CAPD) and automated (APD) peritoneal dialysis in selected peritoneal dialysis centers
Method: VR assistance is provided by a fully immersive VR headset (Pico Neo 3, Pico Immersive Pte. Ltd, Singapore) and two

specific training programs for CAPD and APD, respectively (Weltenmacher GmbH, Düsseldorf in collaboration with Baxter Deutschland GmbH). Patient as well as nurse trainer perceptions of VR-assisted training will be assessed using standardized response questionnaires. Patient perceptions are assessed on the last two days of training, nurse trainer perceptions at baseline as well as after 4, 8 and 12 weeks of training experience.

Results: 3-month data of the ongoing pilot evaluation will be presented. Scientific evaluation of trainer and patient end-user perception are a prerequisite to improve strategic implementation of novel tools in patient education and important means for the subsequent design of prospective end-point trials. Points of interest include duration and staff involvement in patient education, training efficacy and outcome as well as the potential impact on complication rates and patients on therapy in peritoneal dialysis.

Conclusion: VR programs may be a suitable platform to improve patient experience, staff involvement and environmental footprint as well as outcome of patient training in peritoneal dialysis. Critical evaluation of benefits and limitations are key for successful implementation in patient education.

P139**Vereinfachtes Online-Scoring-Tool zur Diagnose der enkapsulierenden Peritonealsklerose**

S. Schricker; P. Fritz; J. Dippon¹; M. Kimmel²; M. D. Alscher; T. Oberacker³; M. Schanz
 Abteilung für Allgemeine Innere Medizin und Nephrologie,

Robert-Bosch-Krankenhaus, Stuttgart;

¹Institut für Stochastik und Anwendungen, Fachbereich Mathematik, Universität Stuttgart, Stuttgart; ²Klinik für Nieren-, Hochdruck- und Autoimmunerkrankungen, Zentrum für Innere Medizin, Alb Fils Kliniken – Klinik am Eichert, Göppingen;

³Dr. Margarete Fischer-Bosch-Institut für Klinische Pharmakologie, Robert-Bosch-Krankenhaus, Stuttgart

Hintergrund: Die enkapsulierende Peritonealsklerose (EPS) ist eine Komplikation der Langzeit-Peritonealdialyse (PD). Obwohl die Inzidenz abnimmt, ist eine frühzeitige Diagnose oder ein Ausschluss entscheidend. Die Unterscheidung von einfacher Sklerose und EPS ist schwierig und stützt sich neben Klinik und Bildgebung auf histologische Kriterien. Ziel der Studie ist es, das histologische Protokoll zu vereinfachen und ein histologisches Online-Scoring-Tool für Verdachtsfälle zu entwickeln.

Methode: Die Studie umfasst 218 Peritonealbiopsien, wovon 85 nach klinischer und radiologischer Klassifizierung zur EPS-Gruppe und 133 zur Kontrollgruppe (nicht-EPS) gehören. Ein Pathologe und zwei Nephrologen analysierten verblindet 15 histologische Variablen nach einem Zwei-Punktesystem (fehlend oder vorhanden (0 oder 1)), einem Vier-Punktesystem (fehlend (0), wenig vorhanden (1), mittelmäßig vorhanden (2) oder viel vorhanden (3)) oder beiden Systemen.

Ergebnisse: Für 15 histologische Variablen wurde die Intra- und Inter-Beobachter-Variabilität (IBV) berechnet (kappa). Gemäß unseren Daten, zeigt sich das Zwei-Punktesystem (kappa mean = 0,6) dem Vier-Punktesystem (kappa mean = 0,44)

überlegen. Variablen mit sehr hoher IBV wurden identifiziert und ausgeschlossen ($\kappa < 0,4$). Somit ergaben sich sieben relevante Variablen mit niedriger IBV zur histologischen Befundung basierend auf dem Zweipunktesystem: 1. azelluläre Areale, 2. Exsudation-Fibrin, 3. Fibrose, 4. Hämmorrhagie, 5. Kalzifikation, 6. mesotheliale Denudation und 7. Vaskulopathie. Auf Grundlage dieser Variablen ergab sich mittels logistischer Regressionsanalyse die Prädiktion der EPS-Diagnose mit einer Genauigkeit von 79,8 % (Sensitivität 73,2 %, Spezifität 83,3 %). Diese vereinfachte Befundung sowie die darauf basierende Prädiktion wurde in ein Online-Scoring-Tool eingearbeitet und mit entsprechenden Referenzbildern auf der Webplattform ipath-network zur Verfügung gestellt.

Zusammenfassung: Die histologische Beurteilung einer EPS-Diagnose konnte durch unser EPS-Online-Scoring-Tool deutlich weiterentwickelt und vereinfacht werden bei suffizienter Sensitivität und Spezifität. Durch die Kooperation mit Webplattform ipath-network entsteht neben der Nutzungsmöglichkeit unseres EPS-Online-Scoring-Tools mit Referenzbildern zur EPS-Befundung auch die Möglichkeit eines Austausches mit bzw. die Einholung einer Zweitmeinung von erfahrenen Nephrologen oder Pathologen, dies kann Zentren mit geringerer Expertise bei der Diagnosefindung unterstützen.

P140

Einstellung von Patienten nach Nierentransplantation zur Videosprechstunde und Kommunikationsplattform

S. Becker; M. Eskinyurt¹; A. Kribben²; W. Kleophas³; A. Mertens⁴; K. Budde⁵; K. Boss²

MVZ DaVita Duisburg, Duisburg; ¹ Head of Marketing & Communications, DaVita Deutschland AG, Hamburg; ² Klinik für Nephrologie, Universitätsklinikum, Universität Duisburg-Essen, Essen; ³ DaVita Clinical Research Deutschland GmbH, Düsseldorf; ⁴ Human Factors Engineering and Ergonomics in Healthcare, Lehrstuhl und Institut für Arbeitswissenschaft, Rheinisch-Westfälische Technische Hochschule Aachen, Aachen; ⁵ Medizinische Klinik mit Schwerpunkt Nephrologie und Internistische Intensivmedizin, Campus Charité Mitte, Charité – Universitätsmedizin Berlin, Berlin

Hintergrund: Digitale Kommunikation hat das Potenzial, die Versorgung nephrologischer Patienten effektiver und effizienter zu gestalten. Das Ziel der aktuellen Umfrage war es, zu erfahren, welchen Stellenwert Kommunikationstechnologien wie Videosprechstunde und Messengersysteme aus Sicht von Patienten nach Nierentransplantation im Rahmen Ihrer nephrologischen Versorgung haben könnten und welche Probleme berücksichtigt werden müssen.

Methode: 36 PatientInnen nach Nierentransplantation (Alter 20-80 Jahre, Median 59 Jahre, männlich 21) füllten in der NTx Ambulanz der Klinik für Nephrologie, Universitätsklinikum Essen und in der Sprechstunde des MVZ Davita Duisburg einen anonymen Fragebogen aus.

Ergebnisse: Mittlerweile nutzen alle Befragten regelmäßig das Internet (n = 36/36), sowie die Mehrheit E-Mail (n = 30/36) und Smartphone (n = 29/36). N = 21/36 Befragten gehen davon aus, dass im Rahmen einer Videosprechstunde und einer Kommunikationsplattform

mit der Praxis unnötige persönliche Vorstellungen in der Sprechstunde reduziert werden könnten, da durch Videosprechstunde und eine Chatfunktion viele Fragen beantwortet werden könnten. Allerdings räumt rund die Hälfte der Befragten (n = 17/36) auch ein, dass eine solche Kommunikation bei akuten Erkrankungen dazu führen kann, dass der Arzt die Gesundheitssituation falsch einschätzt. Grundsätzlich wünschen sich alle Befragten eine persönliche Betreuung, n = 23/36 der Befragten würden gerne über das Telefon mitbetreut werden, n = 17/36 über Videosprechstunde und n = 7/36 über ein SMS System. Fast alle Befragten würden sich wünschen, dass über eine Kommunikationsplattform die Medikation kommuniziert wird (n = 33/36), wie auch Labordaten (n = 33/36), ein Großteil den Austausch von Befunden (n = 23/36), sowie eine Chat-Funktion (n = 23/36).

Zusammenfassung: Die Internetaffinität Nieren-transplantierte PatientInnen hat in den letzten Jahren deutlich zugenommen, nunmehr sind fast alle Befragten mit den entsprechenden Kommunikationsmöglichkeiten vertraut. Prinzipiell kann sich ein Großteil der PatientInnen eine ergänzende digitale Versorgung vorstellen. Insbesondere bei der Kommunikation von Medikations- und Labordaten sowie beim Austausch von Befunden sowie bei einer direkten Chatfunktion gibt es ein Potenzial.

P141

Consilium Care Mobile App und ePROs als Qualitätstool für Hämodialysepatienten

M. Möddel; I. Schuller; M. Peschel; A. Trojan¹

Dialyseabteilung, Klinik Im Park, Zürich/CH; ¹ Onkologie, Klinik im Park, Zürich/CH

Hintergrund: Consilium Care Mobil App (CC-App) digitales Selbst-Monitoring bei internistischen Erkrankungen, insbesondere Krebs. Die App ermöglicht als CE zertifiziertes Medizin Produkt eine Aufzeichnung und Überwachung von Symptomen und selbstberichteten Ereignissen durch Patienten (ePROs), die Reduktion von Symptomen/Schweregrad durch selbstwirksame Massnahmen/Tips, sowie eine Verbesserung von Behandlungsqualität/Outcome durch kollaborativen Patient-Arzt Review von Symptomen. **Methode:** 10 Dialysepatienten konnten die APP während auf dem Smartphone heruntergeladen und installiert. Die CC-App bietet 103 Organsystem-bezogene Symptome. Jeder Patient konnte Symptome selbst auswählen und monitorisieren; dialysespezifisch wurden die Symptome Juckreiz, Müdigkeit, Mundtrockenheit sowie Taubheit und Kribbeln für die Erfassung empfohlen. App-Funktionen wie Vitalwerte Gewicht, Puls, Blutdruck und Blutzucker konnten von dem einzelnen Nutzer optional monitorisiert werden, ebenso die Medikamenten- und Notizfunktion. Die Evaluation war für gesamthaft 4 Wochen vorgesehen. **Ergebnisse:** Bei 8 von 10 Patienten konnten Ergebnisse ausgewertet werden. das Durchschnittsalter betrug 65 Jahre. 4 der 8 Patienten machten über den Testzeitraum weitgehend täglich Einträge in die App, die anderen vier hatten mehrere bis zu mehrtägige Eintragspausen am Stück, ein Teilnehmer nutzte

die App gesamthaft nur über 7 Tage. Insgesamt wurden 259 Vitalzeichen, wie Blutdruck, Gewicht und Puls, eingegeben. Weiterhin 1301 Symptome wie Juckreiz, Müdigkeit, Mundtrockenheit sowie Taubheit und Kribbeln; sowie 38 Einträge zu den verordneten Medikamenten.

Zusammenfassung: Die Consilium Care-App bietet dem Patienten im ambulanten Setting die Möglichkeit einer genauen Symptom- und Vitalwerte-Monitorisierung mit digitaler Übermittlungs- und Überwachungsfunktion sowie mit niederschwelliger Kontaktmöglichkeit zum jeweiligen Behandlungszentrum. Eine gezielte Auswahl der Nutzer und eine gute Einführung sowie aktive Begleitung in der Anfangsphase erhöhen die Compliance und somit den Nutzen bedeutsam. Die App bietet absehbar für Heim-/Peritonealdialysepatienten sowie für das grosse Kollektiv onkologischer Patienten im ambulanten Setting eine sehr gute Monitorisierungs- und Anbindungsmöglichkeit an das Zentrum, da diese Patienten in der Regel nur in grösseren Abständen oder aber in Notfallsituation von dem betreuenden Zentrum gesehen werden

P142

Automatic Analysis of Renal Biopsies with Thrombotic Microangiopathies (TMAs)

P. A. Cicalese¹; S. Rizvi²; S. Seshan¹; S. Sciascia²; B. Schröppel³; N. van de Kar⁴; J. Kers⁵; J. Roelofs⁵; C. Mohan⁶; H. V. Nguyen⁷; J. U. Becker⁷
Department of Electrical & Computer Engineering, University of Houston, Houston/USA; ¹ Department of Pathology, Weill-Cornell Medical Center, New York/USA; ² Dipartimento di Scienze Cliniche e Biologiche, Università degli Studi di Torino, Turin/I;

³ Innere Medizin I, Sektion Nephrologie, Zentrum für Innere Medizin, Universitätsklinikum Ulm, Ulm;

⁴ Department of Pediatric Nephrology, Amalia Childrens Hospital, Radboud University Medical Center, Nijmegen/NL; ⁵ Department of Pathology,

Amsterdam Infection & Immunity, Amsterdam Cardiovascular Sciences, Amsterdam UMC, Amsterdam/NL;

⁶ Biomedical Engineering & Medicine, University of Houston, Houston/USA;

⁷ Institut für Pathologie, Universität zu Köln, Köln

Objective: Thrombotic microangiopathies, comprising atypical hemolytic uremic syndrome (aHUS) and other diseases, can present with a broad clinical and nephropathological spectrum. On our way to finding an evidence-base for the nephropathological work-up of TMAs, we have chosen a machine-learning approach, thus eliminating the considerable lack of reproducibility of individual lesions in the three decisive compartments artery, arteriole and glomerulus with human experts. Here, we present our results towards an end-to-end diagnostic system.

Method: We collected 40 random biopsies with TMAs of various etiologies (including aHUS, hypertension-associated, systemic sclerosis, anti-phospholipid antibody syndrome and others) and 40 biopsies with Mimickers (differential diagnoses of TMA), including severe hypertensive nephropathy, necrotizing arteritis/arteriolitis, cryoglobulinemic vasculitis from the three participating centers Cologne, Weill-Cornell Medical Center, and Turin. Whole slide images (WSIs) from all four nephropathology stainings HE, PAS, trichrome and Jones

were included in this study. We developed an instance segmentation Mask-RCNN model with a Swin Transformer (t) backbone on tissue crops detected using a lightweight variant of the U-Net segmentation architecture. For the classification model we used our own MorphSet++ set transformer architecture to process batches of EfficientNetv2s-encoded tissue crops entered in three separate compartment channels. Batches were chosen with Monte Carlo sampling or using our own soft Markov Chain Monte Carlo (MCMC) approach. Results of the classification model are reported with 5-fold internal cross-validation.

Results: Segmentation performance measured as mIOU, mAP, mAR, mF1, mAS for artery reached .565, .739, .679, .704, .995, for arteriole .342, .531, .488, .490, .996, for glomeruli .818, .880, .919, .896, .993. Classification accuracy reached 90 % with no false positives for TMA.

Missed cases of TMA could be salvaged by an experienced nephropathologist on the display of decisive compartment crops, which were selected using model confidence averaged across each sampling iteration.

Conclusion: We have designed and trained architectures capable of segmenting decisive compartments and diagnosing TMAs on renal biopsy sections. This will enable automatic analysis of clinicopathological datasets with TMA in large cohorts. Our ultimate goal is to use large cohorts from collaborating institutions for weakly supervised, case-level-annotated training of diagnostic, prognostic and theranostic classifiers.

Experimentelle Nephrologie 1

P143

Live cell imaging-based in vitro system enable to characterize loss-of-surface transport as cellular patho-mechanism of mutated slit diaphragm protein Crumbs2

A. Möller-Kerutt; B. Schönhoff; E. Petri; H. Pavenstädt; T. Weide

Allg. Innere Medizin und Notaufnahme sowie Nieren- und Hochdruckkrankheiten und Rheumatologie, Medizinische Klinik D, Westfälische Wilhelms-Universität Münster, Münster

Objective: In contrast to the well-known slit diaphragm protein Nephhrin, Crumbs2 (CRB2) is a more recently identified component of the SD, which bridges the slit between podocyte foot processes with its long extracellular domain (1224 amino acids). Several point mutations of these SD proteins are linked to steroid-resistant nephrotic syndrome and show impaired protein processing from the ER towards the cell surface. Thereby, glycosylation is a central post-translation modification needed for proper folding and processing for both proteins. However, in contrast to Nephhrin mutations, for CRB2 mutations less is known about the cellular patho-mechanism. Here, we tried to characterize novel CRB2 mutants with pathologic potential in a cell-culture based *in vitro* system.

Method: We used HEK293T cells stable expressing BFP-CAAX-signal at the plasma membrane (PM) and transiently expressed GFP-tagged CRB2 wildtype and CRB2 variants with putative pathogenic potential. Using live cell imaging, we analyzed intracellular CRB2 localization

after 48 h of expression and quantified the degree of PM localization of CRB2-GFP signal. In addition, we tested the impact of cellular ER stress induced by chemicals or starvation on the transport of CRB2 wildtype protein.

Results: GFP labeled CRB2 wildtype reference and benign variants are correctly transported via the ER towards the PM. In contrast, CRB2 mutants linked to SRNS like CRB2 C629S, retain predominantly inside the ER. Compared to the wildtype (over 85 %) in most missense mutations only 10–15 % of the cells show any CRB2 signal at the PM. In co-localization analyses, the mutated GFP-CRB2 variants did not show a positive correlation with the blue labeled PM. However, we also found differences between the mutants in their degree of PM localization, which might indicate for differences in pathologic severity. In addition, vice versa, first approaches show that induction of ER stress inhibits the correct transport of CRB2 wildtype protein to the PM.

Conclusion: Our *in vitro* cell culture system based on HEK293T BFP-CAAX cells is well suited to characterize membrane localization of CRB2-GFP variants and thereby their pathologic potential. Proper processing in the ER and ER stress might be so far underestimated injury factors in podocytopathies of SD proteins.

P144

Die Rolle von NK Zellen bei der Clearance seneszenten Tubuluszellen

N. D. Funk; I. Sörensen-Zender; V. C. Wulfmeyer; J. Sinning; H. Haller; K. M. Schmidt-Ott; S. Halle¹; R. Schmitt

Klinik für Nieren- und Hochdruck-erkrankungen, Zentrum für Innere Medizin, Medizinische Hochschule Hannover, Hannover; ¹ Institut für Immunologie, Medizinische Hochschule Hannover, Hannover

Hintergrund: Die Akkumulation seneszenten Zellen trägt zur Progression chronischer Nierenerkrankungen bei. Die natürliche Clearance seneszenten Zellen durch das Immunsystem ist unter bestimmten Bedingungen nicht suffizient, sodass sich weitere seneszente Zellen anhäufen. Zielsetzung des Projektes ist es, die Clearance von seneszenten Tubuluszellen durch NK Zellen darzustellen und diese zu modulieren.

Methode: Nieren aus männlichen C57Bl/6J WT und Perforin-defizienten Mäusen dienten zur Herstellung primärer epithelialer Tubuluszellkulturen (PTEC). Durch Bestrahlung wurden diese in eine synchronisierte Seneszenz versetzt und nach viertägiger Ko-Kultur mit murinen NK Zellen (Ratio 1:10) analysiert. Read-out für die Clearance seneszenten Zellen: Änderung der Zellzahl (DAPI Färbung), Senescence-Associated- β -Galactosidase Färbung, NK Zell-Clusterbildung und die Expression von Seneszenz-Marker-Genen. Durch die Hinzugabe exogener Faktoren wurde die NK Zellfunktion moduliert und mit dem Standardexperiment hinsichtlich der Effektivität der Clearance verglichen.

Ergebnisse: Es konnte gezeigt werden, dass NK Zellen einen robusten senolytischen Effekt auf seneszente PTEC ausüben. Im Vergleich zu nicht-seneszenten PTEC war die NK Zell-Clusterbildung um die seneszenten PTEC signifikant vermehrt. Die senolytische Aktivität ging mit einer signifikanten Reduktion der

Zellzahl und Sa- β -Gal Färbung im Vergleich zur Kontrollgruppe einher. Im Gegensatz dazu war keine Senolyse bei NK Zellen von Perforin-defizienten Mäusen erkennbar, was auf einen Perforin-abhängigen Mechanismus hindeutet. Mehrere mit NK Zellen interagierende Liganden waren auf seneszenten PTEC im Vergleich zu nicht-seneszenten Zellen überexprimiert. Durch die Zugabe des NK Zell Aktivators Interleukin 2 konnte eine verstärkte Senolyse gezeigt werden, während bei den Interleukinen 12 und 15 keine Unterschiede im Vergleich zur unbehandelten Gruppe sichtbar wurden.

Zusammenfassung: Unsere Resultate geben Einblick in Mechanismen der NK Zell-abhängigen Elimination seneszenten Tubuluszellen. Diese Daten können als Basis zur Etablierung NK Zell-abhängiger Strategien zur Reduktion der renalen Seneszenzlast in vivo Anwendung finden.

P145

Hochphosphatdiät führt bei Mäusen zur Stat3/Kim-1-vermittelten Makrophagen-rekrutierung und progredienten tubulären Schädigung und Fibrose

B. Richter; T. Kapanadze¹; N. Weingärtner; I. Vogt; A. Grund; J. Schmitz²; J. H. Bräsen²; F. Limbourg¹; D. Haffner; M. Leifheit-Nestler

Klinik für Pädiatrische Nieren-, Leber- und Stoffwechselerkrankungen, Zentrum für Kinder- und Jugendmedizin, Medizinische Hochschule Hannover, Hannover; ¹ Klinik für Nieren- und Hochdruckerkrankungen, Zentrum für Innere Medizin, Medizinische Hochschule Hannover, Hannover; ² Nephro-pathologie, Institut für Pathologie, Medizinische Hochschule Hannover, Hannover

Hintergrund: Eine hohe diätetische Phosphataufnahme ist in der Allgemeinbevölkerung mit einer erhöhten Gesamt- und kardiovaskulären Mortalität, einem erhöhten Risiko für Typ-2 Diabetes und vorzeitiger Alterung assoziiert. Die renalen Effekte einer chronischen Hochphosphatdiät (HPD) für gesunde Individuen sind unklar.

Methode: C57BL/6N-Mäuse erhielten über den Zeitraum von 1–6 Monaten eine 2 % HPD oder 0,8 % Normalphosphatdiät (NPD). Die Entwicklung einer Nierenschädigung und Parameter der Phosphathomöostase wurden zeitabhängig untersucht und zugrundeliegende molekulare Mechanismen in HK-2-Zellen verifiziert.

Ergebnisse: Die HPD führte bei den Mäusen trotz erhöhten Plasmawerten von FGF23 und PTH und Hyperphosphaturie zu einer Hyperphosphatämie im Vergleich zur NPD. Histologische Analysen zeigten unter HPD beginnend mit Monat 2 eine Schädigung des renalen proximalen Tubulus (PT), die ab Monat 5 rasch voranschritt und mit renaler interstitieller Fibrose verbunden war. Die Expression des Schädigungsmarkers Kim-1 stieg bereits nach Monat 1 signifikant an und kumulierte nach 6 Monaten. Die Kim-1-Synthese war signifikant assoziiert mit dem tubulären Schädigungsgrad, der renalen Fibrose und der Anzahl an pStat3⁺ PT Epithelzellen. Immunfluoreszenzfärbungen zeigten eine erhöhte Synthese von MCP-1 im PT von Mäusen auf HPD. In Mäusen auf HPD fanden wir eine erhöhte MCP-1-Expression nach 3, 5 und 6 Monaten, welche mit der Kim-1-Expression assoziiert war, was auf eine Interaktion zwischen dem pStat3/Kim-1-Signalweg

und MCP-1 hindeutet. Histologisch zeigte sich eine vermehrte Akkumulation von F4/80⁺-Makrophagen um die PT-Läsionen in Mäusen ab 3 Monaten nach HPD-Gabe. Dies wurde quantitativ mittels Durchflusszytometrie bestätigt. Die Makrophagenanzahl korrelierte mit der erhöhten MCP-1-Synthese und dem tubulären Schädigungsgrad. In HK-2-Zellen führte die Stimulation mit FGF23 oder Phosphat, nicht aber PTH, zur Aktivierung von Stat3, während nur Phosphat konzentrationsabhängig die mRNA-Expression von Kim-1- und MCP-1 induzierte.

Zusammenfassung: Unsere Daten zeigen, dass bei gesunden Mäusen eine HPD zur progredienten Schädigung des proximalen Tubulus und interstitiellen Fibrose führt, die wahrscheinlich über den Stat3/Kim-1-Signalweg und vermehrter Makrophageneinwanderung vermittelt wird. Analog dazu könnte übermäßige Phosphataufnahme langfristig auch beim Menschen zur Nierenschädigung führen.

P146

The fibrogenic response with kidney injury in the glomerular and tubulointerstitial compartment follows a YB-1/PAI-1/MMP-2 axis

S. Brandt; A. Bernhardt; S. Häberer; K. Wolters; F. Gebringer; C. Reichardt; R. Geffers¹; J. A. Lindquist; P. R. Mertens
Klinik für Nieren- und Hochdruckkrankheiten, Diabetologie und Endokrinologie, Universitätsklinikum, Otto-von-Guericke-Universität Magdeburg, Magdeburg; ¹ Helmholtz Center für Infektionsbiologie, Technische Universität Braunschweig, Braunschweig

Objective: Extracellular matrix (ECM) is a three-dimensional

protein network that gives structure to the cells and tissues of the body. Accumulation of ECM is an essential feature of tissue repair, however, a dysregulated accumulation leads to organ fibrosis. Recently, the cold shock domain protein Y-box binding protein-1 (*Ybx1*/YB-1) was demonstrated to be a driving factor in kidney and liver fibrosis and immune cell infiltration. YB-1 influences the transcription and translation of many genes (e.g. *Col1a1*, *Mmp2*, *Tgfb1*) via its ability to bind single stranded DNA or RNA. Here, we analyzed for the first time the YB-1-dependent fibrogenic signature.

Method: We used inducible whole body *Ybx1*-deficient mice (*Ybx1*^{ΔRosaCreERT}) and mice selectively lacking YB-1 in myeloid cells (*Ybx1*^{ΔLysMCre}) to explore YB-1's contribution to kidney fibrosis induced by tubular dilation (unilateral ureteral obstruction, UUO). Whole kidney transcriptome analysis, immune histochemistry and histology were performed. Functional analyses include matrix degradation assays, primary tubular cell challenges with TNFα and TGFβ followed by analysis of intracellular signaling, NF-κB activation, pro-survival, and apoptotic cell death gene signatures, ER-stress regulation as well as cell survival assays.

Results: YB-1 confers pathological changes in a pro-fibrotic extracellular matrix composition. In diseased *Ybx1*-deficient kidneys the matrix composition shows enhanced basement membrane components (e.g. type IV collagen and nephronectin) and a reduced interstitial matrix (e.g. collagens I, III, VIII; fibrillin; periostin). Functionally we linked the YB-1-dependent fibrogenic response to an unbalanced matrix production and degradation

that is caused by YAP/TAZ signaling. Furthermore, tubular cell survival is favored in *Ybx1*-deficient animals following UUO. *In vitro* assays demonstrate that the dampened fibrogenic response in *Ybx1*-deficient mice is linked to an altered ER-stress response.

Conclusion: Cold shock protein expression in tubular cells directs the PAI-1-MMP-2 profibrogenic signature and targets kidney injury for organ fibrosis.

P147

Nephron-specific depletion of the small GTPase Rab7 leads to a renal cystic phenotype in mice

K. Vöing; D. A. Braun; T. Weide¹; H. Pavenstädt¹

Molekulare Nephrologie, Medizinische Klinik D, Westfälische Wilhelms-Universität Münster, Münster;

¹ Allg. Innere Medizin und Notaufnahme sowie Nieren- und Hochdruckkrankheiten und Rheumatologie, Medizinische Klinik D, Westfälische Wilhelms-Universität Münster, Münster

Objective: The small GTPase Rab7 is mainly known as a key regulator of endolysosomal trafficking and late endosomal maturation processes. Previous studies have shown that these pathways are required for maintenance of renal glomeruli. In this work, we aimed at investigating the role of disrupted endolysosomal trafficking in renal development and nephron patterning.

Method: We generated a nephron-specific *Rab7* knockout mice line by applying the Cre/loxP system under the *Six2* promotor. Two timepoints were analyzed with regards to phenotype, disease status, and disease progression (2 and 8 weeks). For phenotyping, we

screened for proteinuria and used histological staining, transmission electron microscopy and immunofluorescence. QPCR and proteome analysis were used for the investigating of dysregulated pathways. Further, we used a canine tubulus *Rab7* knockout cell line, created by the crispr/cas9 system, as an *in vitro* model for further examinations and to confirm *in vivo* findings.

Results: Biallelic nephron-specific *Rab7* deletion in mice led to a severe early-onset phenotype affecting the glomerulus and tubular system. We observed polycystic kidneys in 2-week-old mice while kidneys were not enlarged overall (unlike ADPKD). At this timepoint, we did not detect pathogenic effects on the filtration barrier. 8-week-old mice, on the other hand, exhibited severe proteinuria, reduced weight and size and showed global or partial glomerulosclerosis (FSGS-like features). As seen in 2-week-old animals, there were tubular cysts with irregular epithelium and a sclerotic tubular basement membrane. In addition, there was interstitial inflammation and fibrosis. *In vitro* studies of *Rab7* depleted canine tubule cells revealed enlarged lysosomal structures and reduced growth in 2D cell culture as well as a multilumen phenotype in 3D cell culture.

Conclusion: Renal cysts *in vivo* and multilumen formation in 3D cell culture hint at a ciliopathy, polarity defects, or insufficient cell-cell contacts. We hypothesize that *Rab7* depletion interferes with at least one of those processes. Furthermore, we assume that *Rab7* functions in early kidney development, because cysts were observed at an early timepoint and did not increase

in quantity over time. Further studies will deepen the understanding of *Rab7*-related defects in nephron development and renal disease.

P148

Antigen cross-presentation by murine proximal tubular epithelial cells induces cytotoxic and inflammatory CD8⁺ T cells

A. Linke; H. Cicek; A. Müller; C. Meyer-Schwesinger¹; S. Melderis²; T. Wiech³; C. Wegscheid; J. Ridder; O. M. Steinmetz²; L. Diehl; G. Tiegs; K. Neumann
Institut für Experimentelle Immunologie und Hepatologie, III. Medizinische Klinik, Universitätsklinikum Hamburg-Eppendorf, Hamburg; ¹Institut für Zelluläre und Integrative Physiologie, Universitätsklinikum Hamburg-Eppendorf, Hamburg; ²Nephrologie/Rheumatologie und Endokrinologie/Diabetologie, III. Medizinische Klinik, Universitätsklinikum Hamburg-Eppendorf, Hamburg; ³Institut für Pathologie, Sektion Nephropathologie, Zentrum für Diagnostik, Universitätsklinikum Hamburg-Eppendorf, Hamburg

Objective: Immune-mediated glomerular diseases are characterized by infiltration of T cells, which accumulate in the periglomerular space and tubulointerstitium in close contact to proximal and distal tubuli. Recent studies described proximal tubular epithelial cells (PTECs) as renal non-professional antigen-presenting cells, that stimulate CD4⁺ T-cell activation. Whether PTECs have the potential to induce activation of CD8⁺ T cells is less clear. In this study, we aimed at investigating the capacity of PTECs for antigen cross-presentation, thereby modulating CD8⁺ T-cell responses.

Method: Expression of markers associated with antigen

cross-presentation was analyzed in PTECs by quantitative RT-PCR and Western blot analysis. PTECs and ovalbumin (OVA)-specific naïve CD8⁺ T cells were co-cultured in presence of OVA protein. Phenotype of PTEC-activated CD8⁺ T cells was determined by flow cytometry. A cytotoxicity assay was performed to assess the cytotoxic potential of PTEC-activated CD8⁺ T cells. Wild-type and *Cd8a*^{-/-} mice received pristane to induce lupus nephritis and were analyzed 9 months later. Lupus-prone MRL-*lpr* mice were analyzed at an age of 15 weeks. Histological analyses were performed to stain for apoptotic cells and cleaved caspase-3 in renal tissue.

Results: We showed that PTECs expressed proteins associated with cross-presentation, internalized soluble antigen via mannose receptor-mediated endocytosis and generated antigenic peptides by proteasomal degradation. PTECs induced an antigen-dependent CD8⁺ T-cell activation in presence of soluble antigen *in vitro*. PTEC-activated CD8⁺ T cells expressed granzyme B and exerted cytotoxic function by killing target cells. In murine lupus nephritis, CD8⁺ T cells localized in close contact to proximal tubuli. We determined enhanced apoptosis in tubular cells and particularly PTECs up-regulated expression of cleaved caspase-3. Interestingly, induction of apoptosis in the inflamed kidney was reduced in absence of CD8⁺ T cells.

Conclusion: PTECs have the capacity for antigen cross-presentation, thereby inducing cytotoxic CD8⁺ T cells *in vitro*, which might contribute to the pathology of immune-mediated glomerulonephritis.

P149**Hypoxie-induzierbare Faktoren stimulieren die Expression von CKD-assoziierten MUC1-Varianten in humanen renalen Tubuluszellen**

S. Naas; R. Krüger; K. X. Knaup;
S. Grampp; M. Schiffer; M. Wiesener;
J. Schödel

Medizinische Klinik 4, Nephrologie und
Hypertensiologie, Universitätsklinikum,
Friedrich-Alexander-Universität
Erlangen-Nürnberg, Erlangen

Hintergrund: Mehrere genetische Veränderungen im Mucin1-Gen (*MUC1*) prädisponieren Menschen für die Entwicklung einer chronischen Nierenerkrankung. Diese genetischen Varianten umfassen neben dem häufig vorkommenden Polymorphismus rs4072037, der das Spleißen der *MUC1*-mRNA verändert, auch äußerst selten auftretende, autosomal-dominant vererbte Mutationen. Diese Mutationen führen zur Expression eines zelltoxischen Frameshift-Proteins von *MUC1* (*MUC1*-fs), das eine autosomal-dominante tubulointerstitielle Nierenerkrankung (ADTKD-*MUC1*) verursacht. Darüber hinaus ist die Länge einer Region mit Tandemwiederholungen (VNTR) innerhalb des zweiten Exons des *MUC1*-Gens mit Markern der Nierenfunktion assoziiert. Die Regulationsmechanismen, die die Expression von *MUC1* in der Niere beeinflussen, sind bisher unzureichend definiert. **Methode:** Primäre renale Tubuluszellen wurden aus morphologisch gesundem Gewebe einer großen Anzahl von Tumornephrektomie-Präparaten oder aus dem Urin von ADTKD-*MUC1*-Patienten isoliert. Verschiedene pharmakologische Substanzen, die eine

Stabilisierung der Hypoxie-induzierbaren Transkriptionsfaktoren (HIFs) bewirken, sowie Hypoxie wurden verwendet, um die Wirkung von HIF auf die Expression von *MUC1* und dessen pathogene Varianten zu untersuchen. Die Expression von *MUC1* mRNA einschließlich Spleißvarianten wurde mittels qPCR oder RNA-Sequenzierung analysiert. Wildtyp-*MUC1*- und fs-Protein wurden durch Immunoblotting nachgewiesen.

Ergebnisse: Mithilfe eines Assays für Transposase-zugängliches Chromatin (ATAC-seq) sowie Chromatin-Immunpräzipitation DNA-Sequenzierung (ChIP-seq) identifizierten wir eine HIF-Bindestelle in der Promotorregion von *MUC1*, das die *MUC1*-Expression bei Stabilisierung von HIF induziert. HIF verstärkt nicht nur die mRNA-Expression von Wildtyp-*MUC1* sondern auch die der schädlichen Spleiß-, VNTR- und Frameshift-Varianten, wenn tubuläre Zellen Hypoxie oder HIF-Stabilisatoren ausgesetzt wurden.

Zusammenfassung: In dieser Studie zeigen wir eine funktionelle Verbindung zwischen der Regulation der *MUC1*-Expression und dem Hypoxie-induzierbaren Transkriptionsfaktor-Signalweg in menschlichen renalen Tubuluszellen. HIF induziert auch *MUC1* Risikovarianten, die zur Entstehung von Nierenerkrankungen führen. Vor dem Hintergrund der klinischen Zulassung von HIF-stabilisierenden Substanzen zur Behandlung der renalen Anämie sollten die Ergebnisse dieser Studie bei der Auswahl von Patienten mit bekannten *MUC1* Risikovarianten möglicherweise berücksichtigt werden.

P150**Alström Syndrom Protein 1 als neuer Regulator des Zellzyklus in Tubulusepithelzellen**

I.-K. Fehler; G. Nyamsuren; M. Zeisberg
Abteilung Nephrologie und Rheumatologie, Universitätsmedizin Göttingen,
Göttingen

Hintergrund: Fibrose ist die gemeinsame Endstrecke vieler chronischer Nierenerkrankungen, deshalb sind mechanistische Einblicke wichtig, um eine adäquate Therapie zu entwickeln. Das Alström Syndrom ist eine seltene Multisystemerkrankung mit Ausbildung von Multiorganfibrose und wird durch eine Genmutation im *ALMS1*-Gen verursacht. Deswegen basiert das Projekt auf der Annahme, dass das bessere Verständnis der *ALMS1*-Funktion wichtige Einblicke in Mechanismen der Fibrose liefern könnte. Während die meisten Studien aufgrund der Lokalisation des Gens im Basalkörper Assoziationen mit Zilien untersucht haben, basiert diese Studie auf der Hypothese, dass das Gen aufgrund der Lokalisation am Zentrosom eine Rolle bei der Zellzyklusregulation haben könnte.

Methode: Der Zellzyklus von humanen kidney-2-Zellen bzw. humanen Retinaepithelzellen (hRPE) wurde mittels Hunger- bzw. Thymidinblock synchronisiert und sowohl die Synchronisation als auch die Zellzyklusphasen mittels Hoechst-Färbung in der Durchflusszytometrie nachgewiesen. Die Proteinpiegel während der verschiedenen Zellzyklusphasen wurde durch Western Blots bzw. Immunfluoreszenzfärbungen untersucht. Des Weiteren wurden die Unterschiede in der Proliferation mittels Ki67-Immunfluoreszenzfärbung zwischen

im Hungerblock synchronisierten hRPE mit ALMS1-Knockdown und Kontrollzellen untersucht.

Ergebnisse: Die intrazelluläre ALMS1-Quantität ist abhängig von dem Zellzyklusstadium. Während der G1-Phase wird das ALMS1-Level mittels proteolytischer Degradation depletiert. Der Übergang zu G2-/S-/M-Phase ist mit erhöhten ALMS1-Levels assoziiert. Der Knockdown von ALMS1 verzögert in Tubulusepithelzellen den Wiedereintritt in den Zellzyklus.

Zusammenfassung: Unsere Ergebnisse zeigen, dass die Multiorganfibrose-Erkrankung Alström Syndrom mit einer Hemmung des Zellzyklus in Tubulusepithelzellen assoziiert ist. Unsere Ergebnisse weisen auf die Relevanz von der Zellzyklusregulation bei der Progression der Nierenfibrose hin.

P151

Tubular expression of cold shock DNA binding protein A negatively regulates mitochondrial biogenesis and thereby the extent of acute hypoxic kidney injury

C. Reichardt; A. Bernhardt; S. Brandt; S. Sleiman; S. Weinert¹; S. Kahlfuss²; A. Dudeck; B. Isermann³; J. A. Lindquist; P. R. Mertens
Klinik für Nieren- und Hochdruckkrankheiten, Diabetologie und Endokrinologie, Universitätsklinikum, Otto-von-Guericke-Universität Magdeburg, Magdeburg; ¹Klinik für Kardiologie, Universitätsklinikum, Otto-von-Guericke-Universität Magdeburg, Magdeburg; ²Institute of Molecular and Clinical Immunology, Otto-von-Guericke University Magdeburg, Magdeburg; ³Institut für Laboratoriumsmedizin, Klinische Chemie und Molekulare Diagnostik, Uniklinik Leipzig, Leipzig

Objective: DNA binding protein A (DbpA; Y-box binding protein-3, *Ybx3*) belongs to the cold shock protein superfamily with known influence on cell proliferation, transcription, translation and cell-cell communication. DbpA is ubiquitously expressed during development and downregulated following birth. Upregulated DbpA expression is observed in various kidney diseases. Whether DbpA plays a role during renal ischemia reperfusion injury (IRI) is unclear.

Method: Ischemia/reperfusion injury (IRI) *in vivo* as well as a hypoxia/reoxygenation (HR) *in vitro* model with primary tubular cells were established with mice harbouring a *Ybx3*^{+/+}, *Ybx3*^{+/-} or *Ybx3*^{-/-} genetic background and cells harvested thereof. Metabolism was assessed by Seahorse extracellular flux 96 Analyzer (Agilent Technologies). Western blotting, immunohistochemistry and flow-cytometry were carried out to quantify cellular damage, cell infiltration and kidney function.

Results: Contrary to our expectations due to developmental DbpA expression the tubular cell composition (that is principal and intercalating cell numbers, function, channel expression) was unaltered in genetically modified animals (*Ybx3*^{+/+}, *Ybx3*^{+/-} and *Ybx3*^{-/-} mice). Noteworthy, cell analyses revealed that most of the endogenous DbpA protein co-localizes with mitochondrial proteins in primary tubular epithelial cells. Mitochondrial function analyses indicated that the oxygen consumption rates were elevated in cells with *Ybx3*^{-/-} knockout. Furthermore, the expression of voltage-dependent anion-selective channel 1 (VDAC-1), that is located in the outer mitochondrial

membrane and the mitochondrial biogenesis marker nuclear respiratory factor 1 (NRF1) were increased in primary tubular epithelial cells with *Ybx3*^{-/-} knockout. *In vivo* *Ybx3*^{-/-} mice demonstrated a protection from acute hypoxia over 24 hours as well as 28 days. Cellular damage markers (NGAL) were lower following ischemia/reperfusion, cytokine/chemokine release was blunted, less immune cells infiltrated and kidney architecture was preserved in contrast to wildtype animals.

Conclusion: These findings indicate a prominent role of DbpA in cell metabolism, mitochondrial function and demonstrate the relevance of DbpA in maladaptive processes at the physiological filtration barrier of tubular structures.

P152

The CX3CL1/R1 axis limits acute tubulotoxic renal injury by guiding protective CD206+ MHC II+ M2a macrophages

A. Hassinger; A. M. C. Böhner; D. Klaus; M. Eichler; C. Meyer-Schwesinger¹; A. Effland²; S. Brähler³; U. I. Attenberger; C. Kurts
Institut für Experimentelle Immunologie, Medizinische Fakultät, Rheinische Friedrich-Wilhelms-Universität Bonn, Bonn; ¹Institut für Zelluläre und Integrative Physiologie, Universitätsklinikum Hamburg-Eppendorf, Hamburg; ²Institut für Angewandte Mathematik, Universität Bonn, Bonn; ³Nephrologie, Rheumatologie, Diabetologie und Allgemeine Innere Medizin, Klinik II für Innere Medizin, Universitätsklinikum Köln, Köln

Objective: The CX3CR1-L1-axis is known to play an important role in chronic kidney disease. Aristolochic acid nephropathy (AAN) is

a model for kidney tubular injury characterized by proximal tubular epithelial cell (PTEC) loss, tubular-interstitial immune cell infiltration and kidney fibrosis. We investigated the role of this immune cell axis with special emphasis on mononuclear phagocyte subsets and their impact in early AAN. **Method:** CX3CR1-knockout (KO) and wildtype mice were challenged with Aristolochic acid. We employed a low-calcium low-oxalate chow to minimize intrarenal crystal formation and inflammasome activation which was a confounding factor in several previous studies. We analyzed the kidneys with a variety of techniques encompassing Flow Cytometry, bulk-RNASeq, qPCR, ELISA and fluorescence imaging as well as Light-Sheet-Fluorescence microscopy. **Results:** We identified CX3CR1 as a protective chemokine receptor in acute kidney damage in AAN. CX3CR1-KO animals showed higher kidney damage parameters such

as KIM-1, serum creatinine and more severe PTEC loss. Mechanistically, this protection was mediated by recruitment of CX3CR1+ mononuclear-cells, namely M2a macrophages, which produced several potentially protective mediators as identified by RNASeq. **Conclusion:** Injured tubuli up-regulate CX3CL1 as a danger signal, which recruits protective CX3CR1+ M2a macrophages that attenuate kidney damage in AAN.

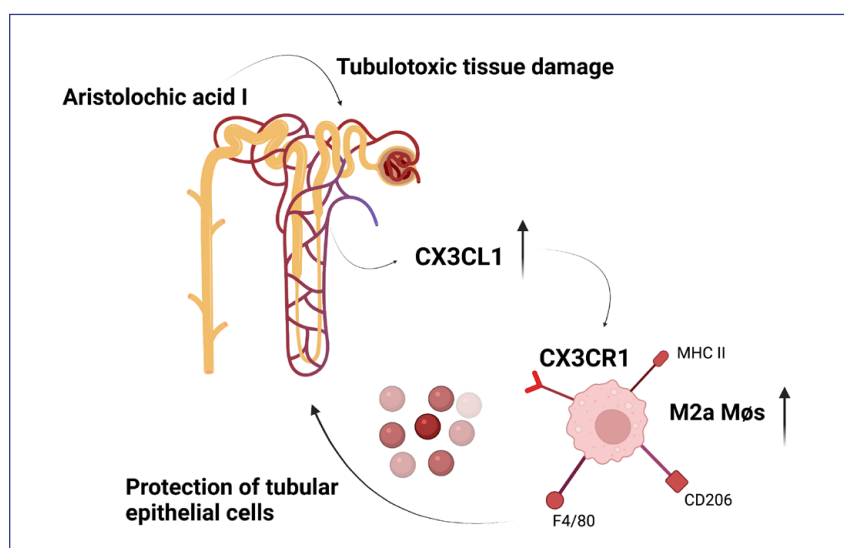
P153

Reduced ANCA-sialylation leads to increased NCGN

D. Lodka; A. Rousselle¹; S. Lucke¹; M. Ebert¹; M. Bieringer²; U. Schneider³; R. Kettritz¹; A. Schreiber
Medizinische Klinik mit Schwerpunkt Nephrologie und Internistische Intensivmedizin, Campus Charité Mitte, Charité – Universitätsmedizin Berlin, Berlin; ¹ECRC-Kooperation von MDC und Charité, Experimental and Clinical Research Center, Berlin; ²Klinik und Poliklinik für Kardiologie und

Nephrologie, HELIOS Klinikum Berlin-Buch, Berlin; ³Medizinische Klinik mit Schwerpunkt Rheumatologie und Klinische Immunologie, Campus Charité Mitte, Charité – Universitätsmedizin Berlin, Berlin

Objective: The glycosylation of IgG and especially of autoantibodies is an important regulator of antibody functionality. It is already described that the binding affinity to Fc receptors is affected by the IgG glycosylation status. Furthermore, it is known that the glycosylation pattern of ANCA is altered during active AAV. However, only few publications describe a direct relationship between glycosylation patterns and cellular functionality in AAV-relevant processes. We tested the hypothesis that B cells from active AAV patients are hypoglycosylated and that hypoglycosylated ANCA enhance neutrophil activation in vitro and lead to more severe MPO-ANCA induced NCGN. **Method:** The glycosylation status of B cells from patients compared to healthy controls was analyzed by flow cytometry. IgG from patients with active AAV were sialylated and desialylated in vitro. These modified antibodies were used in neutrophil stimulation assays to clarify the effect of sialylation on ROS production, NETs induction and IL-1b secretion. Anti-MPO NCGN was induced in WT mice by passive IgG transfer from MPO-immunized mice. The applied IgG were isolated from either MPO^{-/-} (normal IgG) or MPO^{-/-}/St6gal1^{-/-}-mice (hypoglycosylated IgG). Histological evaluation of kidney sections as well as flow cytometric analyses of blood and kidney cells were performed.



P152: Abb. 1

Results: Sialic acid, terminal galactose and fucose levels are about a third lower at B cells from active patients compared to healthy controls. The use of *in vitro* sialylated IgG from active patients resulted in about 64 %, 70 % and 55 % decreased ROS production, NETs formation and IL-1b secretion, respectively, compared to unmodified IgG. Finally, mice receiving hypo-sialylated IgG from MPO^{-/-}/St6gal1^{-/-}-mice had increased proportions of crescentic (20.9 % vs. 8.4 %) and necrotic (10.7 % vs. 4.27 %) glomeruli compared to mice administered IgG from MPO^{-/-}-mice, showing an increased disease course.

Conclusion: Glycosylation, especially sialylation of IgG, affects the severity of AAV disease. While increased IgG-sialylation had a protective effect as evidenced by reduced ROS production, NETs formation and IL-1b secretion, reduced sialic acid content resulted in aggravated ANCA-induced NCGN in a mouse model.

P154

Functional analysis of patient-derived rBAT variants with and without genetic aberration in the candidate modifier SLC7A13/AGT1

L. Pöschla

Medizinische Klinik m. S. Nephrologie und Internistische Intensivmedizin, Charité Campus Mitte, Charité – Universitätsmedizin Berlin, Berlin

Objective: Cystinuria (CU, OMIM 220100) is an inherited tubulopathy based on urinary dibasic amino acid wasting and consecutive cystine stone formation. Today, the great majority of CU patients shows pathogenic variation

in one of the two known disease genes *SLC3A1* and *SLC7A9*, encoding for the heterodimeric amino acid transporter rBAT/BAT1 in renal proximal tubules. In the S3 segment of murine proximal tubules a novel cystine transporter was reported lately, consisting of *SLC7A13/AGT1* and its partner *SLC3A1/rBAT*. Our aim is to evaluate the role of *SLC7A13/AGT1* as novel disease gene or genetic modifier in CU-patients with or without mutations in *SLC3A1/rBAT* or *SLC7A9/BAT1*.

Method: In addition to an initially sequenced discovery cohort (n = 132), we expanded genetic analyses to another 145 CU-patients in collaboration with EU-ROCYS (ERKNet-registry) using targeted next-generation sequencing (MiSeq Illumina) and multiplex ligation-dependent probe amplification (MLPA). Afterwards, transiently transfected cell systems were used to investigate complex formation of identified AGT1/BAT1/rBAT variations.

Results: In the extended CU-cohort (n = 277), we found patients harboring common and rare AGT1 missense variants of interest in addition to diagnostic rBAT or BAT1 variants. However, we did not identify CU-individuals with AGT1 variation only. Altogether, we found two siblings with the common AGT1 N45K variant and three unrelated patients with the common AGT1M452T variant. Moreover, we could identify a potentially new AGT1 variant I174P. Our *in-vitro* analysis showed a comparable efficiency in complex formation of AGT1-rBAT to BAT1-rBAT. In contrast, the complex of rBAT wildtype and patient-derived

AGT1 variants (N45K and M452T) showed functional impairments, indicated by decreased mature N-glycosylation, membrane insertion, and cystine uptake. Especially combinations of the most frequent patient-derived rBAT variation (M467T) with AGT1 variants further aggravated trafficking defects and reduced N-glycosylation.

Conclusion: In this study, we identified CU-patients with variants in AGT1 in combination with either rBAT or BAT1. Based on structural homology and *in vitro* functional analysis, we postulate that germline variation of AGT1 contributes to CU depending on folding, assembly, membrane insertion or uptake defects in concert with its partner rBAT.

P155

Bedeutung von alpha2 A-Adrenozeptoren bei renaler Fibrose und Inflammation

L. Hering; L. Pockardt; M. Rahman; S. A. Potthoff; L. C. Rump; J. Stegbauer
Klinik für Nephrologie, Universitätsklinikum, Heinrich-Heine-Universität Düsseldorf, Düsseldorf

Hintergrund: Sympathischer Stress trägt zur Progression renaler Entzündungsreaktionen und Fibrosierung bei. Präjunktionale α 2A-Adrenozeptoren (α 2A-AR) reduzieren sympathischer Neurotransmitterfreisetzung und schützen von Hypertonie-assoziiertem Nierenschaden. Auf der anderen Seite sind α 2A-AR auch an Immunzell-vermittelten Entzündungsreaktionen beteiligt, die zu Organdysfunktionen führen. Ziel der Studie ist die Beteiligung von α 2A-AR an pro-inflammatorischen und pro-fibrotischen Prozessen in der Niere zu untersuchen.

Methode: Zur Induktion einer tubulointerstitiellen Fibrose wurden α 2A-Adrenozeptor knock-out Mäuse (KO) sowie altersentsprechenden Wildtypen (WT) einer unilateralen Ureterobstruktion (UUO) unterzogen. 14 Tagen nach UUO wurde der Grad der renalen Entzündung, Fibrose und Immunantwort untersucht. Um zwischen der Wirkung präjunctionaler und postsynaptischer α 2A-AR zu unterscheiden, wurden bestrahlten (10 Gy) KOs Wildtyp-Knochenmark transplantiert, sodass der α 2A-AR ausschließlich auf Immunzellen exprimiert (KM-WT) war und vice versa (KM-WT). Letztendlich wurden murine Makrophagen aus dem KM in eine pro-inflammatorische M1 (LPS + IFN γ) polarisiert.

Ergebnisse: Die Expression von renalem Kollagen und Fibronectin war in WT im Vergleich zu KO signifikant erhöht, wodurch sich interessanterweise ein profibrotischer Einfluss des α 2A-AR auf die renale Fibrosierung ableiten lässt. Die Immunzellinfiltration und die renale Inflammation (iNOS, TNF α , IL-6) war ebenfalls signifikant in den UUO von WTs erhöht, was auf eine Beteiligung von α 2A-AR, exprimiert auf Immunzellen schließen lässt. In der Tat, die Entstehung von Nierenfibrose und die renale Immunantwort nach UUO war in KM-KOs signifikant im Vergleich zu KM-WTs abgeschwächt. Letztendlich zeigte sich, dass nach Polarisation in einen pro-inflammatorischen M1 (LPS + IFN γ) Phänotyp murine KO-Makrophagen weniger iNOS, IL-1 β , IL-6 und IL1R1 exprimieren als WT Makrophagen.

Zusammenfassung: Diese Ergebnisse, die im UUO geschädigten Mausmodell erhoben

wurden, sprechen für eine Relevanz des α 2A-AR, welcher einen proinflammatorischen Einfluss auf die Entstehung einer renalen Fibrose zu haben scheint.

Experimentelle Nephrologie 2

P156

YB-1 als Teil von neutrophilen extrazellulären Fallen (NETs) vermittelt Nierenschäden und organübergreifende Effekte

X. Liu; J. Wang; Y. Gu¹; Y. Gao; V. Jankowski²; N. Was³; L. K. Reiss; Y. Yiqin Shi; J. Cai¹; Y. Fang¹; N. Song; J. Floege; T. Ostendorf; X. Ding¹; U. Raffetseder

Medizinische Klinik II, Nephrologie und Klinische Immunologie, Universitätsklinikum, Rheinisch-Westfälische Technische Hochschule Aachen, Aachen;

¹ Nephrology, Affiliated First People's Hospital, Shanghai Jiaotong University, Shanghai/CN; ² Institut für Molekulare Herz-Kreislaufforschung, Universitätsklinikum, Rheinisch-Westfälische Technische Hochschule Aachen, Aachen;

³ Würzburg

Hintergrund: Eine der am häufigsten beobachteten postoperativen Komplikationen einer Operation am offenen Herzen ist die akute Nierenschädigung (AKI). Ein Hauptpathomechanismus ist hierbei die renale Ischämie aufgrund von Hypotonie, Hypoperfusion oder systemischer Entzündung. Die Früherkennung von Hochrisikopatienten könnte eine wirksame Therapie in einem reversiblen Stadium der AKI-Entwicklung ermöglichen.

Methode: In einer Kohorte herzchirurgischer PatientInnen (24 h nach OP klassifiziert als Nicht-AKI- (n = 25) oder AKI-PatientInnen (n = 13)) wurden bei einem Teil

der Nicht-AKI- (n = 4) und AKI-PatientInnen (n = 6) Seren bereits vor AKI-Klassifikation (2, 6 und 24 h nach OP) auf *Neutrophil Extracellular Traps* (NETs) analysiert. In zwei AKI-Mausmodellen, die die renale Hypoperfusion während der Herz-OP nachahmen (bilaterale Ischämie/Reperfusion (I/R) und systemische Lipopolysaccharid (LPS)-Verabreichung), wurde ein neutralisierender Y-Box-Protein (YB)-1-Antikörper verabreicht. Der Einfluss von Hypoxie/NET-Bildung auf die YB-1-Funktion in Neutrophilen und Tubuluszellen sowie bei der Zell-Zellkommunikation wurde *in vitro* analysiert.

Ergebnisse: Nach Operation am offenen Herzen zeigten die AKI- im Vergleich zu Nicht-AKI-PatientInnen eine signifikant höhere Anzahl an Neutrophilen im Blut (AKI: $12,9 \pm 5,4 \times 10^9$ Zellen/IL, n = 13; Nicht-AKI: $10,1 \pm 2,9 \times 10^9$ Zellen/L, n = 25). Bei PatientInnen, die später AKI entwickelten, wurden innerhalb der ersten 24 Stunden erhöhte Serumspiegel von NET-Komponenten wie dsDNA, Histon 3 und YB-1 gefunden. Wir konnten zeigen, dass die NET-Bildung und Hypoxie die Freisetzung von YB-1 auslöst und als Mediator für Nierentubulusschäden fungiert. In beiden murinen AKI-Modellen reduzierte die prophylaktische Gabe eines YB-1-Antikörpers die tubuläre Schädigung signifikant (Schadensscore 1-4, LPS-Modell: IgG, $0,92 \pm 0,23$; anti-YB-1 $0,65 \pm 0,18$; I/R-Modell: IgG $2,42 \pm 0,23$; anti-YB-1 $1,86 \pm 0,44$, n = 5-8). Ebenfalls verbesserte ein therapeutischer YB-1-Antagonismus die Nierenschädigung im I/R-Modell (Schädigungsscore, IgG $3,03 \pm 0,31$; Anti-YB-1 $2,58 \pm 0,18$, n = 6).

Zusammenfassung: Zusammenfassend konnten wir YB-1 als Serumbestandteil bei akuter Nierenschädigung nach Herzchirurgie identifizieren sowie als Teil des NET-Bildungsprozesses. Die Blockade von extrazellulärem YB-1 verringert die durch Hypoxie und NET-Bildung induzierten Prozesse in der Niere und begrenzt AKI signifikant. YB-1 fungiert somit als integraler Mediator in der Niere und extrazellulär zudem bei organübergreifenden Prozessen. XL & JW Erstautor

P157

Gene expression of connexin 43 and pannexin 1 correlates with inflammation activity in experimental models of kidney fibrosis

L. Geis; C. Wagner¹

Abteilung für Nephrologie, Transplantationszentrum, Universitätsklinikum, Universität Regensburg, Regensburg; ¹ Institut für Physiologie, Klinik für Innere Medizin II, Universität Regensburg, Regensburg

Objective: Mammalian kidneys express up to 9 different connexins (Cx) and pannexins (Panx), which form either gap junctions or hemichannels. There is growing evidence that kidneys under inflammatory diseases display noticeable changes in Cx/Panx expression pattern, while their specific role in kidney disease is yet unclear and data is also partly incongruent. As a basis for a better understanding of the potential role of Cx or Panx for the development and progression of kidney disease we aimed to investigate Cx/Panx gene expression in experimental kidney fibrosis systematically.

Method: In two defined mouse models of kidney fibrosis, namely adenine nephropathy (AN) and unilateral ureter obstruction (UUO), we analyzed changes in gene expression of the renal expressed Cx/Panx subtypes by measuring mRNA abundance of whole kidney homogenates. For the Cx/Panx isoforms with significant changes in mRNA levels after induction of fibrosis we performed RNAscope hybridization with various cell marker mRNAs to specifically discriminate Cx/Panx mRNA expression with regard to cellular and zonal localization. Last we examined whether changes in Cx/Panx expression were reversible after cessation of adenine diet.

Results: In both fibrosis models we found clear downregulation of Cx26 mRNA expression (ca. 50 %), while gene expression of Cx43 (3–4 fold) as well as of Panx1 (10 fold) mRNA was significantly increased. Other connexins did not differ significantly from baseline. Attenuation of Cx26 mRNA could be attributed to a decline in expression by injured tubules and did not recover after stop of adenine diet. There was striking upregulation of Cx43 mRNA expression all over the kidney but with emphasis on the outer medulla. Co-expression of collagen I, PDGFR β and α SMA mRNA suggested Cx43 mRNA expression by medullary fibroblasts. Increase in Panx1 mRNA expression was predominantly associated with areas of tubular atrophy and interstitial fibrosis as hybridization signals matched injured tubules and the interstitium in between and also co-located with collagen I mRNA. Although fibrotic scars persisted, increases in Cx43 and Panx1 mRNA

were both reversible after cessation of the detrimental stimulus in AN.

Conclusion: We infer from our findings that experimental kidney fibrosis leads to persistent tubular damage with irreversible decline in Cx26 mRNA expression. Impressive upregulation of Cx43 and Panx1 gene expression however was reversible after cessation of adenine diet, therefore indicating an association with inflammation activity in fibrosis. Further work is demanded to investigate the specific role of Cx43 and Panx1 in fibrosis.

P158

DNA-binding protein A (DbpA) is actively secreted in a calcium and LPS dependent manner by rat mesangial (rMC) and melanoma cells and influences cell migration

G. Hoppstock; A. Bock; S. Stolz;

C. Zhu¹; J. A. Lindquist; P. R. Mertens
Klinik für Nieren- und Hochdruckkrankheiten, Diabetologie und Endokrinologie, Universitätsklinikum, Otto-von-Guericke-Universität Magdeburg, Magdeburg; ¹ University School of Medicine, Hangzhou/CN

Objective: DbpA is a member of the cold shock protein family with known functions in cancerogenesis and organ fibrosis. DbpA messenger RNA is translated and spliced into isoforms, denoted DbpA_a and DbpA_b. DbpA is present in serum and urine samples from patients with glomerular diseases. We hypothesized that DbpA may also be secreted and act as mediator of inflammation as well as cell proliferation. Thus, we asked whether i) DbpA is secreted by mesangial and/or cancer cells? ii) What stimuli induce DbpA secretion? iii) What is the underlying mechanism of

DbpA secretion? and iii) What are the extracellular effects of DbpA?

Method: To investigate the mechanism underlying DbpA secretion we stimulated rMC's with lipopolysaccharide (LPS) and different melanoma cell lines with ionomycin. Cell lysis and fractionation was performed and cell culture medium collected to quantify DbpA by ELISA, immunoblotting, immunofluorescence microscopy and exosome isolation. To look for the extracellular effect of DbpA_a and DbpA_b on cells a scratch assay was examined and recombinant proteins were added. In addition, receptor binding assays with TNF- α were set up in a FACS technique to demonstrate interaction of DbpA with TNF- α -binding to its receptor.

Results: Supernatants precipitated from LPS challenged mesangial cells showed prominent DbpA_a bands 8 h following stimulation. RMC and melanoma cells incubated with LPS or ionomycin and Brefeldin A and Monensin revealed no inhibition of secretion. This led us to hypothesize that DbpA is secreted through a non-classical secretion pathway. Immunofluorescence microscopy of rMC's transfected with GFP-tagged DbpA_a and DbpA_b expression plasmids showed vesicle formation 6 h after LPS exposure. Exosome preparations failed to detect DbpA as major component, however it was detected as non-vesicular protein in conditioned medium. Functional assays with both recombinant DbpA_a and DbpA_b demonstrated a pro-migratory effect cellular "wound closure" in a scratch assay. In an attempt to decipher an extracellular receptor we tested

different assays and thereby identified DbpA_a and DbpA_b as competitors of TNF- α to its receptors.

Conclusion: We identify for the first time that DbpA is an actively secreted protein through a non-classical pathway following LPS and Ionomycin challenge and that intracellular vesicle formation occurs while DbpA is released through rMC. In addition DbpA is secreted in a calcium dependent manner in melanoma and rMC. Extracellular effects are linked with cell migration and antagonism of TNF- α activities.

P159

The Dual Endothelin Angiotensin Receptor Antagonist (DEARA) Sparsentan Protects From Glomerular Hypercellularity and Associated Immune/Inflammatory Gene-Network-Activity in a Model of IgA Nephropathy

C. Reily; Z. Moldoveanu; T. Pramparo¹; S. Hall; L. Novak; R. Komers¹; C. Jenkinson¹; J. Novak
Departments of Microbiology and Medicine, University of Alabama, Birmingham/USA; ¹ Travere Therapeutics, Inc., San Diego/USA

Objective: IgA nephropathy (IgAN) is an autoimmune glomerulonephritis wherein immune complexes (IC) composed of galactose-deficient IgA1 (Gd-IgA1; autoantigen) and Gd-IgA1-specific IgG autoantibodies (AuAb) deposit in the glomeruli (gli) and cause injury. In a mouse model of IgAN induced by IC formed *in vitro* from human Gd-IgA1 and a recombinant AuAb, we used whole-kidney RNA-seq profiling to assess how Sparsentan (Sp) affects the gene expression of pathways dysregulated by IC.

Method: IC were injected intravenously into ~7-week-old nude mice every other day for a total of 6 doses (n = 5/group). Sp (60 or 120 mg/kg) or vehicle (V) were given by gavage once daily from the first day of IC injections. Positive control group mice were injected with IC and gavaged with V and the negative-control mice received only V. Kidney tissue for histopathology and RNAseq was harvested on day 12. RNAseq data, processed using DESeq2, identified differentially expressed genes. WGCNA was used for network-level profiling and to identify co-expressed genes associated with hypercellularity and Ki-67 positivity of gli. GSEA and X2K assessed changes at the pathway level and imputed correlated upstream cell-signaling networks. Pathway enrichment P-values were adjusted with FDR.

Results: Sp ameliorated IC-induced hypercellularity (P < 0.01) and Ki-67-positive gli (P < 0.05). WGCNA clustered genes into co-expressed modules associated with hypercellularity and Ki-67 positivity. GSEA-identified top-5 pathways were enriched for immune processes (FDR < 1×10^{-20}), the top being cytokine signaling pathways. The expression pattern of 95% of the top module genes dysregulated by IC, was corrected by Sp. X2K analysis revealed correlated expression of top hub genes, kinases MAPK14, GSK3B, CSNK2A1 (z-score < 1×10^{-12}) and transcription factors SP1 and RUNX1 (z-score < 0.05), highlighting the role of the ERK1/2-SP1 axis known to regulate cell proliferation.

Conclusion: In a mouse model of IgAN, kidney transcriptomics

revealed gene networks, enriched in immune/inflammatory functions, correlating with IC-induced hypercellularity. The top dysregulated genes were normalized by Sp and were linked to kinases and transcription factors with correlated functional activity. These data suggest a potential anti-inflammatory role for Sp in IgAN.

P160

To model early VHL-defective renal tubular lesions

S. Uebel; S. Naas; R. Krüger; M. Schiffer; J. Schödel

Medizinische Klinik 4, Nephrologie und Hypertensiologie, Universitätsklinikum, Friedrich-Alexander-Universität Erlangen-Nürnberg, Erlangen

Objective: Von Hippel

Lindau (VHL) disease is an inherited, autosomal dominant syndrome caused by mutations of the *VHL* tumor suppressor gene which predispose patients to develop clear cell renal carcinoma (ccRCC), which origin from the proximal tubule. ccRCC are characterized by unrestricted action of hypoxia-inducible transcription factors (HIF). Though progressed stages of ccRCC have been analyzed extensively, early alterations that shape tumor development are incompletely understood. Loss of function of the second *VHL* allele precedes detection of tumors by many years opening a wide window for therapeutic interventions.

Method: We isolated primary tubular cells from the urine (huPTC) of patients with VHL disease and introduced a second genetic hit in *VHL* and other ccRCC-associated genes by CRISPR-Cas9. Editing efficiency was determined by Sanger sequencing, expression

qPCR and immunoblot analyses. To test for epigenetic and transcriptomic changes upon complete loss of *VHL*, we conducted RNA-seq and ATAC-seq on a selection of clones of cells.

Results: In huPTC of a VHL patient carrying a complete deletion of exons two and three on one allele of the *VHL* gene, we achieved a complete knockout of *VHL* in two independent clones of cells using CRISPR-Cas9. Loss of *VHL* led to increased HIF protein comparable to HIF protein levels in the ccRCC cell line RCC4. Functionality of the HIF pathway was confirmed by detecting increased mRNA levels of the HIF target genes *CA9* and *EGLN3*. ATAC-seq data of the knock-out cells showed remarkable differences in open chromatin regions when compared to VHL-competent control cells. In addition, we performed RNA-Seq analyses in lysates from these cells and defined transcriptomic changes in the cells upon VHL-loss. In order to model progression of these cells in tumor evolution, we used CRISPR-Cas9 to knock out additional ccRCC-associated genes. We currently phenotype and analyze these cells.

Conclusion: Loss of *VHL* in patient-derived huPTC results in activation of HIF. We detected epigenetic and transcriptomic alterations in VHL-knock out cells that might open an avenue into researching early tumor evolution in patients at high risk to develop renal cancer. Future analyses will include 3D models and sequential manipulation of important cancer genes to identify mechanisms of tumor development that might affect the HIF pathway and might be susceptible to early therapy.

P161

Entstehung tertiärer lymphoider Strukturen im Rahmen einer Hochphosphatdiät-induzierten Nierenschädigung in gesunden Mäusen

N. Weingärtner; B. Richter; S. Walter; I. Vogt; T. Kapanadze¹; F. Limbourg¹; D. Haffner; M. Leifheit-Nestler
Klinik für Pädiatrische Nieren-, Leber- und Stoffwechselerkrankungen, Zentrum für Kinder- und Jugendmedizin, Medizinische Hochschule Hannover, Hannover; ¹ Klinik für Nieren- und Hochdruckerkrankungen, Zentrum für Innere Medizin, Medizinische Hochschule Hannover, Hannover

Hintergrund: Tertiäre lymphoide Strukturen (TLS) sind Immunzell-aggregate, welche im nicht lymphatischen Gewebe durch verschiedene Stimuli, wie chronische Inflammation entstehen. In ihren Grundfunktionen ähneln sie den sekundären lymphatischen Organen und können adaptive Immunantworten initiieren. Die Entwicklung von TLS wurden bereits bei Autoimmunerkrankungen der Niere wie Lupusnephritis, membranöser Glomerulonephritis oder IgA-Nephritis beschrieben, ihre genaue Herkunft und Funktionsweise ist jedoch unklar. Seit kurzem wird die Rolle von vaskulären Endothelzellen bei der Initiierung von TLS diskutiert. In dem vorliegenden Projekt identifizieren wir erstmals eine chronisch hohe Phosphatlast als Trigger für die Entstehung von renalen TLS in Mäusen.

Methode: Männliche C57BL/6N Mäuse wurden für 1–6 Monate auf eine 0,8 % Normalphosphatdiät (NPD) oder eine 2 % Hochphosphatdiät (HPD) gesetzt und die Entstehung von TLS im Nierengewebe histologisch und mittels

FACS- und Genexpressionsanalysen sowie Zytokinarrays charakterisiert.

Ergebnisse: Bereits nach 2 Monaten bildeten sich in den Nieren der HPD-Tiere größere Immunsammlungen. Parallel dazu waren die renalen mRNA-Level von venösen Markern und Zelladhäsionsmolekülen signifikant erhöht. Nach 3 Monaten HPD-Gabe wurden erstmals ausgeprägte TLS nachgewiesen, welche zu späteren Zeitpunkten bei allen Mäusen perivaskulär in der renalen kortikomedullären Zone und Nierenrinde angelagert waren. Histologischen Färbungen und FACS-Analysen zeigten eine signifikante Zunahme von CD45⁺B-Zellen und CD3⁺T-Zellen in TLS ab 3 Monaten HPD, dabei nahmen CD3⁺CD8⁺ T-Zellen den größten Anteil ein. Weiterhin zeigte sich ab diesem Zeitpunkt eine vermehrte Ansammlung von Kollagen und Podoplanin⁺ fibroblastischen retikulären Zellnetzwerken sowie LYVE⁺Lymphgefäßen und Cxcr4⁺ Zellen. Randständig am TLS waren zusätzlich vermehrt Makrophagen vertreten. In Clustern proliferierende B-Zellen, der Nachweis von Plasmazellen und einer erhöhten IgG-Expression weisen ab Monat 4 auf fortgeschrittene TLS, induziert durch HPD, hin. Auch die Induktion des für die Rekrutierung und Differenzierung von B-Zellen wichtigen Zytokin Cxcl13 konnte histologisch, auf mRNA-Ebene und im Zytokinarray nachgewiesen werden.

Zusammenfassung: Unsere Ergebnisse zeigen, dass allein eine chronisch erhöhte Phosphataufnahme zu einer de novo Formation von voll ausgereiften perivaskulären TLS in Nieren von Mäusen führt, dessen Bedeutung in weiteren Studien näher untersucht werden muss.

P162

FRMD3/Protein 4.1O splice variants regulate Hippo signaling and cell migration

*E. Königshausen; T. Reisewitz; L. Matten; T.E. Vienken; T. Wiech¹; L.C. Rump; L. Sellin
Klinik für Nephrologie, Universitätsklinikum, Heinrich-Heine-Universität Düsseldorf, Düsseldorf; ¹Institut für Pathologie, Sektion Nephropathologie, Zentrum für Diagnostik, Universitätsklinikum Hamburg-Eppendorf, Hamburg*

Objective: FRMD3 has been identified as a candidate gene for diabetic nephropathy and encodes for protein 4.1O. So far, different protein 4.1O splice variants have been identified. The molecular function of these splice variants is unknown. In diabetic kidney disease Hippo signaling (key effectors Yes-associated kinase (YAP) and its paralogue TAZ) is increased. Unphosphorylated YAP/TAZ translocates into the nucleus and activates target genes via different transcription factors (e.g. c-myc). Phosphorylated YAP/TAZ remains within the cytoplasm and is degraded. Activation of YAP/TAZ is increased by Myosin light chain kinase (MLCK). C-myc, YAP/TAZ and growth factors, e.g. EGF, have been shown to promote cell migration.

Method: Human kidney biopsy samples from healthy and diabetic patients were stained for protein 4.1O with immunohistochemistry. Clinical characteristics and laboratory findings were documented. HEK293T cells were stimulated with low (5 mmol/l), high (25 mmol/l) glucose concentrations or an osmotic control (5 mmol/l glucose + 19,5 mmol/l mannitol). RNA was isolated and PCR performed. Using

a c-myc reporter assay we investigated the influence of protein 4.1O. HEK293T cells expressed protein 4.1O splice variants or the control and were stimulated with low, high glucose or mannitol. After cell lysis, western blot was performed for phospho-YAP 397, myosin light chain (MLC), phospho-MLC S-19 and actin. Human podocytes were stably transduced with 4.1O splice variants. For migration assays, human podocytes were stimulated with 10 % FCS or EGF 10 mg/ml.

Results: Protein 4.1O expression is detected in healthy human glomeruli by immunohistochemistry. In diabetic patients with CKD stage 3b to 5 and gross proteinuria protein 4.1O expression seems to be increased in podocytes. High glucose but not its osmotic control leads to enhanced transcription of FRMD3. Under high glucose condition protein 4.1O significantly increases YAP phosphorylation. This effect is abrogated if a splice variant lacking a c-terminal domain is expressed. In line with this finding, protein 4.1O decreases c-myc transactivation. MLC phosphorylation is not altered by 4.1O splice variants in high, low glucose or mannitol. Protein 4.1O (lacking the FERM domain and a c-terminal domain) reduces podocyte migration after EGF stimulation compared to control.

Conclusion: Expression of protein 4.1O is increased in human diabetic kidney disease and under high glucose conditions. Protein 4.1O splice variants have differential effects on c-myc transactivation, YAP/TAZ activation and migration. This improved understanding of protein 4.1O splice variant function helps to better understand its role in diabetic nephropathy.

P163**Calorie restriction ameliorates DNA damage-induced FSGS in *Ercc1* pko mice**

A. M. Mandel; L. Blomberg¹;
F. Braun²; B. Schermer; B. Schumacher;
T. Benzing¹; C. Kurschat¹
Cologne Excellence Cluster on Cellular
Stress Responses in Aging-Associated
Diseases (CECAD), Universität zu
Köln, Köln; ¹ Nephrologie, Rheumatologie,
Diabetologie und Allgemeine
Innere Medizin, Universitätsklinikum Köln,
Köln; ² Nephrologie/Rheumatologie
und Endokrinologie/Diabetologie,
III. Medizinische Klinik, Universitäts-
klinikum Hamburg-Eppendorf,
Hamburg

Objective: Podocytes form the slit diaphragm and are as post-mitotic cells highly susceptible to cell stress. Their injury can lead to albuminuria and glomerulosclerosis. Consequently, we observed differential expression of nucleotide excision repair (NER) genes in glomeruli of patients with FSGS. To study NER in podocytes, we generated a podocyte-specific *Ercc1* knockout mouse (pko), which develops FSGS within weeks. In addition to increased DNA damage, these mice show mTORC1 activation. Inhibition of mTORC1 by rapamycin reduced glomerulosclerosis in this model. Here, we present a calorie restriction study with the *Ercc1* pko model as a different approach to modulate mTORC1 activity, aiming to ameliorate the renal phenotype. **Method:** Four week-old *Ercc1* pko mice were fed with 3.5 g standard diet once daily over 4 weeks (12.5 % calorie restriction; CR). Two control groups were fed once daily with 4 g (single-dose; SD) or *ad*

libitum (AL). Urine analysis was done using the Cayman (urinary) colorimetric assay kit (#500701) and the mouse albumin ELISA quantitation set (#E90-134; Bethyl). Kidneys were analyzed histologically by PAS staining. Glomerular mTORC1 activity was assessed by immunofluorescence staining for downstream phosphorylated S6-ribosomal protein (pS6RP) and counterstaining with synaptopodin.

Results: During treatment, only AL mice gained weight. The amount of albuminuria increased significantly in all groups when comparing 4 weeks (start) vs. 8 weeks (end of treatment); CR mice developed significantly less albuminuria than mice of the AL group. Serum creatinine did not differ between groups at 8 weeks. Histological analysis of kidneys by PAS staining showed significantly less globally sclerotic glomeruli in the CR group, compared with the AL group. By quantifying the immunofluorescence signal for pS6RP, we detected less signal in glomeruli and podocyte-area of the CR group.

Conclusion: *Ercc1*-deficiency causes progeroid syndromes in humans and mice. Deleting *Ercc1* only in podocytes leads to glomerulosclerosis and early death. We previously observed activation of mTORC1 in the *Ercc1* pko model and could ameliorate disease progression by rapamycin-treatment. To study the role of mTORC1 in FSGS, we present a calorie restriction study as a well-established method to slow aging and to inhibit mTORC1 activation. Interestingly, four weeks of calorie restriction were sufficient to ameliorate disease progression, reflected by less albuminuria and less globally sclerosed glomeruli. Quantification

of immunofluorescence stainings confirmed the intended decrease of mTORC1 activity.

P164**Consensus draft of the mouse podocyteome**

A. Hutzfeldt; L. Bonin¹; M. Rinschen
Nephrologie/Rheumatologie und
Endokrinologie/Diabetologie,
III. Medizinische Klinik, Universitäts-
klinikum Hamburg-Eppendorf,
Hamburg; ¹ Laboratory of kidney omics
and metabolism, Aarhus University,
Aarhus/DK

Objective: Here, we aim to establish a common, simplified knowledgebase for the mouse “podocyte-ome” by integrating bulk RNA sequencing and bulk proteomics of sorted podocytes and single cell transcriptomics.

Method: Three datasets of each omics type from three different laboratories, respectively, were integrated, visualized and bioinformatically analyzed.

Results: The procedure sheds light on conserved processes of podocytes, but also on limitations and specific features of the used technologies. High expression of glycan GPI anchor synthesis and turnover, and retinol metabolism was identified as a relatively understudied feature of podocytes, while there are both podocyte-enriched and podocyte-depleted actin binding molecules. We compiled aggregated data in an application that illustrates the features of the dataset and allows for exploratory analyses through individual gene query of podocyte identity in absolute and relative quantification towards other glomerular cell types, keywords, GO-terms and gene set enrichments.

Conclusion: This consensus draft is a first step towards common molecular omics knowledge of kidney cells.

P165

Zyxin is essential for cell adhesion of podocytes exposed to mechanical stress

F. Kliewe; E. Hammer¹; T. Amling; J. Hollemann; C. Weber; K. Amann²; C. Daniel²; U. Völker¹; N. Endlich
Institut für Anatomie und Zellbiologie, Universitätsmedizin Greifswald, Greifswald; ¹ Interfakultäres Institut für Genetik und Funktionelle Genomforschung, Universität Greifswald, Greifswald; ² Institut für Nephropathologie, Universitätsklinikum, Friedrich-Alexander-Universität Erlangen-Nürnberg, Erlangen

Objective: Glomerular hypertension causes mechanical load on podocytes which often leads to podocyte detachment followed by a development of glomerulosclerosis. Although it is well known that podocytes are mechanosensitive, the mechanosensor is still unknown. Zyxin, a zinc-binding phosphoprotein, localized at focal adhesions as well as along the actin cytoskeleton, plays a key role in mechanotransduction and adhesion. Therefore, we hypothesized that zyxin is essential for the outside-in signaling of mechanical stressed podocytes.

Method: Mouse podocytes were cultured on silicone membranes that were connected to the stretch apparatus ("Stretchy", NIPOKA GmbH, Greifswald) for three days at 0.5 Hz and 5 % extension. To study the role of zyxin under mechanical stretch, zyxin was knocked out by CRISPR/Cas9 method. Cell lysates of control and zyxin knockout podocytes

were measured by LC-MS/MS and verified by qRT-PCR, Western blot and immunostaining. Biopsies of patients suffering from diabetic nephropathy were used to study the expression of zyxin *in vivo*.

Results: We found that zyxin which is highly expressed in cultured podocytes, co-localizes with F-actin as well as with the focal adhesion proteins talin, vinculin and paxillin. LC-MS/MS and Western blot analysis showed that a knockout of zyxin significantly reduced the expression of extracellular matrix proteins like nidogen, periostin and fibronectin together with its receptor, integrin $\alpha 5$. Quantification of immunostainings revealed that the size and localization of essential focal adhesion proteins significantly changed due to a knockout of zyxin. In addition, zyxin knockout podocytes showed an increased cell detachment after mechanical stress compared to control podocytes. Furthermore, we found a significant up-regulation of zyxin in biopsies of patients suffering from diabetic nephropathy, particularly in podocytes.

Conclusion: Zyxin plays an important role in podocyte adhesion under mechanical stress due to altered matrix expression.

P166

Die Rolle von MHC-II in der alternden murinen Niere

J. Sinning; N. D. Funk¹; I. Sörensen-Zender; V. C. Wulfmeyer; H. Haller; K. M. Schmidt-Ott; A. Melk; R. Schmitt
Klinik für Nieren- und Hochdruck-erkrankungen, Zentrum für Innere Medizin, Medizinische Hochschule Hannover, Hannover; ¹ Klinik für Pädiatrische Nieren-, Leber- und Stoffwechselerkrankungen, Zentrum für Kinder- und Jugendmedizin,

Medizinische Hochschule Hannover, Hannover

Hintergrund: Daten der letzten Jahre haben gezeigt, dass der Mechanismus der zellulären Seneszenz eine wichtige Rolle bei altersassoziierten Erkrankungen spielt. Vorarbeiten zeigen, dass insbesondere Tubulusepithelzellen, welche prozentual den größten Anteil der Niere ausmachen, im Alter und nach renaler Schädigung einer zunehmenden Seneszenzlast unterliegen. Zielsetzung des Projekts war es, auf Nieren- und Einzelzell-Ebene neue Markergene zu etablieren, um die Seneszenzentwicklung besser zu charakterisieren und mögliche Zielstrukturen für die Elimination seneszenten Zellen zu erarbeiten.

Methode: Zur Identifikation potentieller Kandidatengene wurden Nieren männlicher C57BL/6J-Mäuse unterschiedlichen Alters (3,12, 24 Monate; n = 3), sowie nicht-seneszente und mittels γ -Strahlung induzierte seneszente primäre Tubulusepithelzellen (PTEC), zur RNA-Sequenzierung aufbereitet. Potentielle Kandidatengene wurden mittels quantitativer PCR, In-Situ-Hybridisierung und anhand publizierter Datensätze validiert. Interventionell wurde der Zusammenhang zwischen den Kandidatengen und zellulärer Seneszenz durch pharmakologische Beeinflussung in PTEC überprüft.

Ergebnisse: Die RNA-Sequenzierung zeigte eine altersabhängig zunehmende Expression MHC-II-assoziiierter Gene in der Niere. Diese war nur teilweise auf die Infiltration von Entzündungszellen zurückzuführen. Entsprechende Transkripte ließen sich auch in Epithelzellen des proximalen Tubulus nachweisen. Real- und

Pseudotime-RNA-Sequenzierungs-Analysen ergaben, dass die Expression MHC-II-assoziiierter Gene zeitlich der Entwicklung zellulärer Seneszenz vorgeschaltet war. Interventionell zeigten senolytisch behandelte PTEC eine signifikante Reduktion des MHC-II-assoziierten Gens Cd74 sowie bekannter Seneszenztranskripte. Eine pharmakologische Stimulation bzw. Suppression des Cd74-Gens über den Liganden MIF (Macrophage Migration Inhibitory Factor) führte zu einer Regulation bekannter Seneszenztranskripte wie Cdkn2a.

Zusammenfassung: Die Expression MHC-II-assoziiierter Gene im Zusammenhang mit zellulärer Seneszenz konnte histologisch und funktionell gezeigt werden. Dies ist zum einen technisch in RNA-Einzelzell-Datensätzen relevant, da die Zunahme MHC-II-assoziiierter Genen im proximalen Tubulus zur Fehlannotation führen kann. Zum anderen stellt der prä-seneszente Anstieg von MHC-II-Genen im proximalen Tubulus eine neue potentielle Option für pharmakologische anti-Seneszenz Interventionen dar.

P167

Loss of TrkC in the nephron aggravates chronic kidney disease

C. Lepa; H. Pavenstädt; B. George
Allg. Innere Medizin und Notaufnahme sowie Nieren- und Hochdruckkrankheiten und Rheumatologie, Medizinische Klinik D, Westfälische Wilhelms-Universität Münster, Münster

Objective: Chronic kidney disease has a high prevalence in the Western world, but mechanisms are still incompletely understood. We showed that the neurotrophic tyrosine kinase receptor C (TrkC or

Ntrk3) known to be important for neurite outgrowth and actin-cytoskeletal dynamics in neurons is expressed in podocytes and in a tubular fraction consisting of cortical collecting duct and thick ascending loop in mice (Lepa et al. 2021). In podocytes, TrkC signals to the actin cytoskeleton and mediates migration (Gromnitsa et al. 2018). Loss of TrkC within the nephron of mice (TrkC-KO) results in proteinuria progressing to FSGS while the tubular cell compartment does not show histological alterations in aging mice (Lepa et al. 2021). However, TrkC is differentially expressed in tubuli of biopsy samples of CKD patients of different etiology (Cohen et al. 2002; Martini et al. 2014). This raises the question whether TrkC is important for tubulointerstitial integrity following kidney injury. To elucidate this, we performed an injury model on TrkC-KO mice resulting in tubulointerstitial damage.

Method: Three months old nephron-specific TrkC knockout (TrkC-KO) or littermate controls were fed a 0.2% adenine-enriched or a control-diet for one week. Kidney sections were evaluated by histology, electron microscopy and blood urea and creatinine were quantified.

Results: Adenine-enriched diet causes the precipitation of crystals, tubular injury, inflammation, and fibrosis thereby inducing CKD. Adenine-fed TrkC-KO mice lost more weight than control animals which received adenine diet. Blood urea nitrogen (BUN) was significantly more elevated in adenine-fed TrkC-KO animals compared to adenine-fed controls. Histology

revealed that adenine-fed animals presented with dilated tubules and sclerotic lesions within the kidney cortex which were more severe than in adenine-fed controls. Furthermore, we showed by immunofluorescence analysis that kidneys of adenine-fed TrkC-KO animals expressed more NF- κ B as a surrogate of inflammatory processes compared to adenine-fed controls.

Conclusion: Loss of TrkC in the nephron of mice aggravates adenine-induced CKD.

Experimentelle Nephrologie 3

P168

RAPGEF1 (C3 G) is essential for slit diaphragm integrity.

L. Stöveken; C. Lepa; A. Stöber; H. Pavenstädt; B. George
Allg. Innere Medizin und Notaufnahme sowie Nieren- und Hochdruckkrankheiten und Rheumatologie, Medizinische Klinik D, Westfälische Wilhelms-Universität Münster, Münster

Objective: Podocytes are essential for maintaining proper kidney filter function. Damage to podocytes causes remodelling of the actin cytoskeleton and foot process effacement resulting in proteinuria. Mechanisms leading to proteinuric kidney disease are poorly understood. The cell adhesion protein nephrin is essential for slit diaphragm integrity by building intercellular junctions between two neighbouring podocytes. Nephrin has signalling properties to the actin cytoskeleton of foot processes. We showed that nephrin signals from the slit diaphragm to focal adhesions *via* the small GTPase Rap1 and its activating factor C3G (Dlugos et al., 2019; Maywald et al., 2022). We now hypothesize

that C3G – like nephrin – is necessary for slit diaphragm integrity.

Method: To test our hypothesis, C57BL/6 C3G flox mice were crossed with C57BL/6 Six2-Cre transgenic mice to generate a C3G knockout in the metanephric mesenchyme. Proteinuria, renal histology and glomerular ultra-structure were analysed. Furthermore, we characterized the localization of slit diaphragm and focal adhesion components by immunofluorescence analysis.

Results: Nephron-specific C3G knockout (C3G-KO) mice developed proteinuria 4 to 6 weeks after birth. Ultrastructural analysis revealed foot process effacement in C3G-KO animals which progressed to focal segmental glomerulosclerosis. C3G-KO mice exhibited significant podocyte loss during disease progression. Immunofluorescence analyses with antibodies specific for the slit diaphragm markers nephrin, podocin, zonula occludens (ZO-1) and the focal adhesion protein talin revealed mislocalization of these proteins.

Conclusion: C3G is essential for an intact glomerular filtration barrier. C3G may play a role in anchoring podocytes to the basement membrane as C3G deficiency in the nephron results in podocyte loss.

P169

Alternative splicing in mechanically stretched podocytes as a model of glomerular hypertension

M. Francescapaola; F. Kliewe; E. Hammer¹; S. Ameling¹; O. Tsoy²; C. T. Lio²; J. Baumbach²; U. Völker¹; K. Endlich; N. Endlich
Institut für Anatomie und Zellbiologie, Universitätsmedizin Greifswald, Greifswald; ¹ Interfakultäres Institut für Genetik und Funktionelle Genomforschung, Universität

Greifswald, Greifswald; ² Institute for Computational Systems Biology, University of Hamburg, Hamburg

Objective: As part of the Sys_CARE research network (Systems Medicine Investigation of Alternative Splicing in Cardiac and Renal Diseases), we looked for alternative splicing events that play a role for the development of hypertension induced glomerulopathies.

Method: Differentiated murine podocytes were seeded on a flexible silicone membrane, and mechanically stretched using the *Stretchy* apparatus (NIPOKA GmbH, Greifswald). Cells were stretched for 3 days by an extension of 5 % (physiological stretch conditions) or 8 % (pathological stretch conditions) with a frequency of 0.5 Hz. The mRNA and proteins were isolated and analyzed using RNA-Seq and LC-MS/MS techniques. Gene ontology enrichment analysis for three ontologies (biological process, molecular function and cellular components) of proteomics data was performed to categorize differentially abundant proteins. RNA-Seq data was analyzed by Multivariate Analysis of Transcript Splicing (rMATS) and leafcutter.

Results: Proteomic analysis of cultured podocytes revealed different levels for 134 proteins (63 increased and 71 decreased) and 445 proteins (184 increased and 261 decreased) under physiological and pathological stretch conditions in comparison to unstretched condition. Interestingly, most of the proteins with decreased intensity upon stretch are cytoskeleton and actin-binding proteins. In contrast, the up-regulated proteins are more associated in clusters

affecting transcription and mRNA processing. To identify mRNAs that are the results of alternative splicing induced by mechanical stretch, RNA-Seq of stretched podocytes was performed. In total, over 1000 different splicing events were detected under physiological or pathological stretch conditions, including all types of alternative splicing events. Some candidates that showed an alternative splicing event and are also regulated on protein level after mechanical stretch, are podocyte specific, or show altered expression in glomerulopathies such as diabetic nephropathy. Examples are *Postn*, *Pkm*, *Actn1*, *Myl6*, *Serpinb1*, *Tmem214*, *Flna*.

Conclusion: Our data identified alternative splicing events in mechanical stretched podocytes that may be responsible for podocyte adhesion in cultured podocytes as well as in patients suffering from glomerular hypertension.

P170

TBC1D8B promotes nephrin endocytosis and is required for endosomal cargo processing in *Drosophila*.

J. Milosavljevic; C. Lempicki; K. Lang; L. L. Kampf; T. Hermle
Medizinische Klinik IV/ Abteilung Nephrologie, Universitätsklinikum, Albert-Ludwigs-Universität Freiburg, Freiburg

Objective: Mutations in *TBC1D8B* were recently identified as a monogenic cause of nephrotic syndrome. *TBC1D8B* interacts with nephrin and it was implicated as an inhibitory GAP protein for Rab11 which regulates endocytic recycling. However, the functional spectrum of *TBC1D8B* and its role in trafficking of

nephrin remains poorly understood and requires further investigation.

Method: We generated and analyzed a stable genetic deletion of fly *Tbc1d8b* via CRISPR/Cas9. We successfully introduced a c-terminal HA-tag into the *Tbc1d8b* locus using microhomology-mediated end joining. For overexpression of mouse Tbc1d8b-HA we further generated transgenic flies under control of GAL4/UAS. Endosomal cargo processing was assessed by sequential uptake of two tracers *ex vivo*.

Results: Germline expression of Cas9 and tandem Tbc1d8b-guide RNAs resulted in a stable genetic deletion spanning all functional domains while ending with a frameshift. Surprisingly, homozygous mutant animals were viable without any overt phenotype. However, analysis of the podocyte-like nephrocytes of these flies revealed mislocalization and partial loss of slit-diaphragm proteins with incomplete penetrance. This nephrocyte-restricted phenotype recapitulates the phenotype of human mutations that present exclusively with nephrotic syndrome. Overexpression of murine Tbc1d8b-HA in nephrocytes caused accumulation of endogenous fly nephrin in large vesicles while its binding partner Kirre (Neph1) was not affected. The vesicles containing fly nephrin co-localized with the late endosomal marker Rab7 and disappeared when silencing the early endosomal regulator Rab5. This suggests that mammalian Tbc1d8b specifically promotes nephrin endocytosis. To identify the endogenous subcellular localization of the fly Tbc1d8b we established a knock-in of a c-terminal HA-tag and noted partial co-localization with endosomal

markers including Rab7. To investigate the functional role in the endolysosomal pathway we tracked the fate of two tracers sequentially applied *ex vivo*. A background of both, stable and conditional deletion of Tbc1d8b was associated with defective cargo processing.

Conclusion: Our findings implicate novel functional roles of Tbc1d8b beyond endocytic recycling: promoting nephrin endocytosis and facilitating processing of endosomal cargo.

P171

A slit-diaphragm-associated protein network for dynamic control of renal filtration

M. Kocylowski; H. Aypek¹; W. Bildl; M. Helmstädter²; B. Dumoulin¹; S. Wittösch¹; L. Kühne²; U. Aukschun²; O. Kretz¹; B. Gaal; A. Kulik; A. Köttgen³; B. Göcmen²; J. Schwenk; U. Schulte; T.B. Huber¹; B. Fakler; F. Grammer¹

Institut für Physiologie, Universität Freiburg, Freiburg; ¹Nephrologie/Rheumatologie und Endokrinologie/Diabetologie, III. Medizinische Klinik, Universitätsklinikum Hamburg-Eppendorf, Hamburg; ²Medizinische Klinik IV/Abteilung Nephrologie, Universitätsklinikum, Albert-Ludwigs-Universität Freiburg, Freiburg; ³Medizin IV, Nephrologie und Institut für genetische Epidemiologie, Universitätsklinikum, Albert-Ludwigs-Universität Freiburg, Freiburg

Objective: The filtration of blood in the kidney which is crucial for mammalian life is determined by the slit-diaphragm (SD), a cell-cell junction between the foot processes of renal podocytes. Based on studies of structure and function the SD is thought to operate

as a final barrier or as a molecular sensor of renal filtration.

Method: For comprehensive and quantitative insight into the molecular composition of the rodent SD, we set out to perform multi-epitope affinity purifications with antibodies targeting the known core components Nephrin, Neph1 and Podocin. As a source material we used membrane fractions prepared from glomeruli of both rat and mouse kidney, where all core constituents were highly enriched. To gain functional insights podocyte specific inducible Nephrin, Neph1 and Podocin knockout mice as well as the drosophila nephrocyte system were used.

Results: Using high-resolution proteomic analysis of SDs affinity-isolated from rodent kidney, we show that the native SD is built from the junction-forming components Nephrin, Neph1 and Podocin and a co-assembled high-molecular weight network of proteins. The network constituents cover distinct classes of proteins including signaling receptors, kinases/phosphatases, transporters and scaffolds. Knockout or knockdown of either the core components or the selected network constituents tyrosine kinase MER (MERTK), atrial natriuretic peptide receptor C (AN-PRC) and protein ITM2B resulted in target-specific impairment or disruption of the filtration process.

Conclusion: Our results identify the SD as a multi-component system that is endowed with context-dependent dynamics via a co-assembled protein network. Given that the vast majority of the newly identified SD constituents are either involved in cellular signaling or cell adhesion (by

formation of cellular-junction(s)) it is well conceivable that the podocyte SD operates as a molecular sensor and effector which renders renal filtration dynamic and able to adapt to changing conditions. The molecular details behind such context-initiated dynamics, their exact sites of action as well as their reaction target(s) within or adjacent to the SD must currently remain open and should fuel future research.

P172

Podocyte-derived urinary extracellular vesicles mirror podocyte proteostasis

K. Labme; K. Deheshwar; G. Gloede; O. Kretz¹; S. Zielinski; S. Liu¹; T.B. Huber¹; F. Braun¹; W. Sachs; D. Loreth; C. Meyer-Schwesinger
Institut für Zelluläre und Integrative Physiologie, Universitätsklinikum Hamburg-Eppendorf, Hamburg;
¹ Nephrologie/Rheumatologie und Endokrinologie/Diabetologie, III. Medizinische Klinik, Universitätsklinikum Hamburg-Eppendorf, Hamburg

Objective: Upregulation of the ubiquitin-proteasome system (UPS) within podocytes occurs upon injury and correlates with disease progression in rodent models. During progressive podocyte injury, the proteasome system becomes impaired resulting in the accumulation of non-degraded proteins. Here we tested whether the abundance of urinary extracellular vesicles (EVs) and their content on UPS proteins displays the proteostatic condition of glomerular podocytes.

Method: EVs were isolated from mT/mG and BALB/c mice, and from human urine by differential ultracentrifugation. Isolation of

podocyte-derived EVs from human urine was established and validated. Mouse urine was collected prior to and on different days after disease induction (THSD7A-associated membranous nephropathy (MN), adriamycin nephritis (AN) and diabetic nephropathy (DN)). The abundance and proteostatic content of EVs was analysed by immunoblotting and compared to the proteostatic situation in podocytes. Podocyte-specific urinary EVs from nephrotic patients were investigated for differences in EV amount and abundance of UPS components.

Results: The amount of podocyte-derived EVs increases differentially in murine podocyte injury models. The abundance increases in a dose- and time-dependent manner in THSD7A MN, but not in AN und DN. Both human and murine urinary EVs contain UPS components. The proteostatic content changes in a disease-dependent manner, mirroring the proteostatic situation of podocytes. Human podocyte-specific EVs differentiate in size from total urinary EVs. In nephrotic patients the amount of podocyte-specific EVs differs depending on the underlying podocyte injury.

Conclusion: Analysis of podocyte-specific EVs has the potential to give insight into the proteostatic status of podocytes.

P173

The redundant and unique interactors of YAP and TAZ in podocyte homeostasis and disease

L. Ester; I. Cabrita; M. Ventzke; F. Fabretti; T. Benzing; S. Habbig¹; B. Schermer
Nephrologie, Rheumatologie, Diabetologie und Allgemeine Innere Medizin, Klinik II für Innere Medizin,

Universitätsklinikum Köln, Köln;

¹ Klinik und Poliklinik für Kinder- und Jugendmedizin, Universitätsklinikum, Universität zu Köln, Köln

Objective: The two effector proteins of the Hippo signaling pathway, YAP and TAZ, play a pivotal role in the cellular homeostasis of podocytes and in the pathogenesis of focal segmental glomerulosclerosis (FSGS). The two proteins that share 46 % amino acid identity are often regarded as homolog proteins. However, the podocyte-specific knockout of TAZ results in milder proteinuria and FSGS than the podocyte-specific YAP knockout. We aim to unravel the unique and redundant functions of YAP and TAZ in the podocyte by identifying podocyte-specific interactors in health and disease.

Method: We used murine immortalized podocytes (hsMPs) and co-immunoprecipitated YAP or TAZ with specific antibodies. To overcome possible drawbacks resulting from these two proteins' homology, we further generated hsMPs expressing FLAG-tagged YAP or TAZ using TALEN-based genome editing. For *in vivo* purposes, we generated transgenic mice expressing 3xFLAG.YAP and TAZ.3xFLAG using CRISPR/Cas9 mediated genome editing. YAP or TAZ were pulled down *in vitro* from podocytes and *in vivo* from isolated glomeruli, followed by mass spectrometry analysis. To shed light on the divergent role of YAP and TAZ, we generated YAP or TAZ podocyte-specific knockout mice as well as double knockouts. We are currently performing multi-omic studies to elucidate common, distinct, and possible compensatory

roles of YAP and TAZ in podocyte disease progression.

Results: Within the interactome analyses of the hsMPs, we identified shared and non-shared interacting proteins between YAP and TAZ. Of all interactors found, 60 % overlapped for both, while 40 % were unique. These results comprise known and novel interactors, including Fat1, Actn4, Stat1, or Neph1. Interactome analysis of the nuclear fraction of hsMPs identified specifically nuclear interactors of YAP and TAZ, including known transcription factors like the TEAD protein family and also ~ 30 % of new nuclear interacting proteins. Currently, we are investigating the mechanistic role of novel candidates in FSGS while we are working on the *in vivo* models.

Conclusion: YAP and TAZ are critical proteins in the podocyte's homeostasis with divergent functions and interactors. Overlapping and distinct candidates identified in interactome analyses conducted both in *in vitro* and *in vivo* systems suggest both shared and unique podocyte-specific functions. These novel unique and shared interactors of YAP and TAZ in podocytes will help to understand the specific impact of YAP and TAZ in the development of FSGS and recovery from podocyte injury.

P174

The Immunoproteasome Determines the Fate of Essential Podocyte Proteins in membranous nephropathy

C. Viehmann; A. Kramer; L. Heintz; S. Zielinski; D. Loreth; W. Sachs; C. Meyer-Schwesinger
Institut für Zelluläre und Integrative Physiologie, Universitätsklinikum Hamburg-Eppendorf, Hamburg

Objective: Membranous Nephropathy (MN) is associated with abnormal protein accumulation and an upregulation of the ubiquitin proteasome system (UPS), particularly of the immunoproteasome. This could facilitate effective protein degradation but might also promote disease progression. Previous work has shown that immunoproteasome deficiency in podocytes attenuates progression of glomerular disease in the anti-podocyte nephritis mouse model. Here, we investigated the effect of immunoproteasome deficiency in podocytes, using a more specific mouse model for MN, the passive THSD7A-associated MN.

Method: Podocyte-specific $\beta 5i$ knockout mice ($\beta 5i\Delta$ pod mice) and littermate controls were injected with rabbit anti-THSD7A antibodies to induce passive THSD7A-associated MN. For clinical assessment, bodyweight was monitored, and urine and blood samples were analysed. Western blot analysis of isolated glomeruli and confocal immunofluorescence microscopy were used to study abundance and localisation of podocyte proteins. Protein and gene expression levels of key players of the UPS and autophagosomal/lysosomal pathway (ALP) were determined in isolated glomeruli using Western blot analysis and qPCR. Proteasomal activity was measured using in-gel activity assays and activity-based probes.

Results: Western blot analysis and confocal immunofluorescence microscopy revealed differences between $\beta 5i\Delta$ pod and control mice in abundance and localisation pattern of podocyte proteins, such as α -actinin-4, Neph1, and THSD7A. The effect was most pronounced for THSD7A, with THSD7A linear

signal being significantly more intact but THSD7A aggregate signal enhanced in $\beta 5i\Delta$ pod mice. Protein levels of α -actinin-4, a podocyte-specific protein known to be degraded by the UPS, were higher in $\beta 5i\Delta$ pod mice, hinting at UPS impairment. Interestingly, immunoproteasome deficiency was not compensated by upregulation of the constitutive proteasome but only by activation of the ALP. Clinical manifestation of MN also differed between the experimental groups.

Conclusion: Immunoproteasome deficiency in podocytes alters progression of MN in mice, clinically and on a protein level. Changes in podocyte protein abundance and pattern are particularly striking.

P175

Comparing nephrotoxicity of the calcineurin inhibitors, cyclosporin A and tacrolimus, reveals their differential effects along the nephron in chronic experimental settings

H. Demirci; S. Popovic; J. Hu; I. Amr El Shimy; C. Dittmayer; D. E. Yilmaz; K. Mutig¹; S. Bachmann

Institut für Vegetative Anatomie, Campus Charité Mitte, Charité – Universitätsmedizin Berlin, Berlin;

¹ Institut für Translationale Physiologie, Campus Charité Mitte, Charité – Universitätsmedizin Berlin, Berlin

Objective: Chronic calcineurin inhibitor (CNI) nephrotoxicity is a major drawback in current immunosuppressive regimens. Pathology includes vascular and tubulointerstitial alterations. Although still commonly in use, cyclosporine A (CsA) is increasingly exchanged for tacrolimus (Tac) for a more favorable clinical outcome.

Data on their differential pathogenetic effects in the kidney are still scarce. We asked how CsA and Tac may affect renal pathogenetic responses differentially.

Method: CsA and Tac were administered chronically in wt rats and mice with a megalin-related endocytosis defect using osmotic minipumps (total n = 112). Clinical parameters from plasma and urine samples were controlled. Animals were prepared for high-end morphological analysis, elective immunostaining, and high-throughput technology. Large scale electron microscopy (EM), confocal, stimulated emission-depletion (STED) and 3D-structured illumination (SIM) microscopy were used for pathology. Standard biochemistry, RNA-seq, proteomic and phosphoproteomic technology was used to identify gene expression difference.

Results: In rats, CsA and Tac produced distinct alterations in glomeruli and tubulointerstitium. Both drugs caused α -SMA-positive fibrotic foci with sclerotic glomeruli and damaged tubules to similar extent. With CsA, glomerular damage was milder than with Tac. Proximal tubules showed widespread dysmorphic lysosomes with peripheral LAMP1 signal as well as autophagic and mitophagic vacuoles along with high apoptosis rate and diminished albumin uptake; megalin-dependent endocytosis was causally involved in the changes, and lysosomal exocytosis was sharply stimulated at the luminal cell pole. KIM1 signal was moderate. With Tac, these changes were far less pronounced, but the incidence of focal tubular necrosis along with intense KIM-1 signal was high. High throughput analysis showed differential changes between

CsA and Tac with almost no overlap between the respective spectra. CsA caused upregulation of components of the unfolded protein response and apoptosis, whereas Tac resulted in RAS-associated stimulation and vascular deterioration.

Conclusion: CNI nephrotoxicity presented with fundamentally different effects caused by CsA and Tac. While CsA mostly affected proximal tubular integrity, Tac was primarily acting on vascular components. Results may serve to better adjust immunosuppressive treatment combinations in transplant patients.

P176

A novel quantifiable method in longitudinal 3D intravital microscopy reveals an response to injury feedback system between glomerulus and its renin cell niche

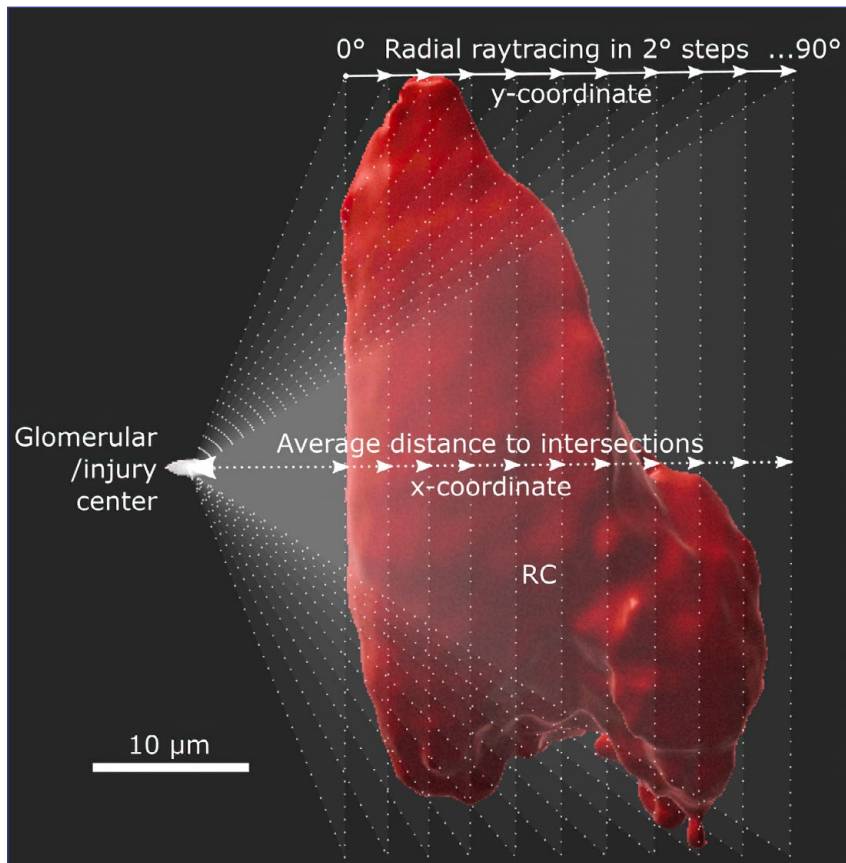
P. Arndt; J. Sradnick; H. Kröger; S. Holtzhausen¹; M. Gerlach²; V. T. Todorov; C. Hugo
Medizinische Klinik III, Nephrologie, Universitätsklinikum Carl Gustav Carus, Technische Universität Dresden, Dresden; ¹ Virtuelle Produktentwicklung, Institut für Maschinenelemente und Maschinenkonstruktion, Technische Universität Dresden, Dresden; ² CFCI Core Facility Cellular Imaging, Universitätsklinikum Carl Gustav Carus, Technische Universität Dresden, Dresden

Objective: Renin cells (RC) reside in the juxtaglomerular apparatus and function as pluripotent progenitors capable of migrating into the glomerulus after injury. While regulation of these complex repair processes is poorly understood, the authors propose the hypothesis that glomerular repair processes in adults underlie an individual

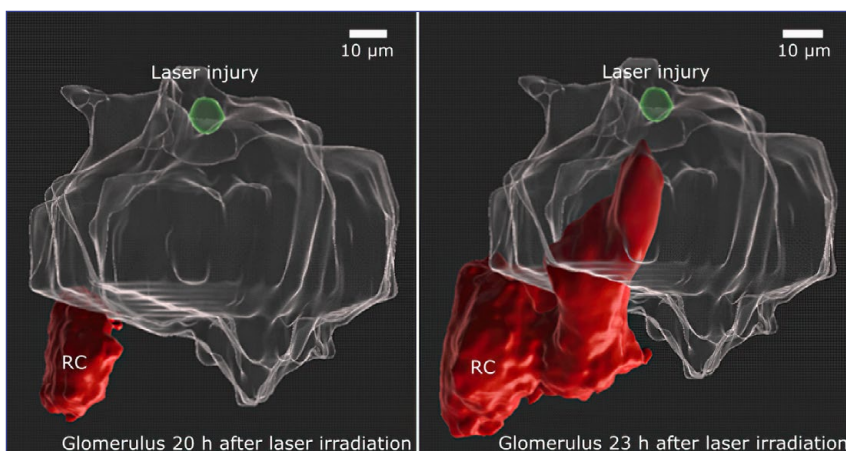
intraglomerular-juxtaglomerular feedback mechanism. Using longitudinal intravital microscopy and an injury model that induces local damage by targeted laser irradiation in individual glomeruli, enables observations of repair processes under controlled conditions. Using virtual ray tracing, an optical object characterization technique, a new method of quantification in longitudinal 3D intravital imaging, especially a detailed characterization of the renin cell niche, was established.

Method: Eight-week-old female mRen-rtTam2/LC-1/tdT renin reporter mice underwent doxycycline pulse induction and 7 days washout. Intravital microscopy was then performed through an implanted body window under an upright Leica SP8 MP/OPO LSM for three hours on up to seven consecutive days. Laser injury was induced by focusing 100 % laser power for 5 seconds at 48x zoom on one Z-plane. 3D processing and analysis were performed with Bitplane Imaris 9.7.2 and novel 3D image quantification was realized by the Marching Cubes algorithm. Image stacks of glomeruli were used to calculate a surface model described by triangles. The calculation of the directional thickness of the renin cells (RC) in relation to a center was based on an adapted ray tracing method, as seen below.

Results: Targeted use of laser irradiation established an inducible, selective and reproducible intraglomerular injury model. Migrating RC (below, left) extended during 3 hours (below, right) towards the injury area, infiltrating the vicinity of this area without losing contact to the juxtaglomerular RC. During these



P176: Abb. 1



P176: Abb. 2

processes the RC first increased in volume outside the glomerulus and then showed an up to three-fold increased area of dynamic migration with up to 344 % compared to their niche of origin area. **Conclusion:** Longitudinal intravital microscopy combined with laser-induced intraglomerular injury and 3D image analysis of site-specific injury directed renin cell migration in transgenic mice was assessed in a quantifiable manner. The combination of these technologies provides a new powerful tool for directly studying the juxtaglomerular feedback system of renin cell recruitment/migration and transdifferentiation as a site-specific response to intraglomerular injury and may promise viable targets for further glomerular regeneration research.

P177

Wild-type heterogeneity is a major driver for clonal variability in genome edited cells

L. Westermann; M. Niedermoser; K. Rhein; I. Cascante; F. Schöler; N. Moser; J. Jahn; B. Neubauer; A. Hofherr; B. Göcmen¹; Y. Li¹; A. Köttgen¹; M. Köttgen; T. Busch
Medizinische Klinik IV/ Abteilung Nephrologie, Universitätsklinikum, Albert-Ludwigs-Universität Freiburg, Freiburg; ¹ Medizin IV, Nephrologie und Institut für genetische Epidemiologie, Universitätsklinikum, Albert-Ludwigs-Universität Freiburg, Freiburg

Objective: CRISPR-based genome editing has simplified the investigation of gene function in cell lines to study kidney diseases, but its widespread use has also revealed challenges of reproducibility. Phenotypic variability among different knockout clones of the same gene is

a frequently observed problem confounding the establishment of robust genotype-phenotype correlations. Even if current state-of-the-art protocols are applied, phenotypic variability persists. In this study we test the hypothesis that inherent differences in wild-type clones might contribute to clonal variability in genome-edited cells when using polyclonal wild-type cells for genomic manipulation.

Method: Wild-type mIMCD-3 cells are isolated by single cell sorting thus generating monoclonal cell lines. These cell lines are tested for phenotypic spectra at the cellular, biochemical, and transcriptomic level. We compare protein abundances of monoclonal wild-type cells for several pathways associated with autosomal-dominant polycystic kidney disease (ADPKD), monitor response to cytotoxic treatment, and study cellular morphology in a 3D organoid assay. In addition, the transcriptomic profiles of mono- vs polyclonal wild-type mIMCD-3 populations are analyzed to uncover the potential contribution of clonal isolation to differential gene expression.

Results: Even in the absence of any genetic manipulation, this study shows significant differences in wild-type clones with several investigated read-outs. Protein levels significantly vary between monoclonal wild-type cells at magnitudes which are usually considered to be biologically relevant. Transcriptomic analysis of mono- vs polyclonal wild-type cells also demonstrates considerable heterogeneity by revealing hundreds of differentially expressed genes (477 up- and 306 downregulated, adjusted $p < 0.05$). We further show that the isolation of single cell

derived wild-type clones prior to genome editing leads to more homogeneous knockout clones compared to traditional CRISPR-protocols thus generating more robust genotype-phenotype relationships.

Conclusion: Clonal isolation of different wild-type cells uncovers an inherent phenotypic spectrum with significant differences at the cellular, biochemical, and transcriptomic level even in the absence of any genetic manipulation. Thus, we demonstrate that heterogeneity of wild-type cells contributes to variability in genome-edited cells when these are generated through isolation of clones. The generation of monoclonal, isogenic wild-type cells prior to genomic manipulation reduces phenotypic variability and increases reproducibility.

P178

CD19 CAR-T cells protect against the development of ANCA-induced NCGN in a mouse model

D. Lodka; M. Zschummel¹; A. Rousselle¹; R. Kettritz¹; M. Bunse¹; U. Höpken¹; A. Schreiber
Medizinische Klinik mit Schwerpunkt Nephrologie und Internistische Intensivmedizin, Campus Charité Mitte, Charité – Universitätsmedizin Berlin, Berlin; ¹ ECRC-Kooperation von MDC und Charité, Experimental and Clinical Research Center, Berlin

Objective: ANCA-induced vasculitis and NCGN are potentially life-threatening and current therapies are mainly based on cytotoxic drugs or B-cell-binding antibodies. Chimeric antigen-receptor T cells (CAR-T cells) are engineered T cells that express a protein consisting of intracellular T-cell receptor domains that are coupled to

an extracellular antibody domain. CAR-T cells bind via that antibody fragment their antigen at target cells and induce target cell lysis. The application of CAR-T cells in autoimmune disorders is a promising therapeutic option. Since ANCA are inducers of ANCA-associated vasculitides (AAVs), depletion of ANCA-producing B cells may be a useful AAV therapy. We hypothesized that administration of CD19 CAR-T cells will lead to depletion of B cells, including ANCA-producing B cells, thereby preventing MPO-ANCA induced necrotizing crescentic glomerulonephritis (NCGN).

Method: An anti-MPO NCGN was induced by immunisation of MPO-/-mice with murine MPO, followed by irradiation and transplantation of hematopoietic cells from WT mice. In addition, CD19 CAR-T cells and SP6 CAR-T cells (control CAR) were administered. Histological examination of renal sections and spleen, blood and bone marrow flow cytometry were done to detect effects on disease severity.

Results: CD19 CAR-T cells were detectable in bone marrow, spleen and peripheral blood after two and five weeks, pointing to their efficient immigration and stable persistence. In addition, mice receiving CD19 CAR-T cells had significantly reduced CD19-expressing endogenous B cells compared to SP6 CAR T mice at 5 weeks in bone marrow (0.03 % vs. 6.68 %), spleen (0.05 % vs. 60.7 %) and peripheral blood (0.004 % vs. 38.3 %) accompanied by faster decreasing anti-MPO titre. Finally, kidney histology showed reduced proportions of crescentic (0.49 % vs. 10.83 %) and necrotic (0 % vs. 6.04 %) glomeruli in mice receiving CD19 CAR-T cells compared to SP6 CAR

T mice at 5 weeks, indicative of protection from NCGN induction.

Conclusion: Our data suggest that depletion of CD19-expressing B cells by administration of CD19 CAR-T cells is an effective therapeutic option in murine anti-MPO-induced NCGN.

P179

Investigation of the VHL-mTORC1 signaling network in ccRCC

E. Neumann-Haefelin; M. Klein; S.-M. Maruhn; I. Frew¹; G. Walz; A. Ganner

Medizinische Klinik IV/ Abteilung Nephrologie, Universitätsklinikum, Albert-Ludwigs-Universität Freiburg, Freiburg; ¹Zentrum für Translationale Zellforschung, Universitätsklinikum Freiburg, Freiburg

Objective: Inactivation of the tumor suppressor von Hippel-Lindau (VHL) gene is a key event in hereditary and sporadic clear cell renal cell carcinomas (ccRCC). pVHL targets hydroxylated HIF- α for proteasomal degradation and this is thought to be a major mechanism for pVHL dependent tumor suppression. Whether pVHL regulates other targets through a similar mechanism is largely unknown.

Method: In our project we combine proteomics technologies with genetic approaches and cellular and *C. elegans* animal models for ccRCC to investigate the relationship between pVHL and mTORC1.

Results: We have previously identified RAPTOR, the central subunit of mTOR complex 1 (mTORC1), as novel target of pVHL. The mTOR signaling pathway is a fundamental regulator of cell growth and proliferation, and hyperactivation of mTOR signaling is a common

finding in VHL-dependent ccRCC. Here, we provide further insight into the mechanism how pVHL regulates RAPTOR/mTORC1 signaling. pVHL targets RAPTOR for proteasomal degradation in an oxygen dependent manner. By Mass Spectrometry analysis, we identified hydroxylated highly conserved proline residues within RAPTOR. Hydroxylation of RAPTOR by prolyl hydroxylase enzymes (PHDs) seems to be prerequisite for pVHL-mediated degradation.

Conclusion: Our work reveals important new functions of the PHD-pVHL in regulating RAPTOR stability and mTORC1 activity. This may represent a novel mechanism where by loss of VHL affects tumor progression.

P180

A novel in vivo tool mimicking Fabry disease in *Drosophila melanogaster*

S. Köhler; L. Strauch¹; B. Cantutan²; X. Tang¹; M. Helmstädter¹; T.B. Huber²
Nephrologie, Rheumatologie, Endokrinologie, Transplantation und Translationale Immunologie, III. Medizinische Klinik und Poliklinik, Universitätsklinikum Hamburg-Eppendorf, Hamburg; ¹Medizinische Klinik IV/ Abteilung Nephrologie, Universitätsklinikum, Albert-Ludwigs-Universität Freiburg, Freiburg; ²Nephrologie/ Rheumatologie und Endokrinologie/ Diabetologie, III. Medizinische Klinik, Universitätsklinikum Hamburg-Eppendorf, Hamburg

Objective: A limitation in the identification and characterization of novel pathways is the lack of suitable *in vivo* tools to mimic Fabry nephropathy and cardiomyopathy. The model organism *Drosophila* could

prove as a novel and advantageous tool for Fabry research. *Drosophila* has an open circulatory system, with only one body fluid, the haemolymph. The heart tube consists out of a single layer of cardiomyocytes and performs pulsatile contractions, which result in haemolymph flow. Due to its' similarity to the mammalian heart, especially high conservation of genes and proteins, the *Drosophila* heart can be used to investigate pathways and mechanisms influencing heart function also in mammals. The *Drosophila* kidney consists of the Malpighian tubules and the nephrocytes. The latter occur in two different populations, the garland nephrocytes, located around the oesophagus and the pericardial cells, which are localized along the heart tube. Nephrocytes filter the haemolymph and present with a highly similar morphology to mammalian podocytes.

Method: We performed morphological and functional readouts in isolated nephrocytes from knockout and controls flies.

Results: Here, we identified the *Drosophila* orthologue of α -GAL, CG7997, and assessed depletion of the enzyme in the fly organism. We were able to reproduce the kidney phenotype observed in Fabry patients, as loss of CG7997 in nephrocytes, the podocyte homologs in flies, caused a severe filtration defect. In addition, we could identify zebroids in nephrocytes and observed increased autophagy, lysosome size and disrupted endosome formation upon CG7997 depletion. Preliminary RNAseq data of nephrocytes also revealed a decrease of mitochondria associated genes, but an increase of mitochondria number and ROS.

Conclusion: Our data presented here describes a novel in vivo model to mimic human Fabry disease. We could show that *Drosophila* nephrocytes express a α -GAL orthologue, CG7997, and its depletion caused a nephrocyte phenotype. Future studies will now focus on other tissues and phenotypes such as the heart, brain and gut. Moreover, *Drosophila* is the ideal tool to reintroduce different human mutations in the fly organisms and perform mechanistic and therapeutic assessment in vivo.

Experimentelle Nephrologie 4

P181

The mechano-sensitive ion channel Piezo activates Rho1 in *Drosophila* nephrocytes

S. Köhler; M. T. Lindenmeyer¹; T. B. Huber¹; B. Denholm²
Nephrologie, Rheumatologie, Endokrinologie, Transplantation und Translationale Immunologie, III. Medizinische Klinik und Poliklinik, Universitätsklinikum Hamburg-Eppendorf, Hamburg; ¹ Nephrologie/ Rheumatologie und Endokrinologie/ Diabetologie, III. Medizinische Klinik, Universitätsklinikum Hamburg-Eppendorf, Hamburg; ² Biomedical Sciences, Edinburgh Medical School, Edinburgh/ UK

Objective: Podocytes constantly face biomechanical forces such as shear stress and hydrostatic pressure. Increasing forces result in morphological changes, detachment from the glomerular basement membrane and loss into the primary urine. This highlights a requirement for podocytes to sense changes in their physical environment and induce a response to react to increased biomechanical force.

Method: Here, we investigated the functional role of the mechano-sensitive ion channel Piezo in *Drosophilanephrocytes*.

Results: First, we confirmed Piezo expression and localisation at the nephrocyte diaphragm. Acute activation of the channel with the chemical compound YODA revealed significantly increased Ca^{++} signalling and Rho1 activation, suggesting a functional role of Piezo in nephrocytes and delineating the putative Piezo mechanosensitive pathway. For further analysis, we used knockout flies and observed a filtration phenotype, while morphology and GTPase activation was not altered. In addition, we also studied the impact of elevated Piezo levels and could show, that in line with the YODA effect, Piezo overexpression revealed severely increased Rho1-GTP levels and FITC uptake, while morphology was not changed. Because of this severe pathological phenotype, we tried to rescue the effects of Piezo overexpression with pharmacological inhibition by using tarantula toxin. Intriguingly, treatment with tarantula toxin reversed the elevated Rho1-GTP levels observed upon Piezo overexpression. Moreover, we were able to confirm Piezo1 and Piezo2 expression in mammalian podocytes and an up-regulation of Piezo2 in glomerular tissue during disease including Lupus, FSGS and hypertension.

Conclusion: Taken together, our data confirms the functional expression of Piezo in nephrocytes, its role in regulating GTPases and the beneficial effect of tarantula toxin to reverse the pathological effects caused by increased Piezo levels.

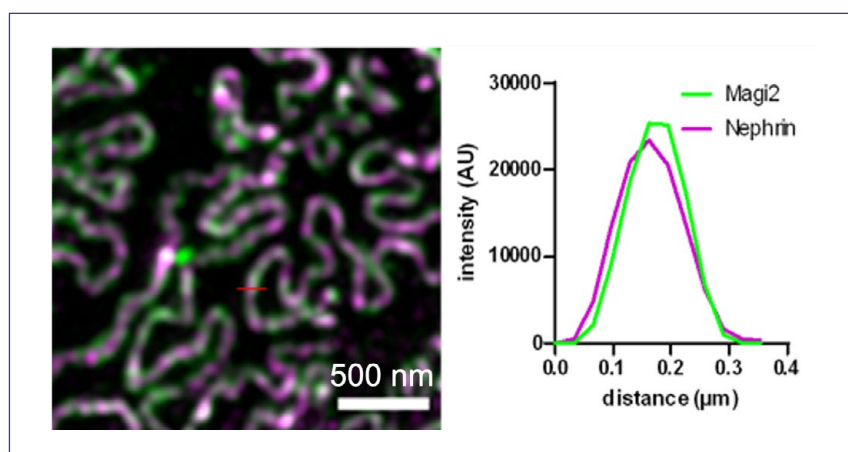
P182

The role of MAGI2 in glomerular disease and its possible role as a diagnostic marker

F. Siegerist; E. Hay; M. Schindler; S.-M. Bach; C. Chatziantoniou¹; C. Chadjichristos¹; T. Wiech²; N. Endlich
Institut für Anatomie und Zellbiologie, Universitätsmedizin Greifswald, Greifswald; ¹ INSERM U702, Hôpital Tenon, Pierre et Marie Curie University, Paris/F; ² Institut für Pathologie, Sektion Nephropathologie, Zentrum für Diagnostik, Universitätsklinikum Hamburg-Eppendorf, Hamburg

Objective: MAGI2 is a tight junction protein and member of the membrane-associated guanylate kinase (MAGUK) family. In the glomerulus, it is exclusively expressed in the slit diaphragm complex in podocytes. Recessive MAGI2 mutations lead to steroid-resistant nephrotic syndrome. The aim of this work was to study the expression of MAGI2 in mouse models, in pharmacogenetic and CRISPR/Cas9-induced zebrafish FSGS models, and in human biopsies of patients suffering from minimal change disease and FSGS.

Method: We used nephrotoxic serum (NTS) as well as uninephrectomy DOCA/salt-induced hypertension as murine models. The podocyte-specific nitroreductase/metronidazole zebrafish model was used to induce FSGS-like disease in zebrafish. MAGI2 expression was evaluated in kidney biopsies of patients affected by minimal change disease (MCD), primary and secondary focal segmental glomerulosclerosis (FSGS) using confocal laser scanning and super-resolution 3D-structured illumination microscopy (3D-SIM). Filtration



P182: Abb. 1

slit density (FSD) was measured on human biopsies by PEMP (podocyte exact morphology measurement procedure). Magi2 expression during glomerular dedifferentiation was studied in the GlomAssay. To evaluate the interaction between magi2 and nephrin in the zebrafish model, the respective proteins were knocked-out using CRISPR/Cas9.

Results: MAGI2 was expressed in a linear pattern along the filtration slit and colocalized with nephrin in all three species investigated (human, mouse, zebrafish) (see Figure). MAGI2 was significantly downregulated in both NTS-induced nephritis and uninephrectomized DOCA/salt-treated mice. In the GlomAssay, Magi2 was significantly downregulated in dedifferentiated podocytes after 6 days primary culture. In addition, we found that magi2 was downregulated in zebrafish larvae using our FSGS-like zebrafish model. When we examined the effect of nephrin on magi2 expression and vice versa, we found that magi2 expression was unchanged in nephrin-KO larvae, whereas nephrin expression was significantly reduced in magi2a-KO

larvae. A significant reduction of MAGI2 was found in human biopsies of patients suffering from primary FSGS, but not in MCD and secondary FSGS, respectively.

Conclusion: Here, we have shown that the expression of MAGI2 in the glomerulus is positively correlated with the expression of nephrin. Using selective knockout of both proteins, we show that nephrin expression is dependent on MAGI2 and not vice versa. Since the expression of MAGI2 seems to be specifically regulated depending on the podocytopathy investigated, we propose a role for MAGI2 to distinguish between different glomerulopathies such as primary and secondary FSGS.

P183 PHD inhibition influences monocyte recruitment in inflammatory chronic kidney disease and protects kidney function in a NR4A1 dependent manner

M. Schauer; G. Schley; V. Schatz¹; M. Schiffer; J. Jantsch¹; C. Willam
Medizinische Klinik 4, Nephrologie und Hypertensiologie, Universitätsklinikum,

Friedrich-Alexander-Universität Erlangen-Nürnberg, Erlangen; ¹Institut für Mikrobiologie und Hygiene, Universität Regensburg, Regensburg

Objective: Progressing kidney inflammation culminates in chronic kidney disease. Hallmarks of progressing inflammation are an increased influx of immune cells into the kidney and declining kidney function. While treatment with prolyl hydroxylase domain enzyme (PHD) inhibitors that stabilise Hypoxia Inducible Factor improves general outcome, the mechanism of PHDi-mediated renoprotection is not fully understood.

Method: Adenine nephropathy (AdNP) was induced in mice by an adenine rich diet. Serum Cystatin C was measured to assess kidney function. Flow cytometry was used to quantify mononuclear phagocytic cells (MNP) in kidney and blood. Kidney samples were used for histologic analysis to assess kidney structure. Protein and RNA were extracted from tissue for Western blot and qPCR analysis. We utilised *in vitro* assays with conditioned medium to investigate migration of bone marrow derived macrophages (BMDMs) and ELISA to assess cytokine expression.

Results: AdNP led to increased serum Cystatin C after two weeks. This was accompanied by an increased influx of CD11b^{hi}; F4/80^{lo} macrophages (MΦ) and Ly6C⁺ monocytes into the kidney and an increase of Ly6C^{hi} monocytes in the blood. Kidney damage was observed in H&E stains. Treatment with PHDi ameliorated kidney inflammation, reducing serum Cystatin C levels to normal. MNPs were reduced in blood and kidney.

Protein levels of CCL2, one of the main chemokines for monocyte recruitment, were reduced in kidneys of PHDi treated mice. Consequently, we investigated the CCL2/CCR2-axis. To test the migration of MΦ *in vitro* we exposed BMDMs to conditioned medium from HT1080 cells stimulated with MSU crystals. Indeed, PHDi treatment reduced MΦ migration *in vitro*, which was dependent on CCR2 expression. Surprisingly, PHDi treatment still reduced the amount of renal MNPs in CCR2^{-/-} mice. To assess circulating MNPs, we conducted experiments with mice lacking NR4A1, a key transcription factor for patrolling monocytes. In NR4A1^{-/-} mice, the PHDi-mediated renoprotection was abrogated. However, deficiency of NR4A1 did not alter the course of AdNP.

Conclusion: Our results show that PHDi treatment ameliorates AdNP and preserves kidney function. We show an effect of PHDi on the CCL2/CCR2-axis. However, it does not seem to be the main way of recruitment to the kidney. We conclude that different migration pathways are dominant in the kidney. Since PHDi treatment was ineffective in NR4A1^{-/-} mice, we conclude that PHDi-mediated renoprotection requires NR4A1. Revealing the function and involvement of NR4A1 in this context is goal for our further research.

P184

Untersuchung der retinalen Gefäßreagibilität bei Patienten mit Morbus Fabry – Eine prospektive Beobachtungsstudie

C. Regenbogen; T. Kuchler;
M. C. Braunisch; R. Günthner;
C. Schmäderer

II. Medizinische Klinik, Nephrologie,
Klinikum rechts der Isar, Technische
Universität München, München

Hintergrund: Morbus Fabry ist eine erbliche, lysosomale Speichererkrankung, bei der es durch fehlende oder mangelnde Aktivität an α-Galaktosidase zu einer Akkumulation von Globotriaosylceramiden (Gb3) in den Zellen kommt. Durch die Ablagerung von Gb3 in Endothelzellen kann es zu einer ausgeprägten Mikrozirkulationsstörung und in der Folge zu Organschäden aller Organsysteme kommen. Die retinale Gefäßreagibilität ist ein Surrogatparameter für die endotheliale Dysfunktion. Das Ziel dieser Studie ist es eine nicht-invasive Untersuchung der retinalen Gefäßreagibilität in einer prospektiven Kohorte von Fabry Patienten zu validieren und Assoziationen mit etablierten klinischen und laborchemischen Parametern zu untersuchen.

Methode: In einer monozentrischen, prospektiven Kohortenstudie wurden 63 Patienten mit Morbus Fabry und 198 gesunde Kontrollen eingeschlossen. Eine dynamische Untersuchung der retinalen Gefäße (DVA) wurde bei 58 Fabry Patienten durchgeführt. Es erfolgte eine paarweise Zuordnung nach Alter und Geschlecht zu den gesunden Kontrollen. Als Surrogatparameter der endothelialen Dysfunktion erfolgte eine Quantifizierung der maximalen arteriellen und venösen Dilatation der Netzhautgefäße als Reaktion auf Flimmerlichtstimulation. Zudem wurden "patient reported outcomes" erhoben, ein KardioMRT, welches als Goldstandard zur Diagnosestellung einer Morbus Fabry assoziierten Kardiomyopathie gilt,

eine Echographie und ein inflammatorisches Bioprofilung durchgeführt. Die Schwere der Erkrankung wurde mittels dem Fabry Outcome Mainz Severity Score Index (FO-MSSI) evaluiert.

Ergebnisse: Vorläufigen Daten lassen einen Unterschied der DVA-Messung, im Sinne einer verminderten Reagibilität der retinalen Gefäße in der Fabry-Kohorte im Vergleich zu unserer Gesundheitskontrolle vermuten. Aktuell werden die Daten der DVA-Messung mit der genetischen Variation, der Schwere der Erkrankung und der Therapie korreliert.

Zusammenfassung: Der Einsatz der retinalen Gefäßanalyse erlaubt es Einblicke in die Pathophysiologie der Mikrozirkulationsstörungen in Patienten mit Morbus Fabry zu gewinnen. Inwieweit sich diese neue, innovative und nicht-invasive Untersuchungsmethode langfristig zum Therapiemonitoring bei Patienten mit Morbus Fabry etabliert, werden weitere Studien untersuchen müssen.

P185

Die Identifizierung von Compound A als Ferroptose-Inhibitor eröffnet neue Therapieoptionen im Verlauf der akuten Nierenschädigung

B. Kolbrink; F. A. von Samson-Himmelstjerna; M. L. Messtorff;
T. Riebeling; R. Nische; J. Schmitz¹;
J. H. Bräsen¹; U. Kunzendorf; S. Krautwald² Klinik für Nieren- und Hochdruckkrankheiten, Campus Kiel, Universitätsklinikum Schleswig-Holstein, Kiel; ¹ Nephropathologie, Institut für Pathologie, Medizinische Hochschule Hannover, Hannover; ² Nephrologisches Forschungslabor, Campus Kiel, Universitätsklinikum Schleswig-Holstein, Kiel

Hintergrund: Die Ischämie-Reperfusion-bedingte Nierenschädigung stellt aufgrund der damit verbundenen *delayed graft function* ein erhebliches klinisches Problem in der Transplantationsmedizin dar. Als zentraler Zelltodmechanismus der ihr zugrunde liegenden Tubulonekrose gilt die Ferroptose. Diese Unterform der regulierten Nekrose ist durch eine eisenabhängige Akkumulation von Lipidperoxiden charakterisiert. Trotz umfassender Forschungsbemühungen existiert bislang kein spezifischer Ferroptose-Inhibitor mit klinischer Anwendbarkeit. Im Sinne eines *drug repurposing* haben wir in dieser Arbeit *Compound A*, welches bereits mit gutem Sicherheitsprofil für andere Indikationen klinisch genutzt wird, aufgrund seiner vorbeschriebenen anti-oxidativen Eigenschaften im Kontext der Ferroptose-Blockade untersucht.

Methode: Für die *in vitro* Versuche wurden transformierte Zelllinien und verschiedene Primärzellen verwendet. Ferroptose wurde durch Inhibition der anti-ferroptotischen Systeme GPX4, FSP1 bzw. DHODH induziert. Per Durchflusszytometrie und Immunoblot wurden der Zelltod und die Expression von Ferroptosemarkern bestimmt. Als murines *in vivo* Modell wurde die bilaterale renale Ischämie-Reperfusion eingesetzt und laborchemisch sowie histopathologisch evaluiert.

Ergebnisse: *Compound A* konnte den ferroptotisch ausgelösten Zelltod bemerkenswerterweise ebenso effizient unterdrücken wie die Referenzsubstanz Ferrostatin-1. Im Tiermodell zeigte sich ein signifikant protektiver Effekt von *Compound A* im Verlauf der renalen Ischämie-Reperfusion. Die Protektion wurde durch eine Verbesserung

der Retentionsparameter, eine histopathologisch verifizierte Abschwächung des Tubulusschadens sowie eine reduzierte Expression verschiedener Ferroptosemarker im renalen Gewebe belegt. Durch Zusatz eines Antagonisten von *Compound A* konnte dieser protektive Effekt im Verlauf der Ferroptose wieder revertiert und somit validiert werden.

Zusammenfassung: Die erstmalige Beschreibung von *Compound A* als protektiver und direkt verfügbarer Inhibitor ferroptotisch-vermittelter Zelltodprozesse eröffnet eine neuartige und klinisch unmittelbar zugängliche Therapieoption für die durch Ischämie-Reperfusion bedingte akute Nierenschädigung. Hieraus ergeben sich vielversprechende translationale Ansätze im Bereich der Transplantationsmedizin.

P186

Gesteigerter Erythrozytenabbau als Ursache der Anämie bei der 5/6 Nephrektomie

R. Bissinger; B. N. Bohnert; M. Z. Kalo; L. Kong; F. Artunc
Sektion Nieren- und Hochdruckkrankheiten, Universitätsklinikum, Medizinische Klinik IV, Eberhard Karls Universität Tübingen, Tübingen

Hintergrund: Die renale Anämie beeinträchtigt die Lebensqualität und Leistungsfähigkeit der betroffenen Patienten in bedeutendem Maße. Frühere Arbeiten aus der eigenen Arbeitsgruppe konnten bei zwei Modellen mit proteinurischer Nephropathie zeigen, dass ein verfrühter Abbau von Erythrozyten durch den Mechanismus der Eryptose maßgeblich zur Anämie beiträgt. Inwiefern die Proteinurie oder die Niereninsuffizienz selbst zur Eryptose

beiträgt, ist nicht bekannt. Daher wurde der Mechanismus der Eryptose nun in einem nicht-proteinurischen Modell der Niereninsuffizienz, der 5/6 Nephrektomie, untersucht.

Methode: Die Untersuchungen wurden in Wildtyp-129S1/SvImJ-Mäusen durchgeführt. Zunächst erfolgte eine unilaterale Nephrektomie, woraufhin nach 2 Wochen die oberen Pole der verbleibenden Niere chirurgisch entfernt wurden. Blut- und Urinproben von 5/6 nephrektomierten (n = 9) und Sham-operierten Kontrollmäusen (n = 12) wurden ab Woche 2 nach Operation bis Woche 8 entnommen. Die PS (Phosphatidylserin)-Exposition der Erythrozytenmembran wurde durch Annexin V-FITC durchflusszytometrisch bestimmt. Die Bestimmung der Retikulozytenzahl erfolgte ebenfalls per Durchflusszytometrie. Die Plasma-Erythropoetin-Konzentration wurde mittels ELISA gemessen.

Ergebnisse: 8 Wochen nach 5/6 Nephrektomie entwickelten die 5/6-Mäuse (n = 9) ein fortschreitendes Nierenversagen (Harnstoff: 153 ± 36 mg/dl). Die Proteinurie war 8 Wochen nach 2. OP nicht signifikant unterschiedlich (5 ± 2 mg/g in der Kontrollgruppe vs. 21 ± 16 mg/g bei den 5/6 Mäusen). Es kam zu einem signifikanten Abfall des Hämoglobins von $15,0 \pm 0,2$ g/dl auf $12,2 \pm 0,6$ g/dl trotz gesteigerter Retikulozytenzahlen ($6,3 \pm 2,0$ % bei den 5/6 nephrektomierten Tieren vs. $2,3 \pm 0,3$ % in der Kontrollgruppe). Der Plasma-Erythropoetin-Spiegel war nicht signifikant unterschiedlich ($4,0 \pm 0,6$ pg/ml bei den Kontrolltieren vs. $5,1 \pm 0,3$ pg/ml bei den 5/6 nephrektomierten Tieren). Parallel dazu konnte nach 8 Wochen eine gesteigerte PS-Exposition ($1,0 \pm 0,2$ %

bei den 5/6 nephrektomierten Tieren vs. $0,6 \pm 0,08\%$ bei den Kontrollmäusen) beobachtet werden.

Zusammenfassung: Die experimentelle 5/6 Nephrektomie führt zur Ausbildung einer Anämie. Möglicherweise trägt der verfrühte Abbau der Erythrozyten durch den Mechanismus der Eryptose zur Anämie bei, da dadurch die Erythrozyten verfrüht aus der Blutbahn eliminiert werden.

P187

Modulation of renal endothelial damage in mice with Gs alpha deficiency in renin producing cells

A. Wegner; A. Steglich; F. Gemhardt; J. Sradnick; M. Schuster; A. Wirth; C. Hugo; V. T. Todorov
Medizinische Klinik III, Nephrologie, Universitätsklinikum Carl Gustav Carus, Technische Universität Dresden, Dresden

Objective: In the kidney, renin synthesis in renin producing cells (RPC) is regulated by physiological cues such as arterial blood pressure or salt intake. The regulatory effect of these stimuli is mediated via cAMP, the generation of which depends on the alpha subunit of the stimulatory G-protein (Gsa). Transgenic mice with an inducible Gsa deficiency in RPC presented an adverse phenotype featuring renal endothelial damage and impaired kidney function. However, it remains unknown whether physiological cues mediating renin production modulate the severity of this phenotype.

Method: Mice with an inducible Gsa knockout in RPC (mRen-rt-Tam2-LC1-tdT-Gsa) and their respective wildtypes (mRen-rt-Tam2-LC1-tdT) were used. Both express the reporter protein tdTomato in

RPC after induction. To induce recombination, 6–8 weeks old mice received doxycycline (625 mg/kg chow) for 21 days. Three months after induction, uninephrectomy was performed. Afterwards, mice were treated with either ACE inhibitor (ACEi; enalapril 10 mg/kg body weight in drinking water) or high-salt diet (4% NaCl in chow) for up to three months. Untreated wildtype and Gsa knockout mice served as controls. Examinations of kidney function were performed before and one month after the start of the treatment. These included transcutaneous measurement of glomerular filtration rate (GFR), sonographic evaluation of renal perfusion, measurement of arterial blood pressure by the tail-cuff method and a 24 h urine collection in metabolic cages.

Results: Preliminary data from the urine analysis showed that one month after the start of the treatment mean albumin excretion was similar in all wildtype groups (approx. 3.7 mcg/24 h). Untreated and high-salt-treated Gsa deficient mice displayed an increased albumin excretion (mean 20.5 mcg/24 h and 18.5 mcg/24 h, respectively). In contrast, albumin excretion in ACEi-treated Gsa deficient mice matched that of the wildtypes (mean 3.5 mcg/24 h). Moreover, these mice also showed a reduced systolic arterial blood pressure compared to their untreated controls ($p < 0.05$). Kidney perfusion and GFR displayed no differences.

Conclusion: Our first data indicates that the extent of renal damage caused by RPC-specific Gsa deficiency is modulated at least by ACE inhibition. We expect to elaborate these initial observations with functional data from later experimental

time points and support them with immunohistochemistry. We therefore suggest that factors regulating renin production, such as treatment with ACEi or high-salt diet, modulate the severity of the adverse kidney phenotype resulting from RPC specific Gsa deficiency.

P188

Proteolytische Aktivität gegen den distalen polybasischen Trakt der Gamma-Untereinheit des epithelialen Natriumkanals ENaC im nephrotischen Urin

M. Wörn; H. Kalbacher¹; F. Artunc
Sektion Nieren- und Hochdruckkrankheiten, Universitätsklinikum, Medizinische Klinik IV, Eberhard Karls Universität Tübingen, Tübingen;
¹ Interfakultäres Institut für Biochemie, Eberhard Karls Universität Tübingen, Tübingen

Hintergrund: Das experimentelle nephrotische Syndrom führt bei Mäusen zu einer proteolytischen Überaktivierung des epithelialen Natriumkanals ENaC, und damit zu den NS-Leitsymptomen renale Natriumretention und Ödembildung. Möglicherweise wird hierbei der distale polybasische Trakt der γ -ENaC-Untereinheit (183RKRK) für die volle proteolytische Aktivierung geschnitten. Wir untersuchten, ob Urinproben sowohl von nephrotischen Mäusen als auch von Patienten eine spezifische proteolytische Aktivität gegen diese γ -ENaC-Sequenz aufweisen.

Methode: Ein Peptidsubstrat (Aminosäuren 180–194 von murinem γ -ENaC) wurde N-terminal an das AMCA-Fluorophor gekoppelt, was AMCA-FTGRKKRKISGKI-IHK ergab. Das Substrat wurde mit gesunden und nephrotischen

Urinproben von Patienten (n = 8) sowie von drei Maus-Modellen (je n = 4: 129S1/SvImJ-Wildtyp (129-WT) und B6-*Nphs2*^{Δipod} mit oder ohne Plasminogen-Knockout (B6-Plg-WT/-KO)) und mit oder ohne den Serinprotease-Inhibitor Aprotinin inkubiert. Die verdauten Peptide wurden auf einer C18-HPLC aufgetrennt, die Fluoreszenz bei 350/450 nm detektiert und die Massen mittels MALDI-TOF-Massenspektrometrie bestimmt. Zusätzlich wurde die Aktivität gegen Peptid-Substrate mit C-terminal gekoppelten AMC (380/460 nm) photometrisch bestimmt, welche die vier unterschiedlichen Spaltstellen bei 183RKRK repräsentieren.

Ergebnisse: In den gesunden Urinproben wurde keine signifikante proteolytische Aktivität gegen die AMCA-/AMC-Substrate gefunden, dafür aber deutlich im nephrotischen Urin. Das dominante Spaltprodukt beim AMCA-Substrat war meist FTGRKR mit 37–58 %, insbesondere in den Human- und B6-Plg-KO-Proben, gefolgt von FTGRK mit bis zu 21 %. Bei Zugabe des Inhibitors Aprotinin blieb ein hoher Anteil des Ausgangssubstrats von 74–96 % erhalten. Dies wurde mit den AMC-Substraten bestätigt. In Human-Proben war hier die Aprotininsensitive Aktivität gegen FTGRKR dominierend. In 129-WT und B6-Plg-WT/-KO ergaben FTGRK und FTGRKR ähnliche hohe Werte, wobei in B6-Plg-KO die Aktivität generell deutlich geringer war.

Zusammenfassung: Nephrotischer Urin sowohl von Menschen als auch von Mäusen enthält Aprotinin-sensitive proteolytische Aktivität gegen den distalen polybasischen Trakt von γ -ENaC, insbesondere gegen FTGRKR. Dies spiegelt

die Ausscheidung aktiver Serinproteasen der Trypsin-ähnlichen S1-Familie vom Plasma in den Urin als sogenannte Proteasurie wider. Diese Serinproteasen könnten eine Rolle in der ENaC-Überaktivierung spielen, was durch weitere Untersuchungen wie an KO-Modellen und *in vivo*-Experimente mit ENaC untersucht werden muss.

P189

Lack of plasminogen relates to a hypercoagulable state in mice with experimental nephrotic syndrome

B. N. Bohnert; M. Xiao; A. Schork; E. Vogel; L. Pelze¹; S. Hammer¹; T. Bakchoul¹; F. Artunc

Sektion Nieren- und Hochdruckkrankheiten, Universitätsklinikum, Medizinische Klinik IV, Eberhard Karls Universität Tübingen, Tübingen;

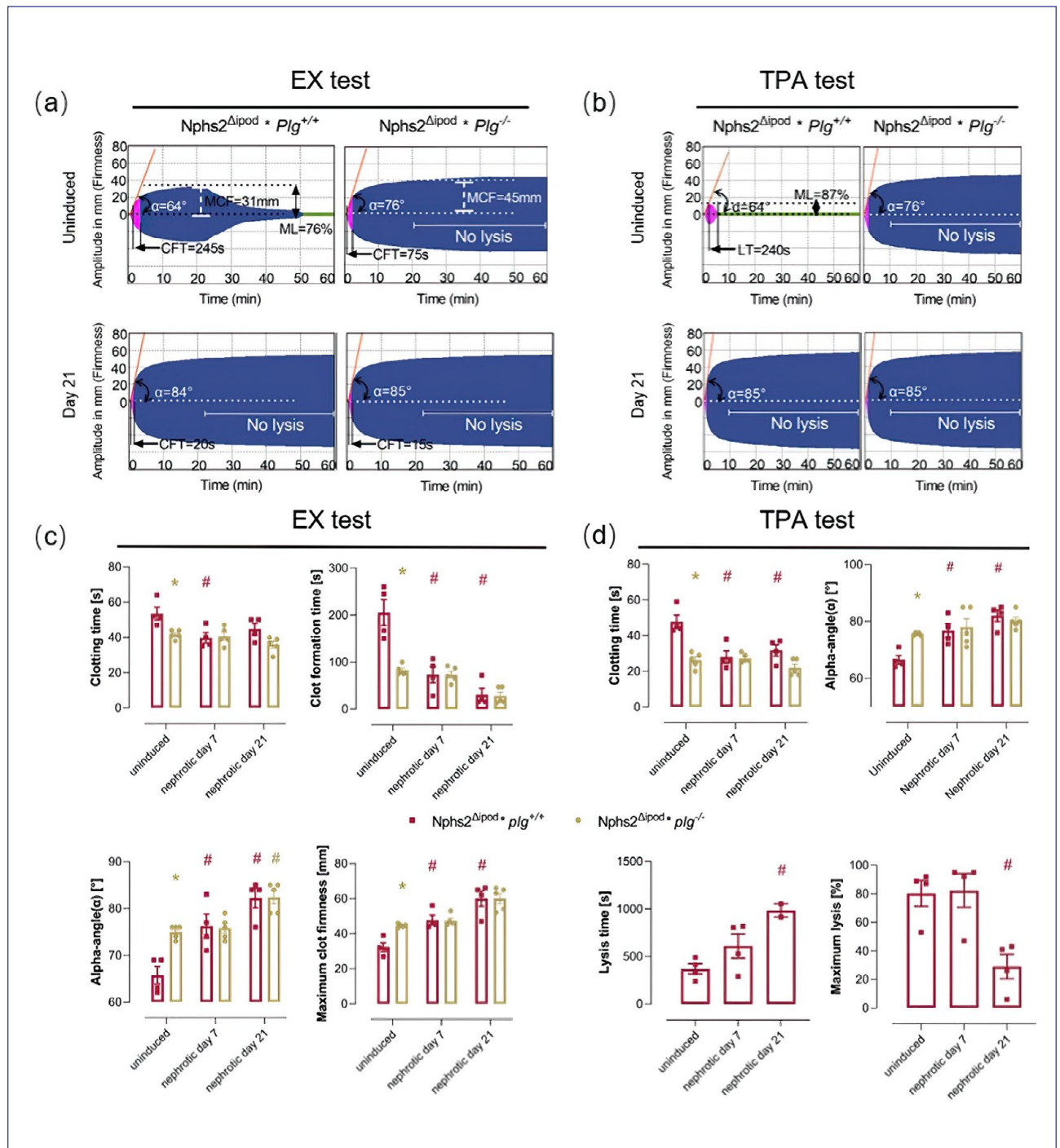
¹Institut für klinische und experimentelle Transfusionsmedizin, Universitätsklinikum Tübingen, Eberhard Karls Universität Tübingen, Tübingen

Objective: Urinary excretion of the fibrinolytic enzyme plasminogen (Plg) has been identified as a characteristic feature of nephrotic syndrome (NS) in both human and experimental mouse models. Lack of plasminogen may lead to a hypercoagulable state and thrombosis. However, the role of plasminogen in mediating the hypercoagulable state in nephrotic syndrome has not been investigated before.

Method: We investigated the relationship between Plg and a hypercoagulable state in a nephrotic mouse model with inducible podocin deletion (*Nphs2*^{Δipod}**Plg*^{+/+}, n = 12). These mice were compared to *Nphs2*^{Δipod} mice with constitutive *Plg* deletion (*Nphs2*^{Δipod}**Plg*^{-/-}, n = 15).

Citrate blood was collected from each mouse before induction of NS, 7 days and 21 days after induction, respectively (*Nphs2*^{Δipod}**Plg*^{+/+} mice, n = 4/timepoint; *Nphs2*^{Δipod}**Plg*^{-/-} mice, n = 5/timepoint). In addition, we collected citrate blood from patients presenting to our department with acute NS (n = 10). Extrinsic coagulation was analyzed using thrombelastography with the ClotPro® system (EX test). In addition, fibrinolysis was tested by adding tissue Plg activator (TPA test).

Results: According to the EX test, uninduced mice with Plg deficiency showed a significantly reduced clotting time (CT, *Plg*^{-/-} vs. *Plg*^{+/+}, 42 ± 1 s vs. 54 ± 4 s, p = 0.0213), and decreased clot formation time (CFT, *Plg*^{-/-} vs. *Plg*^{+/+}, 82 ± 5 s vs. 206 ± 28 s, p < 0.0001) with a larger alpha-angle (*Plg*^{-/-} vs. *Plg*^{+/+}, 75 ± 1° vs. 66 ± 2°, p = 0.0041). The maximum clot firmness (MCF) was significantly increased in uninduced Plg knockout mice (*Plg*^{-/-} vs. *Plg*^{+/+}, 45 ± 1 mm vs. 32 ± 3 mm, p < 0.0001). According to the TPA test, uninduced *Nphs2*^{Δipod}**Plg*^{-/-} mice did not show any clot lysis in contrast to uninduced *Nphs2*^{Δipod}**Plg*^{+/+} mice. After induction of NS, both *Nphs2*^{Δipod}**Plg*^{-/-} mice and *Nphs2*^{Δipod}**Plg*^{+/+} mice developed massive proteinuria to a comparable extent (*Plg*^{-/-} vs. *Plg*^{+/+} on day 21, 218 ± 46 mg/mg crea vs. 203 ± 28 mg/mg crea), and plasminuria was detectable in nephrotic *Nphs2*^{Δipod}**Plg*^{+/+} mice. This was paralleled by a significantly reduced CFT, increased MCF and reduced clot lysis. In nephrotic *Nphs2*^{Δipod}**Plg*^{-/-} mice at day 21, there was also a tendency towards a reduced CT and CFT while clot



P189: Abb. 1

The parameters and visible results of extrinsic coagulation test (EX test) (a) and (TPA test)(b). The summary of results from EX test (c) and TPA test (d). Data were presented as Mean + SEM. * indicated significance between different genotypes; # indicated significance among different time compared to the baseline values. CFT: clot formation time (s); MCF: maximum clot firmness(mm); ML: maximum lysis (%); LT: lysis time (s).

lysis remained absent. In nephrotic patients, clot formation was enhanced in 7 out of 10 patients (EX test), while in the same patients clot lysis was delayed (TPA test). **Conclusion:** The results demonstrate that loss of Plg in the nephrotic state may contribute to a hypercoagulable state by attenuating clot lysis in nephrotic syndrome.

P190

Using isolated mouse glomeruli as an ex vivo model for glomerular disease

M. El Hajami; V. Krausel; H. Bachir¹; H. Pavenstädt; D. A. Braun¹
Allg. Innere Medizin und Notaufnahme sowie Nieren- und Hochdruckkrankheiten und Rheumatologie, Medizinische Klinik D, Westfälische Wilhelms-Universität Münster, Münster;
¹ Molekulare Nephrologie, Medizinische Klinik D, Westfälische Wilhelms-Universität Münster, Münster

Objective: In conventional two-dimensional cell culture systems, podocytes do not form slit diaphragms or foot processes and, due to dedifferentiation, they rapidly lose the expression of specialized slit diaphragm proteins. Therefore, in order to study the impact of extrinsic and intrinsic factors on the integrity of the glomerular filtration barrier and the localization of slit diaphragm proteins, novel model systems are needed. In this study, we aim at establishing an ex vivo system based on isolated mouse glomeruli.

Method: For the isolation of glomeruli from wildtype mice two different approaches were utilized: i) magnetic bead extraction and ii) a sieving method. Isolated glomeruli were maintained in 2D or in

3D Matrigel-based culture. Immunofluorescence analysis of slit diaphragm proteins, including Neph- rin and Podocin, was done to assess their subcellular localization, staining pattern, and expression level. An albumin assay was used to simulate an increased permeability of the glomerular filtration barrier. For the induction of podocyte injury, glomeruli were exposed to protamine sulfate for transient injury and to puromycin aminonucleoside (PAN) for permanent glomerular damage. **Results:** Different culture conditions were tested. In particular, glomeruli were cultured in 2D suspension or in a 3D culture using Matrigel to mimic the extracellular matrix. In 3D conditions, the glomerular architecture was preserved for an extended culture period. Immunofluorescence analysis of slit diaphragm proteins demonstrated staining patterns comparable to renal tissue sections, which were altered upon pharmacologically induced podocyte injury. An ELISA assay for specific measurement of murine serum albumin could detect an increased glomerular permeability for albumin in response to drug stimulation.

Conclusion: Isolated mouse glomeruli can be used as an ex vivo model for glomerular disease that reflects a disruption of slit diaphragm proteins in response to podocyte injury and an increased glomerular leakage of albumin as a functional read-out recapitulating proteinuria. In future applications, this system may enable high-throughput screenings of proteinuric phenotypes and pharmacological treatments capable of mitigating them. Hence, this model has the potential of reducing the need for experimental animals.

P191

The degradation of structural nuclear pore proteins in postmitotic podocytes occurs slowly and causes progressive glomerular disease in mice

H. Bachir; V. Krausel¹; H. Pavenstädt¹; D. A. Braun

Molekulare Nephrologie, Medizinische Klinik D, Westfälische Wilhelms-Universität Münster, Münster;

¹ Allg. Innere Medizin und Notaufnahme sowie Nieren- und Hochdruckkrankheiten und Rheumatologie, Medizinische Klinik D, Westfälische Wilhelms-Universität Münster, Münster

Objective: Recessive mutations in *NUP93* and six other genes that encode structural proteins of the nuclear pore complex, a gated channel across the nuclear envelope of eukaryotic cells, were identified as causing focal segmental glomerulosclerosis (FSGS) in pediatric patients. Surprisingly, despite the essential cellular function, ubiquitous expression, and high evolutionary conservation of nuclear pore proteins, affected patients mostly presented with a kidney-restricted phenotype. Our work aims at understanding the specific vulnerability of glomerular epithelial cells, podocytes, for the disruption of nuclear pores.

Method: A floxed mouse line for the *Nup93* gene was generated and Cre-recombinase driven by the *Six2* or *Nphs2* promotor was used for nephron- or podocyte-specific knockout of *Nup93* (*Nup93-Six2/Pod-ko*). Mendelian ratios in breeding were analyzed and monthly screenings for proteinuria were performed. Proteinuric animals were further evaluated at different time points by laboratory

analysis, renal histology, transmission electron microscopy, and immunofluorescence (IF) staining for nuclear pore proteins, slit diaphragm components, and markers of apoptosis and DNA damage.

Results: Mendelian ratios in homozygous Nup93-Six2-ko mice revealed embryonic lethality. In homozygous Nup93-Pod-ko mice, the knockout of Nup93 was confirmed on the mRNA level. In these mice, proteinuria started at an age of 4 months and increased progressively. At 6 months, renal excretory function declined and mice developed uremia. There was full penetrance of the phenotype in homozygous animals, while heterozygous Nup93-Pod-ko animals were phenotypically healthy. Interestingly, IF staining in knockout animals showed a delayed and gradual degradation of the NUP93 protein. Not until 6 months, parallel to the loss of staining of slit diaphragm proteins and the development of FSGS, the NUP93 signal was focally lost and podocytes depleted for NUP93 underwent apoptosis. Loss of NUP93, a core component of the structural scaffold of nuclear pores caused co-depletion of other nuclear pore proteins, in particular the NUP62 complex, which is essential for nuclear transport.

Conclusion: Our data indicate that, in post-mitotic podocytes, structural nuclear pore proteins, such as NUP93, are very stable and degrade slowly over an extended period. The loss of NUP93 with co-depletion of other nuclear pore proteins induces podocyte injury and ultimately apoptosis. We hypothesize that this may be due to an accumulation of DNA damage upon loss of the barrier function of nuclear pores.

P192

Trajectory Analysis of the Kidney Organoid Proteome Extends its Modelling Potential of Disease

M. Lassé; S. Eddy¹; M. Kretzler¹; J. L. Harder¹; M. Rinschen
Nephrologie/Rheumatologie und Endokrinologie/Diabetologie, III. Medizinische Klinik, Universitätsklinikum Hamburg-Eppendorf, Hamburg; ¹ Internal Medicine, Nephrology, Medical School, University of Michigan, Ann Arbor/USA

Objective: Kidney organoids are a valuable and innovative model to understand genetic diseases, kidney development and transcriptomic dynamics. However, their proteome has not been analyzed so far. It is unclear how their proteome changes during differentiation, and if more complex disease processes such as inflammatory tissue responses could be modelled with this approach.

Method: Here, we used proteomics to compare organoids with existing model systems such as native glomeruli and cultured cells. We characterize the trajectory of organoid differentiation and delineate innate immune responses in organoids to expand its scope as a model system in nephrology. We also compared our proteomics with bulk and single cell transcriptomic data.

Results: Genes involved in podocytopathies and cystic kidney diseases were abundantly expressed on protein level, distinguishing organoids from almost every available cell culture model. On their pathway to terminal differentiation, organoids developed increased deposition of extracellular matrix. Single cell transcriptomic analysis suggests that most changes locate to podocytes and early podocyte

progenitors. This matrix deposition is different from commonly used animal models of glomerular disease. A novel signaling system discovered was the TNF α system, a system also available in podocytes. Incubation of organoids with high concentrations of TNF α led to an activation of NF- κ B signaling, and secretion of cytokines and complement components, alongside with extracellular matrix components.

Conclusion: Interestingly, this signaling system directly links inflammatory signaling, production of cytokines and complement, and production of extracellular matrix. Thus, we provide a repository of human kidney organoid proteins that revealed the potential to model pathophysiological pathways beyond genetic diseases.

Experimentelle Nephrologie 5

P193

Die Behandlung mit Etelcalcetide verbessert die systolische Herzfunktion bei Mäusen unter Hochphosphatdiät

M. Leifheit-Nestler; I. Vogt; A. Grund; B. Richter; D. Haffner
Klinik für Pädiatrische Nieren-, Leber- und Stoffwechselerkrankungen, Zentrum für Kinder- und Jugendmedizin, Medizinische Hochschule Hannover, Hannover

Hintergrund: Hohe Phosphatspiegel stimulieren die Synthese der phosphaturischen Hormone PTH und FGF23 und sind mit einer erhöhten kardiovaskulären Morbidität und Mortalität assoziiert. In der Sekundäranalyse der EVOLVE-Studie senkte Cinacalcet die PTH- und FGF23-Spiegel bei Hämodialysepatienten signifikant, und letzteres

war mit einer geringeren Rate an kardiovaskulären Ereignissen und Todesfällen verbunden. Die intravenöse Gabe von Etelcalcetide führte bei Hämodialysepatienten zu einer Reduktion von FGF23 und einem langsameren Fortschreiten der linksventrikulären (LV) Hypertrophie. In der vorliegenden Studie haben wir die spezifischen Effekte von Etelcalcetide (KP-2326) auf das Herz bei Mäusen unter Hochphosphatdiät (HPD) untersucht.

Methode: Nach einer viermonatigen Gabe einer 2%igen HPD wurden männliche C57BL/6N-Mäuse zwei weitere Monate lang zusätzlich mit Etelcalcetide (1 mg/kg Körpergewicht/Tag) über osmotische Minipumpen behandelt und mit Mäusen verglichen, die eine HPD mit Vehikel oder eine 0,8%ige Normalphosphatdiät (NPD) erhielten. Die Herzfunktion wurde echokardiographisch untersucht und Parameter des Mineralstoffwechsels bestimmt.

Ergebnisse: Mäuse auf HPD hatten im Vergleich zur NPD-Gruppe signifikant höhere Phosphat-, FGF23- und PTH-Spiegel und eine vermehrte Phosphatausscheidung, die mit einer progredienten Nierenschädigung einherging. Mäuse, die HPD erhielten, zeigten einen dilatierten linken Ventrikel mit verminderter anteriorer und posteriorer Wanddicke und vergrößerten LV Durchmesser und Volumina. Die Ejektionsfraktion und fraktionelle Verkürzung waren bei Mäusen auf HPD signifikant reduziert, was auf eine eingeschränkte systolische Funktion hindeutet. Etelcalcetide senkte die HPD-induzierten FGF23- und PTH-Spiegel um 80 % bzw. 75 % und führte zu einer signifikanten Reduktion der Serumkalziumspiegel, hatte allerdings keinen

Einfluss auf die persistierende Hyperphosphatämie und -phosphaturie. Etelcalcetide verminderte effektiv die HPD-induzierte LV Dilatation und systolische Dysfunktion.

Zusammenfassung: Eine HPD führt bei Mäusen zu einer Hyperphosphatämie und hohen FGF23- und PTH-Konzentrationen mit konsekutiver LV Dilatation und systolische Dysfunktion. Die Gabe von Etelcalcetide verhindert trotz bestehender Hyperphosphatämie effektiv den HPD-induzierten pathologischen Herzphänotyp, was zumindest zum Teil auf die Normalisierung der hohen FGF23- und PTH-Plasmaspiegel zurückzuführen ist.

P194

Single-Cell RNA Sequencing reveals renal endothelium heterogeneity during injury and regeneration in a murine model of specific renal thrombotic microangiopathy

*J. Sradnick; A. Wirth; H. Kröger; P. Arndt; V. T. Todorov; C. Hugo
Medizinische Klinik III, Nephrologie,
Universitätsklinikum Carl Gustav
Carus, Technische Universität Dresden,
Dresden*

Objective: Analyses of the marker genes, pathways, and biological functions revealed that endothelial cells (EC) are highly heterogeneous showing plasticity both in normal and pathophysiological conditions. However, the heterogeneity and cellular responses of renal endothelial cells during injury and regeneration have not been well characterized.

Method: Endothelial specific injury was induced in 48 Tie2 eGFP mice by renal arterial perfusion with Concanavalin A (ConA)/anti-ConA.

19 mice served as sham operated controls. Kidneys were harvested 24 h, 48 h, 3 days, 4 days and 7 days after injury induction. For 10x single-cell RNA sequencing, cells were isolated from glomerular and extraglomerular renal tissue. Tie2-eGFP⁺ CD102⁺ (Icam2)/CD105⁺ (endoglin)/CD45⁻ endothelial cells were further separated using FACS cell sorting. After 10x single cell sequencing, Seurat clustering analysis was performed to identify EC cell clusters. Endothelial cell injury was evaluated using periodic acid-Schiff staining and histology in zinc fixed paraffin embedded slices.

Results: Endothelial cell loss was observed 24 h following injury, while the EC number already markedly increased on day 3 and was back to baseline levels after 4–7 days. 10 × single-cell RNA sequencing was performed on 42,000 sorted renal cells. Following quality control measurements almost all sequenced cells expressed endothelial specific genes. In glomerular and peritubular ECs, different cluster (17 and 7, respectively) could be identified following t-distributed stochastic neighbour embedding (t-SNE). In both glomerular and peritubular EC transcriptomics, cell clusters demonstrating predominant regulation of cellular injury genes was seen 24 h but also 48 h after model induction. Gene clusters consistent with cell remodeling and differentiation were mostly identified on day 4–7.

Conclusion: In summary, our study provides a high-resolution atlas of the renal endothelium during EC specific injury and regeneration. Our data highlight the phenotypic heterogeneity and changes of endothelial subtypes which were potentially involved during EC injury

and regeneration/healing after selective renal endothelial cell injury.

P195

Adult human kidney organoids originate from CD24⁺ cells and represent an advanced model for adult polycystic kidney disease

C. Kuppe; Y. Xu; J. Perales-Paton; S. Hayat; J. Kranz; A. T. Abdallah; J. Nagai; F. Peisker; T. Saritas; M. Halder; S. Menzel; K. Hoefft; A. Kenter¹; C. van Roeyen; M. Lehrke²; J. Moellmann; T. Speer³; E. M. Buhl⁴; P. Boor⁴; R. Hoogenboezem¹; J. Jansen; C. Knopp; I. Kurth; B. Smeets⁵; E. Bindels¹; M. Reinders¹; C. Baan¹; J. Gribnau¹; E. Hoorn¹; J. Steffens⁶; I. Costa; J. Floege; J. Saez-Rodriguez⁷; B. Freedman⁸; R. Kramann
Medizinische Klinik II, Nephrologie und Klinische Immunologie, Universitätsklinikum, Rheinisch-Westfälische Technische Hochschule Aachen, Aachen; ¹Erasmus MC, Rotterdam/NL; ²Medizinische Klinik I, Kardiologie, Angiologie und Internistische Intensivmedizin, Universitätsklinikum, Rheinisch-Westfälische Technische Hochschule Aachen, Aachen; ³Nieren- und Hochdruckkrankheiten, Klinik für Innere Medizin IV, Universität des Saarlandes, Homburg/Saar; ⁴Institut für Pathologie, Universitätsklinikum, Rheinisch-Westfälische Technische Hochschule Aachen, Aachen; ⁵Department of Pathology, Radboud University, Nijmegen/NL; ⁶Eschweiler; ⁷Heidelberg; ⁸Seattle/USA

Objective: Adult kidney organoids have been recently described as strictly tubular epithelial organoids and termed tubuloids. While the cellular origin of tubuloids remained elusive, we report here that they originate from a distinct CD24⁺ epithelial subpopulation.

Method: Here we used FACS to isolate CD24⁺ or CD13⁺ cells from human kidneys and performed single-cell RNA sequencing. We extensively characterized tubuloid protocols and performed single cell RNA sequencing at different time points. We established CRISPR-Cas9 in these tubuloids for PKD1 and PKD2 and compared single cell sequencing data from the gene-edited organoids to human ADPKD single cell data.

Results: Long term CD24⁺ derived tubuloids represent a functional human kidney tubule (proximal tubule and Loop of Henle) and we demonstrate that they can be utilized to model the most common inherited kidney disease namely autosomal dominant polycystic kidney disease (ADPKD), reconstituting the phenotypic hallmark of this disease with rapid cyst formation. Single-cell RNA-sequencing of CRISPR/Cas9 gene-edited PKD1 and PKD2 knockout tubuloids and human ADPKD and control tissue showed similarities in up-regulation of disease driving genes. Furthermore, tolvaptan, the only currently approved drug for ADPKD, shows a significant effect on cyst size in tubuloids but no effect in gene-edited iPSC organoids.

Conclusion: Overall, this suggests that tubuloids are a suitable system for compound screening as it resembles human disease pathophysiology.

P196

Der Chemokinrezeptor CCR2 auf myeloiden Zellen fördert die aortale Atherosklerose nach akuter Nierenschädigung

A. M. Breloh; V. C. Wulfmeyer; S. Gaedcke¹; S. Fleig; S. Rong;

D. DeLuca¹; H. Haller; R. Schmitt; S. von Vietinghoff²
Klinik für Nieren- und Hochdruck-erkrankungen, Zentrum für Innere Medizin, Medizinische Hochschule Hannover, Hannover; ¹Deutsches Zentrum für Lungenforschung, Klinik für Pneumologie, Medizinische Hochschule Hannover, Hannover; ²Sektion für Nephrologie, Medizinische Klinik und Poliklinik I, Universitätsmedizin Bonn, Bonn

Hintergrund: Das Risiko kardiovaskulärer Ereignisse steigt nach einer akuten Nierenschädigung (AKI). Wir haben kürzlich ein Mausmodell dafür etabliert, in dem wir jetzt die Rekrutierung von Leukozyten und die mechanistische Bedeutung des Chemokinrezeptors CCR2 untersucht haben.

Methode: LDL Rezeptor defiziente (LDLR^{-/-}) Mäuse, die bei fettreicher Diät Atherosklerose entwickeln, wurden mit CCR2 defizientem, Wildtyp-Kontrollknochenmark oder einer Mischung rekonstituiert. Die aortale Plaquelast und Inflammation unter Kontrollbedingungen und nach unilateraler renaler Ischämie-Reperfusionsschädigung wurden histologisch und per Genexpressionsanalyse untersucht.

Ergebnisse: Das Muster in der atherosklerotischen Aorta nach Nierenschaden differentiell exprimierter inflammatorischer Gene ähnelte dem Zeitverlauf in der Niere nach Ischämie-Reperfusionsschaden. Durch renale Einzelzell-mRNA Sequenzierung wurden renale Zelltypen identifiziert, die nach Nierenschaden lösliche Inflammationsmediatoren, die in der atherosklerotischen Aorta gefunden wurden, exprimierten. Insbesondere fand sich früh nach der Schädigung ein

deutlicher Anstieg in *Ccl2* Expression, vor allem in $CCR2^+$ myeloiden Zellen. Der Chemokinrezeptor $CCR2$ vermittelte das Homing myeloider Zellen in die verletzte Niere auf Einzelzellebene. Eine Rekonstitution mit *Ccr2*^{-/-} Knochenmark verminderte die renale postischämische Inflammation. In der Aorta reduzierte es die *Ccl2* Expression und den Marker inflammatorischer Makrophagen CD11c. Ohne $CCR2$ waren die Tiere vor der erhöhten Plaquelast nach AKI geschützt.

Zusammenfassung: In unserem neuen Mausmodell für proatherogene Effekte eines renalen Ischämieperfusionsschadens zeigen unsere Experimente, dass eine verstärkte aortale Atherosklerose nach Nierenschaden durch myeloides $CCR2$ mediiert wird. Monozyten sollten als potentielle mobile Mediatoren dieses Prozesses weiter untersucht werden.

P197

Leukemia inhibitory factor fördert Verkalkung von Gefäßmuskelzellen durch TYK2/STAT Aktivierung

I. Alesutan; L. Pitigala; T. T. D. Luong; M. O. Estepa Martínez¹; D. Zickler¹; A. Pasch²; J. Holfeld³; A. Vlahou⁴; K.-U. Eckardt⁵; J. Völk

Institute for Physiology and Pathophysiology, Johannes Kepler Universität Linz, Linz/A; ¹ Medizinische Klinik mit Schwerpunkt Internistische Intensivmedizin und Nephrologie, Campus Virchow-Klinikum, Charité – Universitätsmedizin Berlin, Berlin;

² Nephrologie, Allgemeine Innere Medizin, Lindenhofspital, Bern/CH;

³ Universitätsklinik für Herzchirurgie, Innsbruck/A; ⁴ Biomedical Research Foundation, Academy of Athens, Athens/GR; ⁵ Medizinische Klinik mit Schwerpunkt Nephrologie und

Internistische Intensivmedizin, Campus Charité Mitte, Charité – Universitätsmedizin Berlin, Berlin

Hintergrund: Mediale Gefäßverkalkung ist mit Hyperphosphatämie und kardiovaskulärer Mortalität in chronischer Niereninsuffizienz verknüpft. Phosphat-Exposition aktiviert pro-inflammatorische Signalwege in glatten Gefäßmuskelzellen, die dann kalzifizierende Eigenschaften annehmen. In diesem Kontext wurden die Rolle und Signalwege des „leukemia inhibitory factor“ (LIF) untersucht, einem Mitglied der Interleukin-6 Familie.

Methode: Versuche wurden in primären humanen glatten Gefäßmuskelzellen (VSMCs), ex-vivo aortalen Ringen der Maus, in Klotho-hypomorphen (kl/kl) und Cholecalciferol-Injektion Mausmodellen, sowie Serumproben von niereninsuffizienten Patienten und gesunden Kontrollen durchgeführt.

Ergebnisse: Die Expression von LIF wurde durch verkalkende Bedingungen in vivo und in vitro gesteigert. LIF-Supplementation verstärkte die Expression osteogener Marker und Kalzifizierung in verkalkenden VSMCs, wobei Silencing von LIF, LIF-Rezeptor oder des Ko-Rezeptors GP130 die osteogenen Effekte von Phosphat reduzieren konnte. LIF aktivierte TYK2 sowie STAT1/3 Phosphorylierung. Die osteogenen Effekte von LIF wurden reduziert durch Zugabe des löslichen LIF-Rezeptors, ein vermutterter LIF-Inhibitor. Die LIF-Effekte wurden weiterhin durch lösliches GP130 oder Silencing/Inhibierung von TYK2, STAT 1 oder STAT3 gehemmt. Sowohl Zugabe von löslichem LIFR, GP130 oder Hemmung des TYK2/STAT Signalwegs

konnte die Expression osteogener Marker nach Phosphatbehandlung abschwächen. Pharmakologische Hemmung von TYK2 reduzierte die ex-vivo Verkalkung von aortalen Ringen nach Phosphatexposition. Ebenso konnte die Verkalkung und Expression osteogener Marker in Gefäßen von Mäusen nach Cholecalciferol-Behandlung durch TYK2-Hemmung abgeschwächt werden. In Patienten mit chronischer Niereninsuffizienz waren gegenüber gesunden Kontrollen die Spiegel des löslichen LIFR reduziert. Die Spiegel des löslichen LIFR korrelierten mit der „serum calcification propensity“.

Zusammenfassung: Die pro-kalzifizierenden Effekte von LIF identifizieren die kritische Beteiligung eines TYK2-abhängigen Signalwegs bei phosphat-induzierter Verkalkung. Blockade dieses Signalwegs könnte mit der Entstehung und Progression von Gefäßverkalkungen bei chronischer Niereninsuffizienz interferieren.

P198

Pathogenic MAPKBP1 variants impair cilia functionality in nephronophthisis patients

C. Hartig; L. Pöschla; W. Jin; E. Hantmann¹; J. Halbritter¹; R. Schönauer¹

Sektion Nephrologie, Klinik für Endokrinologie und Nephrologie, Universitätsklinikum Leipzig, Leipzig; ¹ Medizinische Klinik mit Schwerpunkt Nephrologie und Internistische Intensivmedizin, Campus Charité Mitte, Charité – Universitätsmedizin Berlin, Berlin

Objective: Nephronophthisis (NPH) is an autosomal-recessive tubulointerstitial kidney disease majorly accounting for end-stage kidney disease in the first

three decades of life. Loss-of-function mutations in *MAPKBP1*, encoding c-Jun N-terminal kinase-binding protein 1 (JNKBP1/MAPKBP1), have previously been identified as an underlying cause of late-onset NPH (Macia et al, *AJHG*, 2017/ Schönauer et al, *Kidney Int*, 2020). Initially, MAPKBP1-causing NPH was thought to have a cilia-independent mechanism (Macia et al, *AJHG*, 2017). However, we previously demonstrated MAPKBP1 localization at the ciliary basal body (Schönauer et al, *Kidney Int*, 2020). In a next step, we aimed to investigate structure and function of primary cilia in NPH patients due to pathogenic *MAPKBP1* variants.

Method: Dermal fibroblasts isolated from NPH patients were observed in fluorescence microscopy studies. Structure of primary cilia were examined by antibody staining and the expression of MAPKBP1 and cilia-associated proteins was observed. The findings were compared with results from RNA sequencing of these primary cells and fluorescence microscopy studies of HeLa and ciliated H69 cells overexpressing GFP-labeled pathogenic MAPKBP1 variants. The effects on ciliary downstream signaling pathways were analyzed by functional assays in primary cells and HEK293T cells transfected with deletion variants of MAPKBP1.

Results: As expected, RNA sequencing yielded reduced MAPKBP1 expression in all patient cells. Immunofluorescence microscopy revealed shorter primary cilia in dermal fibroblasts of NPH patients. Furthermore, endogenous MAPKBP1 localization at the ciliary basal body, as observed in healthy controls, was absent in all primary NPH

patient cells. For confirmation, impaired localization of patient-derived MAPKBP1 variants was replicated in HeLa and ciliated H69 cells by overexpression of GFP-labeled constructs. Functional assays and RNA sequencing revealed altered ciliary downstream signaling pathways upon MAPKBP1 variation.

Conclusion: In the present work, we further demonstrate ciliary defects of MAPKBP1-associated NPH, similar to other NPHs. These defects range from impaired cilia morphology to altered cilia-dependent signalling pathways. Thus, we disproved the original assumption that pathogenic MAPKBP1 variants cause NPH independent from primary cilia anomalies.

P199

An in vivo high-throughput drug screening assay in a zebrafish FSGS model identifies drug 171 as podocyte-protective

M. Schindler; F. Siegerist; T. Lange; S.-M. Bach; J. Gehrig¹; S. Gul²;

N. Endlich

Institut für Anatomie und Zellbiologie, Universitätsmedizin Greifswald, Greifswald; ¹Acquifer Imaging GmbH, Heidelberg; ²Fraunhofer Institute for Translational Medicine and Pharmacology ITMP, Hamburg

Objective: Since causative treatments for FSGS are not available today, there is an urgent need for new drugs. FSGS is strongly associated with podocyte injury and therefore, drugs that prevent podocyte injury are in a high demand. As a small vertebrate model, the zebrafish larva is ideally suited to study glomerular morphology, filtration barrier integrity and response to podocyte injury *in vivo*. Recently, our

group established a reliable pharmacogenetic FSGS-like model in transgenic zebrafish larvae which serves as basis for a high-throughput drug screening system. The aim of this work was the development as well as the utilization of an automated *in vivo* high-content drug screening assay which helps to identify or repurpose drugs for patients suffering from FSGS.

Method: The zebrafish screening strain expresses the bacterial nitroreductase and the fluorophore mCherry exclusively in podocytes as well as the eGFP-vitamin-D-binding protein (78 kDa) in the blood plasma. Addition of the prodrug metronidazole to the medium results in a conversion of metronidazole into a toxin by the nitroreductase resulting in a FSGS-like phenotype and glomerular clearance of the eGFP fusion protein from the vasculature. For the screening, larvae in groups of 12 were treated with the solvent (DMSO), metronidazole or metronidazole together with drugs from a compound library. The zebrafish screening strain provides two readouts: the vitality of podocytes by assessment of the mCherry signal and the degree of proteinuria by assessment of the vascular eGFP signal. Larvae were imaged in a 96-well plate format and target structure detection and fluorescence intensity measurements performed using an automated image analysis workflow at two timepoints. Groups treated with metronidazole plus compound are compared with the metronidazole injury control group. Compounds which ameliorated podocyte injury were considered positive hits.

Results: Screening of an initial 138 compounds drug library provided 36 substances that resulted in

a lethal phenotype in zebrafish larvae in a co-treatment with metronidazole. 9 compounds could be identified as positive hits. Subsequent validation experiments with larger groups confirmed that drug 171 has a protective effect on larval podocytes in this injury model.

Conclusion: This novel assay is an *in vivo* screening platform to identify new drugs that might protect podocytes from injury. Here, we identified drug 171 as a reliable protective agent for larval podocytes and the glomerular filtration barrier in the FSGS-like zebrafish model.

P200

A molecular map of VPS34 activity links nutrient recovery and apical membrane function in the kidney

M. Rinschen; J. L. Harder¹; D. Olganier²; R. Nielsen²; F. Grahammer; F. Theilig³
Nephrologie/Rheumatologie und Endokrinologie/Diabetologie, III. Medizinische Klinik, Universitätsklinikum Hamburg-Eppendorf, Hamburg; ¹Internal Medicine, Nephrology, Medical School, University of Michigan, Ann Arbor/USA; ²Institut for Biomedicine, Aarhus University, Aarhus/DK; ³Anatomisches Institut, Christian-Albrechts-Universität zu Kiel, Kiel

Objective: The lipid kinase VPS34 orchestrates autophagy, endocytosis, and metabolism and is implicated in cancer and metabolic disease. The kidney proximal tubule, recently emerged as a key metabolic organ and drug target, controls abundance of all building blocks of life, including fatty acids, amino acids, sugars and proteins.

Method: Here, we reveal that the *in vivo* molecular landscape of the kidney is controlled by the PI3-kinase VPS34 by integrating metabolomics,

proteomics, phosphoproteomics with functional and super-resolution imaging assays in a novel inducible knock-out model.

Results: In addition to inhibition of pinocytosis and autophagy, VPS34 depletion induces membrane exocytosis and reduces the retromer complex necessary for proper membrane recycling and fate, leading to a loss of fuel and biomass. Integrating omics data into a kidney cell metabolic model demonstrated increased abundance of beta-oxidation, reduced gluconeogenesis, and usage of glutamine for energy consumption. Interestingly, all omics datasets unraveled multi-layered aspects of antiviral cytokine response, and reduction and shedding of apically localized virus receptors such as ACE2. Consequently, VPS34 inhibition abrogated SARS-CoV-2 infection in human kidney organoids and proximal tubule cultured cells, a process relying on sufficient glutamine supply.

Conclusion: In conclusion, this molecular landscape demonstrates that VPS34 *in vivo* is a master switch adjusting endocytosis, nutrient transport, autophagy and the antiviral response. This broad proteometabolic landscape can be exploited in metabolic interventions in health and disease, and suggests that organ-specific maps are necessary to advance VPS34 as a drug target.

P201

The Sphingosine Kinases 1 and 2 Differentially Regulate Erythropoietin Synthesis in Mouse Renal Interstitial Fibroblast-like Cells

R. Manaila; R. Hafizi; F. Imeri; B. S. Tanturovska; S. Schwalb¹; R. H. Wenger²; J. M. Pfeilschifter¹; A. Huwiler

Institut für Pharmakologie, Universität Bern, Bern/CH; ¹Institut für Allgemeine Pharmakologie und Toxikologie, Universitätsklinikum, Johann Wolfgang Goethe-Universität, Frankfurt a. M.; ²Institut für Physiologie, UniversitätsSpital Zürich, Universität Zürich, Zürich/CH

Erythropoietin (Epo) is a crucial hormone regulating red blood cell number and consequently the hematocrit. Epo is mainly produced in the kidney by interstitial fibroblast-like cells. Previously, we have shown that in cultures of the immortalized mouse renal fibroblast-like cell line FAIK F3-5, sphingosine 1-phosphate (S1P), by activating S1P1 and S1P3 receptors, can stabilize hypoxia-inducible factor (HIF)-2 α and upregulate Epo mRNA and protein synthesis. In this study, we have addressed the role of intracellular iS1P derived from sphingosine kinases (Sphk) 1 and 2 on Epo synthesis in F3-5 cells and in mouse primary cultures of renal fibroblasts. We show that stable knockdown of Sphk2 in F3-5 cells increases HIF-2 α protein and Epo mRNA and protein levels, while Sphk1 knockdown leads to a reduction of hypoxia-stimulated HIF-2 α and Epo protein. A similar effect was obtained using primary cultures of renal fibroblasts isolated from wild-type mice, Sphk1^{-/-}, or Sphk2^{-/-} mice. Furthermore, selective Sphk2 inhibitors mimicked the effect of genetic Sphk2 depletion and also upregulated HIF-2 α and Epo protein levels. The combined blockade of Sphk1 and Sphk2, using Sphk2^{-/-} renal fibroblasts treated with the Sphk1 inhibitor PF543, resulted in reduced HIF-2 α and Epo compared to the untreated Sphk2^{-/-} cells.

The upregulation of HIF-2 α and Epo synthesis by loss of Sphk2 was also in the human hepatoma cell line Hep3B, which is well-established to upregulate Epo production under hypoxia. In summary, these data suggest that selective inhibition of Sphk2 is an attractive new option to enhance Epo synthesis and thereby to reduce anemia development in chronic kidney disease.

P202

Sparsentan Improves Glomerular Blood Flow and Augments Protective Tissue Remodeling in Mouse Models of Focal Segmental Glomerulosclerosis (FSGS)

G. Gyarmati; U. Shroff; A. Izuhara; R. Komers¹; P. W. Bedard¹; J. Peti-Peterdi

Zilka Neurogenetic Institute, Keck School of Medicine, University of Southern California, Los Angeles/USA; ¹ Traver Therapeutics, Inc., San Diego/USA

Objective: Aim was to determine glomerular action of sparsentan vs losartan (Los) by direct visualization of renal hemodynamics and tissue remodeling in the intact living kidney.

Method: Intravital multiphoton microscopy (MPM) imaging of the glomerular vasculature and filtration barrier structure and function was performed in multiple genetically engineered mouse models combined with traditional urinalysis and histology-based phenotyping. Glomerular hemodynamic parameters (afferent and efferent arteriole [AA; EA] diameters; single nephron GFR [SNGFR]) and podocyte free calcium (cell injury measure) were quantitatively visualized in the FSGS model Pod-GCaMP5/Tomato TRPC6

transgenic mice (age 1.5 years). Single cell identification and fate tracking of cells of the renin lineage (CoRL) used a second physiologic control mouse model, Ren1d-Confetti mice, that feature a multicolor CFP/GFP/YFP/FP reporter. Three groups of mice in each model received treatment with either vehicle (CTRL), Los (10 mg/kg/day), or sparsentan (120 mg/kg/day) for 6 weeks (FSGS model) or 2 weeks (control physiology model).

Results: Los and sparsentan attenuated the acute ET + Ang II-induced podocyte calcium elevation by ~80 %, and attenuated development of albuminuria, glomerulosclerosis, and tissue fibrosis in the FSGS model. Sparsentan reduced podocyte calcium more than Los and was significantly more effective in dilating AA and EA (Fig 1A, B), increasing SNGFR (Fig 1C) and capillary blood flow 2-fold ($p < 0.0001$ vs CTRL), and decreasing albuminuria by 20 % ($p < 0.05$ vs CTRL). Sparsentan preserved p57+ podocyte number by 50 % vs Los ($p < 0.0001$ vs CTRL). Sparsentan pretreatment was more effective in preventing glomerular arteriolar vasoconstriction induced by acute ET + Ang II IV injection vs Los. In response to 2-week treatment in control healthy Ren1d-Confetti mice, sparsentan resulted in a more robust increase vs Los in the number of Confetti+ cells, clones, and individual cells per clone in the glomeruli and AA (Fig 1D-F). Cortical and medullary tubule segments showed active cellular remodeling in response to sparsentan.

Conclusion: Serial MPM imaging directly visualized several mechanisms underlying beneficial anti-proteinuric and structural effects

of sparsentan in FSGS and normal mouse kidney and potential differences between dual ET/Ang II receptor antagonism and an angiotensin receptor blocker. Sparsentan was more effective in attenuating ET/Ang II-induced podocyte injury and in activation of progenitor cells and tissue remodeling, suggesting multiple renal protective actions by dual ET/Ang II receptor antagonism.

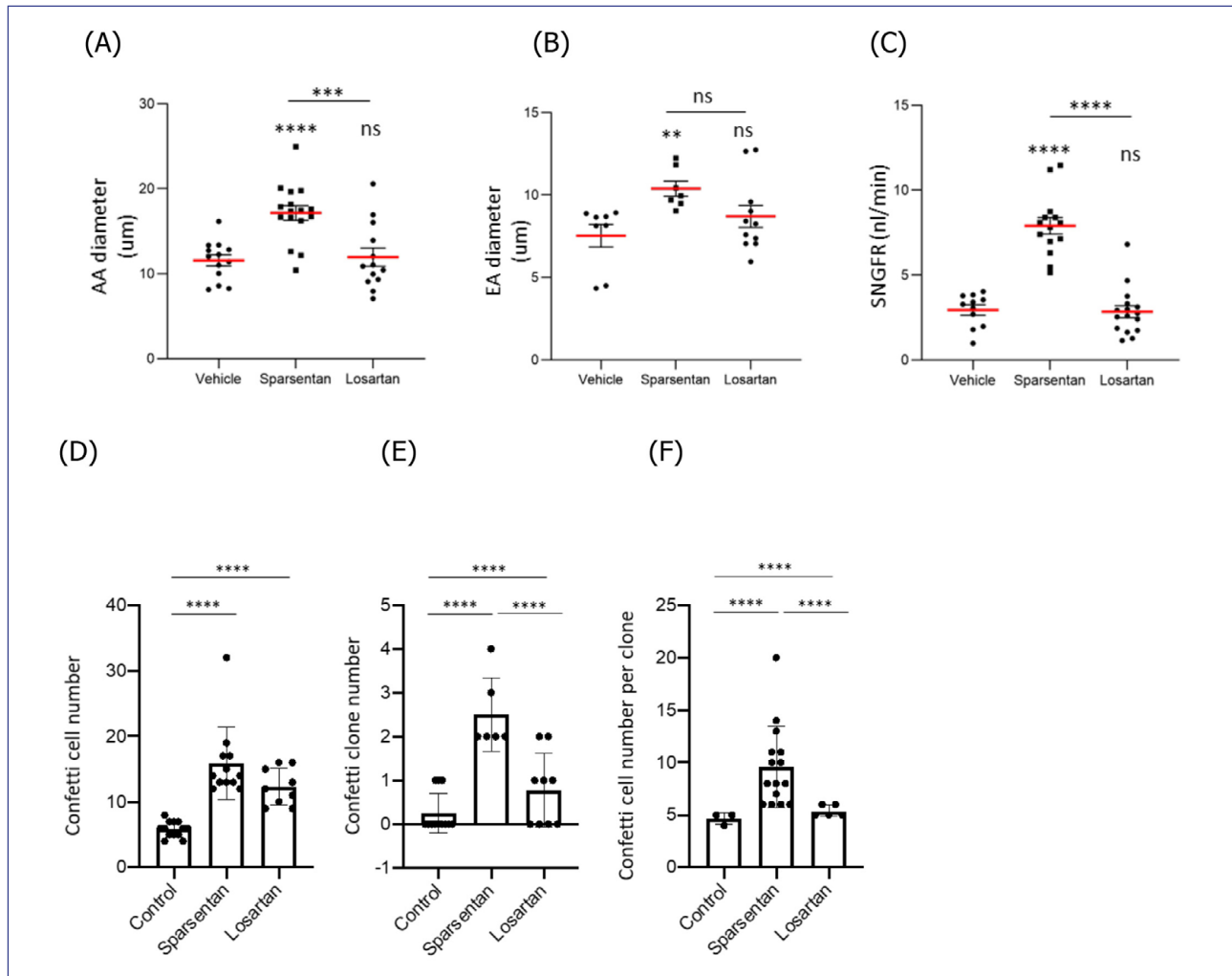
P203

Sparsentan, the Dual Endothelin Angiotensin Receptor Antagonist (DEARA), Improves Kidney Function and Lifespan and Protects Against Hearing Loss in Alport Mice with Developed Renal Structural Changes

D. Cosgrove; M. A. Gratton¹; D. Meehan; D. Vosik; J. Madison; D. Delimont; G. Samuelson; D. Jarocki¹; R. Komers²; C. Jenkinson²
Boys Town National Research Hospital, Omaha/USA; ¹ Washington University School of Medicine, St. Louis/USA; ² Traver Therapeutics, Inc., San Diego/USA

Objective: In Alport syndrome (AS), endothelin type A receptor activation is an important mediator of renal and inner ear pathologies. Sparsentan (SP) administered to COL4A3^{-/-} mice (AS mice) in prevention mode delayed increases in proteinuria, renal structural changes, and hearing loss (HL). Whether these effects translate into preservation of glomerular filtration rate (GFR), increased lifespan (LS), and protection from HL in mice where renal pathology has initiated is unknown.

Method: Wild type (WT) and AS mice were gavaged daily with vehicle (WT-V or AS-V), 60 or 120 mg/



P202: Abb. 1

(A) AA Diameter, (B) EA Diameter, (C) SNGFR, (D-F) Confetti+ cell and clone numbers in the glomeruli and AA. Statistical determined by ANOVA * $p < 0.05$, ** $p < 0.01$, *** $p < 0.001$, **** $p < 0.0001$. ns = not significant.

kg SP (AS-SP60 or AS-SP120) starting at 4 weeks (W) of age or at 5, 6 or 7 W. Glomerulosclerosis (GS) was evaluated in kidney sections stained for fibronectin. GFR was measured using a transdermal device (Medi-beacon) in 9 W mice treated with SP from 4 W. The auditory brainstem response (ABR) was used to assess hearing ability and sensitivity to noise at 8-8.75 W in AS-V or AS-SP120 mice treated from 5 W.

Results: SP begun at 4 W abrogated the decline in GFR at 9 W compared to AS-V mice (GFR $\mu\text{l}/\text{min}$ mean \pm SD; WT-V 159 ± 58 [n = 6], AS-V 54.0 ± 30 [n = 10], AS-SP60 148 ± 21 [n = 6], AS-SP120 145 ± 42 [n = 15]; $P < 0.001$ AS-V vs AS-SP60 or AS-SP120) and provided protection from GS in mice at 10 W ($P < 0.01$ AS-SP120 vs AS-V). For LS studies GS (mean % sclerotic glomeruli) prior to treatment in

AS mice was 0 at 4 W, 5.2 % at 5 W, 23.3 % at 6 W and 47.0 % at 7 W and SP120 extended median LS (MLS) when dosing began even in 5, 6 or 7 W mice with detectable GS (MLS days; AS-V 67.5, AS-SP120 4 W start 118.0, AS-SP120 5 W start 89.0, AS-SP120 6 W start 88.0, AS-SP120 7 W start 83.0). SP120 begun at 5 W improved post noise thresholds with prevention of HL at 16 ($P < 0.05$) and 24 Hz ($P < 0.01$) (Mean \pm SD

dB SPL 16 Hz; WT-V 5 ± 6.1 , AS-V 23 ± 9.7 , AS-SP120 11 ± 4.2).

Conclusion: SP prevents the decline in GFR in AS mice, extends LS, and prevents noise-induced HL noted in AS-V mice, even in mice with developed renal structural changes. If these results are translated successfully into the clinic, SP may offer a novel treatment approach for reducing both renal injury and protecting hearing in AS.

P204

β_2 integrin-dependent adhesion is indispensable for inflammatory HIF1 α activation in human neutrophils

L. Kling; C. Eulenberg-Gustavus¹; U. Jerke¹; A. Rousselle¹; K.-U. Eckardt²; A. Schreiber²; R. Kettritz¹
Klinik für Nephrologie und Intensivmedizin, Charité – Universitätsmedizin Berlin, Berlin; ¹ECRC-Kooperation von MDC und Charité, Experimental and Clinical Research Center, Berlin; ²Medizinische Klinik mit Schwerpunkt Nephrologie und Internistische Intensivmedizin, Campus Charité Mitte, Charité – Universitätsmedizin Berlin, Berlin

Objective: Myeloid cells migrate from blood to inflammatory sites with high cytokine but low oxygen concentrations. Hypoxic but also pharmacologic prolyl hydroxylase-inhibition induces hypoxia-inducible factor 1 α (HIF1 α), and thereby enhances myeloid cell performance. We tested the hypothesis that cytokines and β_2 -integrins co-operate in the HIF1 α activation process. **Method:** We characterized HIF1 α in human blood neutrophils and monocytes using immunoblotting and qPCR. Neutrophil

suspension was achieved on polyhema, adhesion on fibronectin, and migration through transwells. Prolyl hydroxylases were inhibited with Roxadustat (ROX), and HIF1 α translation with YC1. Signaling pathways were analyzed with β_2 -integrin antibodies and the JAK2 inhibitor AZD1480. **Results:** We observed HIF1 α activation in ROX-, but not cytokine-treated neutrophils and monocytes after 4 h incubation in tubes. A 3-fold synergistic effect occurred in neutrophils but not in monocytes with combined GM-CSF and ROX treatment. Neutrophils that interacted with fibronectin showed high HIF1 α protein abundance, whereas HIF1 α protein was completely absent under stringent suspension conditions on polyhema that excluded cell-cell and matrix contacts. Consequently, pre-incubation with blocking β_2 -integrin antibodies prevented neutrophil HIF1 α protein in both tubes and on fibronectin. GM-CSF induced strong HIF1 α mRNA via JAK2/STAT but independent of adhesion. However, an additional β_2 -integrin signal was required for HIF1 α protein upregulation. Adhesion did not accelerate transcription but rather involved post-transcriptional mechanisms stabilizing HIF1 α protein as shown by YC1-mediated inhibitory effects. These novel synergistic mechanisms led to strong HIF1 α protein in neutrophils that migrated towards GM-CSF and ROX in transwell experiments. **Conclusion:** Human neutrophils are unable of activating HIF1 α in suspension. In contrast, cytokine, β_2 -integrin, and prolyl hydroxylase co-operation at inflammatory sites enables strong HIF1 α activation.

Experimentelle Nephrologie 6

P205

P2Y2R fördert das Zystenwachstum in PKD

A. Kraus; K. Skoczynski; S. Grampp; J. Schödel; M. Schiffer; B. Buchholz
Medizinische Klinik 4, Nephrologie und Hypertensiologie, Universitätsklinikum, Friedrich-Alexander-Universität Erlangen-Nürnberg, Erlangen

Hintergrund: Die ADPKD ist charakterisiert durch ein kontinuierliches Zystenwachstum. Hierbei spielt die Flüssigkeitssekretion in das Zystenlumen eine wesentliche Rolle. Wir konnten zeigen, dass hierbei eine ATP- & Ca²⁺-abhängige Chloridsekretion durch den Chloridkanal TMEM16A wesentlich zum Zystenwachstum beiträgt. Bislang war der Mechanismus, der zur Aktivierung von TMEM16A führt unbekannt. Unsere Vordaten legten nahe, dass eine ATP-abhängige Stimulation des purinergen Rezeptors P2Y2R hierfür verantwortlich sein könnte. Deshalb untersuchten wir *in vitro* als auch in einem *in vivo* Mausmodell den Einfluss von P2Y2R auf das Zystenwachstum bei PKD. **Methode:** Unter Zuhilfenahme des bei uns etablierten KspCreERT2;Pkd1^{lox/lox}-Mausmodells konnten wir eine Doppel Knock-out-Linie mit P2y2r^{lox/lox} generieren (KspCreERT2; Pkd1^{lox/lox}; P2y2r^{lox/lox}). Diese Mäuse wurden an Tag 20–22 induziert und die Organe nach 10 Wochen histologisch aufgearbeitet sowie Harnstoff bestimmt. **Ergebnisse:** Die Deletion des purinergen Rezeptors P2Y2 reduzierte das Zystenwachstum in einem induzierbaren tubulusspezifischen Pkd1-Knockout-Mausmodell signifikant. In unseren Analysen zeigte sich ein

verminderter zystischer Index sowie ein geringeres Nierengewicht-Körpergewicht-Verhältnis. Eine verbesserte Nierenfunktion in Form reduzierter Harnstoffwerte zeigte sich passend dazu. Mittels histologischer Färbungen detektierten wir eine verringerte Proliferationsrate (ki67 Färbung), eine verringerte Makrophageninfiltration (F4/80 Färbung) sowie eine verringerte Fibroserate (Sirius Rot Färbung) bei der Doppel Knockout-Linie.

Zusammenfassung: Der purinerge Rezeptor P2Y2 trägt wesentlich zum Zystenwachstum in einem PKD1 orthologen Mausmodell bei. P2Y2R könnte daher ein interessantes therapeutisches Ziel zur Behandlung der ADPKD darstellen.

P206

Modulation und Untersuchung des Zystenwachstums bei ADPKD in einem humanen Gewebe-basierten 3D-Zystenmodell

V. Haller; E. M. Bichlmayer;
L. Mahl; L. Hesse; E. Pion;
A. Möhwald; C. Hackl¹; J. Werner¹;
H. J. Schlitt¹; S. Schwarz²; P. Kainz²;
C. Brochhausen³; C. Groeger⁴;
F. Steger⁴; O. Koelbl⁴; C. Daniel⁵;
K. Amann⁵; A. Kraus⁶; B. Buchholz⁶;
T. Aung; S. Härteis

Lehrstuhl für Molekulare und Zelluläre Anatomie, Institut für Anatomie, Universität Regensburg, Regensburg;

¹ Klinik und Poliklinik für Chirurgie, Universitätsklinikum, Universität Regensburg, Regensburg; ² KML Vision GmbH, Graz/A; ³ Institut für Pathologie, Universität Regensburg, Regensburg; ⁴ Klinik für Strahlentherapie, Universitätsklinikum Regensburg, Regensburg; ⁵ Institut für Nephropathologie, Universitätsklinikum, Friedrich-Alexander-Universität Erlangen-Nürnberg, Erlangen;

⁶ Medizinische Klinik 4, Nephrologie und Hypertensiologie, Universitätsklinikum, Friedrich-Alexander-Universität Erlangen-Nürnberg, Erlangen

Hintergrund: Bei der autosomal dominanten polyzystischen Nierenerkrankung (ADPKD) wachsen zahlreiche Zysten in beiden Nieren, was zur Einschränkung der Nierenfunktion führt. Zellproliferation und Flüssigkeitssekretion sind essenziell für das Zystenwachstum. Aktuell gibt es keine ausreichenden Therapieansätze, um das Zystenwachstum zu inhibieren und so die Nierenfunktion bei der ADPKD zu erhalten. Bisher haben Strategien zur Inhibition des Zystenwachstums in nicht-humanen Modellen ihre klinischen Erfolge verfehlt. Modelle, die Studien humanen Zystenwachstums und die Testung von Medikamenten ermöglichen, sind daher von signifikanter Notwendigkeit. Das ambitionierte Ziel des Projektes ist die Gewinnung dringend benötigter Erkenntnisse zum Ansprechen des Nierengewebes von ADPKD Patienten auf potentielle Therapeutika. Darüber hinaus erhoffen wir uns, durch die Verlaufsbeobachtung Einblicke in die der ADPKD zugrundeliegenden Pathomechanismen zu erhalten und idealerweise neue pharmakologische Targets identifizieren zu können. Diese neue Methode stellt einen wichtigen Schritt für die Entwicklung und Erprobung therapeutischer Ansätze dar, und leistet einen Beitrag zur Reduzierung von Tierversuchen im Sinne der 3R-Prinzipien.

Methode: Nierengewebe von ADPKD-Patienten, das infolge einer Nephrektomie entnommen wurde, sowie Nierenschnitte von adulten Mäusen wurden für eine Woche

auf der Chorion-Allantois-Membran (CAM) kultiviert. Das Volumen des zystischen Gewebes wurde mit mikroskopischen und CT-basierten Anwendungen gemessen. Außerdem wurden Gewicht und Angiogenese quantifiziert. Nach der Entnahme des Gewebes von der CAM wurden morphometrische und histologische Untersuchungen durchgeführt.

Ergebnisse: Humanes Gewebe und Maus-Nierenschnitte verblieben über einen Zeitraum von etwa einer Woche größtenteils vital. Das mittels mikroskopischer und CT-basierter Verfahren erfasste Volumen korrelierte mit dem Gewicht des Zystengewebes und das Gewebewachstum war anhand der Zunahme der Angiogenese ersichtlich. Zusätzlich konnte eine Proliferation zystischer Zellen beobachtet werden.

Zusammenfassung: Das CAM-Modell bietet die Möglichkeit, die „Brücke“ zwischen Tierstudien und klinischen Studien zu humanem Zystenwachstum zu schlagen und stellt außerdem ein Modell für die Testung wachstumsinhibierender Substanzen dar. Echtzeitanalysen von Maus-Nierengewebe ermöglichen zudem eine Untersuchung physiologischer Nierenprozesse bei gleichzeitiger Minimierung des Tiereinsatzes.

P207

Investigating pro-fibrotic impact of the C5aR1/C5a axis on tubular cells after ischemia/reperfusion injury

E. Bleich; M. Chikho; E. Vonbrunn;
M. Büttner-Herold; K. Amann;
C. Daniel

Institut für Nephropathologie, Universitätsklinikum, Friedrich-Alexander-Universität Erlangen-Nürnberg, Erlangen

Objective: Ischemia-reperfusion-injury (IRI) is an inevitable perioperative companion during kidney transplantation and decisively influences immediate and long-term graft function. As a key component of the innate immune response, the complement system plays a crucial role in IRI pathophysiology. We focused on the C5aR1/C5a axis and its suggested impact on profibrotic signaling in tubular cells.

Method: IRI was induced in Dark Agouti rats and kidneys were harvested 10min, 6 h, 24 h, 3d, 5d and 8w post reperfusion (each group n = 10) to investigate the time course of fibrosis. Vimentin, alpha smooth muscle actin, and collagen 1 were detected in kidney sections using immunohistochemistry. Multiplex mRNA analysis was used to analyze different genes coding for matrix molecules and C5aR1. Characterization of C5aR1+ cells in the kidney was performed by immunofluorescence double staining and in situ hybridization. Furthermore, human and rat whole blood, as well as human primary proximal tubular epithelial cells were stained for C5aR1 and analyzed by flow-cytometry. Finally, direct pro-fibrotic effects of C5a on tubular cells were investigated using multiplex RNA analysis after stimulation of proximal tubular cells with 50 nM recombinant C5a.

Results: An early profibrotic reaction emerged by increased staining of vimentin and smooth muscle actin in the rat kidney from d3, peaking on d5 and later diminishing on the final time point of 8w. A concurrently appearing increase in C5aR1 staining and expression, as well as C3d deposition indicated complement activation. C5aR1 mRNA, as

assessed by in situ hybridization, could be detected predominantly in inflammatory cells such as neutrophils and macrophages in the kidney, whereas in tubular cells in general and proximal tubular cells in particular only very scarcely stained positively. This result was consistent with flow cytometry, which failed to detect C5aR1 on the surface of three different human proximal tubular cell lines. Incubation of human proximal tubular cells with C5a had no significant effect on expression of fibrosis related genes.

Conclusion: Although the C5aR1/C5a axis has been reported to have an immediate profibrotic effect on tubular cells, we could not find clear evidence for such activity. Based on our findings, tubular cells do not express C5aR1 in sufficient quantity to be a primary target for C5a signalling. However, neutrophils and macrophages, which are abundant in the kidney after IRI, could be mediators of a C5a-mediated pro-fibrotic response in tubular cells.

P208

Endothelial cell ferroptosis promotes renal damage in ANCA-induced glomerulonephritis

A. Rousselle

ECRC-Kooperation von MDC und Charité, Experimental and Clinical Research Center, Berlin

Objective: Antineutrophil cytoplasmic antibody (ANCA)-associated vasculitides (AAV) are systemic autoimmune diseases characterized by inflammation of small blood vessels and organ damage, including necrotizing and crescentic glomerulonephritis (NCGN). ANCA are circulating immunoglobulin G (IgG) autoantibodies

binding to and activating neutrophil granulocytes and monocytes. The persistent inflammation leads to renal cell necrosis. Ferroptosis is a recently identified form of programmed cell death characterized by the production of ROS- and iron-dependent lipid peroxidation leading to membrane rupture. The Acyl-CoA Synthetase Long Chain Family Member 4 (ACSL4) enzyme regulates the generation of lipid peroxides. We tested the hypothesis that endothelial cell ferroptosis contributes to ANCA-associated NCGN.

Method: To analyse the biological significance of ferroptosis in endothelial cells in vivo, we generated MPO^{-/-} ACSL4^{AEC} mice, which lack ACSL4 specifically in endothelial cells. MPO^{-/-} ACSL4^{AEC} mice were immunized with murine MPO, irradiated and subsequently transplanted with hematopoietic cells from C/57BL6J (WT) mice. Mice were sacrificed and analyzed 6–8 weeks following transplantation. Ferroptosis was investigated in vitro using human umbilical vein endothelial cells and ANCA-stimulated neutrophils. Cell death and lipid peroxidation were detected by flow cytometry. Ferrostatin-1 (Fer-1) and siRNA against ACSL4 were used to inhibit ferroptosis

Results: We found increased lipid peroxidation (4-HNE staining) in kidney section of mice with AAV. MPO^{-/-} ACSL4^{AEC} chimeric mice showed reduced renal damage as indicated by less necrotic and crescentic glomeruli supporting the notion that endothelial cell ferroptosis is important for the development of MPO-ANCA-induced NCGN. In vitro experiments

revealed that ANCA-activated neutrophils induced endothelial cell death and this effect was prevented by ferroptosis inhibition with Fer-1 and siRNA against ACSL4, respectively. In contrast, inhibition of either necroptosis or apoptosis did not prevent endothelial cell death. Finally, ferroptosis inhibition alleviated the accumulation of lipid peroxides and endothelial dysfunction induced by ANCA-activated neutrophils.

Conclusion: ANCA-activated neutrophils induce ferroptosis in endothelial cells in vitro and endothelial cell ferroptosis contributes to ANCA-associated NCGN in a preclinical murine AAV model.

P209

The *Drosophila* nephrocyte as a model to dissect Wnt signaling

L. Bertgen; M. Döser; H. Pavenstädt¹; B. George¹

Molekulare Nephrologie, Medizinische Klinik D, Universitätsklinikum Münster, Münster; ¹ Allg. Innere Medizin und Notaufnahme sowie Nieren- und Hochdruckkrankheiten und Rheumatologie, Medizinische Klinik D, Westfälische Wilhelms-Universität Münster, Münster

Objective: Podocytes are essential for glomerular filter function. Wnt signaling is essential for podocyte development. Furthermore, the Wnt pathway has emerged to play a central role in podocyte injury and consecutive proteinuria. In several proteinuric kidney diseases Wnt signaling is up-regulated and β -catenin is activated. Podocyte-specific deletion of β -catenin protects against proteinuria following kidney injury. Targeted inhibition of components of the Wnt/ β -catenin pathway preserves

podocyte integrity and ameliorates proteinuria in mice models. Thus, exposing molecular targets and identifying potential drugs to down-regulate Wnt signaling during kidney injury is an attractive therapeutic strategy. We propose that the *Drosophila* nephrocyte model may be employed for identifying novel drug targets and screen for inhibitory drugs. It may present a genetically tractable *in vivo* system with short generation times. The initial goal is to assess the Wnt pathway during nephrocyte development, maintenance, and injury to validate whether regulatory mechanisms in nephrocytes are similar to mechanisms in mammalian podocytes *in vivo*.

Method: To test the validity of employing the *Drosophila* nephrocyte model to dissect Wnt pathway signaling, we performed nephrocyte-specific knockdown using *sns::GAL4* and inducible overexpression with the *GAL80ts* system of Wnt pathway components.

Results: To access whether the Wnt pathway is regulated similarly in nephrocytes as in podocytes during nephrocyte development, we generated a nephrocyte-specific knockdown of *wingless* (*Drosophila* orthologue of Wnt) or *armadillo* (*Drosophila* ortholog of β -catenin) employing *sns::GAL4*. We prepared nephrocytes of L3 larvae and the slit-diaphragm proteins sticks-and-stones (*sns*, *Drosophila* orthologue of nephrin) and *pyd* (*Drosophila* orthologue of zonula-occludens-1) were analysed by immunofluorescence analysis. Both the knockdown of *wingless* as well as *armadillo* resulted in significantly reduced slit-diaphragms per μ m basement membrane. *Sns*

and *pyd* were mis-localized with increased cytoplasmic staining.

Conclusion: In *Drosophila* nephrocytes, Wnt signaling is necessary for slit-diaphragm development.

P210

Fibronektin ist von Bedeutung für die tubuläre und glomeruläre embryonale Nierenentwicklung

K. Skoczynski; A. Kraus; M. Schiffer; K. Elsner¹; E. Tamm¹; B. Buchholz
Medizinische Klinik 4, Nephrologie und Hypertensiologie, Universitätsklinikum, Friedrich-Alexander-Universität Erlangen-Nürnberg, Erlangen; ¹ Lehrstuhl für Humananatomie und Embryologie, Universität Regensburg, Regensburg

Hintergrund: Die embryonale Entwicklung des renalen Tubulusapparats und der daran geknüpften Zahl der Glomeruli ist komplex und ein wichtiger Faktor für die spätere Entwicklung von Bluthochdruck und einer chronischen Niereninsuffizienz. Vordaten zeigen, dass die Deletion des Matrixproteins Fibronektin in neugeborenen Mäusen zur Bildung von kortikomedullären Zysten und damit schweren Strukturstörungen in den Nieren führt. Wir folgen der Hypothese, dass Fibronektin eine wichtige Rolle bei der Etablierung und Aufrechterhaltung der tubulären Struktur spielt. Ziel unserer Untersuchungen war es die Rolle von Fibronektin auf die Morphogenese embryonaler Nieren zu analysieren.

Methode: Mausnieren ab Embryonaltag 12 wurden hinsichtlich der Expression von Fibronektin immunfluoreszenztechnisch untersucht. Für die Charakterisierung von Fibronektin abhängigen Effekten wurde eine CAGG-Cre-ERTM/FN^{fl/fl}

Maus etabliert, die eine Deletion von Fibronectin durch Gabe von Tamoxifen induziert. Zur Untersuchung wurden metanephrische Nieren am Embryonaltag 13 entnommen, *ex vivo* mit Hydroxytamoxifen induziert und für 5 Tage kultiviert. Mithilfe kombinierter Färbe- und Mikroskopietechniken wurde die tubuläre Entwicklung und Glomerulogenese analysiert. Zudem untersuchten wir den Einfluss von Fibronectin auf ITGA8 abhängige Signalwege und insbesondere die Expression von GDNF und Wnt11.

Ergebnisse: Fibronectin wird in allen Entwicklungsstufen der Mausniere exprimiert. Auffällig ist eine initial deutliche Expression um die sich aufzweigenden Ureterknospen, die im späteren Verlauf vermehrt im Tubulointerstitium und schließlich in den Glomeruli der ausgereiften Nieren vorzufinden ist. Fluoreszenzfärbungen von ganzen embryonalen Nieren mit einer Fibronectin Deletion zeigten eine signifikante Reduktion in der Nierengröße, der Anzahl der Ureterknospenaufzweigungen und der Zahl der Glomeruli. Ebenfalls ging der Knockout mit einer signifikant reduzierten Proliferation in den sich aufzweigenden Epithelien einher. Passend hierzu zeigte Fibronectin eine signifikante Kolo-kalisation mit ITGA8. Der Knockout von Fibronectin führte zu einer Reduktion der ITGA8 abhängigen Bildung von GDNF sowie zu einer verminderten Expression von Wnt11.

Zusammenfassung: Fibronectin wird in der embryonalen Niere der Maus spezifisch im Bereich der sich aufzweigenden Ureterknospen sezerniert und fördert durch Stimulation von ITGA8 die Bildung von GDNF und Wnt11, die relevant für die

Proliferation und Entwicklung des embryonalen Tubulussystems sind.

P211

Targeting the inflammasome in a mouse model of ADPKD

P. P. Prosseda; J. Liu¹; M. Jain¹; V. Strassl²; S. Brägl¹; T. Kilik¹; B. Saller¹; A. Paolini¹; A. Todkar¹; B. Neubauer¹; C. Schell³; O. Gorka¹; O. Groß¹; W. Kühn¹

Zentrale Klinische Forschung, Universitätsklinikum Freiburg, Freiburg;

¹ Medizinische Klinik IV/ Abteilung Nephrologie, Universitätsklinikum, Albert-Ludwigs-Universität Freiburg, Freiburg; ² Institut für Genetische Epidemiologie, Universitätsklinikum, Albert-Ludwigs-Universität Freiburg, Freiburg; ³ Institut für Klinische Pathologie, Albert-Ludwigs-Universität Freiburg, Freiburg

Objective: Autosomal dominant polycystic kidney disease (ADPKD) is characterized by cyst formation, fibrosis and progression to end stage kidney disease. Recent evidence indicates that inflammation plays an important role in cyst growth and disease progression. Inflammasomes play a role in crystal induced kidney disease and crystals are postulated to contribute to the ADPKD phenotype. IL-18, an inflammasome downstream target, is increased in the urine of ADPKD patients.

Aims: We hypothesized that pharmacologic inhibition of the inflammasome modulates disease severity in ADPKD. MCC950 is an established inhibitor of the NLRP3 inflammasome that is amenable to in-vivo application in mice. We tested if MCC950 treatment attenuates the phenotype in an orthologous mouse model of ADPKD.

Method: Pkd1^{flox/flox} Pax8.rTA TetOcre mice were induced with doxycycline (2 mg/mL) from day 28 to 42. Beginning on day 28, 20 mg/kg MCC950 was repeatedly administered intraperitoneally every other day for a total of 35 injections. The control group with the identical genotype received vehicle. Genotype controls with the genotype Pkd1^{flox/flox} Pax8.rTA (sine TetOcre) received 20 mg/kg MCC950 or vehicle. At day 98, urine and blood of mice were collected for urea, creatinine and interleukin measurements, the kidneys were removed further analysis.

Results: 7 mice per group were examined. MCC950 treatment resulted in a significant reduction of total end kidney weight and kidney-weight-to-body-weight ratio in Pkd1 mutant mice. The treatment was correlated with reduced cystic transformation, kidney weight, and kidney/body weight. Creatinine and urea levels were significantly reduced in the serum of MCC950 treated Pkd1 mutant mice. Caspase-1 expression was decreased in the treatment group. The IL-18/creatinine ratio in urine was reduced in urine, but not the IL-1 β /creatinine ratio. Interestingly, the number of macrophages was not significantly altered between groups.

Conclusion: The inflammasome NLRP3-inhibitor MCC950 ameliorated ADPKD in a mouse model. This resulted in better renal function and decreased excretion of IL-18, but not IL1 β . This may indicate that inflammasomes are active in renal epithelial cells, although direct evidence is lacking. Our data support inflammasomes as a therapeutic target in ADPKD.

Experiments with genetic targeting of inflammasome components in PKD1 k-o mice are ongoing.

P212

Molecular imaging and quantification of smooth muscle cell and aortic tissue mineralization in vitro and ex vivo with a fluorescent hydroxyapatite specific probe

M. Schuchardt; A. Greco; M. R. Gummi; M. Tölle; J. Hermann; M. van der Giet; M. Babic¹; K.-U. Eckardt²

Medizinische Klinik IV, Klinik für Nephrologie, Campus Benjamin Franklin, Charité – Universitätsmedizin Berlin, Berlin; ¹ Medizinische Klinik für Nephrologie – Hochschulambulanz, Campus Benjamin Franklin, Charité – Universitätsmedizin Berlin, Berlin; ² Medizinische Klinik mit Schwerpunkt Nephrologie und Internistische Intensivmedizin, Campus Charité Mitte, Charité – Universitätsmedizin Berlin, Berlin

Objective: The deposition of hydroxyapatite (HAP) crystals within the vessel wall, known as medial arterial calcification (MAC), is a systemic disorder that commonly affects chronic kidney disease (CKD) patients influencing outcomes on life expectancy. Given the clinical importance of MAC as well as the lack of therapeutic approaches, novel tools are needed to improve scientific investigation. Hence, a major challenge in the vascular research field is to sharpen innovative staining methods that permit specific and early evaluation of HAP crystals, yet not reachable via conventional assays. This study aims to establish a rapid and efficient working protocol for specific HAP detection in cells and tissue using the synthetic bisphosphonate fluorescence dye OsteoSense™.

Method: The presence of HAP was assessed through staining via OsteoSense™680EX in the rat thoracic aorta and rat aortic tissue sections as ex vivo settings, and in vitro culturing rat vascular smooth muscle cells (VSMC). High-phosphate medium serves as a positive control to induce calcification of aortic tissue for 7 and 14 days of stimulation. For in vitro detection, a time-response curve from 1 to 7 days was performed. The fluorescence intensity and the calcium content were quantified and compared in both ex vivo and in vitro experiments.

Results: OsteoSense™680EX enables specific whole aorta HAP staining upon 7 days of tissue incubation in a high-phosphate medium. The staining protocol also highlights HAP-rich deposits in rat aortic tissue sections treated with calcification medium for 7 and 14 days. In vitro staining of VSMC via OsteoSense™680EX enables visualization and quantification of micro- and macro-calcification in a time-dependent manner upon 1, 2, 3 and 7 days of incubation in a high-phosphate medium. Additionally, the staining protocols allows co-staining with other markers of interest as shown here for γ H2A.X.

Conclusion: OsteoSense™680EX is a powerful tool for the detection of early subtle-osteogenic activities in the vasculature and reveals in this study its potential of improving calcification assays, especially for quantification in inhibitor studies.

P213

IPC-vermittelte Organprotektion während der SWOP ist ARNT/ALK3 assoziiert

G. Rapp; G. Nyamsuren; B. Tampe; M. Zeisberg

Abteilung Nephrologie und Rheumatologie, Universitätsmedizin Göttingen, Göttingen

Hintergrund: Ischämie und begleitende Hypoxie stellen eine häufige Ursache für eine akute Nierenschädigung (AKI) dar. Strategien zur Prävention und Behandlung des AKI sind limitiert. In verschiedenen Tiermodellen konnte die ischämische Präkonditionierung (IPC) bereits als eine effektive Intervention zur Verhinderung ischämischer Organschädigungen etabliert werden. Eine kurze Ischämie vermittelt im Kontext eines IPC-Protokolls eine für wenige Stunden andauernde Organprotektion. Diese erste Phase der Organprotektion wird gefolgt von einer zweiten, nach 24–48 h, auftretenden protektiven Phase. Die zweite Phase wird als *second window of protection* (SWOP) bezeichnet und kann 3–4d bestehen. Mechanismen und transkriptionelle Mediatoren während der SWOP sind weitestgehend unbekannt. Ziel der zugrunde liegenden Studie war es daher Effektoren und Zielgene während der SWOP zu untersuchen und ein mögliches pharmakologisches Therapieziel zu identifizieren.

Methode: 6–8 Wochen alte C57BL/6-Mäuse wurden einer IPC-Interventionen unterzogen; einer 5-min. Ischämie der A. renalis s. folgte eine 5-min. Reperfusion. Dieser Zyklus wurde fünffach durchgeführt. Es folgte eine Analyse der IPC-Nieren mittels SDS-Page und Western Blot zu den postinterventionellen Zeitpunkten (2, 4, 8, 12, 25, 48 und 72 h). Zwei weitere Mausgruppen wurden über 48 h mit *low dose* FK506 und dem *small molecule* GPI1046 präkonditioniert.

Eine Analyse mittels SDS-Page und Western Blot folgte.

Ergebnisse: Während die frühe Phase nach IPC (2–4 h) durch einen Anstieg der Expression von *hypoxia inducible factor-1α* (HIF1α) gekennzeichnet ist, konnte 48 h nach Durchführung des IPC-Protokolls eine signifikante Zunahme der Expression von *aryl hydrocarbon receptor nuclear translocator* (ARNT) und konsekutiv von *activin receptor-like kinase 3* (ALK3) beobachtet werden. Eine vergleichbare Induktion der Expression von ARNT und ALK3 konnte durch eine pharmakologische Präkonditionierung mit FK506 oder GPI1046 erzielt werden.

Zusammenfassung: Infolge einer Hypoxie induziert HIF1α eine transkriptionelle Hochregulation von ARNT. Aufgrund der verstärkten Expression von ARNT, formieren sich nach 48 h vermehrt ARNT-Homodimere, diese binden an die palindromische E-box 5'-CACGTG-3' im proximalen ALK3-Promoter und induzieren die Expression des renoprotektiven ALK3 während der SWOP. Die organprotektiven Effekte von konstitutiv exprimierten ARNT während der SWOP lassen sich pharmakologisch durch die Gabe von FK506 oder GPI1046 mimieren und könnten sich als künftiges Therapieziel nutzen lassen.

P214

Suppression of enhanced Src/STAT3 signaling inhibits cyst formation by *Pkhd1*-knockout epithelial cells

F. Hassan; H. S. Burmester; J. Westhoff¹; J. K. Scholz²; B. Buchholz²; D. Haffner; W. H. Ziegler

Klinik für Pädiatrische Nieren-, Leber- und Stoffwechselerkrankungen, Zentrum für Kinder- und Jugendmedizin,

Medizinische Hochschule Hannover, Hannover; ¹ Interdisziplinäre Pädiatrische Intensivstation, Kinderklinik, Ruprecht-Karls Universität Heidelberg, Heidelberg; ² Medizinische Klinik 4, Nephrologie und Hypertensiologie, Universitätsklinikum, Friedrich-Alexander-Universität Erlangen-Nürnberg, Erlangen

Objective: Hereditary polycystic kidney diseases are characterized by defective epithelial morphogenesis and/or homeostasis. To study molecular aspects of epithelial defects, genetically modified canine renal tubular epithelial cells, MDCK, provide a well-established model. In 3D culture, monolayered epithelial spheroids with apicobasal polarity and controlled water and ion transport can be employed to analyze consequences of pharmacological intervention. Here, we study epithelial cells with fibrocystin deficiency, the cause of ARPKD, to address the relevance of STAT3 signaling and its inhibition on cyst formation.

Method: We employed pl-MDCK, sub-cloned principal-like cell lines, with CRISPR/Cas9-based genetic knockout of *Pkhd1* and corresponding controls. Cells were grown in matrigel to allow spheroid formation, within 4 days, and treated with forskolin (Fsk) to stimulate cAMP-induced cystic growth, as reported for disease conditions. Lumen and cyst size were determined based on apical and basolateral markers using ImageJ/FIJI. Cyst formation was related to induction of STAT3 signaling.

Results: Enhanced cAMP levels led to massive lumen expansion in epithelial spheroids of *Pkhd1*-KO cell lines as compared to wildtype. While Fsk treatment did not increase

numbers of epithelial cells in cysts, KO cells showed moderately up-regulated proliferation in 2D culture. Cyst formation was accompanied by a rise in pSTAT3 in *Pkhd1*-KO cells. In addition, induction of STAT3 target genes was observed in Fsk stimulated cells, and inhibition of Src kinase reduced pSTAT3 levels. Application of different approved drugs affecting STAT3 signaling strongly reduced lumen size of *Pkhd1*-KO cysts in a dose-dependent manner.

Conclusion: In fibrocystin deficient pl-MDCK cells, induction of cyst formation by enhanced cAMP levels is associated with enhanced Src/STAT3 signaling. Its suppression by approved drugs resulted in inhibition of cystic growth *in vitro*. Thus, targeting enhanced Src/STAT3 signaling could become a useful strategy to attenuate disease progression in ARPKD.

P215

Biomechanical properties of the aortic wall: parameters describing vessel changes during vascular calcification

M. R. Gummi

Medizinische Klinik IV, Klinik für Nephrologie, Campus Benjamin Franklin, Charité – Universitätsmedizin Berlin, Berlin

Objective: Characterizing the biomechanical properties of the aortic wall is essential for understanding the causes of cardiovascular diseases, such as medial arterial calcification (MAC). The contractile vascular smooth muscle cells (VSMC) embedded in an extracellular matrix composed of collagen and elastin are the major microstructural components of the medial layer of the aortic wall and form the basis of

its biomechanical properties. Therefore, knowledge of the biomechanical behavior of the aorta can further advance our understanding of the pathophysiology of MAC and arterial stiffening. However, current research focuses on investigating changes in the expression of collagen and elastin substances in vitro, and there is limited evidence of how these collagen or elastin substances alter the biomechanical properties in ex vivo. The objective of the current study is to establish and validate a method to investigate these biomechanical properties in the process of vascular calcification.

Method: The biomechanical properties of the Wistar rat aorta were evaluated using small vessel myography (SVM) and an ex vivo setting. For induction of vascular calcification, two inducers known from in vitro and in vivo studies were used: high phosphate medium and azathioprine (AZA). Aortic rings were mounted between two jaws in the SVM chamber, the tensile force was recorded, and the stress-stretch curve was quantified. Furthermore, calcium levels were quantified upon decalcification of the tissue.

Results: A protocol for evaluation of the stress-stretch curve via the SVM was established and optimized for rat aortic rings. Induction of mineralization with a high-phosphate medium leads to significant and time-dependent differences in the stress-stretch curve compared to controls. Further changes could be induced by co-stimulation with the known inductor of mineralization as AZA. Decalcification and quantification of the tissue calcium content confirmed the findings of mineralization upon a high-phosphate medium and AZA treatment.

Conclusion: Overall our findings demonstrate that the biomechanical properties change with high effect size between control and stimulation upon vascular calcification. This technique can be utilized to describe the biomechanical properties of arteries caused by vascular calcification.

P216

S1P Stimulates Erythropoietin Synthesis in Mouse Renal Interstitial Fibroblasts by S1P1 and S1P3 Receptor Activation and HIF-2 α Stabilization

*B. S. Tanturovska; R. Hafizi; F. Imeri; R. H. Wenger¹; A. Huwiler
Institut für Pharmakologie, Universität Bern, Bern/CH; ¹ Institut für Physiologie, UniversitätsSpital Zürich, Universität Zürich, Zürich/CH*

Erythropoietin (Epo) is the critical hormone for erythropoiesis. In adults, Epo is mainly produced by a subset of interstitial fibroblasts in the kidney, with minor amounts being produced in the liver and the brain. In this study, we used the immortalized renal interstitial fibroblast cell line FAIK F3-5 to investigate the ability of the bioactive sphingolipid sphingosine 1-phosphate (S1P) to stimulate Epo production and to reveal the mechanism involved. Stimulation of cells with exogenous S1P under normoxic conditions (21 % O₂) led to a dose-dependent increase in Epo mRNA and protein levels and subsequent release of Epo into the medium. S1P also enhanced the stabilization of HIF-2 α , a key transcription factor for Epo expression. S1P-stimulated Epo mRNA and protein expression was abolished by HIF-2 α mRNA

knockdown or by the HIF-2 inhibitor compound 2. Furthermore, the approved S1P receptor modulator FTY720, and its active form FTY720-phosphate, exerted a similar effect on Epo expression as S1P. The effect of S1P on Epo was antagonized by the selective S1P₁ and S1P₃ antagonists NIBR-0213 and TY-52156, but not by the S1P₂ antagonist JTE-013. Moreover, inhibitors of the classical MAPK/ERK, the p38-MAPK, and inhibitors of protein kinase (PK) C and D all blocked the effect of S1P on Epo expression. Finally, the S1P and FTY720 effects were recapitulated in the Epo-producing human neuroblastoma cell line Kelly, suggesting that S1P receptor-dependent Epo synthesis is of general relevance and not species-specific.

In summary, these data suggest that, in renal interstitial fibroblasts, which are the primary source of plasma Epo, S1P₁ and ₃ receptor activation upregulates Epo under normoxic conditions. This may have a therapeutic impact on disease situations such as chronic kidney disease, where Epo production is impaired, causing anemia, but it may also have therapeutic value as Epo can mediate additional tissue-protective effects in various organs.

Experimentelle Nephrologie 7

P217

Molecular nanoscopy in human kidney biopsies using LED-based microscopy

D. Kylies; M. Zimmermann; F. Haas; M. Kuehl; J. Czogalla; S. Hofmann; O. Kretz; M. Schwerk; N. Wanner; N. M. Tomas; T. Wiech¹; C. Kuppe²; R. Kramann²; M. N. Wong; S. Bonn³; T. B. Huber; V. G. Puelles Rodriguez

Nephrologie/Rheumatologie und Endokrinologie/Diabetologie, III. Medizinische Klinik, Universitätsklinikum Hamburg-Eppendorf, Hamburg; ¹Institut für Pathologie, Sektion Nephropathologie, Zentrum für Diagnostik, Universitätsklinikum Hamburg-Eppendorf, Hamburg; ²Medizinische Klinik II, Nephrologie und Klinische Immunologie, Universitätsklinikum, Rheinisch-Westfälische Technische Hochschule Aachen, Aachen; ³Zentrum für Molekulare Neurobiologie (ZMNH), Universitätsklinikum Hamburg-Eppendorf, Hamburg

Objective: Super-resolution microscopy (SRM) enables spatial molecular characterization at a nanoscale, but the access to SRM systems is limited, hindering the applicability of SRM in the scientific and clinical pathology community. Expansion microscopy (ExM) and computational image enhancement algorithms like „super-resolution radial fluctuations“ (SRRF) are alternatives to SRM, but in combination with broadly available LED-based WF systems, the resolution is still limited. Here, we introduce **expansion-enhanced super-resolution radial fluctuations** (ExSRRF), a workflow based on immunofluorescence (IF) labeling of tissues, followed by tissue expansion and subsequent image enhancement using SRRF, enabling nanoscale molecular SRM using LED-based WF systems.

Method: IF-based labeling of tissues is performed, followed by hydrogel embedding and tissue expansion. Next, time-stacked images are acquired using an LED-based WF microscope after which computational processing using the SRRF

algorithm is performed, yielding the final super-resolution image.

Results: In a set of nanorulers (synthetic molecules containing fluorescent dyes at predefined distances), ExSRRF resolved the entire range from 120 nm to 25 nm, thus providing a resolution of at least 25 nm using LED-based wide-field microscopy. ExSRRF is applicable to formalin-fixed paraffin embedded (FFPE) samples in multiple clinical and experimental settings. In human kidney specimens, ExSRRF was combined with a pan-protein label to obtain EM-like images while crossing biological scales from tissue overviews (millimeter) to sub-cellular compartments (nanometer), resolving mitochondria cristae as defined by their morphology, and molecular co-labeling. In an experimental model of ischemia-reperfusion, ExSRRF resolves endoplasmic reticular dilatation in proximal tubular cells. In clinical biopsies, ExSRRF detects diagnostic features of human kidney disease such as foot process effacement in minimal change disease. ExSRRF can be extended as a quantification tool for automated segmentation and analysis of the nephrin slit diaphragm (SD) by implementing algorithms for region of interest and ridge detection in combination with customized SD-density and open source proximity measurement tools, thereby identifying disease signatures in biopsies from patients with nephrotic syndrome.

Conclusion: In summary, ExSRRF is a flexible, scalable, inexpensive and robust method for the molecular characterization of experimental and clinical specimens across large biological scales. ExSRRF thus has the potential to serve

as a bridge between SRM and both clinical and experimental pathology, unlocking molecular nanopathology for the broad community.

P218

Different parts of ETAR N-terminus are involved in the receptor activation depending on the ligand

*M. Adu Gyamfi; R. A. Catar; C. Lucht; G. Kleinau¹; M. Szczepek¹; K. Budde²; P. Scheerer¹; A. L. Philippe
Medizinische Klinik mit Schwerpunkt Internistische Intensivmedizin und Nephrologie, Campus Virchow-Klinikum, Charité – Universitätsmedizin Berlin, Berlin; ¹Institut für Medizinische Physik und Biophysik, Charité – Universitätsmedizin Berlin, Berlin; ²Medizinische Klinik mit Schwerpunkt Nephrologie und Internistische Intensivmedizin, Campus Charité Mitte, Charité – Universitätsmedizin Berlin, Berlin*

Objective: Endothelin-1 type A receptor (ET_AR), a G-protein coupled receptors (GPCR), has multiple ligand binding abilities and may signal upon binding of either its natural peptide agonist, Endothelin-1 (ET-1) or agonistic Immunoglobulin G (ET_AR-IgG). Elucidation of the regions involved in the receptor activation retains the potential to unravel new therapies for vascular pathologies in native kidneys and after organ transplantation.

Method: To investigate the involvement of different ET_AR N-terminal amino acid segments, we generated sequential deletions. Activation of ET_AR mediated by ET-1 or agonistic IgG was assessed in different assays: signalling pathways reporter assays and ELISA. GPCR activation was induced

by the peptide agonist, ET-1, or by IgG isolated from patients with renal vascular pathology.

Results: All deleted receptors were expressed at the plasma membrane of mammalian cells at the wild type receptor level or stronger. $G_{q/11}$, $G_{12/13}$ and ERK 1/2 signalling were activated by ET-1 and only one N-terminal region showed negative effects on these pathways. Interestingly, upon stimulation with ET_AR-IgG, the three signalling pathways were activated milder than with ET-1 albeit significantly and the N-terminal segments involved were different as with ET-1. Furthermore, when cAMP production was analysed, ET_AR-IgG increased cAMP levels stronger as ET-1 and here again, the N-terminal amino acids involved were different according to the ligand used.

Conclusion: We have successfully used models appreciating GPCR functional plasticity to dissect ET_AR activation in response to agonistic antibodies and the receptor's natural peptide agonist. Our data suggest a differential effect of the N-terminal part of the receptor depending on the ligand binding and thus open the way to develop new drugs addressing specifically the immune activation of ET_AR.

P219

The role of local complement expression in renal AL amyloidosis

N. Kriegelstein; M. Reuthelshöfer; G. Rottenaicher¹; F. Ferrazzi; J. Buchner¹; C. Röcken²; C. Daniel; K. Amann

Institut für Nephropathologie, Universitätsklinikum, Friedrich-Alexander-Universität Erlangen-Nürnberg, Erlangen; ¹ Lehrstuhl für Biotechnologie, TU München,

Garching; ² Pathologie, Christian-Albrechts-Universität zu Kiel, Kiel

Objective: Amyloidogenic light chain (AL) amyloidosis is a systemic protein misfolding and deposition disease, which most commonly affects kidney, heart or both. Since the occurrence of C9 and to a lesser extent C3 has been shown within amyloid deposits in the kidney, the aim of this study was to investigate the role of kidney cells as a potential source of the complement integrated into amyloid.

Method: To confirm the presence of complement factors C1q, C3c, C5b9 and C3d in AL kidneys, immunohistochemistry was performed on kidney biopsies from 31 lambda and 10 kappa AL patients. Staining for complement factors and amyloid was evaluated and scored compartment-specifically in glomeruli, tubules and arteries. To further determine whether this complement response could be facilitated by kidney cells stimulated with AL fibrils, human mesangial cells and proximal tubular cells were co-incubated with AL protein fibrils. These fibrils were either mature fibrils isolated from the explanted heart of an AL patient (FibPat-C) or generated under laboratory conditions from the variable domain derived from the same patient (Fib Pat) or the corresponding germline sequence (Fib wt). After 24 h of co-incubation, RNA was isolated and a gene expression of 12 complement related genes was analysed using NanoString (C1s, C3, C5, CCN2, CD44, CD46, CD55, CD59, CFB, CFD, CFH, SERPING1).

Results: In renal biopsies from both lambda and kappa AL patients, the membrane attack complex C5b9 was detected in blood vessels and some

glomeruli, and correlated with amyloid deposition. However, the most prominent staining in all compartments was observed for C3d, while only few cases had deposits positive for C3c and C1q. *In vitro*, the expression of most complement genes was unaffected by co-incubation with either fibril. Yet, in human mesangial cells some activatory and inhibitory complement factors appeared to be downregulated after stimulation with FibPat-C or FibPat compared to cells treated with PBS.

Conclusion: In summary, both C3d and C5b9 detection correlated with amyloid deposition in glomeruli and arteries, but only C3d was also observed in the tubulointerstitium. *In vitro* stimulation of mesangial cells with AL fibrils failed to induce the expression of complement factors, suggesting that they are either expressed locally by other cells or enter the kidney from the bloodstream. However, further studies are needed to investigate the influence of the potential local inhibitory complement response to amyloid fibrils on renal AL pathology.

P220

Humanes Serum von Patienten im septischen Schock induziert eine proinflammatorische Antwort und vaskulären Plasma-proteinverlust in einem in vivo Zebrafisch-Larvenmodell

A. Schultalbers; K. Stahl¹; P. Schroder²; J. Hegermann³; L. Staggs²; B. Schirmer⁴; M. Kosanke⁵; Y. Kiyan; J. Dutzmann⁶; C. Bode⁷; D. Neumann⁴; M. Hoepfer⁸; K.M. Schmidt-Ott; H. Haller; S. David⁹; H. Schenk

Klinik für Nieren- und Hochdruck-erkrankungen, Zentrum für Innere Medizin, Medizinische Hochschule Hannover, Hannover; ¹ Klinik für

Gastroenterologie, Zentrum für Innere Medizin, Medizinische Hochschule Hannover, Hannover; ² Mount Desert Island Biological Laboratory, Bar Harbor/USA; ³ Zentrale Forschungseinrichtung Elektronenmikroskopie, Medizinische Hochschule Hannover, Hannover; ⁴ Institut für Pharmakologie, Zentrum für Innere Medizin, Medizinische Hochschule Hannover, Hannover; ⁵ Research Core Unit Genomics, Zentrum für Innere Medizin, Medizinische Hochschule Hannover, Hannover; ⁶ Universitätsklinik und Poliklinik für Innere Medizin III, Universitätsklinikum, Martin-Luther-Universität Halle-Wittenberg, Halle (Saale); ⁷ Anästhesie und Intensivmedizin, Universitätsklinikum Bonn, Bonn; ⁸ Klinik für Pneumologie, Zentrum für Innere Medizin, Medizinische Hochschule Hannover, Hannover; ⁹ Klinik für Intensivmedizin, Universitätsspital Zürich, Zürich/CH

Hintergrund: Der septische Schock ist durch eine volumenrefraktäre Hypotension mit Laktaterhöhung gekennzeichnet, welcher aus einer fehlregulierten Wirtsantwort auf eine Infektion zusammen mit der Organdysfunktion resultiert. Unser Ziel ist es, ein *in vivo* Zebrafischmodell zu etablieren, das auf der Injektion von Serum von septischen Patienten beruht, welches in die Kardinalvene der Zebrafischlarve appliziert wird. Hierdurch soll evaluiert werden, ob charakteristische Zeichen der Sepsis-assoziierten vaskulären Dysfunktion wie Plasmaproteinverlust bei erhöhter Gefäßpermeabilität und Ödeme im Tiermodell induziert werden können. Darüber hinaus soll beurteilt werden, inwieweit durch Seruminjektionen inflammatorische Prozesse im Zebrafisch hervorgerufen werden können.

Methode: Serum-Proben wurden von Patienten im septischen Schock (< 24 h Dauer, Noradrenalinbedarf > 0.4 µg/kg/min trotz Volumenapplikation) bzw. von gesunden Probanden entnommen. Die Präsenz von Zytokinen bzw. Chemokinen wurde in beiden Gruppen durchflusszytometrisch unter Verwendung eines Bead-Assays bestimmt. Zebrafischlarven wurden mit dem jeweiligen Serum in die Kardinalvene 48 Stunden nach Fertilisation (hpf) injiziert, die Plasmaprotein-Konzentration in *Tg(l-fabp:DBP-EGFP; flk1:mCherry)* Zebrafischen wurde auf Basis der retinalen Fluoreszenzintensität von GFP nach 96 hpf gemessen. Die Expression von Inflammations- und Endothelschädigungsmarkern wurde mittels qPCR evaluiert. Die Morphologie der endothelialen Schädigung wurde durch Transmissions-Elektronenmikroskopie ultrastrukturell beurteilt.

Ergebnisse: Die Injektion von Serum septischer Patienten führt im untersuchten Patientenkollekt zu einer Steigerung des Plasmaproteinverlustes als Indikator der Zunahme der vaskulären Permeabilität. Erhöhte Inflammationsparameter insbesondere des NF-κB-Signalweges sowie eine gesteigerte Genexpression von endothelialen Schädigungsmarkern lassen auf eine gesteigerte Inflammationsreaktion nach Seruminjektion septischer Patienten schließen.

Zusammenfassung: Das Zebrafisch-Larven-Modell zur Evaluation der Effekte von Serum von Patienten mit septischem Schock im Vergleich zu gesunden Probanden ermöglicht es, Effekte vermittelt durch lösliche Faktoren wie Zytokine auf die vaskuläre Permeabilität darzustellen und kann somit als

Werkzeug in der Beurteilung therapeutischer Effekte von Medikamenten aber auch extrakorporaler Verfahren wie der Plasmapherese bei Sepsis-Patienten dienen.

P221

SGPL1 Mangel führt zur podozytären Schädigung durch Endothelzell-derivierte Exosomen

I. Schäfer; H. Haller; K. M. Schmidt-Ott; S. Lovric

Klinik für Nieren- und Hochdruck-erkrankungen, Zentrum für Innere Medizin, Medizinische Hochschule Hannover, Hannover

Hintergrund: Sphingosine-1-phosphate Lyase (SGPL1) ist das finale Enzym im Sphingolipid-Abbau. Mangel von SGPL1 bzw. Loss-of-Function Mutationen des Gens *SGPL1* führen zu einem Steroid-resistenten Nephrotischen Syndrom und zur fokalsegmentalen Glomerulosklerose (FSGS). Die Pathogenese von Mutationen im *SGPL1* Gen ist noch weitestgehend unbekannt. Der Knockout von *Sgpl1* in Mäusen führt ebenfalls zu einer FSGS. Die Mäuse versterben kurz nach der Geburt an Nierenversagen. Ziel dieses Projektes ist es, den Zelltyp des primären Schadens im Glomerulum (Endothel, Podozyten oder Mesangium) und damit die Pathomechanismen, die zur FSGS führen, zu identifizieren.

Methode: Mittels spezifischer SGPL1-siRNA wurde in primären humanen glomerulären Endothelzellen, Mesangialzellen und immortalisierten Podozyten ein SGPL1-Knockdown (SGPL1-KD) generiert. Anhand von Western-Blot und Immunfluoreszenz wurden Autophagie, Zytoarchitektur und Adhäsion sowie Apoptose/Zelltod

analysiert. Weiterhin wurden Exosomen aus dem Zellkultur-Überstand der SGPL1-KD und entsprechenden Kontroll-Endothelzellen isoliert. Podozyten sowie Mesangialzellen wurden mit den Endothelzell-derivierten Exosomen inkubiert und wie oben erwähnt analysiert.

Ergebnisse: SGPL1-KD in Endothelzellen führt zu einer verminderten VE-Cadherin- und erhöhten Icam1-Expression als möglicher Hinweis auf „Vascular Leakage“. Caspase 3/7-Aktivität als Zeichen der Apoptose konnte nicht nachgewiesen werden. Der KD von SGPL1 in Podozyten zeigte einen Defekt im Autophagie-Signalweg. Die Inkubation von Podozyten mit SGPL1-KD Endothelzell-derivierten Exosomen führte ebenfalls zu einem Defekt im Autophagie-Signalweg. Weiterhin konnte ein erhöhtes mTor-Signaling und Veränderungen der Aktin-Strukturen mit einhergehend reduziertem filamentösem Aktin nachgewiesen werden. Caspase 3/7-Aktivität konnte nicht nachgewiesen werden. Allerdings zeigten sich pyknotische Zellkerne mit kondensiertem Chromatin als Hinweise auf mögliche Caspase 3/7-unabhängige Zelltodprogramme. Die podozytäre Schädigung konnte durch gleichzeitige Inkubation mit dem mTor-Inhibitor Everolimus und Vitamin B6/Pyridoxin vermindert werden. Mesangialzellen zeigen weder im direkten SGPL1-KD noch durch Endothelzell-derivierte Exosomen einen Phänotyp.

Zusammenfassung: SGPL1 reguliert krankheitsrelevante endotheliale und podozytäre Signalwege. SGPL1-abhängige Endothelzell-derivierte Exosomen, könnten einen indirekten podozytären Effekt vermitteln und somit ein therapeutisches Target darstellen.

P222

Spezifischer proximal tubulärer Zellzyklusarrest führt zur Abschwächung eines akuten Nierenversagens im Mausmodell

V. C. Wulfmeyer; I. Sörensen-Zender; V. Voß; S. Rong; H. Haller; K. M. Schmidt-Ott; A. Melk; R. Schmitt
Klinik für Nieren- und Hochdruck-erkrankungen, Zentrum für Innere Medizin, Medizinische Hochschule Hannover, Hannover

Hintergrund: Das akute Nierenversagen (AKI) ist ein großes Problem mit steigender Inzidenz. Renale Tubulusepithelzellen befinden sich für gewöhnlich in der G0-Phase des Zellzyklus (ZZ), aber beginnen nach AKI zu cyclen. Studien belegen die Notwendigkeit eines regulierten ZZ nach AKI für eine optimale Regeneration. Cyclin D1 ist essentiell für das Voranschreiten des ZZ von G1- nach S-Phase. In diesem Zusammenhang charakterisierten wir einen proximal tubulär (PT) spezifischen Cyclin D1 Knock-Out (KO) im murinen Ischämie-Reperfusion-Modell (IRI) und einen systemischen siRNA basierten Cyclin D1 Knock-Down (KD). **Methode:** Tamoxifen (TAM) induzierbare proximal tubuläre Cyclin D1 KO Mäuse (Cyclin D1^{flox/flox}::Slc34a1CreERT2) wurden nach Behandlung mit Vehikel (veh) bzw. TAM einer IRI-OP unterzogen. Retentionswerte, Histologie, Immunzellinfiltration, ZZ-Phasen und Fibrosierung wurden evaluiert (2 h, 1 d, 3 d, 7 d, 14 d, 28 d nach OP; n = 8 je Gruppe). Ein Ccnd1-siRNA KD wurde *in vitro* (renal-tubuläre Primärzellkultur) und *in vivo* (1 nmol siRNA/g Maus; 24 h vor und zur IRI) etabliert, sowie zu Tag 14 nach IRI (o.g. Parameter) untersucht.

Zur Evaluation des zugrundeliegenden Mechanismus erfolgten RNAseq Analyse aus isolierten PT (n = 3) sowie MALDI-TOF-MS aus Nieren 1 d nach IRI (n = 5).

Ergebnisse: Cyclin D1 KO Mäuse wiesen eine Abschwächung des AKI auf (S-Krea 312 ± 74 % (relativ zu D0) veh vs. 142 ± 11 % TAM zu d 3 nach IRI; p = 0,036). KD Mäuse zeigten eine ähnliche Abschwächung des AKI (276 ± 69 % WT vs. 144 ± 31 % KD). Neben einer Reduktion des histologischen Schadens (max. 4; 1 d nach IRI: $2,26 \pm 0,1$ veh vs. $1,84 \pm 0,1$ TAM; p = 0,028; 3 d nach IRI: $2,68 \pm 0,1$ veh vs. $2,06 \pm 0,2$ TAM; p = 0,009) zeigte der KO eine 15-fach reduzierte Leukozyteninfiltration (3 d nach IRI; p < 0,0001). 28 d nach IRI zeigten die KO Mäuse keinen Vorteil hinsichtlich Schaden und Regeneration (Histologie und Bürstensaumfärbung). Die RNAseq Analyse erbrachte als Hauptergebnis eine deutlich reduzierte Expression von ZZ-assoziierten Genen in den proximalen Tubuli von KO Tieren.

Zusammenfassung: Die Ablation von Cyclin D1 im proximalen Tubulus oder systemische Antagonisierung von Cyclin D1 bewirkte nach IRI eine Reduktion der Proliferation in der Niere. Damit war in KO und KD Modell ein reduzierter AKI Schaden zu frühen Zeitpunkten nach IRI verbunden. Unsere Daten deuten auf einen direkt Zellzyklus-abhängigen Mechanismus hin, der auch im Hinblick auf translationale Optionen weiter erforscht werden sollte.

P223**Serum uromodulin as a marker for acute kidney injury (AKI) and chronic nephron loss**

E. Vonbrunn; N. Ebert; N. Cordasic¹; J. E. Scherberich²; K. Amann; C. Daniel
Institut für Nephropathologie, Universitätsklinikum, Friedrich-Alexander-Universität Erlangen-Nürnberg, Erlangen; ¹Medizinische Klinik 4, Nephrologie und Hypertensiologie, Universitätsklinikum, Friedrich-Alexander-Universität Erlangen-Nürnberg, Erlangen; ²KfH-Nierenzentrum, KfH Kuratorium für Dialyse und Nierentransplantation e. V., München

Objective: Uromodulin (Umod) is expressed exclusively in the kidney in the thick ascending limb of the loop of Henle. It is secreted in the urine, where it is the most abundant glycoprotein. To a minor degree, Umod is also released basolaterally from cells into the serum. Actually, serum Umod-levels are an established, sensitive and robust marker for chronic kidney disease (CKD). Here, we investigate serum Umod-levels, renal Umod protein and mRNA expression in acute kidney injury (AKI) and in rat models of nephron loss.

Method: Umod was first assessed in AKI using an ischemia-reperfusion (I/R) rat model. Blood and kidney samples were collected 10 min, 6 h, 24 h, 3d, 5d and 8w post reperfusion. To investigate the effect of nephron number on Umod levels, sera and tissue from healthy rats, uni- and 5/6-nephrectomized (Snx) rats were studied. Renal function (serum creatinine), histological changes (acute tubular injury), and renal damage markers (KIM-1) were evaluated in both models.

Serum Umod levels were measured by ELISA and renal Umod mRNA expression by multiplex gene expression analysis. The amount and distribution of Umod protein in the kidney was examined by antibody-based detection methods.

Results: In AKI, serum creatinine increased markedly 24 h after I/R. Serum Umod was also transiently increased, peaking between 6-24 h and correlating with injury. Simultaneously, the amount of Umod-positive kidney cells decreased from $12,4 \pm 7,7\%$ in healthy rats to $1,8 \pm 1,7\%$ in kidneys 24 h after I/R. In healthy kidneys Umod was detected mainly in the inner and outer strips, while it was substantially reduced and homogeneously distributed in the medulla, inner strip, and outer strip 24 h after I/R. Moreover, mRNA expression of Umod decreased continuously after I/R and was lowest on day 1-5. In the models of nephron loss serum Umod correlated positively with nephron number showing highest levels in healthy rats ($2192,2 \pm 323,8$ pg/ml), which were significantly reduced after uni-nephrectomy ($1262,9 \pm 208,8$ pg/ml) and further reduced after Snx ($939,8 \pm 193,5$ pg/ml). The amount of Umod protein per area in the remaining kidney tissue did not change in Snx, the distribution pattern, however, was more diffuse in kidneys harvested 8 weeks after Snx than 12 weeks.

Conclusion: Serum Umod appears to be a sensitive marker for AKI showing a transient increase in serum levels in parallel with loss of Umod-expressing cells. Umod serum level correlated positively with nephron number. Thus, serum Umod

appears as promising marker to assess acute and chronic renal failure.

P224**The three C-terminal domains of FHR1 influence complement activation and FHR1 cooperation with other complement regulators**

P. Luce; S. Selina Stippa; A. Hartmann; M. Miblan; C. Skerka; T. Wiech¹; P. F. Zipfel
Abteilung Infektionsbiologie, Hans-Knöll-Institut, Leibniz Institut für Naturstoff-Forschung und Infektionsbiologie e. V., Jena; ¹Institut für Pathologie, Sektion Nephropathologie, Zentrum für Diagnostik, Universitätsklinikum Hamburg-Eppendorf, Hamburg

Objective: FHR1 is a member of Factor H (FH) protein family which is involved in regulating the innate immune complement system and inflammation. However, the exact interplay between FHR1 and other complement regulators is still not completely understood. Several studies demonstrated that FHR1 competes with FH by binding same cell surface ligands, including complement C3 fragments and glycosaminoglycans, thereby impairing FH regulation and leading to complement activation. Other results showed that FHR1 inhibits complement C5 convertase activity and terminal complex formation. Two common haplotypes of FHR1, respectively having in their SCR3 domain either "YVQ" or "HLE" residue, were found equally distributed in the population but the relevance of the two isoforms is much less documented.

Method: We generated recombinant FHR1 variants, with either "YVQ" or "HLE" in SCR3 and with the FHR1 characteristic "LA" motif

in SCR5. Two modified FHR1 variants were also generated with either “YVQ” or “HLE” motifs and having in their most C-terminal domain the “LA” motif replaced by “SV” motif of FH. All the variants were then assayed for ligand binding to C3 fragments and glycosaminoglycans. Hemolytic assays and complement activation were also assessed, as well as the functional cooperation of FHR1 with FH on the cell surfaces.

Results: We demonstrate that YVQ/HLE exchange influences FHR1 interaction with glycosaminoglycans and cell surfaces as FHR1_{YVQ} binds more efficiently to heparin and modified endothelial cells surfaces compared to FHR1_{HLE}. Furthermore, by changing in SCR5 the FHR1 characteristic “LA” residue with the “SV” residue of FH in SCR20, we observe that, in contrast with modified FHR1_{SV} constructs, FHR1_{LA} significantly reduced erythrocytes lysis showing that the “LA” residue in SCR5 conferred to FHR1a protective role against complement-mediated lysis. Our data also revealed that compared to FH, both FHR1 natural haplotypes binds more efficiently to heparin-C3d suggesting that FHR1 and FH may interact differently to C3-opsinized fragments exposed. In addition, using human FHR1-deficient serum, we observe that FHR1 levels directly affect the degree of FH cell-surface attachment.

Conclusion: Overall, we demonstrate that genetic variations on the FHR1 gene have an impact on its role in complement. Our data also support that FHR1 is not solely a FH competitor but acts as a counterpart with FH in a dynamic control on the innate immunity.

P225

Comparison of cystic liver and kidney damage in a murine *Pkhd1*-knockout model

H. S. Burmester; J. Fox; D. Haffner; W. H. Ziegler

Klinik für Pädiatrische Nieren-, Leber- und Stoffwechselerkrankungen, Zentrum für Kinder- und Jugendmedizin, Medizinische Hochschule Hannover, Hannover

Objective: Loss of fibrocystin function causes autosomal recessive polycystic kidney disease (ARPKD) associated with epithelial defects, cyst formation and fibrosis in kidneys and liver. In the mouse model, liver defects are developing independent of gender, while kidney defects are restricted to female mice. Here, we analyze the liver in relation to the kidney phenotype in *Pkhd1*-knockout mice of different age and observe distinct hallmarks of disease development.

Method: Targeted mutation *Pkhd1*-knockout mice in BALB background were maintained within the line. Kidneys and livers of male and female animals, homozygous and heterozygous for the *Pkhd1*-knockout allele as well as wildtype, were analyzed histologically at 8 weeks, and 3 to 9 months of age with serum and urine samples taken before preparation. We compare progress and characteristics of disease development in both organs.

Results: Analysis of relative organ weights indicates a stronger and earlier increase of liver – than kidney weights in homozygous *Pkhd1*-knockout mice, aged 3, 6 and 9 months, as compared to heterozygous and wildtype controls, with no alterations in lung

and heart weights. In liver, we observe cyst formation originating from the bile ducts at 8 weeks, while female kidneys first show cysts at 3 months. In both organs, cyst development is associated with fibrosis, inflammatory processes and enhanced proliferation. In the liver, recruitment of immune cells comprises T-cells and M2 macrophages, epithelial expression of EGFR is increased, and there is no prominent nuclear localization of phosphorylated STAT3 in cyst lining epithelia as seen in cystic kidneys. Characteristic ductal plate malformation in *Pkhd1*-knockout mice indicates embryonal origin of defects, and cholangiocytes show expression of CK14, a marker of the embryonal stage, in addition to CK7 and CK19, and reduced cilia formation.

Conclusion: Maintenance in defined BALB background leads to a murine *Pkhd1*-knockout model showing progressive cyst formation in liver and kidney. Both organs present with fibrosis, increased proliferation and inflammation, with emphasis on an embryonal defect of the cholangiocytes. The mouse model reliably allows analysis of disease related mechanisms and appears suitable for testing of pharmacological interventions.

P226

Sphingosine 1-Phosphate Receptor 5 (S1P5) Knockout Ameliorates Adenine-Induced Nephropathy

S. Patyna; T. S. Eckes¹; A. Koch¹; A. Oftring¹; S. Gauer; N. Obermüller; S. Schwalm¹; L. Schaefer¹; J. Chun²; H.-J. Gröne³; J. M. Pfeilschifter¹
Medizinische Klinik III, Nephrologie, Universitätsklinikum, Johann Wolfgang Goethe-Universität, Frankfurt a. M.;

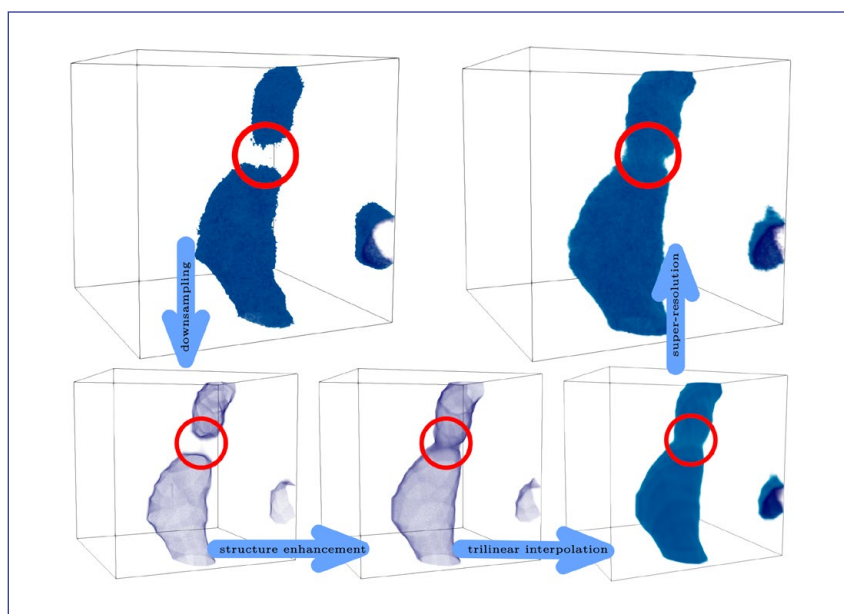
¹ Institut für Allgemeine Pharmakologie und Toxikologie, Universitätsklinikum, Johann Wolfgang Goethe-Universität, Frankfurt a. M.; ² Stanford Burnham Prebys Medical Discovery Institute, La Jolla/USA; ³ Institut für Pharmakologie, Fachbereich Medizin, Philipps-Universität Marburg, Marburg

Objective: S1P and its receptors have been reported to play important roles in the development of renal fibrosis. Although S1P₃ has barely been investigated so far, there are indications that it can influence inflammatory and fibrotic processes. Here, we report the role of S1P₃ in renal inflammation and fibrosis.

Method: Male S1P₃ knockout mice and wild-type mice on a C57BL/6J background were fed with an adenine-rich diet for 7 days or 14 days to induce tubulointerstitial fibrosis. The kidneys of untreated mice served as respective controls. Kidney damage, fibrosis, and inflammation in kidney tissues were analyzed by real-time PCR, Western blot, and histological staining. Renal function was assessed by plasma creatinine ELISA.

Results: The S1P₃ knockout mice had better renal function and showed less kidney damage, less proinflammatory cytokine release, and less fibrosis after 7 days and 14 days of an adenine-rich diet compared to wild-type mice.

Conclusion: S1P₃ knockout ameliorates tubular damage and tubulointerstitial fibrosis in a model of adenine-induced nephropathy in mice. Thus, targeting S1P₃ might be a promising goal for the pharmacological treatment of kidney diseases.



P226: Abb. 1

P226a Improving 3D Light Sheet Fluorescence Microscopy via Machine Learning and Superresolution

A. M. C. Böhner; M. Haas¹; J. Verhülsdonk¹; T. Pinetz¹; C. Kurts; A. Effland¹

Institut für Experimentelle Immunologie, Medizinische Fakultät, Rheinische Friedrich-Wilhelms-Universität Bonn, Bonn; ¹ Institut für Angewandte Mathematik, Universität Bonn, Bonn

Objective: Microscopy is a fundamental corner stone of experimental nephrology and clinical routine alike. In recent years, optical clearing allowed for rapid acquisition of undissected 3D structures in multiple channels via light sheet fluorescence microscopy (LSFM). This approach allows to scan entire organs, but the lateral resolution of these images is significantly lower than in conventional microscopy of paraffin kidney sections. This precludes

application of LSFM to clinical routine. Here, we propose a mathematical method to increase lateral resolution while simultaneously reducing image artefacts using machine learning and superresolution.

Method: We utilized kidneys harvested from untreated wildtype mice. After conducting optical clearing, we imaged identical anatomical regions with a lateral resolution of 5µm (1.3x objective) and 0.6µm (12x objective) with an excitation at 640 nm. Images were registered and a machine learning algorithm was executed to learn the 0.6µm resolution from the 5µm raw data. In addition, a directionality score was introduced to eliminate imaging artefacts concerning the tubular structures and lumina.

Results: Primary results indicated a substantial increase in lateral resolution after superresolution for the 5µm raw images reaching equal contrast distribution as the 0.6µm images. However, the

unavoidable interpolation during superresolution led to errors regarding the tubular lumina. Some tubular lumina seemed to be narrowed or even completely obstructed after superresolution. The underlying causative factors were identified to source from physical limitations of the optical clearing procedure and the technical configuration of the LSMF itself. To counteract these, we implemented a tool based on directionality scores to reconnect and widen tubular lumina in regions, where LSMF imaging at the low resolution of 5µm would lead to systematic errors. The combination of superresolution augmented with directionality score augmentation produced satisfactory results.

Conclusion: In conclusion, we obtained information regarding the usability of varying resolutions in kidney LSMF and propose a method to increase lateral resolution digitally while simultaneously correcting imaging artefacts. 3D image stacks can be recorded ~50 times faster at 5µm lateral resolution than at 0.6µm and allows to acquire the entire murine kidney without necessitating a mosaic of individual image stacks. However, images at 5µm contain systemic artifacts. We were able to satisfactorily reconstruct the 0.6µm resolution images harnessing the superresolution approach augmented with directionality scoring.

P227

Eine chronisch hohe Phosphatbelastung führt zu einer Dilatation des linken Ventrikels mit vermehrter perivaskulärer Fibrose in Mäusen

G. S. Richter; A. Grund; I. Vogt; D. Haffner; M. Leifheit-Nestler

Klinik für Pädiatrische Nieren-, Leber- und Stoffwechselerkrankungen, Zentrum für Kinder- und Jugendmedizin, Medizinische Hochschule Hannover, Hannover

Hintergrund: Patient*innen mit chronischer Niereninsuffizienz weisen erhöhte Serum-Phosphatwerte auf, die u. a. zu einer erhöhten kardiovaskulären Mortalität beitragen. In Industrieländern führt der Verzehr prozessierter Lebensmittel zu einer um bis zu 70 % erhöhten Aufnahme von anorganischen Phosphaten, was auch für die Allgemeinbevölkerung zu einer Erhöhung des kardiovaskulären Risikos führen könnte.

Methode: Um die kardiovaskulären Auswirkungen eines chronischen Phosphatüberschusses näher zu untersuchen, erhielten männliche C57BL/6-Wildtypmäuse sechs Monate lang eine Hochphosphatdiät mit 2 % anorganischem Phosphat (HPD) oder eine Normalphosphatdiät mit 0,8 % Phosphat (NPD). Die Herzfunktion wurde mittels Echokardiographie bestimmt und Herzgewebe für histologische, molekularbiologische und RNA-Sequenzanalysen entnommen.

Ergebnisse: In den echokardiographischen Untersuchungen zeigte sich in den Mäusen mit HPD ein dilatativer Phänotyp mit reduzierter Ejektionsfraktion, erhöhten linksventrikulären Volumina und vergrößerten linksventrikulären Innendurchmessern. HPD-Mäuse zeigten ein leicht erhöhtes Herzgewicht-zu-Tibialängen-Ratio, sowie auf zellulärer Ebene eine Vergrößerung der Kardiomyozytenquerschnittsfläche und Kardiomyozytenlänge, wobei die Transkription der prohypertrophen Gene ANP und bMHC im

Vergleich zur NPD-Gruppe nicht verändert war. Bulk RNA-Sequenzierungen und nachfolgende Pathwayanalysen deuteten auf eine Induktion von Apoptose und Fibrose durch HPD hin. Histologisch zeigte sich keine vermehrte Apoptose, Verkalkung oder beeinträchtigte Kapillarisation in den HPD- Herzen im Vergleich zu den Kontrollen. Die Quantifizierung von Siriusrot-gefärbten Herzschnitten zeigte eine signifikante Induktion perivaskulärer Fibrose in den HPD-Tieren, während keine vermehrte interstitielle Fibrose beobachtet werden konnte. Erste Analysen von isolierten Kardiomyozyten neonataler Ratten, die mit Zellkulturüberständen isolierter und anschließend mit Phosphat stimulierter neonataler Fibroblasten der Ratte inkubiert wurden, deuten auf mögliche parakrine Effekte von pro-fibrotischen Fibroblasten auf Kardiomyozyten hin.

Zusammenfassung: Unsere Daten deuten darauf hin, dass eine chronische HPD in Mäusen zu einem dilatierten Herzphänotyp mit systolischer Dysfunktion und vermehrter perivaskulärer Fibrose führt. Eine chronische Phosphatbelastung könnte demnach zur Erhöhung des kardiovaskulären Risikos in der Allgemeinbevölkerung beitragen.

P228

Auf dem Weg zu einer nachhaltigen Dialysetherapie

J. Beige; H.-P. Barth¹; F. Sommer¹; B. Kitsche²; S. Knöller³; K. de Groot⁴; S. Stracke⁵; S. C. Boedecker-Lips⁶; N. Heyne⁷ Nephrologie und KfH Nierenzentrum, Klinikum St. Georg, Leipzig; ¹ GreenTec Dialysis, Heidelberg; ² Vorstandsbeauftragter Förderung und Entwicklung Heimdialyse, KfH Nierenzentrum Köln-Merheim, KfH

Kuratorium für Dialyse und Nierentransplantation e. V., Köln; ³ Nephrologie, KfH-Medizinisches Versorgungszentrum Bremen-West, Bremen; ⁴ Medizinische Klinik III, Sana Klinikum Offenbach, Offenbach; ⁵ Abteilung für Nephrologie und Hypertensiologie, Klinik und Poliklinik für Innere Medizin A, Universitätsmedizin Greifswald, Greifswald; ⁶ Nephrologie, Rheumatologie und klinische Immunologie, I. Medizinische Klinik und Poliklinik, Johannes-Gutenberg-Universität Mainz, Mainz; ⁷ Sektion Nieren- und Hochdruckkrankheiten, Universitätsklinikum, Medizinische Klinik IV, Eberhard Karls Universität Tübingen, Tübingen

Hintergrund: Der ökologische Fussabdruck (carbon foot print, CFP) von Nierenersatztherapie ist bedingt durch die meist lebenslange, hochtechnisierte Behandlung der absolut größte aller medizinischen Therapieverfahren und entspricht in Deutschland nach bisherigen Schätzungen etwa 6-8 t CO₂-Äqu. pro Patient und Jahr. Zur massiven Reduktion des Dialyse-CFP liegen substanzielle organisatorische und technische Potenziale vor, von denen momentan das nachhaltigste die breite Nutzung von Photovoltaik-Eigenproduktion ist. Für die Einschätzung aller Einsparungseffektivitäten (u. a. Transport, Material, Heizung, Wasser, bauliche Anlagen ...) ist eine IST-Analyse der tatsächlichen Emissionen sehr sinnvoll.

Methode: Weltweit erste Entwicklung eines speziellen Dialyse-zentrierten CFP-Rechners (Greentech Dialysis und Wilderness International). Aus der DGfN-Kommission Nachhaltigkeit, Umwelt und Niere heraus erfolgte Gründung einer Arbeitsgruppe CO₂-Bilanz mit Identifizierung von 5 Pilotzentren

mit aktuell laufender gesamthafter Messung des Dialyse-CFP Ableitung von Standard-CFP-Algorithmen aus diesen Pilotzentren und Darstellung auf der DGfN-Jahrestagung mit dem Ziel der Vereinfachung und Verkürzung der Datenerhebung für alle in der DGfN organisierten Dialysezentren

Ergebnisse: Das Ziel der im Sommer und Frühherbst geplanten Piloterhebungen (mit *break-through* Darstellung auf der Jahrestagung) ist die spätere Einbeziehung (Qu4/2022-Qu3/2023) aller deutschen Dialysezentren und die global erstmalige Erhebung eines verlässlichen nationalen Dialyse-CFP.

Zusammenfassung: Die angestrebte Plattform der Erhebung von teilmodellierten CFP-Daten basierend auf der detaillierten Messung von Pilotzentren soll die Voraussetzung einer Gesamterhebung aller deutschen Dialysezentren schaffen. Mittels eines solchen benchmarks ergibt sich die weltweit erste Möglichkeit, die CFP-Reduktion im Dialysetting im IST-Zustand zu prüfen. Durch ein solches, idealerweise selbstverstärkendes System soll orientiert an den Zielen der Glasgower Klimakonferenz eine Reduktion des Dialyse-CFP um 50 % bis 2030 erreicht werden.

Glomerulonephritis und immunologische Krankheiten (klinisch)

P229

Serodiagnosis of anti-glomerular basement membrane disease using a newly developed chemiluminescence immunoassay

Y. Bestmann; L. Hartwig; A. Kühn; C. Dähnrich; W. Schlumberger
Institute for Experimental Immunology, EUROIMMUN Medizinische Labor-diagnostika AG, Lübeck

Objective: Autoantibodies against the glomerular basement membrane (GBM) are important markers in the diagnosis and monitoring of autoimmune glomerulonephritides. Fast and reliable detection of these autoantibodies is crucial as anti-GBM disease can progress rapidly with fatal outcome.

Here, we investigated the diagnostic performance of a newly developed, standardized anti-GBM chemiluminescence immunoassay (ChLIA).

Method: The diagnostic performance of the EUROIMMUN Anti-GBM ChLIA (IgG), processed on the EUROIMMUN RA Analyzer 10, was assessed using sera from 67 clinically characterized anti-GBM disease patients and 221 disease controls. Results were compared with those obtained by the EUROIMMUN Anti-GBM ELISA (IgG). Inter-assay concordance, measurement range and interference were determined in a subset of samples.

Results: The ChLIA reached 100 % sensitivity at a specificity of 98.6 %, while the ELISA was less sensitive (89.6 %) and more specific (100 %). High qualitative concordance between both assays was evidenced by positive and negative agreement rates of 100 % and 95.6 %, respectively, and a kappa score of 0.901. The ChLIA showed linearity within a measurement range of 3.8-517.3 CU/ml. Coefficients of variation were calculated as 1.2-3.3 % (intra-lot) and 1.6-4.2 % (inter-lot). No interference was observed for hemolyzed, lipemic or icteric samples.

Conclusion: These validation results demonstrate a high quality of the novel Anti-GBM ChLIA. Given its excellent performance compared to the corresponding ELISA, it represents a promising alternative

tool for accurate anti-GBM assessment in routine diagnostic settings with the advantage of rapid turnaround time and fully automated random-access processing. Future studies will address the assay's suitability for monitoring anti-GBM levels during follow-up.

P230

Relevance of anti-PLA2R levels in therapy decision and prediction of therapy outcome using cyclophosphamide and steroids treatment in patients with membranous nephropathy

Y. Bestmann; C. Vink¹;
A.-E. van de Logt¹; A. Kühnl;
C. Dähnrich; W. Schlumberger;
J. F. M. Wetzels¹ *Institute for Experimental Immunology, EURO-IMMUN Medizinische Labor-diagnostika AG, Lübeck; ¹ Department of Nephrology, Radboud Institute for Health Sciences, Radboud University Medical Center, Nijmegen/NL*

Objective: An individualized therapy approach was introduced for anti-phospholipase A2 receptor (PLA2R) positive patients with primary membranous nephropathy (MN). Cyclophosphamide/steroid treatment was stopped when anti-PLA2R results by indirect immunofluorescence assay (IFA) became negative. Here, we evaluated the relevance of anti-PLA2R levels for therapeutic decisions and MN outcome, comparing qualitative and quantitative detection methods.

Method: Anti-PLA2R levels were determined qualitatively by IFA as well as quantitatively by enzyme-linked immunosorbent assay (ELISA) and chemiluminescence immunoassay (ChLIA) at baseline as well as after treatment

and correlated to immunological remission and persistence.

Results: To evaluate the relevance of anti-PLA2R levels at the start of therapy, serum samples of 60 patients were available. Patients sampled at the beginning of therapy were grouped according to tertiles of anti-PLA2R levels determined by ChLIA (each tertile: n = 20). Lower anti-PLA2R levels were seen in patients with relapsing disease. Higher levels were associated with more severe proteinuria. Patients in the lowest tertile were more likely to develop immunological remission after 8 weeks of therapy. In total, 90 % vs. 75 % vs. 45 % of patients in the tertiles turned anti-PLA2R negative after being treated for 8 weeks. In this subgroup with immunological remission after 8 weeks of therapy, only 11 % of patients in the lowest tertile needed renewed immunosuppressive therapy, while this percentage increased in the middle and highest tertiles (11 % vs. 53 % vs. 33 %, p = 0.033).

For the assessment of anti-PLA2R levels before and after therapy, samples at baseline and week 8 of treatment were examined. At baseline, 50/50 (100 %) tested positive in IFA and ChLIA as well as 48/50 (94 %) in ELISA. After 8 weeks on treatment, immunological remission based on IFA was found in 37/51 (73 %) patients. At this point, the overall agreement with IFA was 92 % for ChLIA and 82 % for ELISA. Yet the availability of quantitative levels provided further insight into this group of patients in whom treatment was discontinued. With ChLIA, anti-PLA2R titers > 5 CU/mL after 8 weeks of therapy were found in 4 % of IFA-negative patients with persistent remission,

vs. 55 % of IFA-negative patients with early relapse (p = 0.006).

Conclusion: In the individualized treatment of MN patients, the quantitative anti-PLA2R determination adds further value. Of the examined quantitative methods, ChLIA demonstrated the highest agreement with IFA. Additional studies are needed to evaluate the impact on clinical decision making and outcome.

P231

Mechanical stress and lysosomal increase in the development of Focal Segmental Glomerulosclerosis

J. Promnitz; M. Saudenova; F. Kliewe¹;
N. Endlich¹; F. Theilig
Anatomisches Institut, Christian-Albrechts-Universität zu Kiel, Kiel; ¹ Institut für Anatomie und Zellbiologie, Universitätsmedizin Greifswald, Greifswald

Objective: Focal segmental Glomerulosclerosis (FSGS) is one of the most common causes of nephrotic syndrome (NS) characterized by proteinuria, edema, hyperlipidemia, hypoalbuminemia and hypertension. FSGS is characterized morphologically by sclerotic lesions in a subset of glomeruli. The mechanisms underlying glomerular damage and disease progression are not fully understood and are the aim of this work.

Method: The FSGS mouse model was characterised at different time points during FSGS development. Renal function analysis, immunohistochemistry, western blot, histological analysis were performed. Additionally, immortalized mouse podocytes were used for RT-PCR, western

blot and immunohistochemistry analysis following the application of mechanical stretch.

Results: Morphological analysis of kidney sections of FSGS and control groups revealed augmented number of lysosomes in podocytes of FSGS mice already at day 9 (+104%) as well as at later time points at day 17 and 28 (+185% and +187%) after induction. Moreover, immunohistochemistry analysis revealed increased TFEB, a master regulator of lysosomal biogenesis, and Galectin 3, lysosomal damage marker, in podocytes of FSGS group compared to control. In addition, immortalized podocytes showed significant increase in lysosomal marker LAMP1 5 days after mechanical stress induction.

Conclusion: Our data suggest that mechanical stress leads to lysosomal increase and this lysosomal increase is one of the factors promoting podocyte injury. Additionally, observed increase in lysosomal biogenesis and damage during FSGS development suggest that an additional event is required for the glomerular disease progression in FSGS.

P232

Randomized, multicenter Phase III study evaluating the efficacy and safety of pegcetacoplan in the treatment of C3 G or IC-MPGN

B. P. Dixon; F. Fakhouri¹; M. C. Pickering²; T. Cook²; D. Kavanagh³; G. Remuzzi⁴; P. Walker⁵; C. Licht⁶; G. Appel⁷; M. Vivarelli⁸; Z. Zhang⁹; L. Li⁹; H. Kocinsky⁹
Renal Section, Department of Pediatrics, University of Colorado School of Medicine, Aurora/USA; ¹Service of Nephrology and Hypertension,

Department of Medicine, Lausanne University Hospital, Lausanne/CH; ²Department of Immunology and Inflammation, Hammersmith Campus, Imperial College London, London/UK; ³National Renal Complement Therapeutics Centre, Royal Victoria Hospital, Newcastle University, Newcastle upon Tyne/UK; ⁴Department of Immunology and Clinical Transplantation, Mario Negri Institute for Pharmacological Research, Milan/I; ⁵Department of Pathology and Laboratory Medicine, Arkana Laboratories, Little Rock/USA; ⁶Department of Pediatrics, The Hospital for Sick Children, University of Toronto, Toronto/CDN; ⁷Clinical Nephrology at NewYork-Presbyterian Hospital, University Medical Center in New York, Columbia University, New York/USA; ⁸Division of Nephrology and Dialysis, Bambino Gesù Pediatric Hospital, Rome/I; ⁹Apellis Pharmaceuticals, Waltham/USA

Objective: Complement 3 glomerulopathy (C3 G) and immune complex membranoproliferative glomerulonephritis (IC-MPGN) are rare diseases characterized by excessive deposition of C3 breakdown products in renal glomeruli leading to proteinuria and progressive renal disease. Pegcetacoplan is a targeted C3 investigational therapy for diseases related to complement overactivation. This is a phase 3, randomized, placebo-controlled, double-blind, multicenter study of the efficacy and safety of pegcetacoplan in individuals with C3 G or IC-MPGN.

Method: Approximately 90 patients (age, ≥ 12 years; weight, 20-100 kg) diagnosed with C3 G or IC-MPGN, either as primary disease or posttransplant disease recurrence,

will be recruited. Inclusion criteria include 2+ staining for C3c, global glomerulosclerosis $< 50\%$, urine protein-to-creatinine ratio (uPCR) ≥ 1000 mg/g, and estimated glomerular filtration rate (eGFR) > 30 mL/min/1.73 m². Exclusion criteria include previous pegcetacoplan exposure, C3 G/IC-MPGN secondary to other conditions, and significant infection/malignancy. Patients will be randomized 1:1 to receive subcutaneous infusions of pegcetacoplan (1080 mg/20 mL) or matching volume of placebo twice weekly for 26 weeks (in addition to standard care). Thereafter, in the open-label period, all participants will receive pegcetacoplan twice weekly for 26 weeks. Assessments include first-morning uPCR every 4 weeks and renal biopsies at baseline/screening and weeks 26 and 52. Primary endpoint is proportion of participants with reduction in uPCR $\geq 50\%$ relative to baseline at week 26. Secondary endpoints include proportion of participants with eGFR scores that are stable or improved from baseline; change in C3 G histologic index activity score; and proportion of participants with decreased C3c staining on renal biopsy from baseline at week 26. Safety outcomes will also be monitored throughout the study. Participants may enter a subsequent 8-week follow-up period or long-term extension study.

Results: This is a study design abstract.

Conclusion: C3 G and IC-MPGN are rare, progressive renal diseases due to deposition in renal glomeruli. This study will evaluate the safety and efficacy of complement protein C3 inhibitor pegcetacoplan in treating C3 G and IC-MPGN.

P233**Exploratory diagnostic and prognostic biomarkers in adults with atypical hemolytic uremic syndrome (aHUS): analysis of the phase III study of ravulizumab (NCT02949128)**

W. Hettrich; T.J. Cammett¹; K. Garlo¹; E.E. Millman¹; K. Rice¹; S. Faas¹
 Alexion Pharma Germany GmbH, München; ¹ Alexion, AstraZeneca Rare Disease, Boston/USA

Objective: Validated biomarkers for diagnosis and monitoring of patients with complement-mediated thrombotic microangiopathy (CM-TMA) are not clinically available. Characterization of biomarkers in patients with

aHUS, a form of CM-TMA, may inform diagnosis, treatment decisions and monitoring for patients with other types of CM-TMA.

Method: Using data from the phase III study of ravulizumab (terminal C5 complement inhibitor) in adults with aHUS (NCT02949128), baseline (BL; prior to treatment) serum, plasma and urine biomarker levels in patients were compared with levels in healthy volunteers (HV), and evaluated for associations with kidney function (e.g. estimated glomerular filtration rate [eGFR] and urine protein/creatinine [Cr] ratio [UPCR]) at BL and 26 weeks post-treatment initiation. Regression coefficients and p-values (two-sided t-test) are reported.

Results: This analysis included 55 patients: median age 39 (range 19–76) years; 67 % female; 53 % White, 27 % Asian. Specific BL biomarkers were elevated compared with HV, and associations between BL biomarker levels and both BL eGFR and BL UPCR were identified (Table 1). BL plasma complement factor Ba was associated with eGFR changes after 26 weeks of ravulizumab treatment, while urine sC5b-9, sC5b-9/Cr, Ba and Ba/Cr were associated with UPCR changes after 26 weeks of treatment.

Conclusion: The complement biomarkers Ba (plasma and urine) and sC5b-9 (urine) were associated with kidney function in patients with aHUS at baseline and over 26 weeks

Table 1: Baseline biomarkers

Biomarker	Patients with elevated BL biomarkers* % (n/N)	BL biomarker associations with kidney function measures (BL)		BL biomarker associations with kidney function measures (26-week change from BL)	
		Regression coefficient (p-value)		Regression coefficient (p-value)	
		eGFR	UPCR	eGFR	UPCR
Urine cystatin C/Cr (ng/mg Cr)	100.0 (36/36)	-0.25 (0.0002)	0.42 (0.0048)	-2.28 (0.4290)	-9.72 (0.2385)
Plasma Ba (ng/ml)	97.7 (42/43)	-0.55 (<0.0001)	1.25 (0.0001)	-13.98 (0.0085)	-27.42 (0.1021)
Urine cystatin C (ng/ml)	97.6 (41/42)	-0.25 (<0.0001)	0.51 (<0.0001)	-0.62 (0.7788)	-7.38 (0.2103)
Urine Ba (ng/ml)	97.5 (39/40)	-0.28 (<0.0001)	0.73 (<0.0001)	1.41 (0.5825)	-16.07 (0.0090)
Urine Ba/Cr (ng/mg Cr)	97.1 (34/35)	-0.31 (<0.0001)	0.77 (<0.0001)	2.40 (0.3957)	-17.28 (0.0110)
Urine sC5b-9**/Cr (ng/mg Cr)	96.9 (31/32)	-0.10 (0.0391)	0.45 (<0.0001)	1.91 (0.3650)	-21.46 (<0.0001)
Urine sC5b-9** (ng/ml)	88.1 (37/42)	-0.12 (0.0021)	0.44 (<0.0001)	-0.79 (0.5862)	-16.03 (<0.0001)
Plasma sC5b-9 (ng/ml)	79.1 (34/43)	0.19 (0.1430)	-0.25 (0.3712)	-3.17 (0.5269)	15.91 (0.1830)

*compared with observed maximum for HV; **urine sC5b-9 is undetectable in HV, therefore HV values were set at ½LLOQ

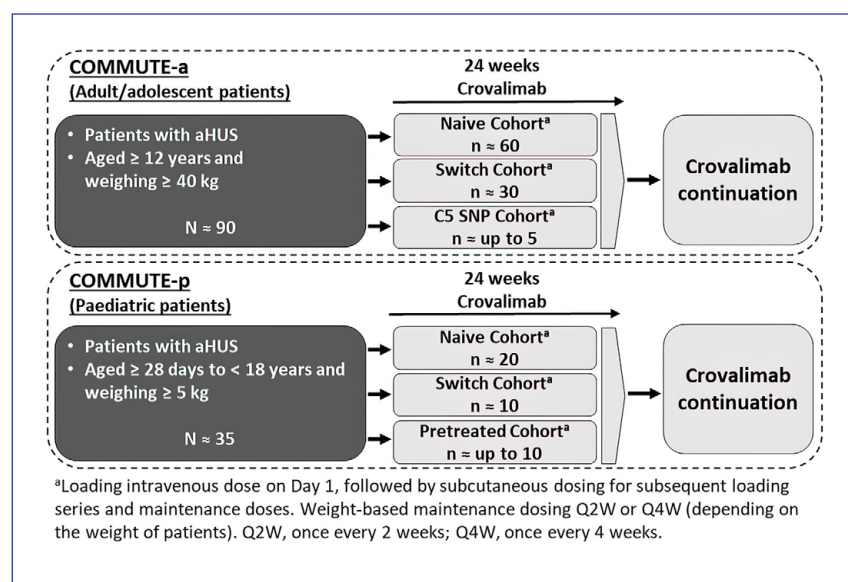
of treatment with anti-C5 therapy. Such biomarkers demonstrate diagnostic potential in CM-TMA and may predict renal response to terminal complement inhibition.

P234

Two Phase III trials evaluating crovalimab in patients with atypical haemolytic uraemic syndrome (aHUS): COMMUTE-a and COMMUTE-p

P. T. Brinkkötter¹; N. S. Sheerin¹;
L. Greenbaum²; S. Ito³; C. Loirat⁴;
S. Maruyama⁵; M.-H. Zhao⁶;
K. Benkali⁷; C. Pieterse⁸; M. D. Shah⁹;
A. Sostelly⁸; S. Sreckovic⁸; F. Fakhouri¹⁰
Nephrologie, Rheumatologie, Diabetologie und Allgemeine Innere Medizin, Klinik II für Innere Medizin, Universitätsklinikum Köln, Köln;
¹ Department of Nephrology, Newcastle University, Newcastle/UK; ² Division of Pediatric Nephrology, Emory University School of Medicine and Children's Healthcare of Atlanta, Atlanta/USA; ³ Department of Pediatrics, Graduate School of Medicine, Yokohama City University, Kanagawa/J; ⁴ University Hospital Robert Debré, Paris/F; ⁵ Department of Nephrology, Nagoya University Graduate School of Medicine, Nagoya/J; ⁶ Renal Division, Department of Medicine, Peking University First Hospital, Beijing/CN; ⁷ Certara, Inc., Paris/F; ⁸ F. Hoffmann-La Roche Ltd., Basel/CH; ⁹ Genentech, Inc., South San Francisco/USA; ¹⁰ Service of Nephrology and Hypertension, Department of Medicine, Lausanne University Hospital, Lausanne/CH

Objective: Atypical haemolytic uraemic syndrome (aHUS) is a life-threatening disease of complement dysregulation, characterised by thrombotic microangiopathy (TMA). While treatment with C5 inhibition



P234: Abb. 1

is effective, currently approved therapies require regular intravenous infusions. Crovalimab, a novel anti-C5 monoclonal antibody, allows for small-volume, subcutaneous self-injections. Crovalimab is being tested for treatment of aHUS in two global, Phase III single-arm trials: COMMUTE-a and COMMUTE-p. **Method:** COMMUTE-a (NCT04861259) will enrol 3 cohorts of patients with aHUS aged ≥ 12 years (Figure): **Naive:** complement inhibitor-naïve patients; **Switch:** patients switching from eculizumab/ravulizumab; and **C5 SNP:** patients with a known single-nucleotide polymorphism (SNP). COMMUTE-p (NCT04958265) will enrol three cohorts of patients with aHUS aged ≥ 28 days to < 18 years (Figure): **Naive:** complement inhibitor-naïve patients; **Switch:** patients switching from eculizumab/ravulizumab; and **Pretreated:** patients who received and discontinued prior eculizumab/ravulizumab treatment. In both the COMMUTE-a

and COMMUTE-p trials, patients will receive weight-based crovalimab as a weekly loading series (Weeks 1-4), followed by self-administered, subcutaneous maintenance doses (Weeks 5 and after; once every 4 weeks or once every 2 weeks if < 20 kg). The primary objective for both studies is to evaluate the efficacy of crovalimab in Naïve patients, based on the proportion of patients with complete TMA response any time from baseline to Week 25. **Results:** COMMUTE-a and COMMUTE-p are currently enrolling. **Conclusion:** Both COMMUTE-a and COMMUTE-p will assess the efficacy and safety of crovalimab in patients with aHUS.

P235

Interstitial ANCA-associated vasculitis associates with severe kidney injury independent of glomerulonephritis

S. Hakroush¹; B. Tampe¹
Institut für Pathologie, Universitätsmedizin Göttingen,

Georg-August-Universität, Göttingen;
¹ Klinik für Nephrologie und Rheumatologie, Universitätsmedizin Göttingen, Georg-August-Universität, Göttingen

Objective: Antineutrophil cytoplasmic antibody (ANCA)-associated vasculitis (AAV) is a small vessel vasculitis affecting multiple organ systems, including the kidney. Small vessels in the kidney include small-sized arteries (interlobular artery, afferent and efferent arteriole), capillaries (glomerular and peritubular capillary) and venules. Although crescentic ANCA glomerulonephritis (GN) is a common histological finding reflecting glomerular small vessel vasculitis, it is reasonable that manifestation of AAV could also contribute to interstitial small vessel vasculitis. Therefore, we here aimed to expand our current knowledge focusing on interstitial vasculitis in ANCA GN by systematic histological scoring of vascular lesions analogous to Banff.

Method: A total number of 49 kidney biopsies with confirmed renal involvement of AAV at the University Medical Center Göttingen were retrospectively included between 2015 till 2020. A renal pathologist evaluated all biopsies and was blinded to clinical data collection and analysis.

Results: Among all active and chronic tubulointerstitial lesions analogous to the Banff scoring system, the only association between severe kidney injury requiring kidney replacement therapy (KRT) was observed for interstitial vasculitis in AAV reflected by peritubular capillaritis (ptc, $p = 0.0002$) and arteritis (v, $p = 0.0069$), affecting 5/49 (10.2%) and 11/49 (22.4%) of renal biopsies, respectively.

Interestingly, no association between interstitial vasculitis (ptc and v correlating with severe kidney injury) and any glomerular lesion in ANCA GN (also correlating with severe kidney injury) was observed, thereby confirming that interstitial vasculitis contributes to severe kidney injury independent of ANCA GN. By contrast, short-term renal recovery from KRT was equal in both groups, suggesting a distinct association with acute decline of kidney function at disease onset.

Conclusion: Taken together, by using the Banff scoring system we here expand our current knowledge of renal interstitial lesions in AAV revealing peritubular capillaritis and arteritis as important histological alterations associated with severe kidney injury in a considerable subset of AAV. Furthermore, our findings that interstitial vasculitis did not correlate with crescentic ANCA GN implicate that the characteristics of each vasculitis manifestation are independent and could further improve our understanding of mechanisms contributing to renal injury.

P236

Systematic characterization of histopathological lesions in association with anemia in ANCA-associated renal vasculitis

E. Baier; D. Tampe; I. A. Kluge; S. Hakroush¹; B. Tampe
 Klinik für Nephrologie und Rheumatologie, Universitätsmedizin Göttingen, Georg-August-Universität, Göttingen;
¹ Institut für Pathologie, Universitätsmedizin Göttingen, Georg-August-Universität, Göttingen

Objective: Anemia in anti-neutrophil cytoplasmic antibody (ANCA)-associated renal vasculitis is a

severe complication depicting a predictor of renal survival. Decline of kidney function tightly corresponds with anemia severity, thus implying renal causation to be mainly contributory in the pathogenesis of anemia. However, histopathological implications directly associated with anemia in ANCA-associated renal vasculitis remain elusive. Therefore, we performed survival-curve analyses to assess the effects of anemia on short-term survival in hospitalized patients suffering from ANCA-associated renal vasculitis and conducted correlative analyses to scrutinize correlations of low hemoglobin levels and histopathological characteristics.

Method: A total number of 52 patients with biopsy proven ANCA-associated renal vasculitis were retrospectively enrolled between 2015 and 2020 in a single-center observational study. Laboratory parameters on blood cell count, iron and vitamin status were assessed in addition to clinical data. Renal biopsies were classified according to Berden *et al.* (focal, crescentic, mixed, and sclerotic), Brix *et al.* (ARRS low, intermediate, or high risk), and the Banff scoring system for allograft pathology. Survival-curve analyses using the Kaplan-Meier method and curve comparison by log-rank testing were performed. Additionally, correlative analyses utilizing Spearman's correlation and linear regression was conducted.

Results: We here show that renal anemia predominantly occurred with a prevalence of 86.2%, and significantly affected clinical recovery of hospitalized patients with ANCA-associated renal vasculitis ($p = 0.0041$, HR: 2.2, 95% CI: 1.2-4.1), especially within the initial

phase of critical illness ($p = 0.0415$, HR: 2.5, 95 % CI: 0.5-11.8). By performing correlative analyses, low serum hemoglobin levels were identified to correlate with extensive rupture of Bowman's capsule ($p = 0.014$, $\beta = -0.374$) and peritubular capillaritis ($p = 0.013$, $\beta = -0.358$), thus providing evidence of distinct histopathological lesions to be associated with anemia in ANCA-associated renal vasculitis.

Conclusion: In summary, we here provide evidence that clinical recovery of hospitalized patients with ANCA-associated renal vasculitis is significantly impaired by anemia represented by serum hemoglobin levels below the median of 9.6 g/dL. We here identified distinct histopathological lesions (including extensive rupture of the Bowman's capsule and peritubular capillaritis) to be associated with anemia, predominantly in MPO-ANCA-positive renal vasculitis, thus improving our current knowledge of anemia etiopathogenesis in ANCA-associated renal vasculitis.

P237

Clinical relevance and histopathological implications of low albumin serum levels and hyperuricemia in ANCA-associated renal vasculitis

E. Baier; D. Tampe; S. Hakroush¹; B. Tampe

Klinik für Nephrologie und Rheumatologie, Universitätsmedizin Göttingen, Georg-August-Universität, Göttingen; ¹Institut für Pathologie, Universitätsmedizin Göttingen, Georg-August-Universität, Göttingen

Objective: Low albumin levels predict renal outcome in antineutrophil cytoplasmic

antibody (ANCA)-associated renal vasculitis. Despite growing insights on the relevance of albumin and uric acid serum levels for the regulation of oxidative conditions, implications of hypoalbuminemia and hyperuricemia on a) clinical aspects encompassing short-term recovery and long-term renal survival and b) correlative analyses comprising proteinuria and histopathological associations in the pathophysiology of ANCA-associated renal vasculitis remain elusive.

Method: A total number of 53 biopsy-proven cases of ANCA-associated renal vasculitis were retrospectively enrolled between 2015 till 2020 in a single-center observational study. The primary endpoint, composite kidney failure, was defined as having reached a stable creatinine threshold 50 % higher than baseline creatinine. Secondary endpoints were all-cause mortality, CKD G5 or dependency on permanent dialysis. Correlative analyses were performed regarding serum parameters, proteinuria and histological characteristics.

Results: We here show that low albumin levels below the median of 2.4 g/dL at timepoint of initial hospitalization promote composite kidney failure, especially in MPO-ANCA-associated renal vasculitis. Short-term clinical recovery in hospitalized patients is impaired by hyperuricemia and low albumin levels, especially in critically ill patients. Low platelet count and systemic complement C3c decrease were associated with hyperuricemia, wherein low albumin levels also associated with low platelets. Urinary markers of glomerular and tubular damage correlated with low albumin levels. On a histopathological level, low albumin

levels were associated with eosinophilic and plasmacytic immune-cell infiltrates, wherein interstitial fibrosis correlated with hyperuricemia.

Conclusion: In summary, we here provide evidence that nephrogenic loss of albumin contributes to low albumin serum levels that promote composite kidney failure, especially in MPO-positive ANCA-associated renal vasculitis. Hyperuricemia may favor systemic complement C3c activation, which is particularly relevant in the state of critical illness in hospitalized ANCA-associated renal vasculitis patients. Low albumin levels were associated with low platelet counts and distinct tubulointerstitial immune-cell infiltrations as a histopathological correlate, wherein hyperuricemia correlated with interstitial fibrosis and glomerular sclerosis. We hence show that systemic components that engage in regulation of oxidative conditions in the pathophysiology of ANCA-associated renal vasculitis contribute to disease progression.

P238

Two-Year Efficacy and Safety of Ravulizumab in Adults and Children with Atypical Hemolytic Uremic Syndrome (aHUS): Analysis of Two Phase 3 Studies

N. Heyne; B. P. Dixon¹; A. D. Madris-Aris²; B. Adams³; D. Kavanagh⁴; H. G. Kang⁵; J. Wang⁶; K. Garlo⁶; K. Tanaka⁷; L. Greenbaum⁸; M. Ogawa⁶; S. H. Kim⁹; S. Cataland¹⁰; S.-S. Yoon¹¹; Y. Miyakawa¹²; Y. Luque¹³; M. Muff-Luett¹⁴

Sektion Nieren- und Hochdruckkrankheiten, Universitätsklinikum, Medizinische Klinik IV, Eberhard Karls Universität Tübingen, Tübingen; ¹Renal Section, Department of Pediatrics, University of Colorado School of

Medicine, Aurora/USA; ² Children's Nephrology and Renal Transplantation Service, Children's Maternity Hospital

Sant Joan de Déu, University of Barcelona, Barcelona/E; ³ Department of Pediatric Nephrology, Children's

Hospital Queen Fabiola, Université libre de Bruxelles, Brüssel/BE; ⁴ National Renal Complement Therapeutics

Table: Efficacy data from baseline to 26 wks and from baseline through 2 yr in the phase 3 studies of ravulizumab in adults and children naïve to complement inhibition

	Adults naïve to terminal complement inhibition (N=56)		Children naïve to terminal complement inhibition (N=20)	
	Initial evaluation period	Extension period	Initial evaluation period	Extension period
	26 wk	All data through 2 yr	26 wk	All data through 2 yr
Treatment duration, median (range) weeks	26.1 (0.6, 27.1)	114.4 (0.6, 162.4)	26.1 (3, 26.6)	134.7 (3, 154)
Complete TMA response, n (%)	30 (53.6)	34 (60.7)	15 (75.0)	18 (90.0)
Time to complete TMA response, median (95% CI) days	86.0 (42.0, 401)		30.0 (22.0, 88.0)	
Platelet count normalization, n (%)	47 (83.9)	48 (85.7)	19 (95.0)	19 (95.0)
LDH normalization, n (%)	43 (76.8)	49 (87.5)	18 (90.0)	19 (95.0)
≥25% improvement in serum creatinine, n (%)	33 (58.9)	35 (62.5)	16 (80.0)	18 (90.0)
Hematologic normalization, ^a n (%)	41 (73.2)	48 (85.7)	18 (90.0)	19 (95.0)
Hemoglobin response, ^b n (%)	40 (71.4)	45 (80.4)	17 (85.0)	18 (90.0)
Change in eGFR, median mL/min/1.73 m ² (range)	29 (-13, 108)	35 (-6, 95)	80 (0, 222)	82.5 (5, 149)
Dialysis discontinuation from baseline, ^c n/N (%)	16/24 (66.7)	12/18 (66.7)	5/6 (83.3)	6/6 (100)
Dialysis initiation from baseline, ^d n/N (%)	4/25 (16.0)	4/20 (20.0)	0/11 (0)	0/9 (0)
CKD stage improvement, ^e n/N (%)	32/47 (68.1)	25/35 (71.4)	15/17 (88.2)	15/16 (93.8)
CKD stage worsening, ^f n/N (%)	2/13 (15.4)	1/10 (10.0)	0/11 (0)	0/10 (0)
Change in FACIT-Fatigue score from baseline, ^g median (range)	20.0 (-16, 48)	12.0 (-7, 49)	10.0 (4, 48)	8.0 (7, 48)
Change in EQ-5D-3L score from baseline, ^h				
Mean VAS (SD)	32.3 (29.6)	32.9 (29.5)	N/A	N/A
Mean TTO (SD)	0.32 (0.32)	0.31 (0.32)		

^aplatelet count and LDH normalization;

^b≥20 g/L increase;

^cn refers to the number of patients who came off dialysis who were on dialysis at baseline, N includes only those patients who remained in the study, had available data at the given timepoint and who were on dialysis at baseline;

^dn refers to the number of patients who started dialysis who were not on dialysis at baseline, N includes only those patients who remained in the study, had available data at the given timepoint and who were not on dialysis at baseline;

^eimprovement means a decrease from baseline by at least 1 stage according to standard eGFR thresholds per CKD stage, N includes only those who remained in the study at the given timepoint and excludes patients with stage 1 CKD at baseline as they cannot improve;

^fworsening means an increase from baseline by at least 1 stage according to standard eGFR thresholds per CKD stage, N includes only those who remained in the study at the given timepoint and excludes patients with stage 5 CKD at baseline as they cannot worsen;

^gpediatric FACIT-Fatigue questionnaire used to assess HRQoL in patients ≥5 years of age in ALXN1210-aHUS-312;

^hTTO value set for the USA.

aHUS, atypical hemolytic uremic syndrome. CI; Confidence interval. CKD, Chronic kidney disease. eGFR, Estimated glomerular filtration rate. FACIT, Functional assessment of chronic illness therapy. HRQoL, Health related quality of life. LDH, Lactate dehydrogenase. N/A, Not applicable. SD, Standard deviation. TMA, Thrombotic microangiopathy. TTO, Time trade-off. VAS, Visual analog scale.

Centre, Royal Victoria Hospital, Newcastle University, Newcastle upon Tyne/; ⁵ Division of Pediatric Nephrology, Department of Pediatrics, Seoul National University College of Medicine, Seoul/ROK; ⁶ Alexion, AstraZeneca Rare Disease, Boston/USA; ⁷ Department of Nephrology, Aichi Children's Health and Medical Center, Obu/J; ⁸ Division of Pediatric Nephrology, Emory University School of Medicine and Children's Healthcare of Atlanta, Atlanta/USA; ⁹ Department of Pediatrics, Pusan National University Children's Hospital, Yangsan/ROK; ¹⁰ Division of Hematology, Department of Internal Medicine, Ohio State University, Columbus/USA; ¹¹ Department of Internal Medicine, Seoul National University Hospital, Seoul/ROK; ¹² Department of General Internal Medicine, Saitama Medical University, Saitama/J; ¹³ Renal Intensive Care Unit, Nephrology Department, Tenon Hospital, Assistance Publique – Hôpitaux de Paris, Sorbonne Université, Paris/F; ¹⁴ Division of Pediatric Nephrology, University of Nebraska Medical Center, Omaha/USA

Objective: Ravulizumab, a humanized anti-complement C5 monoclonal antibody designed by targeted modification of eculizumab to achieve an extended half-life, is approved to treat aHUS in the USA (2019), EU and Japan (2020). Data at 26 weeks (wk) and 1 year (yr) from the phase 3 studies of ravulizumab in adults and children with aHUS have been published. Here we report 2-yr data from these trials.

Method: Efficacy and safety data from ravulizumab clinical trials in adults naïve to complement inhibitor treatment (NCT02949128), and

in children either naïve to (naïve) or switched from (switch) eculizumab (NCT03131219), were assessed at 2 yr and presented alongside data from the initial 26-wk evaluation periods. No statistical comparisons between data at 26 wk and 2 yr, or between trials, were conducted.

Results: Efficacy data in adults and treatment-naïve children are presented in the Table. Complete thrombotic microangiopathy (TMA) response was achieved in more patients at 2 yr vs 26 wk in both studies (adult: 34 [61 %] vs 30 [54 %]; naïve: 18 [90 %] vs 15 [75 %]). All complete TMA response components were either numerically improved or maintained at 2 yr vs 26 wk. Kidney function continued to improve, with the median change in estimated glomerular filtration rate from baseline numerically increasing at 2 yr vs 26 wk in both adults (35 vs 29 mL/min/1.73 m²) and naïve children (82.5 vs 80 mL/min/1.73 m²). Most patients receiving dialysis at baseline were able to discontinue dialysis at 26 wk; this was sustained in adults (67 % vs 67 %) while all naïve children receiving dialysis at baseline had discontinued by 2 yr (83 % vs 100 %). No patients who discontinued dialysis by 26 wk subsequently restarted. Chronic kidney disease (CKD) stage improved in most patients through 26 wk in both studies (adult, 68 %; naïve, 88 %); improvements were sustained at 2 yr (adult, 71 %; naïve, 94 %). No naïve children experienced a worsening of CKD stage at 2 yr. Most adverse events (AEs) and serious AEs (SAEs) occurring in these studies were reported during the initial 26-wk evaluation period, with

a general reduction in the number of patients with any new S/AE events being reported at 2 yr. No patients discontinued either study due to treatment-emergent AEs after 26 wk. No meningococcal infections were recorded in either study at any timepoints.

Conclusion: The data suggest that long-term treatment with ravulizumab is well tolerated and may be associated with continuing improvements in TMA parameters and renal function in adults and children with aHUS.

P239

Immunosuppressive therapy and its effect on renal involvement in IgA vasculitis (Henoch-Schönlein purpura)

S. Bettag; P. Zgoura; A. Doevelaar; S. Bertram; D. Racovitan; B. Rohn; M. Seidel; S. Rieckmann; J. Braun¹; N. Babel; T. H. Westhoff; F. S. Seibert
Centrum für Translationale Medizin, Medizinische Klinik I, Marien Hospital Herne, Ruhr-Universität Bochum, Herne; ¹ Rheumazentrum Ruhrgebiet, Herne

Objective: Data on therapeutic effects of immunosuppression in IgA-vasculitis (Henoch-Schönlein purpura; IgAV) are conflicting. It remains elusive, whether glucocorticosteroids (GS) with/without additional immunosuppressive therapy with cyclophosphamide, rituximab or azathioprine have a significant impact on either clinical symptoms or renal function.

Method: This retrospective monocentric study investigates 27 adult patients with IgAV and biopsy proven IgA nephropathy (IgAN), who were either under GS mono-therapy or in combination

with cyclophosphamide, rituximab or azathioprine. Next to score responsiveness of the immunosuppressive regimen on arthritis, skin rash and abdominal pain, we analysed the progression of eGFR loss and reduction of proteinuria over a time course of 3-6 months and after at least 1 year after treatment initiation.

Results: 26 out of 27 (96,3 %) patients reported an overall improvement of their symptoms ($p = 0.001$). Score based analysis for cutaneous manifestations ($p = 0.0001$), arthritis ($p = 0.0001$) and abdominal pain ($p = 0.002$) showed significant differences after one year of treatment. Renal function showed a short-term (3-6 months) increase in eGFR ($\Delta\text{eGFR} +15.1 \pm 23.2 \text{ ml/min/1.73 m}^2$, $p = 0.0189$), which attenuated after 12 months ($\Delta\text{eGFR} +6 \pm 21.7 \text{ ml/min/1.73 m}^2$, $p = 0.1355$). After 1 year, albuminuria and overall proteinuria declined by $-547.3 \pm 866.6 \text{ mg/l}$ ($p = 0.0059$) and $-579 \pm 788 \text{ mg/l}$ ($p = 0.0134$), respectively. Comparing the subgroup of patients under steroid monotherapy ($n = 13$) to a combination therapy ($n = 14$), no additional beneficial renal effect could be seen with cyclophosphamide, rituximab or azathioprine ($p > 0.05$ for eGFR and proteinuria). Noteworthy, in case of renal involvement of IgAV, cyclophosphamide ($n = 4$, median $\Delta\text{eGFR} +34 \text{ ml/min/1.73 m}^2$) showed a renoprotective tendency compared to rituximab ($n = 4$, median eGFR $-6.5 \text{ ml/min/1.73 m}^2$, $p = 0.0571$).

Conclusion: Immunosuppressive therapy in IgAV improves clinical symptoms, proteinuria, and eGFR. Its long-term effect remain uncertain.

P240

Analyse von Nierenbiopsien und Rebiopsien bei Patienten mit IgA-Nephropathie – eine retrospektive monozentrische Analyse

A. Gribaudo; K. Herfurth; M. Schlosser; G.B. Wolf; M. Busch

Abteilung für Nephrologie, Klinik für Innere Medizin III, Friedrich-Schiller-Universität Jena, Jena

Hintergrund: Der klinische Nutzen von renalen Rebiopsien und deren Relevanz für die Prognose bei IgA-Nephropathie ist unklar. Ziel dieser retrospektiven Studie war es, die Anzahl von Rebiopsien, deren Indikationen und ihre potentielle Bedeutung für den Krankheitsverlauf zu erfassen.

Methode: Im Universitätsklinikum Jena wurden von 2001–2021 159 Patienten mit IgA-Nephropathie betreut, 127 mit vorliegendem Biopsiebefund. Bei 33 Patienten (26 %) wurde mind. eine weitere Nierenbiopsie, entweder vor Diagnosestellung der IgAN ($n = 5$, 15,2 %) und/oder im weiteren Verlauf ($n = 30$, 90,9 %) durchgeführt. Es wurden histologische, laborchemische und klinische Parameter, die Therapie-regime (Supportivtherapie vs. Immunsuppression) sowie die Endpunkte Nierentransplantation, Dialysebeginn und Tod untersucht.

Ergebnisse: Es handelte es sich um 27 Männer und 6 Frauen im Alter von 40 (18–72) Jahren zum Zeitpunkt der ersten Biopsie. Bei 22 Patienten wurden zwei, bei 8 drei und bei 3 Patienten vier Biopsien durchgeführt. Gründe für die erste Rebiopsie waren, allein oder in Kombination, eine progrediente Proteinurie (69,7 %), eine GFR-Abnahme (57,6 %) inkl. eines ANV (6,1 %) und die Durchführung

im Rahmen einer Studie (6,1 %). Fünf Patienten (15,2 %) erhielten in der ersten und zwei (6,1 %) in der zweiten Biopsie eine andere oder nicht klar einer IgAN zuordenbare Diagnose. Ein Patient (3 %) zeigte in beiden Biopsien frische Nekrosen. In 21 Fällen (63,6 %) erfolgte nach der ersten Rebiopsie eine Therapieanpassung (48,5 % erhielten Immunsuppression, 15,2 % eine Verstärkung der RAAS-Blockade). In 12 Fällen (36,4 %) wurde die Therapie unverändert fortgeführt. Bei 13 Patienten (39,4 %) trat 8,1 (1,6–23,2) Jahre nach der Erstbiopsie, im Alter von 51 (24–67) Jahren, eine dauerhafte Dialysepflichtigkeit ein. Ein Patient (3 %) verstarb im Alter von 80 Jahren an einer Sepsis und 19 Patienten (57,6 %) erreichten bis zum Beobachtungsende im Jahre 2021 keinen Endpunkt.

Zusammenfassung: Bei mehr als einem Fünftel zeigte sich in der zweiten Biopsie eine nicht der Erstbiopsie entsprechende Diagnose. Des Weiteren führte die erste Rebiopsie in nahezu zwei Drittel der Fälle zu einer Änderung oder Anpassung des Therapieregimes. Dies lässt vermuten, dass eine Rebiopsie in bestimmten Fällen, v. a. bei einer schnellen Verschlechterung von GFR und/oder Proteinurie, im Hinblick auf die korrekte Diagnosestellung und eine Änderung des Therapieregimes sinnvoll sein kann.

P241

Successful long term plasma exchange therapy in recurrent focal segmental glomerulosclerosis in a living renal transplant recipient

I. Menasria; S. Freim von Rheinbaben; T. Kuschnereit; S. Stracke

Abteilung für Nephrologie und Hypertensiologie, Klinik und Poliklinik

für Innere Medizin A, Universitätsmedizin Greifswald, Greifswald

Objective: Focal segmental glomerulosclerosis (FSGS) is a proteinuric glomerulopathy caused by renal podocyte injury. FSGS recurs in 14 %-60 % of first renal transplants, likely associated with a circulating permeability factor. Primary FSGS in adults is often resistant to multiple immunosuppressive agents, which is associated with ongoing complications of nephrotic syndrome and a high risk of progression to end-stage renal disease.

Results: In 2011, a 19 yr old female was admitted with edema in both legs. Laboratory analyses revealed nephrotic proteinuria > 20 g/d and normal eGFR. Renal biopsy showed primary FSGS. Genetic analysis was negative. Steroid therapy initially led to a decrease in proteinuria before relapsing in 2012. Over the next 3 years and despite sequential treatments with tacrolimus, rituximab, mycophenolate mofetil and plasma exchange, renal function deteriorated and in 2015, hemodialysis was initiated. In 2018, the patient received a living renal transplant from her mother (CMV-/CMV-). Immunosuppression then consisted of cyclosporine, prednisolone and MMF. Only 2 weeks after transplantation, heavy proteinuria recurred, and transplant biopsy confirmed FSGS recurrence. Intensified immunosuppressive therapy with 2 cycles of obinutuzumab followed by repeated plasma exchange was initiated. Primarily, plasma exchange was carried out 2-3 x/week. After 8 weeks, CMV infection occurred. MMF and plasma exchange had to be stopped for 6 weeks, CMV infection was treated with valganciclovir.

The frequency of plasma exchange was then reduced to 1x/week and later to every other week. In 2019, stable low level proteinuria was achieved (0,5 g/d), maintained through prednisolone, tacrolimus and MMF combined with plasma exchange. However, eGFR gradually decreased without the former massive proteinuria. In 2020, a repeat transplant biopsy showed normal podocytes and no typical features for FSGS. Instead, tubular toxicity and a low grade chronic humoral reaction were described. We increased tacrolimus target levels and MMF doses and stopped cotrimoxazole which the patient had been taking on her own. Since 2021, proteinuria recurred (3-5 g/d), most likely due to low patient compliance and resulting reduced frequency of plasma exchange.

Conclusion: Underlying mechanisms of primary FSGS are not completely understood. Therefore, therapy is limited to unspecific immunosuppression and often is unsuccessful. The elimination of a soluble, still unknown factor via plasma exchange may be an alternative. In this case, we demonstrate a stable disease after recurrence of FSGS in a living renal transplant using continuous plasma exchange for over 3 years.

P242

An interdisciplinary diagnostic approach to guide therapy in C3 glomerulopathy

T. Schmidt; S. Afonso¹; L. Perie¹; K. Heidenreich²; S. Wulf³; C.F. Krebs⁴; P.F. Zipfel¹; T. Wiech³
Abteilung für Nephrologie/Osteologie, III. Medizinische Klinik, Universitätsklinikum Hamburg-Eppendorf, Hamburg; ¹ Abteilung Infektionsbiologie, Hans-Knöll-Institut, Leibniz

Institut für Naturstoff-Forschung und Infektionsbiologie e. V., Jena; ² Eleva GmbH, Freiburg; ³ Institut für Pathologie, Sektion Nephropathologie, Zentrum für Diagnostik, Universitätsklinikum Hamburg-Eppendorf, Hamburg; ⁴ Sektion für Translationale Immunologie, III. Medizinische Klinik, Universitätsklinikum Hamburg-Eppendorf, Hamburg

Objective: Since the re-classification of membranoproliferative glomerulonephritis the disease entity C3 glomerulopathy is diagnosed if C3 deposition is clearly dominant over immunoglobulins in immunohistochemistry or immunofluorescence. Although this new definition is more orientated at the pathophysiology C3 glomerulopathy remains a heterogeneous group of disorders. Prognosis is poorly predictable. Current biopsy based diagnostic approaches sometimes combined with complement profiling are not sufficient to guide clinicians neither (i) whether to treat an individual patient nor (ii) to choose the best therapy. We present here an approach that might in future help to guide therapy of renal diseases with relevant complement activation.

Method: With this work, we propose an interdisciplinary diagnostic approach, including detailed analysis of the kidney biopsy for morphological alterations and immunohistochemical staining, for genetic analyses of complement genes, complement activation patterning in plasma, and furthermore for applying novel approaches for convertase typing and complement profiling directly in renal tissue. Such a combined diagnostic approach was used here for a 42-year-old female patient with C3 glomerulopathy and signs of chronic endothelial damage.

Results: Genetic testing revealed a heterozygous mutation of the Factor H gene affecting expression of one allele both of Factor H and of the FHL1 protein. Using ELISA, a series of complement markers and activation product were analyzed in plasma to follow the complete complement pathways. We found strong activation of the terminal complement cascade in sera of our patient and in detailed analysis of the renal biopsy. Based on these effects we finally decided to start treatment with Eculizumab. After 13 weeks of treatment, again a kidney biopsy was performed, allowing us to reevaluate the inhibitory effect in the target organ. Upon treatment we observed some reduction of C3 and considerable reduction of C5b-9 deposition in the glomeruli. During treatment the serum creatinine levels stabilized and the patient presented without significant albuminuria (< 100 mg/g creatinine), up to 20 weeks follow-up.

Conclusion: We believe that C3 G is not only too rare but also too heterogeneous for larger, controlled, randomized, prospective therapy studies. Thus, C3 G is a perfect example of a disease, in which unravelling the exact pathogenesis by combining morphological *in situ*, genetic, autoimmune, and functional *in vitro* data of single patients likely will be the clue to the best, personalized therapy.

Pädiatrische Nephrologie

P243

Erhöhte postnatale Zufuhr von Omega-3 Fettsäuren verhindert die Entwicklung einer proinflammatorischen und prokoagulatorischen Protein-

signatur in der Niere nach intrauteriner Wachstumsrestriktion

J. Voggel; G. Fink; M. Zelck; M. Wohlfarth; L. Bindila¹; M. Rauh²; K. Amann³; M. A. Alejandre Alcázar; J. Dötsch; K.-D. Nüsken; E. Nüsken
Klinik und Poliklinik für Kinder- und Jugendmedizin, Universitätsklinikum, Universität zu Köln, Köln; ¹ Institut für Physiologische Chemie, Universitätsmedizin Mainz, Mainz; ² Kinder- und Jugendklinik, Pädiatrische Nephrologie, Universitätsklinikum, Friedrich-Alexander-Universität Erlangen-Nürnberg, Erlangen; ³ Institut für Nephropathologie, Universitätsklinikum, Friedrich-Alexander-Universität Erlangen-Nürnberg, Erlangen

Hintergrund: Eine intrauterine Wachstumsretardierung (IUGR) erhöht das Risiko für chronische Nierenerkrankungen, unter anderem durch Aktivierung proinflammatorischer Signalwege. Mehrfach ungesättigte Omega-3 Fettsäuren (n-3 PUFAs) haben antiinflammatorische Eigenschaften. Wir untersuchten den Einfluss eines erhöhten n-3/n-6 PUFA Verhältnisses von 1:1 im Rattenmodell auf (1) die Zusammensetzung der Phospholipide (PLs) und den Gehalt von Arachidonsäure (AA)-Metaboliten in der Niere und (2) den Einfluss der Nahrungsintervention auf die Proteinsignatur von IUGR- und Kontrolltieren.

Methode: Eine IUGR wurde durch bilaterale Uterusgefäßligatur (LIG) oder intrauterinen Stress (IUS) durch Scheinoperation 3,5 Tage vor Geburt induziert. Als Kontrollen (C) dienten Tiere nach unauffälliger Schwangerschaft. Zwischen dem postnatalen Tag (P) 2 und P39 erhielten die Ratten entweder eine Kontrollnahrung (CONTR, n-3/n-6 PUFA Verhältnis 1:20) oder eine

Interventionsnahrung (N3PUFA, n-3/n-6 PUFA Verhältnis 1:1). Im frühen Erwachsenenalter wurden bei weiblichen Nachkommen Plasma-parameter (P33), Nierencortex-Lipidomics und -Proteomics, sowie Nierenhistologie (P39) untersucht.

Ergebnisse: Die Interventionsnahrung verdreifachte Docosahexaensäure (DHA)-haltige PLs (PC40:6; $p < 0.01$) und verminderte sowohl AA-haltige PLs (PC38:4 und LPC20:4; $p < 0.05$) als auch AA-Metaboliten (HETEs, DiHETEs, EETs) auf bis zu 25 % in allen Gruppen. String-Netzwerkanalysen der durch LIG in ihrer Expression veränderten Proteine ($n = 170$, $p < 0.05$, $fc > 1.5$) des Nierencortex identifizierten eine Entzündungs- und Koagulationsneigung bei LIG im Vergleich zu C. Die Interventionsnahrung hatte auf einen 61 dieser Proteine einen gegenläufigen, also normalisierenden Effekt. Morphologische Veränderungen zwischen den Gruppen waren nicht nachweisbar.

Zusammenfassung: Ein erhöhter Anteil von n-3 PUFAs in der frühen Ernährung reduziert proinflammatorische PLs und Mediatoren in der Niere, während antiinflammatorische PLs erhöht wurden. Des Weiteren wird die Entwicklung einer proinflammatorischen und prokoagulatorischen Proteinsignatur in der Niere verhindert. Unsere Studie unterstreicht das Potential von Ernährungsinterventionen während der Nierenentwicklung zur Prävention von Nierenerkrankungen.

P244

Urämietoxine and extrazelluläre Vesikel als Mediatoren kardiovaskulärer Morbidität in chronischer Nierenerkrankung

F. Behrens; J. B. Holle¹; C.-Y. Chen²; B. C. Krause³; U. Brüning²;

M.-F. Mashreghi⁴; D. Müller¹;
N. Wilck⁵; W. Kübler; S. Simmons
Institut für Physiologie, Campus
Charité Mitte, Charité – Universitäts-
medizin Berlin, Berlin; ¹Klinik für
Pädiatrie mit Schwerpunkt Nephro-
logie, Campus Virchow-Klinikum,
Charité – Universitätsmedizin Berlin,
Berlin; ²Max-Delbrück-Centrum für
molekulare Medizin (MDC), Berlin;
³Abteilung für Chemikalien- und
Produktsicherheit, Bundesinstitut
für Risikobewertung (BfR), Berlin;
⁴Deutsches Rheuma-Forschungszentrum,
Berlin; ⁵Medizinische Klinik mit Schwer-
punkt Nephrologie und Internistische
Intensivmedizin, Campus Virchow-
Klinikum, Charité – Universitätsmedizin
Berlin, Berlin

Hintergrund: Kardiovaskuläre Ereignisse (CVD) sind die Hauptursache der erhöhten Morbidität und Mortalität bei chronischer Nierenerkrankung (CKD). Die zugrunde liegenden Mechanismen sind jedoch bisher nur unvollständig geklärt. In dieser Studie untersuchen wir, ob mikrobiell produzierte Urämietoxine (UT) die Freisetzung extrazellulärer Vesikel (EVs) endothelialen und Immunzell-Ursprungs bedingen, die endothelialen Schaden und in der Folge CVD verursachen.

Methode: Es wurde eine Kohorte von 94 Kindern (mittleres Alter 10,9 Jahre) in unterschiedlichen CKD-Stadien rekrutiert, inklusive Patient*innen an Dialyse und nach Nierentransplantation, sowie eine alters-gematchte Kontrollgruppe. Das Fehlen altersassoziierter Komorbiditäten wie Diabetes und metabolischem Syndrom in pädiatrischer CKD ermöglicht die spezifische Analyse kardiovaskulärer Effekte von

CKD. Plasma-Metabolomics für Tryptophan-UTs wurden durchgeführt und Plasma-EVs wurden mittels Nanoparticle Tracking Analysis, Durchflusszytometrie und small RNA sequencing analysiert. EV-Freisetzung aus Leukozyten (PBMCs) nach UT-Exposition wurde gemessen.

Ergebnisse: Konzentrationen von UTs aus den Indol- und Kynurenin-Stoffwechselwegen sind im Blut von CKD-Patient*innen stadienabhängig erhöht, insbesondere Indoxylsulfat (IS) mit einem 21-fachen Anstieg in Peritonealdialyse (PD) im Vergleich zu gesunden Spendern. Ähnliche Effekte können bei Hämodialyse beobachtet werden, während die Unterschiede in CKD ohne Dialyse geringer sind und UT-Konzentrationen in Transplantierten annähernd normal. PD-Patient*innen zeigten erhöhte EV-Gesamtkonzentrationen im Vergleich zu Gesunden und Transplantierten. Makrophagen- (3-fach) und T-Zell-EVs (6-fach) waren in CKD ohne Dialyse erhöht im Vergleich zu Gesunden, während endotheliale EVs nach Transplantation sowohl longitudinal als auch im Querschnitts-Vergleich von HD und Transplantierten vermindert waren (3-fach). Mittels sequencing konnten mehrere in Patient*innen-EVs differentiell regulierte microRNAs identifiziert werden, u. a. miR-16-5p, miR-19b-3p, miR-106a-5p, miR-451a und miR-4485. In vitro induzierte IS einen dosisabhängigen Anstieg der EV-Freisetzung aus PBMCs. **Zusammenfassung:** Erhöhte Konzentrationen mikrobieller Urämietoxine und die folgende Freisetzung von EVs endothelialen und Immunzell-Ursprungs könnten sowohl als Biomarker dienen als

auch pathophysiologisch an der Entstehung von CVD als CKD-Komplikation beteiligt sein.

P245

Fingerpiks – Monitoring der Nierenfunktion und der immunsuppressiven Behandlung bei nierenkranken Kindern mittels Trockenblutkarte

L. Brunkhorst; M. Gutting;
N. Kanzelmeyer

Klinik für pädiatrische Nieren-, Leber- und Stoffwechselerkrankungen, Zentrum Kinderheilkunde und Jugendmedizin, Medizinische Hochschule Hannover, Hannover

Hintergrund: Ein engmaschiges Monitoring der Nierenfunktion sowie der immunsuppressiven Therapie ist bei Kindern und Jugendlichen nach Nierentransplantation oder im Rahmen einer schweren Glomerulopathie essentiell. Die Patienten müssen sich daher regelmäßig im entsprechenden kindernephrologischen Zentrum vorstellen, was für einen Großteil der Patienten weite Anfahrtswege bedeutet. Durch die Möglichkeit die relevanten Laborparameter heimatnah zu bestimmen, könnten die Vorstellungen in unserer Ambulanz reduziert werden. Ziel dieser Arbeit ist die Validierung von Trockenblutkarten, welche die Immunsuppressiva Spiegel und den Kreatininwert aus Kapillarblut bestimmen.

Methode: Es erfolgte eine Pilotstudie an der Kinderklinik der MHH. Prospektiv wurden Patienten < 18 J., die aufgrund einer Nierentransplantation oder einer Glomerulopathie eine immunsuppressive Therapie mit Ciclosporin A, Tacrolimus, Everolimus oder Mycophenolat Mofetil einnehmen,

eingeschlossen. Die Bestimmung der Immunsuppressiva und des Kreatinins erfolgte aus venösem Blut. Zusätzlich wurde venöses Blut auf die Trockenblutkarte getropft und an unser Partnerlabor verschickt. Statistisch erfolgte eine Berechnung der Mittelwertsdifferenz nach Bland-Altman. Im Anschluss an die Pilotstudie ist eine prospektive Studie geplant, bei der Kapillarblut auf die Trockenblutkarten getropft wird (Bestimmung von Kreatinin und Immunsuppressiva) und mit der zeitgleich abgenommenen venösen Laborprobe verglichen.

Ergebnisse: Insgesamt wurden 79 pädiatrische Patienten (weiblich 42 %) eingeschlossen. Das mediane Alter lag bei 15 Jahren (Min. 4 Jahre; Max. 17 Jahre). 65 Patienten waren nierentransplantiert und bei 14 Patienten besteht eine Glomerulopathie. Die Berechnung der Mittelwertsdifferenz der beiden angewandten Messmethoden (Trockenblutkarte vs. EDTA/Serum Blut) ergab folgende Ergebnisse: Kreatinin $7 \mu\text{mol/l}$; Everolimuspiegel $0,71 \text{ in } \mu\text{g/L}$; Tacrolimus $0,75 \mu\text{g/L}$ und CSA $7 \mu\text{g/L}$.

Zusammenfassung: Die Pilotstudie zeigte eine gute Übereinstimmung zwischen den Bestimmungen der Serum-Kreatinin und Immunsuppressiva-Spiegel aus venösem Blut und den Trockenblutkarten. Eine erfolgreiche Etablierung dieser Methode bei der Kapillarblut verwendet wird, würde es Patienten ermöglichen die Blutentnahme im häuslichen Umfeld durchzuführen und per Post ins Labor zu schicken. Die ambulante Vorstellung könnte durch eine Televisite ersetzt werden. Eine erfolgreiche

Etablierung der Methode könnte die Anzahl an Vorstellungen in unserer Ambulanz reduzieren.

Transplantation 1

P246

Kidney transplant patients generate varicella zoster-reactive T cell and humoral immunity following protein-based varicella zoster vaccination

T. Roch; P. Webler; A. Blazquez-Navarro¹; F. Bachmann²; I. E. Neumann¹; S. Kaliszczyk¹; C. Thieme¹; M. Anft; U. Stervbo; T. H. Westhoff; N. Babel; M. Choi²
 Centrum für Translationale Medizin, Medizinische Klinik I, Marien Hospital Herne, Ruhr-Universität Bochum, Herne; ¹Berlin-Brandenburger Center für Regenerative Therapien, Charité – Universitätsmedizin Berlin, Berlin; ²Medizinische Klinik mit Schwerpunkt Nephrologie und Internistische Intensivmedizin, Campus Virchow-Klinikum, Charité – Universitätsmedizin Berlin, Berlin

Objective: Reactivation of latent varicella zoster virus (VZV) might lead to serious complications in immunocompromised patients including pneumonia, cerebellar ataxia, encephalitis and hepatitis with a fatality rate of 5–10 %. VZV vaccination is recommended for healthy individuals above the age of 60, in chronically ill patients above the age of 50 years. However, only few reports exist, whether VZV vaccinations can induce humoral and cellular immunity in immunosuppressed transplant patients. Here, we characterized the humoral and cellular immunity following two VZV vaccinations in kidney transplant patients (KTX).

Method: In a cross-sectional study, we analyzed VZV-specific IgG and T cells in 39 immunosuppressed KTX vaccinated with two doses of a recombinant protein-based vaccine (Shingrix®), containing the VZV envelope glycoprotein E as immunogenic domain. To elaborate T cell assays for clinical utility, VZV-reactive T cells were compared in whole blood and in isolated peripheral blood mononuclear cells (PBMC) after VZV vaccine stimulation.

Results: The vaccination was well tolerated and did not influence kidney allograft function, since eGFR remained stable in all individuals in the follow. In patients with pre-vaccination titers available, we observed an average 1.8 fold titer increase, indicating humoral responsiveness. Both protocols used for the detection of VZV glycoprotein E-reactive T cells allowed the characterization of CD4+ and CD8+ T cell responses. In PBMC and whole blood 67 % and 59 % of vaccinated KTX showed a positive VZV-reactive T cell response, respectively. CD8+ VZV-reactive T cells were observed in 47 % and 60 % of PBMC and whole blood assay, respectively. Polyfunctional VZV-reactive CD4+ T cells – as characterized by simultaneous expression of TNF- α , IFN- γ , and IL-2 – were detected in PBMC and whole blood in at least 40 % of the KTX. The amounts of VZV-reactive CD4+ and CD8+ T cells did not correlate with VZV IgG titers.

Conclusion: Despite under chronic immunosuppression, the majority of KTX developed humoral and T cells responses after VZV vaccination, which could be evaluated using whole blood and PBMC-based protocols.

P247**Viroimmunologisches Monitoring als Prädiktor für Komplikationen im ersten Jahr nach Nierentransplantation: eine erste Ad-hoc-Auswertung der VIRENO-Studie**

P. Affeldt; K. Burkert; G. Dieplinger¹; C. Holzmann-Littig²; J. Anders³; K. Tuschen; M. Kann⁴; F. Grundmann; R. R. Datta⁵; R. Kaiser⁶; O. Adams⁷; U. Bauerfeind⁸; V. Ditt⁸; B. Wilde⁹; C. Kurschat; A. Weidemann¹⁰; L. Renders²; D. Stippel¹; F. Klein⁶; V. di Cristanziano⁶; R.-U. Müller

Nephrologie, Rheumatologie, Diabetologie und Allgemeine Innere Medizin, Klinik II für Innere Medizin, Universitätsklinikum Köln, Köln;

¹ Klinik für Allgemein-, Viszeral- und Tumorchirurgie, Universitätsklinikum, Universität zu Köln, Köln;

² II. Medizinische Klinik, Nephrologie, Klinikum rechts der Isar, Technische Universität München, München;

³ Medizinische Klinik I, Krankenhaus Köln-Merheim, Kliniken der Stadt

Köln gGmbH, Köln; ⁴ Nephrologisches Forschungslabor, Universitätsklinikum, Klinik II für Innere Medizin, Universität zu Köln, Köln; ⁵ Klinik für Viszeralchirurgie, Uniklinik Köln, Universität zu Köln, Medizinische Fakultät, Köln; ⁶ Institut für Virologie, Universitätsklinikum Köln, Köln; ⁷ Institut für Virologie, Universitätsklinikum, Heinrich-Heine-Universität Düsseldorf, Düsseldorf; ⁸ Institut für Transfusionsmedizin, Krankenhaus Köln Merheim, Kliniken der Stadt Köln, Köln; ⁹ Klinik für Nephrologie, Universitätsklinikum, Universität Duisburg-Essen, Essen; ¹⁰ Nephrologie und Dialyse, Medizinische Klinik III, St. Vinzenz Krankenhaus, Paderborn

Hintergrund: Die multizentrische, nicht-interventionelle VIRENO-Studie hat zum Ziel, viroimmunologische Parameter als Risikoprädiktoren für infektiöse und immunologische Komplikationen nach Nierentransplantation (NTX) zu identifizieren.

Methode: Das viroimmunologische Monitoring der Kohorte wurde vor NTX, 3 Wochen und 6 Monate nach NTX durchgeführt. Bei Organempfänger*innen und -spender*innen wurde die humorale Immunität gegen das BK-Polyomavirus (BKPyV) durch Messung der IgG-Antikörper untersucht. Die zelluläre CMV-Immunität wurde mittels T-SPOT®.CMV (Oxford Immunotec) und QuantiFERON-CMV (Qiagen) quantifiziert. Zusätzlich wurde bei allen Teilnehmenden die Torque Teno Virus (TTV)-Viruslast gemessen. Klinische Parameter wurden 3 Wochen, 6 und 12 Monate nach NTX erfasst, wobei der Fokus auf relevanten Infektionen und Abstoßungsreaktionen lag. **Ergebnisse:** Insgesamt wurden 196 Nierentransplantierte ein Jahr nach NTX nachverfolgt und in die Auswertung einbezogen. Hinsichtlich der primären Endpunkte traten 113 infektiöse Komplikationen (davon 52 CMV-assoziiert,

	Genauigkeit	Sensitivität	Spezifität	Einbezogene Variablen		
				Klinische Parameter	Viroimmunologisches Monitoring vor NTX	Viroimmunologisches Monitoring 3 Wochen nach NTX
Infektiöse Ereignisse	73 %	87,1 %	50,8 %	Alter bei NTX* Geschlecht Spender* Präemptive NTX* Nicht-immunologische Grunderkrankung* Verstorbenenspende	TTV-Viruslast (Plasma) TTV-Viruslast pro 1 Mio Zellen* BKPyV IgG	TTV-Viruslast (Plasma und Vollblut) TTV-Viruslast (Urin) BKPyV IgG
Immunologische Ereignisse	93,1 %	91,7 %	93,5 %	Genetische Nierenerkrankung	ELISPOT IE1* BKPyV IgG (Spender)	ELISPOT Positivkontrolle CMV Quantiferon PBMC* ELISPOT IE1*

P247: Tab. 1

Logistisches Regressionsmodell für infektiöse und immunologische Ereignisse; soweit nicht anderweitig gekennzeichnet, beziehen sich alle Werte auf Organempfänger; *p > 0,1

17 EBV-assoziiert, 40 BKPyV-assoziiert und 59 zur Hospitalisierung führende Infektionen) und 34 immunologische Komplikationen (davon 30 Abstoßungen und 8 de-novo donorspezifische Antikörper) auf. In einer ersten Ad-hoc Analyse konnte unter Verwendung eines binären logistischen Regressionsmodells eine Kombination klinischer und viroimmunologischer Parameter identifiziert werden, die immunologische Komplikationen mit einer hohen Sensitivität (91,7 %) und Spezifität (93,5 %) vorhersagt (s. Tab. 1). Hinsichtlich infektiöser Komplikationen konnten ebenfalls Parameter identifiziert werden, deren kombinierte Betrachtung diese mit einer hohen Sensitivität (87,1 %), jedoch niedrigen Spezifität (50,8 %) vorhersagt.

Zusammenfassung: Die Ergebnisse unserer ersten Ad-hoc Analyse deuten darauf hin, dass viroimmunologisches Monitoring die Abschätzung des Infektions- und Abstoßungsrisikos nach NTX und damit die Steuerung der Immunsuppression verbessern kann. Nächste Schritte sind eine Validierung an anderen Kohorten sowie eine prospektive Studie mit angepasster Steuerung der Immunsuppression.

P248

Age at transplantation, immunosuppression and underlying kidney disease influence the risk of de novo malignancies after kidney transplantation

A. Baum; T. H. Lindner; A. Bachmann; A. Weimann¹; B. Popp²; J. Münch³; J. Halbritter³

Sektion Nephrologie, Klinik für Endokrinologie und Nephrologie, Universitätsklinikum Leipzig, Leipzig; ¹Klinik für Viszeral-, Transplantations-, Thorax- und

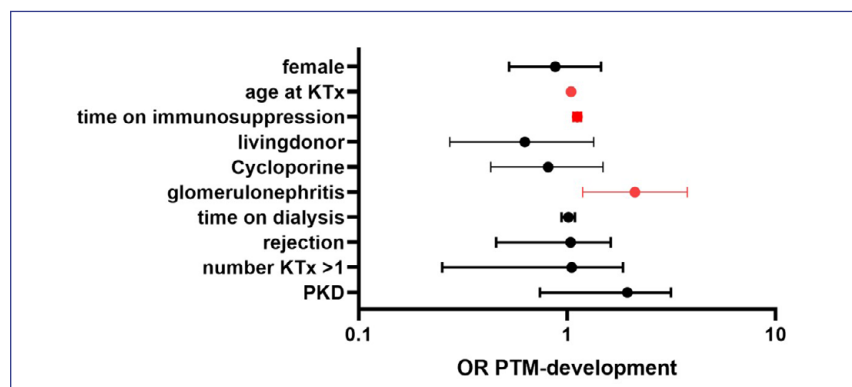
Gefäßchirurgie, Universitätsklinikum, Universitätsklinikum Leipzig, Leipzig; ²Institut für Humangenetik, Universitätsklinikum Leipzig, Leipzig; ³Medizinische Klinik mit Schwerpunkt Nephrologie und Internistische Intensivmedizin, Campus Charité Mitte, Charité – Universitätsmedizin Berlin, Berlin

Objective: Kidney transplant (KTx) recipients are at increased risk for developing cancer, reducing both graft and patient survival. To date, systematic evaluation of post-transplant malignancies (PTM) and its determinants is missing in Germany. Therefore, this study aimed to exemplarily assess PTM frequency, single cancer entities, and associated risk factors at our transplant center.

Method: We retrospectively collected clinical data from electronic health records and prospectively obtained updates on all patients undergoing KTx since 1993. This data was assessed for PTM

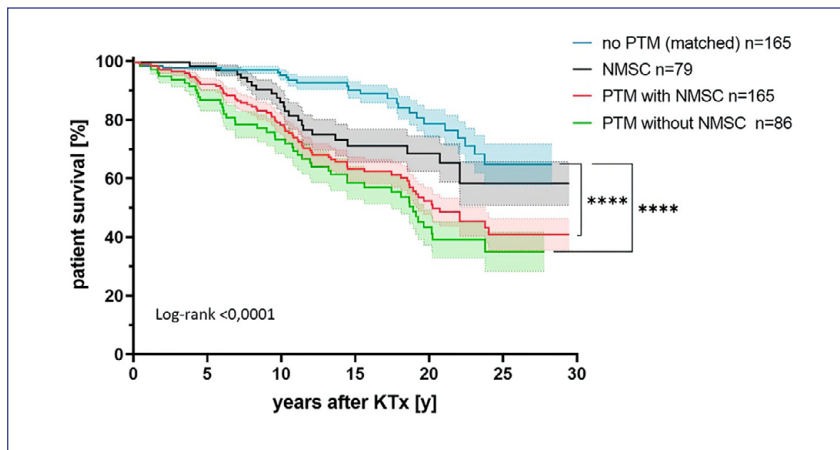
occurrence and associated risk factors in a case-control design.

Results: Between 1993 and 2019, a total of 1,035 KTx were performed in 901 patients, of which 788 patients (female 39.9 %) matched the inclusion criteria. 206 PTM were diagnosed in 165 patients (20.9 %) of our cohort. Almost one-fourth (23.6 %) of patients with PTM had more than one tumor manifestation. Mean age at cancer diagnosis was 60.9 years. Median time from KTx to PTM was 8.6 years and the average time between the diagnosis of PTM and patients' death was 4.1 years. The most common PTM was non-melanoma skin cancer (NMSC – 51.4 %), followed by renal cell carcinoma (RCC) with a frequency of 11.2 %. We identified age at KTx (odds ratio (OR) 1.05; $p < 0.0001$), time on immunosuppression (OR 1.12; $p < 0.0001$) and underlying glomerulonephritis (OR 2.12; $p = 0.0108$) as risk factors for PTM-development. While the latter was mainly associated



P248: Abb. 1

Forrest Plot of risk factors for PTM-development: age at KTx (OR 1.046; CI 1.023 to 1.071), time on immunosuppression (OR 1.118; CI 1.074 to 1.167) and glomerulonephritis (IgA-nephropathy, chronic glomerulo-nephritis, membranous nephropathy, pANCA glomerulonephritis) as underlying kidney disease (OR 2.116; CI 1.190 to 3.781) are significant risk factors (red)



P248: Abb. 2

Cumulative patient survival rates of PTM without NMSC (green; $n = 86$), PTM with NMSC (red; $n = 165$), only NMSC (black; $n = 79$) and no PTM (matched) cohort (blue; $n = 165$) analysed by Log-rank test. We matched age at KTx and time of follow-up. Patients who died in the first 4 months after KTx (e.g. due to (sub-) acute rejection) were excluded to keep a bias low by a too short follow-up period.

with RCC (OR 7.36; $p = 0.0014$), age at KTx was the greatest risk factor for the NMSC-development (OR 1.08; $p < 0.0001$). We found significantly poorer patient survival in the PTM group with and without NMSC compared to a matched cohort (Log-rank < 0.0001).

Conclusion: The development of PTM constitutes a devastating condition in the course of KTx and is associated with poor survival rates, notably beyond NMSC. In accordance with data from other European transplant centers (Pendón-Ruiz et al., *Transplant Proc* 2015; Wimmer et al., *Kidney Int* 2007). NMSC represents the most common entity. Older patients and patients with long-time immunosuppression are at greater risk of developing PTM. The interesting association between glomerulonephritis and RCC was observed previously (Al-adra et al., *CJASN* 2022) and requires assessment in further studies. Our findings may

contribute to improved PTM surveillance in KTx recipients.

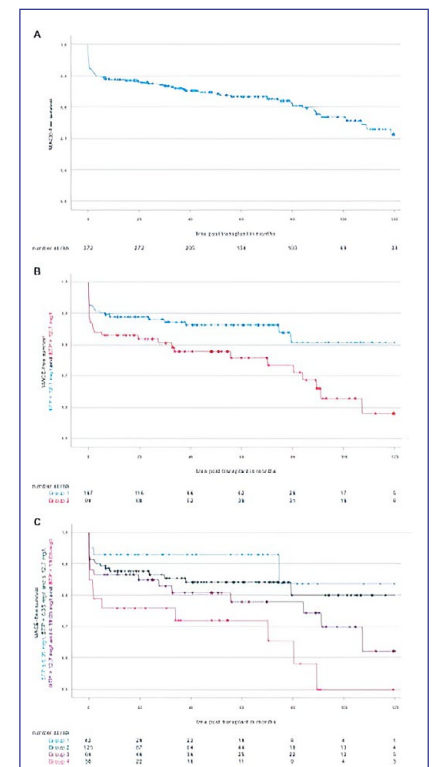
P249 Pre-Transplant Serum Beta Trace Protein indicates risk for post-transplant MACE

S. Schwab; D. Pörner; C. E. Kleine; R. Werberich; L. Werberich; S. Reinhard; D. Bös¹; C. P. Strassburg; S. von Vietinghoff; P. Lutz; R. Woitas²
Sektion für Nephrologie, Medizinische Klinik und Poliklinik I, Universitätsmedizin Bonn, Bonn; ¹ KfH-Nierenzentrum am Universitätsklinikum Bonn, KfH Kuratorium für Dialyse und Nierentransplantation e. V., Bonn; ² Diaverum Deutschland GmbH, München

Objective: Beta Trace Protein (BTP) is a biomarker for residual kidney function which has been linked to cardiovascular and all-cause mortality in hemodialysis patients. Following renal transplantation, recipients remain at

increased risk for cardiovascular events compared to the general population. We aimed to determine the relationship of pre-transplant BTP to major adverse cardiac events (MACE) in patients following kidney transplantation.

Method: We included 384 patients with end-stage renal disease who received a kidney transplant. MACE was defined as myocardial infarction (ST-segment elevation [STEMI] or non ST-segment elevation [NSTEMI]), stroke or transient ischemic attack), coronary artery disease requiring intervention or bypass or death for cardiovascular reason. The association between pre-transplant serum BTP concentration and post-transplant major cardiovascular events (MACE)



P249: Abb. 1

was evaluated by Kaplan-Meier and Cox regression analyses.

Results: Post-transplant MACE occurred in 70/384 patients. Pre-transplant BTP was significantly higher in patients with post-transplant MACE (14.36 ± 5.73 mg/L vs. 11.26 ± 5.11 mg/L; $p < 0.01$). Next to smoking (HR 1.98) and pre-existing coronary heart disease (HR 8.76), BTP above the cut off value of 12.7 mg/L was confirmed as independent risk factor for MACE (HR 2.16, all $p < 0.05$). MACE-free survival inversely correlated with pre-transplant BTP levels.

Conclusion: Pre-transplant serum BTP concentration may identify renal transplant recipients with higher risk of post-transplant MACE.

P250

Der Kidney Donor Profile Index (KDPI) korreliert mit Ergebnissen der Histopathologie in post-Reperfusion Protokollbiopsien und prognostiziert das Transplantatüberleben

Q. Bachmann; F. Haberkellner; M. Büttner-Herold¹; C. Torrez; B. Haller; V. Aßfalg²; R. I. Hausinger; L. Renders; K. Amann¹; U. Heemann; C. Schmaderer; S. Kemmner
II. Medizinische Klinik, Nephrologie, Klinikum rechts der Isar, Technische Universität München, München; ¹ Institut für Nephropathologie, Universitätsklinikum, Friedrich-Alexander-Universität Erlangen-Nürnberg, Erlangen; ² Klinik und Poliklinik für Chirurgie, Klinikum rechts der Isar, Technische Universität München, München

Hintergrund: Die zunehmende Organknappheit bei Nierentransplantationen macht die Verwendung vormals als ungeeignet

eingestufte Organe notwendig. Dabei haben zahlreiche Studien illustriert, dass die häufig genutzte Klassifizierung nach den Kriterien „standard“ und „expanded“ Spender (SCD/SCD-Klassifikation) keine ausreichende Aussage über die Qualität des Transplantates ermöglicht. Der „Kidney Donor Profile Index“ (KDPI) nutzt eine deutlich höhere Anzahl an Spenderereigenschaften. Zudem ermöglichen Transplantatbiopsien eine Einschätzung des Transplantates.

Methode: Von 363 im Klinikum rechts der Isar zwischen Januar 2006 und Dezember 2016 durchgeführten Nierentransplantationen wurde retrospektiv der KDPI erhoben. Bei Postmortalspenden wurde der KDPI, bei Lebendspenden der „living“ KDPI (LKDPI) erhoben. Gemeinsam ist dies in der weiteren Analyse als (L)KDPI beschrieben. Die 10 Minuten nach Beginn der Reperfusion entnommenen Nullbiopsien wurden auf akute und chronische Veränderungen untersucht. Überlebensanalysen bis zu 5 Jahren Verlauf wurden mit Kaplan-Meier und Cox-Regression durchgeführt.

Ergebnisse: Der (L)KDPI korrelierte mit Glomerulosklerose ($r = 0,30$, $p < 0,001$), Arteriosklerose ($r = 0,33$, $p < 0,001$), interstitieller Fibrose und tubulärer Atrophie ($r = 0,28$, $p < 0,001$) sowie akutem Tubuluschaden ($r = 0,20$, $p < 0,001$). Die C-Statistik des (L)KDPI für das todeszensierte 5-Jahres-Überleben war 0,692. 48 % der ECD-Nieren wurden mit einem (L)KDPI < 85 % klassifiziert. In einem multivariaten Cox-Regressionsmodell mit präformierten Panel-reaktiven Antikörpern, kalter Ischämiezeit, (L)KDPI und der SCD/ECD-Klassifikation war der (L)KDPI signifikant

assoziiert mit dem Risiko der Organverlustes (HR pro 10 % (L)KDPI: 1,185, 95 % KI: 1,033–1,360, $p = 0,025$). Für (L)KDPI-Gruppen < 35 %, 35–85 % und > 85 % zeigten sich abnehmendes todeszensiertes ($p < 0,001$) und nicht-todeszensiertes ($p < 0,001$) Transplantatüberleben mit steigendem (L)KDPI.

Zusammenfassung: Durch seine höhere Auflösung und die Fähigkeit einen Großteil von ECD-Nieren besser einzuordnen ist der KDPI ein vielversprechendes Werkzeug. Zum ersten Mal konnte eine Assoziation von Nullbiopsien und dem (L)KDPI gezeigt werden. Die dennoch stark limitierte prognostische Vorhersagefähigkeit unterstreicht die Notwendigkeit eines noch präziseren Instrumentes.

P251

Dickkopf 3 – ein neuer Indikator für die Verschlechterung der Transplantatfunktion nach Nierentransplantation

A. Schuster; L. Steines; K. Müller¹; F. Zeman¹; B. Banas; T. Bergler
Abteilung für Nephrologie, Transplantationszentrum, Universitätsklinikum, Universität Regensburg, Regensburg; ¹ Zentrum für Klinische Studien, Universitätsklinikum, Universität Regensburg, Regensburg

Hintergrund: Der Nachweis einer tubulären Atrophie und interstitiellen Fibrose (IF/TA) nach NTx ist prognostisch ungünstig und oft mit einem vorzeitigem Transplantatverlust assoziiert. Zurückliegend wurde in tierexperimentellen und klinischen Studien gezeigt, dass Dickkopf 3 (DKK3), ein profibrotisches Glykoprotein, das von gestressten tubulären Epithelzellen freigesetzt wird, eine tubulointerstitielle

Fibrose verursacht, indem es das Wnt/ β -Catenin-Signal reguliert. Ziel unserer Studie war es zu untersuchen, ob eine Korrelation zwischen den DKK3-Werten und der nachfolgenden Transplantatfunktion – jenseits bekannter Einflussfaktoren – besteht und ob DKK3 als nicht-invasiver Marker herangezogen werden kann, um Patienten mit einem hohen Risiko für eine nachfolgende Verschlechterung der Transplantatfunktion zu identifizieren.

Methode: Alle Patienten, die zwischen 2016 und 2018 in unserem Zentrum transplantiert wurden, wurden eingeschlossen (n = 122). Wir analysierten die Transplantatfunktion, die durch Kreatinin, eGFR und Albuminurie repräsentiert wird, und bestimmten parallel die DKK3-Werte im Urin über einen Beobachtungszeitraum von 3 Jahren.

Ergebnisse: In einer multivariaten Analyse, in die andere bekannte, die Transplantatfunktion beeinflussende Variablen (Donor-Alter, -Hypertonie, etc.) mit einbezogen wurden, konnte sowohl der 3 als auch der 12-Monats-DKK3-Wert die nachfolgende Nierenfunktion – dargestellt durch Kreatinin, eGFR und Albuminurie – bis zum Zeitpunkt 36 Monate statistisch signifikant vorhersagen. Ein Anstieg von DKK3 von Monat 3 auf 12 von $\geq 25\%$ bedeutete ein höheres Risiko einer beeinträchtigten Transplantatfunktion (Reduktion der eGFR um etwa 7–10 ml/min, 5–7-fach höhere Albuminurie) im Gegensatz zu Patienten ohne verstärkten DKK3-Anstieg. Die Induktionstherapie (Basiliximab vs. T-Zell-Depletion) ließ einen Einfluss auf DKK3 erkennen, da Patienten, die mit einer T-Zell-depletierenden Therapie induziert wurden, einen Trend

zu niedrigeren DKK3-Werten (3 und 12 Monate postNTx) hatten.

Zusammenfassung: Unsere Studie zeigt erstmalig, dass DKK3 im Urin signifikant mit der nachfolgenden Transplantatfunktion korreliert und somit als neuer Prädiktor für eine Veränderung der Transplantatfunktion weiterentwickelt werden kann.

P252

Genomic two-field HLA typing identifies significantly more mismatches and is less prone to error in living kidney transplantation

S. Pehnke; C. Lehmann¹; A. Weimann²; A. Bachmann; F. Petzold; D. Fürst¹; J. de Fallois; R. Landgraf¹; R. Henschler¹; T.H. Lindner; J. Halbritter³; I. Doxiadis¹; B. Popp⁴; J. Münch³

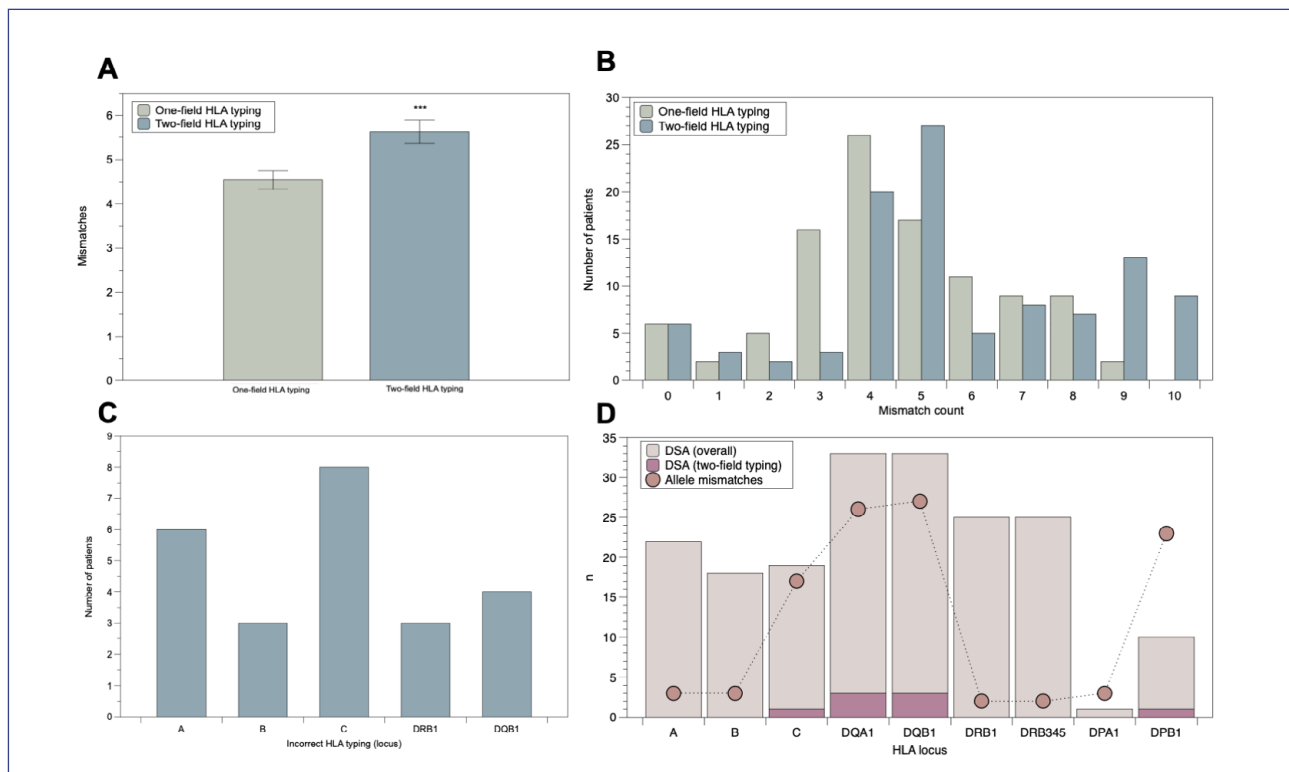
Sektion Nephrologie, Klinik für Endokrinologie und Nephrologie, Universitätsklinikum Leipzig, Leipzig; ¹Institut für Transfusionsmedizin, Universitätsklinikum Leipzig, Leipzig; ²Klinik für Viszeral-, Transplantations-, Thorax- und Gefäßchirurgie, Universitätsklinikum, Universitätsklinikum Leipzig, Leipzig; ³Medizinische Klinik mit Schwerpunkt Nephrologie und Internistische Intensivmedizin, Campus Charité Mitte, Charité – Universitätsmedizin Berlin, Berlin; ⁴Institut für Humangenetik, Universitätsklinikum Leipzig, Leipzig

Objective: Antibody mediated rejection (ABMR) is the most common cause of long-term allograft loss in kidney transplantation (KT). Therefore, a low human leukocyte antigen (HLA) mismatch count is favorable for KT outcomes. Hitherto, serological or low-resolution molecular HLA typing have been adapted in parallel. Here, we aimed

to identify previously missed HLA mismatches and corresponding antibodies by high resolution HLA genotyping including the not yet commonly used DQA1, DPA1, and DPB1 in a living-donor KT cohort.

Method: We typed 103 donor/recipient pairs at University of Leipzig Medical Center between 1998 and 2018 by next generation sequencing (NGS) of the HLA loci -A, -B, -C, -DRB1, -DRB345, -DQA1, -DQB1, -DPA1, and -DPB1. Using these data, we compiled a genomic HLA mismatch formula and comparatively evaluated genomic HLA-typing with previous serological/low-resolution HLA mismatches recorded in the Eurotransplant Network Information System (ENIS). In case of discrepancy, confirmatory typing was performed. Obtained high-resolution HLA typing data was used for reclassification of de novo HLA antibodies as “donor-specific”.

Results: By molecular HLA re-typing, we were able to identify additional mismatches in 64.1 % (n = 66) of cases. The mean calculated mismatch count for serological and genetic HLA typing was 4.54 and 5.63, respectively (t-test p < 0.001) (Figure A). 8.7 % (n = 9) of donor/recipient pairs had a highest possible mismatch count, that was missed by serological and low-resolution HLA typing methods (Figure B). We further observed, that in 10.2 % of individuals (n = 21), the HLA typing results in ENIS were incorrect (Figure C). With respect to HLA specific antibodies, we observed additional incompatibilities in HLA-DRB345 (n = 33), -DQA1 (n = 25), -DPA1 (n = 1), -DPB1 (n = 10). Among these DSA, 4.3 % (n = 8) could only be detected via two-field typing (Figure D).



P252: Abb. 1

Conclusion: Our results indicate that genomic HLA-typing using NGS is feasible and provides significantly more sensitive HLA mismatch recognition in living-donor kidney transplantation. A higher accuracy in pre-transplant HLA-typing might enhance adequate donor selection. Furthermore, accurate HLA typing can influence graft management during ABMR and HLA induced immunological rejection in general, as it may improve discrimination between donor and non-donor HLA directed cellular and humoral alloreactivity in the long-range allowing a better risk assessment. The inclusion of additional loci towards which antibodies are detected, HLA-DRB345, -DQA1, -DQB1, -DPA1, and -DPB1 will allow a better and precise virtual

crossmatch and prediction of possible DSA which might jeopardize the transplantation outcome.

P253 No association between pre-transplant BK virus-specific antibodies and post-transplant viral burden

A. Blázquez-Navarro; T. Roch; P. Wehler; C. Bauer¹; K. Wolk²; R. Sabat²; C. Dang-Heine; C. Thieme; U. Stervbo³; M. Anft³; S. Neumann⁴; S. Olek⁵; O. Thomusch⁶; H. Seitz⁷; P. Reinke; C. Hugo⁸; B. Sawitzki⁹; M. Or-Guil; N. Babel³

Berlin-Brandenburger Center für Regenerative Therapien, Charité – Universitätsmedizin Berlin, Berlin;

¹ MicroDiscovery GmbH, Berlin;

² Abteilung für Dermatologie, Charité – Universitätsmedizin Berlin, Berlin;

³ Centrum für Translationale Medizin, Medizinische Klinik I, Marien Hospital Herne, Ruhr-Universität Bochum, Herne; ⁴ numares AG, Regensburg;

⁵ Ivana Türbachova Laboratory for Epigenetics, Berlin; ⁶ Abteilung für Endokrine Chirurgie, Universitätsklinikum Freiburg, Freiburg im Breisgau; ⁷ Fraunhofer-Institut für Zelltherapie und Immunologie, Potsdam-Golm; ⁸ Medizinische Klinik III, Nephrologie, Universitätsklinikum Carl Gustav Carus, Technische Universität Dresden, Dresden; ⁹ Institut für Medizinische Immunologie, Campus Virchow-Klinikum, Charité – Universitätsmedizin Berlin, Berlin

Objective: BK virus (BKV) reactivation is a very common complication after renal transplantation, which can lead to graft loss

in 1–10 % of the cases. While occurrence of reactivation seems to be associated with certain immunosuppressive regimes, particularly the use of calcineurin inhibitors, risk factors have not been sufficiently defined yet. Particularly, it is still unclear whether pre-transplant serostatus is associated with protection from BKV reactivation.

Method: Therefore, we characterized a large, multi-centre cohort (N = 397) for the presence of IgG antibodies against the structural BKV protein VP1, using an ELISA assay. In parallel, BKV viral load in serum was monitored two weeks and one, two, three, six, nine and twelve months post renal transplantation. A total of 2092 samples were analysed for BKV viral load.

Results: 395 (99.5 %) patients had detectable pre-transplant anti-BKV antibodies, with a median [IQR] IgG concentration of 23 [13–38] µg/ml. BKV load over the detection limit (> 250 copies/mL) was observed in 196 (49.4 %) patients. Importantly, no association between anti-BKV IgG concentrations and the occurrence of detectable BKV was observed (no reactivation: 22 [14–38] µg/ml, reactivation: 25 [13–38] µg/ml; P = 0.886). Similarly, no significant difference was found when comparing patients without reactivation with those demonstrating a viral load > 10,000 copies/mL (24 [16–35] µg/ml; P = 0.764). Finally, we evaluated whether the peak viral load during the first post-transplant year correlates with the anti-BKV concentration; no correlation was found ($p = 0.00$, $P = 0.955$). Similarly, no correlation was observed between pre-transplant anti-BKV IgG concentration and

renal function one year post-transplant ($p = 0.00$, $P = 0.950$).

Conclusion: Our results support a lack of protection against BKV reactivation through pre-existing antibodies, as patients were similarly affected by BKV reactivation regardless of their pre-transplant serostatus. Further characterization efforts – including the donor – are needed to better understand the risk constellation of BKV reactivation.

P254

High incidence and viral load of HHV-6 A in a multi-centre kidney transplant cohort

A. Blázquez-Navarro; T. Roch; P. Wehler; S. Kaliszczyk; C. Bauer¹; C. Thieme; U. Stervbo²; M. Anft²; P. Reinke; C. Hugo³; P. Zgoura²; R. Viebahn⁴; F. S. Seibert²; T. H. Westhoff²; M. Or-Guil; N. Babel²
 Berlin-Brandenburger Center für Regenerative Therapien, Charité – Universitätsmedizin Berlin, Berlin;
¹ MicroDiscovery GmbH, Berlin;
² Centrum für Translationale Medizin, Medizinische Klinik I, Marien Hospital Herne, Ruhr-Universität Bochum, Herne; ³ Medizinische Klinik III, Nephrologie, Universitätsklinikum Carl Gustav Carus, Technische Universität Dresden, Dresden; ⁴ Chirurgische Klinik, Knappschafts-Krankenhaus Bochum, Ruhr-Universität Bochum, Bochum

Objective: Human herpesvirus 6 (HHV-6) is a common opportunistic pathogen in kidney transplant recipients. HHV-6 reinfections and reactivations of a latent infection are common in the early post-transplant period. Especially reactivations are associated with symptoms ranging from fever to life-threatening hepatitis and bone marrow suppression.

Two different variants of HHV-6, HHV-6 A and HHV-6 B, have been identified, of which the latter seems to be dominant. However, it is unclear whether they increase the likelihood of other viral reactivations.

Method: We characterized a multi-centre cohort of 93 patients along nine study visits for viral load in peripheral blood; the study visits were scheduled pre-transplant, one and two weeks post-transplant and one, two, three, six, nine and twelve months post-transplant. We tested for the following viruses: HHV-6 A and HHV-6 B, the herpesviruses cytomegalovirus (CMV) and Epstein-Barr virus (EBV) and the polyomavirus BK (BKV), with a detection limit of 250 copies/mL.

Results: We detected HHV-6 A viral load in 48 (51.6 %) patients; the incidence of HHV-6 B was much lower, being detected in 7 (7.5 %) patients. Median peak viral load among HHV-6 A positive patients was 13,600 [1484–2,378,4040] copies/mL; for HHV-6 B it was 1350 [419–31,280] copies/mL. As a comparison, incidence of CMV was 27.7 %, 7.7 % for EBV and 29.2 % for BKV. There was a strong association between HHV-6 A and HHV-6 B ($P = 0.066$, $OR = 6.2$), the lack of significance can be explained by the low incidence of HHV-6 B. Importantly, we did not find any evidence of increased incidence of other viruses among patients with HHV-6 A reactivation (CMV: $P = 0.386$, $OR = 1.4$; EBV: $P = 0.882$, $OR = 0.5$; BKV: $P = 0.297$, $OR = 1.6$). No negative effect of high HHV-6 A load (10000 copies/mL) on markers of graft renal and hepatic function or blood count six months post-transplant.

Conclusion: Our results show a clear dominance of HHV-6A in peripheral blood when compared to HHV-6B, with higher incidence and viral loads. Despite the high HHV-6A loads observed, we did not identify any negative effects on graft renal function, hepatic function or in the haematopoiesis.

P255

Herpes-Zoster-Impfung ist nach Nierentransplantation effektiv

C. Baumann; M. Lindemann¹; B. Wilde²; A. Gäckler²; A. Kribben²; L. Meller; P. A. Horn¹; A. Krawczyk; O. Witzke

Klinik für Infektiologie, Universitätsklinikum, Universität Duisburg-Essen, Essen; ¹ Institut für Transfusionsmedizin, Universitätsklinikum Essen, Universität Duisburg-Essen, Essen; ² Klinik für Nephrologie, Universitätsklinikum, Universität Duisburg-Essen, Essen

Hintergrund: Nierentransplantierte (NTX) Patienten haben ein deutlich höheres Risiko für die Reaktivierung des Varizella-Zoster-Virus. Aufgrund der lebenslangen immunsuppressiven Therapie kann die von der STIKO empfohlene Impfung gegen Herpes Zoster mit dem Totimpfstoff Shingrix® weniger wirkungsvoll sein. Ziel der Studie ist es zu untersuchen, ob NTX Patienten nach Shingrix® Impfung eine Varizellen-spezifische, zellulären Immunantwort aufbauen können.

Methode: Dazu wurden 17 Männer und 12 Frauen, mit einem Durchschnittsalter von 61 Jahren, im Durchschnitt 7,2 Jahre nach Nierentransplantation zweifach mit dem rekombinanten, adjuvanten Subunit-Impfstoff Shingrix® geimpft. Der Impfstoff enthält das

VZV-Glykoprotein E (gE) und das AS01_B Adjuvans. Die zelluläre Immunität gegen verschiedene VZV-Antigene wurde zu unterschiedlichen Zeitpunkten mittels Interferon-gamma ELISpot bestimmt.

Ergebnisse: Die größten impfbedingten Veränderungen der zellulären Immunität wurden nach Stimulation mit einem gE Peptid-Pool beobachtet. Nach der zweiten Impfung konnte eine auf das Zweifache angestiegene Immunantwort auf das gE-Peptid bei 22 von 29 Patienten (76 %) im ELISpot beobachtet werden. Die mittlere Immunantwort einen Monat nach der zweiten Impfung war 8,0-fach höher, verglichen mit den Reaktionen vor den Impfungen ($p = 0,0006$) und 4,8-fach höher verglichen mit den Reaktionen nach der ersten Impfung ($p = 0,0007$). Männliches Geschlecht, gute Nierenfunktion, ein früher Zeitpunkt nach der Transplantation sowie die Einnahme von Tacrolimus oder Mycophenolat-Mofetil korrelierten mit signifikant höheren ELISpot Reaktionen, wohingegen Patienten mit Diabetes Mellitus schwächere Reaktionen zeigten.

Zusammenfassung: Diese Einflussfaktoren, die durch univariante Analyse nachgewiesen wurden, konnten alle in einer multivariaten Analyse bestätigt werden. Die Daten zeigen, dass die Impfung die Varizellen-spezifische, zelluläre Immunität bei NTX Patienten steigert, und es konnten verschiedene Einflussfaktoren dieser zellulären Immunität definiert werden.

P256

GNB3 c.825C > T (rs5443) polymorphism is associated with increased risk for acute

cardiovascular events after transplantation in renal allograft recipients

T. Peitz; B. Möhlendick¹; W. Siffert¹; F. M. Heinemann²; A. Kribben; U. Eisenberger; J. Friebe-Kardash
Klinik für Nephrologie, Universitätsklinikum, Universität Duisburg-Essen, Essen; ¹ Institut für Pharmakogenetik, Universitätsklinikum Essen, Universität Duisburg-Essen, Essen; ² Institut für Transfusionsmedizin, Universitätsklinikum Essen, Universität Duisburg-Essen, Essen

Objective: The c.825C > T single-nucleotide polymorphism (rs5443) of the Guanine Nucleotide-Binding protein subunit $\beta 3$ (GNB3) results in generation of a splice variant of GNB3 implicating a gain of function and increased intracellular signal transduction via GNB3 in diverse human tissues. Multiple disease-association studies showed a link between homozygous TT genotype of β -adrenergic system and occurrence of essential hypertension, atherosclerosis, coronary diseases, and cerebrovascular events. The present study was aimed to investigate the effect of GNB3 c.825C > T polymorphism on cardiovascular events appearing in renal allograft recipients posttransplant.

Method: Our retrospective study included 436 renal allograft recipients in which GNB3 c.825C > T polymorphism as well as frequency of cardiovascular events, *de novo* formation of donor-specific antibodies (DSA), and clinical outcome up to 8 years after transplant were analyzed. GNB3 c.825C > T polymorphism was detected restriction fragment length polymorphism (RFLP)-PCR.

Results: The TT genotype of GNB3 was identified in 43 (10 %) of 436 recipients. Death due to acute

cardiovascular event occurred more frequently in recipients having TT genotype (4 (9 %) vs. 7 (2 %), $p = 0.003$). The frequency of myocardial infarction and acute peripheral artery occlusive disease (PAOD) posttransplant was significantly higher among TT genotype carriers than noncarriers (8 (19 %) vs. 27 (7 %), $p = 0.007$; 7 (16 %) vs. 21 (5 %), $p = 0.006$). Myocardial infarction-free survival ($p = 0.003$) and acute PAOD-free survival ($p = 0.004$) rates significantly decreased in T homozygous patients. However, there was no difference regarding chronic cardiovascular diseases such as coronary heart disease and chronic PAOD occurring pretransplant between TT genotype carriers and noncarriers. Otherwise, pretransplant diabetic nephropathy based on preexisting diabetes mellitus type II appeared more frequently in TT genotype than CT/CC genotypes. Adjusting for covariables in a multivariate analysis revealed only a mild effect of homozygous GNB3 C825 T polymorphism as a heritable risk factor for occurrence of myocardial infarction and acute PAOD after renal transplantation (relative risk 2,2 $p = 0.065$; relative risk 2,4 $p = 0.05$). **Conclusion:** Our results suggest that homozygous GNB3 c.825C > T allele has a slight impact on the risk for myocardial infarction and acute PAOD in renal allograft recipients after transplantation displaying noticeable effects only in presence of additional nonheritable risk factors.

P257

Belatacept in kidney transplant patients with severe BK-Polyomavirus (BKPyV) infection

U. Jehn; S. Siam; V. Wiening; P. Berning; H. Pavenstädt; S. Reuter

Allg. Innere Medizin und Notaufnahme sowie Nieren- und Hochdruckkrankheiten und Rheumatologie, Medizinische Klinik D, Westfälische Wilhelms-Universität Münster, Münster

Objective: In order to avoid allograft rejection on the one hand and infectious complications on the other, it is essential to balance the immune system in kidney transplant recipients by choosing the appropriate immunosuppressive treatment. BKPyV-associated nephropathy (BKPyVAN) is a viral complication of immunosuppression that seriously threatens kidney allograft survival. Until now, the main treatment strategy of BKPyVAN is to reduce immunosuppression, but this is associated with an increased risk of rejection. Belatacept is an immunosuppressant that blocks the CD80/86-CD28 co-stimulatory pathway of effector T-cells with marked effects on the humoral response but increased risk of acute T-cell mediated rejection. There are limited data to date on the use of belatacept in BKPyV infection.

Method: We evaluated the outcomes of nine kidney transplanted patients who were switched from a standard immunosuppressive regimen consisting of tacrolimus, mycophenolate mofetil or everolimus and prednisone to a belatacept-based regimen after the development of severe BKV-associated complications (five of them with biopsy proven BKPyVAN).

Results: After conversion, all patients showed significantly improved control of BKPyV DNAemia and stabilized or improved graft function, with no allo-immunologic complications, despite increased immunologic risk

in 4/9 patients (3x pre-existing donor-specific antibodies, 1x severe T-cell-mediated rejection).

Conclusion: The presented cases suggest that a switch to a belatacept-based immunosuppressive regimen is a safe treatment option in patients with severe BKPyV infection without exposing them to increased immunological risk.

P258

Multiple infectious events early after renal transplantation increase the risk for rejection – an analysis of the German transplant cohort (DZIF)

C. Sommerer; I. Schröter; K. Gruneberg; D. Schindler¹; C. Morath; P. Schnitzler²; L. Renders¹; U. Heemann¹; M. Zeier; T. Giese³

Medizinische Klinik I, Sektion Nephrologie, Medizinische Fakultät, Ruprecht-Karls-Universität Heidelberg, Heidelberg;

¹ II. Medizinische Klinik, Nephrologie, Klinikum rechts der Isar, Technische Universität München, München;

² Molekulare Virologie, Zentrum für Infektologie, Ruprecht-Karls-Universität Heidelberg, Heidelberg; ³ Institut für Immunologie, Medizinische Fakultät, Ruprecht-Karls-Universität Heidelberg, Heidelberg

Objective: An analysis of the German transplant cohort (DZIF) revealed renal allograft recipients in Germany experience a high burden of infectious events throughout the first posttransplant year.

Method: In this prospective multicenter study of the German Center of Infectious Diseases (DZIF), all infectious events and rejections episodes observed during the first year after renal transplantation were evaluated. Characteristics of multiple infections (> 2 infections/

patient/year) were analyzed. Our cohort comprised all adult renal transplant recipients included in the DZIF-Cohort from April 2011 to November 2019 (n = 804). **Results:** Multiple infections were detected in 17.0 % (137/804) of recipients. Prevalence increased with age (25.5 % in recipients in > 65 years vs. 10.5 % in recipients < 55 years, $p < 0.001$). Univariate analysis revealed that recipient age, deceased donor, donor age, delayed graft function and the number of postoperative inpatient days were significantly associated with their occurrence. Multivariate analysis confirmed that recipient age (OR = 1.02 [1.00;1.04], $p = 0.038$) and number of postoperative inpatient days (OR = 1.25 [1.10;1.43], $p < 0.001$) were independent risk factors. Recipients infected with *Candida albicans* were frequently affected by multiple infections (mean: 5 infections/patient, range 1–10), but also with bacterial resistance (66.7 % [12/18]). Incidence rates of nosocomial pathogens (e. g. *Enterococcus* spp.) were significantly higher in recipients with multiple infections compared to recipients with 1-2 infections. Bacterial infection increased the risk of fungal infection (HR = 6.45 [3.23;12.90], $p < 0.001$) and fungal infection increased the risk for bacterial infection (HR = 3.50 [1.44;8.49], $p = 0.006$). Mean eGFR (month 3) was 51 ± 20 , 45 ± 20 , and 39 ± 21 ml/min/1.73 m² in recipients with no infection, 1-2 infections and multiple infections, respectively. Allograft rejection occurred in 15.1 % (55/365) of recipients with no infection, in 24.8 % (75/302) with 1-2 infections and in 40.9 % (56/137) with multiple infections. Rejections were most

prevalent in recipients experiencing *Candida* spp. (38.5 % [10/26]), CMV (35.4 % [35/99]) or *Enterococcus* spp. (33.6 % [40/119]) infection within first year.

Conclusion: Depending on age about 10.5 to 25.5 % of all renal transplant recipients suffer from more than two infections per year. Nosocomial pathogens and rejections are highly prevalent, especially in recipients with *Candida* spp. infection. Age and number of postoperative inpatient days were identified as independent risk factors. Multiple infections increased the risk for renal allograft rejection.

Transplantation 2

P259

High similarity of T cell-receptor repertoires in Epstein-Barr-reactive T cell cultures despite immunosuppressive treatment

C. Thieme; M. Schulz¹; S. Kaliszczuk; L. Amini; A. Blázquez-Navarro; U. Stervbo²; J. Hecht³; M. Nienen⁴; A.-B. Stittrich⁴; M. Choi⁵; R. Viebahn⁶; M. Schmuck-Henneresse; P. Reinke; T. H. Westhoff²; N. Babel²

Berlin-Brandenburger Center für Regenerative Therapien, Charité – Universitätsmedizin Berlin, Berlin;

¹ Hochschule für Technik und Wirtschaft Berlin (HTW), Berlin; ⁰ Berlin-Brandenburger Center für Regenerative Therapien, Charité – Universitäts-

medizin Berlin, Berlin; ² Centrum für Translationale Medizin, Medizinische Klinik I, Marien Hospital Herne, Ruhr-Universität Bochum, Herne; ³ Centre for Genomic Regulation, Barcelona Institute of Science and Technology, Barcelona/E;

⁴ Institute of Medical Immunology, Campus Virchow-Klinikum, Charité – Universitätsmedizin Berlin, Berlin;

⁵ Medizinische Klinik mit Schwerpunkt

Nephrologie und Internistische Intensivmedizin, Campus Virchow-Klinikum, Charité – Universitätsmedizin Berlin, Berlin; ⁶ Chirurgische Klinik, Knappschaftskrankenhaus Bochum, Ruhr-Universität Bochum, Bochum

Objective: Chronic and acute Epstein-Barr virus infection can cause serious complications in kidney transplant patients due to the suppression of T cells by the immunosuppressive medication. One important determinant of successful viral control is the T-cell-receptor (TCR) repertoire diversity. However, the influence of different clinically used immunosuppressants on the phenotype of EBV-reactive T cells and their TCR repertoire diversity has not been well defined thus far.

Method: We isolated EBV-antigen-specific T cells of six healthy donors using FACS and then expanded and characterized the cells in the absence or presence of tacrolimus (TAC), cyclosporin A (CSA), prednisolone (PRED), rapamycin (RAPA), and mycophenolic acid (MPA). Proliferation, viability, and phenotypes of T cells were assessed by flow cytometry. TCR repertoires were analyzed by next-generation sequencing.

Results: Proliferation of EBV-reactive T cells was strongly decreased by MPA and to a lesser extend by RAPA-treatment, but not by other immunosuppressants. Viability of T cell cultures, however, was increased by RAPA and strongly decreased by MPA, as most MPA-treated T cells appeared to be dead. EBV-reactive CD8⁺ T cells were slightly more frequent than CD4⁺ T cells *ex vivo*, but their ratio changed after three-week cultivation, and CD4⁺

T cells dominated most cultures. The majority of *ex vivo* EBV-reactive T cells were terminally differentiated T_{EMRA} in some, and of effector memory (T_{EM}) memory phenotype in other donors. However, after three weeks T_{EM} cells dominated the cultures of all donors. The reduced proliferative capacity of CD8⁺ T_{EMRA} cells could explain this shift. RAPA treatment maintained CD8⁺ T cells in culture, possibly benefiting cytotoxicity. The Morisita-Horn-indices for T cell cultures with and without immunosuppressants was relatively high, indicating that immunosuppression did not significantly impact T cell clonality.

Conclusion: Different immunosuppressants have diverse effects on EBV-reactive T cell proliferation, viability, and phenotype. MPA strongly impaired proliferation and viability, while RAPA reduced proliferation but had positive effects on viability and cytotoxicity. Of interest, immunosuppressive treatment did not affect the diversity of TCR repertoires in our cell-culture model. Thus, the immunosuppressive treatment studied here impairs the functionality of T cells, but does not seem to specifically target certain clones and does not lead to a shift in TCR repertoires.

P260

Evaluation of plasma chemokine levels in renal transplant patients with delayed graft function

A. Müskes; C. Thieme; P. Wehler; A. Blázquez-Navarro; P. Zgoura¹; R. Viebahn²; M. Anft¹; P. Reinke; U. Stervbo¹; T. H. Westhoff¹; T. Roch; N. Babel¹

Berlin-Brandenburger Center für Regenerative Therapien, Charité – Universitätsmedizin Berlin, Berlin;

⁰ Berlin-Brandenburger Center für Regenerative Therapien, Charité – Universitätsmedizin Berlin, Berlin;

¹ Centrum für Translationale Medizin, Medizinische Klinik I, Marien Hospital Herne, Ruhr-Universität Bochum, Herne; ² Chirurgische Klinik, Knappschafts Krankenhaus Bochum, Ruhr-Universität Bochum, Bochum

Objective: Renal inflammation after transplantation can manifest as delayed graft function, which is associated with increased risk for transplant rejection and graft loss. DGF is most commonly defined as the need for dialysis within the first week after kidney transplantation. The incidence of DGF in kidney transplant patients with post-mortem organ donation varies ranging from 19 % to 71 %, while the incidence of DGF living donor organ transplantation is only about 5 %. Risk factors for the DGF include cold ischemia time, donor creatinine, recipient body mass index (BMI), donation after cardiac death, and donor age. The ischemia-reperfusion injury can lead to the release of danger associated molecular pattern, which facilitate inflammatory reaction including the production of chemokines. Thus, we hypothesize that plasma chemokine levels are associated with the occurrence of the DGF.

Method: We compared age-, sex-, immunosuppression regime-, and BMI-matched kidney transplant patients (KTX) with DGF (n = 22) with KTX without DGF (n = 20) for their plasma levels of thirteen chemokines before (day 0) and after (day 3) kidney transplantation. Chemokines such as CXCL1, CXCL5, CXCL8, CXCL9, CXCL10, CXCL11, CCL2, CCL3, CCL4,

CCL5, CCL11, CCL17 and CCL20 were determined in plasma using a bead based multiplex assay. Additionally clinical parameters such as the glomerular filtration rate (eGFR) were monitored up to one year post transplantation.

Results: As expected, patients with DGF showed a significantly longer hospitalization after kidney transplantation compared to non-DGF patients (30 days (DGF) vs 13 days (nonDGF), mean). One month and one year after transplantation, the eGFR was a significantly lower in patients with DGF compared to patients without DGF (1 month: 29 (DGF) vs 45 (nonDGF) ml/min/1.72²; 1 year: 45 (DGF) vs 60 (nonDGF) ml/min/1.72²). The level of the analyzed chemokines before and after transplantation did not differ between the two KTX groups.

Conclusion: Levels of CXCL1, CXCL5, CXCL8, CXCL9, CXCL10, CXCL11, CCL2, CCL3, CCL4, CCL5, CCL11, CCL17 and CCL20 in plasma of KTX are not associated with DGF. The DGF is associated with an impaired eGFR, indicating that measures avoiding the DGF should be further explored.

P261

FOXP3 splice variants in kidney transplant recipients

Q. Saleh; S. Nagarajah; M. Rasmussen; M. E. Tepel

Department of Nephrology, Odense University Hospital, Odense/DK

Objective: The master gene regulator of T regulatory cells, the forkhead box P3 (FOXP3) transcription factor, is expressed in three different isoforms in humans. This variation is achieved

by exon skipping during ribonucleic acid splicing. The two most common variants include the variant that expresses all exons (FOXP3fl) and a variant in which exon 2 is skipped (FOXP3Δ2). The impact of the different distribution of these variants and their specific effects are only partly known. Now we determined the distribution of these variants in kidney transplant recipients.

Method: We collected blood samples from incident kidney transplant recipients at the first post-operative day. We isolated peripheral blood mononuclear cell ribonucleic acid. Complementary deoxyribonucleic acid was then utilized in quantitative reverse transcription polymerase chain reaction. Three specific primer sets were used to quantify total FOXP3, FOXP3fl and FOXP3Δ2. Finally, we calculated efficiency adjusted percentage of each splice variant relative to total FOXP3 expression. Data is presented as median [Interquartile range].

Results: 474 kidney transplant recipients were included. 58 received an allograft from an ABO-incompatible donor, 145 from an ABO-compatible donor, and 265 from a deceased donor. The relative distribution of FOXP3fl was 33.9 % [26.8–38.8] in ABO-incompatible donor graft recipients, 36.4 % [30.9–41.1] in

ABO-compatible donor graft recipients, and 34.9 % [28.7–41.3] in deceased donor graft recipients. The relative distribution of FOXP3Δ2 in ABO-incompatible, ABO-compatible, and deceased donor graft recipients was 66.1 [61.2–73.2], 63.6 [58.9–69.1] and 65.1 [58.6–71.3], respectively.

Conclusion: We observed a large scatter of the relative distribution of FOXP3 splice variants which may be associated to different outcomes after kidney transplantation.

P262

Vaccination status in renal transplant recipients

N. Paproth

Infektiologie, Universitätsklinikum Essen, Duisburg-Essen, Essen

Objective: The aim of this study was to examine the frequencies and titers of documented vaccinations in a cohort of renal transplant patients.

Method: Patients were recruited from the outpatient renal transplantation unit of the university hospital Essen. In addition to their yearly check-up at the outpatient renal transplantation unit patients are regularly seen by their nephrologist and/or family doctor. 105 renal transplant patients were included into this cross-sectional study (63 % male, 37 % female). Vaccination cards were

evaluated at check-up. Patients were asked to answer a questionnaire and blood samples were taken to determine vaccination titers.

Results: 18 of the 105 patients (17 %) had no vaccination card. With respect to the upcoming option of vaccination against SARS-CoV-2 patients were asked whether they wanted to get vaccinated if an approved vaccine would be available. 22 % were against vaccination, 66 % were in favor and 12 % were unsure. 44 % of the patients with vaccination cards had no valid registered tetanus vaccination and 15 % had no valid registered measles vaccination. 53 % of the patients with vaccination cards lacked vaccination against pneumococci, 18 % lacked proof of vaccination against hepatitis B virus (HBV) and 44 % against poliomyelitis. Only 52 % of the patients had protective antibody titers against diphtheria and 89 % had protective antibody titers against tetanus. 3 % of the patients had no protective antibody titers against measles. 82 % of the patients had three documented HBV vaccinations but only 25 % thereof had titers exceeding 100 IU/l.

Conclusion: Patients following renal transplantation were not sufficiently vaccinated in a cross-sectional cohort of the year 2020. Missing vaccination cards, incomplete vaccinations and failure to check titers of immunity add up to this result. Even though the vaccination

Pathogen	Tetanus	Measles	Pneumococci	HBV	Poliomyelitis	Pertussis	Diphtheria	Influenza
No valid vaccination	45 %	15 %	53 %	18 %	44 %	55 %	47 %	75 %
Protective antibody titers	89 %	97 %	76 %	37 %	Not measurable	Not measurable	52 %	Not measurable

P262: Tab. 1

Proportions of registered vaccinations and proof of immunity through titer determination against different pathogens

rates measured in this study are still below the set goals they all surpass the general population vaccination rates of Nordrhein measured in the epidemiological bulletin 50/2021 by the Robert Koch Institute.

P263

Mental Health of Living Kidney Donors before Donation – First Data from the German Living Donation Register SOLKID-GNR (Safety of the Living Kidney Donor-German National Register)

J. Jedamzik; J. Wegner¹; L. Greulich²; E. Bormann³; M. Dugas⁴; J. Gerß³; C. Sommerer⁵; M. Koch⁶; B. Suwelack¹; SOLKID-GNR Registry Group⁷
Sektion für Psychosomatische Medizin und Psychotherapie, Klinik für Psychische Gesundheit, Universitätsklinikum Münster, Münster; ¹ Allg. Innere Medizin und Notaufnahme sowie Nieren- und Hochdruckkrankheiten und Rheumatologie, Medizinische Klinik D, Westfälische Wilhelms-Universität Münster, Münster; ² Institut für Medizinische Informatik, Westfälische Wilhelms-Universität Münster, Münster; ³ Institut für Biometrie und Klinische Forschung, Westfälische Wilhelms-Universität Münster, Münster; ⁴ Institut für Medizinische Informatik, Universitätsklinikum Heidelberg, Heidelberg; ⁵ Medizinische Klinik I, Sektion Nephrologie, Medizinische Fakultät, Ruprecht-Karls-Universität Heidelberg, Heidelberg; ⁶ Klinik für Allgemein-, Viszeral- und Transplantationschirurgie, Universitätsmedizin, Johannes-Gutenberg-Universität, Mainz; ⁷ Transplantationszentren Deutschland

Objective: The aim of the SOLKID-GNR is to provide a prospective data collection for the scientific evaluation of long-term effects of living kidney donation (LD)

on the physical and mental health of living kidney donors (LKD).

Method: Since 2020, SOLKID-GNR prospectively collects demographic, medical and psychosocial data of LKD at German transplant centers (Tx-centers). Amongst other things, the register captures established psychosomatic self-assessment questionnaires for health-related quality of life (SF-12), depression (PHQ-9), somatization (PHQ-15), psychosocial stress factors (PHQ-stress), anxiety (GAD-7), resilience (RS-13), fatigue (MFI-20) and ambivalence (Simmons's Ambivalence Scale) in the population of LKD before and at regular intervals after LD. The ascertained scores before LD were compared with published German normative data using one-tailed t-tests.

Results: As of March 2nd, 2022, complete data of the first measure point (0–4 weeks before LD) of 335 LKD from 28 Tx-centers are available. 66.1 % of the LKD are female and the mean age is 54.3 (SD ± 10.2) years. 43.5 % donate to their life partner, 34.5 % to their child. Across the entire population, LKD significantly showed scores in a more favorable range (higher or lower, depending on the polarity), compared to values of the German normative data, with predominantly medium and strong effect sizes. Deviating from this pattern, the group of < 40-year-old female LKD (n = 15) showed significantly increased scores in the MFI-20-subscale „Reduced Motivation“ and „Physical Fatigue“.

Conclusion: The group of LKD included in this survey, showed a disproportionately good mental health before donation. In the group of < 40-year-old female LKD the

MFI-20-subscale „General fatigue“, „Reduced Activity“ and „Mental Fatigue“ revealed no significant differences compared to the normative data. An increased everyday stress in this group (e.g. high workload/child care) could have led to increased fatigue scores of the MFI-20-subscale „Reduced Motivation“ and „Physical Fatigue“, especially considering the data collection during the Covid-19 pandemic. The small number of cases should be regarded when interpreting these findings.

P264

Characterization of Living Kidney Donors in Germany – First Results from the German Living Donation Register SOLKID-GNR (Safety of the Living Kidney Donor-German National Register)

C. Sommerer; J. Wegner¹; L. Greulich²; E. Bormann³; M. Dugas⁴; J. Gerß³; J. Jedamzik⁵; M. Koch⁶; B. Suwelack¹; SOLKID-GNR Registry Group⁷
Medizinische Klinik I, Sektion Nephrologie, Medizinische Fakultät, Ruprecht-Karls-Universität Heidelberg, Heidelberg; ¹ Allg. Innere Medizin und Notaufnahme sowie Nieren- und Hochdruckkrankheiten und Rheumatologie, Medizinische Klinik D, Westfälische Wilhelms-Universität Münster, Münster; ² Institut für Medizinische Informatik, Westfälische Wilhelms-Universität Münster, Münster; ³ Institut für Biometrie und Klinische Forschung, Westfälische Wilhelms-Universität Münster, Münster; ⁴ Institut für Medizinische Informatik, Universitätsklinikum Heidelberg, Heidelberg; ⁵ Sektion für Psychosomatische Medizin und Psychotherapie, Klinik für Psychische Gesundheit, Universitätsklinikum Münster, Münster; ⁶ Klinik für Allgemein-, Viszeral- und Transplantationschirurgie,

Universitätsmedizin, Johannes-Gutenberg-Universität, Mainz; ⁷ Transplantationszentren Deutschland

Objective: Living kidney donation (LKD) represents the optimal treatment for patients with end-stage renal failure. There is a lack of prospective multicenter studies evaluating the physical and psycho-social outcome of living kidney donors (LD) in Germany. Since 2020 German transplant centers can participate at the prospective National Living Donation Register SOLKID-GNR.

Method: 28 of 38 transplant centers in Germany evaluated LD in an interdisciplinary approach (01/2020 to 01/2022). Clinical baseline data collected prior and 8–14 weeks after LKD were summarized to characterize LD in Germany.

Results: 305 LD were enrolled (33 % male, mean age 55 ± 10 years, range 29–83 years) representing 84 % of the recruitable LDs in Germany. Pre-emptive LKD was performed in 30 %, ABO-incompatible LKD in 27.3 %, and 8.6 % immunized LKD with donor-specific antibodies. Prior LKD S-creatinine was 0.8 ± 0.14 mg/dl and CKD_{epi} eGFR was 91 ± 13 ml/min. Alb/Crea ratio was 11 ± 28 mg/g; microalbuminuria showed 6.6 % of the LD and 3 LDs with an BMI > 35 kg/m² (mean BMI 25.9 ± 3.6 kg/m², range 17–39 kg/m²). Most of the LDs (82.4 %) reported to be completely healthy. Medical history revealed 26.6 % hypertension, 1.0 % diabetes, 3.6 % cardiovascular diseases, 9.0 % hyperlipidemia, 4.3 % autoimmune/immunological diseases and 3.3 % former malignancies. 3.6 % of LD reported about chronic pain, 3.7 % sleeping disorders, 1.7 % restlessness,

4.0 % psychological/psychosomatic diseases and 0.7 % depressive symptoms. 26.8 % of LDs without any medical history revealed to take medication. 8 to 14 weeks after LKD S-creatinine increased to 1.2 ± 0.26 mg/dl and CKD_{epi} decreased to 59 ± 12 ml/min. 42.1 % of the LDs were in CKD stage 2, 57.0 % in CKD stage 3 and one LD in CKD stage 4. There was no significant increase of microalbuminuria, or blood pressure after LKD.

Conclusion: LDs in Germany are not only healthy young persons but also persons with pre-existing medical problems. About 35 % reduction of renal function after LKD was confirmed. To evaluate any negative effect on biological and physical influence due to the nephrectomy all LDs need a regular follow-up at the transplant center. Especially LDs with a medical history should have close and comprehensive check-up visits.

P265

Herpes and polyoma virus infections and effects on the renal allograft – an analysis of the Transplant Cohort of the German Center for Infection Research (DZIF)

C. Sommerer; I. Schröter; K. Gruneberg; D. Schindler¹; C. Morath; P. Schnitzler²; L. Renders¹; U. Heemann¹; M. Zeier; T. Giese³

Medizinische Klinik I, Sektion Nephrologie, Medizinische Fakultät, Ruprecht-Karls-Universität Heidelberg, Heidelberg;

¹ II. Medizinische Klinik, Nephrologie, Klinikum rechts der Isar, Technische Universität München, München;

² Molekulare Virologie, Zentrum für Infektologie, Ruprecht-Karls-Universität Heidelberg, Heidelberg; ³ Institut für Immunologie, Medizinische Fakultät,

Ruprecht-Karls-Universität Heidelberg, Heidelberg

Objective: Herpes and polyoma virus infections are the most common infections after renal transplantation. Incidence-rates and timelines of posttransplant infection episodes and its consequences on the renal allograft have not been comprehensively documented in a German transplant cohort.

Method: In this prospective multicenter study of the German Center for Infection Research (DZIF), all herpes and polyoma virus infectious events and rejection episodes observed during the first year after renal transplantation as well as renal function were evaluated. Our cohort comprised all adult renal transplant recipients included in DZIF-Cohort from April 2011 to February 2021 (n = 1035).

Results: 1035 renal transplant recipients (64.6 % male, age: 51 ± 14 y) were enrolled. Nearly all (99.7 %) received the present standard immunosuppression consisting of an CNI, MPA and low-dose steroids. Within the first 12 months post-transplantation, 268 patients suffered 380 herpes- and polyomavirus infections, demonstrating a cumulative incidence rate of 26.4 %, 95 %CI = [23.8;29.2]. CMV accounted for the highest viral incidence-rate, affecting 14.2 % [12.2;16.5] of patients. Replication mainly occurred between month 4 and 6 at a median of 138 days (IQR = 77–219) after transplantation and after a median of 59 days (IQR = 0–140) after discontinuation of prophylaxis. The incidence rate of the high-risk group (D+/R-) was 28.3 % [22.7; 35.3] compared to 1.8 [0.7; 4.8] in the low-risk group (D-/R-). Other

herpes virus infections were rare (incidence-rates: HSV-1:1.4 % [0.8;2.3]; VZV: 0.9 % [0.5;1.7]; EBV:

0.7 % [0.3;1.4]; HSV-2: 0.6 % [0.3;1.3]; HHV-6: 0.1 % [-]). BKV incidence rate accounted for 13.1 % [11.2;15.4]).

JC-Virus was rare (n = 3); exclusively occurring in the final quarter of the first year and in all cases following CMV or BKV infection.

23 (2.2 %, 54.5 % D+/R-) patients suffered both, BKV and CMV, infection within first year. There were 6 co-infections, 11 patients with preceding BKV infection and 6 patients with preceding CMV infection. Cox Regression analysis revealed an increased rejection risk after experiencing CMV or BKV infection (HR = 3.66 [2.45;5.49], $p < 0.001$, HR = 2.151 [1.32;3.50], $p = 0.005$, respectively). Renal function was 45 ± 21 , 44 ± 20 , and 52 ± 20 mL/min in patients with CMV, BKV, or no infection 12 months after transplantation, respectively.

Conclusion: In the current era of immunosuppression and prophylaxis, renal allograft recipients in Germany experience a high burden of Herpes- and polyoma-virus infections. CMV and BKV are predominating, thereby increasing risk for rejection and lowering allograft function.

P267

The effect of tacrolimus formulation (prolonged-release vs. immediate-release) and pharmacogenetics on its susceptibility to drug-drug interactions with St. John's Wort

D. Czock; K. Gümü; A. Teegellbecker; K. I. Foerster; J. Burhenne; A. D. Meid; J. Weiss; W. Haefeli
Klinische Pharmakologie und Pharmakoepidemiologie, Innere Medizin VI,

Universitätsklinikum Heidelberg, Heidelberg

Objective: Tacrolimus is metabolized by cytochrome P450 (CYP) 3A4 and 3A5 isozymes and is susceptible to interaction with the CYP3A4 and P-glycoprotein inducer St. John's Wort (SJW, *Hypericum perforatum*). CYP3A enzymes are expressed predominantly in the small intestine and in the liver. When using prolonged-release ("once-daily") tacrolimus formulations, tacrolimus is absorbed in more distal intestinal sections, thereby potentially bypassing intestinal first-pass metabolism. Envarsus®, a prolonged-release formulation with predominant tacrolimus absorption in the colon, is considerably less susceptible to CYP3A inhibition by voriconazole. We analyzed the effect of tacrolimus formulation (immediate release, IR-Tac, Prograf® vs. prolonged release, PR-Tac, Envarsus®), CYP3A5 genotype (rs776746), and CYP3A4 phenotype (estimated with a midazolam microdose) on the extent of induction by SJW.

Method: 18 healthy volunteers (7 CYP3A5 expressors) were included in a randomized, cross-over, pharmacokinetic trial. A single oral tacrolimus dose (IR-Tac or PR-Tac, 5 mg) was administered without or with SJW (Jarsin® 300 mg TID, starting 10 days before tacrolimus and continued for 3 more days). Concentrations were quantified using validated UPLC-MS/MS methods and pharmacokinetics were analyzed by non-compartmental methods.

Results: Tacrolimus exposure (AUC) after IR-Tac was decreased 0.73-fold (90 % CI 0.60–0.88) and maximum concentration (C_{max}) was decreased 0.61-fold (0.52–0.73) by

SJW. With PR-Tac, the decrease in AUC was 0.67-fold (0.55–0.81) and C_{max} 0.69-fold (0.58–0.82), with no statistical difference between the two formulations ($p = 0.60$). In CYP3A5 non-expressors with low CYP3A4 activity the tacrolimus AUC was decreased 0.57-fold (0.47–0.70), whereas in CYP3A5 expressors with high CYP3A4 activity the AUC was decreased only 0.93-fold (0.73–1.18) by SJW.

Conclusion: Enzyme induction by SJW showed a similar extent of interaction with both tacrolimus formulations. A higher metabolic capacity and presence of a functional CYP3A5*1 allele appeared to attenuate the extent of induction by SJW, possibly due to pre-systemic SJW metabolism or limited inducibility in individuals with already high CYP3A activity.

P268

CC genotype of GNAS c.393C > T (rs7121) polymorphism has a protective impact on development of BKV viremia and BKV-associated nephropathy after renal transplantation

T. Peitz; B. Möhlendick¹; U. Eisenberger; W. Siffert¹; F. M. Heinemann²; A. Kribben; J. Friebe-Kardash
Klinik für Nephrologie, Universitätsklinikum, Universität Duisburg-Essen, Essen; ¹ Institut für Pharmakogenetik, Universitätsklinikum Essen, Universität Duisburg-Essen, Essen; ² Institut für Transfusionsmedizin, Universitätsklinikum Essen, Universität Duisburg-Essen, Essen

Objective: The GNAS gene encodes alpha-subunit of the stimulatory G-protein (G α) which is ubiquitously expressed in various tissues. The single-nucleotide

polymorphism (rs7121) of *GNAS*, c.393C > T, is associated with occurrence of a splice variant leading to elevated production of Gsα and subsequent increase of the second messenger cAMP. In the current study, we analyzed the prevalence of *GNAS* polymorphism in renal allograft recipients and its impact on allograft outcome.

Method: We screened for the *GNAS* c.393C > T polymorphism in a cohort of 436 renal allograft recipients and retrospectively studied its relationship with *de novo* formation of donor-specific antibodies (DSA), rejection events, allograft survival and appearance of viral infection in particular BKV viremia up to 5 years after transplant. *GNAS* polymorphism was determined using restriction fragment length polymorphism (RFLP)-PCR.

Results: While *GNAS* c.393C > T polymorphism was prevalent in 319 (73 %) recipients, 117 recipients (27 %) were negative. The lack of *GNAS* polymorphism correlated with significantly lower posttransplant frequency of BK polyomavirus (BKV) viremia and BKV-associated nephropathy (17 (15 %) vs. 84 (26 %), $p = 0.01$; 3 (3 %) vs. 27 (8 %), $p = 0.03$). BKV-associated nephropathy-free survival was significantly improved in noncarriers compared with *GNAS* polymorphism carriers ($p = 0.043$). Multivariate analysis indicated an independent protective effect of CC genotype on development of BKV viremia and BKV-associated nephropathy after renal transplantation (relative risk 0.54, $p = 0.04$; relative risk 0.27, $p = 0.036$). High dose BKV viremia with $\geq 10^4$ copies/mL was linked to significantly reduced allograft survival and rapid progression to

BKV-associated nephropathy compared to low dose viremia ($< 10^4$ copies/mL). However, low dose BKV viremia was more prevalent in *GNAS* polymorphism noncarriers than in carriers. On the other hand, we found a trend towards lower portion of *de novo* DSA in recipients without evidence of the *GNAS* c.393C > T polymorphism than in polymorphism carriers. With respect to rejection and allograft loss, no difference was observed between the carriers and noncarriers.

Conclusion: Lack of *GNAS* c.393C > T polymorphism corresponding to the CC genotype seems to represent a protective factor in terms of development BKV-viremia and BKV-associated nephropathy in renal allograft recipients.

P269

Differential effects of CYP3 A4*22 and POR*28 on tacrolimus metabolism and alloimmunization after kidney transplantation in contrast to CYP3 A5 genotype

J. Friebus-Kardash¹; B. Möhlendick¹; F.M. Heinemann²; E. Nela; A. Kribben; W. Siffert¹; U. Eisenberger
Klinik für Nephrologie, Universitätsklinikum, Universität Duisburg-Essen, Essen; ¹ Institut für Pharmakogenetik, Universitätsklinikum Essen, Universität Duisburg-Essen, Essen; ² Institut für Transfusionsmedizin, Universitätsklinikum Essen, Universität Duisburg-Essen, Essen

Objective: In our previous work we saw a significant effect of CYP3 A5 expresser status on the development of *de novo* donor-specific antibodies (DSAs) and antibody-mediated rejection (ABMR). Besides CYP3 A5, other enzymes such as CYP3 A4 and POR are involved in the tacrolimus

metabolism. The impact of single nucleotide polymorphism (SNPs) in the genes of CYP3 A4 and POR on alloimmunization after kidney transplantation is less understood.

Method: We retrospectively studied 400 kidney transplant recipients treated with a tacrolimus-based immunosuppression regimen to detect CYP3 A4*22 and POR*28 and to analyze the association of the two SNPs with *de novo* formation of human leukocyte antigen (HLA) antibodies and DSAs, and clinical outcome up to 5 years after transplant.

Results: In 38 (10 %) recipients expressing CYP3 A4*22 significantly higher concentration-to-dose ratios of tacrolimus than in nonexpressers were observed in the first six months posttransplant. Concentration-to-dose ratios of tacrolimus were comparable in 35 (9 %) homozygous expressers of POR*28, 158 (40 %) heterozygous expressers and nonexpressers. CYP3A4 and POR genotypes had no impact on the development of *de novo* DSAs, allograft failure and T-cell mediated as well as ABMR. Indeed, *de novo* anti-HLA antibodies occurred more frequently and *de novo* anti-HLA antibody free-survival rates were significantly decreased in homozygous carriers of POR*28. Coexpression of CYP3 A4*22 with CYP3A5 genotype was detected in only 4 (1 %) recipients. Coexpression of POR*28 with CYP3 A4 in 23 (6 %) recipients and with CYP3 A5 genotype in 31 (8 %) recipients, respectively, was not associated with significant changes in concentration-to-dose ratios of tacrolimus. Additionally, recipients with coexistence of POR*28 with CYP3 A5 genotype showed similar rates of *de novo* DSAs, *de novo* anti-HLAs and rejection as recipients

having only the *CYP3 A5* genotype. However, regarding separately the subgroup of *CYP3 A5* nonexpressers, a significantly increased number of patients with *de novo* DSAs and *de novo* anti-HLAs was found among recipients homozygous for *POR*28* compared to *POR*28* nonexpressers. **Conclusion:** Our results indicate a little effect of the SNPs, *CYP3 A4*22* and *POR*28* on alloimmunization and occurrence of ABMR compared to *CYP3 A5* genotype. Coexpression of *POR*28* had no synergistic effect on *CYP3 A5* genotype.

P270

25(OH)D- but not 1,25(OH)₂D – is an Independent Risk Factor Predicting Graft Loss in Stable Renal Transplant Recipients

S. Zeng¹; Y. Yang¹; S. Li²; C. Chu³; C.-F. Hoher⁴; Z. Zheng²; B. K. Krämer⁴; B. Hoher⁴ Guangzhou/CN; ¹ Changsha/CN; ²

Department of Nephrology, Center of Kidney and Urology, The Seventh Affiliated Hospital, Shen Zhen/CN; ³ Medizinische Klinik mit Schwerpunkt Nephrologie, Campus Charité Mitte, Charité – Universitätsmedizin Berlin, Berlin; ⁴ Nephrologie, Endokrinologie, Rheumatologie, V. Medizinische Klinik, Universitätsmedizin Mannheim, Mannheim

Objective: Vitamin D deficiency (VDD) or vitamin D insufficiency is common in kidney transplant recipients (KTRs). The impact of VDD on clinical outcomes in KTRs remain poorly defined and the most suitable marker for assessing vitamin D nutritional status in KTRs is unknown so far.

Method: We conducted a prospective study including 600 stable KTRs (367 men, 233 women)

and a meta-analysis to pool existing evidence to determine whether 25(OH)D or 1,25(OH)₂D predicted graft failure and all-cause mortality in stable KTRs.

Results: Compared with a higher 25(OH)D concentration, a low concentration of 25(OH)D was a risk factor for graft failure (HR 0.946, 95 %CI 0.912–0.981, *p* = 0.003), whereas 1,25 (OH)₂D was not associated with the study end-point graft loss (HR 0.993, 95 %CI 0.977–1.009, *p* = 0.402). No correlation was found between either 25(OH)D or 1,25 (OH)₂D and all-cause mortality. We furthermore conducted a meta-analysis including 8 studies regarding the association between 25(OH)D or 1,25(OH)₂D and graft failure or mortality, including our study. The meta-analysis results were consistent with our study in finding that lower 25(OH)D levels were significantly associated with the risk of graft failure (OR = 1.04, 95 %CI: 1.01–1.07), but not associated with mortality (OR = 1.00, 95 %CI: 0.98–1.03). Lower 1,25(OH)₂D levels were not associated with the risk of graft failure (OR = 1.01, 95 %CI: 0.99–1.02) and mortality (OR = 1.01, 95 %CI: 0.99–1.02).

Conclusion: In conclusion, baseline 25(OH)D concentrations but not 1,25(OH)₂D concentrations were independently and inversely associated with graft loss in adult KTRs.

P271

Indikationsbezogene Umstellung von IR-Tac auf LCP-Tac führt zur Verbesserung der Nierentransplantatfunktion

G. Thölking; F. Tosun; U. Jehn¹; H. Pavenstädt¹; B. Suwelack¹; S. Reuter¹

Innere Medizin und Nephrologie, UKM Marienhospital Münster; Westfälische Wilhelms-Universität, Steinfurt; ¹ Allg. Innere Medizin und Notaufnahme sowie Nieren- und Hochdruckkrankheiten und Rheumatologie, Medizinische Klinik D, Westfälische Wilhelms-Universität Münster, Münster

Hintergrund: Tacrolimus (Tac) ist der Eckpfeiler der immunsuppressiven Therapie nach Nierentransplantation (NTx), kann allerdings zu nephrotoxischen Nebenwirkungen führen. Aufgrund einer unterschiedlichen Pharmakokinetik der erhältlichen Tacrolimus-Präparate, untersucht diese Studie, ob sich die Nierenfunktion nach einer indikationsbezogenen Umstellung von immediate-release Tac (IR-Tac) auf LCP-Tac erholt.

Methode: Achtzig Patienten wurden in die Studie eingeschlossen, die eine initiale Immunsuppression mit IR-Tac (Prograf®), Mycophenolat und Prednisolon erhielten. Alle Patienten wurden von IR-Tac auf LCP-Tac einen Monat nach Transplantation oder später umgestellt (4,5 (1,0–253,1) Monate). Die Nierenfunktion und Komplikationen wurden für 36 Monate nach Umstellung beobachtet.

Ergebnisse: Die wesentlichen Gründe für die Umstellung auf LCP-Tac waren Spiegelschwankungen bzw. die Vermeidung von Nebenwirkungen bei 64 Patienten (84 %). Die glomeruläre Filtrationsrate (GFR in ml/min/1,73 m²) stieg bereits 10 Tage nach Umstellung von 41,7 auf 44,8 (*P* = 0,001), nach 12 Monaten auf 46,6 (*P* < 0,001, *N* = 78) und nach 36 Monaten auf 47,4 (*P* = 0,065, *N* = 60) an. Folgende Komplikationen traten während der Nachbeobachtung auf: CMV Infektionen:

5 (6,3 %), BKV Infektionen: 1 (1,3 %), kein Posttransplantationsdiabetes, akute Rejektionen: 10 (12,5 %).

Zusammenfassung: Unsere Studie zeigt, dass NTx-Patienten von einer indikationsbezogenen Umstellung von IR-Tac auf LCP-Tac profitieren können. Prospektive Multicenter-Studien mit pharmakokinetischen Analysen sind notwendig, um unsere Ergebnisse zu bestätigen und zu erklären.

AUTORENVERZEICHNIS

A

Adams, B. P238
 Adams, O. P247
 Adu Gyamfi, M. P218
 Affeldt, P. P247
 Afonso, S. P242
 Ahmed, A. P057
 Aigner, F. FV03, P116
 Alabdo, A. FV06
 Alba-Schmidt, E. P136
 Alber, J. P119, P120
 Albert, A. P088
 Albert, C. P088, P107
 Alejandro Alcázar, M. A. P243
 Alesutan, I. P197
 all GCKD Investigators, P031
 Alscher, M. D. FV10, P004, P139
 Alter, C. P128
 Altini, N. FV29
 Alvarez, C. FV33
 Aly, M. FV33
 Amann, K. FV12, P055, P067, P131, P132, P165, P206, P207, P219, P223, P243, P250
 Ameling, S. P169
 Amini, L. P259
 Amling, T. P165
 Amr El Shimy, I. P175
 Anan, Y. P113
 Anders, J. P247
 Anderson, D. P028, P033
 Anft, M. P070, P071, P072, P073, P074, P246, P253, P254, P260
 Angermann, S. FV02, P097
 Antignac, C. FV26
 Appel, G. P232
 Arifaj, D. FV36, P128, P130
 Arndt, P. P176, P194
 Arntjen, B. P138
 Arsiwala, A. H. P038
 Artunc, F. FV01, P049, P059, P109, P186, P188, P189
 Ashby, D. FV35
 Ashraf, M. I. FV03, P116
 Assali, T. P078
 Aßfalg, V. P250
 Attenberger, U. I. P152
 Auber, B. P022

Auge, I. FV24
 Aukschun, U. P171
 Aung, T. P206
 Avaniadi, D. P081
 Aypek, H. P171

B

Baan, C. P195
 Babel, N. P008, P055, P066, P070, P071, P072, P073, P074, P077, P080, P107, P126, P239, P246, P253, P254, P259, P260
 Babic, M. P047, P051, P212
 Bach, D. P098
 Bach, S.-M. P182, P199
 Bachir, H. P190, P191
 Bächle, H. P031
 Bachmann, A. P248, P252
 Bachmann, F. P246
 Bachmann, M. P066
 Bachmann, N. FV17
 Bachmann, Q. P083, P250
 Bachmann, S. P121, P175
 Bader, B. P138
 Baecker, M. P138
 Baier, E. P236, P237
 Bakchoul, T. P189
 Balasubramanian, P. P017
 Balcerek, B. P032
 Baleanu-Curaj, A. P127
 Bamukhaiar, F. P057
 Banas, B. FV34, P251
 Banne, E. FV31
 Barghouth, M. FV13, FV18, P040
 Barone, S. P034
 Barratt, J. FV25, P035, P036, P037
 Bartenschlager, R. FV05
 Barth, H.-P. P228
 Bartolomaeus, H. FV07, P135
 Bartolomaeus, T. U. P. FV07, P135
 Bauer, C. P253, P254
 Bauerfeind, U. P247
 Baukrowitz, T. P118
 Baum, A. P248
 Baumann, C. P255
 Baumbach, J. P169
 Bazua-Valenti, S. P121
 Becker, J. U. FV29, P002, P142

Becker, S. P140
 Bedard, P. W. P202
 Bedenbender, S. FV08
 Beer, K. P005
 Behrens, F. FV07, P244
 Beige, J. P098, P228
 Bekheirnia, M. R. FV31
 Belavgeni, A. P005
 Benkali, K. P234
 Benmerah, A. FV26
 Benning, L. FV05, FV33, FV35, P106
 Benz, K. FV12
 Benzing, T. FV27, P163, P173
 Berg, A. H. P045
 Berg, T. P041
 Bergler, T. P251
 Bergmann, C. FV17, P041, P053
 Berloco, F. FV29
 Berndt, N. P115
 Bernhardt, A. P146, P151
 Berning, P. P257
 Bertgen, L. P209
 Bertram, S. P055, P080, P107, P239
 Bestmann, Y. P229, P230
 Bethke, N. P096
 Bettac, L. P089
 Bettag, S. P008, P239
 Betz, C. P081
 Beutel, G. P003
 Bevilacqua, V. FV29
 Bichlmayer, E. M. P206
 Bieringer, M. FV04, P153
 Bildl, W. P171
 Billing, A. FV20
 Billot, K. FV26
 Bindels, E. P195
 Bindila, L. P243
 Biolik, K. P103, P104, P105
 Birkenfeld, A. L. P058
 Bissinger, R. P049, P186
 Blank, A. FV05
 Blankenberg, S. FV06
 Blázquez-Navarro, A. P071, P072, P073, P074, P246, P253, P254, P259, P260
 Bleich, E. P207

- Bleich, M. FV20, P110, P121, P123
 Blomberg, L. P163
 Bock, A. P158
 Bode, C. P220
 Bodegard, J. P028, P033
 Boedecker-Lips, S. C. P228
 Böger, C. A. P052
 Bøgh, N. FV20
 Böhmig, G. A. FV33
 Böhner, A. M. C. P152, P226a
 Bohnert, B. N. FV01, P059, P109, P186, P189
 Boivin, F. P111, P116, P122
 Bollmann, A. P028, P033
 Bolten, K. P134
 Boltengagen, A. FV22
 Bonin, L. P164
 Bonn, S. P217
 Bonnie Shen, Y. P091
 Boor, P. P195
 Bormann, E. P263, P264
 Börries, M. FV17
 Bös, D. P249
 Boss, K. P020, P064, P065, P093, P140
 Bothe, T. FV13, FV18, P024, P040
 Bothe, T. L. P133
 Bouvain, P. P128
 Boyer, O. FV26
 Bräg, S. P211
 Brähler, S. FV27, P152
 Brand, E. P027
 Brand, J. P014
 Brandt, A. P089
 Brandt, S. P146, P151
 Bräsen, J. H. P057, P065, P117, P145, P185
 Braumann, M. FV27
 Braun, D. A. P147, P190, P191
 Braun, F. P163, P172
 Braun, J. P239
 Braunsch, M. C. FV02, FV15, P021, P078, P091, P092, P184
 Brauns, N. P117
 Breiderhoff, T. P110
 Breloh, A. M. P117, P196
 Brenner, S. P023
 Brenner, T. FV21, P066
 Brensing, K. A. FV38
 Brinkkötter, P. T. FV27, P234
 Brinkmann, L. P032
 Brochhausen, C. P206
 Brohammer, E. P019
 Brown, R. P062
 Brucker, A. P002
 Brüder, N. P003
 Brunetti, A. FV29
 Brüning, U. P244
 Brunkhorst, L. P245
 Buchholz, B. P205, P206, P210, P214
 Buchner, J. P219
 Buckenmayer, A. P095
 Budde, K. FV39, P140, P218
 Budde, U. P066
 Buerger, F. FV31
 Buhl, E. M. P195
 Bunse, M. P178
 Burgun, A. FV26
 Burhenne, J. P267
 Burkert, K. P247
 Burkhardt, T. P106
 Burmester, H. S. P214, P225
 Busch, M. P031, P240
 Busch, T. P177
 Busch, V. P094
 Büttner-Herold, M. FV12, P021, P052, P067, P207, P250
 C
 Cabrita, I. P173
 Cai, J. P156
 Callewaert, F. P086
 Cammett, T. J. P233
 Cantutan, B. P180
 Cao, S. P111, P122
 Cao, Y. P039
 Cardoso, J. P091
 Carr, S. P121
 Cascante, I. P177
 Caskey, F. P045
 Cataland, S. P086, P238
 Catar, R. A. FV39, P090, P218
 Cejka, V. P023
 Chadjichristos, C. P182
 Chatziantoniou, C. P182
 Chen, C.-Y. P135, P244
 Chen, L. P013
 Chen, X. P039
 Chen, X. FV26
 Chenot, J.-F. O. P024, P040
 Chesnaye, N. P045
 Chikho, M. P207
 Cho, S. P001
 Choi, M. P246, P259
 Choukroun, G. P035, P036, P037
 Chrysopoulou, M. FV20
 Chu, C. P039, P082, P270
 Chun, J. P226
 Chung, W. K. P053
 Cicalese, P. A. FV29, P142
 Cicek, H. P148
 Ciesek, S. P076, P081
 Cinkilic, O. P071, P072, P073
 Clasen, W. P054
 Clausmeyer, J. FV23
 Comic, J. FV15, P021
 Cook, T. P232
 Coppo, P. P086
 Cordasic, N. P131, P223
 Coresh, J. P038
 Cosgrove, D. P203
 Costa, I. P195
 Crone-Rawe, T. P083
 Czock, D. FV33, P267
 Czogalla, J. P217
 D
 Dabers, T. FV19, P029, P056
 Dahlke, E. P113
 Dahlmann, A. FV37
 Dahmen, L. P069
 Dähnrich, C. P229, P230
 Dammann, E. P003
 Dang-Heine, C. P253
 Daniel, C. FV12, P067, P165, P206, P207, P219, P223
 Daniel, V. FV33
 Datta, R. R. P247
 David, S. P220
 de Fallois, J. P030, P053, P252
 de Groot, K. P061, P076, P228
 de la Rubia, J. P086
 De Nicola, L. P035, P036, P037

de Passos Sousa, R. P086
 Decker, E. FV17, P053
 Dehde, S. FV09
 Deheshwar, K. P172
 Delanaye, P. FV16
 Delimont, D. P203
 Dellanna, F. P035, P036, P037, P101
 Dellmann, A. P057
 Delprete, C. FV29
 DeLuca, D. P196
 Demir, F. FV20
 Demirci, H. P110, P175
 Denholm, B. P181
 Devane, J. FV17
 di Cristanziano, V. P247
 Diefenhardt, P. FV27
 Diehl, L. P148
 Dieplinger, G. P247
 Dihazi, G. H. P129
 Dihazi, H. P129
 Dilz, J. FV24
 Dimkovic, N. P035, P036
 Ding, X. P156
 Dippon, J. P139
 Ditt, V. P247
 Ditting, T. P131, P132
 Dittmayer, C. P175
 Dittmer, R. P066
 Dittmer, U. P066
 Dixon, B. P. P232, P238
 Doebeis, C. P039
 Doevelaar, A. P008, P055, P066, P077, P080, P107, P239
 Dogan, I. P042, P099
 Dolff, S. P065
 Döllner, J. P131
 Dorn, C. FV14
 Dörr, M. FV19, P043
 Döser, M. P209
 Dötsch, J. P243
 Doxiadis, I. P252
 Draganova, D. P084
 Drechsler, C. P045
 Dröge, L. P024
 Dudeck, A. P151
 Dugas, M. P263, P264
 Dumoulin, B. P171

Duttlinger, J. FV38
 Dutzmann, J. P220
 Duvnjak, B. P134
 Dvela-Levitt, M. P121

E

Eberbach, M.-L. FV01
 Ebert, M. P153
 Ebert, N. FV13, FV16, FV18, P024, P040
 Ebert, N. P223
 Eck, C. P067
 Eckardt, K.-U. FV22, P031, P038, P051, P096, P197, P204, P212
 Eckermann, M. P091
 Eckert, P. FV28
 Eckes, T. S. P081, P226
 Eddy, S. P192
 Eder, M. P003
 Effland, A. P152, P226a
 Eiber, M. P052
 Eichler, M. P152
 Einloft, J. FV08
 Eisenberger, T. FV17
 Eisenberger, U. P026, P256, P268, P269
 El Hajami, M. P190
 Elitok, S. P082
 Eller, P. P010
 Elsaesser, A. P017
 Elsner, K. P210
 Endlich, K. P029, P169
 Endlich, N. P029, P165, P169, P182, P199, P231
 Enghard, P. FV04, FV22, P006, P096
 Engler, C. P103
 Epting, D. FV17
 Erdogan, C. FV03, P108
 Eskinyurt, M. P140
 Esser, A. P031
 Esser, G. P087
 Essigke, D. P109
 Estepa Martínez, M. O. P197
 Ester, L. P173
 Eugen-Olsen, J. FV21
 Eulenberg-Gustavus, C. P204
 Evans, M. P045

F

Faas, S. P233
 Fabretti, F. P173
 Fähling, M. P032, P114, P115, P116
 Fährndrich, M. P096
 Fakhouri, F. P232, P234
 Fakler, B. P171
 Fang, Y. P156
 Feger, M. P119, P124
 Fehler, I.-K. P150
 Felderhoff, T. P094
 Felix, S. B. FV19
 Ferrazzi, F. P219
 Ferreira, J. O. P. P017
 Fichtner, F. P078
 Fink, G. P243
 Fischer, J. P041
 Fischer, K.-D. FV31
 Fischereder, M. P063
 Flade, K. P002
 Flechsig, M. P117
 Fleig, S. P196
 Fliser, D. FV06
 Floege, J. P156, P195
 Flögel, U. P128
 Foerster, K. I. P267
 Föllner, M. P119, P120, P124, P125
 Foltmann, T. P045
 Forer, L. P031
 Forslund, S. P135
 Fox, J. P225
 Frahnert, M. P074
 Francescapola, M. P169
 Franke, U. P004
 Freedman, B. P195
 Frein von Rheinbaben, S. FV19, P029, P043, P056, P241
 Freund, P. FV22
 Frew, I. P179
 Fricke, L. P074
 Friebus-Kardash, J. P026, P256, P268, P269
 Friedl, F. FV35
 Friedrich, A. FV17, P041
 Friedrich, N. FV19
 Fritsche, R. FV03
 Fritz, P. P139

Füeßl, L. P063
 Funk, N. D. P144, P166
 Fürst, D. P252

G

Gaal, B. P171
 Gäckler, A. P064, P065, P255
 Gaedcke, S. P196
 Gairing, S. J. P007
 Galle, P. R. P007
 Ganner, A. P179
 Ganser, A. P003
 Gao, Y. P156
 Garcelon, N. FV26
 Garlo, K. P233, P238
 Gast, L. FV37
 Gastmeier, P. FV23
 Gauer, S. P226
 Geffers, C. FV23
 Geffers, R. P146
 Gehlen, F. P019, P084
 Gehrig, J. P199
 Gehringer, F. P146
 Geis, L. P157
 Geißler, S. P126
 Gembardt, F. P018, P187
 George, B. P167, P168, P209
 Gerdes, N. FV36
 Gerhardt, L. P001
 Gerlach, M. P176
 Gerß, J. P263, P264
 Geßner, R. P069
 Gesualdo, L. FV29
 Ghavampour, S. P023
 Giese, T. P258, P265
 Giglio, T. P071, P072
 Girndt, M. P050
 Gloede, G. P172
 Göbel, K. P098
 Göbel, N. P004
 Göcmen, B. FV28, P171, P177
 Goepfert, M. FV19
 Gohl, M. P054
 Gohlisch, C. P047
 Gollasch, B. P042, P099
 Gollasch, M. P042, P048, P099
 Gorka, O. P211
 Görlich, N. FV04, FV22

Gorski, M. FV32
 Göth, D. FV35, P106
 Göttfried, K. P006
 Graf-Allgeier, C. FV23
 Grahammer, F. P171, P200
 Grampp, S. P149, P205
 Grams, M. P038
 Gratton, M. A. P203
 Greco, A. P212
 Greenbaum, L. P234, P238
 Greipel, L. P060
 Greka, A. P121
 Grenz, J. P106
 Greulich, L. P263, P264
 Grgic, I. FV08
 Gribaudo, A. P240
 Gribnau, J. P195
 Griesmann, B. P061
 Groeger, C. P206
 Gröne, H.-J. P226
 Groß, O. P211
 Großewinkelmann, C. FV15
 Grothgar, E. FV04, FV22
 Grund, A. P119, P145, P193, P227
 Grundmann, F. P247
 Grune, T. P048
 Gruneberg, K. P258, P265
 Grünewald, I. FV17
 Gu, Y. P156
 Gul, S. P199
 Gummi, M. R. P212, P215
 Gümüs, K. P267
 Gunawardena, S. P086
 Günthner, R. FV02, FV15, P091, P184
 Günzel, D. P110
 Guthoff, M. P058
 Gutting, M. P060, P245
 Gyarmati, G. P202

H

Haas, C. S. P069, P085, P095
 Haas, F. P217
 Haas, M. P226a
 Haase, N. P135
 Habbig, S. P173
 Häberer, S. P146
 Haberfellner, F. P250

Hackl, C. P206
 Haefeli, W. P267
 Haesner, M. P107
 Haffner, D. P119, P145, P161, P193, P214, P225, P227
 Hafizi, R. P201, P216
 Hafner, M. P010
 Hahm, E. FV21
 Hakroush, S. FV30, P235, P236, P237
 Halbritter, J. P030, P041, P053, P198, P248, P252
 Halder, M. P195
 Hall, S. P159
 Halle, S. P144
 Haller, B. FV02, P091, P250
 Haller, H. P022, P117, P144, P166, P196, P220, P221, P222
 Haller, V. P206
 Hammer, E. P165, P169
 Hammer, S. P189
 Hannane, N. P083
 Hannemann, L. P092
 Hanssen, H. FV02
 Hantmann, E. P041, P198
 Hänzelmann, S. FV06
 Harder, J. L. P192, P200
 Härteis, S. P206
 Hartig, C. P198
 Hartmann, A. P224
 Hartner, A. P116
 Hartwig, L. P229
 Hassan, F. P214
 Hassinger, A. P152
 Hatzl, S. P010
 Haug, A. P045
 Hauser, I. A. P076, P081
 Hausinger, R. I. FV02, P083, P091, P092, P250
 Hausmann, F. FV06
 Hay, E. P182
 Hayat, S. P195
 Hayek, S. FV21
 Hecht, J. P259
 Heckel-Kratz, E. P076
 Heemann, U. FV02, FV15, P021, P052, P078, P083, P091, P092, P097, P250, P258, P265

- Hegermann, J. P220
 Heid, I. FV32
 Heidenreich, K. P242
 Heidet, L. FV26
 Heinemann, F. M. P256, P268, P269
 Heintz, L. P014, P174
 Heintze, C. P040
 Heinze, L.-M. P003
 Heister, D. J. FV01, P058, P059
 Helmstädter, M. P171, P180
 Hemmersbach, A. P080
 Henschler, R. P252
 Herber, A. P041
 Herfurth, K. P240
 Hergesell, O. P084
 Hering, L. FV36, P128, P130, P155
 Hermann, J. P212
 Hermans-Borgmeyer, I. FV09
 Hermle, T. P044, P170
 Herrmann, H. P089
 Hesse, L. P206
 Hettler, S. P015
 Hettrich, W. P233
 Heuser, M. P003
 Heyne, N. FV01, P058, P059, P138, P228, P238
 Hildebrandt, F. FV31
 Hilgers, K. F. P131, P132
 Hillebrandt, J. P068
 Himmerkus, N. FV20, P110, P121, P123
 Hindricks, G. P028, P033
 Hinze, C. FV22, P111, P122
 Hochar, B. P039, P082, P270
 Hochar, C.-F. P270
 Hoeft, K. P195
 Hoeper, M. P220
 Höfele, J. FV15, P021
 Hoffmann, R. P029
 Hofherr, A. P177
 Hofmann, S. P217
 Hofmeister, A. FV08
 Hogeweg, M. P008, P055, P077
 Hohenstein, B. P019, P084
 Holfeld, J. P197
 Holle, J. B. FV07, P244
 Hollemann, J. P165
 Hollerieth, K. P009
 Holtzhausen, S. P176
 Hölzer, B. P066, P107
 Holzmann-Littig, C. P078, P091, P092, P247
 Hoogenboezem, R. P195
 Hoorn, E. P195
 Höpken, U. P178
 Hoppenz, P. P005
 Hoppstock, G. P158
 Horn, P. A. P255
 Hornung, S. P091
 Hoyer, J. P069, P085, P095
 Hu, J. P175
 Huang, M. FV09
 Huber, T. B. FV06, FV09, P014, P136, P171, P172, P180, P181, P217
 Hückelhoven-Krauss, A. FV33
 Hugo, C. P002, P005, P018, P176, P187, P194, P253, P254
 Huscher, D. P040
 Hussain, S. P062
 Hussein, N. P067
 Hutzfeldt, A. P164
 Huwiler, A. P201, P216
I
 Ibrahim, E. FV33
 Imeri, F. P201, P216
 Inzucchi, S. E. P017
 Isermann, B. P151
 Ito, S. P234
 Ittermann, T. FV19, P043
 Ivens, K. P068
 Izuhara, A. P202
J
 Jackisch, C. P061
 Jägers, J. FV20
 Jahn, J. P177
 Jahn, M. P026
 Jain, M. P211
 Jakobs, C. E. M. P080
 Jankowski, J. P127
 Jankowski, V. P156
 Jansen, J. P195
 Jantsch, J. P183
 Jarocki, D. P203
 Jarquin-Diaz, V. H. P135
 Jeanpierre, C. C. FV26
 Jedamzik, J. P263, P264
 Jehn, U. P137, P257, P271
 Jenkinson, C. P159, P203
 Jens, A. P030
 Jensen, B.-E. O. P080
 Jerke, U. P204
 Jiletcovici, A. P036, P037
 Jin, W. P198
 Joosten, M. FV31
 Jost, J. S. P022
 Jürgens, C. P065
 Jüttner, K. P098
K
 Kächele, M. P089
 Kaczmarek, A. P138
 Kahl, A. L. P025
 Kahlfuss, S. P151
 Kainz, P. P206
 Kaireit, T. F. P022
 Kaiser, R. P247
 Kalampoka, V. P007
 Kalbacher, H. P188
 Kälble, F. FV21, FV33, FV35, P106
 Kaliszczyk, S. P246, P254, P259
 Kalk, P. P088
 Kalo, M. Z. P109, P186
 Kamalanabhaiah, S. P069, P085
 Kampf, L. L. P170
 Kang, H. G. P238
 Kann, M. P247
 Kantauskaite, M. P068, P130, P134
 Kantzow, B. P138
 Kanzelmeyer, N. FV14, P060, P245
 Kapanadze, T. P145, P161
 Kaps, L. P007
 Kashihara, N. FV25
 Kavanagh, D. P232, P238
 Kawka, E. P090
 Kayser, N. FV28
 Kedziora, S. P135
 Keller, C. P069, P085
 Keller, K. P121
 Kelterborn, S. P116
 Kemmner, S. P009, P063, P250
 Kenter, A. P195

- Kers, J. P142
 Kessel, F. P018
 Ketteler, M. FV10, P004
 Kettritz, R. P153, P178, P204
 Khadzhynov, D. P096
 Khedkar, P. H. P108
 Kiel, S. P024
 Kielstein, J. T. P003, P057
 Kilik, T. P211
 Kim, S. H. P238
 Kim, S. J. FV22
 Kimmel, M. FV10, P139
 Kindelan Lohse, A. P127
 Kirschner, K. M. P116
 Kirwan, J. FV07
 Kispert, A. FV31
 Kitsche, B. P228
 Kittel, M. P068
 Kiyan, Y. P220
 Klämbt, V. FV31
 Klaus, D. P152
 Klein, F. P247
 Klein, M. P179
 Kleinau, G. P218
 Kleine, C. E. P249
 Kleinschnitz, C. P093
 Kleist, C. FV33
 Klemm, K. P082
 Kleophas, W. P079, P101, P140
 Klie, L. P113
 Kliewe, F. P165, P169, P231
 Kling, L. P204
 Klocke, J. FV04, FV22
 Kluge, I. A. P236
 Knauf, F. P042, P099, P116
 Knaup, K. X. P149
 Knöbl, P. P086
 Knöller, S. P228
 Knopp, C. P195
 Koch, A. P226
 Koch, B. F. P081
 Koch, M. P263, P264
 Kocinsky, H. P232
 Kocks, C. FV22
 Kocylowski, M. P171
 Koelbl, O. P206
 Köhler, M.-B. P048
 Köhler, S. P180, P181
 Köhler, S. P003
 Kohlhasse, J. P044
 Kohmer, N. P076, P081
 Kolb, T. P068, P134
 Kolbrink, B. P087, P185
 Kollins, D. FV25
 Köllner, S. FV09
 Komers, R. P159, P202, P203
 Kong, L. P186
 König, J. FV17
 König, S. P028, P033
 Königshausen, E. P068, P134, P162
 Konik, M. J. P064, P065
 Konrad, M. FV17
 Kopp, C. FV37
 Koppitch, K. P001
 Kosanke, M. P220
 Kost-Alimova, M. P121
 Kotliar, K. FV02
 Kotsis, F. K. P031
 Köttgen, A. FV28, P031, P044, P171, P177
 Köttgen, M. P177
 Kowall, B. P020
 Koziolk, M. J. P129
 Kramann, R. P195, P217
 Kramer, A. P174
 Kramer, T. FV23
 Krämer, B. K. P015, P039, P082, P270
 Kranke, P. P078
 Kranz, J. P195
 Kraus, A. P205, P206, P210
 Krause, B. C. P244
 Krausel, V. P190, P191
 Krautkrämer, E. FV21
 Krautwald, S. P185
 Krawczyk, A. P255
 Krebs, C. F. P242
 Kremer, W. M. P007
 Kremer Hovinga, J. P086
 Kretz, O. FV09, P171, P172, P217
 Kretzler, M. P192
 Kreuzberger, N. P083
 Kreuzer, L. P063
 Kribben, A. P020, P025, P026, P064, P065, P093, P140, P255, P256, P268, P269
 Krieglstein, N. P219
 Kriuchkova, N. P110
 Kröger, H. P018, P176, P194
 Kron, J. P102, P103, P104, P105
 Kron, S. P102, P103, P104, P105
 Kronenberg, F. P031
 Krug, P. FV26
 Krügel, U. P048
 Krüger, A. P096
 Krüger, B. M. P030
 Krüger, R. FV32, P149, P160
 Krüger, T. P079, P101
 Kuang, F. P026
 Kübler, W. P244
 Kuchle, C. P092
 Kuchler, T. P184
 Kuehl, M. P217
 Kuhlen, R. P028, P033
 Kuhlmann, M. K. FV13, FV16, FV18
 Kuhn, P.-H. P021
 Kühn, T. FV05
 Kühn, W. P211
 Kühne, L. P171
 Kühnl, A. P229, P230
 Kulik, A. P171
 Kulow, V. A. P032, P114, P115
 Kumar, S. P034
 Kunz, J. V. P096, P099
 Kunzendorf, U. P087, P185
 Kuppe, C. P195, P217
 Kurek, J. P070
 Kurschat, C. P163, P247
 Kurth, I. P195
 Kurts, C. FV27, P152, P226a
 Kusch, A. FV03
 Kuschnereit, T. P056, P241
 Kylies, D. P217

L
 Labenz, C. P007
 Labes, R. P032, P114, P115
 Lahme, K. P172
 Lai, E. FV31
 Lamberti, J. P068

- Landgraf, R. P252
Landmann, S. P068
Lang, A. FV36
Lang, K. P170
Lang, K. S. P026
Lange, T. P199
Lanznaster, J. P080
Lassé, M. P192
Lauer, V. FV32
Lautsen, C. FV20
Lech, M. P091
Lehmann, C. P252
Lehrke, M. P195
Leifheit-Nestler, M. P119, P145, P161, P193, P227
Leimbach, T. P103, P104, P105
Leiner, J. P028, P033
Leiz, J. P111, P122
Lempicki, C. P170
Lendeckel, U. P029
Lenders, M. P027
Lepa, C. P167, P168
Lettermann-Nass, I. P069, P085
Lewandowski, N. P025
Li, J. FV21
Li, L. P232
Li, S. P270
Li, Y. P177
Licht, C. P232
Lichtenberger, F. B. P108
Lienkamp, S. FV31
Lifton, R. FV31
Limbourg, F. P145, P161
Lin, J. P086
Lindemann, M. P064, P255
Lindenmeyer, M. T. FV06, P181
Linder, N. P041
Lindner, T. H. P248, P252
Lindquist, J. A. P146, P151, P158
Linke, A. P148
Linkermann, A. P002, P005
Linz, P. FV37, P131, P132
Lio, C. T. P169
Liu, J. P211
Liu, S. P014, P172
Liu, T. P042, P099, P100
Liu, X. P156
Löber, U. FV07, P135
Lodka, D. P153, P178
Loirat, C. P234
Lojko, D. P084
Loos, S. FV14
Lorenz, G. FV02, P091
Loreth, D. P014, P172, P174
Lovric, S. P221
Loyen, M. P054
Lucas, R. FV09
Luce, P. P224
Lücht, C. P218
Lucke, S. P153
Lüders, S. P129
Ludwig, U. P089
Luft, F. C. P042, P099
Lühnen, J. P078
Luong, T. T. D. P197
Luque, Y. P238
Lürken, K. P075
Lutz, P. P249
- M**
- Madison, J. P203
Madris-Aris, A. D. P238
Maes, B. FV25
Magirr, A. FV25
Mahl, L. P206
Mahler, C. F. FV35
Manaila, R. P201
Mandel, A. M. P163
Mane, S. FV31
Manfredini, S. P101
Marcy, F. P006
Maremonti, F. P005
Markau, S. P050
Marko, L. P048
Markus, M. P043
Martirosian, P. P058
Maruhn, S.-M. P179
Maruyama, S. P234
Masanneck, M. P098
Mashregghi, M.-F. FV22, P244
Mathia, S. P032
Matschkal, J. FV02
Matten, L. P162
Mausberg, A. K. P093
Maybaum, J. FV09
Mayr, S. P052
McClure, C. P101
McMahon, A. P001
McParland, V. FV07
Meehan, D. P203
Meerpohl, J. J. P078
Mehrabi, A. FV33, FV35
Meid, A. D. P267
Meier, M. FV25
Meier, N. P044
Meinitzer, A. P010
Meiselbach, H. P031
Meiser, B. P063
Meister, T. L. P071, P072, P073, P074
Melderis, S. P148
Melk, A. P166, P222
Meller, L. P255
Menasria, I. P241
Menke, M. FV15
Menzel, S. P195
Merle, U. FV33
Mertens, A. P140
Mertens, P. R. P146, P151, P158
Messer, J. P098
Messtorff, M. L. P185
Metjian, A. P086
Metzger, P. FV17
Metzke, D. FV04, FV22
Meyer, C. P005
Meyer, T. M. P057
Meyer-Schwesinger, C. FV09, P014, P148, P152, P172, P174
Mielke, N. FV13, FV18, P024, P040
Mieth, M. FV35
Mihlan, M. P224
Millman, E. E. P233
Milosavljevic, J. P170
Milster, M. P079
Minkue Mi Edou, J. P086
Miyakawa, Y. P238
Möddel, M. P141
Moellmann, J. P195
Mohan, C. FV29, P142
Möhlendick, B. P256, P268, P269
Möhwald, A. P206
Moldoveanu, Z. P159
Möller, B. P095
Möller-Kerutt, A. P143

Monsef, I. P083
 Moore, L. P062
 Morath, C. FV05, FV21, FV33, FV35, P106, P258, P265
 Morinière, V. FV26
 Moser, N. P177
 Mrowka, R. FV24
 Mueller, N. P094
 Muff-Luett, M. P238
 Müller, A. P138
 Müller, A. P020
 Müller, A. FV11, P148
 Müller, D. FV07, FV14, P110, P244
 Müller, D. N. P135
 Müller, K. P251
 Müller, L. P068
 Müller, R.-U. P247
 Müller, S. P094
 Müller-Tidow, C. FV33
 Mülling, N. P025
 Münch, F. D. R. FV22
 Münch, J. P248, P252
 Münz, S. P125
 Mursic, I. P010
 Müskes, A. P260
 Mutig, K. P110, P121, P175

N

Naas, S. FV32, P149, P160
 Naert, T. FV31
 Nagai, J. P195
 Nagarajah, S. P261
 Nagel, A. FV37
 Nagel, M. P007
 Nauck, M. P043
 Nela, E. P269
 Neubauer, B. P177, P211
 Neumann, D. P220
 Neumann, I. E. P246
 Neumann, K. FV11, P148
 Neumann, S. P253
 Neumann-Haefelin, E. P179
 Nguyen, H. V. FV29, P142
 Niedermoser, M. P177
 Nielsen, R. P200
 Nienen, M. P259
 Nierychlewski, K. P063
 Nische, R. P185

Novak, J. P159
 Novak, L. P159
 Nürnberg, B. P048
 Nüsken, E. P243
 Nüsken, K.-D. P243
 Nußhag, C. FV21, FV33, FV35, P106
 Nyamsuren, G. P150, P213

O

Oberacker, T. FV10, P004, P139
 Obermüller, N. P226
 Ofstad, A. P. P017
 Oftring, A. P081, P226
 Ogawa, M. P238
 Ögel, N. P116
 Ohrenschall, G. P118
 Olganier, D. P200
 Olek, S. P253
 Olinger, E. FV17
 Omran, H. FV38
 Opelz, G. FV33
 Or-Guil, M. P253, P254
 Ostendorf, T. P156
 Ostermaier, C. P069, P085, P095
 Ott, C. P131, P132
 Ott, E. FV17
 Öttl, K. P093
 Ovcara, E. P076

P

Paar, M. P093
 Paniskaki, K. P066, P071, P072
 Paolini, A. P211
 Pape, L. FV14
 Paproth, N. P262
 Pasch, A. P197
 Passfall, J. P107
 Pastene Maldonado, D. O. P015
 Patyna, S. P076, P081, P226
 Patzak, A. FV03, P108, P133
 Paul, V. P056
 Pavenski, K. P086
 Pavenstädt, H. P137, P143, P147, P167, P168, P190, P191, P209, P257, P271
 Peach, E. P034
 Pego da Silva, L. FV33

Pehnke, S. P252
 Peisker, F. P195
 Peitz, T. P026, P256, P268
 Pellisier, V. P028
 Pellissier, V. P033
 Pelze, L. P189
 Perales-Paton, J. P195
 Perie, L. P242
 Perkovic, V. FV25
 Persson, P. B. P032, P108, P110, P114, P115
 Pesce, F. FV29
 Peschel, M. P141
 Peters, H. P096
 Petersen, E. L. FV06
 Peti-Peterdi, J. P202
 Petri, E. P143
 Petsch, T. P029
 Petzold, F. FV26, P252
 Peyvandi, F. P086
 Pfab, T. P107
 Pfaender, S. P071, P072, P073, P074
 Pfefferkorn, A. M. FV03
 Pfeilschifter, J. M. P081, P201, P226
 Pfister, F. P092
 Pflanzl-Knizacek, L. P010
 Philippe, A. L. P218
 Pickering, M. C. P232
 Pieper, D. P129
 Pieterse, C. P234
 Pigorsch, M. P096
 Pilz, N. P133
 Pinckert, L. P123
 Pinetz, T. P226a
 Pion, E. P206
 Pitigala, L. P197
 Platzer, K. P053
 Pockardt, L. P155
 Pollmann, S. P027
 Pontrelli, P. FV29
 Popatenko, O. P135
 Popovic, S. P175
 Popp, B. P248, P252
 Popp, M. P078
 Pörner, D. P249
 Porto, G. P045

Portoles, J. P035, P036, P037
 Poschenrieder, A. P091
 Pöschla, L. P154, P198
 Pottel, H. FV16
 Potthoff, S. A. P155
 Pramparo, T. P159
 Pratschke, J. FV03
 Prencipe, B. FV29
 Preuß, S. P009
 Preussner, M. FV08
 Promnitz, J. P231
 Prosseda, P. P. P211
 Prskalo, L. FV04, FV22
 Puelles Rodriguez, V. G. P217
 Pul, R. P093
 Pustlauk, W. P126

Q

Quach, K. P127
 Queisser, L. P010
 Quintanova, C. P123

R

Rabenau, H. P076, P081
 Racovitan, D. P008, P239
 Raffetseder, U. P156
 Rahman, M. FV36, P128, P130, P155
 Rahmel, A. FV34
 Rajewsky, N. FV22
 Rapp, G. P213
 Rasmussen, M. P261
 Rauh, M. P243
 Regenbogen, C. P184
 Reichardt, C. P146, P151
 Reichardt, J. P042
 Reichel, H. FV38
 Reichel, M. P116
 Reily, C. P159
 Reinders, M. P195
 Reinhard, S. P249
 Reinhardt, W. P025
 Reinke, P. P253, P254, P259, P260
 Reiser, J. FV21, FV33
 Reisewitz, T. P162
 Reiss, L. K. P156
 Remuzzi, G. P232

Renders, L. FV15, P021, P078, P092, P247, P250, P258, P265
 Renné, T. FV06
 Renschler, G. FV17
 Rettig, R. P029
 Reusch, M. P035, P036, P037
 Reuter, S. P137, P257, P271
 Reuter, S. FV24
 Reuthelshöfer, M. P219
 Rhein, K. P177
 Ribeiro, A. P091
 Ribitsch, W. P010
 Rice, K. P233
 Richter, B. P145, P161, P193
 Richter, G. S. P227
 Richter, S. P088
 Ridder, J. P148
 Riebeling, T. P185
 Rieckmann, S. P008, P055, P077, P239
 Riedhammer, K. M. FV15, P021
 Rifai, K. P057
 Rilinger, N. P061
 Rinschen, M. FV20, P164, P192, P200
 Rizk, D. V. FV25
 Rizvi, S. FV29, P142
 Roch, T. P070, P071, P073, P074, P126, P246, P253, P254, P259, P260
 Röcken, C. P219
 Rodionova, K. P131, P132
 Rodriguez-Niño, M. A. P015
 Roelofs, J. P142
 Rögner, K. P032, P114, P115
 Rohn, B. P008, P066, P071, P107, P239
 Rohn, H. P064
 Rong, S. P196, P222
 Rosenberger, C. P032, P114, P115, P116
 Rossini, M. FV29
 Roth, K. FV08
 Rothe, M. P042, P099
 Rottenaicher, G. P219
 Rousselle, A. P153, P178, P204, P208
 Rovin, B. FV25
 Rüb, M. P019

Rump, L. C. FV36, P068, P128, P130, P134, P155, P162
 Rüthrich, M. M. P080

S

Sabat, R. P253
 Sachs, W. P014, P172, P174
 Saez-Rodriguez, J. P195
 Salama, A. FV04
 Saleh, Q. P261
 Saller, B. P211
 Samadova, A. P056
 Samuelson, G. P203
 Sandersfeld, M. FV12
 Saritas, T. P195
 Saudenova, M. P118, P231
 Sauer, I. M. FV03
 Saunier, S. FV26
 Sawitzki, B. P253
 Sayer, M. P138
 Schaaf, A. FV14
 Schaaf, C. P021, P078, P092
 Schaefer, L. P226
 Schaefer, L. P049
 Schaefer, M. P048
 Schäfer, A.-K. P129
 Schäfer, H. P052, P097
 Schäfer, I. P221
 Schöffner, E. FV13, FV16, FV18, P024, P040
 Schaier, M. FV05, FV33, FV35
 Schanner, C. P028, P033
 Schanz, M. FV10, P004, P139
 Schattenberg, J. M. P007
 Schatz, V. P183
 Schauer, M. P183
 Scheerer, P. P218
 Scheid, C. P091
 Schell, C. P211
 Schenk, H. P220
 Scheppach, J. P038
 Scherberich, J. E. P223
 Scherer, S. FV33
 Schermer, B. FV27, P163, P173
 Scheuch, M. P029
 Schewe, M. P118
 Schierbaum, L. FV31

- Schiffer, M. FV32, FV37, P131, P132, P149, P160, P183, P205, P210
 Schilcher, G. P010
 Schindler, D. P258, P265
 Schindler, M. P182, P199
 Schirmer, B. P220
 Schleicher, E. M. P007
 Schlevogt, B. FV17
 Schley, G. P116, P183
 Schlitt, H. J. P206
 Schlosser, M. P240
 Schlumberger, W. P229, P230
 Schmaderer, C. FV02, FV15, P021, P046, P052, P078, P083, P091, P092, P097, P184, P250
 Schmid, N. P004
 Schmidt, C. P134
 Schmidt, S. P107
 Schmidt, T. P136, P242
 Schmidt-Lauber, C. FV06
 Schmidt-Ott, K. M. FV22, P022, P111, P116, P122, P144, P166, P220, P221, P222
 Schmieder, R. E. P131, P132
 Schminke, U. FV19
 Schmitt, A. FV33
 Schmitt, C. P. FV14
 Schmitt, M. FV33
 Schmitt, R. P022, P144, P166, P196, P222
 Schmitz, J. P065, P117, P145, P185
 Schmitz, P. P028, P033
 Schmuck-Henneresse, M. P259
 Schneditz, D. P102, P104, P105
 Schneider, A. FV13, FV18, P040
 Schneider, M. P. P034, P038
 Schneider, S. FV31
 Schneider, U. FV04, P153
 Schneppenheim, S. P066
 Schnitzler, P. FV05, FV33, P258, P265
 Schödel, J. FV32, P149, P160, P205
 Schöler, F. P177
 Scholten, D. P077
 Scholz, H. P116
 Scholz, J. K. P214
 Schömig, T. FV27
 Schönauer, R. P030, P041, P198
 Schönbrunn, A. P082
 Schönherr, S. P031
 Schönhoff, B. P143
 Schörghuber, M. P010
 Schork, A. FV01, P189
 Schreiber, A. FV04, FV25, P153, P178, P204
 Schrick, S. FV10, P004, P139
 Schroder, P. P220
 Schröder, T. P006
 Schröppel, B. P089, P142
 Schröter, I. P258, P265
 Schuchardt, M. P047, P051, P212
 Schüler, M. P030
 Schuller, I. P141
 Schultalbers, A. P220
 Schulte, K. P087
 Schulte, U. P171
 Schulte-Kemna, L. S. P089
 Schultheiß, U. T. P031, P044
 Schulz, A.-M. P047
 Schulz, M. P062
 Schulz, M. P259
 Schumacher, B. P163
 Schüssel, K. P087
 Schuster, A. P251
 Schuster, M. P187
 Schwab, C. FV33
 Schwab, F. FV23
 Schwab, S. P249
 Schwalm, S. P201, P226
 Schwarz, M. P063
 Schwarz, S. P206
 Schwelberger, H. G. FV03
 Schwenk, J. P171
 Schwerk, M. P217
 Sciascia, S. P142
 Scully, M. P086
 Seeber, C. P078
 Segelmacher, M. P077
 Seibert, E. P019, P084
 Seibert, F. S. P008, P055, P066, P077, P080, P094, P107, P239, P254
 Seidel, M. P008, P107, P239
 Seifert, L. FV09
 Seith, F. P058
 Seitz, H. P253
 Sekula, P. P031
 Selina Stippa, S. P224
 Sellin, L. P162
 Servais, A. FV26
 Seshan, S. P142
 Shah, M. D. P234
 Shao, F. P002
 Sheerin, N. S. P234
 Shril, S. FV31
 Shroff, U. P202
 Siam, S. P257
 Sieckmann, T. P116
 Siegerist, F. P182, P199
 Sierks, D. P041
 Sierocinski, E. P024
 Sierra-Gonzalez, C. FV27
 Siffert, W. P256, P268, P269
 Sikora, A. P019
 Simmons, S. P244
 Sinning, J. P144, P166
 Skerka, C. P224
 Skoczynski, K. P205, P210
 Skoetz, N. P083
 Skopnik, C. FV04, FV22
 Sleiman, S. P151
 Smeets, B. P195
 SOLKID-GNR Registry Group, P263, P264
 Sommer, F. P228
 Sommerer, C. FV33, P031, P106, P258, P263, P264, P265
 Song, N. P156
 Sonnemann, J. FV04
 Sörensen-Zender, I. P144, P166, P222
 Sostelly, A. P234
 Speer, C. FV05, FV21, FV33, FV35, P106
 Speer, T. P195
 Spinner, C. P080
 Spitthöver, R. M. P025
 Sprangers, B. FV25
 Sradnick, J. P018, P176, P187, P194
 Sreckovic, S. P234
 Srugies, F. P134
 Stadler, D. FV02, P046
 Staggs, L. P220
 Stahl, K. P220

Stang, A. P020
 Stanzick, K. J. FV32
 Stark, K. FV32
 Stecher, M. P080
 Steckelberg, A. P078
 Steffens, J. P195
 Stegbauer, J. FV36, P068, P128, P130, P134, P155
 Steger, F. P206
 Steglich, A. P187
 Steinbrenner, I. P031
 Steiner, R. P081
 Steines, L. P251
 Steinmetz, O. M. P148
 Stervbo, U. P070, P071, P072, P073, P074, P246, P253, P254, P259, P260
 Stettner, M. P093
 Steubl, D. P091
 Steveling, A. P043
 Stippel, D. P247
 Stittrich, A.-B. P259
 Stöber, A. P168
 Stock, K. P009
 Stockmann, H. P031, P096
 Stolpe, S. P020
 Stolze, S. P158
 Stöveken, L. P168
 Stracke, S. FV19, P024, P029, P043, P056, P228, P241
 Strassburg, C. P. P249
 Strassl, V. P211
 Strauch, L. P180
 Streese, L. FV02
 Streis, J. P094
 Sudowe, S. P081
 Süsal, C. FV33
 Suwelack, B. P263, P264, P271
 Szczepek, M. P218
 Szepanowski, F. P093
 Szymczak, M. P. P045

T

T. Abdallah, A. P195
 Talbot, S. R. P003
 Tamm, E. P210
 Tampe, B. FV30, P213, P235, P236, P237

Tampe, D. P236, P237
 Tanaka, K. P238
 Tang, X. P180
 Tangri, N. P034
 Tanturovska, B. S. P201, P216
 Tauber, R. P052
 Taylan, C. FV14
 Teegelsbekkers, A. P267
 Temme, S. FV36, P128
 Tepel, M. E. P261
 Terlinden, M. P027
 Terness, P. FV33
 Theilig, F. P113, P118, P200, P231
 Thieme, C. P246, P253, P254, P259, P260
 Thölking, G. P271
 Thomusch, O. P253
 Thumfart, J. FV14
 Thürmer, A. FV07
 Tiegs, G. FV11, P148
 Tieken, I. FV34
 Tillmann, F.-P. FV38
 Timm, J. P068
 Timmesfeld, N. P080
 Todkar, A. P211
 Todorov, V. T. P018, P176, P187, P194
 Tölle, M. P047, P051, P212
 Toller, W. P010
 Tomas, N. M. FV09, P136, P217
 Tometten, I. P068
 Tonnus, W. P002, P005
 Torrez, C. P250
 Tory, K. FV26
 Tosun, F. P271
 Tran, T. H. FV05, FV33
 Trimarchi, H. N. FV25
 Trinsch, B. FV27
 Trojan, A. P141
 Tsoy, O. P169
 Tsvetkov, D. P048
 Tun, Z. M. P062
 Tuschen, K. P247
 Twerenbold, R. FV06

U

Uder, M. FV37
 Uebel, S. P160

Ulrich, C. P050

V

van de Kar, N. P142
 van de Logt, A.-E. P230
 van den Born, J. P015
 van der Giet, M. FV13, FV16, FV18, P047, P051, P212
 van Roeyen, C. P195
 Vecera, V. P135
 Veelken, R. P131, P132
 Veenstra, A. C. FV28
 Vehreschild, M. P080
 Ventzke, M. P173
 Verhülsdonk, J. P226a
 Vidal Blanco, E. P071
 Viebahn, R. P254, P259, P260
 Viehmann, C. P174
 Vienken, T. E. P162
 Vigolo, E. P116
 Vink, C. P230
 Vivante, A. FV31
 Vivarelli, M. P232
 Vlahou, A. P197
 Vo-Cong, M.-T. P009
 Vogel, E. P189
 Voggel, J. P243
 Vogt, I. P145, P161, P193, P227
 Vöing, K. P147
 Volbracht, L. P020
 Völker, U. P165, P169
 Völkl, J. P197
 Volland, K. P069, P085
 Völzke, H. FV19, P043
 von Baehr, V. P039, P082
 von Mäßenhausen, A. P005
 von Samson-Himmelstjerna, F. A. P087, P185
 von Vietinghoff, S. P117, P196, P249
 Vonbrunn, E. P067, P207, P223
 Vosik, D. P203
 Voß, V. P222

W

Wadewitz, J. FV34
 Wagner, C. P157
 Wagner, F. P010

- Wagner, L. FV04, FV22
Wagner, M. FV15
Wagner, T. P053
Waldherr, R. FV33
Walker, P. P232
Wallbach, M. P129
Walter, S. P161
Walz, G. FV28, P179
Wang, C. FV31
Wang, H. FV28
Wang, J. P156
Wang, J. P238
Wang, L. FV33
Wang, M. P014
Wang, W. FV25
Wanner, C. P011, P012, P017, P023, P045
Wanner, N. P217
Was, N. P156
Weber, C. P165
Weber, L. T. FV14
Weckbach, O. P138
Wegner, A. P187
Wegner, J. P263, P264
Wegscheid, C. P148
Wehler, P. P126, P246, P253, P254, P259, P260
Wei, C. FV21
Weide, T. P143, P147
Weidemann, A. P247
Weikert, B. FV23
Weimann, A. P248, P252
Weinert, S. P151
Weingärtner, N. P145, P161
Weinmann-Menke, J. P007
Weinreich, T. P019, P084
Weiss, A.-C. FV31
Weiss, J. P267
Weiß, L. P081
Weissensteiner, H. P031
Wellenkötter, J. P071, P072
Wenger, R. H. P201, P216
Wenzel, U. P136
Werberich, L. P249
Werberich, R. P249
Werner, J. P206
Westergaard Rasmussen, C. FV20
Westermann, L. P177
Westermann, M. P118
Westhoff, J. P214
Westhoff, T. H. P008, P055, P066, P070, P071, P072, P073, P074, P077, P080, P094, P107, P126, P239, P246, P254, P259, P260
Westphal, F. P137
Wetzels, J. F. M. P230
Wiech, T. P014, P054, P136, P148, P162, P182, P217, P224, P242
Wiening, V. P257
Wiesener, M. P149
Wilck, N. FV07, P135, P244
Wilde, B. P247, P255
Wilhelm, J. P066
Willam, C. P183
Wille, K. P080
Wimmer, M. I. P135
Wirth, A. P187, P194
Witowski, J. FV39, P090
Wittösch, S. P171
Witzke, O. P064, P065, P066, P255
Wohlfarth, M. P243
Woitas, R. P249
Woitas, R. P. P088
Wolf, G. B. P240
Wolf, L. P124
Wolf, R. P056
Wolk, K. P253
Wolters, K. P146
Wong, M. N. P217
Wörn, M. P188
Wörns, M.-A. P007
Wu, D. FV39, P090
Wu, S. P016
Wulf, S. P242
Wulfmeyer, V. C. P022, P144, P166, P196, P222
- X**
Xiao, M. P189
Xie, S. P013
Xiong, Y. P039
Xu, M. FV03, P108
Xu, Y. P048
Xu, Y. P195
- Y**
Yakoub, M. FV36, P128, P130, P134
Yakulov, T. A. FV28
Yang, Y. P270
Yard, B. A. P015
Yilmaz, A. FV17
Yilmaz, D. E. P110, P175
Yilmaz, S. P066
Yiqin Shi, Y. P156
Yoon, S.-S. P238
Young, J. P035, P036, P037
- Z**
Zacharias, H. U. P031
Zahner, G. FV09
Zaidan, M. FV26
Zaiser, F. FV28
Zamora Gonzalez, N. P005
Zecher, D. FV34
Zegers, M. FV31
Zeier, M. FV05, FV21, FV33, FV35, P106, P258, P265
Zeiler, M. P046
Zeisberg, M. P150, P213
Zelck, M. P243
Zeller, T. FV06
Zellner, A. P021
Zeman, F. FV34, P251
Zeng, S. P270
Zgoura, P. P066, P080, P107, P138, P239, P254, P259, P260
Zhang, C. P058
Zhang, H. FV25
Zhang, X. P112
Zhang, Z. P232
Zhao, H. FV39, P090
Zhao, L. FV03
Zhao, M.-H. P234
Zheng, Z. P270
Zheng, Z. P048
Zhu, C. P158
Zickler, D. FV39, P197
Ziegler, W. H. P214, P225
Zielinski, S. P014, P172, P174
Zimmermann, M. P217
Zinman, B. P017
Zipfel, P. F. P224, P242

Zitta, S. P010
Zou, W. P013
Zschummel, M. P178

IMPRESSUM

Mitteilungen der Deutschen
Gesellschaft für Nephrologie e. V.

Der Bezug ist im Mitgliedsbeitrag
enthalten.

Herausgeber

Deutsche Gesellschaft
für Nephrologie (DGfN) e. V.
Sitz: Heidelberg
Geschäftsstelle:
Großbeerenstraße 89, 10963 Berlin
Telefon: +49 30 258 009 40
Telefax: +49 30 258 009 50
gs@dgfn.eu
www.dgfn.eu

Verantwortlich für den redaktionellen Inhalt

Prof. Dr. U. Heemann
(Tagungspräsidium)
Prof. Dr. J. Lutz
(Tagungspräsidium)
Prof. Dr. C. Schmaderer
(Tagungskoordination)

Verlag, Layout, Anzeigenverwaltung

Aey Congresse GmbH
An der Wuhlheide 232A,
12459 Berlin
Telefon: +49 30 2900 6594
Telefon: +49 30 2900 6595
info@aey-congresse.de

Bildrechte im Heft

Von den Autorinnen/Autoren,
so nicht anders ausgewiesen.
Bilder Titelseite: © U. Heemann;
© khmelev, stock.adobe.com;
© gpointstudio, stock.adobe.com

Hinweis

Der Verlag und die herausgebende
Fachgesellschaft übernehmen trotz
sorgfältiger Kontrolle keine Gewähr
für die Richtigkeit von Dosierungs-
anweisungen und Applikations-
formen. Diese sind immer anhand

der Fachinformationen und/oder
Packungsbeilagen zu prüfen.

Copyright

Alle Rechte, wie Nachdruck
auch von Abbildungen, Vervielfältigungen jeder Art, Vortrag,
Funk, Tonträger und Fernseh-
sendungen sowie Speicherung in
Datenverarbeitungsanlagen,
auch auszugsweise, behalten wir uns
vor. Trotz sorgfältiger Bearbeitung
aller termingerecht eingegangenen
Unterlagen kann der Hersteller
keine Gewähr für vollständige
und richtige Eintragungen über-
nehmen. Schadenersatz für fehler-
hafte und unvollständige oder nicht
erfolgte Eintragungen und Anzeigen
ist ausgeschlossen. Erfüllungsort
und Gerichtsstand ist Berlin.

